

This electronic thesis or dissertation has been downloaded from the King's Research Portal at <https://kclpure.kcl.ac.uk/portal/>



The clay mineralogy, weathering and mudslide behaviour of coastal cliffs.

Moore, Roger

The copyright of this thesis rests with the author and no quotation from it or information derived from it may be published without proper acknowledgement.

END USER LICENCE AGREEMENT



Unless another licence is stated on the immediately following page this work is licensed

under a Creative Commons Attribution-NonCommercial-NoDerivatives 4.0 International

licence. <https://creativecommons.org/licenses/by-nc-nd/4.0/>

You are free to copy, distribute and transmit the work

Under the following conditions:

- Attribution: You must attribute the work in the manner specified by the author (but not in any way that suggests that they endorse you or your use of the work).
- Non Commercial: You may not use this work for commercial purposes.
- No Derivative Works - You may not alter, transform, or build upon this work.

Any of these conditions can be waived if you receive permission from the author. Your fair dealings and other rights are in no way affected by the above.

Take down policy

If you believe that this document breaches copyright please contact librarypure@kcl.ac.uk providing details, and we will remove access to the work immediately and investigate your claim.

**THE CLAY MINERALOGY, WEATHERING AND MUDSLIDE BEHAVIOUR
OF COASTAL CLIFFS.**

by

Roger Moore

March 1988

A thesis submitted to the University of London
for the degree of Doctor of Philosophy

Department of Geography
King's College London

In memory of Mike Purser
Colleague and friend

ABSTRACT

Reviews of geomorphological and geotechnical literature suggest that the physico-chemical properties of clay are important in processes of soil deformation but in practice such properties are seldom considered in explanations of slope instability. This thesis establishes the importance of clay mineralogy and solute geochemistry upon the seasonal behaviour of coastal mudslides.

Analyses of the 'static' and 'dynamic' properties of mudslides include a regional survey of landslide-prone geological strata and on-site analyses of two mudslides at Warden Point, north Kent, and Worbarrow Bay, Dorset. Twenty soil parameters were determined for 95 samples, and the results correlated to establish the degree of association between variables and residual shear strength. Laboratory simulation tests established the importance of clay mineralogy and chemistry upon shear strength.

The seasonal behaviour of mudsliding was monitored at one site over 20 months. Automated techniques recorded movement, pore water pressure and weather conditions, along with periodic assessments of soil moisture, atmospheric and pore water chemistry. Data were collated at several time-scales and correlated to identify relationships between parameters; antecedent time-lags were established between the variables. Seasonal fluctuations in pore water chemistry were related to simulated results which suggested that residual strength was naturally sensitive to change.

The nature and chemistry of clays were found to have important effects upon the location and behaviour of landslides. Such effects were exacerbated by weathering reactions; these were modelled using WATEQF and PHREEQE and applied to a process-response flow diagram. The temporal and spatial controls of residual shear strength were fundamentally related to the physico-chemical properties.

Fluctuations in shear strength were not only found to be a major cause of the seasonal reactivation of mudslides but also the primary control of the underlying mechanisms of behaviour. Infinite slope models revealed that the pore water pressures and undrained loading were less sensitive to change than the residual strength of mudslides: realistic factors of safety were only obtained when the seasonal changes in strength were considered by the model.

SUMMARY OF CONTENTS

	Abstract	3
	Summary of Contents	4
	Chapter Contents	5
	List of Figures	10
	List of Tables	16
	List of Plates	21
	List of Appendixes	22
	Acknowledgements	23
Chapters		
One	Mudslide form, behaviour and materials	26
Two	The physico-chemical properties of landslip clays	74
Three	Methodology and field-site description	152
Four	Results of the static analysis: the properties of mudslides with respect to weathering and slope morphology	263
Five	Results of the dynamic analysis : the dynamics of seasonal mudslide behaviour	428
Six	Analysis and discussion of results : solute geochemistry and slope stability analysis	513
Seven	Conclusions	612
	References	640
	Appendixes	666

CHAPTER CONTENTS

Chapter One

MUDSLIDE FORM, BEHAVIOUR AND MATERIALS

1.1	Aims and organisation of the thesis	27
1.2	What is a mudslide ?	31
1.3	The development and morphology of mudslides	39
1.4	The mechanics of mudslide behaviour	51
1.5	Material properties	61
1.6	Conclusions	73

Chapter Two

THE PHYSICO-CHEMICAL PROPERTIES OF LANDSLIP CLAYS

2.1	Introduction	75
2.2	The inherent properties:	
2.21	Composition	76
2.22	Clay Mineralogy	81
2.23	Clay chemistry:	88
	2.231 Particle interactions and bonding mechanisms	89
	2.232 Water chemistry and exchange reactions	96
2.24	Plasticity, cohesion and the phase relationships	102
2.3	The mechanical properties:	
2.31	Weathering:	110
	2.311 Weathering of clay minerals	111
	2.312 Reaction of sea-water with clay minerals	117
2.32	Shear strength	120
2.33	Volume change behaviour	131
2.34	Permeability	139
2.4	Conclusions	148
2.5	Research objectives	150

Chapter Three

METHODOLOGY AND FIELD SITE DESCRIPTION

3.1	Introduction	153
3.2	Field survey, photogrammetry and site description:	157
3.21	Geomorphological mapping and survey techniques	158
3.22	Photogrammetric survey:	163
3.221	Field-survey	166
3.222	Analysis	170
3.23	Site description, morphology and lithology:	
3.231	Manor Lane	175
3.232	Worbarrow Bay	183
3.3	Field instrumentation and sampling techniques:	191
3.31	Field sampling techniques	193
3.32	Field instrumentation:	199
3.321	Weather and climate	202
3.322	Pore water pressure	205
3.323	Soil moisture	213
3.324	Surface movement	217
3.325	Salt deposition	224
3.326	Pore water chemistry	227
3.33	Monitoring framework and site maintenance	231
3.4	Laboratory methods:	236
3.41	Physico-chemical analysis of core-samples:	
3.411	Core-sample processing	240
3.412	Soil description and sub-sampling	241
3.413	Physical analyses	245
3.414	Mineralogical and chemical analyses	247
3.42	Routine analysis of rain and pore water samples	254
3.43	Residual strength simulation	257
3.5	Conclusions	262

Chapter Four

PROPERTIES OF MUDSLIDES WITH RESPECT TO WEATHERING AND SLOPE MORPHOLOGY

4.1	Introduction	264
4.2	Characterization of mudslide materials:	
4.21	Site morphology and sampling resolution	266
4.22	Core sample descriptions	269
4.23	Particle size distributions	277
4.24	The phase relationships:	
4.241	Moisture content	288
4.242	Specific gravity, void ratio and porosity	296
4.243	Unit weight and particle density	303
4.3	Geotechnical properties:	310
4.31	Plasticity and activity	311
4.32	Shear strength:	
4.321	Drained residual shear strength	319
4.322	Drained peak shear strength	322
4.4	Soil chemistry:	
4.41	Chemical characterization of mudslide materials:	
4.411	pH and conductivity of soil solution	327
4.412	Organic matter content and loss on ignition	337
4.42	Cation balance:	
4.421	Interstitial free water	341
4.422	Soluble ions and exchangeable bases	351
4.43	Cation exchange capacity and exchange reactions	361
4.44	Bulk chemistry of the clay-size fraction	371
4.45	Anisotropic particle and solute chemistry	381
4.46	Semi-quantitative analyses of clay minerals	394
4.5	Conclusions of the laboratory analysis	405
4.6	Regional variations in clay and landslide distribution:	
4.61	Southern and south-eastern England	409
4.62	The London Clay Basin	423
4.63	Conclusions	426

Chapter Five

THE DYNAMICS OF SEASONAL MUDSLIDE BEHAVIOUR

5.1	Introduction	429
5.2	Morphological change and mudslide development:	
5.21	Photogrammetric analyses	430
5.211	Planimetric comparison	431
5.212	Profile change	435
5.213	Contours and DTM of difference	438
5.214	Target and instrument fix	442
5.3	Field monitoring	447
5.31	Weather and climate:	
5.311	Rainfall	448
5.312	Net hydrological flux	451
5.313	Wind speed and direction	453
5.314	Salt deposition	456
5.32	Soil water relations:	
5.321	Soil moisture	464
5.322	Pore water pressure	472
5.323	Pore water chemistry	476
5.33	Surface movement:	
5.331	Automatic movement sensors	484
5.332	Association of movement with other variables	494
5.4	Shear strength simulation	497
5.41	Pure clay minerals:	
5.411	Effect of mineral type and quantity	499
5.412	Effect of exchangeable cations	502
5.42	Natural samples:	
5.421	Effect of sea-salts on residual strength	505
5.5	Conclusions	509

Chapter Six

SOLUTE GEOCHEMISTRY AND SLOPE STABILITY ANALYSIS

6.1	Introduction	514
6.2	The physico-chemical variability and behaviour of mudslides:	
6.21	Static properties and residual strength:	515
6.211	Particle and density characteristics	517
6.212	Mineralogical and chemical properties	527
6.22	Dynamic behaviour:	534
6.221	Climatic controls upon slope instability	537
6.222	Soil water relations	542
6.223	Shear strength	545
6.3	Geochemical modelling:	552
6.31	Phase equilibria:	552
6.311	Weathering reactions	554
6.312	Effects of salt deposition and pore water dilution	568
6.32	Geochemical interactions	575
6.4	Slope stability analyses:	578
6.41	Choice of model	579
6.42	Local and global Factor of Safety:	
6.421	Peak and residual conditions	581
6.43	Seasonal fluctuations in Factor of Safety:	
6.431	Effect of pore water pressure	589
6.432	Effect of residual shear strength	595
6.433	Effect of undrained loading	606
6.5	Conclusions	

Chapter Seven

CONCLUSIONS

7.1	Original contribution to the study of mass movement	613
7.2	Suggestions for future research	620
7.3	Epilogue:	
7.31	Regional associations between landslides and clay minerals	621
7.32	The spatial variability of physico-chemical properties	622
7.33	Effects of weathering	630
7.34	Association of geochemical properties with shear strength	632
7.35	The seasonal behaviour of mudslides	634

LIST OF FIGURES

Chapter One

- Figure 1.1 Morphological characteristics of mudslides.
- Figure 1.2 Mudslide form in relation to the intensity of toe erosion of London Clay cliffs 30-40 metres in height.
- Figure 1.3 The cyclic development of deep-seated mudslides on London Clay cliffs exposed to rapid marine erosion.
- Figure 1.4 The location of deep-seated mudslides with respect to structural dip and sea-level.
- Figure 1.5 A process-response system of the form, stresses and rate of operation of a mudslide system.
- Figure 1.6 Relationship between pore water pressure and 'graded' slip displacements of a mudslide at Worbarrow Bay.
- Figure 1.7 Variation in soil properties of mudslides on St. Lucia.
- Figure 1.8 Pattern of mudflow movement and montmorillonite-illite to kaolinite ratios.

Chapter Two

- Figure 2.1 Relationship between water and clay content required to fill voids in a granular soil.
- Figure 2.2 The coordination of alumino-silicate clays into tetrahedral and octohedral sheet structures.
- Figure 2.3 Double layer repulsive and attractive energy in relation to particle separation and electrolyte concentration.
- Figure 2.4 Effect of cation valence on double layer interactions.
- Figure 2.5 The phase relationships.
- Figure 2.6 Relation between the plasticity index and clay fraction.
- Figure 2.7 Typical chemical weathering environments.
- Figure 2.8 Classification of UK overconsolidated clays and mudrocks in relation to plasticity and clay content.
- Figure 2.9 The relation between water flux and the hydraulic gradient.
- Figure 2.10 The relation between hydraulic conductivity and void ratio.

Chapter Three

- Figure 3.1 Location of the field study sites.
- Figure 3.2 Geomorphological mapping symbols with computer coding for photogrammetric analyses.
- Figure 3.3 Geomorphological map of Worbarrow Bay.
- Figure 3.4 Geomorphological map of Manor Lane.
- Figure 3.5 Schematic diagram of photo and object coordinate systems.
- Figure 3.6 Computational procedure used in photogrammetric analyses.
- Figure 3.7 1:500 scale plan of the Manor Lane field-site.
- Figure 3.8 1:250 scale plan of the Worbarrow Bay field-site.
- Figure 3.9 Core-sampler design.
- Figure 3.10 Instrument and sampling locations at Manor Lane.
- Figure 3.11 Instrument and sampling locations at Worbarrow Bay.
- Figure 3.12 Installation procedure used for electrical and standpipe piezometers.
- Figure 3.13 Calibration curves for the automatic water depth sensors.
- Figure 3.14 Interface design to control the water depth sensor battery-transducer link.
- Figure 3.15 Access tube installation and the principle of the neutron soil moisture meter.
- Figure 3.16 Automatic movement sensor design.
- Figure 3.17 Typical calibration of movement sensors.
- Figure 3.18 Salt gauge design.
- Figure 3.19 Typical rainfall calibration of each salt gauge.
- Figure 3.20 Typical Flame Photometer calibrations for sodium and potassium.
- Figure 3.21 Typical Atomic Adsorption Spectrometer calibrations for magnesium and calcium.
- Figure 3.22 Typical Ion Chromatograph calibrations for chloride and sulphate.
- Figure 3.23 Modified Bromhead ring-shear apparatus.

Chapter Four

- Figure 4.1 Particle-size distribution and frequency histogram for sample 5A₃.
- Figure 4.2 Percent clay profiles for selected core samples.
- Figure 4.3 The distribution of clay at the shear surface.
- Figure 4.4 Natural moisture content profiles of selected core samples.
- Figure 4.5 The distribution of moisture content at Manor Lane.
- Figure 4.6 The distribution of moisture content at Worbarrow Bay.
- Figure 4.7 Void ratio depth profiles for selected core samples.
- Figure 4.8 The distribution of the void ratio at the shear surface.
- Figure 4.9 The distribution of porosity with depth and along the basal shear surface.
- Figure 4.10 Unit weight profiles of selected core samples.
- Figure 4.11 Distribution of unit weight at the shear surface.
- Figure 4.12 Bulk density profiles of selected core samples.
- Figure 4.13 Distribution of bulk density at the shear surface.
- Figure 4.14 Distribution of the liquid limit at the shear surface.
- Figure 4.15 Distribution of the plasticity index at the shear surface.
- Figure 4.16 Distribution of the activity ratio at the shear surface.
- Figure 4.17 Residual strength Mohr envelopes at the shear surface.
- Figure 4.18 Residual stress ratio at the basal shear surface.
- Figure 4.19 Peak strength Mohr envelopes for *in situ* materials.
- Figure 4.20 Distributions of the peak and residual friction angles in relation to the Manor Lane and Worbarrow mudslide sections.
- Figure 4.21 Hydrogen ion activity profiles of selected core samples.
- Figure 4.22 Distribution of pH at the shear surface.
- Figure 4.23 Electrical conductivity with depth of selected profiles.
- Figure 4.24 Distribution of conductivity at the basal shear surface.
- Figure 4.25 Loss-on-ignition with depth of selected profiles.
- Figure 4.26 Distribution of LOI at the basal shear surface.

- Figure 4.27 Distribution of dominant free-water anions at the basal shear surface.
- Figure 4.28 Distribution of free-water calcium at the shear surface.
- Figure 4.29 Distribution of free-water sodium at the shear surface.
- Figure 4.30 Distribution of free-water iron at the shear surface.
- Figure 4.31 Distribution of the total free-water cations at the shear surface.
- Figure 4.32 Concentration of water-soluble cations of selected core profiles.
- Figure 4.33 Distribution of water-soluble cations at the shear surface.
- Figure 4.34 Concentration of exchangeable cations for selected core profiles.
- Figure 4.35 Distribution of exchangeable cations at the shear surface.
- Figure 4.36 Cation exchange capacity profiles of selected core samples.
- Figure 4.37 Distribution of CEC at the basal shear surface.
- Figure 4.38 Percent base-saturation profiles of selected core samples.
- Figure 4.39 Distribution of base-saturation at the basal shear surface.
- Figure 4.40 Crystal lattice aluminium profiles for selected samples.
- Figure 4.41 Distribution of aluminium oxide at the basal shear surface.
- Figure 4.42 Distribution of crystal lattice iron at the shear surface.
- Figure 4.43 Distribution of lattice silica at the basal shear surface.
- Figure 4.44 Anisotropic silica deposition across the shear surface.
- Figure 4.45 Anisotropic aluminium deposition across the shear surface.
- Figure 4.46 Anisotropic iron deposition across the shear surface.
- Figure 4.47 Distribution of micaceous clay minerals at Manor Lane.
- Figure 4.48 Distribution of montmorillonite clays at Manor Lane.
- Figure 4.49 Distribution of micaceous clay minerals at Worbarrow Bay.
- Figure 4.50 Distribution of montmorillonite clays at Worbarrow Bay.
- Figure 4.51 The geological formations of the study area.
- Figure 4.52 Frequency histograms of the total and youthful number of landslides reported for each geological formation.

- Figure 4.53 The total and inland density of youthful landslides reported for each geological formation.
- Figure 4.54 The number of translational mudslides and unclassified landslides reported for each geological formation.
- Figure 4.55 The distribution of mica and montmorillonite clay minerals associated with each geological formation.
- Figure 4.56 The density of youthful landslides in association with the proportion of micaceous and montmorillonite clay minerals.
- Figure 4.57 The inland density of youthful landslides in association with the proportion of mica and montmorillonite clays.
- Figure 4.58 The distribution of landslides in the London Clay Basin with respect to the proportion of montmorillonite clays.

Chapter Five

- Figure 5.1 Morphological change at Worbarrow Bay revealed in plan by photogrammetric analyses between March 1986 and May 1987.
- Figure 5.2 Change in surface profile of the main mudslide at Worbarrow Bay between March 1986 and May 1987.
- Figure 5.3 Change in surface profile of the perched mudslide system at Worbarrow Bay between March 1986 and May 1987.
- Figure 5.4 Contour map of the Worbarrow site from the March 1986 DTM.
- Figure 5.5 DTM of difference of the Worbarrow mudslides between March 1986 and May 1987.
- Figure 5.6 Movement trajectories of targets installed at Worbarrow.
- Figure 5.7 Total monthly rainfall throughout the study.
- Figure 5.8 Daily rainfall histograms of peak winter rainfall in the 1985/86 and 1986/87 seasons.
- Figure 5.9 Net monthly hydrological flux during the study.
- Figure 5.10 Prevailing wind directions at the coastal cliffs of Worbarrow Bay.
- Figure 5.11 Maximum monthly wind speed during the study.
- Figure 5.12 Monthly weight of salt deposited on the coastal cliffs at Worbarrow Bay.
- Figure 5.13 Relationship between effective south-westerly precipitation and salt deposition.
- Figure 5.14 Total monthly rainfall with respect to micro-climate.
- Figure 5.15 Deposition of sea-salts with respect to micro-climate.

- Figure 5.16 Moisture volume fraction depth profile within the backcliff at Worbarrow Bay.
- Figure 5.17 Moisture volume depth profiles within the Worbarrow mudslide.
- Figure 5.18 Mean monthly soil moisture in the back-cliff and accumulation lobe at Worbarrow Bay.
- Figure 5.19 Soil moisture at the shear surface in the source and lobe between December 1986 and March 1987.
- Figure 5.20 Mean monthly phreatic levels in the source and accumulation lobe throughout the study.
- Figure 5.21 Daily rainfall and phreatic level during August 1986 illustrating associated time-lagged responses.
- Figure 5.22 Pore water salt concentration at the shear surface of the accumulation lobe throughout the study.
- Figure 5.23 Distribution of pore water salt concentrations at the shear surface of the Worbarrow mudslide on the 30th January 1987.
- Figure 5.24 Release of aluminium oxide during 1986/7 in relation to the seasonal intensity of weathering and erosion of the cliff and source units of the Worbarrow mudslide.
- Figure 5.25 Maximum monthly movement throughout the study.
- Figure 5.26 Cumulative pattern of movements during the winters of 1985/86 and 1986/87.
- Figure 5.27 Daily movement of pin 3 from November 1986 to May 1987.
- Figure 5.28 An example of a low-intensity 'multiple' mechanism of movement from 0900 hours on the 14th November 1986.
- Figure 5.29 An example of a 'graded' mechanism of movement from 0600 hours on the 22nd January 1987.
- Figure 5.30 An example of a high-intensity 'surge' mechanism of movement from 0300 hours on the 1st January 1987.
- Figure 5.31 Daily summary of maximum movement (pin 3) and pore water pressure throughout the 1986/87 winter period.
- Figure 5.32 Relationship between clay mineral content, the type and concentration of pore water cations and residual strength.
- Figure 5.33 Residual stress transmitted in relation to pore water chemistry and time.
- Figure 5.34 The effect of sea water concentration upon the residual strength of weathered and unweathered London and Wealden Clay.

Chapter Six

- Figure 6.1 Fluctuation in strength attributed to pore water chemistry at Worbarrow Bay.
- Figure 6.2 Fluctuation in strength attributed to pore water chemistry at Manor Lane.
- Figure 6.3 Mineral stability diagram for the activities of aluminium and amorphous silica.
- Figure 6.4 Mineral stability diagram for the activities of divalent magnesium and calcium.
- Figure 6.5 Mineral stability diagram for the activities of monovalent sodium and potassium.
- Figure 6.6 Physico-chemical process-response model of mudslide activity.
- Figure 6.7 Worbarrow Bay slope slices used in stability analyses.
- Figure 6.8 Summary of parameters influencing the seasonal instability of mudslides at Worbarrow Bay.

LIST OF TABLES

Chapter One

- Table 1.1 Hutchinson's classification of landslides (1969).
- Table 1.2 Classification of landslides by Varnes (1975).
- Table 1.3 Classification of mass movements adapted from Terzaghi (1950) and Brunsden (1986).
- Table 1.4 Classification of mass movement phenomena by Chorley *et al* (1984).
- Table 1.5 Summary of reported velocities of mudslide displacements.
- Table 1.6 Typical material properties of mudslides.

Chapter Two

- Table 2.1 Classification of phyllosilicates related to clay minerals.
- Table 2.2 Structure and properties of the clay minerals.
- Table 2.3 Calculated diffuse double layer thickness in relation to electrolyte concentration.
- Table 2.4 Relationship between the Atterberg limits, clay mineralogy and chemistry.

Table 2.5	Exchange of cations on reaction of clays with sea-water.
Table 2.6	Engineering properties of weathered and unweathered over-consolidated clays.
Table 2.7	Variation in residual friction and solution chemistry.

Chapter Three

Table 3.1	Laboratory equipment used for the measurement and analysis of photographs.
Table 3.2	Stratigraphic sequence of the north-Kent coast.
Table 3.3	Lithology of the Sheppey cliff sequence.
Table 3.4	Stratigraphy of the Cretaceous in Dorset.
Table 3.5	Lithology of the Wealden Beds at Worbarrow Bay.
Table 3.6	Core identification and sampling efficiency.
Table 3.7	Pore water depth sensor technical details.
Table 3.8	Summary of parameters, record interval and total length of data-set established from field-monitoring at Worbarrow.
Table 3.9	Summary of parameters, techniques and total tests performed in the laboratory analysis of materials from both sites.
Table 3.10	Chemical composition of solutions derived from different pre-treatment methods.
Table 3.11	Solutions used in laboratory simulations of residual shear strength.

Chapter Four

Table 4.1	Morphological indices and sampling resolution.
Table 4.2	Soil catalogue and description for core sample 2B.
Table 4.3	Soil catalogue and description for core sample W2.
Table 4.4	Computer output from laser particle-size analysis.
Table 4.5	Particle-size distribution back-calculation.
Table 4.6a	Manor Lane particle-size data summary of cores 1A - 4A.
Table 4.6b	Manor Lane particle-size data summary of cores 4B - 7U.
Table 4.7	Worbarrow particle-size data summary for all cores samples.
Table 4.8	Moisture content relations for all Manor Lane core samples.

Table 4.9	Moisture content relations for all Worbarrow core samples.
Table 4.10	Data summary of the phase relationships at Manor Lane.
Table 4.11	Data summary of the phase relationships at Worbarrow Bay.
Table 4.12	Unit weight and bulk density results for Manor Lane.
Table 4.13	Geotechnical properties at the basal shear surface for all Manor Lane core samples.
Table 4.14	Geotechnical properties at the basal shear surface for all Worbarrow core samples.
Table 4.15a	Chemical characteristics and percent organic matter for Manor Lane cores 1A - 4A.
Table 4.15b	Chemical characteristics and percent organic matter for Manor Lane cores 4B - 7U.
Table 4.16	Chemical characteristics and percent organic matter for all core samples from Worbarrow Bay.
Table 4.17	Interstitial free water chemistry at the basal shear surface for all Manor Lane core samples.
Table 4.18	Interstitial free water chemistry at the basal shear surface for all Worbarrow Bay core samples.
Table 4.19a	Water soluble and exchangeable cations for Manor Lane cores 1A - 3B.
Table 4.19b	Water soluble and exchangeable cations for Manor Lane cores 4A - 7U.
Table 4.20	Water soluble and exchangeable cations at Worbarrow Bay.
Table 4.21a	Cation exchange capacity and ion-exchange relations for Manor Lane cores 1A - 4B.
Table 4.21b	Cation exchange capacity and ion-exchange relations for Manor Lane cores 5A - 7U.
Table 4.22	Cation exchange capacity and ion-exchange relations for all Worbarrow cores.
Table 4.23a	Bulk chemistry of clay-size material for Manor Lane core samples 1A - 3B.
Table 4.23b	Bulk chemistry of clay-size material for Manor Lane core samples 4A - 7U.
Table 4.24	Bulk chemistry of clay-size material at Worbarrow Bay.
Table 4.25a	Anisotropic surface and fissure chemistry for Manor Lane core samples 1A - 4A.

Table 4.25b	Anisotropic surface and fissure chemistry for Manor Lane core samples 4B - 7U.
Table 4.26	Anisotropic surface and fissure chemistry at Worbarrow Bay.
Table 4.27	Clay mineralogy of weathered materials at Manor Lane.
Table 4.28	Clay mineralogy of weathered materials at Worbarrow Bay.
Table 4.29	Reported number of landslides occurring on the geological formations of southern and south-east England.
Table 4.30	Reported clay mineralogy of landslide-prone geological strata.

Chapter Five

Table 5.1	Summary of target movements between September 1986 and May 1987.
Table 5.2	Chemical composition of precipitation, interstitial pore water and sea-water.
Table 5.3	Profile variations in moisture volume fraction throughout the study.
Table 5.4	Release of iron, aluminium and silica upon weathering of the backcliff, source and mudslide accumulation lobe.
Table 5.5	Relationship between residual shear strength and solution chemistry from simulation tests on pure clay minerals.
Table 5.6	Relationship between residual shear strength and solution chemistry from simulations on weathered and unweathered London and Weald Clay.

Chapter Six

Table 6.1a	Correlation matrix of soil properties at Manor Lane established at the basal shear surface.
Table 6.1b	Correlation matrix of mean soil properties at Manor Lane.
Table 6.2a	Correlation matrix of soil properties from the shear surface at Worbarrow Bay.
Table 6.2b	Correlation matrix of mean soil properties at Worbarrow.
Table 6.3	Correlation matrix of monthly summary of dynamic mudslide variables at Worbarrow Bay.
Table 6.4	Correlation of dynamic variables with slope movement with associated time-lags from continuous recordings between November to May 1987 at Worbarrow Bay.

Table 6.5	Calculation of the change in residual shear strength attributed to fluctuations in pore water concentration at Worbarrow.
Table 6.6	Description of aqueous and mineral phase geochemistry for each slope unit at Worbarrow Bay.
Table 6.7a	Description of aqueous and mineral phase geochemistry for slope units 1A - 3B at Manor Lane.
Table 6.7b	Description of aqueous and mineral phase geochemistry for slope units 4A - 7U at Manor Lane.
Table 6.8	Simulated effect of weathering and mineral stability with an increasing concentration of sea water at Worbarrow Bay.
Table 6.9	Simulated effect of weathering and mineral stability of an increasing concentration of sea water at Manor Lane.
Table 6.10	Computed factor of safety at Worbarrow assuming zero pore water pressure.
Table 6.11	Computed factor of safety at Manor Lane assuming zero pore water pressure.
Table 6.12	Computed factor of safety at Worbarrow assuming zero pore water pressure and cohesion.
Table 6.13	Computed factor of safety at Manor Lane assuming zero pore water pressure and cohesion.
Table 6.14	Computed factor of safety at Worbarrow assuming worst case pore water pressure.
Table 6.15	Computed factor of safety at Manor Lane assuming worst case pore water pressure.
Table 6.16	Seasonal fluctuation in F at Worbarrow attributed to pore water pressure.
Table 6.17	Seasonal fluctuation in F at Manor Lane attributed to pore water pressure.
Table 6.18	Seasonal fluctuation in F at Worbarrow attributed to pore water pressure and shear strength.
Table 6.19	Seasonal fluctuation in F at Worbarrow attributed to shear strength alone.
Table 6.20	Seasonal fluctuation in F at Manor Lane attributed to pore water pressure and shear strength.
Table 6.21	Seasonal fluctuation in F at Manor Lane attributed to shear strength alone.
Table 6.22	Simulated effect of a reduction in cohesion with pore water pressures upon the stability of mudslides.

- Table 6.23 Reduction in F with the inclusion of undrained loading in November 1986 with measured pore water pressures and shear strength at Worbarrow Bay.
- Table 6.24 The effect of undrained loading and other variables on the stability of the Worbarrow mudslide in November 1986.

LIST OF PLATES

Chapter Three

- Plate 1 Diapositive contact print of the Worbarrow field-site.
- Plate 2 Carl Zeiss Elta 2 Electronic Recording Tacheometer.
- Plate 3 Carl Zeiss Jena UMK Terrestrial Photogrammetric Camera.
- Plate 4 Stecometer used for the observation and extraction of points from photographs.
- Plate 5 Colour image of the Manor Lane mudslide site.
- Plate 6 Colour image of the Worbarrow Bay mudslide site.
- Plate 7 Didcot Automatic Weather Station installed at Worbarrow.
- Plate 8 Epsilon data-logger and interface unit.
- Plate 9 The Pitman soil moisture meter or neutron probe in use at Worbarrow Bay.
- Plate 10 Gantry installed at Worbarrow for monitoring surface movement.
- Plate 11 Cable and channel port link to movement sensors.
- Plate 12 Pore water sampler design.
- Plate 13 Exposed core-sample illustrating the nature of shear surfaces and the location of sub-sampling zones.

Chapter Four

- Plate 14 Platy and wave-like form of mixed clays.
- Plate 15 SEM print showing the presence of fissures and slickensides and the preferential orientation of clays.
- Plate 16 SEM prints showing the anisotropic deposition of iron.

LIST OF APPENDIXES

- Appendix 1 Field sampling method.
- Appendix 2 Particle size analysis procedure.
- Appendix 3 Moisture content and field bulk density.
- Appendix 4 Specific gravity, porosity and void ratio.
- Appendix 5 Atterberg limits.
- Appendix 6 Drained peak and residual shear strength.
- Appendix 7 Mineralogical and micro-fabric identification.
- Appendix 8 Determination of organic matter.
- Appendix 9 Soil chemical analyses.
- Appendix 10 Core sample log-sheets.
- Appendix 11 Salt concentrations and chemical equilibria.
- Appendix 12 Manor Lane displacement and phreatic level data summary.
- Appendix 13 Corrections to FORTRAN 4 programme WATEQF.

ACKNOWLEDGEMENTS

In the course of this research I have been very fortunate to meet many distinguished scientists and friends. Much of the success of this work was due to the willingness of several university departments and government institutions to provide laboratory facilities and loan equipment. Additionally, many people have helped in the compilation and presentation of this thesis. It is with great pleasure that I recognise all who have contributed to this research but because it was not practical to name everyone in person a few are unavoidably omitted. To those not mentioned below I am extremely grateful for your help.

Special thanks first to Professor Denys Brunsten for initially suggesting the research, to the Natural Environment Research Council for supporting the on-going expenditure of the project and for providing technical expertise through the NERC Equipment Pool; in particular thanks to Tom Dean, Mike Walker and Mike Stroud of the Institute of Hydrology without whom the quality and efficiency of field-monitoring would not have been achieved. It was comforting in times of crisis to have advice and solutions so readily at hand, so thanks Mike. Thanks also to the Geography Department, King's College, for providing equipment and 'home' for the last three years, and especially to the staff and technicians who gave freely of their time and advice and made me feel very welcome. In particular, thanks to John Harper for helping out with the design and construction of much of the equipment developed as part of this research.

In the early days of the project valuable advice was sought from Professor John Hutchinson, Dr Peter Loveland, Professor John Thornes, Dr Malcolm Anderson, Dr Eddie Bromhead and Dr John Cripps to whom I am

greatly indebted. With their wisdom and the advice of my predecessor, Dr Bob Allison, the project unfolded and I began to collect field and laboratory data to support the research objectives. Again many friends and institutions were involved at this stage, a few of which deserve special mention. The M.O.D. for allowing access to the Lulworth Camp Ranges and to Majors Payne and McLucas and the 'Range Wombles' for their enthusiastic support during the on-going fieldwork. The Institute of Terrestrial Ecology at Furzebrook for allowing the storage of equipment and the use of their facilities. To the Burton family, Isle of Sheppey, for providing accommodation, light relief and for putting up with the dirt. To Rick Pipkin and Tom Carroll, my hard and trusted field-staff (and all for real ale), to the King's geography postgraduates for helping out on numerous occasions and to the geomorphology fieldclasses who showed interest in the work.

For assistance in surveying and the development of photogrammetry in this study thanks to Mike Cooper, Jim Chandler and the team at the City University for field and laboratory support, and for XRD and SEM work thanks to Tim Linsey, Kevin Shrapel and the staff of Earth Sciences at Queen Mary College. For use of their particle-sizer and for initially developing my interest in geomorphology thanks to Dr Dave Robinson, Dr Helen Rendell and the Geography Laboratory of the University of Sussex. Thanks also to Geomorphological Services Limited for providing data for the regional survey in Chapter Four. In the final stages of this work I was extremely grateful for the assistance of Mark Stuart on computing matters and to Dr Eddie Bromhead for advice and assistance on slope stability modelling. Much of the success of Chapter Six may be attributed to their expertise.

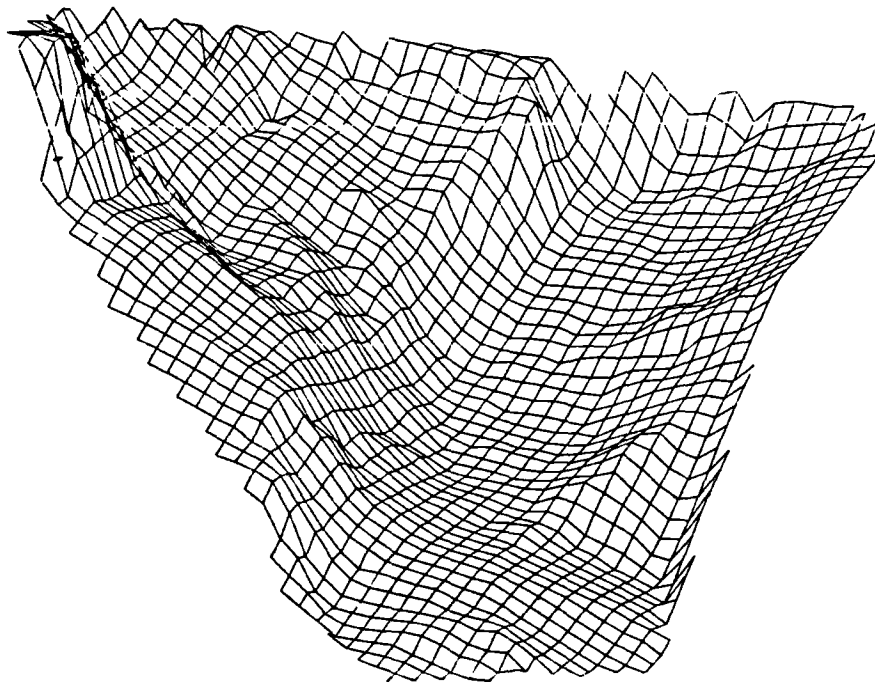
In the process of writing the project a number of people have read and influenced me on the final product and special thanks go to my supervisor Professor Denys Brunsden and to Julia Davy for their patience and encouragement in the early stages. Thanks also to Alan Moore for proof reading the second draft.

For help with production, my special thanks to Roma Beaumont and Gordon Reynell for their time and cartographic skills in drawing many of the diagrams, to John Payne of Van Dyke Design for work on the geomorphological maps and plans, and to Peter Howard and Jim Hooker for their advice and assistance with photography.

Finally, I would like to thank my examiners, Dr John Gerrard and Prof. Clifford Embleton for their time in assessing this work, and especially to several people who have guided me to the completion of the research. Firstly, Denys Brunsden for his enthusiastic support throughout the study; his experience as a research supervisor can only be rivalled by few and his guidance within the discipline of geomorphology were especially appreciated. Secondly, my thanks to Julia Davy for her unyielding patience with me since undertaking this work. Her involvement was quite considerable from the occasional 'muddy' holiday to thoroughly reading all the text. Thirdly, thanks to my parents who have always shown considerable interest in my work and for providing endless encouragement and support whilst at university.

Chapter One

MUDSLIDE FORM, BEHAVIOUR AND MATERIALS



1.1 Introduction : aims and organisation of the thesis.

Recent reviews of mass movement processes (Brunsden 1984; Crozier 1986; Sidle *et al* 1985; Anderson and Richards 1987) have all emphasised the clay mineralogy and chemistry of soils as important factors in landslide development. They also report a growing cooperation between geomorphologists, geologists, soil scientists and civil engineers in mass movement studies. Consequently any research design for landslide investigations must now be multi-disciplinary to enable an accurate assessment and explanation of the role of physico-chemical properties in landslide behaviour.

The complete literature review (see sections 1.2 - 2.4) isolated a number of research objectives (section 2.5) that should be satisfied by investigations within this field. These were to:

1. evaluate the nature of the physico-chemical properties of slope forming materials;
2. determine whether these properties sufficiently control shear strength to affect slope stability;
3. isolate the spatial and temporal scales of mass movement behaviour;
4. monitor seasonal changes in weather conditions and slope behaviour with respect to soil moisture, pore water chemistry and aerial salt deposition;
5. determine the probable influence of pore water chemistry on the seasonal weathering and behaviour of coastal mass movements and the factor of safety against landsliding;

6. include a static and dynamic analysis of soil properties within independent landslides;
7. to develop a dynamic model of the role of environmental chemistry on the seasonal degradation of landslides.

To provide consistency this study concentrates on one mass movement form. Mudslides were chosen for this purpose because they are commonly found on the coastal slopes of Britain, and because their form and behaviour is well known from both geomorphological and soil mechanics viewpoints. In addition the mudslides are well developed on several different soil types facilitating comparative studies.

Results are presented from analyses of two coastal mudslides in south-east England; one developed on the Eocene London Clay outcropping in the Thames Estuary, and the other on the Wealden Beds outcrop of the Isle of Purbeck, Dorset. The fieldwork associated with the study was undertaken from October 1985 to March 1987.

The findings of laboratory and field investigations showed that soil variability was highly associated with weathering processes and the morphology of mudslides. Furthermore, the presence of densely-packed shear zones within the slope were found to self-preserve mudsliding across highly orientated slickensided surfaces. Shear strength was not constant and was found to reduce within the mudslides according to the density of shear surfaces and the chemistry of clays and pore water solutions. These associations were verified by laboratory simulation tests which suggested that the type of clay mineral, the valency of the dominant cation and the concentration of the pore water solution were directly related to the residual shear strength of clay soils.

Significant variations in residual strength were found depending on the concentration of sea-water and the weathered state of soil clays. The lowest strengths coincided with dilute solutions increasing in strength with salt concentration. Within mudslides, seasonal fluctuations in pore water chemistry were thus considered to correspond with changes in residual shear strength. Actual changes in residual strength were calibrated from simulation results and applied to slope stability models to determine the sensitivity of the variable as a causal factor of mudslide behaviour.

This contribution to the study of mass movement is supported by a regional survey of landslide-prone geological strata and comprehensive analyses of the spatial distribution of mudslide properties, the identification of dominant weathering reactions, the assessment of temporal variations in atmospheric, soil water and movement parameters, and analyses of the stability of each site using the properties and behaviour of soils prevailing throughout the study.

Thus, the following thesis presents a review of the literature from which the research objectives were based, the methodology adopted during the investigation, the presentation of results, statistical analyses of soil variability and behaviour, and the derivation of a dynamic model of the role of environmental chemistry and other factors on the seasonal degradation of mudslides.

The layout of the thesis is as follows: in Chapter One the classification and definition of mass movements are briefly introduced, followed by a more detailed account of the ideas and concepts describing the location, morphology and development of mudslides. The seasonal behaviour exhibited

by landslides is discussed in relation to material properties. The importance of clay mineralogy and solute geochemistry is noted and isolated for further study.

The role of physico-chemical properties in the weathering and behaviour of mudslides is discussed in detail in Chapter Two with respect to clay mineralogy, particle interactions, the mechanical properties of soils, and shear strength. The methodology used in site selection, survey, field monitoring, sampling, and laboratory analyses are outlined in Chapter Three.

The results of laboratory and field investigations are presented in Chapters Four and Five respectively, forming the basis of the discussion and analysis of results in Chapter Six. The findings are related to the physical behaviour of mudslides to establish to what extent they explain residual shear strength and seasonal slope instability.

Chapter Seven outlines the conclusions of the research in relating the physico-chemical properties to observed behaviour with respect to weathering processes and the location, form and development of coastal mudslides. Further research is suggested along with the original contributions made by this thesis to the study of mass movement.

1.2 What is a mudslide ?

Mass movement may be considered simply as the detachment and downslope transport of soil and rock material under the influence of gravity. Scientists are in reasonable agreement with this definition, although in classifying the types of mass movement there is great disparity within the literature.

Hansen (1984), Crozier (1986), Craig (1979) and McConchie (1986) provide detailed reviews of the classification of mass movements pertinent to this study. The most recent classifications are those of Varnes (1958, 1975), Hutchinson (1969 and 1984), Nemcok *et al* (1972), and Brunsten (1985). Tables 1.1 and 1.2 show the schemes of Hutchinson (1969) and Varnes (1975) respectively. These and most other schemes consider the mode and rate of movement, the shape of the sliding surface, and the type of material involved. Further criteria are often used for the purpose of recognition, avoidance, control, correction, or for other reasons of the classification. The combination of materials, slopes and agents responsible for movement produce considerable opportunities for the classification enthusiast (Terzaghi 1950) and are the primary reason for the absence of a standard in the literature.

Hansen (1984), in conclusion to her discussion stated:

"It is the geotechnical properties which reflect the characteristics of the moving mass which are of greatest importance, but as yet there are no comprehensive classifications based on such properties."

Table 1.1 Hutchinson's classification of landslides (1969).

CREEP	<ol style="list-style-type: none"> 1. Shallow, predominantly seasonal creep; <ol style="list-style-type: none"> (a) Soil creep (b) Talus creep 2. Deep-seated continuous creep; mass creep 3. Progressive creep
FROZEN GROUND	<ol style="list-style-type: none"> 4. Freeze-thaw movements <ol style="list-style-type: none"> (a) Solifluction (b) Cambering and valley bulging (c) Stone streams (d) Rock glaciers
LANDSLIDES	<ol style="list-style-type: none"> 5. Translational slides <ol style="list-style-type: none"> (a) Rock slides; block glides (b) Slab, or flake slides (c) Detritus, or debris slides (d) Mudflows <ol style="list-style-type: none"> (i) Climatic mudflows (ii) Volcanic mudflows (e) Bog flows; bog bursts (f) Flow failures <ol style="list-style-type: none"> (i) Loess flows (ii) Flow slides 6. Rotational slips <ol style="list-style-type: none"> (a) Single rotational slips (b) Multiple rotational slips <ol style="list-style-type: none"> (i) In stiff, fissured clays (ii) In soft, sensitive clays; clay flows (c) Successive, or stepped rotational slips 7. Falls <ol style="list-style-type: none"> (a) Stone and boulder falls (b) Rock and soil falls 8. Sub-aqueous slides <ol style="list-style-type: none"> (a) Flow slides (b) Under-consolidated clay slides

Table 1.2 Classification of landslides by Varnes (1975).

TYPE OF MOVEMENT		TYPE OF MATERIAL		
		Bedrock	Soils coarse	fine
FALLS		Rockfall	Debris fall	Earth fall
TOPPLES		Rock topple	Debris topple	Earth topple
SLIDES				
ROTATIONAL	few units	Rock slump	Debris slump	Earth slump
TRANSLATIONAL	many units	Rock glide	Debris glide	Earth glide
		Rock slide	Debris slide	Earth slide
LATERAL SPREAD		Rock spread	Debris spread	Earth spread
FLOWS		Rock flow (deep creep)	Debris flow (soil creep)	Earth flow
COMPLEX		Combination of two or more types		

the causes of

Table 1.3 Classification of landslides adapted from Terzaghi (1950) and Brunsden (1985).

EXTERNAL CHANGES IN STABILITY CONDITIONS

1. Geometrical: Undercutting, erosion, stream incision, artificial changes in slope height, length or steepness.
 2. Unloading: Erosion, incision, artificial excavation.
 3. Loading: Addition of material, increase in volume such as through undrained loading (Hutchinson, 1971).
 4. Shocks and Vibrations: Man-induced, earthquakes, collapse of structure and physical disruption.
 Associated processes
 and mass movements:
 (a) Expansion (mudslides and flows)
 (b) Remoulding (quick-clay flowslides.)
 (c) Liquefaction (wet flowslides.)
 (d) Fluidization (cataclysmic rock and
 (e) Air lubrication flow-slides.)
 (f) Grain impact (cohesionless grain flows.)
 5. Drawdown: Lowering of water levels in lakes and reservoirs.
 6. Water-regime Rainfall, increase in weight, pore water pressure.
-

INTERNAL CHANGES IN STABILITY CONDITIONS

1. Progressive failure: Lateral expansion, fissuring and erosion.
 2. Weathering: Freeze-thaw, desiccation, changes in bonding mechanism between particles, reduction in cohesion, removal of cement.
 3. Seepage erosion: Solution, piping, etc.
-

She suggests that a system like Table 1.3 provides a framework for such a classification because it reproduces the causal factors behind changes in the internal and external stability of the slope. A move towards a geotechnical descriptive base using properties, such as measures of remoulding, liquefaction, undrained loading and excess pore pressure, will provide the most valuable answer to the problem of classifying mass movements.

Yatsu (1967) recognised the difficulties in classifying mass movements of slide and flow types, commenting:

"In general, slips and some of the flows seem to be conspicuously associated with the materials composing the slopes, especially with the type of clay minerals."

Although geological conditions are of primary importance to slope instability, Yatsu (1966) suggested more important aspects that overly 'superficial concepts such as geologic conditions': What type of rocks form landslipped areas? Why? How are they decomposed? What kind of surface chemical and mechanical behaviours are debris exhibiting?

"These are fundamental characteristics of geological pre-dispositions".

Many of these early suggestions have since been answered and included in classification schemes; the mechanical behaviour of landslips, in particular, has received much attention. However, the geochemical processes operative in landslide systems have generally been ignored.

Craig (1979) and McConchie (1986) have reviewed the relevant literature on the definition of mudslides within the classifications of mass

movement, and it is felt unnecessary to repeat their findings here, since it would only serve to confuse the debate as it has in past years.

Brunsdon (1984) provides the clearest and least ambiguous definition of mudslides as being:

"A form of mass movement in which masses of softened argillaceous, silty or very fine debris advance chiefly by sliding on discrete boundary shear surfaces in relatively slow moving, lobate or elongate forms."

This statement illustrates the past confusion in the definition of mudslides, since there was considerable disagreement about the mechanism of movement: does it flow or slide? Before the term 'mudslide' was accepted and used as the correct definition by Hutchinson *et al* (1971, 1974); Chandler (1972a); Hutchinson (1981, 1973); Brunsdon (1974, 1979a, 1984); Prior *et al* (1975, 1979, 1980) and Craig (1979, 1981), the process was referred to as 'mudflow' by Hutchinson (1968, 1970); Grove (1953); Zaruba and Mencl (1969); Prior *et al* (1968, 1970, 1971, 1972); Brunsdon (1973); Conway (1976); Balteanu (1976) and Sharpe (1938). The term 'earthflow' was used by Putnam *et al* (1940); Crandell and Varnes (1961); Campbell (1966); Cunningham (1972); Sharpe (1938); Prior *et al* (1972) and Varnes (1958) and is still being used in the latest work from New Zealand (McConchie, 1986). Occasionally the term 'mud-glacier' has been used (Moorman, 1939; Lang, 1944) but is now regarded as redundant. It is noted that there may still be a tendency not to use 'mudslide' with confidence in recent classifications, as seen for example in Table 1.4, after Chorley *et al* (1984, p.234).

Table 1.4 Classification of mass movement phenomena by Chorley et al (1984)

DIRECTION OF MOVEMENT	TYPE OF MOVEMENT	TRANSPORTING AGENT	TYPES OF MASS MOVEMENT
VERTICAL	FALL	None	Rockfall, earthfall, debris-fall and topples.
	SUBSIDENCE	None	Collapse and settlement
LATERAL	SLIDE	Minor along shear surface	Block-slides
	SPREAD	Moderate along shear surface	Spread, cambering, sacking
DIAGONAL	CREEP	Minor	Soil, rock and talus creep
	SLIDE	Minor to Moderate	Rock slide, debris slide, soil slips and slumps
	FLOW	Moderate	Earth flows, debris flows
		Major	Solifluction, mudflows, sturzstrom, rock avalanche and rock glaciers

Varnes (1958) discussed the use of the term flow-slide for classification purposes and stated that movement within the displaced mass is such that the form taken by the moving material or the apparent distribution of velocities and displacements resemble those of a viscous fluid. The boundary between the moving and the stationary material may be sharp or it may be a zone of plastic flow. The material itself must be unconsolidated at the time of flow, although Varnes argued that it may consist of rock fragments, fine granular material, mixed debris, and water or plastic clay. 'Mudslides' can occur in plastic or predominantly fine-grained material and yet become 'mudflows' at higher water contents. Varnes recognised that a continuum of processes exists within fine-grained materials, ranging from slumps to mudslides, with true mudflows being the liquid end member. More often than not, he argued, any one mass movement feature shows several types of movement within its various parts or at different times in its development.

The distinction between 'slide' and 'flow' types was emphasised by Skempton and Hutchinson (1969) in suggesting that 'slides' were primarily features of shear failure at the boundaries of the moving mass, while flows form a neglected, and little understood group of movements with correspondingly confused terminology. The problem is compounded when distinguishing mudslides from debris-slides and debris-flows. The correct classification often depends on the experience of the researcher because both phenomena may be observed in the same landslide. Debris-flows are, however, generally developed in coarse materials whereas mudslides consist of predominantly fine sediments.

In summary, it is evident that a standard classification of mass movement still requires definition. Problems have arisen in the past from confused

terminology and from combining at least three independent complex causal factors. The consequent variety of slope movements led Hutchinson (1968) to believe that a rigorous classification is hardly possible, and Yatsu (1967) wondered whether a complicated classification is of any practical use. Hansen (1984) has suggested a move towards developing a geotechnical based classification and clarified the terminology. Thus, the initial reason for much of the confusion in the slide-flow debate is now resolved, and it is accepted that mudslides advance chiefly by sliding on discrete boundary shear surfaces, with some degree of internal deformation. The recent definition of Brunsden (1984) makes this clear in relation to the materials involved and the resultant form of a mudslide.

1.3 The development and morphology of mudslides.

Despite the frequent mis -classification of mudslides, it is generally agreed that they possess three distinct morphological units (Figure 1.1):

1. Source. The source is the uppermost section of a mudslide in which slumped and weathered material is thoroughly mixed and softened before moving downslope (Figure 1.1a).
2. Track. Material derived from the source is transported via the track, which may be a direct connection between the source and accumulation lobe, or elongated in form (Figure 1.1b). Movement rates are typically greatest in this zone.
3. Lobe. Better termed the accumulation zone, the lobe is located at the foot of the mudslide and is the depositional area for mudslide material. The lobate feature is less steep and consequently more stable than the other units. The edge or 'toe' of the lobe may become undermined or truncated by erosion.

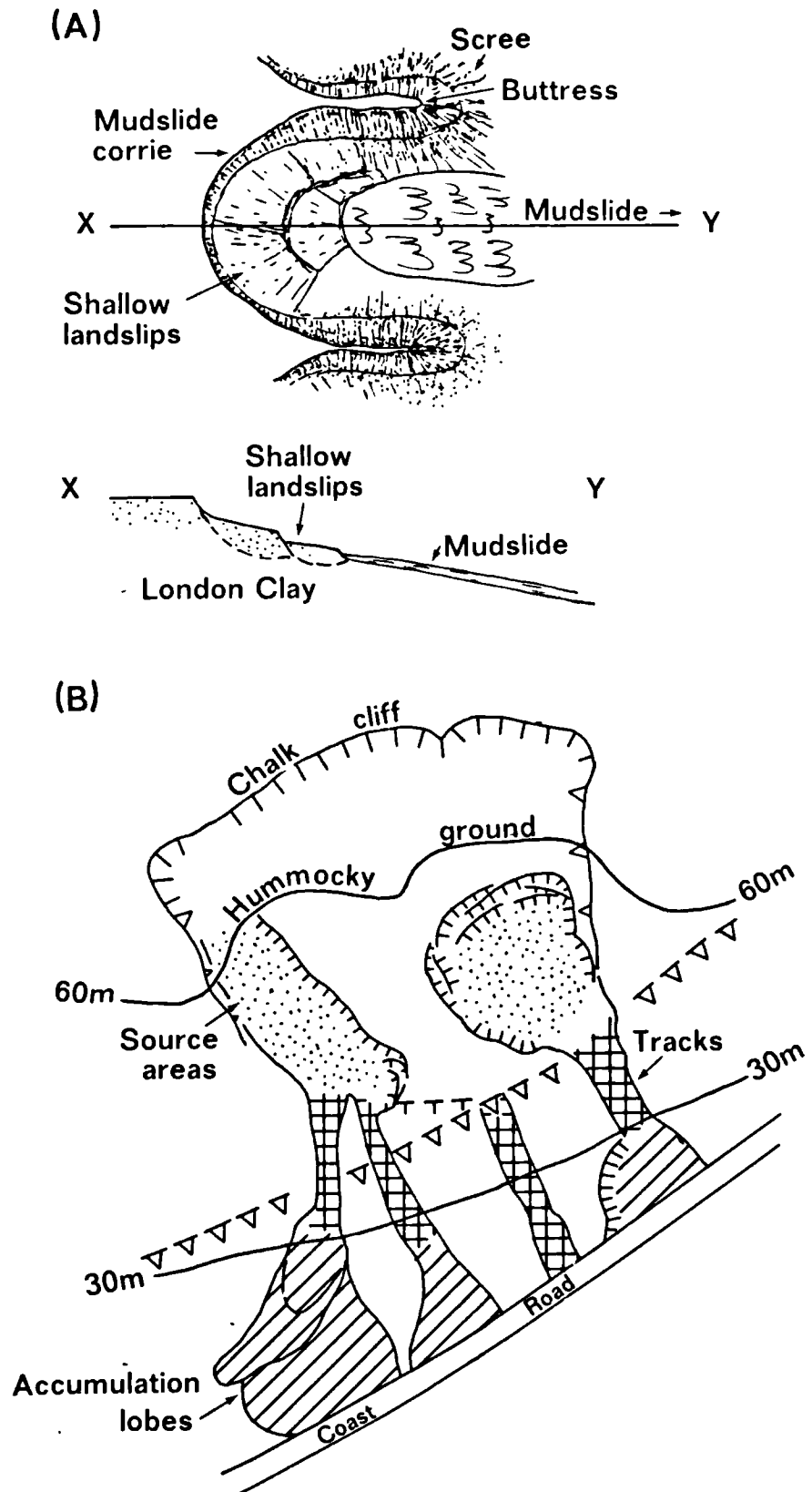
Within the literature there is considerable agreement in the descriptions of mudslide morphology worldwide (Hutchinson, 1968, 1970, 1973; Prior et al 1968, 1970, 1971, 1975, 1977, 1980; Brunsden 1973, 1974, 1984; Quigley et al 1976; Campbell 1966 and Kelsey 1980). This seems surprising given the problems encountered in defining the process. In the discussion of the morphology of mudslides, many early writers noted their similarity to glaciers. Analogous terms such as cirque, crevasse and pressure ridge are frequently used: Brunsden (1984); Putnam and Sharp (1940); Kelsey (1978); Prior (1977) and Campbell (1966). The likeness in form has also led to suggestions of similarity in process.

Brunsdén (1984) provides the most comprehensive description of the characteristic morphological units of a mudslide. A summary of his description is included here since a clear explanation of form is required in the subsequent debate on the development and behaviour of mudslides. With reference to Figure 1.1:

"...The source area consists of failure scars, disturbed slumps, rotational slips or translational failures, debris slopes and complex depositional areas of softened, weathered and fissured debris. This zone usually has a confused groundwater distribution and depressions which often contain water. The headwalls are usually steep, occasionally vertical, arcuate in plan, and form a basin, bowl, or 'cirque', with adjacent source areas separated by sharp crested ridges and buttresses. The source area serves as a mixing bowl in which material from upslope accumulates and softens before moving downslope.

...During active periods mud is delivered by sliding to the zone below. The track of a mudslide is usually a steep, straight or gently concave channel, or a series of channels through which material is transported from the source to the accumulation zone. Mudslides occur as either short, lobate forms (20-80m long, 5-20m

Figure 1.1. Morphological characteristics of mudslides.



Source: Brunsten et al (1984) p.368.

wide and 1-5m deep), or as an elongated variety, which tend to be steep and very narrow. Typically the lobate forms occur on small, steep coastal cliffs and the track is often terminated by an abrupt break of slope at the foot. The elongated forms may occur on long, steep mountain slopes. The track is always very sharply defined by boundary shear surfaces at their sides and base. Common features of this zone include the development of minor scarps, en echelon edge cracks, Reidel shears and transverse tensional or pressure cracks and ridges reflecting the pattern of movement and the general slope form in profile. These cracks are very similar to those developed in glaciers with tension cracks forming at steep convex breaks in slope and pressure ridges on benches or concave sections of the profile. Rills and gullies caused by direct runoff may develop during inactive periods, but these channels are quickly erased in the saturation and movement of the clays.

...The accumulation zone consists of debris delivered from upslope forming a single or several overlapping lobes that may occupy as much as 75 per cent of the slope as it degrades. The expanded lobes are usually irregular with steps and pressure ridges marking the positions of successive phases of deposition at the head, and in the lower areas radial cracks form as the mass spreads out onto flatter ground. Thus, the lobe profile consists of two parts, an upper, flatter tread at 1-5° and an almost continuously convex curved distal toe which maintains a steep (10-25°) angle. The lobe is further characterised by a complex micro-relief caused by surface cracking of the crust during dry periods, mud vents, dry season gullying and tension cracks related to toe erosion. Such surface features reflect the internal structure which typically demonstrates a sharp basal shear surface. It is noted that material within this zone is attempting to come to rest at a new stable angle, with respect to the type of material, drainage and geometrical conditions."

Although this characteristic morphology has been described by numerous workers, the site conditions of individual mudslides determine whether

all three units will be present. Studies in the United Kingdom tend to show all three components. The majority of these studies are in coastal locations, the accumulation zone forming on the beach where it is eroded by wave action. In other situations mudslides may form on valley slopes where streams actively remove material from the lower slope units, preventing the development of accumulation lobes. The development of the lobe would appear to be dependent on location and whether the opportunity exists for the material to collect on flatter slopes.

During the past two decades attempts have been made to model both the location and development of coastal mudslides. Several authors (Hutchinson, 1968, 1973; Prior *et al*, 1968, 1980; Brunsden, 1974) have noted that mudslide basins may combine in a series of embayments with intersecting headwalls to form the cliff itself. This form of development is related to mass balance conditions in which the supply of debris at the source is equal to the rate of unloading at the toe by erosion (Hutchinson 1968, 1973; Prior 1977; Prior *et al* 1975, 1980; Brunsden 1973; Quigley *et al* 1976, 1977, and Moore 1986). The latter provokes renewed evacuation of the track and further weathering and subsidence in the source, and are thus self-generating in nature.

The most comprehensive studies have been published by Hutchinson (1970, 1973, and 1983), which are worthy of further discussion although a more detailed account is given by Moore (1986). Observations of coastal cliff development in north Kent, led Hutchinson (1970, 1973) to note the tendency for mudslides on relatively uniform slopes undergoing moderate toe erosion to develop in a regular series of embayments. Lateral mudslides characteristically formed around the margins of deep-seated landslides. The subsequent degradation of the slipped block through

mudslide processes occurred in a cycle leading once more to slope failure.

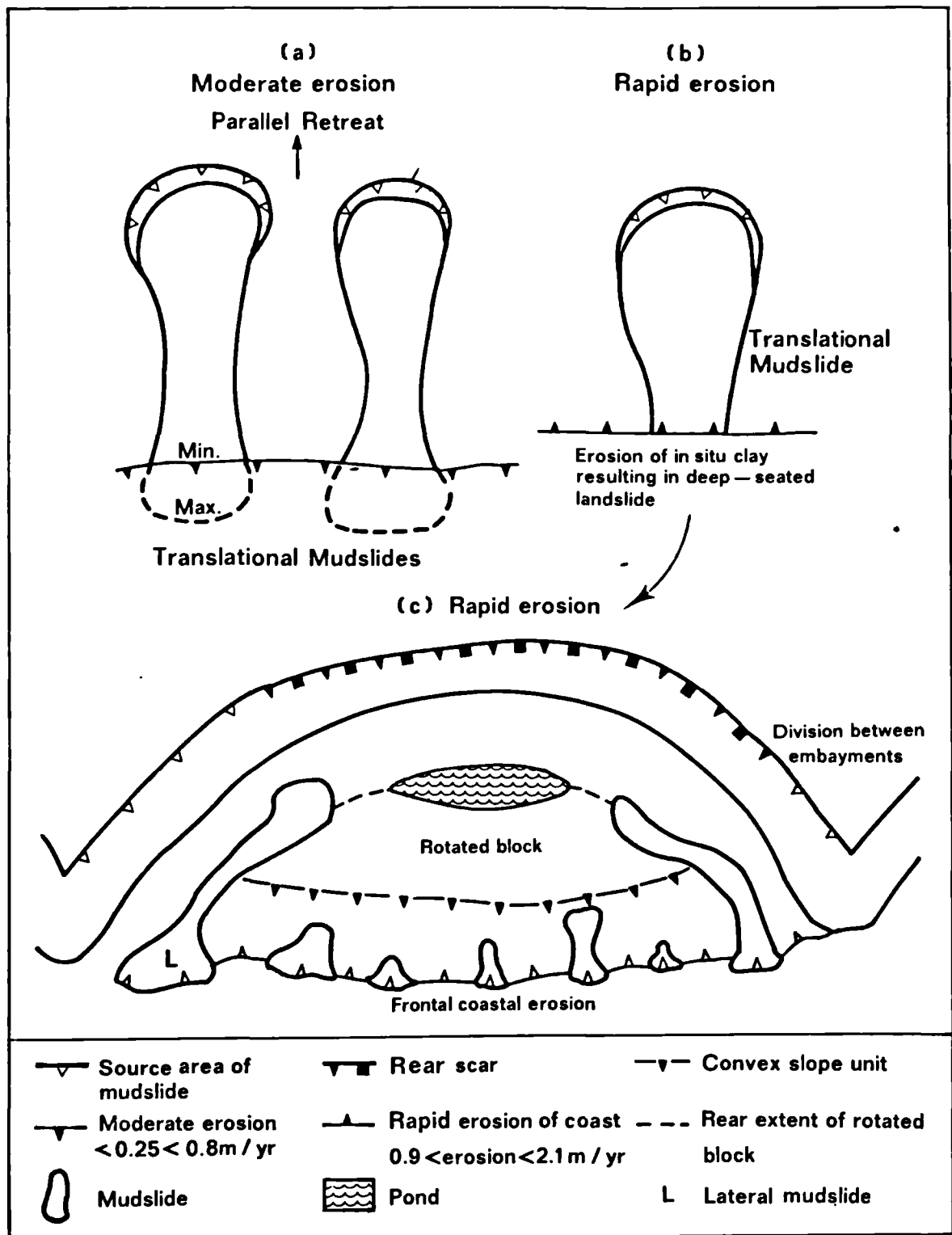
A second model states that in other situations, hydrogeological factors are important in slope instability, particularly where cliff sections show marked variations in permeability. Due to such variability many coastal mudslides do not conform to one model although Hutchinson (1983) recognised that certain dominant mudslides stand out against a general background of lesser mudslides and other forms of failure.

In the first model Hutchinson proposed that the form of a mudslide is related to the severity of toe erosion. Three categories were distinguished:

1. Erosion broadly in balance with the rate of weathering;
2. Erosion more rapid than weathering;
3. Zero erosion.

The removal of weathered material from cliffs exposed to moderate erosion occurs in the form of translational mudslides as portrayed in Figure 1.2a, and where a number of source units co-exist, the cliff evolves by a process of parallel retreat. For cliffs experiencing rapid erosion, a point will arise when the discharge of the slope is less than the amount of debris removed. Oversteepening then occurs with the removal of *in situ* clay. This causes deep-seated cliff failures, represented by a transition from b to c in Figure 1.2. The land lost in such failures occurs rapidly, but infrequently, along shear surfaces that may be either planar or rotational, and generally involve a greater loss of ground than occurs with smaller translational mudslides. Subsequent degradation of

Figure 1.2. Mudslide form in relation to the intensity of toe erosion of London Clay cliffs 30-40 metres in height.



Based on Hutchinson (1973).

the deep-seated slip may be observed in a cycle, as summarised in Figure 1.3, leading once more to the erosion of *in situ* clay and oversteepening of the lower slopes.

In the second model, a pattern in the location of major mudslide complexes is said to exist where cliffs of stiff fissured clay are underlain by a more competent stratum with an element of coastal dip. Up the coastwise dip the more competent stratum forms a sea cliff which suffers only moderate erosion: zone S in Figure 1.4. It was suggested that this probably results from diminishing thickness and some under-drainage, while the overlying clay is subject only to shallow slips and minor mudslides. Down the coastwise dip the more competent stratum lies below beach level, allowing oversteepening of the clay by wave attack to bring about deep-seated rotational or multiple rotational slips (zone M). The transitional zone Z, occurs where the base of the clay stratum lies at or close to sea level and is characterized by major active mudsliding. Movements will tend to be greatest in this zone where optimum conditions exist for the stimulation of mudslide activity by toe erosion.

Although these models provide the clearest statements on the development and evolution of coastal mudslides in terms of erosion, shear failure, and subsequent degradation through weathering and mudslide processes, they have received little debate in the literature. Quigley *et al* (1977) applied the first model to explain the development of the Lake Erie north shore bluffs in North America, while Brunsden (1984) considers the model as generally applicable in view of evidence from north Kent, Dorset, and Antrim in the British Isles:

Figure 1.3. The cyclic development of deep-seated mudslides on London Clay cliffs exposed to rapid marine erosion.

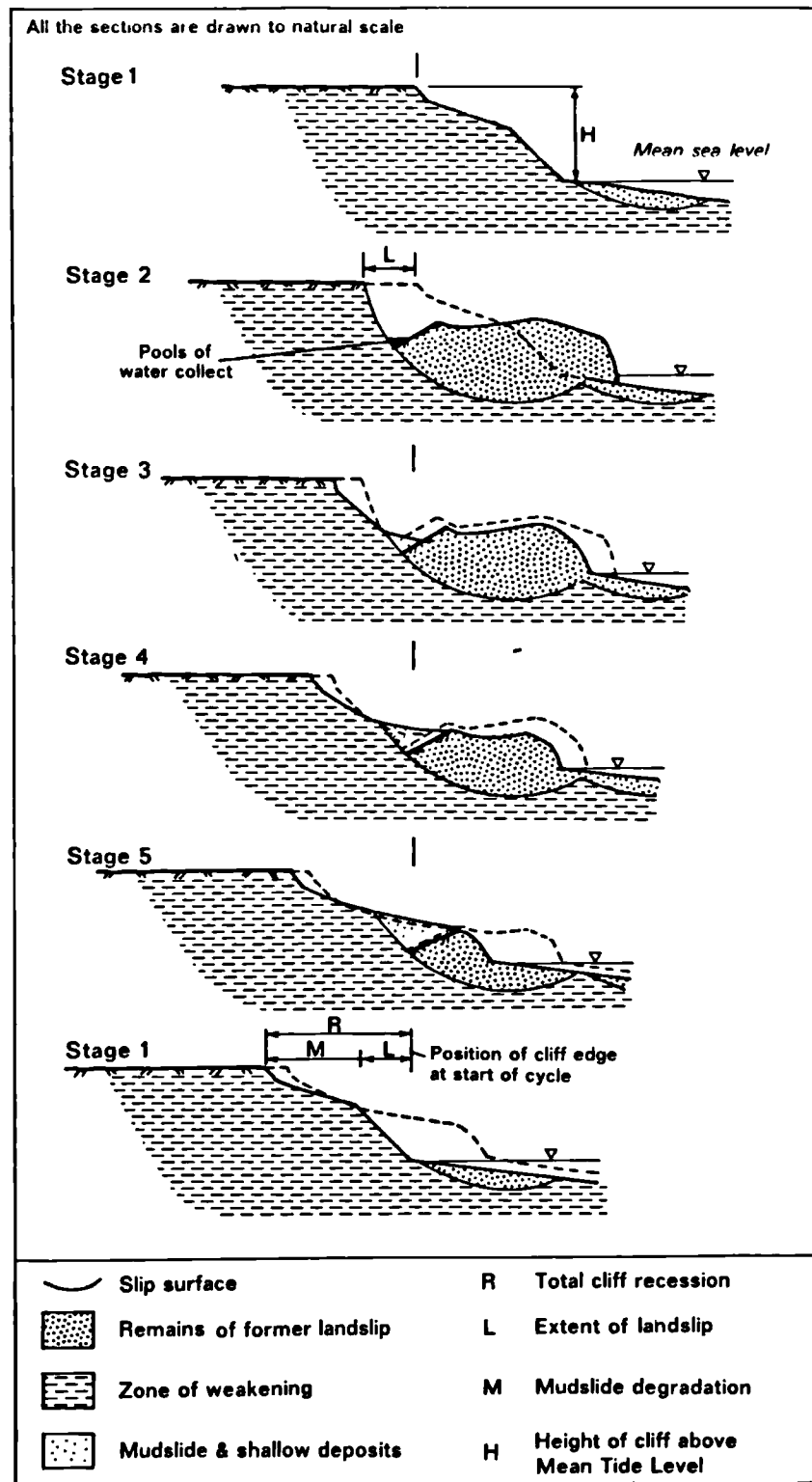
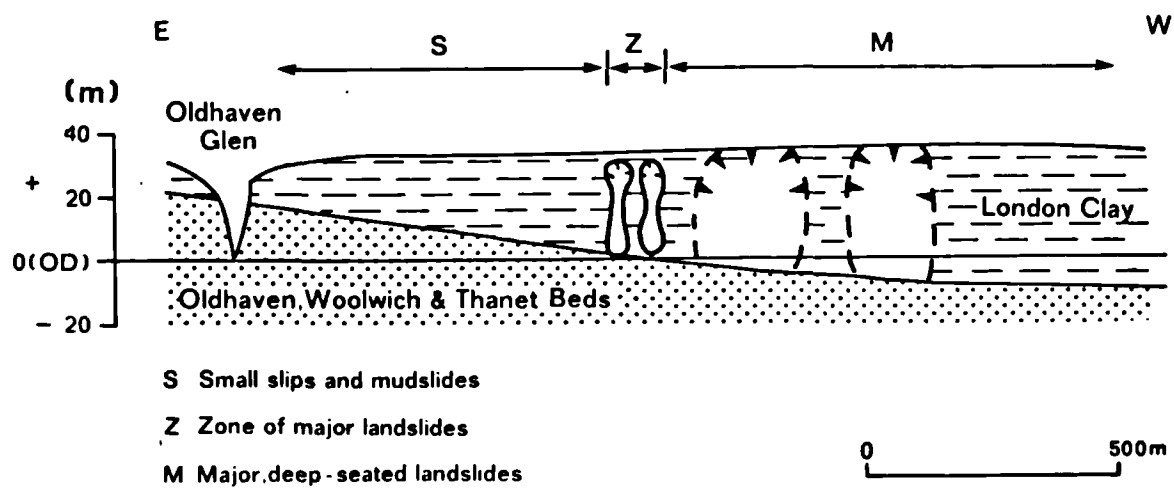


Figure 1.4. , The location of deep-seated mudslides with respect to structural dip and sea-level.



Source: Hutchinson (1983) p.393.

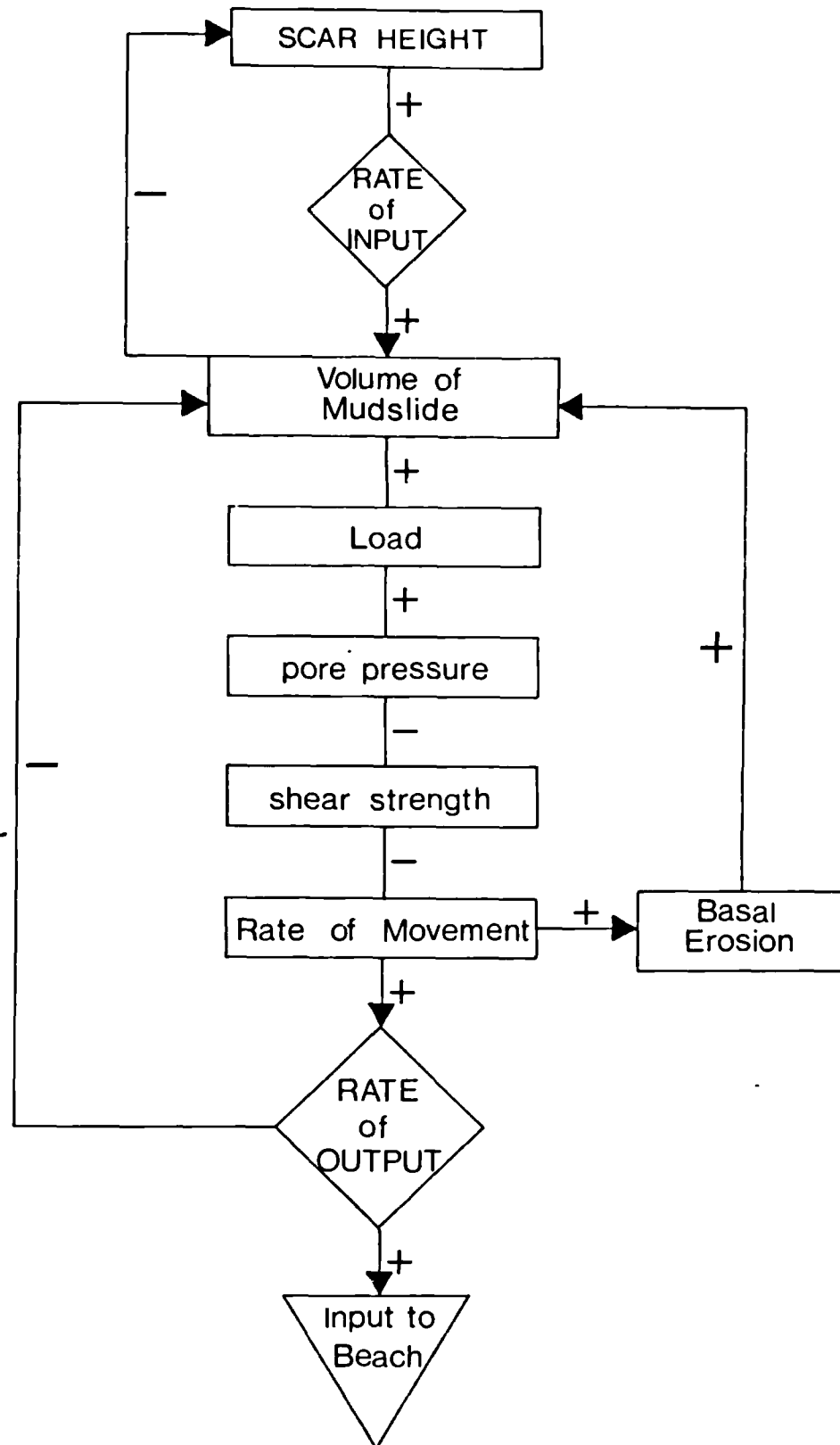
"...In all these examples basal erosion is found to be more rapid than weathering, steepening the slope profile and generating deeper slips. Only subsequently does mudsliding become important as one of the agents of degradation of the slipped mass. The form of the cliff is determined by the nature, size and spacing of the deep-seated slides, and the mudslide source is only one unit of the bigger landslide complex. Occasionally a mudslide occurs as a single feature on a hillside. In these cases the source consists of a more simple arcuate embayment with a headwall, failure scar, tension cracks, slipped units and depressions."

Mudslide sources are commonly located in the headward depressions and along the sides of earlier deep-seated landslides which led Prior et al (1971) to suggest that existing slides are a prime determinant of mudslide location, since the natural groundwater regime is altered promoting their self-generating behaviour. Moore (1986) demonstrated a wider application of the models than first thought to sites developed in heterogeneous lithologies.

The two models clarified from the studies of Hutchinson indicate an attempt by geomorphologists and engineers to isolate the complex interplay between the processes of erosion or destabilization and slope failure. The balance between debris supply and unloading of the slope offers a simple process-response model (Figure 1.5), originally proposed by Brunsden (1973), that explains the subsequent development of mudslide form.

As Hutchinson (1973) has shown, in situations where the balance is dominated by processes of loading or unloading, significant changes in mudslide morphology would be expected. Furthermore, in temperate climates there is a distinct seasonal trend in the activity of mudslides

Figure 1.5. A process-response system of the form, stresses and rate of operation of a mudslide system.



Source: Brunsden (1973) p.198.

that is related to the wetter months of the year. Where toe erosion is greater than the supply of debris, the slope is undermined, and deep-seated landslides are provoked. If the supply of weathered debris is greater than erosion, significant extension of the accumulation lobe occurs, protecting the cliff from the likelihood of large failures.

The second model demonstrated the importance of the hydrogeology of coastal cliffs with an element of dip, and the location of large coastal mudslides. The influence of geologic structure, lithology, and ground-water conditions were noted. Given the causal processes of the location and evolution of landslides, mudslide behaviour is governed by the properties of soil and the interaction with ground-water.

1.4 The mechanics of behaviour.

The slope behaviour exhibited by mudslides is governed by the nature and properties of soils. By far the most important property is shear strength, although it is necessary to understand the influences thereupon by groundwater pressures and saturation in both space and time. The properties of soils pertinent to mudslides are introduced in section 1.5 and Chapter Two, following a discussion of the nature and development of mudslide movements.

In temperate climates, the seasonal activation of shallow translational mudslides show a distinct relationship with an increase in soil water or the phreatic level coincident with the wetter months of the year. The association is so marked that the phrase 'mudslide season' may be used to refer to this unstable period.

The condition of a mudslide through the seasons was aptly described by Prior (1977):

"In summer, when the material dries out, the flows (slides!) can be examined on foot with ease, but in spring they are extremely unstable. During spring the material has a very high water content and very low strength, and some low angled areas are virtually pools of mud."

Many investigations have noted the importance of precipitation in promoting slope movements (Zaruba & Mencl 1969; Prior et al 1968, 1971, 1972, 1977, 1980; Brunsden 1973, 1984; Hutchinson 1970; Prior et al 1975; Craig 1979; Moore 1986; Balteanu 1976; Allison 1986; McConchie 1986; Chandler 1984). All indicate clear winter-summer cycles, with movement occurring in late autumn (November-December) through to March, and cessation of movement during the summer. Wet summers may control continued slow movements, and particularly dry periods may cause a lag effect by delaying new movements until the moisture deficit or groundwater storage has been restored.

Prior et al (1971) correlated slope movements directly with rainfall and found significant associations. More recent work (Craig, 1979; Crozier, 1986; McConchie, 1986) has similarly attempted such correlations, although these were improved when 'effective' rainfall or hydrological flux parameters were used. Correlations of greater significance were found when associating movement with soil moisture content and pore water pressures; it is considered unlikely that movement would immediately follow rainfall since time-lags exist between the initial event, a rise in ground water levels, and the trigger of movement. This process is further delayed through complex subsurface lithology with significant variations in permeability in the vertical cliff section. Thus rainfall

is more frequently indirectly associated with slope movements, as a result of an increase in soil water and pore water pressure and the saturation of the clay materials.

Hutchinson (1970), Hutchinson and Bhandari (1971), Hutchinson et al (1974) and Bhandari and Hutchinson (1982) have shown that the most important expression of climate on slope movement is the fluctuation in groundwater pressure. Brunsden (1984) proposed a model in which the basic climatic parameter is the seasonal balance of water surpluses and deficits related to precipitation and evapotranspiration, and the estimation of 'effective rainfall', soil moisture and pore water pressures and tensions. Movement usually occurs in periods of rainfall surplus ~~over losses~~ with high pore water pressures. More typically pore water pressure variations are explained by the concept of undrained loading, originally suggested by Hutchinson and Bhandari (1971), which is now considered to be a primary mechanism of mudslide degradation. The concept explains why the lower sections of mudslides may advance by shearing on slopes of lower angle than the corresponding limiting equilibrium for residual strength and pore water pressure. Movement is initiated by undrained loading in the headward regions and to the rear of the accumulation lobe from an increase in the weight or volume of material and ground water coincident with a rise in pore water pressures. Although the concept is supported by considerable empirical evidence, few studies have published experimental and field data to substantiate this process.

Past work has shown that mudslide tracks move, with slight time-lags, during periods of water surplus, although the accumulation lobes may show lags of up to 1-4 months (Hutchinson 1970). This led to the conclusion

that there was no clear relationship between movement and pore water pressure except where rapid loading of debris onto the accumulation area was found. Brunsden (1984) suggests there is an inadequacy of instrumentation and sensitivity to detect the pressures generating movement. Hutchinson and Bhandari (1971) and Hutchinson et al (1974) employed electrical diaphragm piezometers with improved response times to pressure fluctuations. They found strong artesian and near-geostatic pressures in the 'loading zone' of the accumulation lobe, while pressures upon the basal shear surface were assumed to be greater than hydrostatic. The findings were not correlated with rainfall.

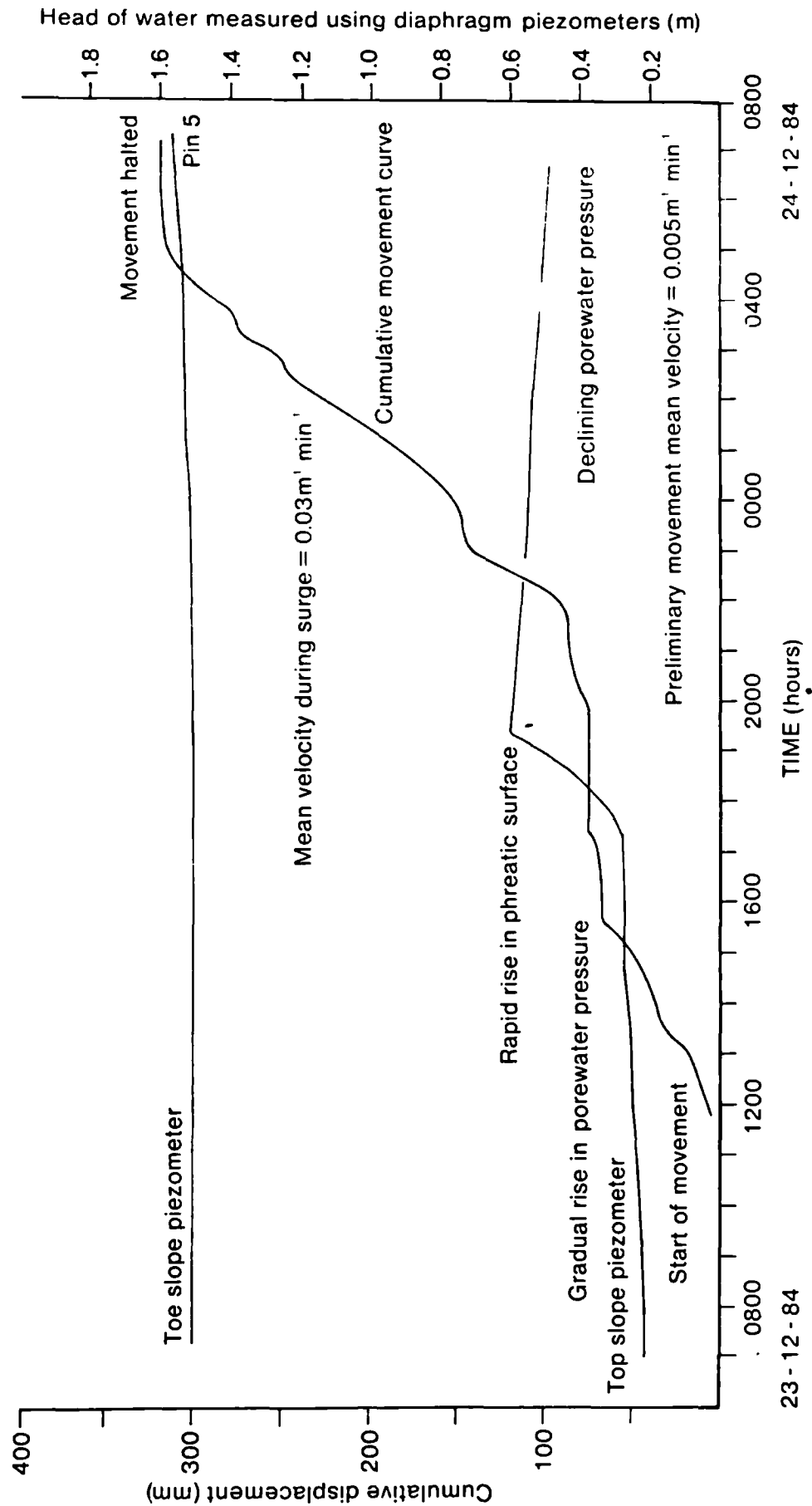
In recent years our understanding of this process has been improved with new instrumental techniques. Allison (1986) and McConchie (1986) used electrical piezometers to monitor the temporal variability in pore water pressures. McConchie inserted eight piezometers based on the design of Hutchinson and Bhandari (1971) recording on dataloggers, while Allison developed an automatically recording system using two sensitive pressure transducer tensiometers, sited in the source and accumulation zones.

The findings of Allison are particularly relevant to this study. In monitoring the porewater pressures in the source and accumulation areas of a mudslide in Dorset, England, he demonstrated that there was a seasonal rise in pore water pressure in both these zones:

"The toe and top slope records tend to mirror each other in their seasonal trend but with some clear weekly fluctuations."

Pressures in the accumulation lobe remained high all year whereas fluctuations recorded in the source area reflected short-term climatic variations, mudslide movements and back-slope loading (Figure 1.6). The

Figure 1.6 Relationship between pore water pressure and 'graded' slip displacements of a mudslide at Worbarrow Bay.



tensiometer in the accumulation lobe only registered a change, following severe movement in the source, often with a time-lag, suggesting that instability is generated from the source with movement in the accumulation zone only occurring in extreme cases of toe-slope loading. It was noted that the cost and effort of using electrical piezometers is only justifiable when detailed short term variations are required. The results provided new data in explaining resultant movements, which hitherto, have been poor as a result of the inadequate sensitivity of standpipe piezometers.

During the wetter months of the year the soils of mudslides become progressively more saturated causing a reduction in shear strength and an increase in the likelihood of movement. This is a little understood process and as such has received little attention in explanations of the seasonal movement of mudslides. The properties of the material fabric, and the minerals therein, show different degrees of affinity for water which strongly influences the physical behaviour of soil particles. Such properties are discussed in the next section and in greater detail in Chapter Two.

Brunsdon (1984) like many of the other studies previously mentioned, states that mudslides occur in saturated clays of all types. More recently it has been noted that mudslide materials are associated with expansive clay minerals such as montmorillonite in addition to illite and kaolinite (Prior and Ho 1970, 1972; Handy and Williams 1966; Yatsu 1966, 1967). The latter state (Yatsu, 1967):

"If bedrock contains some components of swelling clay minerals it swells with pressure when afforded with water and it is apt to

become unconsolidated clayey debris. Such detritus is easily affected by mass-movement of slip or flow types."

Herein lies a complex relationship that ultimately is responsible for mudslide instability. Yet, in practice it is difficult to isolate the separate influences of pore water pressure and saturation for they are interdependent. Swelling caused through a rise in soil moisture exerts a positive pressure on the soil mass in the process of saturation, whereas it may also be construed that the rise in pressure causes the progressive saturation and breakdown of the soil fabric, which is further accentuated by movement itself. It is clear there is a need for further research in this field to establish the separate influences of soil water and pore pressures on the properties of mudslide materials.

Numerous types and speeds of movement have been reported, most of which relate the stage of development, the water content, and the slope of the feature to the rate of activity. Reported velocities (Table 1.5) vary from day to day and season to season, at different locations on and within the mudslide, and some show that there is a positive correlation between velocity and effective precipitation (Campbell 1966; Crozier 1968; Prior *et al* 1968, 1971, 1972; Hutchinson *et al* 1974). Brunsdon summarizes typical velocities, and suggests that mudslides should generally be classified as slow mass movement types. Movements average 5-25 metres per year with exceptional records of 85 metres per year.

Traditional methods of measurement do show weekly movements of several metres, suggesting that annual averages may conceal the underlying mechanism of sudden movements interspaced with long periods of slow movement or quiescence. Prior *et al* (1971, 1972), Hutchinson (1974),

Table 1.5 Summary of reported velocities of mudslide displacements.

AUTHOR	METHODS	TYPE OF MOVEMENT	REPORTED VELOCITIES
Von Moss (1953)	Stakes	-	7.0 m/yr (av)
Fukuoka (1953)	Stakes, FT + Incln.	-	25 cm/day (max), and 25 m/yr (av)
Crandell and Varnes (1961)	Stakes	-	5 m/yr (av)
Auger and Mary (1968)	Stakes	-	1.75 m/day
Skempton and Hutchinson (1969)	Stakes FT + Incln.	Plug	25 cm/day (max) 8 m/yr (av)
Hutchinson (1970)	40 mm ² blocks on 60 mm pins FT + Incln. Strain Gauge	Plug and sharp shears	Intermittent 0-260 mm/day 9-86 m/yr (av)
Brunsdon (1973)	40 mm ² blocks on 300 mm pins FT + Incln.	Plug, complex	>0.5 m/day (max) 18 m/year (av)
Prior <i>et al</i> (1971) + Prior and Stephens (1974)	Stakes, MONRO CR (IH 130) FT re-excav.	Plug	Surge 8 m/min (max) 100 m in 14 months 5 m/month (av) 251.4 cm in 7 days 35.9 cm/day 1.49 cm/hour 7.6-248.9 cm/week 1-20 cm/hour
Hutchinson and Bhandari (1971)	Stakes	Plug	1.9 mm/hour.
Craig (1981)	Painted line MONRO CR and FT re-excav.	Plug	$2.6 \times 10^{-6} \text{ms}^{-1}$ $8.0 \times 10^{-7} \text{ms}^{-1}$ $1.1 \times 10^{-6} \text{ms}^{-1}$ $7.7 \times 10^{-6} \text{ms}^{-1}$ $100 \times 10^{-7} \text{ms}^{-1}$
Moore (1986)	Stakes	Complex	131 cm/day (max)
McConchie (1986)	Stakes and Lea water-level FT + Incln.	Plug	45 cm/15 months 3 mm/day
Allison (1986)	Gantry+Rotary Potentiometers	Complex	18-30 m/7 months 2-3 m/20 minutes

FT: flexible tubing used with inclinometer CR: chart recorder for MONRO

Based on Brunsdon (1984) p.392.

Craig (1981), McConchie (1986) and Allison (1986) have all reported a complex erratic pattern of pronounced accelerations and decelerations with sudden surges and long periods of stability.

Measurements of edge displacements (Hutchinson 1965, 1970; Prior et al 1968, 1972; McGreal and Craig 1977; Craig 1979, 1981) demonstrated that mudslide movements may be described as 'plug-flow'. Craig (1979) confirmed this belief, although noted that it is possible for mudslides to become so saturated and disturbed that all the debris may truly flow by continuous internal deformation. This may occur either at different times in one movement or in different sections of the same mudslide, and Craig suggests that these should be taken into account in conventional stability analyses.

More recently Allison (1986) has provided new details of the nature and pattern of mudslide movements from continuously recording 'unwinding potentiometers' suspended from a gantry spanning the slope. Three types of movement event were identified:

1. Multiple; small individual spatial movements;
2. Graded; gradual spatial movements and;
3. Surge; rapid movements in space and time.

The three types of movement occurred with different frequency and at different times in the overall record and were considered to reflect the influence of undrained loading and pore pressure conditions. All were separated by periods of no displacement.

In summary, the physical behaviour of mudslides during the wetter months of the year is related to an increase in the stresses promoting movement and a decrease in the strength that resists movement. Ultimately the stability of the slope is reduced to a critical condition for failure. In the event of slope failure and movement, stresses are relieved and the materials establish a new state of equilibrium by consolidation. The seasonal movement of mudslides is no longer explainable as flow caused by continuous deformation, but by a series of movement types, predominantly sliding, although flow may subsequently be important depending on the magnitude of the stresses promoting movement.

The onset of movement is generated by an increase in winter rainfall and water surplus, a decrease in evapotranspiration, a general rise in groundwater and soil moisture levels, clay saturation, an increase in pore water pressure, and a decrease in shear strength. It was noted that the interdependence of these processes on the properties of materials makes their separate influences difficult to isolate in practice. There may be a tendency when faced with such problems to ignore these interrelationships for those which are easily measured and accountable. It is the intention of this study to investigate the role of soil properties in strength reduction and the seasonal behaviour of mudslides.

1.5 Material properties.

A wide variety of materials are found in mudslides, involving clays of all types from soft intact clay to stiff fissured clays which are progressively softened, weathered and broken up by movement. They may include mudstones, marls, shales, fine sands and silts, and often support massive boulders overlying and moving on a softened clay matrix. Clays have large surface areas and are very reactive in soil; surface forces significantly influence the properties and behaviour of clays.

The destructive processes in the development and formation of mudslide materials may be either physical or chemical. Physical disintegration caused by movement and water results in soil particles retaining the same composition as the parent rock, whereas chemical processes result in changes of mineral form due to the action of water, salts, oxygen and carbon dioxide. Water is the major agent in chemical weathering and is also the primary factor in the internal causes of mass wasting.

Reduction in material strength occurs by weathering, swelling, fracture development, removal of cement and softening of rock by increased water content. Most unconsolidated materials become susceptible to failure when water is added. In time, weathering of slope materials produces a progressively less-stable condition as more clay is released and formerly coherent materials become increasingly disaggregated and even plastic.

Kenney (1984) categorises the properties of soils into two groups, and these shall be adopted in this thesis:

1. Inherent properties; these are related to the nature of the constituent particles such as mineralogy, particle-size and plasticity.
2. Mechanical properties; describe the physical behaviour of soils under various conditions and include shear strength, compressibility and permeability.

In explanations of slope stability, geotechnical engineers consider the mechanical properties in standard formulations of the factor of safety, in terms of shear strength, slope angle and effective stress. However, soil behaviour is more a function of the inherent properties of materials such as the amount and type of clay minerals. For instance, as clay content increases there are corresponding increases in plasticity, volume, cohesion and saturation potential, with lower permeability and frictional resistance. The inherent properties are fundamental to the mechanical behaviour of soils, and yet in geotechnical applications little consideration is given to the variability of soil properties in space and time, such assessments often being made on few 'standard' samples. Stability calculations based on few well-tested specimens may subsequently give rise to significant errors in explanations of slope behaviour.

The strength of the soil mass depends partly on the strength of the minerals composing the aggregates, but also on the forces holding the aggregates together. Selby (1982) suggests that an equation describing the factors determining the shearing resistance of soil might take the form:

$$\tau = f [e, \phi, C, \sigma', c', H, T, \epsilon, \dot{\epsilon}, S \dots]$$

where

- τ is the shearing resistance;
- e is the void ratio
- ϕ is the frictional property of the material
- C is the composition
- σ' is the effective normal load
- c' is the effective cohesion of the material
- H is the stress history
- T is the temperature
- ϵ is the strain
- $\dot{\epsilon}$ is the strain rate
- S is the structure of the material

Many of these parameters are not independent, and many cannot be evaluated quantitatively. Consequently, cohesion and friction are usually evaluated under various conditions of water content, load, rates of loading, confining pressures and stress history during controlled measurements. The cohesive forces are derived largely from cementing agents that bind rock and soil particles together, whereas the frictional properties are derived from the resistance of grains to sliding, crushing, rearrangement and volume change.

Brunsden (1984) provides the most comprehensive review of the range and type of properties reported in the literature and noted the consistency of the reported values (Table 1.6):

"The clay content of mudslide materials generally exceeds 50 per cent in the <2 μ group and up to 80 per cent in the <5 μ group. They possess typical index properties of liquid limits 56-80 per cent, plastic limits 22-36 per cent, a plasticity index of approximately 20-30 per cent, a liquidity index of 0.02-0.5, an activity of 0.7-0.8 and a unit weight of 1.7-2.0 g/cm³."

Table 1.6. Typical material properties of mudslides.

AUTHOR	LOCATION	LITHOLOGY	CLAY MINERALS	CF(%) 2µm < 5µm	W(%)	LL(%)	PL(%)	PI(%)	LI(%)	c' (kN/m ²)	c _r ' (kN/m ²)	φ' (degrees)	φ _r ' (degrees)	UNDRAINED STRENGTH (kN/m ²)	Af	UNIT Wt (kN/m ³)
Hutchinson (1970)	Bellingue, UK	London Clay	—	67-71	38-49	85	30		0.15 0.35					4.8-7.2	0.8	16.7-17.6 (SG=2.74)
Stampton & Hutchinson (1979)	Savenoaks, UK	Soft Allerfield Clay Weald Clay Gouge (soft)	—	55 60 58	31 25 34	72 65 71	29 26 31		0.40 0.02 0.44	0 0 0		12-15 15.5-16.5 16				
Prior & Stevens (1972)	Minnis North	Liasic clay & till	Montmorillonite	50-56	41-43	56-63	22-24		0.38	0-2	0	24-27	14.5-15.0	0.5	0.73-0.77	17.5-17.6
Prior et al. (1971)	Antrim, NI		Illite Kaolinite													
Prior & Ho (1970) Hutchinson et al. (1974)																
Prior (1974)	Drummagraigh	Soft			40	43	27		0.62	2.1	0	24	14.0			2.0g/cm ³ 1.76-1.81t/m ³
Hutchinson & Bhandari (1971)	Isle of Wight	Stiff fissured Oligocene clay Hursthead Beds	—	67	32-55 50	67-80 66	27-33 28		0.41 0.42		0		13.5	0-1.6 t/m ² 0.08 t/m ² Remoulded		
Prior & Renwick (1980)	Normandy, France	Jurassic clay Shales-mudstones	Illite Kaolinite Montmorillonite		50 55-60	58	23	3	0.40		0		14.0	0.05-4.0 t/m ²		1.85 g/m ³
Prior & Renwick (1980)	Denmark	Eocene soft plastic clay & silt	Montmorillonite Kaolinite Illite Chlorite	65-76	Crust 12 60	60	33	27	0.55	0.09 kg/cm ²	0	12	11	0.02-7.8 t/m ²		1.86g/cm ³
Prior (1973), Prior & Eves (1975) Hansen & Mose (1964)	Denmark Rosnaes Helgenæs Røje Flint	Eocene	Chlorite	59 52 63	65-80 28-48	63-(273)	25-(55)		0.40 0.59 0.53	0.097 kg/cm ²	0	12	11			2.09 1.71
Sukarya & Prior (1978)	Mississippi Delta, USA	Subaqueous deltaic clays	—		70 surface 50-60 depth					0.00- 3.35-9.58		20-24		4.8-23.9 KPA		14.00-16.00

Source: Brunnsden (1984) p. 382-383.

Nevertheless, there are discrepancies in the range and type of parameters reported. For example quantitative assessments of clay mineralogy are rarely determined although its importance is recognised. The results reported are usually based on one or more samples taken from just below the ground surface at unspecified localities with disregard to the variations that might exist within the mudslide. This is offset to some extent by increasing the number of sampling sites, although the variability is lost by averaging the results. Samples are rarely taken from the shear surface, the zone most critical for movement. The properties reported are of general use in establishing the nature, type and range of properties reported in mass movement studies worldwide. Care must be taken, however, in using generalised properties for specific explanations of slope behaviour since variations in soil properties due to weathering and the continual processes of material degradation are not considered.

Since the mid 1960s a number of workers have suggested the importance of the mineralogical and chemical properties of soils in the behaviour of shallow landslides. Yatsu (1966, 1967) with his theories on rock control in geomorphology, is the major proponent for the incorporation of geochemical properties as promoters of slope instability. The importance of such properties had also been stressed by Yong and Warkentin (1966) and Zaruba and Mencl (1969), and it is interesting to note that the introductions of most soil mechanics textbooks begin with a consideration of the properties of clays and the chemistry of particle interaction (Lambe and Whitman 1969; Mitchell 1976; Craig 1983 and Das 1985).

Mudslide materials are often associated with swelling clay minerals such as montmorillonite together with illite and kaolinite (Handy and Williams

1966; Prior et al 1970, 1971, 1972, 1973, 1977 and 1980). The work of Prior has provided quantitative data of both geotechnical and geochemical nature that suggests a close association between clay minerals and mudslide distribution. Many mudslide materials are characterised by the presence of swelling clays within the matrix. Increasingly this has led to explanations of mudslide behaviour due to the 'hydration or saturation of swelling clay minerals' mentioned in section 1.4, p56, and also as a main factor in promoting mudsliding. Craig (1979), however, has refuted the evidence of Prior et al (1971) that suggested a relationship between mudslide movement and the presence of montmorillonite clays. Little work has subsequently been published to clarify the argument. McConchie (1986) assessed both the inherent and mechanical properties of an earthflow in New Zealand but did not report any association between the clays and chemistry of the system. Brunsden (1984) in response to the dilemma, drew attention to the presence in coastal areas of hydrated sodium and magnesium exchangeable cations and subsequent changes in the chemical and physical properties of mudslide materials prompting the need for further research.

In the phenomenon of landslips, clay minerals seem to play important and fundamental roles of rock control (Yatsu 1966). The presence of ten per cent clay in soils may completely alter their mechanical behaviour (Mori 1964). Such changes in the properties of material depend on the total content and the species of clay minerals, adsorbed ions, and surface chemical characteristics of the boundary between clays and water. If this is realised, states Yatsu (1966):

"There is no doubt for the necessity of mineralogical, physico-chemical and mechanical research on landslide clays.....Generally, swelling clay minerals are more or less contained in landslide

clays. The ratio of clay to water, the type of clay minerals and adsorbed cations on the surface of clay minerals are reflected in the mechanical properties of the clays or clayey soils."

The strength and plasticity of soils will be affected by the type of clay mineral. The plastic limit and plasticity index decrease in order of montmorillonite, attapulgite, illite, halloysite and kaolinite. In ranges of low water content, the shearing strength is mainly influenced by water content, while with high moisture contents, the kind of clay minerals and exchangeable ions play an important role in this property although their effects are time-dependent.

According to Kerr (1963), clay minerals in glacial tills are illite, montmorillonite, chlorite, and kaolinite, but they are very different from one another in mineral composition, even in adjacent areas, which might account for local occurrences of mass movement. For example, Leda clay, near Ottawa, consists mainly of illite; clay minerals of landslide areas in Manitoba consist of illite and montmorillonite (Warkentin 1961). The clays are thought to be a marine deposit saturated with calcium and magnesium ions, giving rise to their unique properties of sensitivity*. Surface chemistry must be a powerful method in an attempt at complete solution of sensitivity problems (Yatsu 1966).

Anderson et al (1969) proposed that bentonite debris flows characterised by easily hydrated interbedded bentonite deposits, slopes of 5-20°, and abundant water, are unique to arctic environments. This partly contradicted the evidence provided by Yatsu (1966, 1967), Handy and Williams (1966), which led Prior and Ho (1970, 1972) to suggest the

* The more reversible the hydration and dehydration of clay minerals, the greater their sensitivity. Sensitivity may be expressed by a ratio of undisturbed to disturbed shear strength.

presence of other bentonite landslides in widely differing climatic conditions. In Northern Ireland, for instance, mudslides are seasonal and related to the hydration of swelling clays. Coastal landslides in St. Lucia ^(Prior and Ho, 1972) are related to pure swelling montmorillonite and move erratically in response to soil saturation during periods of heavy rainfall. In Barbados, clay minerals again contribute to widespread landslide activity.

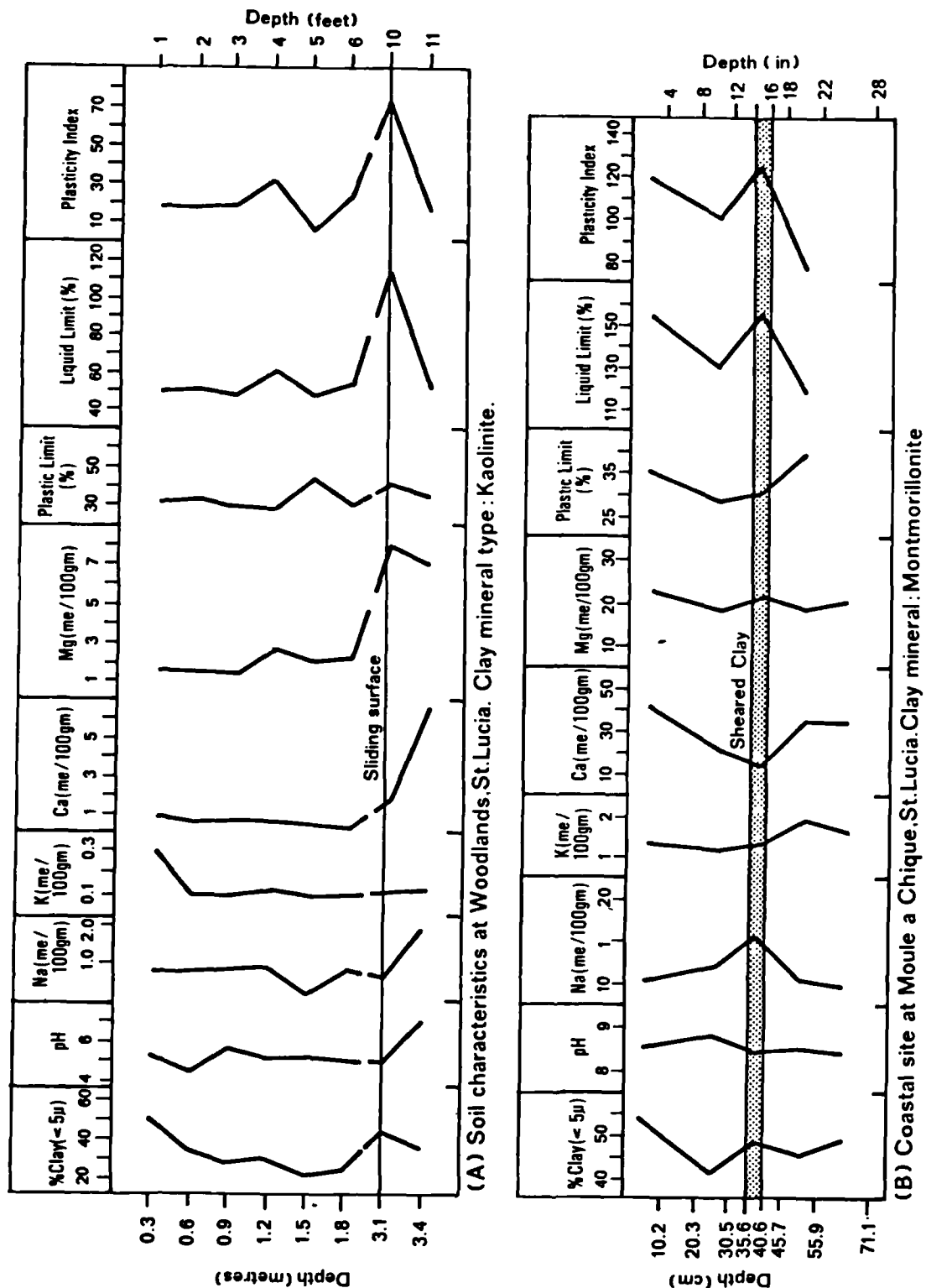
Prior and Ho (1972) reported that the type of mass movement on the islands of St. Lucia and Barbados were related to the presence of certain clay minerals:

"Rotational, translational, complex slides and slump earthflows are present...Complex slides involving pure montmorillonite clays occur only on coastal sites. Mixtures of kaolinite, montmorillonite, illite and chlorite clay minerals occur at rotational slides and slump earthflow sites, while pure kaolinite soils are associated with translational slides."

They also found that the geochemistry was important in explaining the properties of material in the translational slides (Figure 1.7):

"The type and concentration of exchangeable cations determined the plastic properties of the unstable soil and there was an association between the type of clay mineral and the liquid limits. The presence of basal shear planes were coincidental with discrete layers of soil which differed physically and chemically from the overlying materials. In these zones there were high concentrations of divalent calcium and magnesium cations affecting the index properties of the kaolinite. Landslide activity appeared to be directly related to the development of this clay rich, plastic layer at depth. Adsorption of water by the plastic clay reduces strength and contributes to the instability. The depth of movement is therefore controlled by the position of the plastic layer which in turn reflects the degree of horizonation."

Figure 1.7. Variation in soil properties of mudslides in St. Lucia.



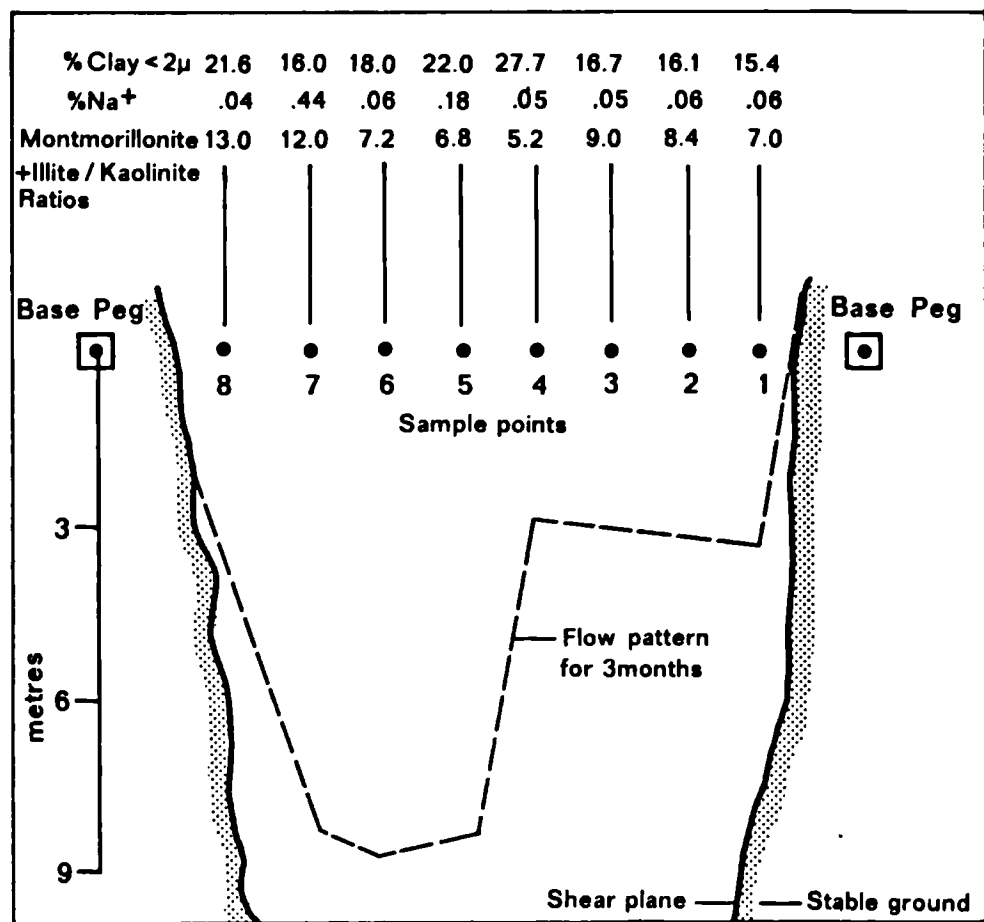
In their conclusion, Prior and Ho (1970) point out that the association between landslides and the presence of montmorillonite-rich clays in Northern Ireland, St. Lucia and Barbados is not incidental. The clays are susceptible to the processes of weathering which are further enhanced by the presence of hydrated sodium and magnesium exchangeable ions (Yong and Warkentin 1966). According to Prior and Ho (1970) there is a limit to the relevance of climatic criteria:

"...The primary factor in the location of flow and slide type landslides is not a climatic one, but rather due to the presence of bentonite clay minerals."

Prior et al (1971) again note the contribution of studies relating climatic variables as promoters of slope instability, but state that the geotechnical and geochemical properties cannot be disregarded. The paper describes examples of mudslide and rockfall activity in Northern Ireland, instability being explained by the high adsorptive capacity of montmorillonite for ions and water, particularly in the presence of sodium causing expansion to several times their dry volume (Yong and Warkentin 1966). Such hydration accounted for the association between movement and rainfall. Attention was drawn to the variation in clay abundance, clay minerals and exchangeable ions in solution within the track (Figure 1.8). The variations were not found to be consistent, although high ratios of montmorillonite plus illite to kaolinite ratios corresponded with greatest movement...

"...demonstrating the importance of the mineralogical properties of materials; instability is largely determined by the presence of montmorillonite and to the degree of hydration of the material by rainfall."

Figure 1.8. Pattern of mudflow movement and montmorillonite-illite to kaolinite ratios.



Source: Prior, Stephens and Douglas (1971) p.135.

Craig (1979) re-considered their findings and found the data inconclusive in explaining accelerated movement in relation to clay mineral content.

Prior (1973) has also analysed the landslide clays of Denmark and confirmed the presence of swelling minerals. Montmorillonite, illite, chlorite and kaolinite were present with some quartz. The chemistry of the clays showed a decreasing abundance of Ca, Mg, Na and K, and were generally alkaline. Prior (1977) extended these findings to relate mudslide processes to specific coastal localities in Denmark, where there are outcrops of clay-rich sediments of Eocene age. The clay content exceeded fifty per cent and Prior was in no doubt that the Danish mudslides clearly reflect the properties of the over-consolidated Eocene clay:

"Weathering and softening of the clays is promoted by fissures and excess water penetrating along them. This process is encouraged by the mineralogy and geochemistry of the clays. Montmorillonite swelling clay minerals favour the adsorption of water provided by precipitation and groundwater. Present slope instability is, thus, the result of geotechnical and geochemical properties of the clays together with climatically induced pore water pressures on slopes which are subject to variations in rates of coastal erosion."

In summary, there seems little doubt that mass movements are associated with the materials composing the slopes, especially with the amount and type of clay minerals. The presence of swelling clays can change the mechanical properties of mudslide material while the clays themselves may be modified by chemicals in the pore solution. Most studies report the presence of swelling clay minerals although a few indicate that mudslides may develop in non-swelling kaolinite clays. In ranges of low moisture content, material strength is influenced by water, while with larger

moisture levels the type of clay minerals and exchangeable cations determine the loss or gain of strength.

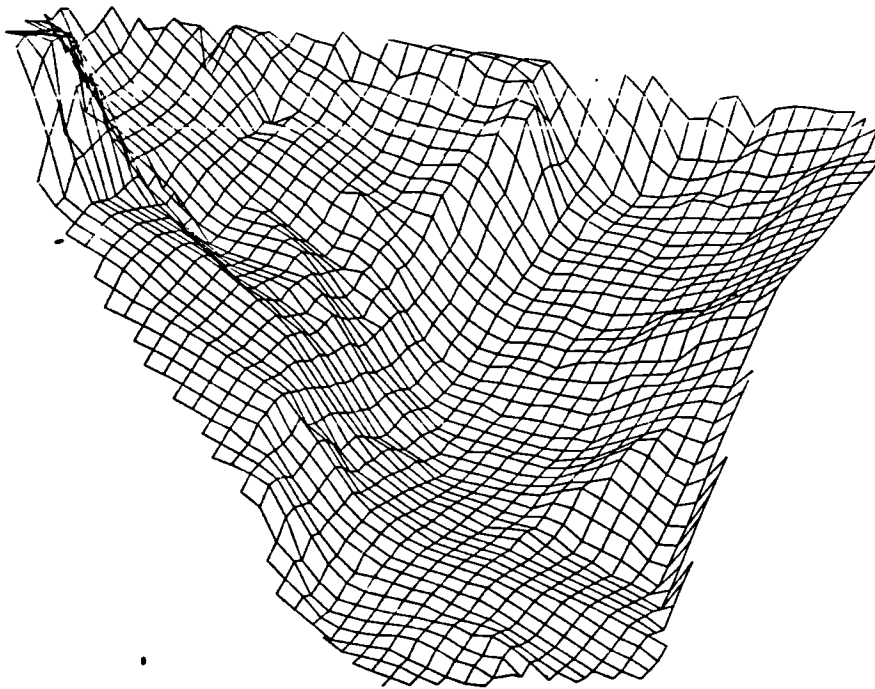
1.6 Conclusions

It is clear that the past two decades have seen considerable advances in the study of mass movement by developing standards for both the description and measurement of slope processes. These years have also seen the incorporation of electronic sensor and recording techniques which have significantly improved the resolution and response times for monitoring critical properties in the field and laboratory.

The mechanical behaviour of mudslides is well known, but the geochemistry of landslipped clays has, in comparison, received little attention. The interdependency of the mechanical and inherent properties point to a necessity for mineralogical, physico-chemical and geotechnical analyses of clays in landslip studies. The purpose of this thesis is, thus, to evaluate these interrelationships and at the same time combine the disciplines of geomorphology, pedology, hydrology and engineering geology to assess the physico-chemical properties of materials with respect to weathering processes and the location, form and behaviour of mudslides.

Chapter Two

THE PHYSICO-CHEMICAL PROPERTIES OF LANDSLIP CLAYS



2.1 Introduction.

To determine the importance of the mineralogical and chemical properties of landslipped materials it is necessary to understand the physico-chemical behaviour of clays. Clays usually make up greater than 50 per cent of mudslide materials (p.63), and so any explanation of the weathering and behaviour of mudslides should be related to the properties of clays. This is widely recognised by soil scientists and engineers alike, and Dixon and Weed (1977) concluded:

"Since the same underlying mechanisms are apparently responsible for the influence of clays on the physical properties of soil, it is not surprising that good correlations are found between these parameters and those used to quantify the physical behaviour of soils."

Thus, the purpose of this chapter is to introduce the physico-chemical properties of clay materials relevant to mass movement studies using the classification of Kenney (1984;p.61). In section 2.2, the 'inherent' properties are sub-divided into composition, clay mineralogy, clay chemistry, plasticity and the phase relationships. These are discussed with respect to their importance in determining the physical condition and behaviour of clay soils.

Alterations to the properties of clays are initiated by weathering processes which are introduced in section 2.3, followed by a discussion of the 'mechanical' properties of soils. The shear strength, volume and permeability characteristics pertinent to mudslide behaviour are outlined with respect to the role of the physico-chemical properties and weathering of clay materials.

The outcome of the review is summarised in section 2.4, indicating the importance of the mineralogy and chemistry of clays in mass movement studies. The conclusions of Chapters One and Two enable the formulation of the research objectives of this study, clearly outlined in section 2.5. The methodology used in the investigation is then discussed in Chapter Three.

2.2 The inherent properties:

2.21 Composition.

A knowledge of soil mineralogy is essential for an understanding of soil behaviour. Mineralogy is the major factor controlling the size, shape and physico-chemical properties of soil particles (Mitchell, 1976; Yong and Warkentin, 1975).

Materials involved in mass movements include a wide variety of rock fragments from boulder size to gravel and the very small particles produced by weathering processes. These rock-forming minerals may be sub-divided into two groups (Kenney, 1984; Blyth and De Freitas, 1974):

1. Massive or primary minerals;
2. Clay minerals.

Each group may be distinguished on the basis of particle size and the specific surface area or surface area per unit mass of mineral. The massive or primary minerals may be defined as any particle within the size-range 2.0-0.002 mm, and Fripiat (1965) demonstrated that they have

relatively low specific surface areas ($0.01-1.0 \text{ m}^2\text{g}^{-1}$). Quartz minerals dominate the group although feldspar and calcite are further examples.

The clay minerals may be defined as fine-grained, crystalline, hydrous silicates with structures of the layer-lattice type. They are effective ion-exchangers and the most common products of water-rock interactions. The term 'clay' is also used to denote a grain-size of less than $2 \mu\text{m}$ (or occasionally less than $4 \mu\text{m}$). Clay particles smaller than $1 \mu\text{m}$ are classed colloidal. Although clay materials in nature contain clay minerals, and most clay minerals are clay-sized, the correspondence between the terms is not exact. The clay fraction of soils usually contains quartz, feldspars, iron oxides, and carbonates in addition to the clay minerals whereas some clays such as kaolinite and chlorite often occur with grain sizes larger than $2 \mu\text{m}$. Therefore it is necessary to use the term clay-size when referring to particle size and clay type when describing mineral composition.

Clay mineralogy refers to the types of clay mineral, each of which differ considerably with respect to grain-size, specific surface area and physico-chemical characteristics (section 2.22). Thus, the large minerals of kaolinite and chlorite have lower specific surface areas ($5-100 \text{ m}^2\text{g}^{-1}$) than hydrous mica and illite ($100-200 \text{ m}^2\text{g}^{-1}$), vermiculite ($300-500 \text{ m}^2\text{g}^{-1}$) and montmorillonite ($700-800 \text{ m}^2\text{g}^{-1}$). The increase in surface area corresponds with a reduction in the particle size of each mineral.

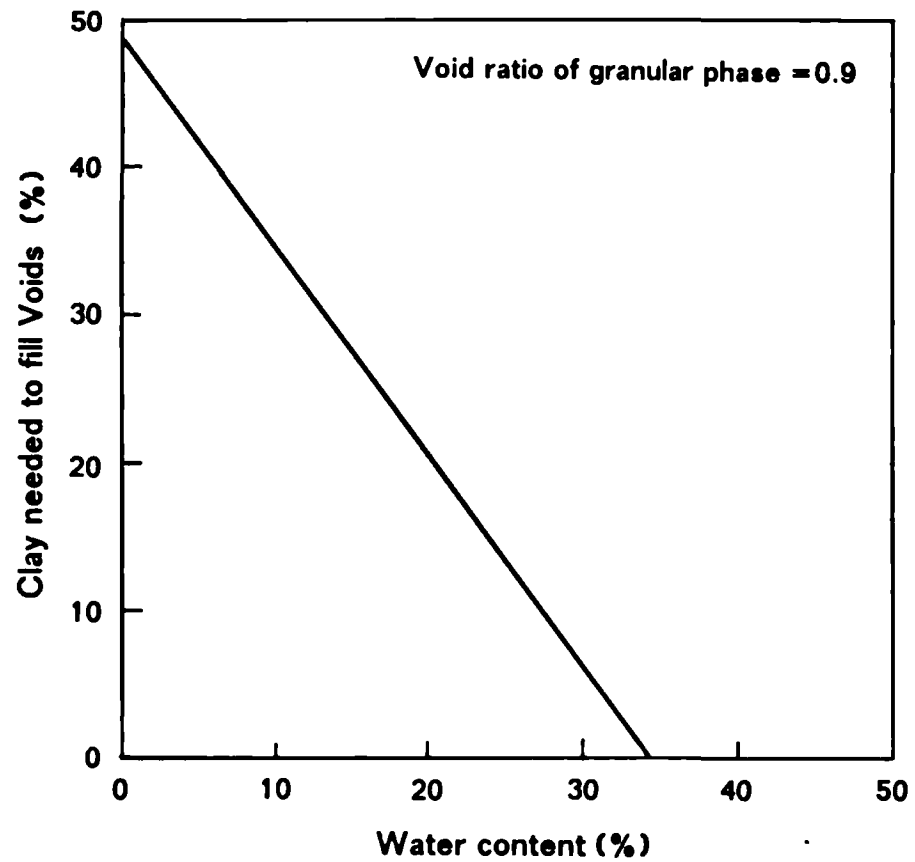
The role of soil mineralogy in the behaviour of mass movements is best seen when the particles interact with soil water. The surfaces of the massive minerals are inactive to soil moisture and only support thin layers of water. Thus the non-clay massive minerals may be regarded as

relatively inert materials whose interactions are predominantly physical in nature. The surfaces of clay minerals, however, are chemically reactive to soil moisture and attract hydrated cations and water molecules. Water layers around each particle form diffuse ionic double layers; the nature of such layers is highly dependent on the type of mineral and the chemistry of the solution (section 2.23).

The size of clay particles is so small and the surface area to volume relationship large, that physico-chemical interactions with each other and with the water-electrolyte soil phase may be substantial. The influence of such interactions on the properties of soils was recognised in the 1950s by Mielenz and King (1955) and Rosenqvist (1959). The diffuse double layers bonded to each clay mineral cause assemblages of clays to exhibit plasticity, cohesion and swelling (section 2.24), fundamental properties of landslipped materials. A second consequence of bonded water is to reduce the frictional properties of the clays when compared with the massive minerals. The clay phase may exert an influence on physical properties far exceeding its relative abundance in the soil (Yong and Warkentin, 1975; Mitchell, 1976; Kenney, 1984).

Clay content is important in determining the influence of clays upon the mechanical properties and the degree of plasticity exhibited by soil (Figure 2.6). It has been suggested by Mori (1964) that only 10 percent clay-size material may completely alter the mechanical behaviour of soil. For example, Mitchell (1976) calculates that at typical natural moisture contents it is only necessary for one third of the soil solids to be clay to have a condition where clays dominate soil behaviour by preventing direct inter-particle contact between the granular minerals (Figure 2.1). Since clay particles line the surfaces of the larger particles, clay may

Figure 2.1. Relationship between water and clay content required to fill voids in a granular soil.



Source: Mitchell (1976).

exert a significant influence on the mechanical properties even when present in quantities less than shown in Figure 2.1.

The structure and orientation of the clay particles is also important in the resistance to soil deformation. The development of slickensides and shear surfaces during the genesis or remoulding of clays will result in the alignment of clay minerals and the destruction of inter-particle bonds (section 2.231). During the 1970s a number of workers (Barden, 1972; Matsuo and Kamon, 1977; Morgenstern and Tchalenko, 1967; Mckyes and Yong, 1971; Calladine, 1971; Chandler, 1972b; Sankaran, 1972; Krizek, 1977; Sergeyev and Osipov, 1977 and Aylmore and Quirk, 1967) demonstrated the importance of anisotropic behaviour and interparticle bonding on the strength and deformation of clays. Matsuo and Kamon (1977) state:

"We have many soil engineering problems because soils are multi-phase complexes. And it will be one of the most important points to reveal the physico-chemical properties of soils and to establish their microscopic stress-strain relations. It is evident that clay soils must be regarded from the microstructural point of view."

The directional-dependent mechanical properties of clay soils are governed to a large extent by their 'structure' or 'micro-structure', which consist of complex combinations of particle arrangements and inter-particle bonds. The geometrical aspects of these particle arrangements at a microscopic level are usually termed 'fabric' or 'micro-fabric' which are more amenable to study and evaluation. Bennett and Hulbert (1986) provide a good review of the importance of micro-structure in relation to soil mechanics while Rowe (1972) suggested the incorporation of fabric studies into site investigation practice. Assessments of the

micro-fabric properties of clays are required to improve our understanding of the anisotropic mechanical behaviour of clay soils.

In summary, the presence of 50 per cent or more clay-size particles in mudslides suggests that the mechanical properties will be controlled by the type of clay minerals, the chemistry of clays and pore solution, the development of diffuse double layers and the affinity of minerals for soil water, and by the destruction of inter-particle bonds along shear surfaces.

2.22 Clay mineralogy.

The small size of clay particles precluded their direct study prior to the mid 1920s when the first X-ray diffraction techniques were used. Since then clay mineral research has produced a wealth of scientific literature, particularly during the 1960s, so that the inclusion of a review would not only be extensive but inappropriate for this thesis. The reader is referred to Fowden (1984), Grim (1953, 1959, 1968), Gillott (1987), Baver (1972), Bear (1964), Brewer (1964), Van Olphen (1977), Weaver and Pollard (1975), Dixon and Weed (1977), Bolt (1979), Yariv and Cross (1979), Sposito (1984), and Brindley and Brown (1984) for comprehensive reviews of clay mineral structure, composition and physico-chemical behaviour. Such properties will be discussed, however, in the context of their effects on the mechanical properties of landslipped clays.

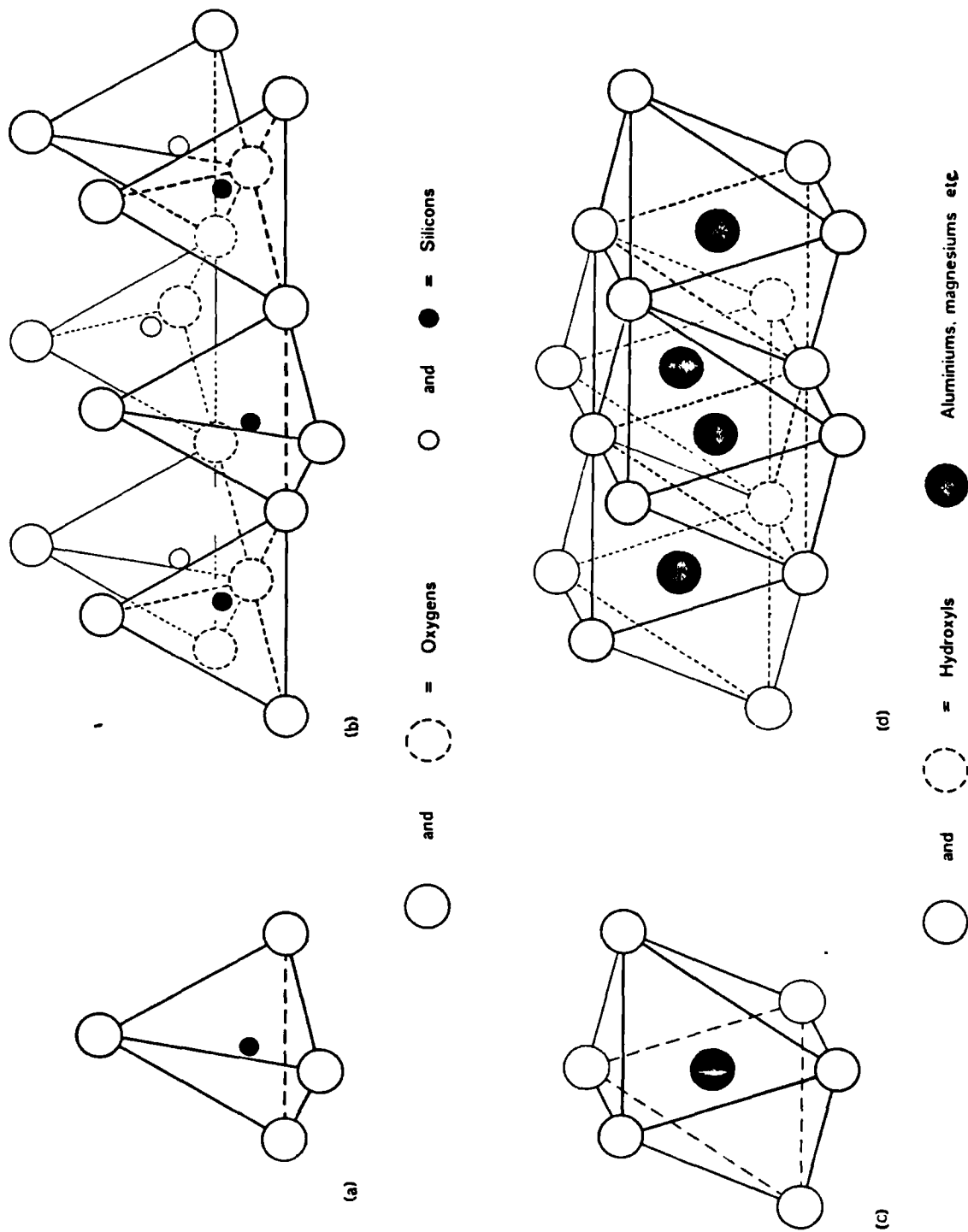
Chemically the clay minerals are silicates of aluminium, iron and magnesium. Occasionally they may contain alkalis such as sodium and potassium, or alkaline earths such as calcium or magnesium as essential constituents (Grim, 1968). Clay particles are mostly crystalline with the constituent atoms arranged in well known geometric patterns. The majority of these particles are 'semi-colloidal' because their mineral thickness is only a few millimicrons compared to their length, which exceeds the upper size limit of colloids. If the crystalline structure is irregular the solid phase is termed amorphous (Sposito, 1984), although the presence of amorphous material cannot be used in explanations of clay mineral behaviour (Grim, 1959).

The majority of clay minerals have sheet or layered 'platy' structures with a few having tubular or fibrous forms. The layered structures may be considered in terms of two simple structural units:

1. Silica tetrahedral unit. Four oxygens or hydroxyls combine in the configuration of a tetrahedron enclosing a silicon atom (Figure 2.2a). The tetrahedra combine in a sheet structure in a common plane where each oxygen bonds with two opposing tetrahedra (Figure 2.2b).
2. Octahedral unit. A unit in which an atom of either aluminium, iron or magnesium, is enclosed by six hydroxyls or oxygens having the configuration of an octahedron (Figure 2.2c). The octahedral units combine into a sheet structure (Figure 2.2d) with two layers of densely packed hydroxyls surrounding the cations between the sheets in octahedral coordination.

The octahedral sheet is termed di-octahedral when the internal cation is trivalent since only two thirds of the possible cationic spaces are filled and if the cation is Al^{3+} the layer is called a gibbsite sheet.

Figure 2.2. The coordination of aluminosilicate clays into tetrahedral and octahedral sheet structures.



Based on Grim (1968) and White (1979).

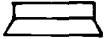
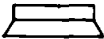


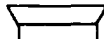
When the cation is divalent, as with Mg^{2+} , the structure is tri-octahedral and termed a brucite sheet.

All clay minerals are formed by various combinations of these structural units which is convenient for classification purposes since each group has similar physico-chemical properties. The groups vary markedly in plasticity, cohesion and adsorptive capacity for ions and water. Thus, it is important to know which clay mineral dominates any particular soil.

The structural units of the clay minerals are best classified in Table 2.1 after Bailey *et al* (1971) and Bailey (1986). The structures shown are idealized; in natural clay minerals irregular substitutions and inter-layering are common and they are not necessarily formed by the direct assembly of the basic units. All the minerals have unit cells consisting of two, three or four sheets. The 1:1 sheet minerals consist of one tetrahedral sheet bonded to an octahedral unit. The 2:1 clay minerals are formed of either a di-octahedral or tri-octahedral sheet sandwiched between two tetrahedral sheets. The latter may be stacked closely together but water layers may penetrate the sheet layers. The most common group of minerals in soil clays are the micas (illite, hydrous mica); amorphous materials are found but are not classified because they have no identifiable crystal structure.

The 2:1 sheet clay minerals have greater affects on the physico-chemical properties of soil when associated with water. The minerals within the group differ from one another by the type and amount of inter-layer attraction. Smectites for example, contain loosely bonded cations between the sheets, the micas are strongly bonded with potassium, and vermiculites by one or two layers of water and cations. The variability

Table 2.1. Classification of phyllosilicates related to clay minerals.

Type	Group (x = charge per formula unit)	Subgroup	Species ^a	Basic Structure
1 : 1	Kaolinite - serpentine x ~ 0	Kaolinites	Kaolinite, halloysite	
		Serpentines	Chrysotile, lizardite, antigorite	
2 : 1	Pyrophyllite - talc x ~ 0 Smectite - or Montmorillonite - Saponite x ~ 0.25 - 0.6	Pyrophyllites	Pyrophyllite	
		Talcs	Talc	
		Diocahedral	Montmorillonite	
		Smectites or	beidellite nontronite	
		Montmorillonites	Saponite, hectorite, saunonite	
2 : 1	Vermiculite x ~ 0.6 - 0.9 Mica ^b x ~ 1 Brittle mica x ~ 2	Diocahedral vermiculites	Diocahedral vermiculite	
		Triocahedral vermiculites	Triocahedral vermiculite	
		Diocahedral micas	Muscovite, paragonite	
		Triocahedral micas	Biotite, phlogopite	
		Diocahedral brittle micas	Margarite	
2 : 1:1	Chlorite x variable	Diocahedral chlorites	Donbassite	
		Di, triocahedral chlorites		
		Triocahedral chlorites	Cookeite, sudoite Pennite, clinochlore, prochlorite	

^a Only a few examples are given

^b The status of illite (or hydromica) sericite etc. are left open because it is not clear at what level they would enter the table. many materials so indicated may be interstratified















Source: Bailey et al (1971).

of the charge per formula unit (Table 2.1) is a reflection of the wide range of compositions arising from isomorphous substitution, the origin of the surface electric charge; the structure always remains electrically neutral. The boundaries between the groups are thus somewhat arbitrary.

Isomorphous substitution is an important concept in the structure and behaviour of clay minerals. Elements of the same valency frequently substitute for one another in the crystal lattice. However, when elements of a different valency are exchanged for one another there is an imbalance of electric charge, de-stabilizing the clay mineral. Common substitutions include aluminium for silicon, magnesium for aluminium and ferrous iron for magnesium. The excess negative charge is neutralised by the attraction of cations to the surface of mineral lattices such as Na^+ , K^+ , Mg^{2+} , and Ca^{2+} , or by structural re-arrangements which allow for the internal compensation of charge. Isomorphous substitution may only occur during initial formation and not by later replacement.

Depending on the extent of isomorphous substitution, the groups have quite different physico-chemical properties (Table 2.2) some being inactive and others being very reactive and responsive to changes in the chemical composition of the pore fluid (Van Olphen, 1977; Yong and Warkentin, 1975; Mitchell, 1976; Kenney, 1984; Grim and Guven, 1978; Grim, 1968). The unique properties of clays in aqueous suspensions has stimulated considerable research into applications for industry and commerce (Nadeau, 1987). The variability in properties arises from the specific surface area (particle size and shape) and the cation and anion exchange capacity (surface electric charge).

Table 2.2. Structure and properties of the clay minerals.

Mineral	Structure symbol	Isomorphous Substitution (nature & amount)	Linkage between sheets (type & strength)	Specific surface (m ² /g)	Charge density (Å ² /ion)	Potential exchange capacity (me/100g)	Actual exchange capacity (me/100g)	Particle shape	Particle size
Serpentine		none	H-bonding + secondary valence			1	1	Platy or fibrous	
Kaolinite		Al for Si 1 in 400	H-bonding + secondary valence	10-20	83	3	3	Platy	d=0.3 to 3μ thickness = 1/3 to 1/10 d
Halloysite (4H ₂ O)		Al for Si 1 in 100	Secondary valence	40	55	12	12	Hollow rod	OD=0.07μ IC=0.04μ L=0.5μ
Halloysite (2H ₂ O)		Al for Si 1 in 100	Secondary valence	40	55	12	12	Hollow rod	OD=0.07μ ID=0.04μ L=0.5μ
Talc		none	Secondary valence			1	1	Platy	
Pyrophyllite		none	Secondary valence			1	1	Platy	
Muscovite		Al for Si 1 in 4	Secondary valence + K linkage			250	5-20	Platy	
Vermiculite		Al Fe for Mg Al for Si	Secondary valence + Mg linkage	5-400	45	150	150	Platy	t=1/10 d to 1/5 d
Illite		Al for Si, 1 in 7 Mg, Fe for Al Fe, Al for Mg	Secondary valence + K linkage	80-100	67	150	25	Platy	d=0.1 to 2μ t=1/10 d
Montmorillonite		Mg for Al, 1 in 6	Secondary valence + exchangeable ion linkage	800	133	100	100	Platy	d=0.1 to 1μ t=1/100 d
Nontronite		Al for Si, 1 in 6	Secondary valence + exchangeable ion linkage	900	133	100	100	Lath	l=0.4 to 2μ t=1/100 d
Chlorite		Al for Si, Fe Al for Mg	Secondary valence + brucite linkage	5-50	700	20	20	Platy	

Source: Mitchell (1976).

The specific surface area of clays was shown to be greatest with the smallest particles (p.76). The second factor, cation exchange capacity, is dependent on both the specific surface area and the density of the surface electric charge arising from isomorphous substitution. Neutrality is restored when the hydrated cations and water molecules are attracted to the mineral surfaces to form diffuse double layers. Thus, depending on such factors as concentration and valence, cations in diffuse double layers can be exchanged for other types of cation (see section 2.232). Clay minerals possessing large specific surface areas and charge densities attract large numbers of cations and water molecules and, thus, have large cation exchange capacities. Such clay minerals have layers of attracted ionic water which are large in comparison to the thickness of the particle. The thickness and nature of these water layers can be significantly altered as a result of changes in the chemistry of pore fluids (Kenney, 1984 and Rosenqvist, 1984).

2.23 Clay chemistry:

Interactions between soil particles, adsorbed cations and water arise because there are unbalanced forces at the interfaces between mineral contacts. A variety of interparticle attractive and repulsive forces control the flocculation-deflocculation behaviour of clays with water and hence the mechanical properties shear strength, volume and permeability (Van Olphen, 1986). Furthermore, changes in the mechanical properties will be affected by changes in the physico-chemical forces of interaction (Mitchell, 1976).

2.231 Particle interactions and bonding mechanisms.

The combination of silica, gibbsite and brucite sheets in the basic clay mineral types involves very strong inter-sheet bonding of a primary valence type (Figure 2.2). Several types of inter-layer and inter-particle bonds hold the clay sheets and minerals together. These may be classified as electrostatic or Coulombic forces and Van der Waals' forces of attraction. Both groups may be sufficiently weak that the physical and chemical behaviour of clays may be influenced by the response of these bonds to changes in environmental conditions (Hay, 1981).

Five mechanisms of inter-layer bonding are recognised decreasing in order of strength (Marshall, 1964):

1. Neutral parallel layers are held by Van der Waals' forces of attraction between individual atoms in opposing particles. The sum of all the inter-atomic forces can be appreciable decreasing less rapidly with distance than the electrostatic forces.
2. Where opposing layers of oxygen and hydroxyl, or hydroxyl and hydroxyl exist, as in kaolinite, hydrogen bonding and Van der Waals' forces between layers provide fairly strong bonds that do not separate in the presence of water, but they may be sheared or cleaved.
3. Neutral silicate layers may be separated by layers of highly polar water molecules giving rise to hydrogen bonding.
4. Cations required to provide electrical neutrality may occupy positions that control inter-layer bonding. This bond is sufficiently strong in the micas where potassium becomes non-exchangeable between the tetrahedral layers. In other situations such electrostatic bonds are weak and liable to change through exchange reactions.

5. When the surface charge density is moderate, as for smectite and vermiculite, the silicate layers may readily adsorb polar water and bonding cations may hydrate, resulting in the separation of the layers and expansion. The strength of the inter-layer bond is low and a sensitive function of charge distribution, hydration energy of the cation, cation shape, surface ion configuration and the structure of the polar molecule.

The type of bond present between mineral particles will depend on the mode of particle association. It is assumed that three different modes exist: face to face (FF), edge to face (EF) and edge to edge (EE). In addition the sheet layers may become broken; the charged surface exposed may not be parallel to the unit layers or be completely compensated by the adsorption of cations and water. These surfaces are called broken-bond or edge surfaces and may occupy an appreciable proportion of the total bonds between colloidal particles (Yariv and Cross, 1979). Attention is also drawn to the role of amorphous materials such as iron oxide in the bonding of soil particles (Taylor, 1959; Torrance, 1983; Deshpande *et al*, 1964 and Yong and Sethi, 1977).

The destruction of bonds and associated activation energies during weathering (section 2.31), soil deformation and creep processes has been considered by Andersland and Douglas (1970), Culling (1983), Mitchell (1964), El-Hiti (1985), Piper (1987) and Mitchell *et al* (1969). Andersland and Douglas (1970) found that the free energy of activation of the bonding mechanism was due to ionic bonds at the points of direct mineral to mineral contact and that these were dependent on temperature. Piper (1987) demonstrated that the shear moduli of $<2\mu\text{m}$ clays was best described by the forces of interaction between particles and found the shear modulus increased in order of $\text{Ca}^{2+} \approx \text{Mg}^{2+} < \text{K}^+ < \text{Na}^+$ ionic forms. Mitchell (1976) provides values of activation energy for a wide range of

materials and supported the concept that soil deformation was a thermally-activated process. It was also found that the activation energy and creep-rate are stress dependent. Culling (1983) has noted the application of rate process theory to physical processes involving the re-arrangement of particulate matter. The progressive breaking of bonds and the lowering of the activation energy will be fundamental in explanations of the physico-chemical deformation of clay soils.

The electrical energy of the various bonding mechanisms and particle associations is described by the concept of diffuse double layers (Van Olphen, 1977, 1986). The net negative layer charge is compensated by the accumulation of counter-ions on the mineral surfaces. Double layers consist of ions more or less attached to the solid surface (the fixed or Stern layer) and an ionic layer in which the ions are free to move (the Gouy layer). At the same time, however, the ions in the Gouy layer have a tendency to diffuse away from the mineral surface to the pore water, their concentration decreasing exponentially from the Stern layer. Ions in the fixed layer are held by electrostatic forces or by the formation of complexes on the surface of the clay minerals.

The effective thickness of the double layer is sensitive to variations in surface charge density or surface potential, electrolyte concentration, cation valence, temperature and the dielectric constant of the medium (Mitchell, 1976). When two particles interact, the Gouy layers effectively repel one another separating the particles, and a stable suspension results. As concentration increases, the Gouy layer becomes compressed close to the mineral surface. When this happens the electrostatic repulsion separating the particles is insufficient to counteract the Van der Waals' force which attracts the minerals together,

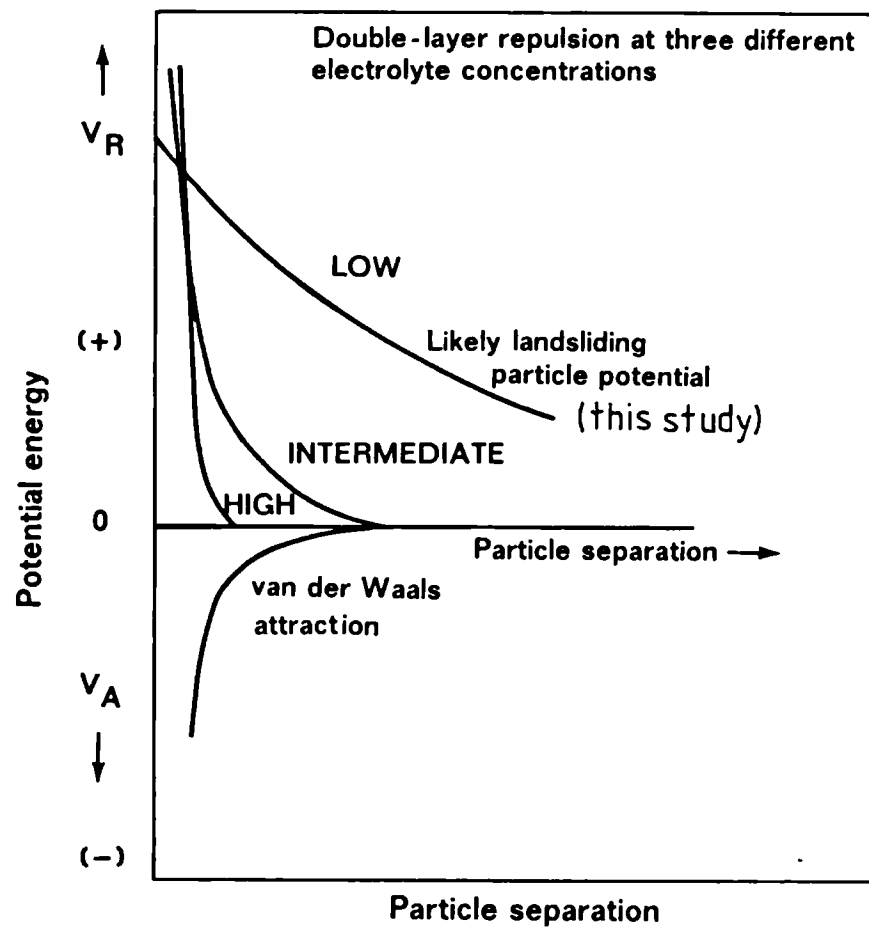
and the suspension is no longer stable (Drever, 1982). This explains why clay minerals form stable suspensions in fresh water but flocculate in more saline solutions such as sea-water. At equilibrium double layer repulsion is balanced by attractive forces which must be comparable in range and magnitude. Generally, the thicker the double layer the less the tendency for the particles to flocculate and the greater the repulsive potential, dispersion and swelling pressure in cohesive soils (Van Olphen, 1977).

Double layer repulsions and Van der Waals' electromagnetic attractions interact in the manner shown in Figure 2.3. At high electrolyte concentrations, the potential curve shows a deep minimum at close separation, where attraction predominates except at very close range. If repulsion dominates (at medium and low salt concentrations), the diffusion will be counteracted by repulsive forces (Lerman, 1981). Initially flocculation is retarded, but at low electrolyte concentrations the coagulation process is retarded to such an extent by long-range repulsion that it may take weeks or months for flocculation to re-establish (Van Olphen, 1977). Low pore water salt concentrations will enhance dispersion and any change in system chemistry may have important consequences when soil is disturbed or subjected to changes in environmental conditions.

With reference to Table 2.3, it may be seen that the valence or type of cation and the concentration of the solution is extremely important in determining double layer thickness. White (1979) concludes:

"In short, as the valency of the cation increases and the solution concentration increases, the diffuse layer is compressed"...and the bonding force of attraction is enhanced.

Figure 2.3. Double layer repulsive and attractive energy in relation to particle separation and electrolyte concentration.



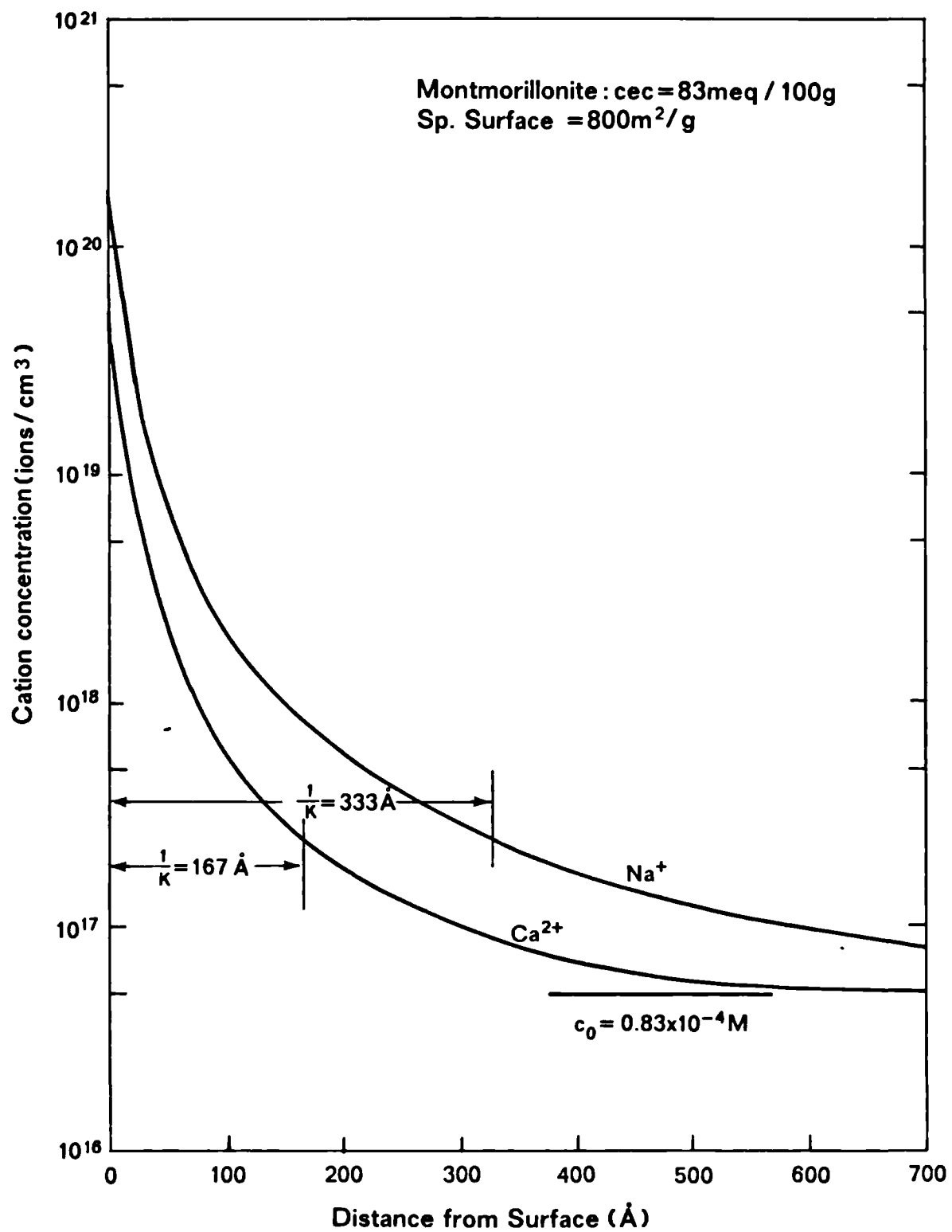
Source: Van Olphen (1977).

Table 2.3. Calculated diffuse double layer thickness in relation to electrolyte concentration.

Electrolyte concentration (me cm ⁻³)*	Double layer thickness, <i>d</i> (nm)	
	NaCl	CaCl ₂
0.1	1.94	1.0
0.01	6.20	3.2
0.001	19.40	10.1

* A solution containing 1 me (milliequivalent) of salt per cm³ is defined as a normal (N) solution.

Figure 2.4. Effect of cation valence on double layer interactions.



Source: Mitchell (1976).

The double layer is particularly sensitive to changes in concentration: an increase in concentration of 10^2 Meq/cm³ can cause a ten-fold reduction in layer thickness (Table 2.3) and as Figure 2.3 shows, not only is the diffuse layer reduced for the condition of constant charge, but also the decay with distance is much more rapid.

For solutions of the same concentration and surface charge, a change in cation valence affects both the surface potential and the thickness of the double layer (Mitchell, 1976). The layer distributions of sodium and calcium are shown in Figure 2.4, and it follows that an increase in valence suppresses the concentration of ions between the minerals and interacting layers. It is known that relatively small additions of di- or trivalent cations added to clay-water-monovalent electrolyte systems can have significant influences on the mechanical properties of soils (Rosenqvist, 1984; Bolt, 1979; Grim, 1959; Blackmore and Miller, 1961; Sridharan and Jayadeva, 1982).

2.232 Water chemistry and exchange reactions.

In order to understand the character of the inherent properties and the physical behaviour of soils, it is necessary to establish the nature of clay-water systems (Kazda, 1979). The association between clay minerals and soil water gives rise to a wide variety of soil behaviour, plasticity, shear strength and soil deformation. Generally, the strength of water adsorption decreases away from the surface of the particles, while in a parallel direction it is practically identical.

The unusual shape of clay minerals and the dual character of their surfaces strongly influence the inter-particle forces on contact with water in creating large swelling pressures and in building colloidal structures (Van Olphen, 1977 and Fripiat *et al*, 1984). Two ranges of interaction are distinguished:

1. The hydration of dry clay mineral surfaces;
2. Double layer repulsion.

In the first stage water is adsorbed in successive monolayers on the surface and pushes the particles or layers of the 2:1 clays apart. Inter-layer cation exchange may occur with swelling after a threshold pressure or activity is reached (Barrer, 1984). The principal force is the adsorption energy or affinity for water of the clay mineral surface. The water molecules are highly oriented in the first adsorbed layer, the structure becoming less orderly and more like that of free pore water as the layers multiply.

At the charged planar surfaces of the 2:1 type clay minerals the water is strongly attracted to the exchangeable cations and only weakly bonded, if at all, to the oxygen surfaces. The electric field of the cation orientates the polar water molecules around the ion to form a hydration shell (Havlicek and Kazda, 1961). The energy of hydration per mole of cation depends upon its radius and charge and for the common cations this decreases in order of:



The greater the hydration energy of the cation, the larger is the reduction in free energy of the water molecules in its hydration shell.

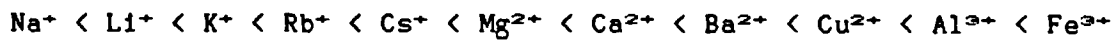
Thus, the small amount of water present in a dry soil is mainly associated with exchangeable cations.

The second stage of swelling is due to double layer repulsion whereby the particles and layers may be pushed further apart. This is often referred as osmotic swelling which depends on such factors as particle orientation and interaction and can involve large volume changes (Van Olphen, 1986). Measured swelling pressures, as a function of water content (or plate distance), are the magnitude of calculated double layer repulsion and therefore dominate the swelling process. In practical situations, the force of repulsion amounts to several atmospheres (Van Olphen, 1977).

It has been noted (p87) that the type and amount of cations in clay-water-electrolyte systems can have a major influence on double layer interactions (Ma, 1985; Alther, 1986; Sposito, 1986; Ogwada and Sparks, 1986). The thermodynamics of ion-exchange is discussed by Townsend (1984) and Bolt (1979). Clays naturally adsorb cations with a fixed total charge. Exchange reactions involve the replacement of such ions with other ions having the same total charge (Helfferich, 1962; Anderson and Rubin, 1981), although the exchange process does not affect the structure of clay minerals themselves. The most common cations found in soils are Ca^{2+} , Mg^{2+} , Na^+ , and K^+ usually in decreasing order of abundance. The most common anions are SO_4^{2-} , Cl^- , PO_4^- , and NO_3^- .

Ions of one type can be replaced by ions of another, thus Ca^{2+} for Na^+ , Na^+ for Ca^{2+} , Fe^{3+} for Mg^{2+} and so on. The ease with which an ion of one species can replace another depends mainly on the valence, the relative abundance of the various ions, the ion size, and charge density (Brady, 1984; Shainberg, 1987). The ratio of the valence to ionic

radius is referred to as the ionic potential (Webb *et al*, 1986) which is directly related to the energy of hydration of the ion-exchanged minerals. The specific adsorption of various cations to montmorillonite clays was reported by Nir *et al* (1986) who confirmed the importance of these factors during ion exchange. Generally, trivalent cations are held tighter than divalent and similarly divalent tighter than monovalent. However small cations displace larger cations increasing in order of size:



However, it is possible to displace a cation of higher replacing power for one of lower by mass action, such as Al^{3+} for Na^+ , where the concentration of Na^+ is very much greater than Al^{3+} .

The rate of ion exchange will vary with clay mineral type, the availability of ions, pore water concentration, pH and temperature. The mobility of cations in soils has been studied by Siyag (1984) and Kerpen and Scharpenseel (1967) where it was found that an increase in activity results in faster reaction rates. Cations located in the Gouy layer exchange rapidly relative to the Stern layer, which might exchange rapidly or slowly depending on the strength of bonding to the mineral surface (Drever, 1982). Typically, it is found that reactions in the kaolin minerals are almost instantaneous, whereas in illite the speed of reaction may take a few hours, because a small part of the exchange capacity is located between the unit layers. The rate of reaction in the smectites is slower still because much of the exchange takes place in the inter-layer region (White 1979).

A number of theories of ion exchange have been proposed to account for concentrations of different cations in the adsorbed double layer relative to the bulk solution. For instance the Gapon equation enables an assessment of the proportion of monovalent to divalent cations (White, 1979). For example, if the proportions of Na^+ and Ca^{2+} in the adsorbed complex are equal and the concentration of Na^+ in the pore water is doubled, then the concentration of Ca^{2+} in the pore water must be quadrupled if the proportions are to remain the same. The resultant equation has proved widely applicable to cation exchange in soils:

$$\frac{\text{Na}^+ \text{ exchanger}}{\text{Ca}^{2+} + \text{Mg}^{2+} \text{ exchanger}} = \frac{K * \text{Na}^+}{(\text{Ca}^{2+} + \text{Mg}^{2+})^{1/2}}$$

The concentrations of ions are in milliequivalents per litre. The term:

$$\frac{\text{Na}^+}{(\text{Ca}^{2+} + \text{Mg}^{2+})^{1/2}} = \text{S.A.R. (Meq l}^{-1}\text{)}$$

is called the sodium adsorption ratio (SAR), which can be determined by chemical analyses of pore water or from saturation extracts. The Gapon constant (K) has a value of 0.017 for most soils (Mitchell, 1976). Thus the relative abundance of monovalent and divalent ions in the adsorbed cation complex may be easily calculated.

Of further importance to the structural status of the soil, is the proportion of sodium in the adsorbed layer. This is often described as the exchangeable sodium percentage (ESP):

$$\text{ESP} = \frac{\text{Na}^+ * 100\%}{\text{CEC}}$$

A number of studies have shown that the ESP and SAR provide a good indication of the stability of clay structures to breakdown and particle dispersion. Soils with ESP values greater than 3 per cent are susceptible to spontaneous dispersion on reaction with water (Lerman, 1981; Emerson and Bakker, 1973; Emerson and Chi, 1977). Soils with high pore water salt contents up to and exceeding 100 Meq l^{-1} are likely to be dispersive.

Analyses of the physico-chemical properties of clays provides insight into the long-range repulsive and attractive forces of particle interaction, and the influence of system variables such as pore water chemistry, the type of adsorbed cations and the type of clay minerals. The importance of pore water chemistry and exchange reactions upon the mechanical properties of soil have been noted by Rosenqvist (1984), Keil and Striegler (1961), Moum and Rosenqvist (1961), Taylor (1959) and Brooks et al (1956). Double layer theory and colloid geochemistry explain the dynamics and development of soil fabric, structure and plasticity, which in turn exert a major influence on the mechanical properties. Changes in shear strength and compressibility are found to occur with replacement of one type of cation for another.

Moum and Rosenqvist (1961) concluded:

"The shear strength in an undisturbed clay is a function of the Van der Waals' forces between the adsorbed cations of one mineral and the ions of the adjacent minerals. By substitution of the sodium ion with potassium, the attractive forces and bonds of the flocculated system are increased. This increase seems to be the same for illitic and montmorillonitic clays. By remoulding, where the short distance contacts are broken by the mechanical treatment, the residual shear strength is no longer a function of the stress history of the sediment, but depends mainly upon the mineralogical and chemical composition as well as the volume ratio between the mineral phase and liquid phase."

Chemical methods of soil stabilisation have utilised such properties (Moore, 1985), and Sherwood (1961) provides a review of the earlier developments in this field. More recent work by Handy and Williams (1966), Ingles (1968, 1970), Mearns (1973), Broms and Boman (1977), Broms (1984, 1985), and Larsson and Jansson (1982), have shown that chemical treatments of slopes may be successfully used to improve soil stability. Most techniques report an increase in amorphous cements as responsible for strength improvement, although little is known about the natural and artificial ion exchange reactions. Chemical stabilisation techniques have not been used in UK engineering practice.

In his conclusion, Taylor (1959) suggested that the diffuse double layer theory provides a satisfactory basis for the study of many types of clay soils and may be used to derive useful information about probable mechanical behaviour from the results of chemical tests. Modern research continues to support this contention.

2.24 Plasticity, cohesion and the phase relationships.

The plasticity, cohesion, dispersion, flocculation, swelling and shrinkage properties of colloidal clays assume considerable importance on the mechanical behaviour of soils. All are mineral-surface phenomena and their intensity depends upon the amount and nature of clay interfaces.

Plasticity is exhibited by soils containing an excess of 15 per cent clay, and is due primarily to the platy nature of clay particles and the binding influence of adsorbed water (Brady, 1984). Plastic behaviour

occurs when particles slide over one another across thin films of water and by definition is only exhibited when soils are wet. The influence of clay mineralogy and chemistry upon plasticity is further detailed below.

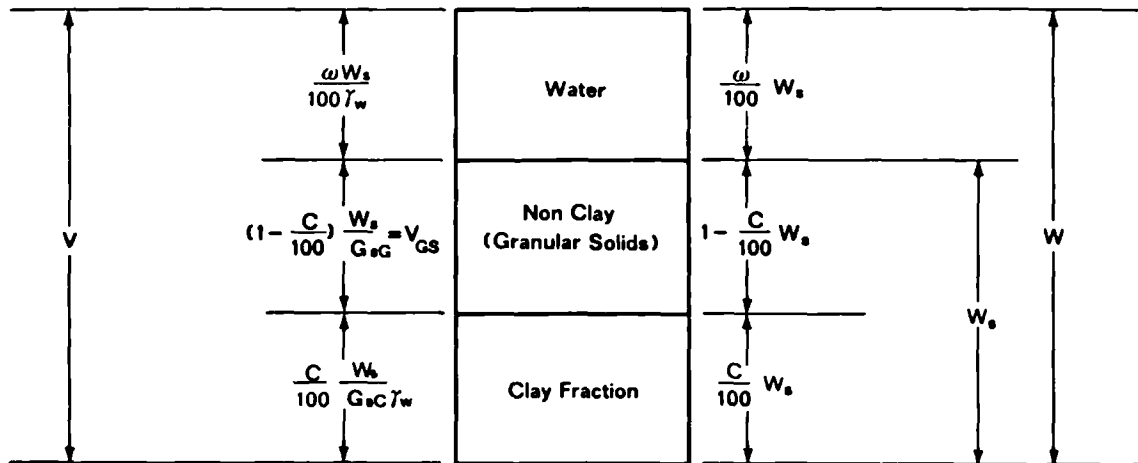
Cohesion is somewhat related to plasticity. Hydrogen bonding between clay and water and among water molecules is the attractive force responsible for cohesion. As the water content of a saturated clay is reduced, there is an increase in the force of attraction between clay minerals for each other. This tendency for particles to bind together is due to the attraction of the particles to the remaining water molecules held between them. Generally, the cohesion and plasticity of the clay minerals decreases in order of attapulgite, montmorillonite, halloysite- $4H_2O$, illite, halloysite- $2H_2O$ and kaolinite (Grim, 1968). Iron-rich clays such as nontronite tend to have lower values than the aluminous varieties.

If clay has expanding minerals and very small grain-sizes extreme swelling may occur upon wetting, and following prolonged dry spells soils may become highly fissured, cracked and broken through shrinkage, allowing the rapid penetration of rain and surface water. Swelling is induced by water movement between crystal layers and inter-crystalline expansion. Most swelling is accounted for by water attracted to ions adsorbed to clay mineral surfaces (White, 1979). Swelling, shrinkage, cohesion and plasticity are closely related; they are dependent not only on the clay mixture and the dominant adsorbed cation, but also on the amount and nature of humus associated with organic colloids.

Dispersion is a typical condition of a dilute colloidal suspension in water: minerals tend to repel each other permitting each particle to act independently. Such behaviour is encouraged by small particle sizes, negative charges, and hydration enhanced by hydrated cations around each mineral. Thus, dispersion is greatest in alkaline solutions where the electro-negativity is maximum, and by hydrated monovalent ions (Na^+) loosely bonded to mineral surfaces. Dispersion-flocculation processes are dynamic such that changes in particle interactions occur through exchange processes and changes in the valency and concentration of cations. Alterations in the mechanism and strength of bonding determines the status of dispersion or flocculation processes.

The interaction between soil particles, air and water is conveniently described by the phase relationships. Soils can be of either two phase in composition, as in situations of dryness or saturation, or three phase in composition during conditions of partial saturation. The components of a soil may be represented by a phase diagram shown in Figure 2.5. The formulation and measurement of the phase parameters are detailed in BS 1377 (1975) and many soil mechanics texts (Lambe and Whitman, 1969; Vickers, 1983; Sutton, 1984; Das, 1985 and Craig, 1979). The porosity, voids ratio, degree of saturation, water content, bulk density and unit weight are considered the most important factors in quantitative soil description for geotechnical purposes and shall thus be adopted in this study. They may easily be calculated from a knowledge of the specific gravity of the soil particles and the natural and saturated water contents.

Figure 2.5. The phase relationships.



C : % Clay by weight
 G_{sc} : Specific gravity of clay particles
 G_{sg} : Specific gravity of granular particles
 W : % Water content

γ_w : Unit weight of water
 W_{sc} : Saturated moisture content
 V_{GS} : Volume of voids in granular phase

The theory of elasticity and plasticity applied to soils is described by Atkinson (1973) and it is accepted that plasticity is one of the most fundamental properties in soil mechanics. The range of moisture contents in which plastic behaviour is evident is determined by two consistence limits:

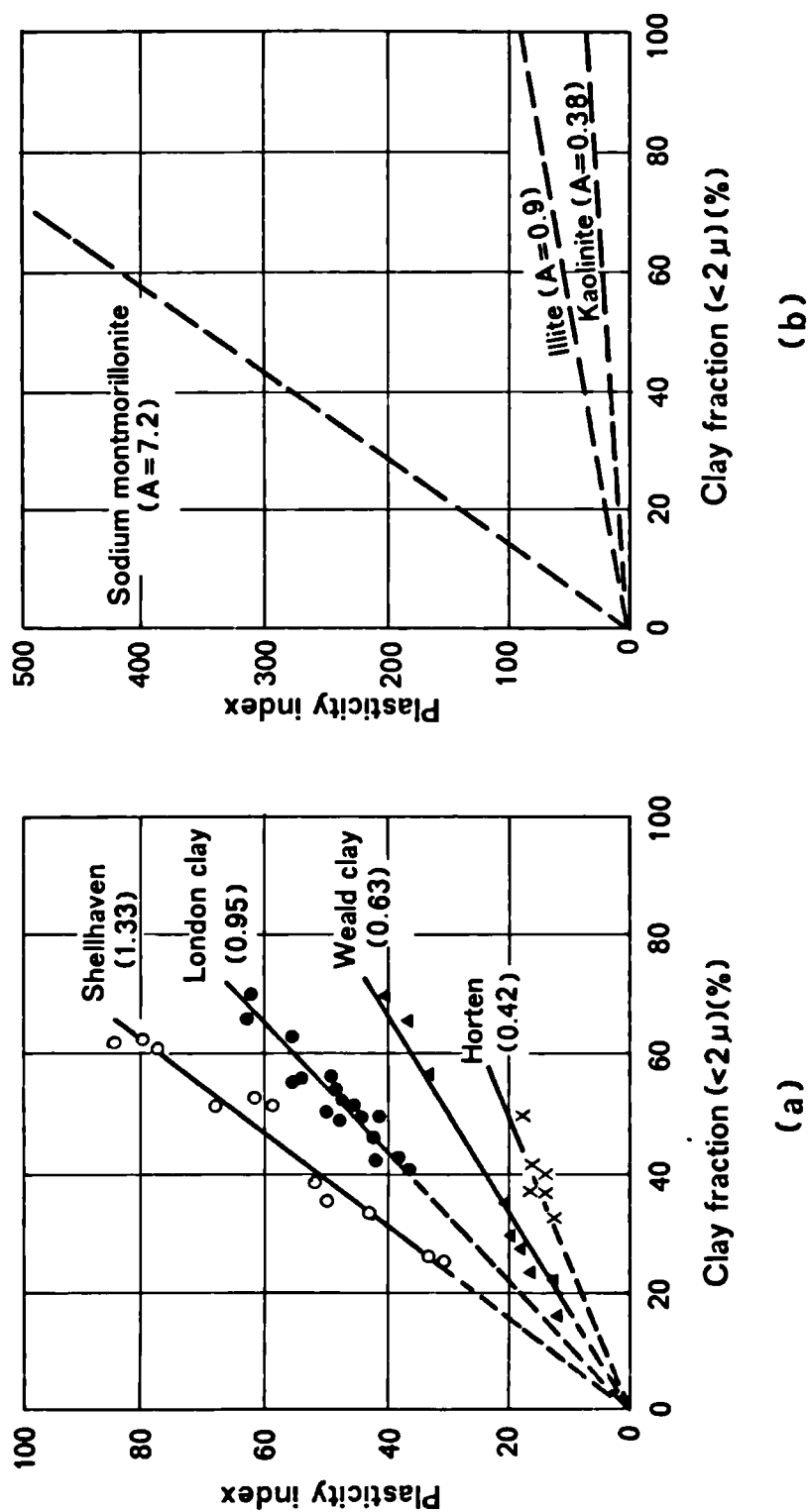
1. The plastic limit (PL) is the moisture content below which the soil can no longer be moulded;
2. The liquid limit (LL) is the moisture content at which the soil tends to flow like a liquid.

The range of moisture contents over which a soil exhibits plasticity is defined as the plasticity index (I_p) and may be calculated by subtracting the plastic limit from the liquid limit. Skempton (1950; 1953) showed that the plasticity index was related to the amount of clay size particles and to the type of clay mineral (Figure 2.6). Dumbleton (1966) has also shown that plasticity is dependent on the type of clay minerals. The former association led to the definition of the activity ratio (A):

$$A = \frac{I_p}{\% < 2 \mu m}$$

The values of activity are quite constant for particular soil units and they provide some indication of the identity of the predominant clay mineral. The gradient of the line is a measure of the activity of surface forces on the clay particles (Kenney, 1984). Work by Seed *et al* (1964) has shown that the activity may not always be linear, but can be approximated by two straight lines; one for clay contents above 40 per cent where the line passes through the origin and another for clay contents between 10 and 40 per cent where the line intersects the clay content axis at 10 per cent.

Figure 2.6. Relation between the plasticity index and clay fraction.



Source: Skempton (1953).

White (1955) presented data on the relationship between cation type and the plasticity characteristics of the common clay minerals (Table 2.4). In the 1:1 layered clays the nature of the exchangeable cation was found to cause relatively little change to the plastic limit; this would be expected because of their low cation exchange capacity. In the 2:1 clay minerals, exchangeable Na^+ and Li^+ cations were found to support higher plastic limits. The presence of Al^{3+} and Fe^{3+} exchangeable cations produced lower plastic limits. In natural materials variations in the plastic limits are probably affected by the presence of non-clay minerals rather than any differences in the exchangeable cation composition. An important exception to this is Na^+ which causes a slight decrease in the plastic limits of the 1:1 clay minerals whereas it substantially increases the plasticity of montmorillonite 2:1 layered minerals.

Table 2.4. Relationship between the Atterberg limits, clay mineralogy and chemistry.

Clay	Ca ⁺⁺			Mg ⁺⁺			K ⁺			NH ₄ ⁺			Na ⁺			Li ⁺		
	Pw	Lw	Ac	Pw	Lw	Ac	Pw	Lw	Ac	Pw	Lw	Ac	Pw	Lw	Ac	Pw	Lw	Ac
Montmorillonite																		
Pontotoc Miss.	65	166	1.26	59	158	1.24	57	161	1.30	75	214	1.74	93	344	3.14	80	638	6.98
Cheto Ariz.	65	155	1.20	51	199	0.97	57	125	0.91	75	114	0.52	89	443	4.72	59	565	6.75
Belle Fourche S. Dakota	63	177	1.34	53	162	1.24	60	297	2.79	60	323	3.09	97	700	7.09	60	600	6.35
Oksted Ill.	79	123	0.44	73	138	0.65	76	108	0.32	74	140	0.66	86	280	1.12	82	292	2.10
Attapulgitte																		
Quincy Fla.	124	232	1.08	109	179	0.70	104	161	0.57	97	158	0.61	100	212	1.12	103	226	1.23
Illite																		
Fithian Ill.	40	90	0.50	39	83	0.44	43	81	0.38	42	82	0.40	34	61	0.27	41	68	0.27
Jackson County Ohio	36	69	0.33	35	71	0.36	40	72	0.32	37	60	0.23	34	59	0.25	38	63	0.25
Grundy County Ill.	42	100	0.58	43	98	0.55	41	72	0.31	39	76	0.37	41	75	0.34	40	89	0.49
Kaolinite																		
Anna Ill.	36	73	0.37	30	60	0.30	38	69	0.31	34	75	0.41	26	52	0.26	33	67	0.34
Dry Branch Ga.	26	34	0.08	28	39	0.11	28	35	0.07	28	35	0.07	28	29	0.01	28	37	0.09
Halloysite(2H ₂ O)																		
Eureka Utah	38	54	0.16	47	54	0.07	35	39	0.04	32	43	0.11	29	36	0.07	37	49	0.12
Halloysite(4H ₂ O)																		
Bedford Ind.	58	65	0.07	60	65	0.05	55	57	0.02	56	61	0.05	54	56	0.02	47	49	0.02

Ac: Activity values of montmorillonites 1,2,3 are greater than (Lw-Pw)/100 because they contain nonclay minerals

Montmorillonites contains about 25% Illite in mixed layers

Illite contains about 5% montmorillonite in mixed layers

Source: White (1955).

2.3 The mechanical properties:

2.31 Weathering:

The frequency distribution or relative abundance of clay soils varies in accordance with the five principal factors governing soil formation (after Dokuchaev c1870). The minerals of soil '*parent material*' undergo alteration over varying lengths of '*time*' in response to '*climate*', '*relief*' and '*biotic*' factors. Transformations occur in particle energy states in conjunction with exposure to the atmosphere, water and the various chemical and biological agents. These result in processes of weathering in which rock and clay materials are disrupted to form new compositions, often with very different properties. The new state is usually more stable than the old and involves a decrease in the internal energy of the materials. The change is largely irreversible.

The study of weathering has become somewhat isolated as a separate discipline within the geomorphic literature. Brunsden (1979b), Chorley *et al* (1984), Selby (1982), Cooke and Doornkamp (1978), Loughnan (1969), Ollier (1969) and Statham (1979), describe weathering in terms of several causative factors, and as Chorley *et al* (1984) state, the study has been isolated because of the apparent dominance of chemistry over physics and the subordination of gravitational forces to inter-molecular ones. Thus geochemists (Krauskopf, 1967; Bear, 1964; Drever, 1985; Holdren and Berner, 1979) have contributed widely to the study of weathering.

Typically weathering is considered systematically as a series of separate processes (most commonly physical, chemical and biological) although in reality rock disintegration is effected by a complex interplay of these

factors. Physical processes mostly reduce particle size, increase surface area and bulk volume, and decrease particle density. Chemical and biological processes may cause complete changes in both the physical and chemical properties and result in the formation of new minerals. Chorley *et al* (1984) provide a comprehensive account of such processes, but it is felt necessary for the purposes of this study to isolate predominant weathering reactions of clay minerals and to describe the likely effects of the intrusion of sea-salts on exchange processes, mineral stability and weathering behaviour in coastal environments.

2.311 Weathering of clay minerals.

Parent materials contain the initial suite of minerals present in soil. These minerals in turn influence soil mineralogy by their relative susceptibility to weathering, and as a consequence, the physico-chemical nature of the '*inherent*' properties of clay soils will be affected by weathering processes. The susceptibility of minerals to chemical weathering may be estimated by the bond strengths between oxygen and associated cations in the sheet structures (Chorley *et al*, 1984):

K⁺299; Na⁺322; H⁺515; Ca²⁺839; Mg²⁺912; Fe²⁺919; Al³⁺1793; Si⁴⁺3110-3142.

These values (Kcal/mol) only provide a guide to the likely strength of cation linkages within the mineral structures described in section 2.22. Generally, silicon-oxygen bonds are the most resistant to weathering.

Physical processes of weathering influence clays by the disruption of minerals through thermal, biological and geological stresses. Internal stresses exist in all rocks which have been subjected to high

temperature, tectonic and overburden pressures during their formation. Weathering causes stress relief and enhances the development of fissures and joints. For instance Callabresci and Scarpelli (1985) have noted the swelling tendency of recently unloaded over-consolidated clays. The development of such discontinuities to a large extent determines the rapidity of breakdown by allowing the ingress of water and associated weathering processes into the rock mass. The effects of physical and chemical weathering are complementary, but physical processes are usually more rapid controlling the rate of chemical activity and decomposition.

Hydrofracturing and frost action are two of the most widely recognised processes of physical weathering, and these will be significant where water is closely bound to clay surfaces. The formation of ice crystals causes an increase in specific volume of 9.08 per cent and the direct heaving of pebbles, soil aggregates and particles (Selby, 1982). Such movements will involve inter-particle fracturing and bond breaking and may indirectly cause fissures along rock pores. However, by far the most important process of clay weathering involves the hydration and hydrolysis of minerals and associated chemical reactions.

In clay dominated soils of temperate environments the presence of soil moisture is the single most important factor in weathering processes. Mineral hydration and internal swelling of the crystal lattice is responsible for much surface disintegration of shales, mudrocks and over-consolidated clays, particularly with respect to the 2:1 layered minerals. Soil water holds in solution free-oxygen, carbon dioxide, various hydrated salts, and organic and nitric acids close to mineral surfaces, which are important agents in promoting physico-chemical reactions and weathering behaviour. The inclusion of water and the

hydration of clay minerals is also an important prerequisite for subsequent weathering by oxidation when elements loose electrons to oxygen ions in solution. The process is governed by the redox potential (Eh which is inversely related to pH), the amount of organic matter and the accessibility of oxygen. The process is particularly relevant where over-consolidated clays become normally-consolidated and saturated, and wherever a high degree of mottling is observed.

The weathering of alumino-silicates is primarily a process of hydrolysis (Krauskopf, 1967). Dissociated H^+ ions in soil water readily penetrate mineral lattices displacing inter-sheet cations which then combine with OH^- ions in solution. The reaction is enhanced by the tendency for H^+ to unite with silicate groups to form weak silicic acid. The reaction is relatively slow and complicated in which the overall effect is the removal of inter-particle and inter-layer K^+ , Na^+ , Ca^{2+} and Mg^{2+} cations and some Si^{4+} in solution, while aluminium and the remaining silica precipitate as clay minerals or products of weathering.

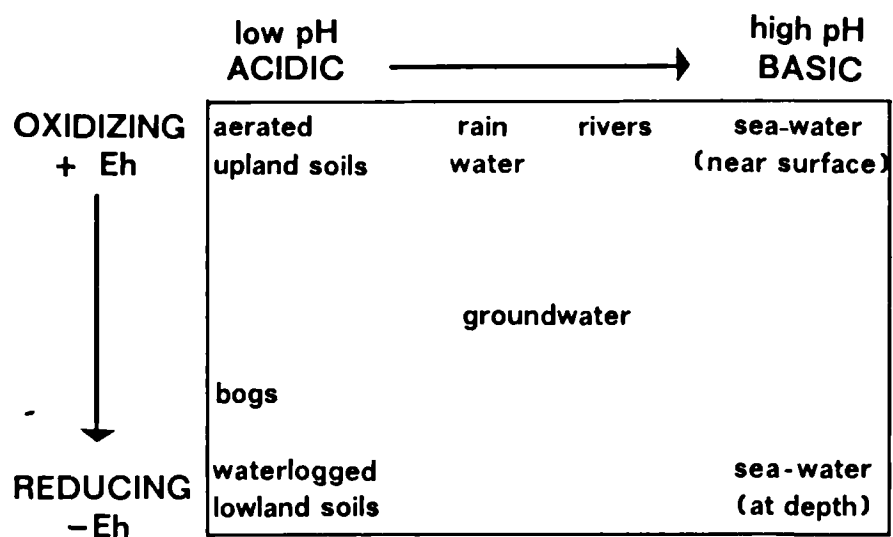
The nature of the clay minerals following alteration or formation depends on the conditions of weathering, such as pH, the composition of rain and soil water, the presence of organic acids and the nature of the exchange reactions. Kaolinite favours acidic solutions and good drainage, montmorillonite by alkaline solutions containing Ca^{2+} , Mg^{2+} and Fe^{2+} , and illite by abundant K^+ (White, 1979). Although inter-lamellar K^+ in illite is non-exchangeable, it is found that upon weathering and depletion of K^+ in solution the clay crystals slowly exfoliate from the edges, exposing the inter-sheet cations to exchange with others in solution.

As base cations are removed from soil by leaching, the clay minerals and organic matter gradually become saturated with H^+ ions. However, H-clays are unstable and slowly disintegrate from the crystal edges inwards to release Al^{3+} and SiO_2 , the silica going into solution as $Si(OH)_4$ while the aluminium is adsorbed by both clay minerals and humified organic matter. The hydrolysis of Al^{3+} produces more H^+ ions, the neutralization of which is achieved by further lattice decomposition so that the resultant pH is higher than that of pure H-clay or organic acid. Ultimately, clay minerals are completely destroyed to yield gibbsite and the basic sheet structures (section 2.22) leaving hydrated oxides of iron and aluminium as the principal inorganic residues. Natural pH is thus dependent upon reactions with minerals, rate of leaching of cations, and the nature and exchange capacity of the residual mineral products.

Chemical weathering is clearly very complex and depends on the reagents present and temperature. In practice, however, the chemical environment may be described by the acidity (pH) and the redox potential (Eh), represented in Figure 2.7. These parameters are important since all weathering reactions involve the loss or gain of H^+ or OH^- ions, the loss or gain of electrons from ions, or both. Thus, changes in these factors influences almost all reactions, particularly at clay mineral surfaces, and will indicate particular chemical environments. .

The influence of the amount, circulation and periodicity of water flow on the rate and products of weathering has been stressed by Trudgill (1976). Weathering rates depend on the solubility of ions at mineral interfaces and the rate of waterflow. Reactions will be proportional to the flow of water because increased turbulence aids the diffusion of dissolved ions away from mineral surfaces (Statham, 1979). Indeed the removal of

Figure 2.7. Typical chemical weathering environments.



Source: Statham (1979) p.30.

weathered products assists in the continuation of weathering processes (Trudgill, 1986).

Changes in the mechanical properties, shear strength, volume and permeability, are associated with the weathering behaviour of clay slopes, although it must be remembered that there is a large degree of inter-dependence between these properties (Kowalski, 1970). Inferences concerning these properties can be based on a knowledge of the stress history because of the strong dependence of deformation and strength on both past and present states of stress (Mitchell, 1976; Russell and Parker 1979). Anisotropic consolidation of clay occurs with the rotation of platy clay minerals and often forms cleavage planes and fissures. Diagenesis bonds the particles together, often with amorphous cements, in the form of strong ionic bonds and the weaker Van der Waals' forces acting at very close mineral separations. The action of weathering reverses these processes by altering the anisotropic structure and by breaking and weakening inter-particle bonds. Changes in chemical environment will cause changes in the inter-particle forces of attraction in fine-grained soils, although the degree of homogeneity and anisotropy are related to its formational mode and subsequent history.

The long-term effects of weathering were recognised by Skempton (1948) when a series of first-time slips in artificial cuttings of over-consolidated London Clay implied that slope stability was time-dependent. It was noted that shallow-angled slopes could fail up to one hundred years after excavation. The strength at failure in all cases was much less than expected. Progressive weathering, strain softening and creep processes were all considered to be responsible for the failure of the slope.

The publication was followed by many studies reporting similar responses on natural and artificial slopes (Skempton, 1953, 1957, 1964, 1970; Henkel and Skempton, 1955; Skempton and Delory, 1957; Skempton and Hutchinson, 1969; Skempton and Weeks, 1976; Skempton and Chandler, 1974; Chandler, 1969, 1972b; Bjerrum, 1967; Weeks, 1969; Spears and Taylor, 1972) and generated a whole body of geomorphological literature on threshold slopes (Young, 1961; Carson, 1969, 1971, 1975; Carson and Petley, 1970; Carson and Kirkby, 1972; Rouse, 1975; Rouse and Farhan, 1976; Kirkby, 1987; Hutchinson, 1967; Chandler, 1982; Hutchinson and Gostelow, 1976). Francis (1987) provides a good review of the threshold slope concept, and rather than include an extensive review of this literature the reader is also referred to Taylor and Cripps (1987) for a comprehensive account of the weathering effects on UK mudrocks and over-consolidated clays. However, aspects of the weathering of clays will be discussed with respect to the *mechanical* properties in section 2.32-2.34.

2.312 Reaction of sea-water with clay minerals:

Salts in coastal environments are known to promote weathering processes. However, previous work (Goudie *et al*, 1970; Goudie, 1974; Cooke, 1979; Williams and Robinson, 1981; Mottershead, 1982; Trenhaile and Mercan, 1984; McGreevy and Whalley, 1984) has tended to concentrate on the breakdown of hard rocks, particularly sandstones. In comparison, there are few published geomorphological studies on the effects of sea-salt on the weathering of clays. Within the geochemical literature, however, much attention has been given to the chemistry of sea-water and associated sediments (Riley and Chester, 1971; Drever, 1977; Broecker, 1974; Holland, 1978; Drever, 1982). The specific effects of reacting sea

water with different clay minerals was reported by Carroll and Starkey (1960), Roberson (1974), Manglesdorf and Sayles (1975) and Sayles and Manglesdorf (1977).

Each study shows considerable alterations to exchange equilibria following the addition of sea-salts to clay minerals. In fresh (dilute) terrestrial waters, the dominant exchangeable cation is Ca^{2+} , whereas in the ocean (concentrated) the dominant cation is Na^+ (Sayles and Manglesdorf, 1979). When clays encounter sea water calcium ions are replaced by sodium, potassium and magnesium (Table 2.5). The net ion-exchange effect is the adsorption of monovalent sodium ions from sea water in place of divalent calcium.

The monovalent-divalent effect is important in nature because the weathering of clays (dilute) in coastal environments may be viewed as a change from a divalent to a monovalent form with consequent dispersion amongst the particles (section 2.232). When completely submerged in sea water flocculation occurs due to the much greater concentration of salts. Moreover, Sayles and Manglesdorf (1977) found that the common analytical procedure of washing sediments with distilled water causes the removal of monovalent cations from clay minerals. This increases their stability and suggests that laboratory tests should receive careful thought if realistic estimations of the behaviour of clay-soils are to be obtained.

Table 2.5. Exchange of cations on reaction of clays with sea water.

MINERAL	ΔX.CATION*				
	Na ⁺	K ⁺	Mg ²⁺	Ca ²⁺	H ⁺
Arizona Montmorillonite	+0.22	+0.03	+0.13	-0.37	-0.02
Dakota Montmorillonite	+0.47	+0.02	-0.03	-0.44	-0.02
Texas Montmorillonite	+0.52	+0.02	-0.01	-0.52	-0.02
Wyoming Montmorillonite	+0.50	+0.04	+0.12	-0.61	-0.05
Bath Kaolinite	+0.32	+0.05	+0.14	-0.27	-0.25

* Data presented as change in equivalent cation fraction.

Sign convention: + = cation gain by mineral

- = loss of cation from mineral.

Source: Sayles and Manglesdorf (1977) p.958.

2.32 Shear strength.

The compressibility and strength of soil depends on the force required to distort or displace particles or groups of particles relative to one another. In clays the resistance to deformation is provided by the chemical and physical forces of interaction in addition to the gravitational force associated with the weight of the soil mass. Relationships have been derived to describe the strength and stress-deformation properties of soils: the Mohr-Coulomb equation is the most widely used:

1. $\tau = c + \sigma \tan \emptyset$ and in terms of effective stresses;

2. $\tau' = c' + \sigma' \tan \emptyset'$

where τ is the shear stress or shear strength, c is the cohesion, σ is the normal stress and \emptyset is the friction angle. Consideration must be given to the proportion of stress carried by the grain assemblages and the portion carried by the fluid phase. Hence, equation 1 is defined as a total stress because pore water pressures are implicit, but unknown. Equation 2 is defined as an effective stress, where c' and \emptyset' are effective stress parameters because pore water pressures (μ) are accountable by the effective normal stress (σ'), where:

3. $\sigma' = \sigma - \mu.$

This is a deduced quantity and cannot be ascertained without a more detailed examination of all the inter-particle forces in a soil mass (Mitchell, 1976). Thus, Terzaghi's (1931) principle of effective stress was extended by Lambe (1960) to include all the forces which exist in a clay-electrolyte system subject to unloading. Sridharan (1968) examined

Lambe's equation and concluded that the inter-particle effective stress (\bar{c}) may be formulated as follows:

$$4. \quad \bar{c} = \sigma \cdot a_m = \sigma - u_w - u_a - R + A$$

where: σ = mineral to mineral contact stress
 a_m = fraction of the total inter-particle contact area that is mineral to mineral contact
 σ = total normal pressure
 u_w = effective pore water pressure
 u_a = effective pore air pressure
 R = total inter-particle repulsion divided by the total inter-particle area
 A = total inter-particle attraction divided by the total inter-particle area.

If the clay is fully saturated then equation 4 may be expressed:

$$5. \quad \bar{c} = \sigma' + A - R$$

where σ' is the conventional effective stress and $A - R$ determines the net electrical attractive force or 'intrinsic' effective stress. When A and R are both small, as would be for the massive minerals, and clays of low plasticity, or in cases where $A \approx -R$, the inter-granular and effective stress would be approximately equal (Mitchell, 1976). This is assumed in most conventional analyses. However, where A or R are large, or differ in magnitude, the total and effective stress will vary significantly. This would be likely in highly plastic soils, for reasons this chapter has outlined (sections 2.23 and 2.24). The forces of attraction and repulsion between clay minerals affect the resistance of soil to deformation and give rise to physico-chemical swelling (Taylor and Smith 1986) discussed in section 2.33.

The fundamental properties of shear strength are friction and cohesion, as outlined in sections 1.5 and 2.24. Terzaghi (1936) first described the relationship between the shearing resistance of soils and the friction angle between the planes of shear. The basic factor responsible for the strength of a soil is the frictional resistance between soil particles and mineral to mineral contacts (Hvorslev, 1960). Frictional strength will be influenced by the number of point contacts in the zone of shear, and also by the physico-chemical forces of interaction and volume change tendencies of soils. Cohesion is caused by the direct chemical bonding between particles and the attraction for hydrated ions between particles and mineral layers (section 2.24). Cohesion can be quite considerable when amorphous oxides are present. The bonds are primarily molecular and ionic and are very strong when ions are shared between crystal units (p82). The electrostatic and electromagnetic forces between clay particles can produce cohesive strengths as large as 7 kPa at close distance (Selby 1982).

Reductions in strength may occur by weathering, swelling, fracture development, bond breaking, physico-chemical interaction and softening of materials by increased water content. Skempton (1964) suggested that the shear strength of first-time slips in over-consolidated clays was controlled by the fully softened strength, or the critical pre-failure state, roughly corresponding to zero cohesion and peak ϕ_{cv}' .

Residual strength is attained after larger strains or movements when the materials become gradually remoulded. The residual condition represents deformation under constant volume and fabric where ϕ_r' bears a more direct relationship to true friction than ϕ_{cv}' or ϕ_p' . The process of slow loss of strength through time is termed progressive failure

(Bjerrum, 1961, 1967), and clearly, it is vital that the relevant strength parameters are used in concurrent stability analyses. If existing slip surfaces are present then residual strength parameters must apply.

Taylor and Cripps (1987) summarize the significant fall in shear strength of indurated mudrocks and over-consolidated clays as a consequence of *in situ* weathering (Table 2.6). All show significant reductions in effective cohesion and friction. Chandler (1969) found that for Keuper Marl, cohesion fell from over 28 to 17 kPa and peak ϕ' dropped from more than 40° to 32° as weathering progressed. The residual strength showed a similar reduction when ϕ_r' declined from 32° to 18° through weathering.

Russell and Parker (1979) observed reductions in shear strength for weathered profiles of Oxford Clay. They suggested that this was due to the destruction of calcite cementing agents and the rupture of mineral to mineral contacts by solution of diagenetic bonds and by the degradation of illite clay minerals. They also noted that the most intense weakening of bonds occurred near the base of the weathering profiles, where percolating fluids were acidic and capable of bond destruction. At depth soil solutions would normally be neutralised by salts leached from the surface horizons (Pitman, pers.com.).

The fall in peak effective shear strength to a lower bound value as a result of weathering indicates a return towards a normally-consolidated state, where cohesion is essentially not greater than zero and with shear strength supported mainly by true particle friction. Chandler and Skempton (1974) warn of the problems in assuming cohesion to be zero in post-failure conditions from the mechanical point of view, and contrary

Table 2.6. Engineering properties of weathered and unweathered over-consolidated clays.

FORMATION		London Clay	Bearpaw Shale	Lower		Upper Lias Clay	Keuper Marl	Coal Measures			
GEOLOGICAL AGE		Tertiary	Upper Cretaceous	Oxford Clay	Upper Jurassic	Lower Jurassic	Triassic	Mudrock			
Lab. pre-consolidation pressure (kN/m ²)		1436-4137	>18100	9583-14504	9540-10510	11850-21450		c.48 500			
Depth to base of Zone III weathering (m)		5.0-15.0	14.9	0.0-10.0	2.9-5.5	5.6-8.5		2.0-4.0			
Clay mineralogy %	Kaolinite	10-40	27	20-35	15	15-85	20	6-10	5	35	
	Illite/mica	20-60	43	65-80	52	5-90	58	28-93	70	43	
	Smectite/mixed layer	0-70	27	44-100	29	0-55	15	13		15	
	Chlorite	0-20	3	0-17	0-5	1	0-10	5	0-23	7.5	7
Natural water content %		19-28 23-49	19-27 29-36	15-25 20-33	11-23 20-38	5-15 12-40		3-8 3-32			
Liquid limit %		50-105 66-100	70 82	80-150	45-75 —	20-38 56-72	54	12-40 25-35	30-51 27-72	42 57	
Plasticity index %		41-85 36-55	47 44	62-123	12-50 —	32 —	19-40 24-42	33 32	10-15* 10-35	18-33 18-42	30
Clay size fraction (<2µm,%)		48-61	<5µm 30-65 30-65	30-70 52	18-65 38	10-35	12-29				
Bulk density Mg/m ²		1.92-2.04 1.70-2.00	1.90	1.84-2.05 2.03	—	1.87-2.09 1.79-1.96	1.90	2.20-2.50 1.80-2.30	2.15-2.76 1.86-2.18	2.23 1.92	
Undrained shear strength kN/m ²		80-800 40-190	100-400 175	276-874	96-12000 360-1100 52-93	40-1200 110-240	130-2800 300-1200 70-200	100-150 15-335	80-150		
Effective shear strength		c' 31-252 φ' 20-29	10-152 25-30	10-216 23-40	27 24	>30 >40		Cac' ≈ 131 ≈ 2000-3200 φ' ≈ 46 φ' ≈ 28-39			
c', ca kN/m ²											
φ', φs Degrees		1-18 17-23	0-41 20-28	0-20 21.5-28	1-17 18-25	2-80 25-42		0-25 26-39			

* May be non-plastic 150 Average values

Source: Taylor and Gripps (1987) p.426-427.

to experience, suggest the inclusion of a small value so that shear strength may not be construed as being independent of depth. Bruckl and Scheidegger (1973) found that the cohesive force acting on the shear surface may be 50-100 per cent of the cohesion of the sliding material, which is very high for modern principles of geotechnical engineers.

Since the work of Skempton in 1948, considerable attention has been given to the residual strength properties of landslip soils, both in the field and laboratory (Skempton 1985; Noble 1973; Bishop *et al* 1971; Lupini *et al* 1981; Bromhead 1979; Hawkins 1985). They stress the importance of the development of one or more shear zones in the soil mass. For example, Hawkins (1985) states:

"It is not the rock or soil mass itself which is at residual strength, but a zone or number of zones within the mass."

Rates of strain or displacement on pre-existing shear surfaces may vary quite markedly, but tests by Petley (1966) and Lupini (1980) showed that on average, the change in strength for a ten fold increase or decrease in displacement was less than 2.5 per cent. True residual strength is thus independent of strain rate, although it is standard practice to test at low strains ($0.002-0.01 \text{ mm min}^{-1}$) to ensure fully drained conditions and the prevention of excess pore water pressures.

When movement occurs it is recognised that the stress required to cause displacement will depend very much on particle size and shape. Skempton (1985) notes that when the clay fraction is about 50 per cent, residual strength is controlled almost entirely by sliding friction of the clay minerals; between 25-50 per cent there is a transitional type of

behaviour when residual strength is dependent on the nature and quantity of clay-size particles.

Chattopadhyay (1972) related residual strength to the mode of cleavage of the constituent minerals of soils, and also to particle shape. He found that low residual friction angles were associated with platy minerals, and that sub-angular and needle-shaped particles gave higher values. Wesley (1977) confirmed that ϕ_r' was governed by composition and that the adsorption of water to mineral surfaces further reduced particle friction (Horn and Deere, 1962). This process is most important for clay minerals with associated double layer activity (p77).

Lupini *et al* (1981) confirmed the importance of the proportion of platy to rotund particles and noted the influence of the coefficient of inter-particle friction ($\phi_r = \tau' / \sigma'$) of platy minerals in controlling the type of residual shearing mechanism. Three modes of residual shear behaviour were recognised:

1. Turbulent shear, where $\phi_r' = \phi_{cv}'$: when soil deformation is dominated by rotund particles or when the coefficient of inter-particle friction between minerals is high, residual strength is high and there is no preferred particle orientation. ϕ_r' depends on the shape and packing of the soil particles and is affected by stress history.
2. Sliding shear, occurs when the behaviour is dominated by platy, low-friction particles. A low strength shear surface of orientated particles develops. ϕ_r' depends primarily on mineralogy, pore water chemistry and the coefficient of inter-particle friction, but is independent of stress-history.

3. Transitional shear, occurs when there is no dominant particle shape, and involves both turbulent and sliding behaviour in different parts of a shear zone. ϕ_r' is sensitive to small changes in soil fabric.

The sliding mode of behaviour will dominate in mudslides containing more than 50 per cent clay-size particles. Mesri and Olson (1970), Olson (1974), Kenney (1966;1977), Ramiah et al (1970), Shridharan et al (1971), Moore et al(1977), Steward (1983), and Steward and Cripps (1983), have looked at the role of clay minerals and chemistry on shear strength properties. Much of this work has been confined to experimentation on pure clay minerals and is somewhat divorced from the earlier literature; but as Mesri and Olson (1970) point out:

"A clear understanding of the fundamental factors controlling the physical and chemical properties of clay minerals is necessary for comprehending their behaviour, before, and after slope failure."

Kenney (1966) tested three groups of clays for residual strength using a reversible direct shear box: the clays included a very sensitive marine clay, an over-consolidated clay and an inter-bedded clay from a limestone series. The test data indicated that small values of ϕ_r' were obtained for soils containing large amounts of montmorillonite or mixed-layer minerals containing montmorillonite, whereas soils exhibiting large residual strengths contained large quantities of massive minerals, small quantities of montmorillonite, large quantities of chlorite, or clay minerals of the mica family.

Where clay was orientated in shear zones, Kenney (1977) showed that the residual strength of this mode of failure was strongly dependent on the mineralogy of the platy particles and upon pore water chemistry.

Typically among the tests, friction angles were lowest for montmorillonite soils and highest when the mineralogy was dominated by illites and kaolinites.

Ramiah *et al* (1970) reported the influence of changes in pore water chemistry on residual strength for flocculating and dispersive conditions where residual friction angles reduced from 33° to 28°. It was concluded that the influence of pH on inter-particle repulsions and the existence of positive edge charges in low pH environments are of greatest importance in kaolinite, of lesser importance in illite, and relatively unimportant in montmorillonite.

Moore *et al* (1977) demonstrated the influence of leaching and solute processes on the shear strength and compressibility of an over-consolidated marine sediment. They treated samples to remove the organic and inorganic cations and when tested against a control differences in behaviour were noted. During shear and consolidation, the control sample exhibited behaviour characteristic of an over-consolidated clay. Sodium leached samples showed no over-consolidated behaviour and it was concluded that the over-consolidated state was due to physico-chemical effects, and particularly to cementation or primary bonding between particles. The failure of chemical bonds binding clay aggregations and particles together occurred only at high shear stresses, resulting in the over-consolidated behaviour.

Steward (1981) and Steward and Cripps (1983) studied the effects of acid weathering on the engineering properties of pyritic shale. In order to quantify these effects in terms of the residual shear strength, a Bromhead ring shear was modified so that pore water compositions could be

controlled during strength testing. This experimental design eliminated the risk of sample variation or errors in preparation techniques. They concluded:

"The residual strength of shale appears to be subject to modification during weathering because it is sensitive to pore water chemistry and mineralogical composition, both of which are altered by weathering reactions."

σ_r' was sensitive to cation composition and concentration (Table 2.7). Potassium increased and sodium decreased residual strength in comparison with values obtained for distilled water. Salt applications were both reversible and reproducible.

The mineralogy and pore water chemistry of clays which control the shearing resistance of the sliding type of residual behaviour have not been reflected in attempts to correlate σ_r' with the index properties (Kenney 1977): in cohesive soils, where the influence of pore water chemistry can be assumed constant, σ_r' should correlate with the clay fraction and activity. Similarly, if clay mineralogy is constant or uniform, residual strength should correlate with the proportion of clay and plasticity. According to Lupini (1981), if tests are plotted in this manner they correlated well.

This section has demonstrated the influence of weathering on shear deformation processes. Slope instability may result from the long-term reduction in friction from peak to the fully softened strength or the critical pre-failure state. The progressive chemical weathering of diagenetic bonds were considered responsible for such effects because in principle, particle friction must remain constant in undisturbed

Table 2.7. Variation in residual friction and solution chemistry.

SOLUTION	CONCENTRATION (Molar)	ϕ_r' (degrees)
Distilled water	-	22°
NaNO ₃	0.1	20°
NaNO ₃	1.0	19°
KNO ₃	0.1	23°

Values are averages for two experimental runs.

Effective normal stress = 294 kN/m² and $c_r' = 0$.

Source: Steward and Cripps (1983).

materials. Residual conditions prevail in pre-existing landslides and for materials following movement, disruption and remoulding. Cohesion is essentially zero and friction is governed by ϕ' . Three mechanisms of shear were proposed with respect to the amount of movement or strain exhibited by materials.

True residual conditions are dependent on the mineralogy, pore water chemistry, and the coefficient of inter-particle friction, and are independent of stress history. In principle the bonding mechanisms and clay-water-exchange reactions will have important effects on particle interaction, cohesion and the influence of residual friction along shear surfaces. The presence of montmorillonite and sodium ions in natural sediments will potentially give rise to the lowest residual shear strengths, particularly along shear-induced fabric and highly orientated clay surfaces. For such reasons it was considered that greater attention should be given to these properties in soil-testing procedures. The advent of the ring-shear apparatus has enabled a better understanding of the physico-chemical nature of shear strength and is now used in standard laboratory testing.

2.33 Volume change behaviour.

Swelling, shrinkage, collapse, consolidation and compression are all terms used to describe volume changes. During weathering, swelling will occur as a result of three processes:

1. Stress relief;
2. Intra-particle swelling of the 2:1 clay minerals; and

3. Inter-particle or osmotic swelling between particles.

The stresses associated with volume changes are important in determining the resistance of soil to compression, expansion and deformation. The forces of interaction involved were outlined in section 2.32 (p120), where it was noted that volume changes affect the intrinsic normal stress of soils; expansion will reduce shear strength whereas compression will result in an increase in shear strength.

The mechanisms of swelling processes may be sub-divided into:

1. Mechanical processes; these include the bending, sliding, rolling and crushing of mineral particles, elastic and time-dependent stress unloading and the rupture of particle bonds coupled with shear displacements.
2. Physico-chemical processes; involve intra-particle hydration (section 2.232) in response to weathering by unloading and erosion, or following surface desiccation. Intra-particle swelling is confined to the 2:1 layered clays and to within 10 Å of the mineral surface. Inter-particle swelling results from the development of double layer repulsive forces (section 2.231). Large volume increases are due to osmotic forces associated with exchangeable cations.

The mechanical processes were initially considered by Terzaghi (1929) whereas Bolt (1956) and Olson and Mesri (1970) have contributed widely to the second model. Bolt (1956) found that the degree of compression between Ca^{2+} and Na^+ illites and montmorillonites could be explained by the concentration and valency state of the clay-electrolyte system:

"The compressibility of pure clay suspensions and pastes can be accounted for very well by the consideration of the interaction between the electric double layers formed on the clay particles."

And Olson and Mesri (1970) state:

"It should be possible to perform experiments to determine which of the two models better describes the consolidation characteristics of clays. For example, the physico-chemical model predicts that large variations in pore water electrolyte concentration will cause great changes in the position of the swelling curves whereas the mechanical model predicts either no change, or a very small change, depending on whether or not the electrolyte concentration is assumed to influence surface friction. Tests on clays with a wide variation in electrolyte concentration should then show which model is most applicable...The two models predict quite the opposite effect."

Particle shape is important in the physico-chemical model since platy particles allow the maximum interaction of double layers. Meade (1964) and Quirk (1968) suggested that particle size is the single most important factor influencing the void ratio and the effects of physico-chemical and mechanical factors on the process of consolidation and swelling. Particle size is a direct manifestation of mineralogical composition, with increasing colloidal activity and expansion associated with decreasing particle sizes. Studies such as Schafer and Singer (1976) and Franzmeier et al (1968) support the influence of clay mineralogy, the intensity of volume change depending on both compositional and environmental factors.

Osmotic swelling and double layer repulsions are greatest where particles align. In addition to promoting the physico-chemical effects, discontinuities tend to reduce the influence of the mechanical processes (Warkentin and Bozozuk, 1961; Aylmore and Quirk, 1959). The adsorption of cations by clays and the formation of double layers are responsible for long range repulsive forces between particles (p91). Quantitative

prediction of these forces is possible in some cases, and the extent to which they account for the swelling and compression behaviour of clays is known. The works of Bolt (1954, 1956, 1979), Olson and Mesri (1970), Shridharan and Venkatappa Rao (1973), Sridharan and Jayadeva (1982), Foster (1953), Davidtz and Low (1970), Blackmore and Miller (1961), Madsen (1979), Aylmore and Quirk (1959), Yong and Warkentin (1975) and Mitchell (1976), give a reasonably clear picture of the extent to which the osmotic pressure concept can account for the compression and swelling behaviour of fine-grained soils.

Their findings show that for the mechanical model, Kaolinite, illite and muscovite can be considered as stiff elastic plates, whereas those of montmorillonite may be thought of as highly flexible films. The mechanical properties tended to exert the most influence on volume change behaviour when the average angle of contact between adjacent particles was large. The displacement of particles and the influence of adsorbed fluid on the coefficient of friction rapidly decreased as the surface roughened (Horn and Deere, 1962).

The results suggest that the larger clay minerals such as kaolinite, are not subject to physico-chemical swelling, which is supported by Mitchell (1960) and Shridharan and Venkatappa Rao (1973). The latter workers consolidated smectites and kaolinite minerals with 'non-wetting' fluids, and showed that both minerals had similar magnitudes of rebound. Smectite expansion was physico-chemically based, although only Na-montmorillonite expanded according to predicted double layer theory. Aylmore and Quirk (1959) provided a reason for this, when they found that Ca-montmorillonite minerals compacted to form irreversible domains which cannot expand beyond 19 Å. Dead volume corrections can be applied to

compensate for this behaviour (Blackmore and Miller 1961). In practice, cations of low concentration and valency generate the largest diffuse layers and therefore greater swelling pressures, particularly with the expansive 2:1 clay minerals (Norrish, 1954).

In conclusion, Olson and Mesri (1970) stated:

"The compressibility characteristics of clays, in general, are influenced by both mechanical and physico-chemical effects. Although they must occur simultaneously in all soils, the experiments indicate that one or other usually dominates and this depends on the spacing between the particles. Since physico-chemical properties control the original soil structure in clays, they exert an immediate influence on the virgin compressibility of all clay soils. Kaolinite is controlled by the mechanical effects whereas the swelling behaviour of smectites are physico-chemically controlled. Illite occupies an intermediate position with both mechanical and physico-chemical effects evident during swelling."

Clay swelling may result from changes in pressure, temperature and chemical environment. In the context of physico-chemical swelling these will be greatest near the ground surface where the water percolating downwards from precipitation and groundwater is likely to be different in composition from *in situ* pore water. If the concentration of the soil water is less than that of the double layer, swelling will occur until equilibrium is attained.

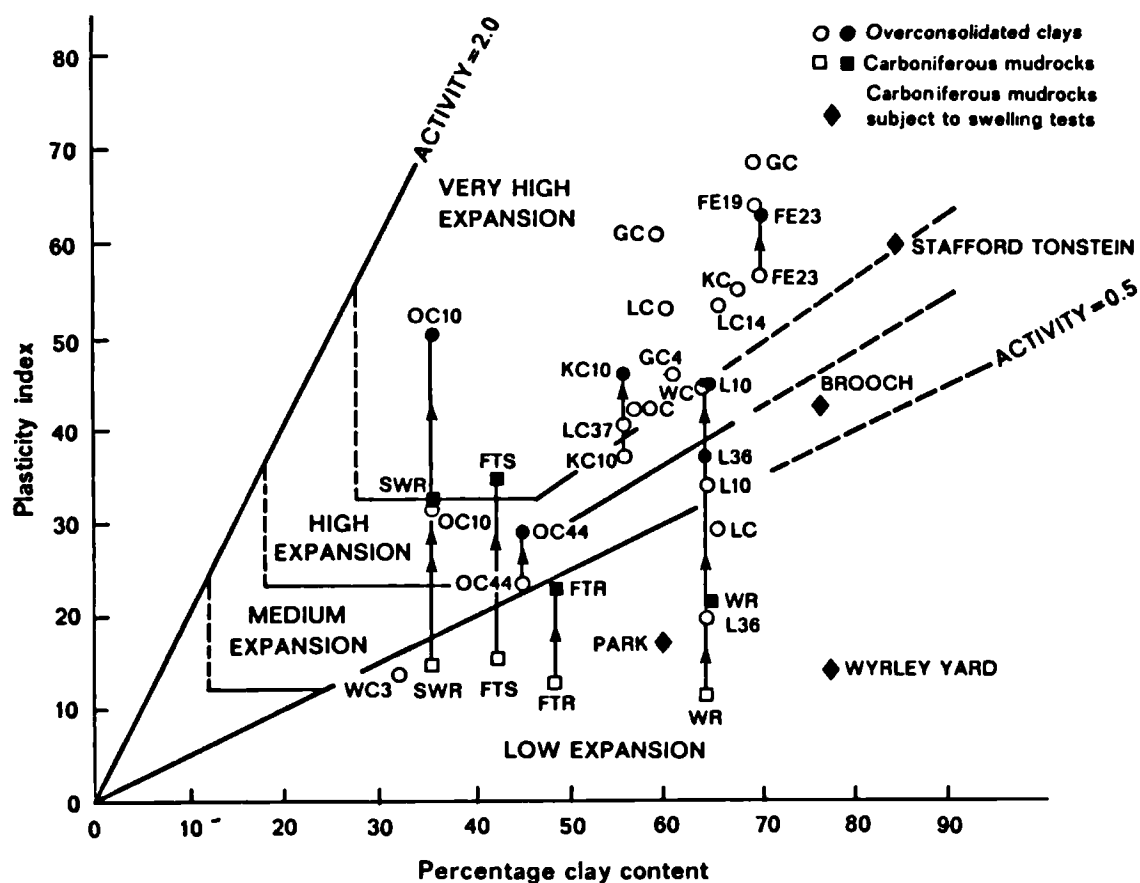
Temperature variations can cause significant changes in the volume and effective stresses of saturated soils. This is achieved through thermal expansion of the mineral solids, pore water, and thermally induced changes in soil structure. Two effects may be distinguished:

1. Pore water tensions will result from rapid increases and decreases in temperature, due to differences in the volumetric expansion and shrinkage of soil grains and water, respectively. With an increase in temperature pore water pressures may develop, and where permeability is low, a much greater time is required to restore equilibrium.
2. An increase in temperature causes a decrease in the shearing strength of the individual particle contacts. Consequently, there is a partial collapse of the soil structure and decrease in the void ratio, until a sufficient number of additional bonds are established to carry the new stress level.

A 'swell sensitivity' has been observed in some clays, wherein the swell index for remoulded clay is higher than that for undisturbed clay. The increased swelling of disturbed material can result from both the rupture of inter-particle bonds, which inhibit swelling, and differences in fabric. Old, unweathered, over-consolidated clays, may be particularly swell-sensitive. It is found that over-consolidated soil is usually less compressible, but more expansive, than the same material at the same void ratio, but normally-consolidated. In the case of a soil containing expansive clay minerals, any change in pore water chemistry that promotes double layer repulsion will lead to an increase in swell or swell pressure.

Skempton's (1953) activity concept has been used as a means for establishing the expansiveness of clay soils. With reference to Figure 2.8, Taylor and Smith (1986) collated data from Williams and Donaldson (1980) and Driscoll (1984), to classify the expansive nature of U.K. over-consolidated clays and mudrocks. The classification provides reasonable agreement with predictions using standard data. Taylor and Cripps (1987) concluded that in the United Kingdom, clay and mudrock

Figure 2.8. Classification of UK over-consolidated clays and mudrocks in relation to plasticity and clay content.



GC : Gault Clay OC : Oxford Clay KC : Kimmeridge Clay FE : Fuller's Earth LC : London Clay
 L : Lias Clay WR : Widdrington roof Shale WC : Weald Clay FTR, FTS : Flockton thin roof & seam
 SWR : Swallow Wood seam roof shale

Source: Taylor and Smith (1986).

disintegration is unlikely to be exacerbated by intra-particle swelling in sediments older than the Silurian.

Kimmeridge Clay, Oxford Clay, Lias Clay and the Carboniferous mudrocks may be seen to vary between one or more classes (Figure 2.8). This was considered to reflect different methods used for the assessment of plasticity. It was found that using particles <75 μm gave higher values of plasticity, although the <425 μm is used in standard soil mechanics practice (BS 1377, 1975). London, Gault, Kimmeridge and Oxford Clay, and Fullers Earth were predominantly highly expansive in comparison to Weald Clay which varied from very highly expansive to low expansion. Clearly, further data are required to supplement this classification.

A knowledge of the nature and conditions enhancing the volume change behaviour of clay soils can be applied in a number of ways:

1. the relationship between soil type, overburden pressure, and void ratio, can be used to make preliminary estimates of compression, and swell index values;
2. the osmotic pressure theory of swelling is useful to estimate the effects of environmental changes;
3. examinations of differences in mineralogy may be necessary if differences in the swelling behaviour of apparently similar soils are to be explained;
4. delayed compression may have important consequences on the longer-term compression behaviour of clays *in situ*. A knowledge of stress history and careful laboratory testing are required if useful deformation and settlement analyses are to be made in such materials;

5. the previous considerations on temperature point to a need for temperature controls on soil testing and suggested that soil deformation is a thermally activated process.

2.34 Permeability.

Soil permeability may be defined as the ability of the soil medium to transmit water. Hydraulic conductivity refers to the flux or volume of water flow through soil and is dependent on the hydraulic gradient and permeability. For instance, if permeability is held constant the hydraulic conductivity is the ratio of the flux of water to the hydraulic gradient, as depicted in Figure 2.9.

For water movement through clay materials flow is assumed to be laminar and the rate of flow is directly proportional to the driving force and inversely proportional to the resistance. This relationship was expressed by Darcy in the 1850s which subsequently became known as Darcy's Law:

$$1. \quad V = -K \text{ grad } \psi$$

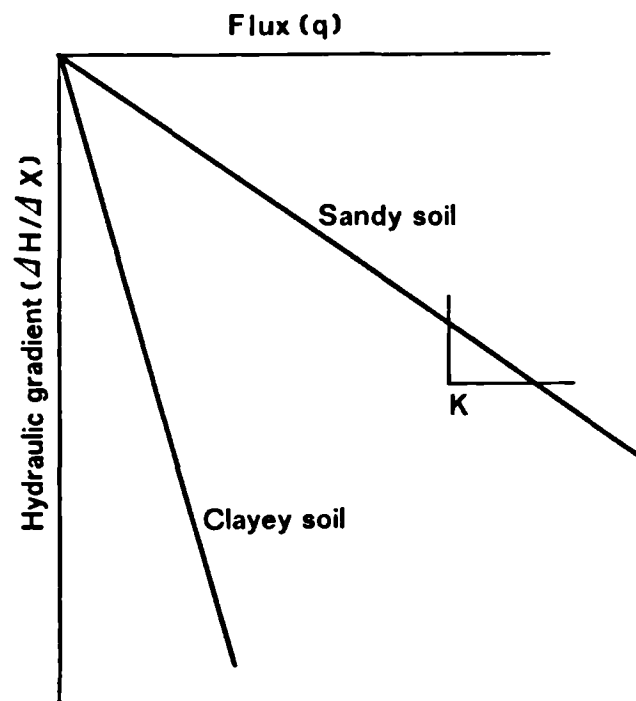
where: V = the volume of flow in relation to area and time;

K = hydraulic conductivity;

ψ = denotes the change in water potential per unit distance in the direction of flow.

However, K is not an exclusive property of the soil because it depends not only on the inherent properties but also on the nature of the pore water fluid. It is possible in theory, and occasionally in practice, to separate hydraulic conductivity into two factors known as the intrinsic permeability and the fluidity which are described by the equation:

Figure 2.9. The relationship between water flux and the hydraulic gradient.



Source: Hillel (1971).

$$2. \quad K = \bar{k} \cdot \mu / \rho g = \bar{k} \cdot f$$

where: K = hydraulic conductivity (cmsec^{-1});

k = intrinsic permeability (cm^2);

f = fluidity ($1/\text{cmsec}^{-1}$);

μ = fluid viscosity;

ρ = fluid density,

g = gravitational constant.

It is not surprising, therefore, that the term 'permeability' has been applied synonymously or alternatively to K , and has often been loosely applied to describe the readiness with which porous media transmit water or various other fluids. The nature and ability of soil to store and transmit water is determined by the intrinsic permeability, \bar{k} , the property of concern in this section. Thus, in the following discussion hydraulic conductivity refers to K and permeability to \bar{k} .

It is the intention of this section to describe permeability in relation to the inherent physico-chemical properties and the weathering behaviour of landslipped clays. For further discussion on the formulation of the laws of hydraulic conductivity the reader is referred to Hillel (1971), Freeze and Cherry (1979), Tavenas *et al* (1983), Mitchell (1976), Yong and Warkentin (1975) and Kenney (1984). Similarly, the processes of hill-slope hydrology, infiltration and solute processes will not be discussed for these are somewhat dependent on the permeability of soil even though permeability may be affected by them. The reader is, thus, referred to Kirkby (1978), Anderson and Burt (1978), McCaig (1986) and Trudgill (1986).

Numerous papers have been published in the past dealing with the fundamental aspects of soil permeability, such as the validity of Darcy's

Law, and the factors governing the magnitude of hydraulic conductivity. The majority of past work was concerned with artificial or remoulded soils, while *studies* of intact natural clays have been few in number. Tavenas *et al* (1983) provides the most recent review of both the theoretical and practical aspects of the permeability of natural clays.

The factors responsible for determining soil permeability may be listed:

1. Particle size, void ratio and porosity;
2. Anisotropy of structure and fabric;
3. Shear and Volume change behaviour;
4. Physico-chemical reactions between clays and water;
5. Temperature.

Permeability is primarily a function of the average size of the pores, which in turn is related to the distribution of particle sizes, particle shape and soil structure. Soils containing a large proportion of clay minerals have small average particle sizes and low values of permeability. It was noted in section 2.21 (p78), that only small quantities of clay are necessary to influence the properties of coarser particles. The permeability of soils will be greatly reduced where clays coat coarse particles, reducing the pore size by clogging *in situ* pore space.

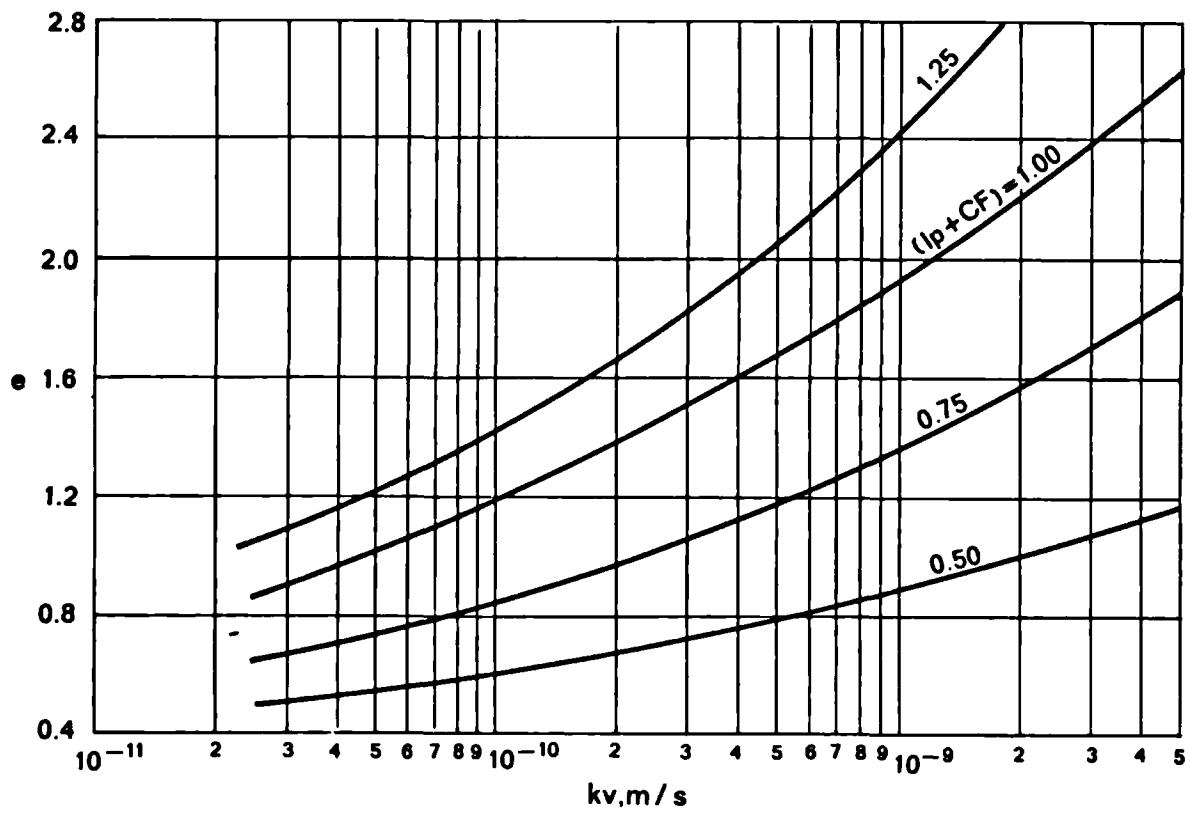
The total porosity and the size of the conducting pores are, thus, the two most important factors governing soil permeability. For example, a sandy soil with large pores can have a much greater hydraulic conductivity than a clay soil with narrow pores though the total porosity

or permeability of clays is typically greater than that of a sandy soil. The presence of cracks and holes will increase the total permeability in different ways, depending on the direction and condition of the flow process.

Tavenas *et al* (1983) reviewed the relationship between void ratio and the hydraulic conductivity and noted that the majority described in the literature do not take into account the probable complex behaviour of the structure of intact natural clays when they become normally-consolidated. However, a linear void ratio verses log K relationship, shown in Figure 2.10, was proposed to describe the permeability behaviour in terms of initial conditions and of the permeability change index (the gradient of the e versus log K function). The relationship showed a high degree of linearity and correlation with the grain size and plasticity characteristics of clays, which was thought to be evidence of both the validity of Darcy's Law and the conditions of saturated and laminar flow.

Weathering processes cause an increase in the void ratio and porosity of disturbed materials and the development of secondary structural features such as fissures and joints (section 2.31). Anisotropic permeability may also occur from the preferred orientation of elongated or platy particles along bedding planes in heterogeneous lithologies and along shear surfaces during weathering and soil deformation. Permeability will be dependent on the direction of flow, and will be greatest in the direction parallel to preferred orientation, and least in the direction normal to particle alignment. It is important to note the differences in permeability in the horizontal plane to the vertical dimension.

Figure 2.10. The relationship between hydraulic conductivity and void ratio.



Source: Tavenas (1983).

Most geological formations display spatial variations in k : Greenkorn and Kessler (1969) developed a set of definitions to describe the degree of heterogeneity in soil and rock formations and found that the homogeneous condition was very unlikely. However, it was possible to define a uniform formation where the mean hydraulic conductivity was found to be monomodal, compared to the multimodal condition for heterogeneous lithologies (Freeze and Cherry, 1979). This concept is important in explanations of slope instability, where large variations in permeability have often been suggested as a primary causal factor. In such slope sections it is often found that there is a greater conductance of water in the horizontal plane.

Ratios of horizontal to vertical permeability may vary from 1 to 7 for undisturbed samples of several different clays (Mitchell, 1956). Laboratory tests have shown that for one-dimensionally consolidated kaolinite the ratios are of the order 1.3 to 1.7 and for illite 0.9 to 4.0 (Olson 1962); although it was computed that if all the particles were orientated to the horizontal, permeability ratios for kaolinite would increase to 20 and for other 2:1 clay minerals by up to 100. It may thus be concluded that the permeability along fissures and shear surfaces will be very much greater than the overlying undisturbed material. Preferential solution and movement of particles in this zone may give rise to the development of piping (Jones, 1981; Wooding and Schafer, 1979; Schafer and Trangmar, 1981; Sherard et al, 1976).

The effects of volume change behaviour will cause changes in permeability (Pane et al 1983). Shrinkage, swell, collapse, and compression all reduce the size and available pore space by the destruction of inter-particle contacts. In section 2.32, it was noted that soil deformation

depends both on the arrangement of particles and particle groups, and on the forces of bonding. It has also been noted that swelling is strongly dependent on the physico-chemical interaction between particles. The processes governing the properties of volume change and shear deformation apply equally to permeability and suggest a close association between clay mineralogy and chemistry.

Because of the various physico-chemical processes, the hydraulic conductivity may change as water permeates and flows through soil (Hillel, 1971). Changes in pore water chemistry may affect both the permeability and the fluidity (equation 2, p141). When water entering the soil is of a different solute composition to the pore water, ion-exchange reactions will occur that may greatly influence the hydraulic conductivity (Reeve *et al*, 1954; Quirk and Schofield, 1955; Brooks *et al* 1956). Such effects will be exacerbated during volume and deformation behaviour.

The influence of ion concentration and valency on the saturated hydraulic conductivity of clay soils was reported by Quirk and Schofield (1955). They found decreases in K , immediately after the application of water containing low concentrations of electrolytes. Reeve (1957) also found that the hydraulic conductivity decreases with a lowering of the electrolyte concentration, due to swelling and dispersion. McNeal *et al* (1966a) have since demonstrated that the decrease in hydraulic conductivity is predominantly related to the expansion of the clay and thus a reduction in the intrinsic permeability \bar{k} . McNeal *et al* (1966b) also studied the effects of electrolyte concentration and composition on the unsaturated K of smectitic and kaolinitic soils. It was found that for smectite there was a decrease in the unsaturated K with a decrease in

electrolyte concentration and with an increase in the sodium adsorption ratio of the leaching water. The kaolinitic soils were much less sensitive to changes in pore water composition.

The influence of pore water electrolytes on both the saturated and unsaturated hydraulic conductivity and permeability of soils containing swelling clays may be explained by a decrease in pore volume as a consequence of the ~~the~~ swelling process and due to the blockage of small pores by clay particles which may disperse as the thickness of double layers increase.

Due to the electrical nature of the clay-water-electrolyte system, it is known that the hydraulic conductivity may be affected by electro-kinetic phenomena (Mitchell, 1976; Freeze and Cherry, 1979). The process involves the relative movements of electricity, charged clay surfaces, and polar cations and liquid phases, a fact utilised by soil engineers in electro-osmosis to facilitate the movement of water and salts through soil media. It is not intended to describe such processes, these may be found in the references, but simply to indicate the fundamental nature of the physico-chemical basis of solute and soil water conductance.

The charged surface of the clay minerals and the consequent adsorption of balancing cations behave as 'imperfect' semi-permeable membranes. In fine-grained soils the flow of salts is restricted near to the clay surfaces where the force of attraction for cations is greater. As for the development of diffuse double layers (p91) the 2:1 layered clays are more active and produce a much greater effect. The porosity of the diffuse layers is reduced, such that soils with large active diffuse double layers will also have the lowest permeability.

2.4 Conclusions.

The physico-chemical properties of clay soils, as found in mudslides, will promote slope instability under the following circumstances:

1. where there has been a weakening or breaking of inter-layer and inter-particle bonds due to weathering and soil deformation processes; the progressive loss of strong covalent and ionic bonds between minerals will be superseded by weaker electrostatic bonds, and there will be a corresponding drop in the activation energy of the bonding mechanism. The change is largely irreversible and dependent on temperature.
2. where there is a high degree of anisotropy along structural discontinuities, joints and fissures and where weathering has resulted in shear surfaces and tension cracks. These zones are characterised by a significant loss of ionic bonds, residual shear strength, increased permeability, and a greater swell tendency. The mechanical properties are not dependent on stress history, but upon the physico-chemical properties of clay minerals.
3. where there is a predominance of the 2:1 layered clay minerals. This group of clays gives rise to the highest plasticity, the weakest inter-layer and inter-particle bonds, the lowest residual shear strengths, the largest potential for volume change, and greatly reduced permeability. This condition will be worst when montmorillonite is present, even in small quantities, especially in association with sodium cations.
4. when the pore water concentration promotes the development of large diffuse double layers. Its associated repulsive energy causes deflocculation and the dispersion of clay particles. This tendency will be greatest in monovalent 2:1 layered clay systems. High concentrations of pore fluid compress double layers bonding opposing mineral layers and particles by Van der Waals' forces of attraction, otherwise termed flocculation.

5. where pore water is dominated by low valency cations with great affinity for water. These may be specifically adsorbed to mineral surfaces in exchange for cations of higher valency. For monovalent cation dominated clay minerals, it would be expected that the clays would support the lowest residual shear strengths, cause the largest volume changes and the lowest permeability. For di- or multivalent clays, there would be a correspondingly higher residual shear strength, suppression of swell tendency, and an improved soil permeability.

The influence of the type and quantity of clay is evidenced in the bulk physical properties of all soils. The physico-chemical nature of the clay minerals is exacerbated during processes of weathering and along pre-existing shear boundaries. High surface area clays, and especially those saturated with monovalent cations, have the greatest influence on the engineering properties of soils. The physico-chemical processes by which clays influence the mechanical properties are fairly well understood, although predictions of the exact response of a given fabric are not possible because of the complexity of the bonding mechanisms between the sheet minerals and clay particles.

From the foregoing reviews a fairly consistent picture has materialised which suggests without doubt that the mineralogy and chemistry of clays are fundamental in controlling the mechanical properties of mudslide materials. Research in this field has largely been isolated in the faculties of clay geochemistry, geomorphology, pedology and geotechnical engineering. The findings have not been applied to studies of the seasonal behaviour of mudslides in the United Kingdom.

2.5 Research objectives.

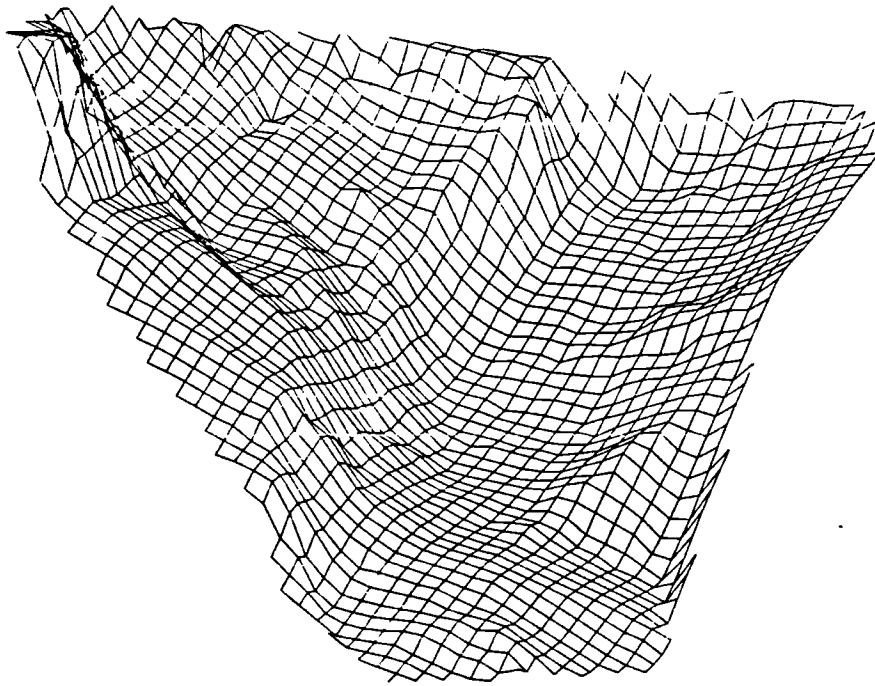
On the basis of the conclusions of Chapters One and Two, a wealth of unanswered questions are raised concerning the natural physico-chemical properties of mudslide materials. From a practical viewpoint this development is new, and the research objectives proposed can only further our understanding of the true significance of these factors within the study of mass movements, and serve as a basis for future research. Thus, the following areas of research are outlined to assess the physico-chemical nature of mudslide behaviour:

1. to collate information on the distribution of mudslides and clay minerals in south-east England to test whether their distributions are related to the presence of 2:1 layered clay minerals.
2. to determine the regional variation in lithology and mass movement of a landslide-prone geological formation with respect to the distribution of mudslides.
3. to compare the variability in clay mineralogy between *in situ* clay and the weathered profiles of two sites of differing lithology.
4. to establish the variability of the type and quantity of clay minerals forming the basal shear surface of the two sites.
5. to establish the variability of physical and chemical properties at the shear surface and overlying mass of weathered debris.
6. to test whether the natural clay mineralogy, pore water composition and concentration, can account for the residual shear strength characteristics of mudslides.
7. to determine the origin and flux of pore water chemicals through a mudslide catchment.

8. to monitor the seasonal physical behaviour of the same mudslide.
9. to test whether seasonal fluctuations in pore water chemistry and weathering behaviour can account for shear strength reduction of an order to facilitate seasonal slope failure.

Chapter Three

METHODOLOGY AND FIELD SITE DESCRIPTION



3.1 Introduction.

The methods of study underlying this research are predominantly site-specific, although as stated in the research objectives (section 2.5), a regional appraisal of the distribution of mudslides and their association with specific clay minerals was warranted. South-east and southern England provides a distinctive and varied area for such a regional survey, and thus formed the basis of the study. The findings of the survey identified the lithologies most prone to mudsliding (see section 4.61) enabling the selection of field sites for further monitoring.

The main aim of the survey was to collate the known distribution of mudslides and clay minerals in southern England from published sources with some supplementary field data. The literature available for such analysis includes a recent 'State-of-the-Art' report to the Department of the Environment (1987) by Geomorphological Services Limited to establish the causes, frequency and scale of landsliding in Great Britain. This analysis provides the most recent and comprehensive survey of landsliding in southern England and serves as a template for the addition of clay mineral data.

A complementary analysis of the distribution of clay minerals was not available and was determined from several sources. Probably the most extensive is Perrin's (1971) '*Clay mineralogy of British sediments*'. Notable additional sources include Avery and Bullock (1977) and Loveland (1984).

Following the regional appraisal (presented in section 4.6), at least two field sites were required for sampling and monitoring to satisfy the

requirements of the remaining research objectives. Care was needed at this stage for the subsequent results can only be as representative as the site itself. To enable the selection of suitable sites a number of criteria were formulated:

1. the sites chosen must be either primary or secondary translational mudslides of characteristic morphology;
2. the size of each field site must be such that allows a reasonable resolution of sampling and instrumentation points, but not so small as to be uncharacteristic of mudslides;
3. the lithology of the mudslides must be generally susceptible to landsliding;
4. the lithology of each site must be different so that the effects of material variability may be assessed;
5. one site should be developed in as uniform a deposit as possible to enable the isolation of the separate influences of the physical and chemical properties on soil behaviour;
6. the sites should be reasonably inaccessible to avoid vandalism;
7. the sites should be reasonably topical to geomorphologists, geotechnicians and geologists.

The importance of lithology or composition is stressed for the reasons concluded from the literature reviews (section 2.21). The regional survey (section 4.6) catalogued the types of lithologies prone to landsliding in south-east and southern Britain (Table 4.29). In south-east England the greatest number of landslides recorded within the region occur on the London Clay and the Weald Clay-Lower Greensand geological units. The London Clay appeared to be particularly susceptible and has been the

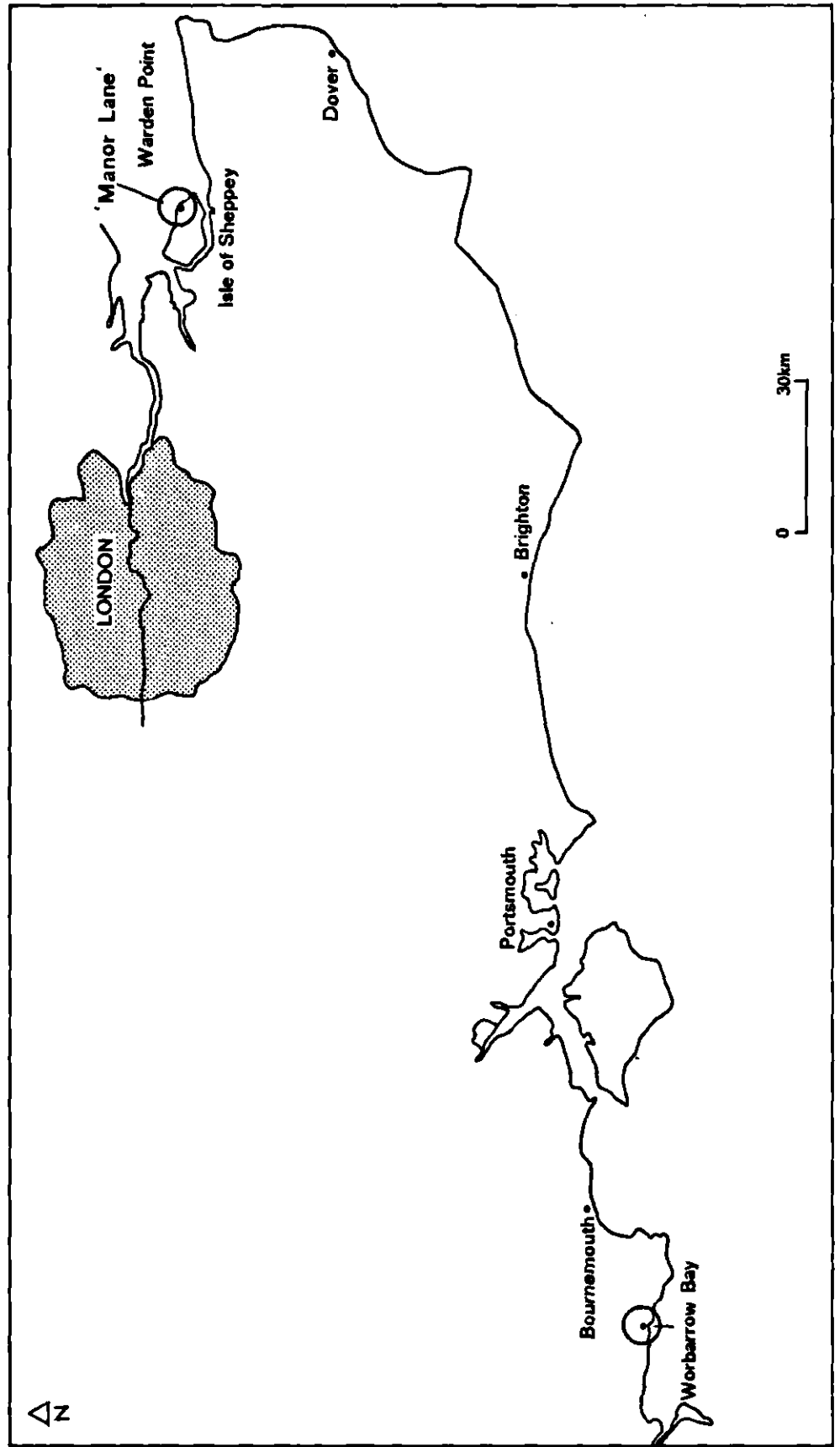
subject of much research in the literature. Lithologically, the London Clay is very suitable for this study, meeting criteria 3, 5 and 7.

On the Isle of Sheppey, north Kent (Figure 3.1), the London Clay forms an extensive section of landslipped cliffs. The style of failure is predominantly deep-seated and rotational, but a reconnaissance of the coastal section between Minster and Warden revealed several suitable translational mudslides meeting criteria 1 and 2. Thus, a site was chosen 1 km west of Warden Point at Manor Lane (TR 015727), although it was noted that the whole coastal stretch is heavily visited by the public and prospecting geologists.

In contrast, the Wealden series are exposed in the Weald of south-east England and the Hampshire Basin. Recently Allison (1986) has surveyed the geological controls on mass movements on the Isle of Purbeck, Dorset, which included a study of mudslides on the Wealden Beds. An opportunity arose to continue working with the same mudslide-site established at Worbarrow Bay, Dorset (SY 871798), and shown in Figure 3.1. This site complements the previous choice, since the lithology of the Wealden Beds is heterogeneous and highly susceptible to landsliding of both rotational and translational types. The site is relatively small and manageable, and has restricted public access.

Reduced public access to Worbarrow Bay meant it was possible to comprehensively instrument the site without the usual fears of vandalism. The site was automatically monitored using electronic sensors and data loggers, and routinely sampled to assess slope instability with respect to seasonal fluctuations in environmental conditions (section 3.32). In addition, a comprehensive set of core samples was extracted from both

Figure 3.1. Location of the field study sites.



sites (section 3.31) and subsequently tested in the laboratory using the methods outlined in section 3.4. Field instrumentation at the Manor Lane site was kept to a minimum for the purposes of stability analysis, owing to public interference, limited resources and time. It was thus only feasible to assess surface movements, pore water pressures and soil properties in relation to weathering and slope morphology at Manor Lane.

Before outlining the field and laboratory methods adopted in this investigation, section 3.2 details the field survey and photogrammetric techniques used to describe the geomorphology and lithology of each site, and the production of site plans for morphological analyses.

3.2 Field survey, photogrammetry and site description:

The objectives of this study required that variations in the morphology and location of sampling sites be established in both space and time. It was necessary to identify various fixed points of reference against which heights, changes in position and absolute position could be coordinated. Survey and photogrammetric techniques were employed to facilitate the production of geomorphological maps and detailed site plans.

The purpose of geomorphological mapping was to:

1. assess the spatial distribution of landsliding of the chosen cliff sections;
2. assess the style and magnitude of failures, and;
3. identify translational mudslides suitable for further study.

Site plans were then produced to enable:

4. the morphological description of the site, and;
5. the design of equipment installation and sampling strategies.

In addition, a new terrestrial photogrammetric technique was used at Worbarrow Bay to provide accurate planimetric and elevation measurements, which together enabled the computation of:

6. contour plans and digital terrain models (DTM);
7. profiles;
8. accurate locations of instrument and sampling sites;
9. assessment of surface movement targets, and;
10. morphological change between surveys over the period of study.

3.21 Geomorphological mapping and survey techniques.


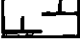



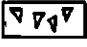


The purpose of geomorphological mapping is clearly described by Cooke and Doornkamp (1978):

"It leads to the recognition of properties that vary across an area, or those found in association with each other. The location and spatial patterns may be as important in planning a project as the height and width dimensions of a particular feature. A map of the relevant landforms, materials and processes is invaluable."






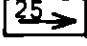

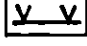
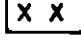
Detailed geomorphological maps (Demek and Embleton, 1978) can provide information about landform genesis, age, lithology, structure and morphology (Goudie, 1981). As a result much attention has been paid in recent years to developing a standard mapping system for geomorphologists

Figure 3.2. Geomorphological mapping symbols and computer coding used for photogrammetric analyses.

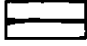
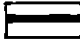

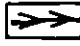
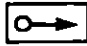
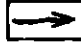
GEOLOGICAL AND SLOPE INSTABILITY FEATURES:

	1100 mudslide		1200 rotational block with backtilt
	1300 shallow translational slide		
	1400 landslipped block		1500 soil creep
	1600 rockfall		1700 in situ bedding
	1800 earth slump		

MORPHOLOGICAL DETAIL:

	2000 backscar with extent undefined		
	2100 rear scarp		2200 rockfall scar
	2300 tension cracks		2400 knife-edged ridge
	2500 angle and dip of slope		2600 convex slope unit
	2700 concave slope unit		2800 survey station

COASTAL AND HYDROLOGICAL FEATURES:

	3100 high water mark		3200 sea-cliff
	3300 ancient sea cliff		3400 gully
	3500 spring		3600 stream

INSTRUMENT CODES:

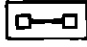


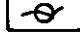



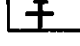
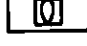
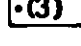
	4100 gantry for movement		4200 movement targets
	4300 standpipe piezometer		4400 electrical piezo
	4500 soil moisture tube		4600 lysimeter
	4700 salt gauge		4800 weather station
	4900 event recorder		5000 core sample

Figure: 3.3

GEOMORPHOLOGICAL MAP OF WORBARROW BAY

DATE 86:04

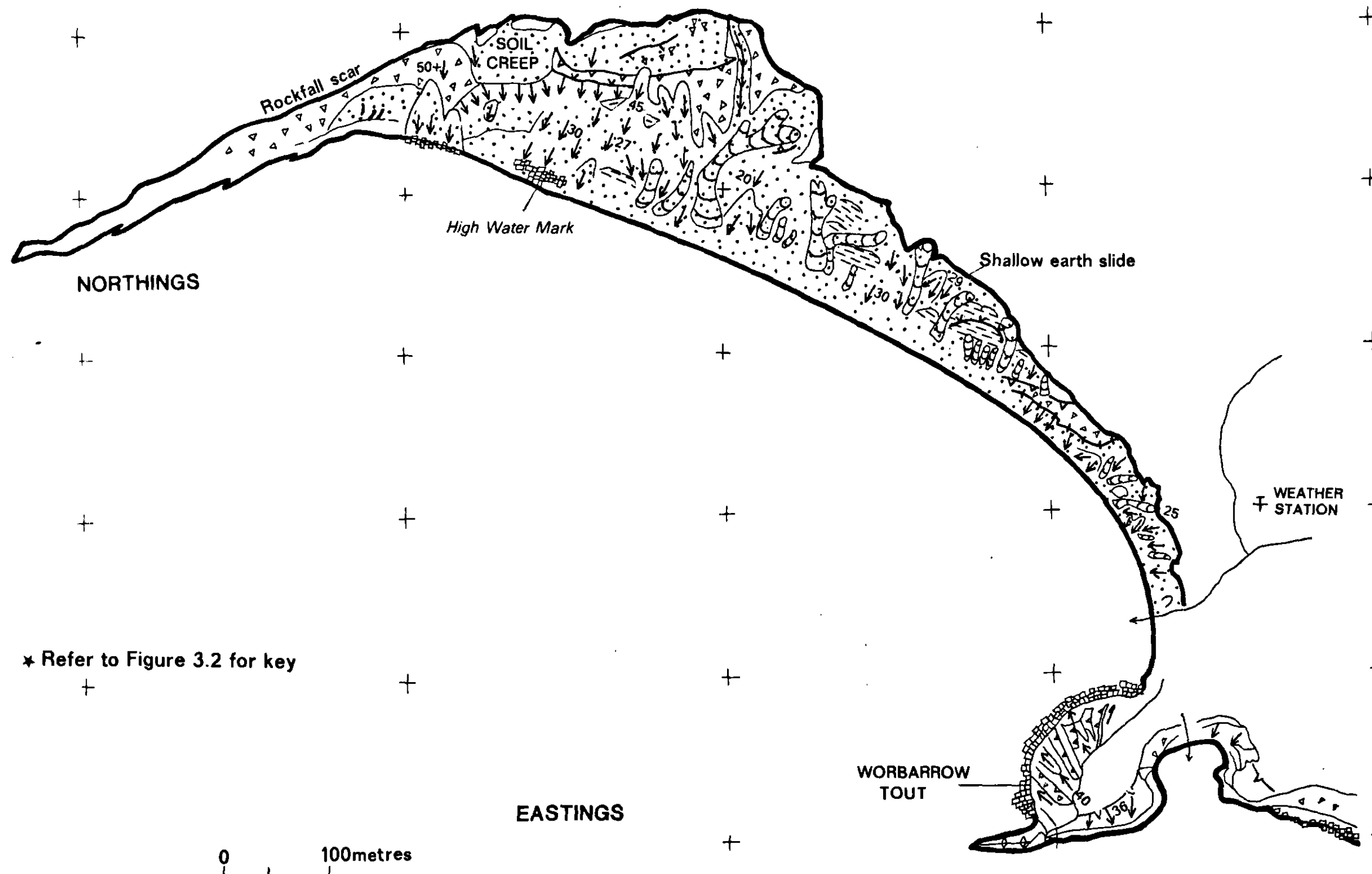
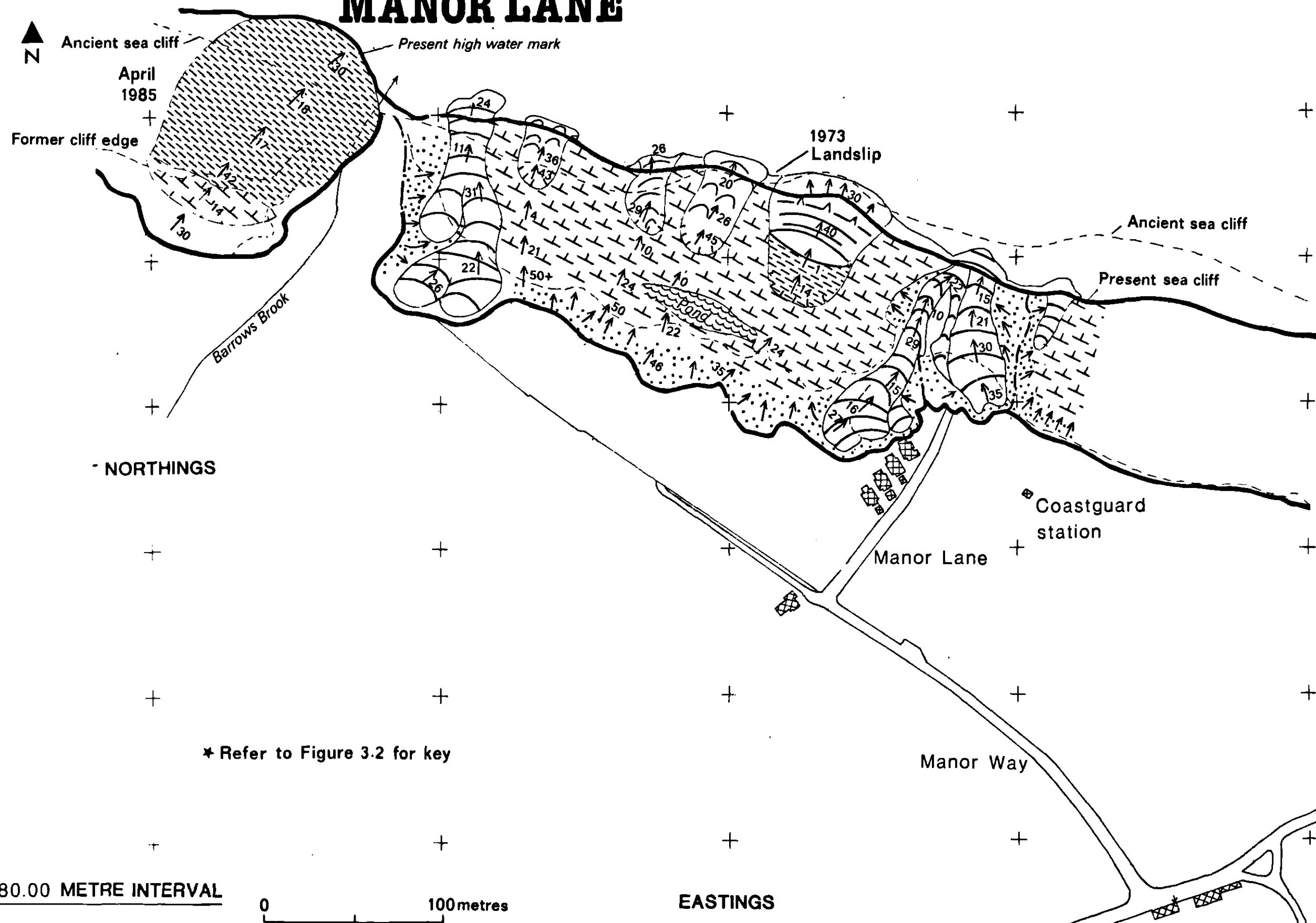


Figure: 3.4

GEOMORPHOLOGICAL MAP OF MANOR LANE

DATE 86:04



(Cooke and Doornkamp, 1974; Gardiner and Dackombe, 1983). The mapping symbols used will vary for different applications and the system designed for this study is presented in Figure 3.2. The legend was used in the compilation of the maps and detailed plans presented in this section, and for the identification and notation of geomorphological detail in photogrammetric analyses.

Geomorphological maps are usually compiled from existing topographic maps and plans, field survey and aerial photographs. Allison (1986) describes the suitability of Ordnance Survey (OS) maps and notes that the OS 1:2500 scale sheets provide the most suitable base maps. Adopting the genetic-morphological technique of Brunnsden and Jones (1972), Allison (1986) has mapped the coastal cliffs of Worbarrow Bay, presented here in Figure 3.3 with minor modification.

This approach to geomorphological mapping was extended to the Manor Lane site, where a large section of cliffs is currently undergoing active landsliding. The base map was found to be sufficiently out of date to warrant a more accurate ground survey. Using a Wild Topcon (TC1) tachometer with data logger, the current location of the cliff edge and a detailed site plan were established, which subsequently served as a base map for the addition of geomorphological detail. The resultant geomorphological map is presented in Figure 3.4.

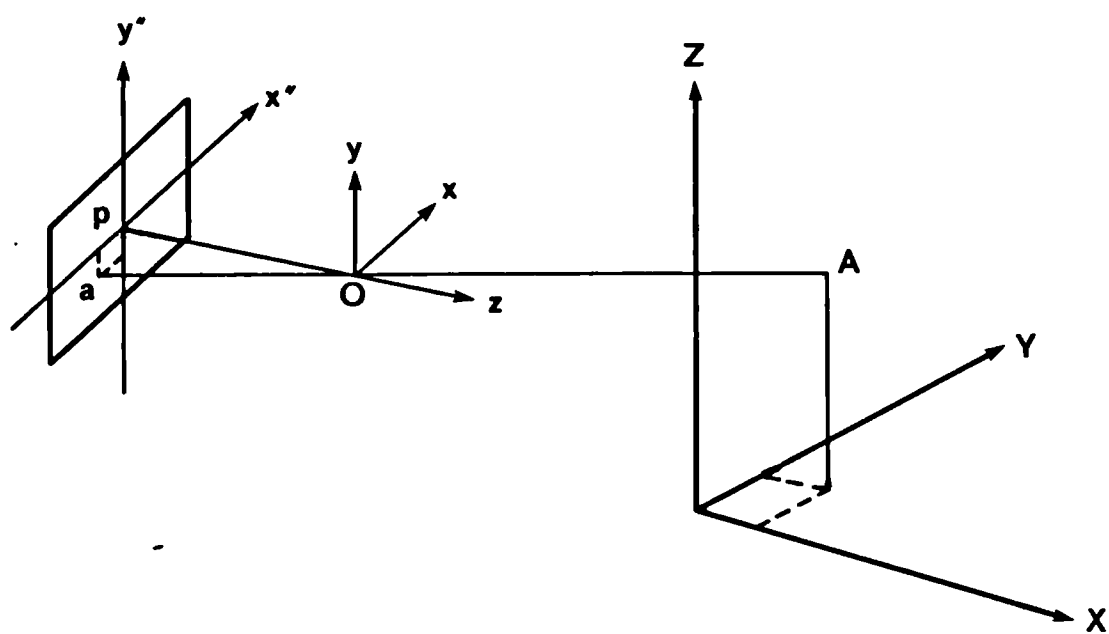
3.22 Photogrammetric survey:

To enable a more accurate and detailed assessment of slope morphology a new technique of Terrestrial Photogrammetry was applied at Worbarrow Bay. Three surveys (epochs) were taken during the study from which changes in slope form were quantified as a result of the seasonal behaviour of mudslides. Each epoch involved the establishment of a control survey followed by a series of photographic exposures of the site.

Traditionally photogrammetric techniques involve the use of analogue stereo-plotters from near-vertical photography (McConchie, 1986) or obliques (Grainger *et al*, 1988), while Collins and Madge (1985, 1981) describe a method applicable to mass movements based on photo-radiation. Analytical photogrammetry, used in this study, allows the use of terrestrial, oblique and vertical photography significantly improving the versatility of the technique for field survey. Analysis of the survey takes place in the laboratory, where the images are processed, read by a stereo-comparator, digitized, and transferred to a Fortune micro-computer. Analysis procedures have subsequently been greatly enhanced by the Intergraph Map Analytic (IMA) linked to a Vax mainframe. The method has only recently been applied to geomorphology (Cooper *et al*, 1986; Chandler *et al*, 1987).

Details of the principles and methods of analytical photogrammetry may be found in Cooper (1987), Methley (1986) and Wolf (1985). In principle, a photograph is an approximation of a central projection of a three dimensional object space onto a two-dimensional image space. Cooper *et al* (1987) describe two sets of coordinate systems that determine the position of a point on the object and the position of its image (Figure

Figure 3.5. Schematic diagram of photo and object coordinate systems.



Source: Cooper *et al* (1986) p.54.

3.5). X,Y,Z is the object or ground coordinate system, and x,y,z the photograph coordinate system. Providing the focal length of the camera is known, and the X,Y,Z coordinates established from a control survey (with at least three non-col linear control points visible in the photographs), it is possible to establish the 'camera parameters' or camera position. The analytical approach is thus not constrained by the location or orientation of the camera providing a minimum of three control targets are visible on the image. If the same control is visible on re-survey the location of the cameras may be different and left to the discretion of the surveyor.

The analytical solution is totally numerical and in effect replaces optical and mechanical stereo-plotters. The method also accommodates the use of non-calibrated cameras because the numerical model can correct for lens and film distortions associated with cheaper conventional cameras. The model is totally rigorous and a full 'error analysis' can be performed and the quality of the final coordinates estimated. The analytical approach requires the use of computers to ensure accuracy, speed and flexibility of analysis, and once the camera parameters are established using the control survey further measurements may be taken from the photographs using a stereo-comparator and digitizer interfaced with a computer. Because the camera parameters are derived from the original field survey the accuracy of the technique is dependent on the quality of the field survey.

3.221 *Field-survey.*

There are two stages to the field survey:

1. the installation of a control survey with clearly visible control points, and;
2. the photography.

The control grid established at Worbarrow is partly shown in Plate 1, indicated by the targets located on the tripods and gantry posts. It is important to obtain from the control survey the coordinates of at least three targeted points to enable a numerical solution. If additional points are available the least squares estimation of the camera parameters (or space resection) is possible with greater confidence and redundancy. In addition, an object coordinate datum must be defined. Where possible this would normally be OS datum, but at Worbarrow Bay it was not possible within reasonable distance to intersect an OS bench mark or pillar. Thus, a local coordinate datum was established.

Once sufficient control targets had been set up, a standard ground survey was used to establish the object coordinates of the control targets. This was achieved with a Carl Zeiss Elta 2 electronic recording tacheometer (Plate 2). Observations consisted of horizontal angles, zenith angles and slope distances between datum stations and control targets. Each control point target was surveyed from at least two datum stations, ensuring reasonable triangulation and redundancy.

The photographs were then taken using a Carl Zeiss Jena UMK Terrestrial Photogrammetric Camera (Plate 3). The camera positions were chosen to

Plate 1.

Diapositive contact print of the Worbarrow field-site.



Plate 2.

Carl Zeiss Elta 2 Electronic Recording Tacheometer.

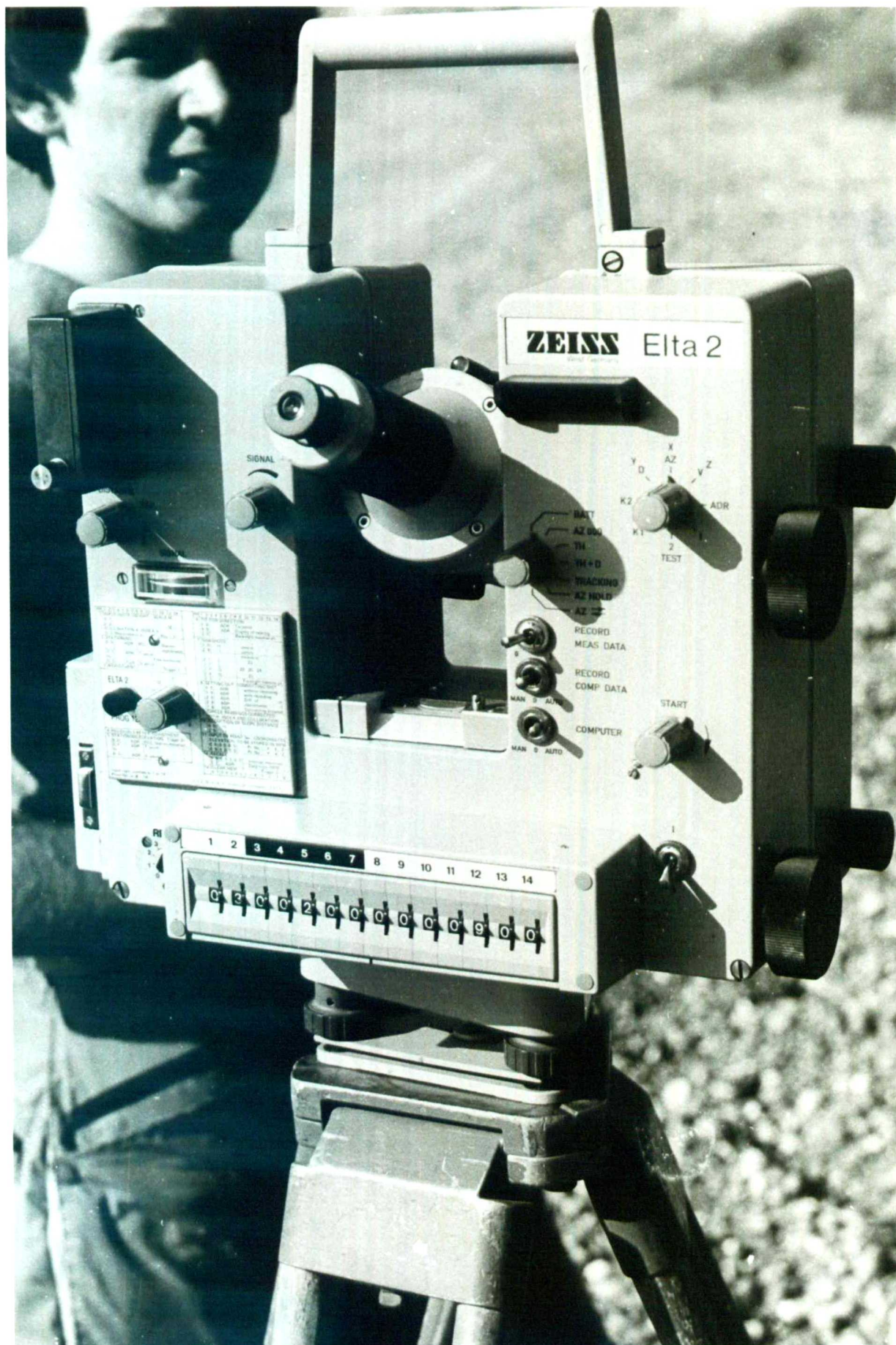
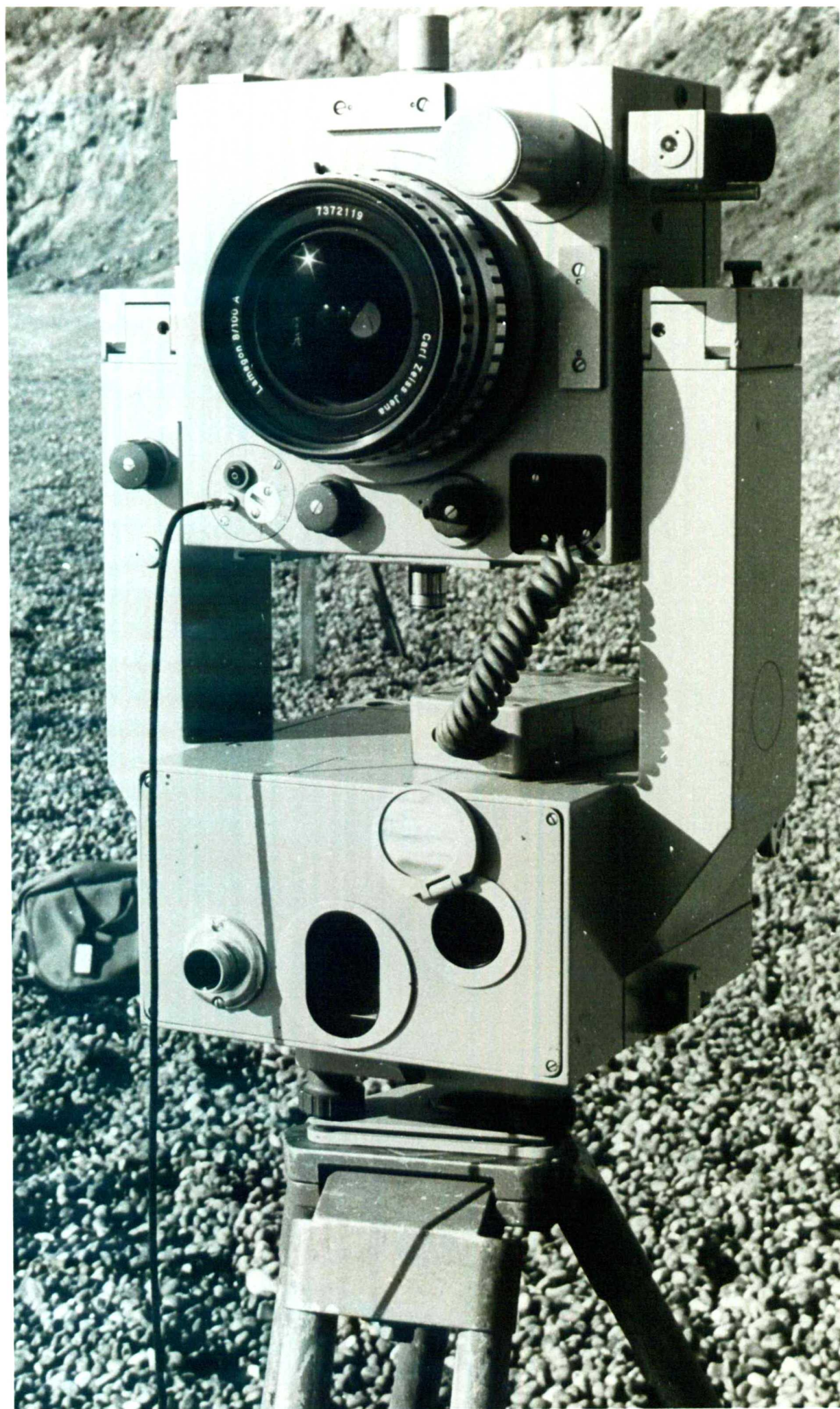


Plate 3.

Carl Zeiss Jena UMK Terrestrial Photogrammetric Camera.



provide the best views of the site and did not require surveying, the only essential criterion was to include a minimum of three control points in each exposure. Pairs of photographs were taken with some degree of overlap to produce a stereo image of the mudslide. However, a number of precautions needed to be considered when taking the photographs; for example the quality of the plates varied between epochs due to the following factors:

1. very bright conditions caused shadows and glare over parts of the slope with a resultant loss of detail;
2. dull conditions reduced the amount of contrast on the images making the identification of surface detail very difficult;
3. when developed some photographic plates were unsuitable for measurement so it was essential to take several exposures at each camera position, and;
4. dead ground may be included within the image with subsequent loss of detail; this is particularly true of terrestrial photographs where sharp breaks of slope may obscure flat ground behind. Oblique aerial photography will reduce this effect, and is preferable at such sites.

3.222 Photogrammetric analysis.

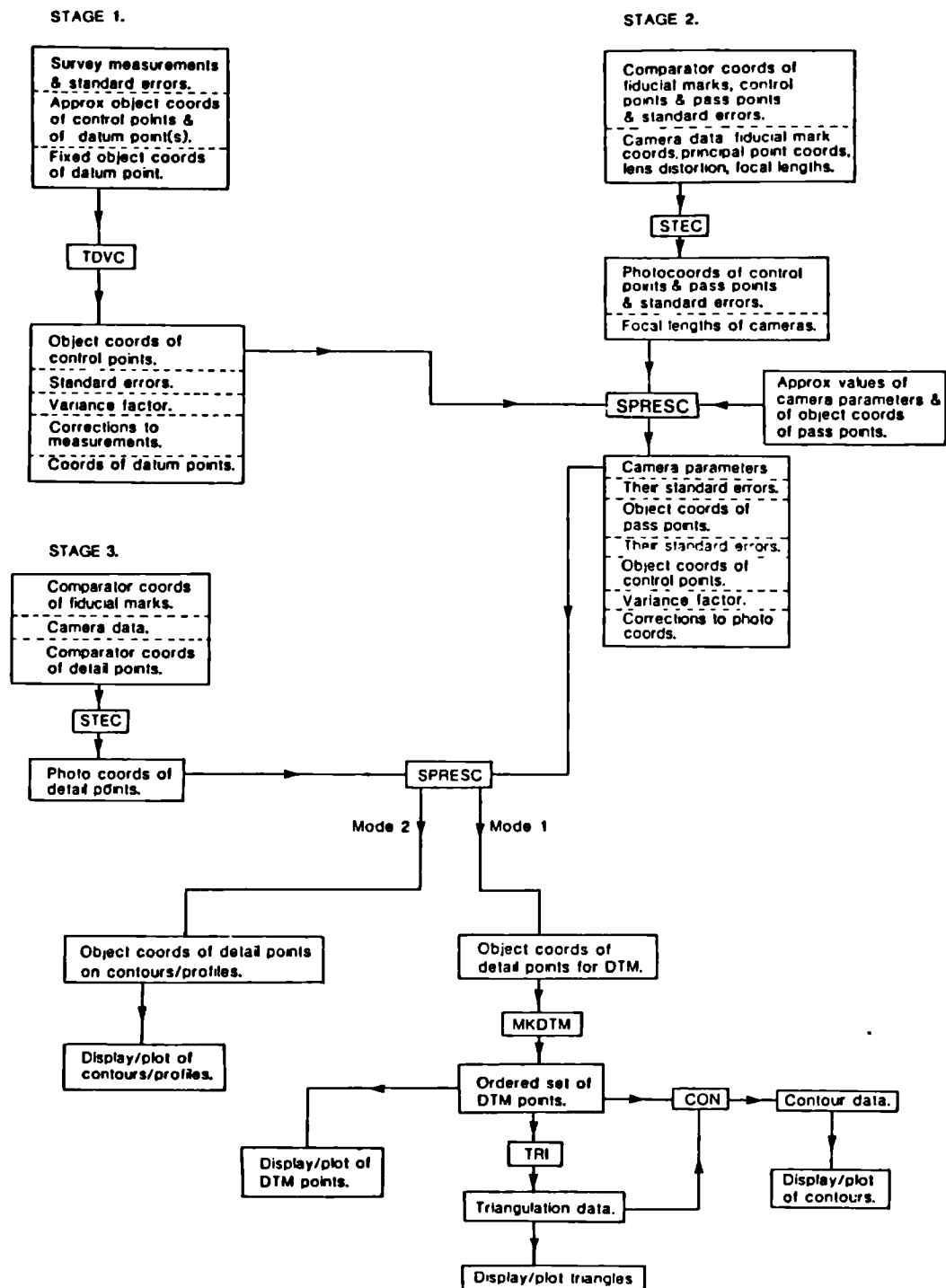
The photographic plates were processed in the laboratory. Glass plate negatives were used in this study in preference to diapositive plates, so that errors arising from the developing process were kept to a minimum.

The equipment used for the measurement and analysis of the survey is presented in Table 3.1. The procedure followed in the laboratory for

Table 3.1. Laboratory equipment used for the measurement and analysis of photographs.

EQUIPMENT	PURPOSE
Zeiss Jena Stecometer (stereo-comparator)	Measurement of comparator coordinates x, y, py, px.
MDR-1s/4 Registration unit (digitiser)	Displays comparator coordinates to the nearest 1 μm , with an 8-digit code number.
Fortune 32:16 micro-computer operating under UNIX with C and fortran compilers.	Linked to digitiser to allow transfer of coordinates to database, and subsequent analysis with existing software.
Two computer terminals with keyboards and monitors.	One dedicated to the steconeter/MDR-1s/4 combination to run program SPRESC, and another for data processing.
Gould PN 9005 super minicomputer.	Accessed by the Fortune for data processing.
Tektronix 4010 graphics screen	Displays graphics.
Hitachi 672 plotter	DTM and planimetric output.
Epson dot-matrix printer.	Coordinate data listing.

Figure 3.6. Computational procedure used in photogrammetric analyses.



Source: Cooper et al (1986) p.56.

each epoch consisted of three main stages illustrated by the block-diagram in Figure 3.6 and summarized below:

1. the computation of the control survey;
2. the derivation of the camera parameters, and;
3. the detailed point-by-point measurement of the site from stereo-pairs.

The computer program TDVC was used to establish the object coordinates of the control points. Pairs of photographs were selected to give adequate cover of the area to be processed. The first pair were placed on the Stecometer or stereo-comparator Plate 4 and the camera parameters computed from the plate coordinates of the control points and from the object coordinates of the control points seen in the photograph.

Program SPRESC allows the on-line transformation, point-by-point, of two pairs of photo coordinates to three object coordinates. Surface features can be measured as single points or strings of points, each point or string being assigned a code of up to eight digits. Thus, with reference to Figure 3.2, codes were assigned to features such as breaks of slope, and instrument locations.

Program SPRESC may be used in either of two modes. Firstly, all points measured are stored with their object coordinates to form a digital terrain model (DTM). Secondly, only those points lying close to the intersection of the ground surface with a specified horizontal or vertical plane are accepted and stored. Graphical representation of the morphology of slopes can be obtained by a planimetric plot of the DTM, contours from the DTM, or by contours and skew profiles from the second mode (see Figure 3.6).

Plate 4.

**Stecometer used for the observation and extraction
of points from photographs.**



The analytical approach to photogrammetry provides a wide range of opportunities for the field geomorphologist for several reasons:

1. the technique may be applied at a variety of scales from regional (aerial) down to the site (terrestrial and oblique);
2. the position of the camera is relatively unimportant as long as the photograph contains coordinated control points;
3. the type of camera and film is unimportant provided the lens calibration and film distortions are known;
4. the opportunity exists to use archive photography, both aerial and oblique, for comparison with present day photography, emphasising time rather than space in geomorphic explanations;
5. the technique enables the measurement of surface features at a much greater resolution and accuracy than possible in conventional geomorphological and field surveys, and;
6. the results of each survey are easily stored by computer and compared with different epochs.

3.23 Site description, morphology and lithology:

3.231 Manor Lane.

The coastal section west of Warden Point is subject to severe coastal erosion through mass movement processes. The style of cliff failure is predominantly deep-seated and rotational as identified on the geomorphological map in Figure 3.4. This mode of failure is in agreement with the works of Hutchinson (et al 1971, 1973, 1986) and Bromhead (1979a) on the north Kent coast of the Isle of Sheppey.

The geomorphological map shows a large rotational landslide at Manor Lane extending 290 metres across and 120 m deep which was first thought to have failed in 1973 (Bromhead, 1979a). Further west, to the other side of Barrows Brook, a deep-seated rotational failure occurred during the period of study in April 1985, and was included in the mapping exercise. The area covered in the map has been undergoing rapid slope development for some time, and when compared with the Ordnance Survey 1:2500 plan (1965), the recession of the cliff has been considerable (\approx 50 metres).

The large rotational block has gradually slipped northwards into the Thames Estuary, advancing the High Water Mark (HWM) further seaward. Lateral mudslides seen at the extremities of the landslip have excavated a considerable amount of debris and are largely responsible for the rapid retreat of the cliff-line. At Manor Lane one of the lateral mudslides has undermined a series of cottages, some of which have been lost and others have recently been deserted.

At the apex of Manor Lane (Figure 3.4), there is a distinctive primary translational mudslide that intersects the lateral mudslide towards the HWM. This shallow landslide has resulted in the excavation of a 'corrie-like' feature (Plate 5) at the eastern extremity of the deep-seated failure and is currently retreating towards the coastguard station. This distinctive mudslide was selected for further analysis, and was subsequently surveyed in detail to produce a plan of the site, shown in Figure 3.7.

The mudslide is 85 m in length and at its maximum 30 m wide. There are two separate source regions (labelled 1 and 2 in Figure 3.7), one of which (1) contains a large deposit of gravel and superficial material.

Plate 5.

Colour image of the Manor Lane mudslide site.



During very wet periods water seeps out of the currently most active source (2). There is no accumulation lobe since the severe undercutting sustains a small 4 m sea-cliff (Plate 5) over which material is transmitted through a narrow 14 m wide track. Marine erosion actively disperses the debris overflowing on to the poorly developed beach.

The coastal cliffs are almost entirely developed in London Clay. A small outcropping of Head gravel is apparent in the source regions of the site, and large nodules of silica identified in the back-cliff (of the large rotational slip) indicate the presence of the lower facies of the Claygate Beds (Table 3.2). The uniformity of London Clay is well known (Holmes, 1981), and it is thus not surprising that considerable attention has been given to this lithology by geologists, geomorphologists and geotechnical engineers. The London Clay forms a major part of the London Basin and the best outcrops are found on the north Kent coast where marine erosion sustains short 25-40 m coastal-cliffs.

The geology of the region is described by Dines *et al* (1971), Holmes (1981), Sherlock (1960), Davis and Elliot (1957) and Williams (1971), with other notable contributions by Davis (1936, 1937), Wooldridge and Linton (1955), Burnett (1972) and Burnett and Fookes (1974).

The geological succession is given in Table 3.2. The London Clay is a marine deposit laid down in Eocene times between 40 and 50 million years ago (Sherlock 1960). The deposition environment initially transgressed south-west across Europe although later a northern arm of the warm Tethys sea joined the London Clay sea in the Wealden area to form the Hampshire Basin (Davis and Elliot, 1957).

Figure: 3.7

SHEPPEY FIELD SURVEY~ MANOR LANE

DATE 86:04

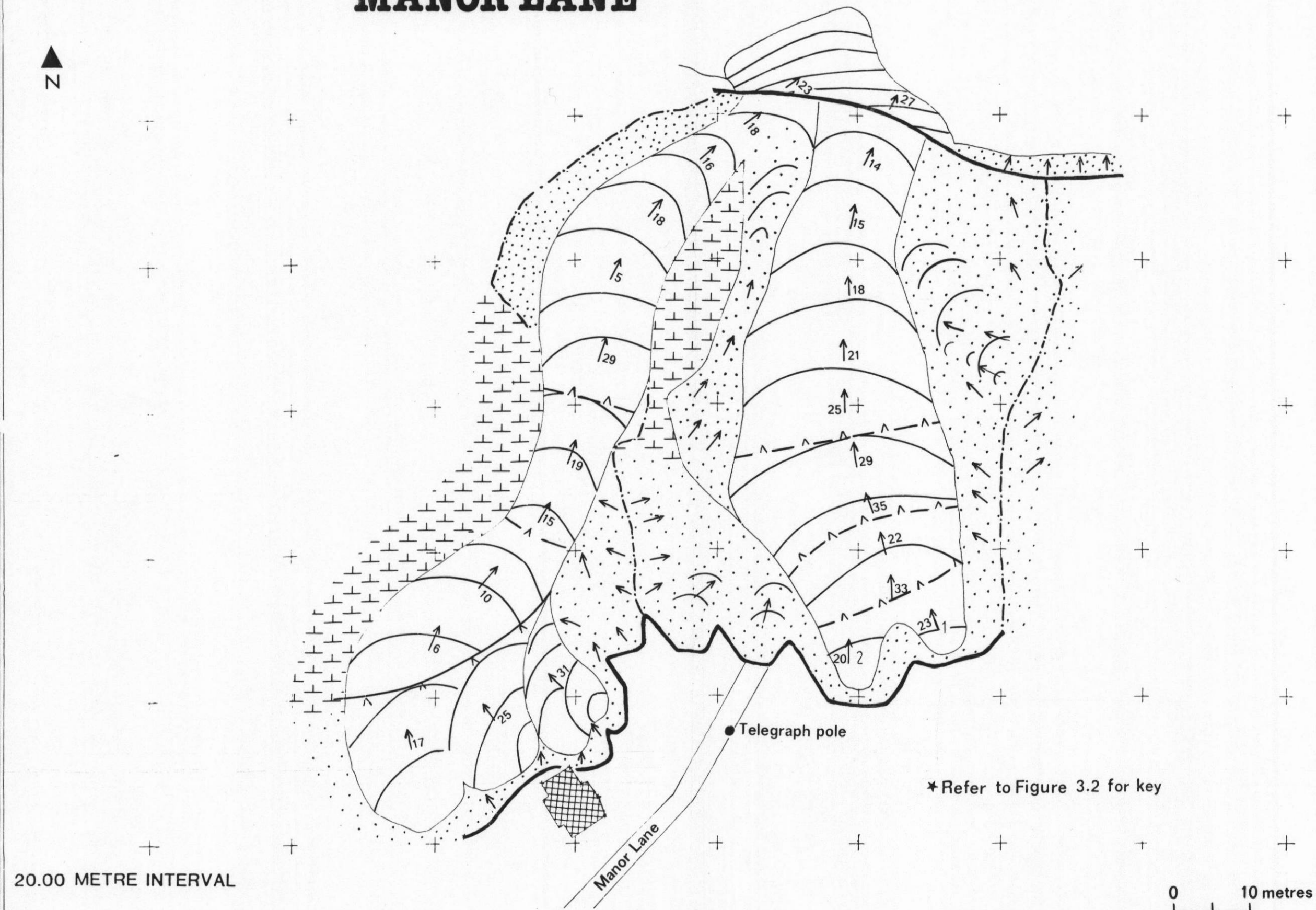


Table 3.2. Stratigraphic sequence of the north Kent coast.

AGE	FORMATION	ROCK TYPE	MAX THICKNESS (metres)
Recent Pleistocene	Head	Loam, sand, chalk rubble, silts and clayey loam.	9.1
	Clay with flints	Loamy clay with unworn flints - Tertiary deposit	4.6
Eocene	Bagshot Beds	Sands with pebble beds	12.2
	Claygate Beds	Thin alternating beds of clay and sand.	6.1
	London Clay	Stiff blue clay	137.1
	Blackheath and Oldhaven Beds	Pebble beds, sands and clays	7.6
	Woolwich Beds	Sands and clays	18.3
	Thanet Beds	Fine grained sands/clay	39.6
Upper Cretaceous	Upper Chalk	White chalk with flints	30.5
	Middle Chalk	Chalk, hard and rough, or blocky-flints top 15.2	70.1
	Lower Chalk	Massive tough chalk	71.6
Lower Cretaceous	Gault	Stiff blue-grey clay	71.6
	Folkestone Beds	Fine grained sands	51.8

Source: Dines *et al* (1971).

Since deposition, the London Clay has undergone a period of uplift and erosion which has caused considerable loss of material, reducing the thickness of the clay and in some places removing it entirely. In addition it has also been gently folded, giving rise to the synclinal structure of the London Basin. Upon this structure there are many superimposed minor faults and folds (Wooldridge and Linton, 1955).

Holmes (1981) provides a good description of the clay:

"The clay usually has at the base only a thin sandy bed, with a few pebbles; above this the clay may be somewhat shaly for a metre or so but rapidly passes into a compact, stiff fine-grained tenacious dark blue clay of entirely uniform lithology. Towards the top however, the beds tend again to contain a certain amount of fine-grained sand, either as seams or admixed with clay, even at some 50 m below the level at which they grade into the Claygate Beds."

It is also noted that calcareous concretions, termed claystones, may vary in abundance according to the horizon and may be present in numerous bands only 0.6-0.9 m apart. In weathered clay, pyrite and selenite are common and most of the clay weathers to a dark brown or chocolate colour, or at the surface sometimes to a yellow shale.

In the Sheppey cliffs approximately 60 m of London Clay is present below the discontinuous Claygate Beds and they are much disturbed by periodic mudsliding. At Manor Lane the cliff is entirely developed in London Clay, with a small overlying deposit of head gravel. The lithological details of the site are given in Table 3.3, including a summary by Davis (1936) of the Sheppey cliff sequence.

Table 3.3. Lithology of the Sheppey cliff sequence.

LITHOLOGY (London Clay)	THICKNESS (m)
Stiff brown clay with few fossils	up to 15
Stiff grey and brown clays with the fauna and flora of Sheppey in the lower part	18
Stiff blue clays with very few fossils (only seen in gaps, for both the overlying divisions are subject to extensive landsliding which obscure the beds below)	15
Barren clays, blue or lead-coloured (on foreshore)	-

Source: Davis (1936) p.331.

Clay minerals to be found within London Clay were reported by Grim (1948) as illite (70%), kaolinite(20%) and montmorillonite (10%), while Burnett (1972) has shown that there is a decrease in the proportion of kaolinite from west to east across the basin, and conversely a steady increase in montmorillonite to 35% towards the Kent coast. From a regional review of the literature (section 4.61; Figure 4.30), an average of 62 analyses showed that the mineralogy of the London Clay approximates to 40 percent mica-illite minerals, 40 percent smectite, 20 percent kaolinite with traces of Chlorite, suggesting that the presence of montmorillonite clays may have been underestimated.

3.232 Worbarrow Bay.

The geomorphological map of Worbarrow Bay (Figure 3.3) reveals a wide variety of slope forms and mass movement processes. The style of cliff failure varies from rockfalls to rotational and translational slides, and Allison (1986) has conclusively shown that the underlying geology of the region is the major control on the type of mass movements.

The variable resistance of the rocks to marine erosion gives rise to the distinctive form of the coastline between Durdle Door and Worbarrow Tout (Brunsden and Goudie, 1982). The excavation of the weak Wealden Beds by marine attack following the breach of the resistant Portland limestone fronting the coastal section, gives rise to the formation of bays. The process of erosion is accelerated by the susceptibility of the Wealden Beds to rotational and translational mudslides.

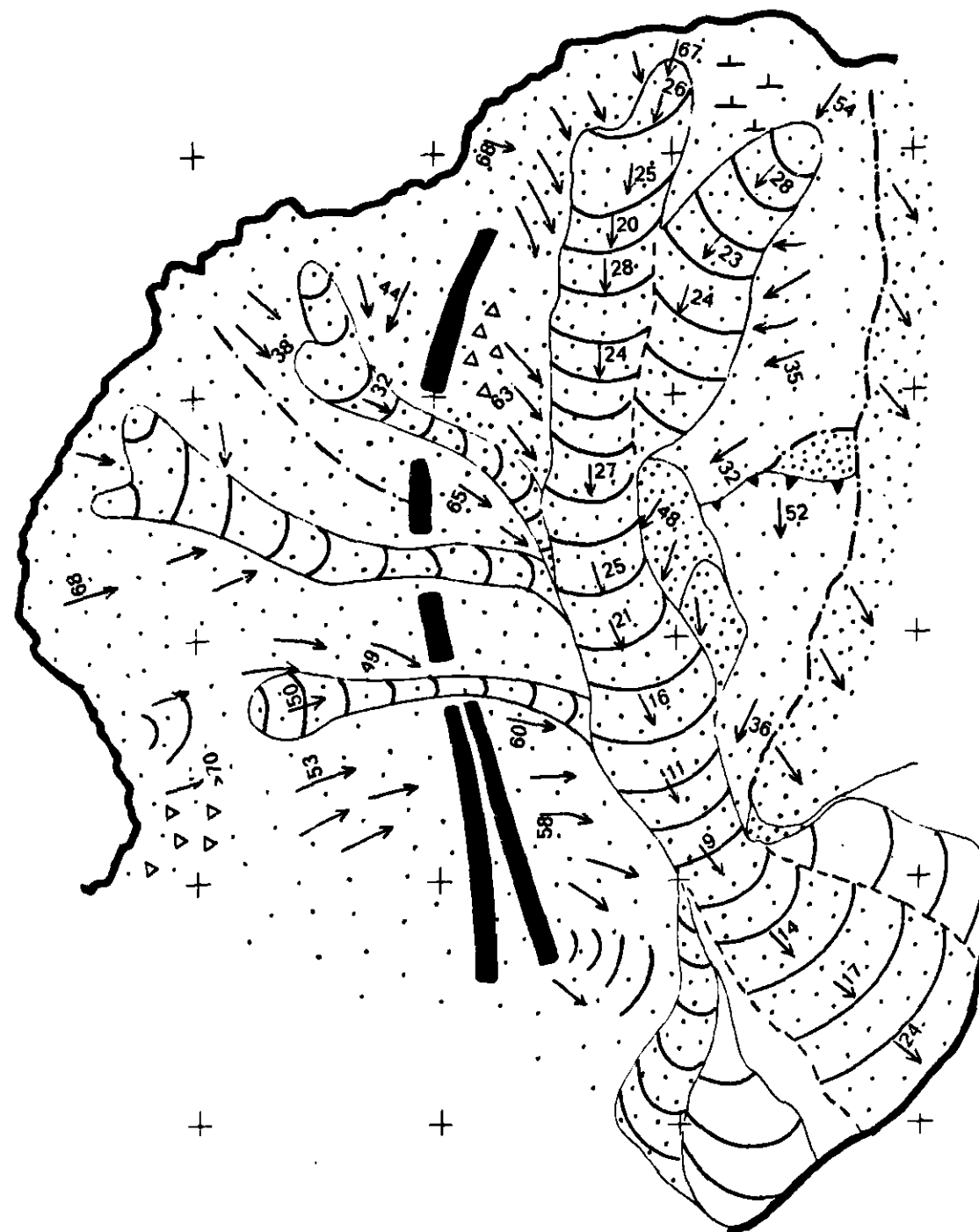
The density of slope failures revealed on the geomorphological map are indicative of the severity of erosion and cliff retreat within Worbarrow Bay. Since the Bay is predominantly formed of Wealden sands and clays the most common styles of landsliding are rotational and translational, although where the coastal cliffs are formed of Chalk rockfalls and rockslides are more common.

Eight rotational landslides can be identified, each of which vary in size and the degree of interrelation with other slope failures. Two groups of landslides are examples of multiple rotational slips but each differ in character. One group shows a sequence of successive failures, where each slipped mass has gradually moved towards the beach, unloading the upper slope, initiating further landslips in the upper reaches. The second rotational unit contains two successive rotated blocks with well developed lateral and frontal mudslides similar in style to the Manor Lane examples.

Translational mudslides are the most frequent form of erosion in the Wealden Beds and throughout the Isle of Purbeck (Allison, 1986). As the cliff-section thins towards Worbarrow Tout mudslides and soil creep are the main erosive features. One such translational mudslide (SY 871798) is currently undergoing quite rapid development and was selected for further study. With reference to the 1:250 site plan (Figure 3.8), it is immediately apparent that this mudslide is not independent, unlike the Manor Lane site. The main feeder track is supplied with debris from smaller perched mudslides to the west forming an overall 'corrie' complex (Plate 6). The main mudslide is 48 m in length, an average 7.6 m in width, and like Manor Lane has two separate source units. The most active source area, to the west, shows considerable seepage of water from

WORBARROW FIELD SURVEY

2



10.00 METRE INTERVAL

0 10 metres

Plate 6.

Colour image of the Worbarrow Bay mudslide site.



a sandstone facies in the back-cliff overlying clays during the wetter periods of the year. During the most active seasonal phases, as experienced in March 1987, the second source area which is mostly developed in Wealden Clays became active.

The shape of the mudslide is determined by the structure of the underlying geology, where resistant beds of sandstone confine the lateral shear surfaces to sharply defined narrow tracks. Sandstone beds are also responsible for the perched mudslides to the west of the corrie, where slurries of clay and debris overflow onto the main slide during very wet periods. The alternate bedding of sand and clay controls slope form and drainage and gives rise to some very unstable slopes.

The major outcrops of the Wealden Clays are found in the Weald and Hampshire Basins (Jones, 1981). It is only along the Purbeck fold of the Hampshire Basin and the Isle of Wight that the Wealden Beds outcrop extensively along the coastal fringe, giving rise to more recent and active mudsliding than can be found in the Low Weald of south-east England.

The geology of the region was considered by Arkell (1947), Allen (1972), Melville and Freshney (1982) and Jones *et al* (1983), but the reader is referred to Allison (1986) and Brunsden and Goudie (1982) for the most recent reviews of the geology and geomorphology of Worbarrow Bay. With the availability of these recent and comprehensive works it is not intended to discuss the regional geology and geomorphology, except where it is felt necessary to clarify site details.

Table 3.4. Stratigraphy of the Cretaceous in Dorset.

AGE	FORMATION	ROCK TYPE	MAX THICKNESS (m)
Upper Cretaceous	Upper Chalk	Chalk with flint	310
	Middle Chalk	Chalk with some flint	78
	Lower Chalk	Muddy chalk on sandy phosphatic basement bed	64
Lower Cretaceous	Upper Greensand and Gault	Shallow marine sands and clays	76
	Lower Greensand	Shallow marine sands and clays	250
	Wealden	Well bedded shales, brackish to marine at top	94
		Brightly coloured marls with cross-bedded sand- stones and coarse grits	600
	Durlston Beds	Non-marine limestones and clays marine at base	62

Source: Melville and Freshney (1982).

The geological succession of the Isle of Purbeck is presented in Table 3.4. Broadly, the topography of the region is characterised by the underlying geology, the result of variable rock strength. Substantial variations exist within each of the stratigraphic units (Melville and Freshney 1982) which gives rise to variations in slope form and stability at a local scale. For example, within the Wealden, hard sandstone bands separate softer argillaceous material (Arkell, 1947; Allen, 1972) which promotes the initiation of failures along the clay-sandstone interface.

The Wealden Beds consist of 716 m of clays and sands deposited in a lacustrine environment during the Cretaceous period 105-130 million years ago. The Beds outcrop throughout the area forming subdued relief, including the 'central core' of the Isle of Purbeck. However, despite the spectacular coast sections, where up to 50 per cent of the total thickness is exposed, the Wealden Beds are probably the least studied formation in the region. From work in the Isle of Wight, it has been possible to divide the Wealden into two distinct units; the lower unit comprises the Wealden Marls or variegated clays and the upper unit the Wealden Shales (Melville and Freshney, 1982).

Generally, lithology is highly variable, comprising sands, marls, clays and shales with inter-bedded sandstones and coarse, quartz-rich pebbly grits (Allen, 1972). More specifically, lithology may include red, purple and green marls, with variegated clays and marls, bands of sandstone, sand and sandy limestone. The Shales are dull blue or blackish clays with layers of clay ironstone, sandstone and shelly limestone which is considered evidence of the return of marine conditions during times of deposition (Melville and Freshney, 1982). The resultant

Table 3.5. Lithology of the Wealden Beds at Worbarrow Bay.

LITHOLOGY (Wealden)	THICKNESS	
	(m)	(Total)
Sandrock, orange and white in colour, with some clay	2.6	423.0
Ironstone, blood-red and purple	0.1	420.4
Red, purple and orange sandrock	5.5	420.3
White sands and clays	20.7	414.8
Red sands with blood-red and purple iron bands	10.1	394.1
Gritstone, coarse	0.6	384.0
Clays, mainly slipped	65.2	383.4
Yellow sand	3.1	318.2
Clays, partly dark	21.3	315.1
Yellow, false-bedded sand and coarse gritstone	2.3	293.8
Clay, sand and sandrock	18.3	291.5
Gritstone, dark, iron, impersistent	0.3	273.2
Mottled clays	18.5	272.9
Conglomerate	0.6	254.4
Clays, sandy towards base	18.3	253.8
Sandy clays with sulphur, blackish to pale	19.8	235.5
Coarse quartz grit, false bedded ironstone	6.1	215.7
Pink, white and orange sandstones, some clay	11.0	209.6
Clay, sand and thin sandstones, with seams of grit	35.0	198.6
Clay, largely red	14.3	163.6
Sand and grit, white and yellow	7.3	149.3
Clay, red, purple and mottled	18.0	142.0
Coarse yellow and brown sand and sandrock	4.3	124.0
Clays, sulphurous towards base	19.2	119.7
Lignite beds	1.5	100.5
Clays and subordinate beds of sand to end of exposure	57.9	99.0
Gap, unexposed at stream, then wealden clays	41.1	41.1

Source: Arkell (1947).

similarity in stratigraphy has led the Shales to be correlated with the upper part of the Weald Clay of the Weald (Anderson, 1967).

At Worbarrow Bay, nearly the whole formation is exposed, dipping to the north. The section was measured by Wright (Arkell, 1947) which is presented in Table 3.5. The Worbarrow field-site is located on the Wealden clays and sands at approximately 198 m from the base of the exposure.

The clay mineralogy of the Wealden Beds has received little attention in comparison to the London Clay, although if the formation is assumed to be similar to the Weald Clay, the mineralogy would include 25-80 per cent illite-mica, 33-50 per cent smectite and 15-25 per cent Kaolinite (Perrin, 1971). The large range of proportions probably reflects the heterogeneous nature of the lithology. From a more comprehensive review of the literature (section 4.61; Table 4.30) an average of 35 reported analyses showed smectites to dominate the mineralogy of the clay fraction ($\approx 70\%$) in comparison with kaolinite (20%) and illite-mica (10%).

3.3 Field instrumentation and sampling techniques:

It is often considered in the earth sciences that the results of laboratory experimentation are only as good as the methods used to obtain representative field samples. An understanding of geomorphological processes involves the analysis and interpretation of accurate and representative data, using standard procedures wherever possible. This is particularly true in studies of mass movements, since an understanding of mudslide processes will depend on the measurement of parameters

concerned with the interaction of soil with water, and how these vary in space and time.

The collection of both field and laboratory measurements is invariably constrained by the availability of equipment, the remoteness of the sites and time. Thus, the sampling and instrumentation techniques used in this study were considered carefully in an attempt to balance what was feasible and practical against the ideal, given the constraints on resources and time.

To meet the aims of the research objectives two programmes were designed to enable:

1. the collection of samples for laboratory analysis, and;
2. the installation of monitoring equipment.

Once implemented, these programmes provided the framework for the acquisition of data for:

Model A. the 'static' analysis of the physico-chemical variability of mudslide materials, and;

Model B. the 'dynamic' analysis of the role of pore water chemistry and environmental conditions upon the seasonal weathering and behaviour of mudslides.

It may be seen that in principle these programmes satisfy the research objectives; objectives 1-5 refer to the static model, and objectives 6-8 to the dynamic model. The results of these models are presented in Chapters Four and Five, respectively.

The purpose of the remainder of this chapter is to outline the field and laboratory methods used in this study. This begins in section 3.31, with a consideration of the sampling methods, the location of sampling sites, and the field procedure. Sampling took place at both Worbarrow Bay and Manor Lane to assess Model A for two sites of contrasting lithology. In section 3.32, the range of instrumentation and techniques used for field monitoring are introduced.

The laboratory methods used in this investigation are described in section 3.4. These are considered in three groups; the physico-chemical analyses of the field samples, the routine analysis of rain and pore water chemistry, and the simulation of residual strength to establish the influence of weathering and geochemical processes on soil behaviour.

3.31 Field sampling techniques.

With reference to the research objectives, a sampling technique was required that would:

1. preserve both the weathered and unweathered profiles of the mudslide materials;
2. obtain a sample as undisturbed as possible for geotechnical purposes;
3. preserve the basal shear surface intact;
4. prevent contamination of the sample once removed from the ground;
5. be economical to produce, and;
6. be practical for the conditions at the time of sampling.

To obtain such a sample it was recognised that core-sampling would be the most appropriate technique (Loveday, 1974; Okumura, 1981; La Rochelle *et al* 1981; Begemann, 1977; Raymond *et al*, 1971; Hodgson, 1978).

The main problem of all sampling techniques is the resultant disturbance to the extracted soil (Okumura, 1981). In soil mechanics however, it has been found that if certain precautions are taken, one can isolate a core with very little distortion: the so-called 'undisturbed' sample (La Rochelle *et al*, 1981). Attention to sampler design and the method used to drive the sampler into the soil, can result in the removal of cores substantially undisturbed. This may be achieved provided the *in situ* stresses and fabric are retained within the sampler, and by ensuring that the stresses and strains that occur during insertion and extraction of the core do not cause significant distortion of the sample.

The characteristics of the sampler may be described by two ratios (Loveday, 1974):

$$\text{Area ratio} = \frac{\text{area annulus of displaced soil}}{\text{area of the sample at the cutting edge}}$$

$$\text{Soil recovery ratio} = \frac{\text{length of sample obtained in tube}}{\text{depth of hole from which removed}}$$

To obtain an 'undisturbed' core the area ratio should be <0.15 and the soil recovery ratio >0.98.

An open-drive thin-walled sampler was designed to meet the aims and precautions outlined above. Loveday (1974) states that the diameter

should ideally be 100 mm, or more, and the longer the core the greater the time needed for the sample to reach equilibrium moisture content.

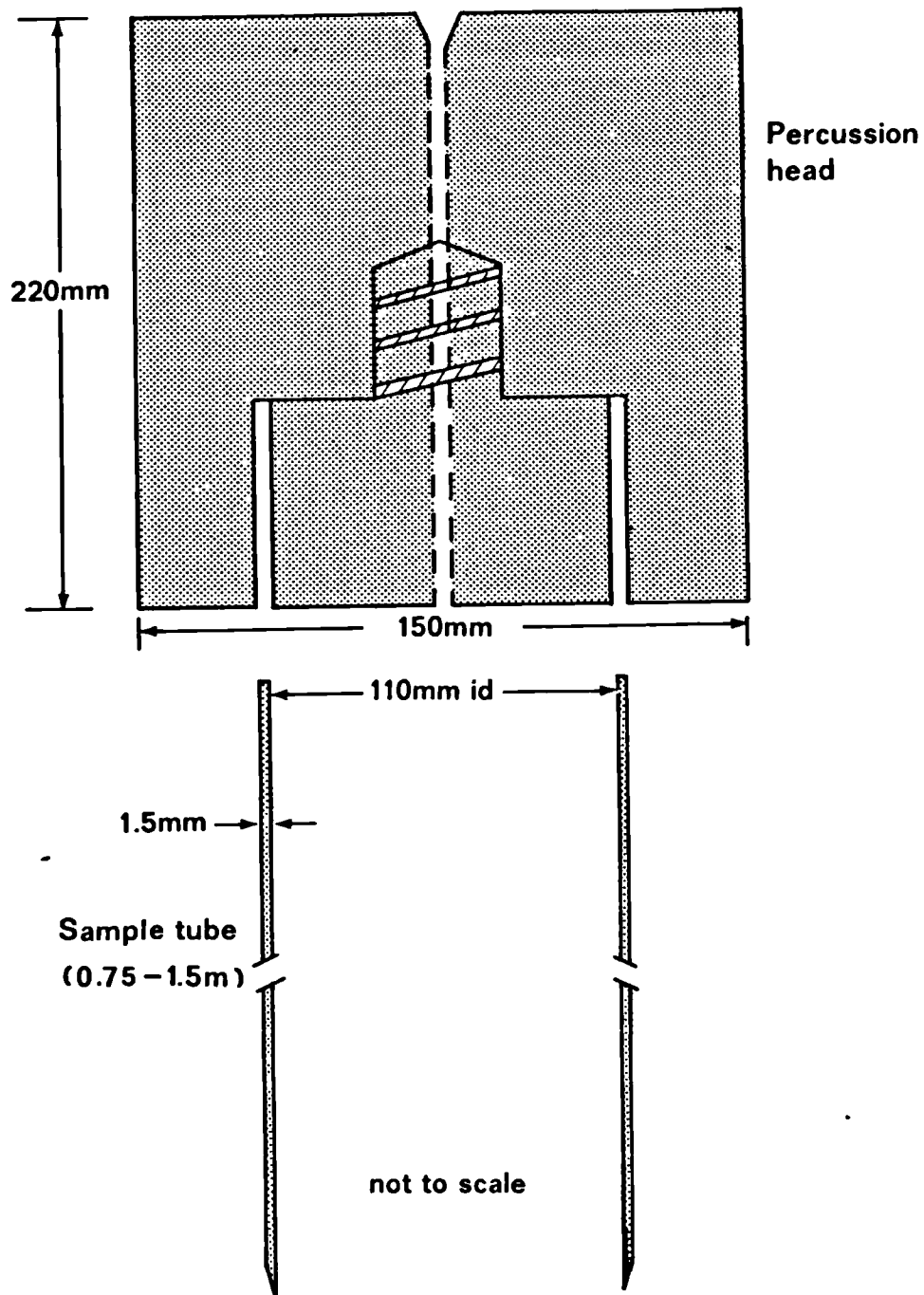
The core sampler designed is shown in Figure 3.9, and is based on the 110 mm diameter Terrain soil piping. The specifications of the piping are stated, in addition to the calculated area ratio; the value of 0.12 is less than the value specified above and the method may be classified as 'thin-walled'.

Sample tubes were prepared from 4 m lengths of piping; lengths of pipe were cut between 0.75-1.5 m long with the assumption that the depth of the basal shear surface would be less than 2 m and average about one metre. This meant that problems encountered in driving long tubes into the ground would be minimized. A 5° bevelled cutting edge was made, and each tube was thoroughly polished, inside and outside, to reduce wall friction.

To enable quick and efficient penetration into the ground a percussion head was designed to fit the sample tubes (Figure 3.9). Aluminium was chosen because it is easy to machine, cost effective, reasonably heavy, and unlikely to fracture when stressed. An air vent allowed air to escape from the sample tube when driven into the ground. The operating method adopted in the field is detailed in Appendix 1, which includes a description of the preparation of cores for transportation.

The sampling locations established at each site are shown in Figures 3.10 and 3.11. The sites were chosen before the field work to provide as even a network as possible and to maximize the area of mudslide sampled. The sites were identified in the field from the site plan and re-surveyed.

Figure 3.9. Core-sampler design.



SPECIFICATIONS:

Terrain soil piping (4 metre lengths).

Area ratio of tube = 0.12, with 5° cutting edge.

Percussion head - machined 150 mm diameter aluminium alloy bar, with guide and air vent.

Table 3.6. Core identification and sample efficiency.

CORE #.	LEVEL O.D. (m)	(A) DEPTH OF HOLE	(B) DEPTH OF SHEAR SURFACE	(C) LENGTH OF CORE (cm)	(D) LENGTH OF <i>IN-SITU</i> CLAY	TOTAL SRR C/A	<i>IN SITU</i> SRR D/A-B
MANOR LANE							
1A	10.31	141.1	125.2	126.5	15.6	0.90	0.98
1B	10.29	99.8	72.7	77.3	26.5	0.78	0.98
2A	15.43	96.2	82.4	70.6	12.9	0.73	0.94
2B	15.48	77.3	55.0	60.1	21.7	0.78	0.97
3A	21.17	90.3	59.3	75.6	29.8	0.84	0.96
3B	22.09	74.4	43.0	64.7	30.5	0.87	0.97
4A	30.17	75.9	53.4	63.0	21.7	0.83	0.96
4B	29.00	92.0	67.8	64.5	23.8	0.70	0.98
5A	36.59	55.1	33.1	49.4	21.1	0.90	0.96
5B	36.57	83.7	62.5	72.4	20.6	0.87	0.97
6	37.12	83.2	62.7	61.0	19.8	0.73	0.97
7U	43.73	159.5	-	142.9	-	0.90	-
$\bar{X} =$						0.82	0.97
WORBARROW BAY							
L.D.							
W0	13.45	136.8	125.7	118.4	10.5	0.87	0.95
W1	16.66	136.4	120.4	102.0	15.7	0.75	0.98
W2	20.60	87.1	69.6	83.2	16.4	0.96	0.94
W3	22.00	85.5	49.1	67.3	35.1	0.79	0.96
W4	24.10	86.5	60.5	63.5	25.5	0.73	0.98
W5	26.45	84.2	68.2	63.8	15.6	0.76	0.98
WU	26.74	145.6	-	137.2	-	0.94	-
$\bar{X} =$						0.83	0.97

L.D. = Local Datum

O.D. = Ordnance Datum

SRR = Sample recovery ratio

U = Unweathered/unslipped core-sample

The total number of core samples feasible for post-sampling analysis was set at 20. At Manor Lane 12 core samples were extracted at the end of March 1986, and a further 7 core samples were extracted from Worbarrow Bay in April 1986. The analysis of the core samples will be discussed in section 3.41.

The efficiency and success of the sampling method is assessed in Table 3.6. The technique was found to be highly practical in view of the very saturated conditions at the time of sampling. Duck boards were required at most sites to prevent both equipment and operators from sinking into the mudslide. The penetration of cores to the required depth was achieved within five minutes. Extraction took much longer, the maximum period being 90 minutes, but more generally 30 minutes. The sample tubes and percussion head were sufficiently strong for the materials sampled in this study. However, on one occasion at the Manor Lane site, the sample tube splintered on contact with a selenite crystal. In this case the core sample was discarded and the location re-sampled.

Of interest in Table 3.6 is the sample recovery ratio, since this is an estimation of the degree of sample disturbance. The ratio varied between 0.7 to 0.96, averaging 0.82 for the set. This is lower than the 0.98 specified for an undisturbed core. The variance may be explained by differences in saturation, soil type and stratification. It is noted that the greater part of the compression experienced occurred in the saturated overlying material, and that the *in situ* clay recovered from below the shear surface was relatively undisturbed, varying between 0.94 to 0.98 and averaging 0.97 (see Table 3.6).

3.32 Field instrumentation:

In section 1.4, the parameters pertinent to the study of the seasonal behaviour of mudslides were reviewed. These may be summarised as follows:

1. weather and climate;
2. pore water pressure;
3. soil moisture, and;
4. slope movement.

In addition it was concluded in section 1.5 that clay chemistry is an important factor in determining shear strength and the hydration and swelling behaviour of landslipped materials. This was confirmed in the detailed review of the physico-chemical properties of clay materials in Chapter Two. Thus, it is likely that the type and concentrations of exchangeable cations in the pore water may play a significant role in the swelling and shear strength properties of mudslide materials. The input of sea salts to coastal cliffs was considered to promote the weathering and shear strength reduction of coastal slope materials (section 2.312). Thus, the instrumentation programme was extended to include:

5. salt deposition, and;
6. pore water chemistry.

Before discussing the techniques used to monitor these variables, consideration was given to the use of electronic sensor and recording devices. It was concluded from Chapter One, that advanced methods of data acquisition had significantly improved our understanding of field

processes. However, it was noted that they are not without their limitations. They are not only expensive, but the sensitivity of data recordings may to some extent offset the ruggedness and durability of the equipment. This led Peck (1972) to state:

"The simpler device is likely to have the greatest chance of success - the more complicated the equipment the greater the likelihood of malfunction."

However, in our quest for knowledge and explanation, the need for long-term records and a better resolution of data is often reported (Thornes and Brunsden, 1977; Chorley, et al 1984).

Recent work (Allison, 1986; McConchie, 1986) on mass movements suggests that the use of data loggers is now a standard tool of the field geomorphologist. Allison (1986) and McConchie (1986) both used comprehensive networks of electronic sensor and data logging techniques. Thus, it was considered important to establish the advantages and disadvantages of using such equipment in place of more traditional methods. The advantages noted in these studies include:

1. the opportunity to record the chance event, seldom measured or observed by the field researcher;
2. the measurement of parameters at a resolution and frequency greater than attained by previous methods;
3. a variety of different parameters to be recorded simultaneously for future correlation;
4. a more sensitive analysis of processes operating in the natural environment and often in very remote locations, and;
5. a permanent record of events which may be stored on magnetic tape via a computer, analysed and reused as required.

However, both studies report problems involved in the design and running of the equipment. Data were occasionally lost through logger malfunction, amounting to 10 per cent of McConchie's data-base. For this reason the limitations of using data loggers must be borne in mind:

1. they generate vast quantities of data which requires rational methods of handling for the selection of significant parameters;
2. there are many reasons for malfunction, the most common being the loss of battery power. For whatever reason data may be lost for periods of weeks;
3. data loggers are not a replacement for traditional fieldwork; the possibility exists to ignore the latter for the more hi-tech methods. Data loggers can only be a tool of the trade;
4. they are expensive to purchase and maintain, and;
5. they are a liability where the public have access to the site.

For reasons of continuity with Allison's (1986) study and the remoteness of the Worbarrow site (208 km from London), it was considered that the advantages of using data logging facilities far outweighed the disadvantages. Subsequently, the instrumental techniques used by Allison (1986) have largely been adopted in this study, with slight adaptation, strengthening and redesign (see section 3.324), allowing a much greater emphasis on the monitoring of the geochemical aspects of mudslide processes.

3.321 *Weather and climate.*

The weather parameters of most importance in this study were:

1. precipitation;
2. wind direction;
3. wind speed, and;
4. the net hydrological flux.

For this purpose a Didcot Automatic Weather Station (Plate 7) was used at Worbarrow Bay throughout the monitoring period. For safety reasons, the station was located away from the cliff edge, 102 metres inland of the mudslide (Figure 3.3). Allison (1986) noted differences in the rainfall record between the station and mudslide, but it was felt that this climatic variation was not sufficient to invalidate the results.

In this study it was important to note the variable deposition of rain and air-borne salts. Thus, a digital event recorder was sited on the cliff-edge to the rear scarp of the mudslide (Figure 3.11), in addition to 6 salt gauges (section 3.325) located in a line, roughly 15 metres apart, from the beach up the mudslide and towards the weather station. This series of gauges supplemented the automatic data record to assess the influence of micro-climate. The weather station, event recorder, and salt gauges were installed using standard procedures and precautions (Ward, 1975; Bruce and Clark, 1980; Meteorological Office, 1982).

Plate 7.

Didcot Automatic Weather Station installed at Worbarrow.

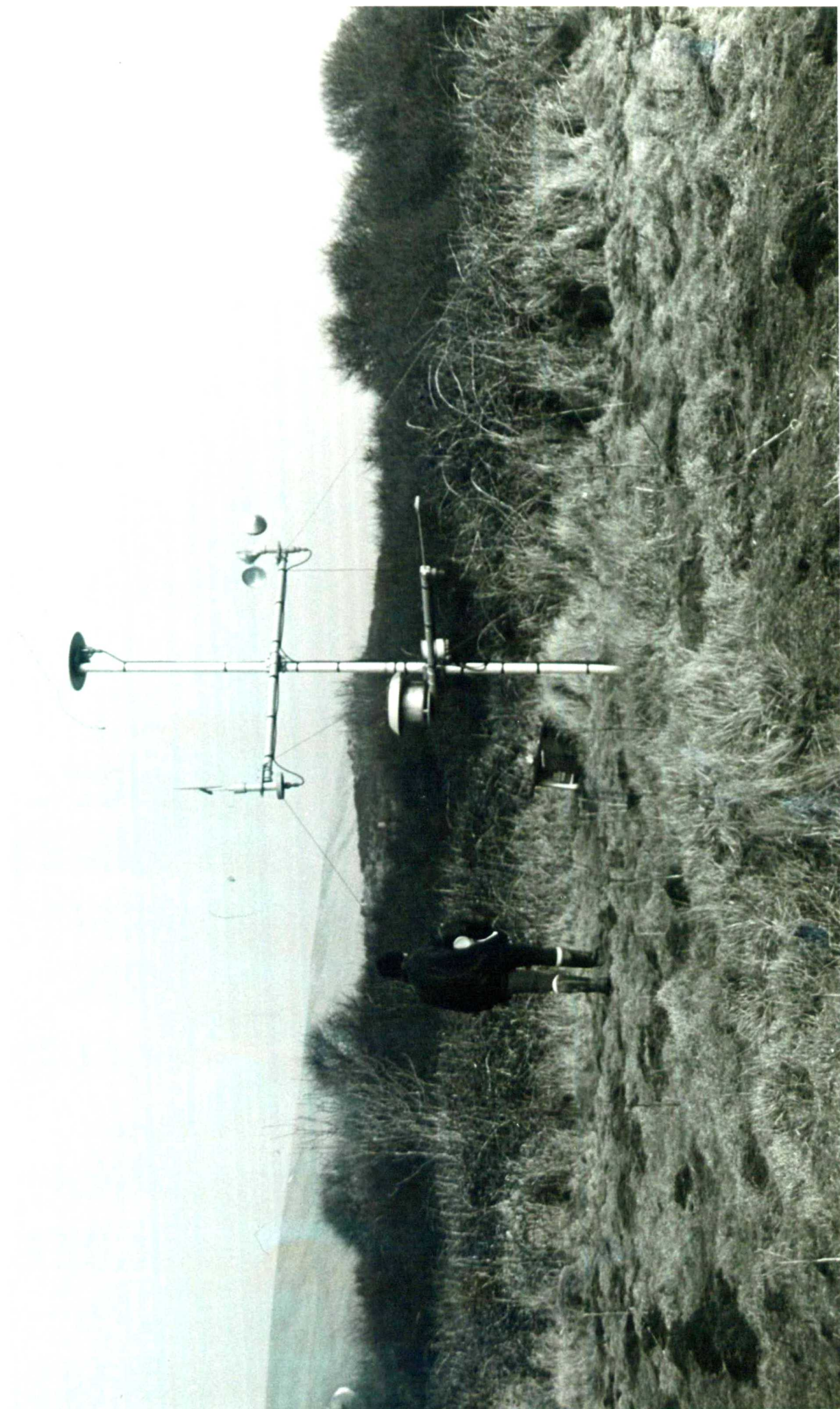
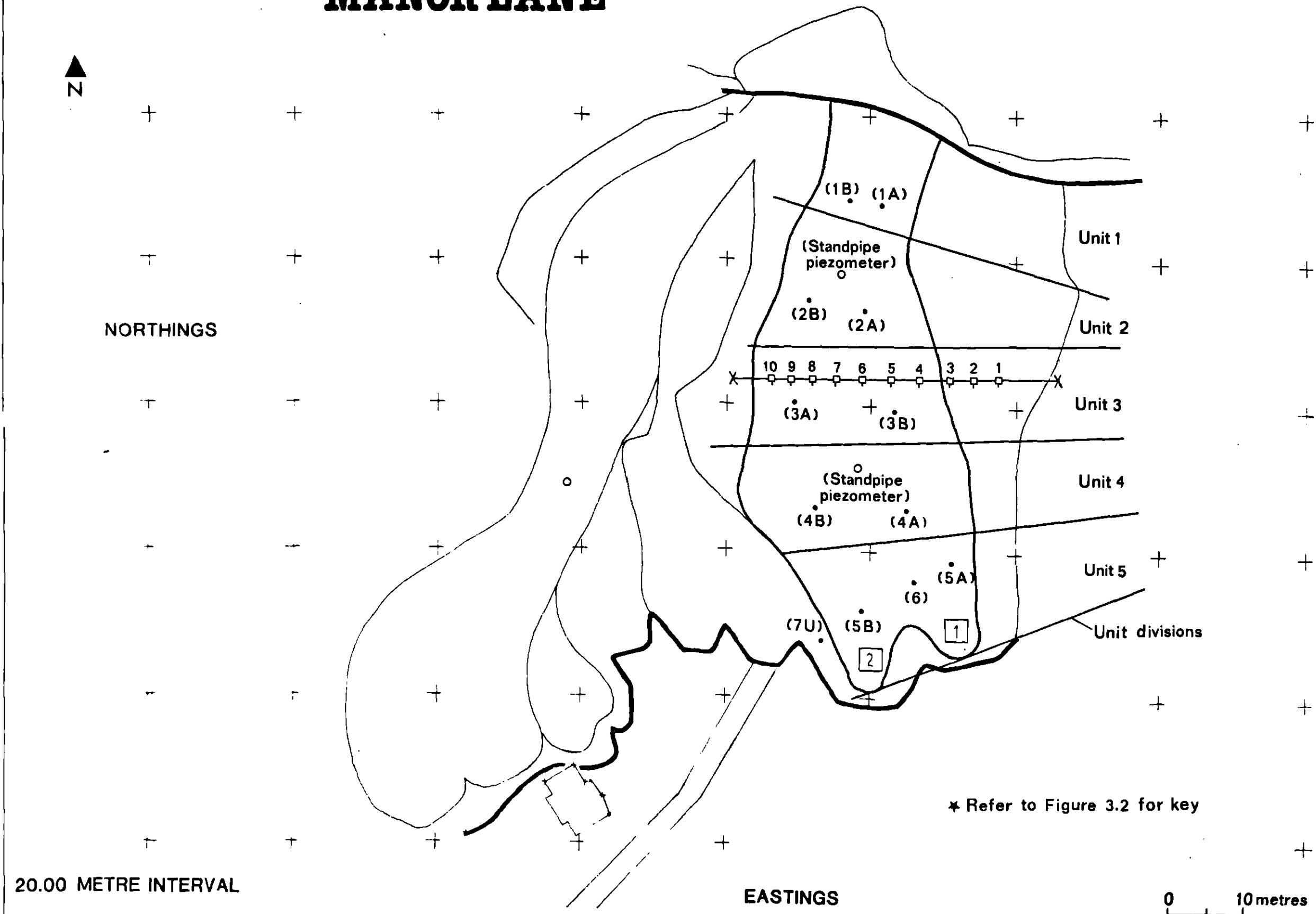


Figure: 3.10

INSTRUMENT AND SAMPLING LOCATIONS - MANOR LANE

DATE 86:04



Weather station data were controlled by a Microdata M200L data logger with an M200U interface unit and recorded on standard magnetic cassette tape, translated and analysed using a PDP11-23 computer. Likewise, bucket tips were logged every five minutes onto cassette tape by the digital event recorder. On return to the laboratory, the tapes were translated using a Microdata M200TR2 Cassette Translation System and a purpose written BASIC program for an Apple micro-processor. Manual records were kept for the salt gauges (see section 3.325) using the guidelines of the Meteorological Office (1982).

3.322 Pore water pressure.

The methods and techniques used to measure pore water pressures are widely reported (Anderson and Kneale, 1980; Anderson and Richards, 1987; Hutchinson, 1970; Vaughan, 1973), and the problems associated with its measurement and explanation were discussed in section 1.4. Two methods of measuring pore water pressure were chosen that were considered to be the most practical and useful for this study:

1. Casagrande porous plastic standpipe piezometers, and;
2. steel diaphragm pressure transducer water depth sensors.

Casagrande piezometers were located at Manor Lane and Worbarrow Bay, shown in Figures 3.10 and 3.11, respectively. Where piezometers were located on the mudslides, 6" diameter boreholes were augered down to the shear surface. A piezometer was also installed in the back-cliff of the Worbarrow site, but owing to resistant beds of sandstone, a Holman 1½" auger was used to excavate a borehole 3 metres deep. This was widened

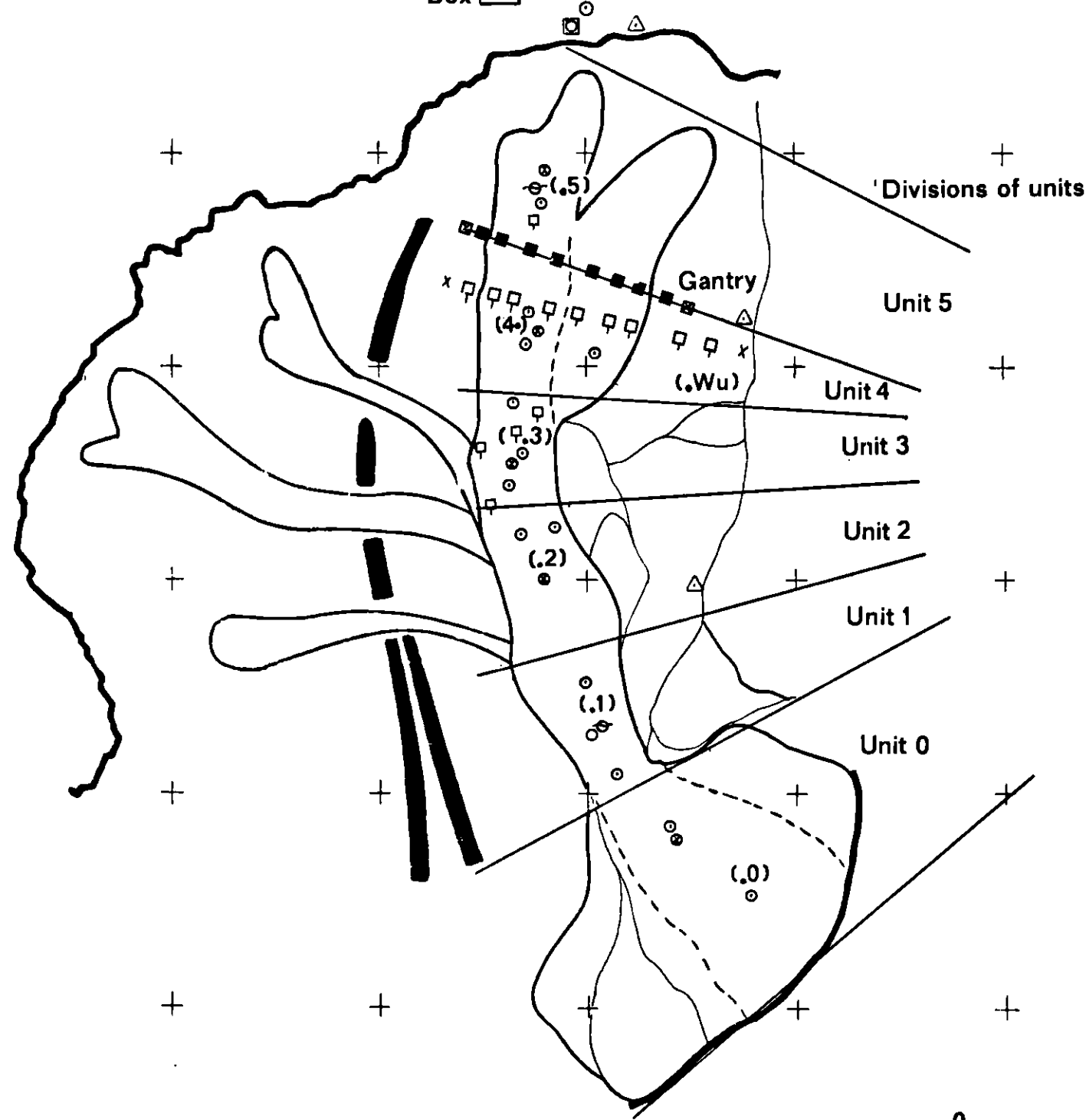
Figure: 3.11

INSTRUMENT AND SAMPLING LOCATIONS ~ WORBARROW

DATE 86:04



Datalogger
Box



* Refer to Figure 3.2 for key

10.00 METRE INTERVAL

0 10 metres

using a 2" bit, and the piezometer inserted. Each borehole was back-filled with sharp sand to act as a filter, and a bentonite clay mixture was used to create a water seal (Figure 3.12). The remaining cavity was filled with previously excavated material. Subsequent measurement of piezometric water levels was made to the nearest 0.5 cm using a dipmeter fitted with an 11 mm diameter PTFE brass probe (Figure 3.12).

At Worbarrow, two automatically recording water depth sensors were installed in boreholes in a similar fashion to the standpipe piezometers. One was located in the source and the other in the accumulation zone of the mudslide (Figure 3.11). The specifications of the sensors are given in Table 3.7. An Epsilon data logger and interface unit (Plate 8) were used to record data onto magnetic tapes, which were later translated using a PDP8 computer. Using previously measured calibrations for each sensor (Figure 3.13) the head of water at each location was obtained.

Allison (1986) notes many problems in the initial design and functioning of this equipment, which continued through the early stages of this project. The problems were caused by the requirement of the sensors to be continually energised. Data loggers only require power at the time of recording, so an interface unit was built to regulate a constant 15 volt DC supply to the transducers (Figure 3.14). An improved source of battery power was also provided in the form of an 8 volt, 25 ampere hour, lead acid battery unit per transducer (Plate 8). Following these alterations, the data record was considerably more reliable.

Figure 3.12. Installation procedure used for electrical and standpipe piezometers.

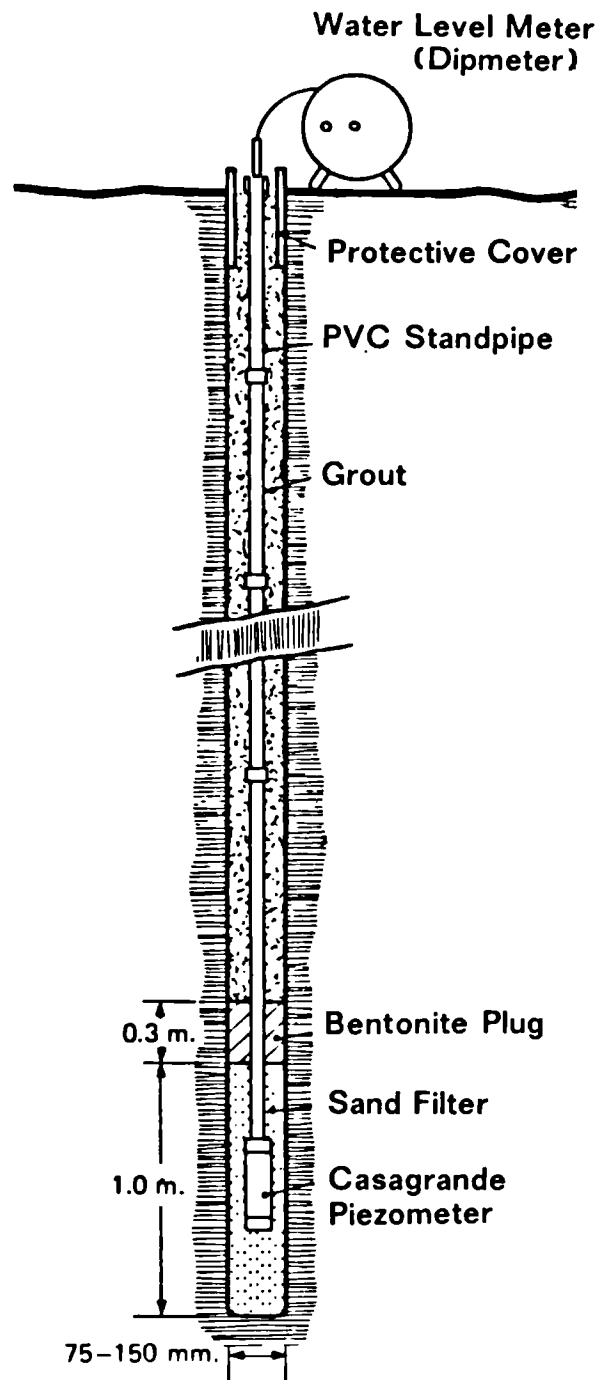


Table 3.7. Pore water depth sensor technical details.

TECHNICAL DETAILS	(A) SENSOR 1A-845-A	(B) SENSOR 1A-846-A
Range (Bar G)	0-1	0-1
Supply (Volts A.C.)	+10.0	+10.0
Sensitivity (mV/V ⁻¹ Bar G ¹)	5.88	5.84
Non-linearity and hysteresis (% F.S.)	±0.02	±0.10
Full range output (mV)	58.8	58.4
Input resistance	1761	1726
Output resistance	434	455
Manufacturer:	Shape Instruments Limited	
Transducer type:	Water depth sensor	
Type Number:	SH2-P5300-SP65L-15MO	
(A):	Source piezometer	
(B):	Accumulation piezometer	

Plate 8.

Epsilon data-logger and interface unit.

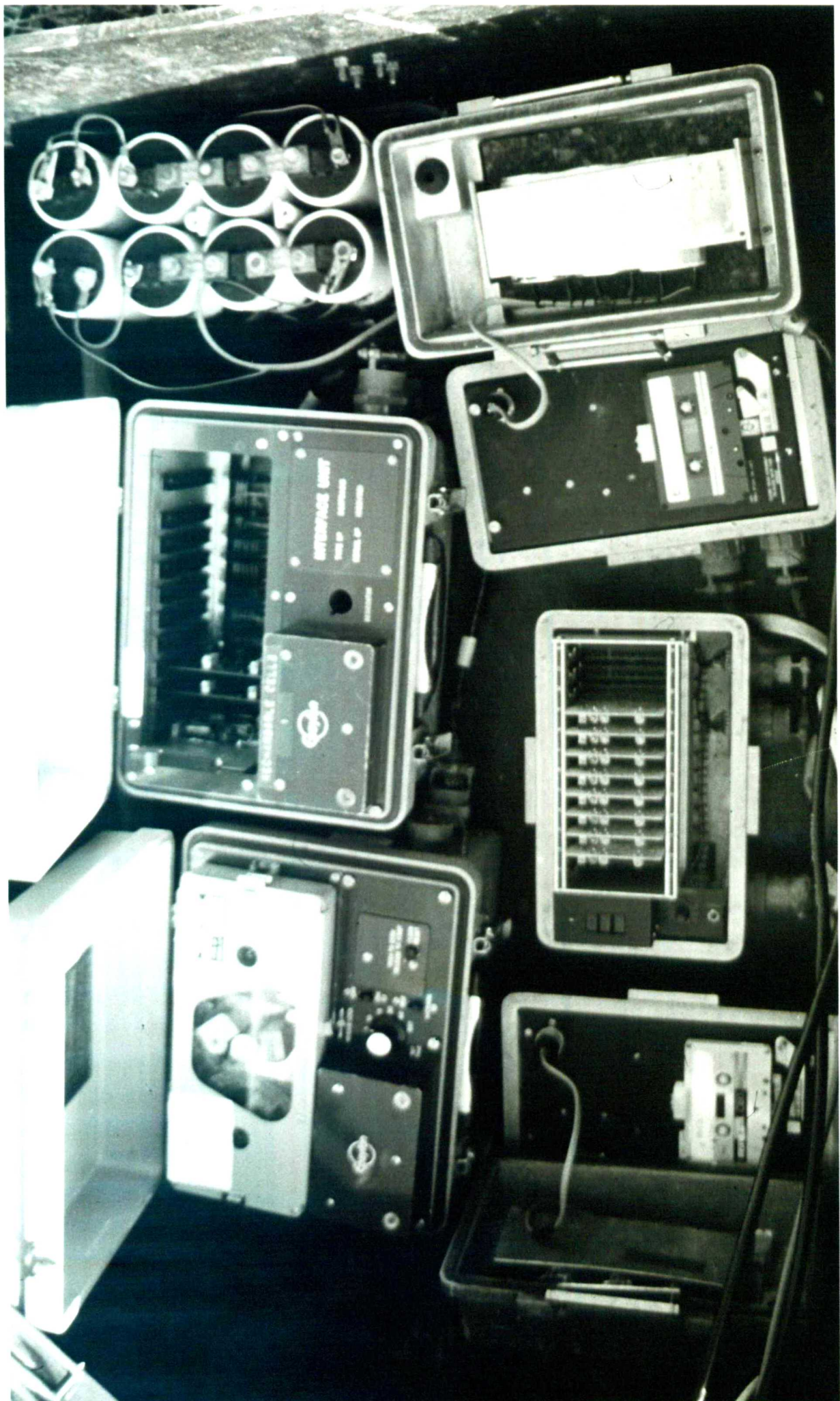


Figure 3.13. Calibration curves for the automatic water depth sensors.

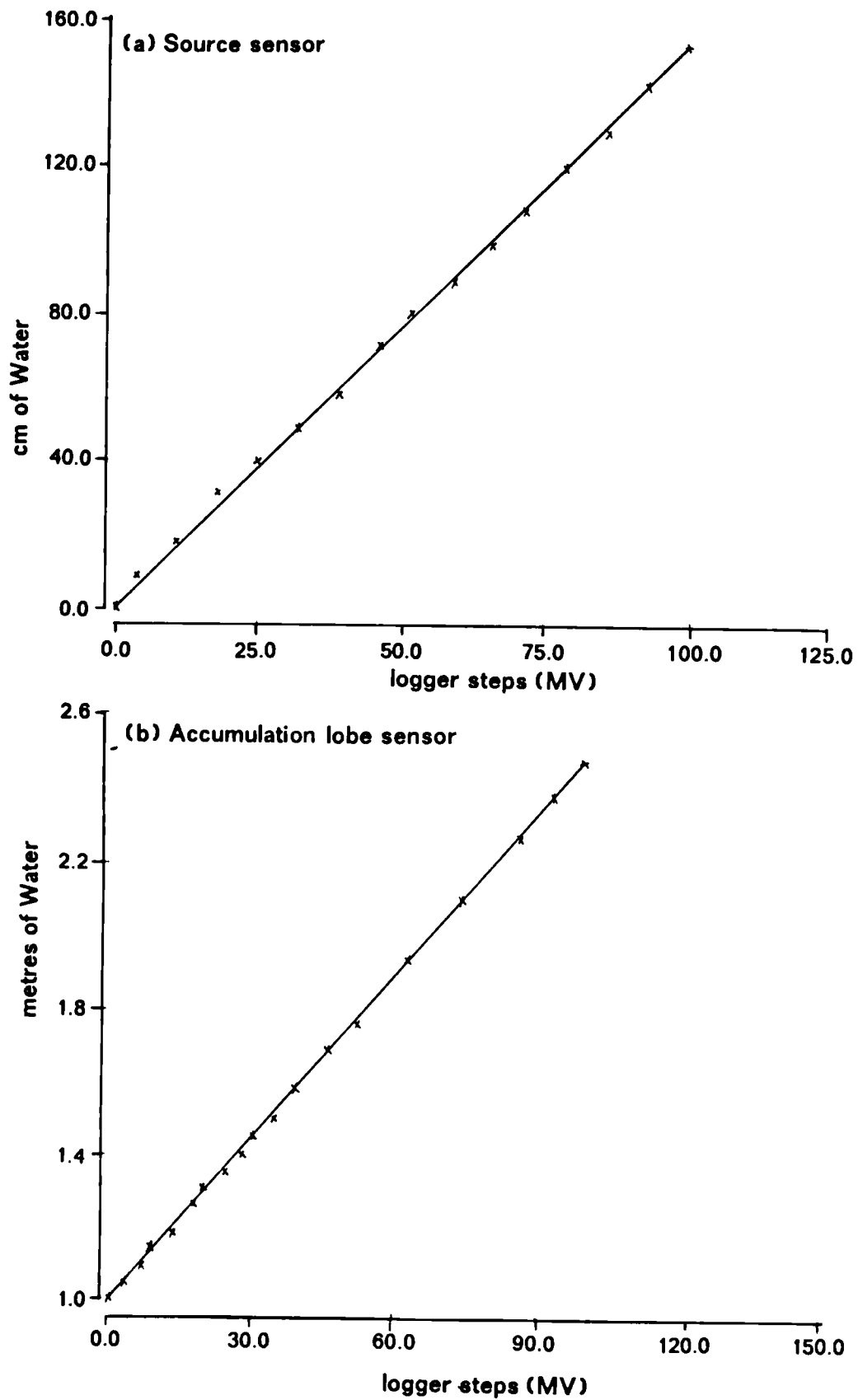
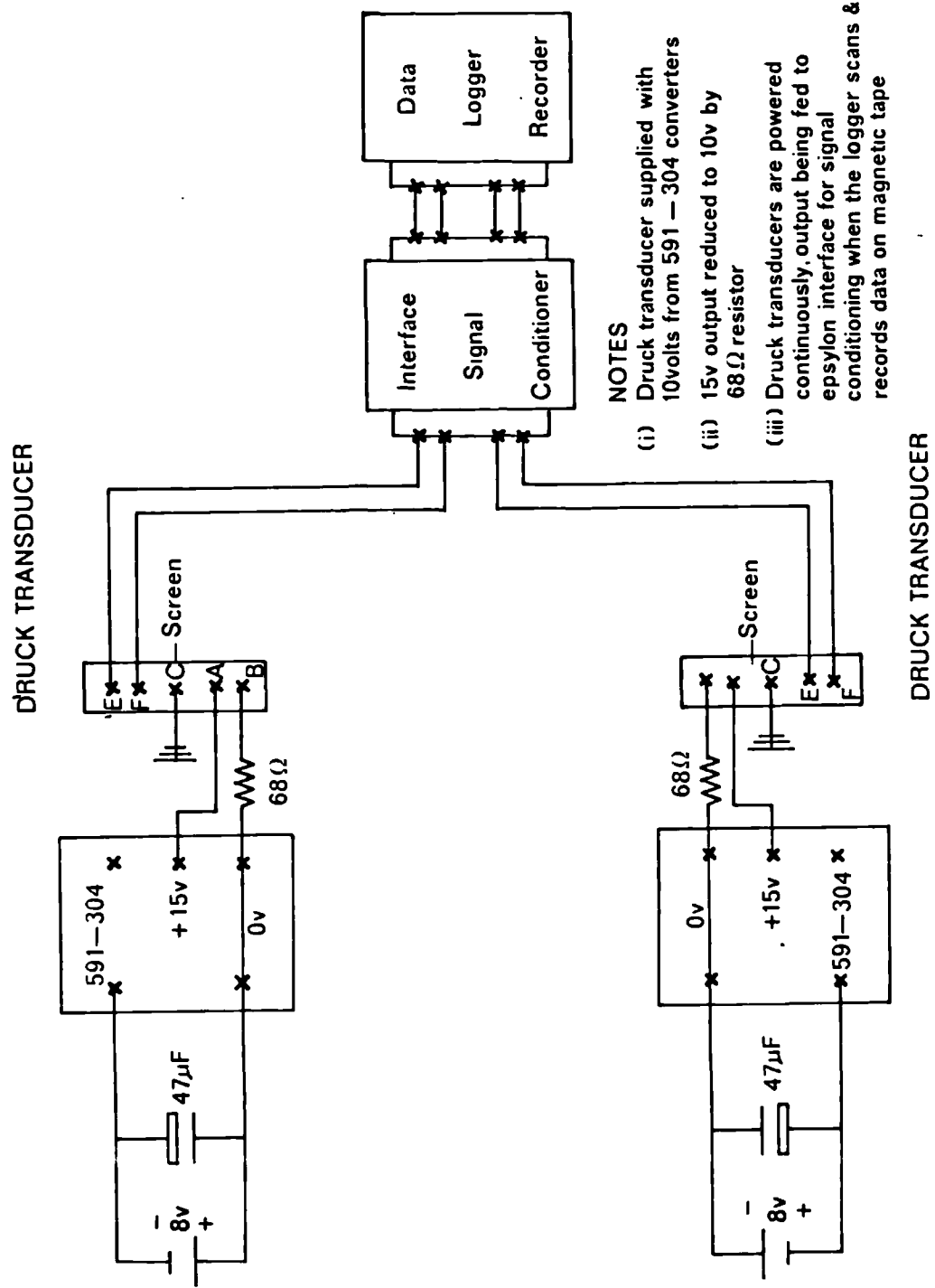


Figure 3.14. Interface design to control the water depth sensor battery-transducer link.



3.323 Soil moisture.

A Pitman soil moisture meter or Neutron Probe (Plate 9) was used to provide the precise measurement of soil moisture profiles within the Worbarrow mudslide via a network of 14 access tubes (Figure 3.11). The technique was discussed by Bell and McCulloch (1969), Greacen *et al* (1981) and Visvalingham and Tandy (1972). Both Allison (1986) and McConchie (1986) have used the technique in mass movement studies. The advantages of the technique were recognised and include:

1. a record of a continuous soil moisture profile;
2. little disruption to the site, since measurements are taken via previously installed access tubes;
3. the measurement of soil moisture *in situ*, reducing errors inherent in other extractive methods;
4. a moisture profile is measured over a sphere of influence, eliminating the errors incurred by point sampling due to lithological variability, and;
5. measurements taken periodically for each access tube, may be compared over time to assess the temporal change in the soil moisture status.

However, the technique is known to have some sources of error which are considered in a report by the Institute of Hydrology (1981). It is known that the count rates (readings) can be affected by the following:

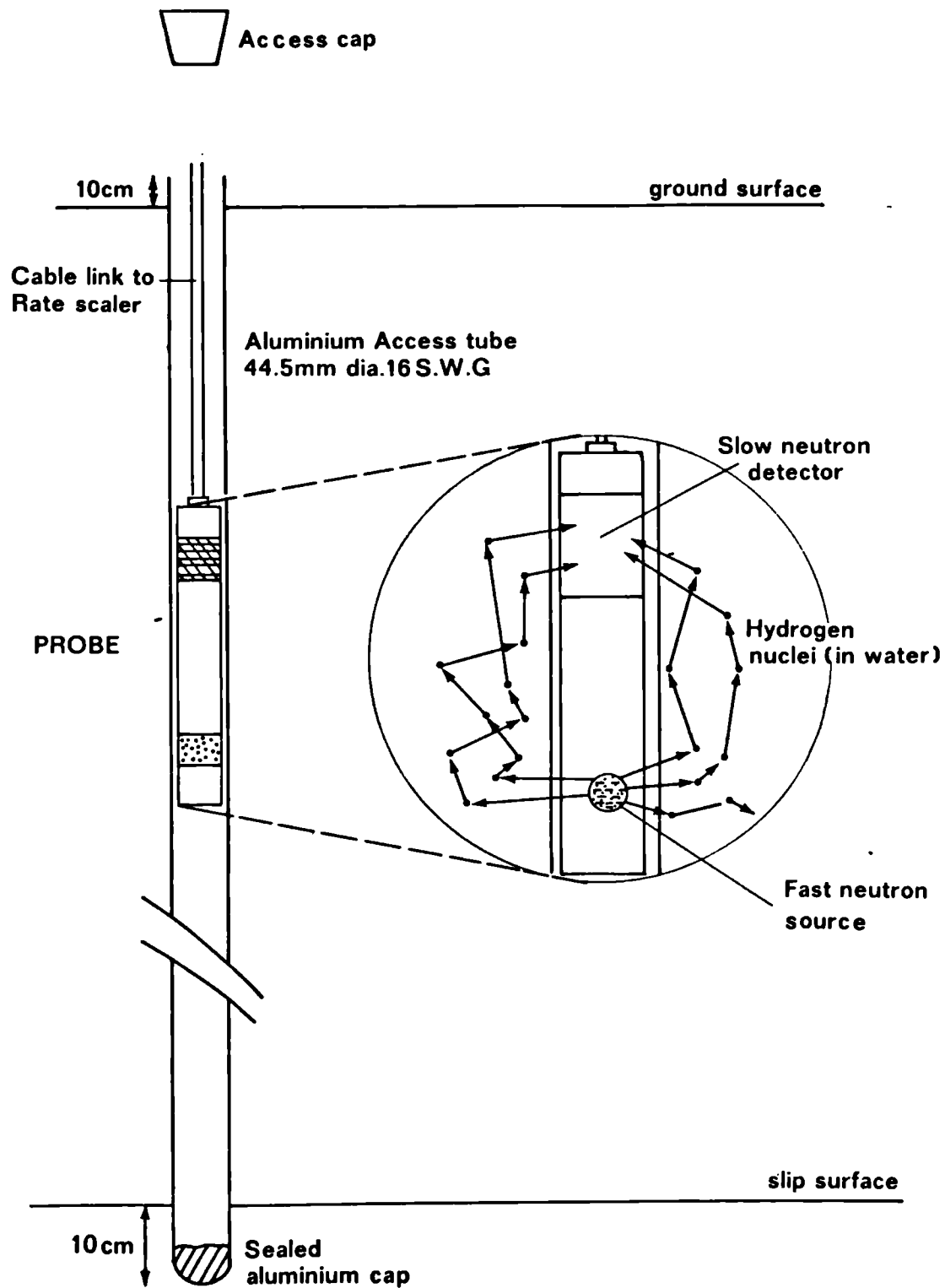
- a. hydrogen ions in association with bound water and humus, and not free water;
- b. neutron adsorbing elements such as boron, cadmium and chlorine;

Plate 9.

**The Pitman soil moisture meter or neutron probe
in use at Worbarrow Bay.**



Figure 3.15. Access tube installation and the principle of the neutron soil moisture meter.



- c. variations in soil density, and;
- d. variable soil texture.

In addition, the use of this technique requires abidance with the Radioactive Substances Act (1960), the Health and Safety at Work Act (1974), and the guidelines of the Ionising Radiations Regulations (1985) issued on the 1st January 1986.

With careful consideration to the limitations of the use of the Neutron Probe, the assessment of *in situ* soil moisture profiles was considered advantageous to this study. The principle of the probe is that hydrogen in the soil scatters fast neutrons, converting them to slow neutrons, which are then counted by the probe detector (Figure 3.15). The number of slow neutrons detected is related to the number of water molecules. The readings are calibrated for soil density, and standard counts are obtained before and after each site visit by measuring a moisture profile via an access tube suspended in a drum full of water.

The 14 access tubes established at Worbarrow were inserted by augering a tight-fit hole using a technique described by the Australian Water Resources Council (1974). Care was required during installation not to destroy the natural particle arrangement around each access tube, and to ensure that there was no air space between the tube and soil. All access tubes were located in the mudslide except for one 3 m length tube inserted in the back-cliff (Figure 3.11).

During each site visit measurements were taken at 10 cm intervals down each tube, from 20 cm below ground level, using a 16 second count rate.

The readings were recorded manually and analysed by a purposely written BASIC computer programme.

Following slope movement, the access tubes became progressively distorted, and some were even broken. These required replacement each season and it was noted that as movement took place the positions of the tubes changed, although it was felt that the moisture profiles measured were consistent for the slope sections in which the tubes were initially set.

3.324 Surface movement.

Many techniques have been used to monitor slope movements, the most common being the location and survey of targets on the surface of unstable slopes (Bentley, 1985). The problems associated with obtaining movement records usually centre around two factors:

1. targets can only provide cumulative or average rates of movement, and it is rarely possible to derive single-event movements or a continuous record, and;
2. assessment of surface movements may not necessarily reflect the movement occurring along the basal shear surface.

Attempts have been made to obtain a continuous record since the 1970s when Prior and Stevens (1972) developed a mechanical technique in the form of a modified Monro water level recorder. This technique was further used by Craig (1979) but Brunsden (1984) noted that there is much scope for improvement in these techniques by using electrical sensors and micro-processors.

Alternatively, Bentley (1985) has suggested ways in which target movements can provide a great deal more than simply 'watchdog' information such as locating shear boundaries, while Allison (1986) has pioneered a continuously recording micro-processor based movement sensor technique. As a result mudslide movements were assessed in three ways:

1. the direct measurement of targets from a fixed datum line;
2. the photogrammetric measurement of targets in object coordinate space with terrestrial photographs (see section 3.22), and;
3. by an automatic unwinding pulley and rotary potentiometer system spanning the slope on a gantry.

Movement targets were established at Manor Lane and Worbarrow Bay. The automatic technique of Allison (1986) was improved and redesigned for use at Worbarrow, while the photogrammetric analysis of a number of field surveys at Worbarrow has already been discussed in section 3.221.

With reference to Figure 3.10, a line of movement stakes were installed at Manor Lane, and surveyed to a reference datum during the 1985-1986 winter season. The stakes were 0.7 m long and constructed of 2:1" pine wood with small aluminium plates bolted into a groove at the top of the peg. Identification numbers were painted onto the plates. The reference datum was re-established every site visit, and the stakes re-measured using a 30 m tape, normal to the datum line (see Appendix 12).

At Worbarrow a similar line of stakes was established and measured (Figure 3.11). These were installed for a number of reasons; to support the automatic technique in case of malfunction, to test the accuracy of the various techniques, and to provide control points for the photogrammetric survey.

Figure 3.16. Automatic movement sensor design.

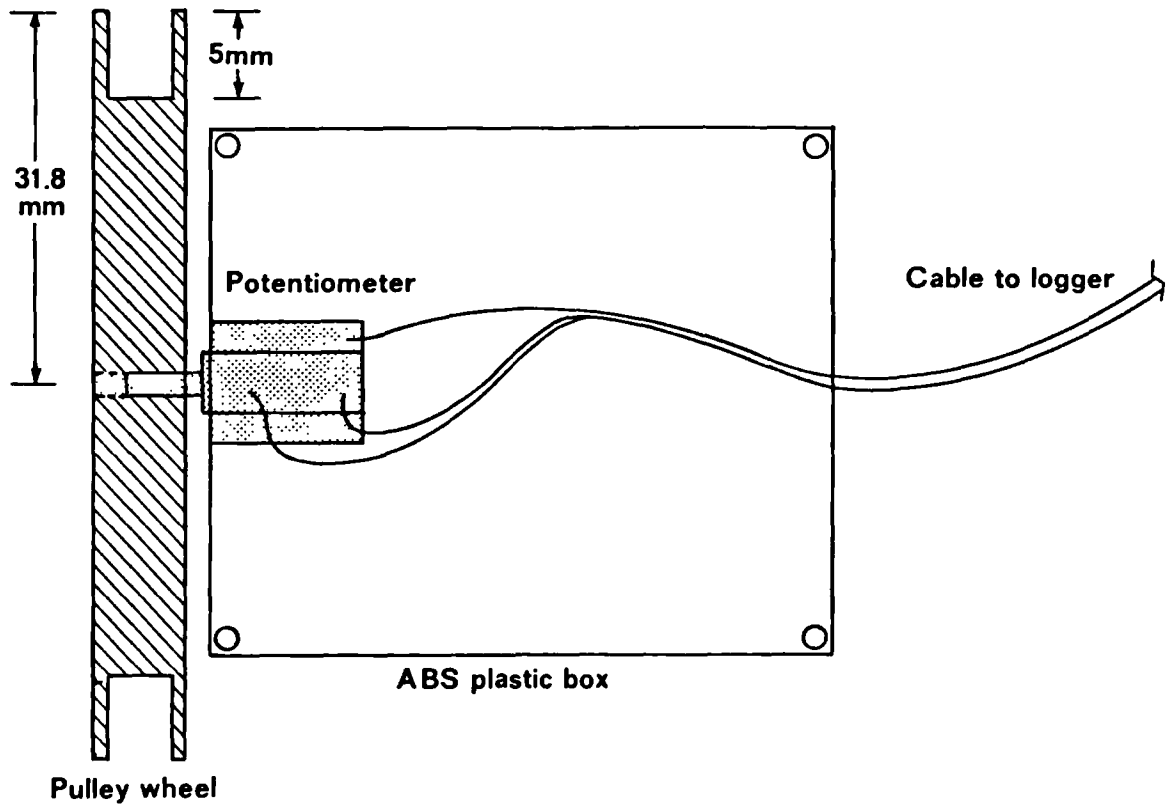
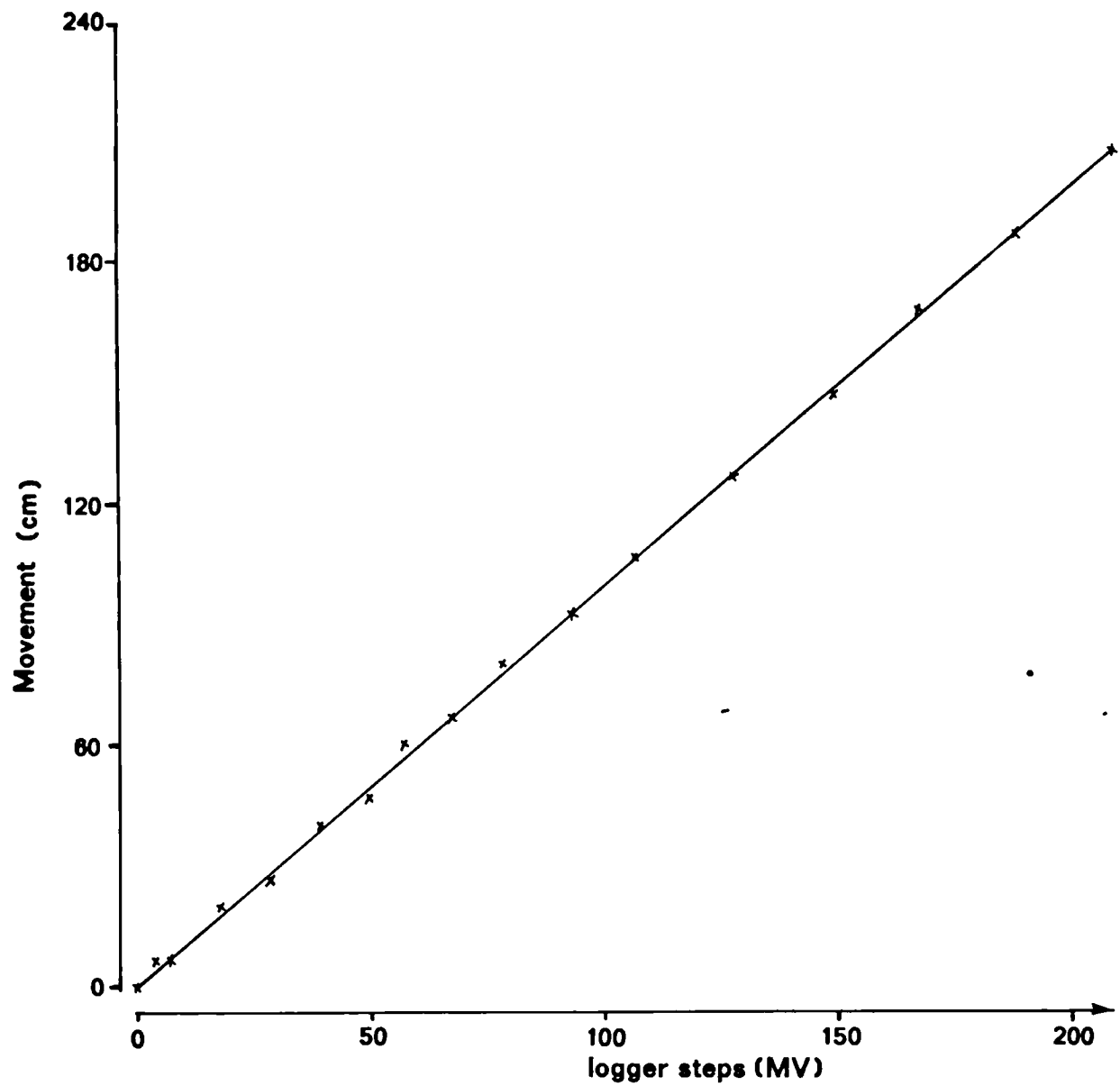


Figure 3.17 Typical calibration of movement sensors.



Movement was automatically recorded using a micro-processor based system with rotating potentiometers as movement sensors. Eight sensors supported on a gantry were attached to the surface of the mudslide with nylon wire fixed to 10" pins inserted into the ground. Each sensor consisted of a rotating potentiometer secured in a protective A.B.S. box with the potentiometer shaft extending through an end wall (Figure 3.16). A pulley wheel was joined to the shaft to carry the nylon wire. The pulleys were machined to a precise calibration (Figure 3.17), so that a loss of 1 cm of wire was equivalent to 1 logger step recorded on the data logger. Data were recorded on standard cassette tape via a Microdata M200L data logger and interface. Using purposely written software, data were transferred to disc and analysed using an Apple II micro-processor.

Problems were encountered with the initial design (Allison, 1986), such as excessive loss of wire from the pulleys, flexure of the gantry during strong winds, and the seizure of the potentiometers. Improvements were made to the equipment which included:

1. the installation of a firm 11 m span scaffolding gantry (Plate 10), following the destruction of earlier prototypes during slope movement (Allison, 1986), and;
2. a completely new and improved cable link and wiring design, including a channel port link (Plate 11) on the gantry, and the separation of 8 sensors into 4, two-channel units. This meant that individual sensors could be serviced without dismantling the entire device.

It is also recommended that better quality potentiometers and sealed metal boxes be used in future designs, to prevent seizures of the potentiometers and damage to the plastic boxes as the wire is pulled by the moving mudslide.

Plate 10.

Gantry installed at Worbarrow for monitoring surface movement.

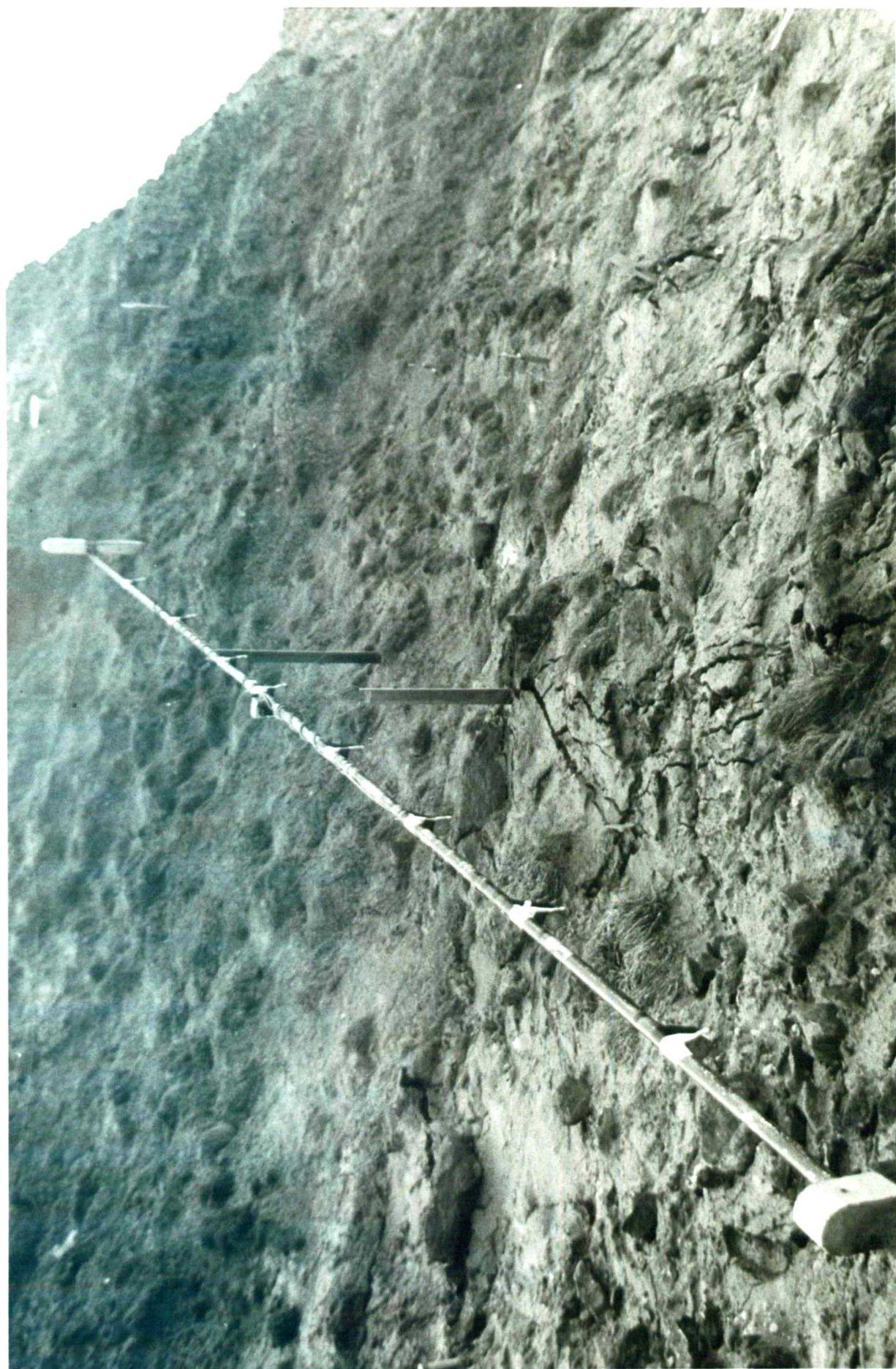
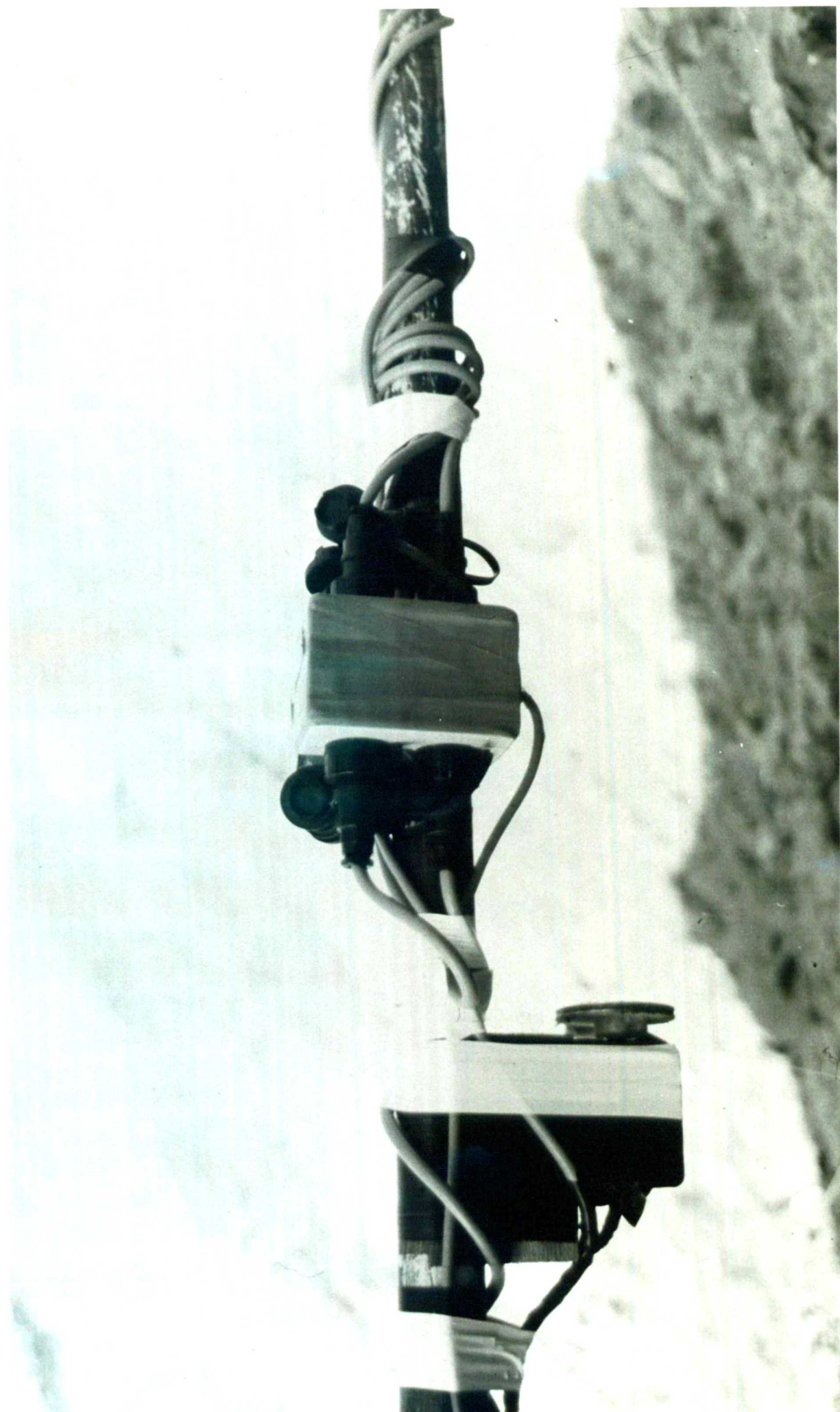


Plate 11.

Cable and channel port link to movement sensors.



3.325 *Salt deposition.*

To facilitate the assessment of the magnitude and seasonal pattern of salt deposition on the mudslide and surrounding cliffs, a large number of rain gauges were required. The gauge had to be accurate, constructed of materials that would not contaminate the sample, and cost effective to produce in bulk. These requirements meant that conventional gauges were unsuitable, so it was decided to build the gauges from basic materials.

The gauge design as shown in Figure 3.18 was based on a similar gauge used by Likens (1967). The materials used in its construction, consisted of two bottles and lids of one and half litre capacities, a funnel 16.9 cm in diameter, three sizes of tubing of 6 mm, 12 mm and 19 mm inside diameters, and various tube connectors. During the monitoring programme the sample bottle capacity was increased to 2 litres. The component specifications are given in Figure 3.18, and were mostly made of polyethylene plastic.

The design was such that it would reduce errors arising from the evaporation of the sample; the sample tube contained a U-bend full of water and an evacuation tube, leading to a smaller bottle full of water, to allow air to escape from the sample bottle during infilling. This reduced the total evaporation surface from 72.4 cm² to 2.3 cm².

The efficiency of the gauge was tested for a variety of adaptations before field installation, such as the use of different funnel and tube sizes and splash suppressors. The final design (Figure 3.18) was chosen since it conformed most closely to the standard gauge (Meteorological

Figure 3.18. Salt gauge design.

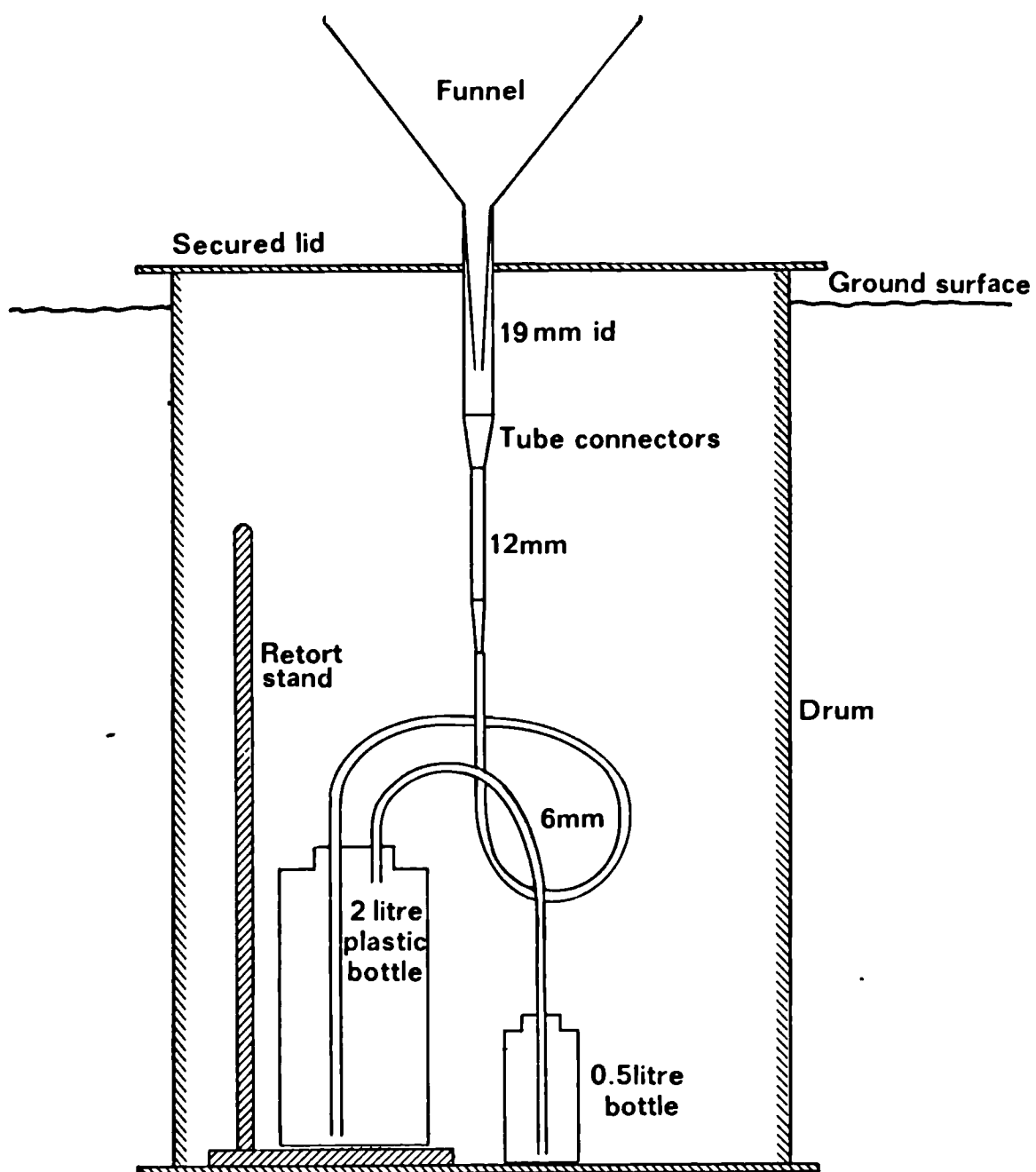
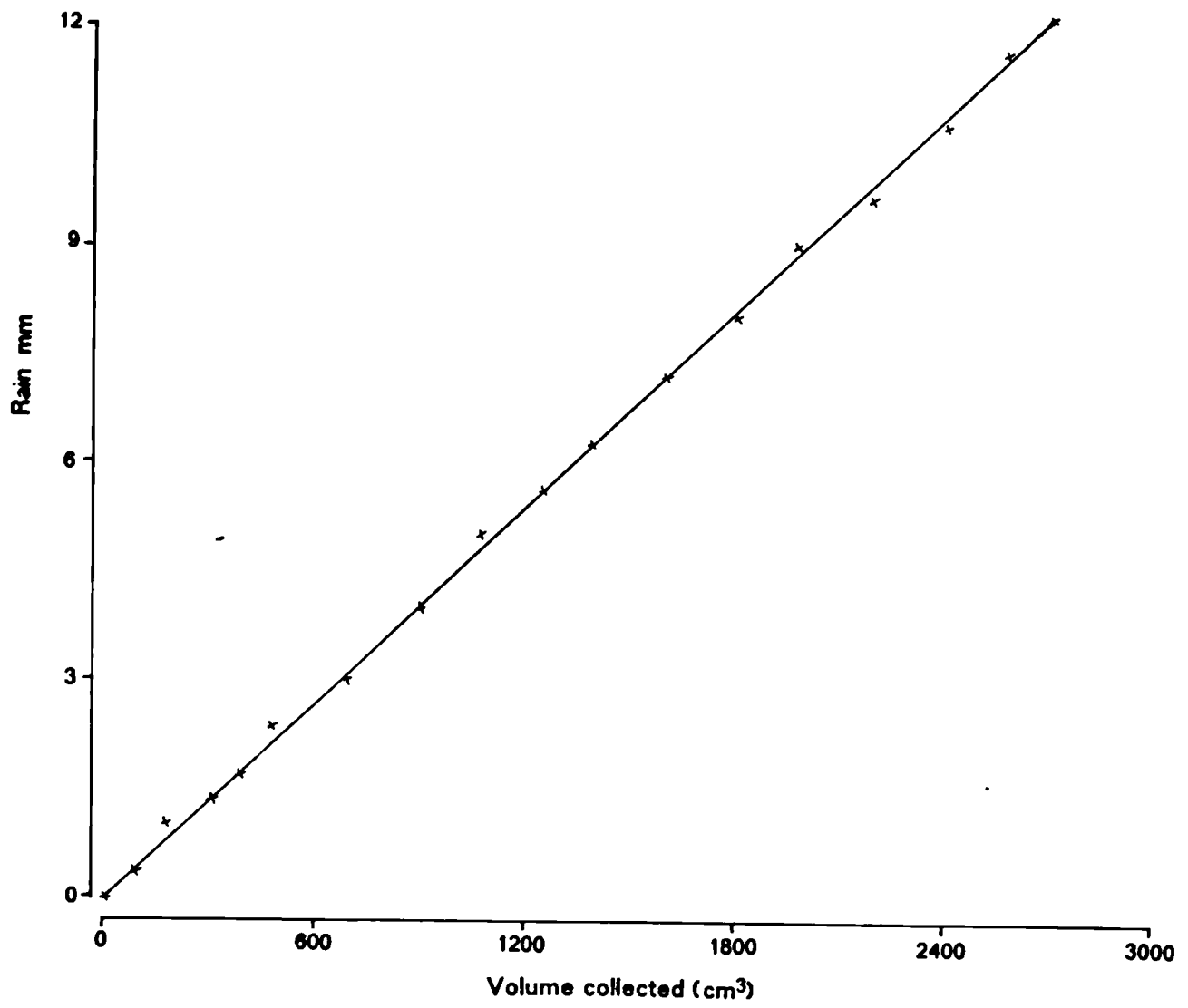


Figure 3.19. Typical rainfall calibration of each salt gauge.



Office, 1982). The addition of splash suppressors was found to make no improvement to the accuracy of the gauge during trials.

Before field installation the gauge was mounted in a cylindrical drum with base, as shown in Figure 3.18, to secure the funnel and internal bottles from damage. The whole gauge was thoroughly washed with a 10 per cent solution of nitric acid before use and after each sampling. Control samples were initially taken in the field; 250 cm³ of distilled water was poured into the gauge, and the funnel covered with cling-film. After 24 hours a sample was measured and taken back to the laboratory and tested for contamination. This was subsequently found to be negligible.

During each site visit, the volume of rain collected was measured using a clean 250 cm³ plastic measuring cylinder. When the gauge was empty the funnel was washed with 200 cm³ to assess dry-salt deposition. On each occasion a small 100 cm³ sample was saved in a polyethylene bottle. The pH and conductivity readings were measured in the field and samples returned to London for analysis. Using the calibration of the gauge, shown in Figure 3.19, the total rainfall (in mm) was calculated from the volume collected over the period between site visits.

3.326 Pore water chemistry.

Sampling pore water from the basal shear surface of a mudslide presents a number of logistical problems:

1. the sampler has to be sufficiently robust to withstand the stresses involved during slope movements;

2. the sampler has to remain at the shear surface;
3. the sampler must contain a representative, uncontaminated, sample of interstitial free water at the shear surface, and;
4. in the event of loss and breakage, the equipment must be replaceable and inexpensive.

Traditionally, lysimeters are used in soil science for the collection of leachates and ground water (Brady, 1984). In addition, there is a variety of soil water equipment available on the market (Soil Instruments, 1986), such as soil water samplers, although these are expensive and usually constructed with ceramic cups. Ceramics should be used with care since they cause slight contamination of solutions (Richards, 1954).

With these considerations a variety of techniques were used at Worbarrow to extract pore water from the shear surface:

1. casagrande porous plastic standpipe piezometers;
2. porous plastic piezometer tips attached to reinforced nylon tubing;
3. specially constructed lysimeters, and;
4. the extraction of saturated clay samples from the basal shear surface using a Hiller auger.

The most successful and consistent technique was the extraction of clay samples since no instrumentation was required. However, the clay extracted had to be further analysed in the laboratory to extract the interstitial pore water from the clay (section 3.42). Ideally, pore water solutions needed to be obtained from the field to substantially reduce the time required for laboratory analysis. A lysimeter was

designed and built for this purpose, although once installed in the field, their performance was very disappointing for two reasons:

1. during movement, the connecting tubing was sheared from the lysimeter, and;
2. during installation, some lysimeters rotated so that the connecting tube was at the top of the sampler, reducing the ability to extract solution.

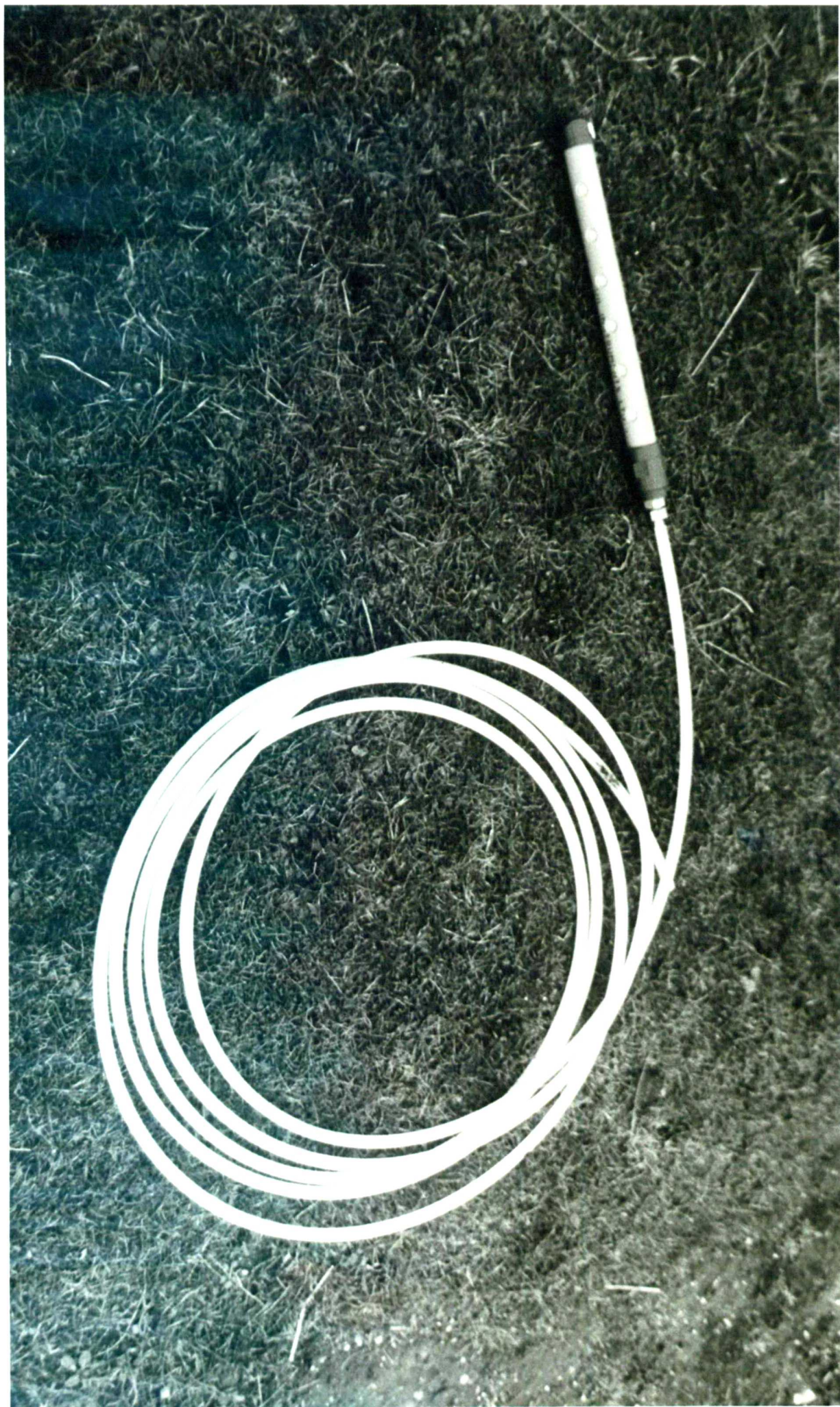
As a result of this initial attempt, attention was given to the use of porous plastic piezometer tips. Standpipes can be used for the extraction of solution, although the longevity of the equipment is usually foreshortened by slope movement. It was the intention of this technique to extract pore water before, during and after slope movements.

Success was eventually achieved by designing a piezometer tip attached to reinforced nylon tubing (Plate 12). Using strong cleated nuts the tubing was firmly glued, locked and sealed to the piezometer tip using a specially machined plug. Once installed in conventional boreholes (section 3.322), the tubing was pulled into the slide as movement took place, the sampler maintaining its position at the shear surface.

Six samplers were installed, including one towards the rear of the mudslide to collect ground water (Figure 3.11). During sampling a clean rigid plastic micropore tube was inserted down the nylon tubing into the piezometer. Solution was extracted using a 50 ml capacity syringe and stored in polyethylene sample bottles. The nylon access tube was then resealed. Conductivity and pH were measured in the field and samples taken to the laboratory for analysis (section 3.42).

Plate 12.

Pore water sampler design.



Inevitably, some of the gauges were buried, which required supplementing the data record with pore water extracted from clay samples. Controlled experiments were performed to test the results of the chemical tests from solutions obtained by the different techniques (section 3.42). They were found to be in reasonable agreement, so that the extraction of clay from the shear surface was considered a reliable compromise to the loss of samplers.

3.33 Monitoring framework and site maintenance.

A network of three data loggers recording weather, movement and pore water pressure, one digital event recorder, and the periodic measurement of soil moisture, movement, pore water pressure, salt deposition and pore water chemistry, formed the basis of the monitoring programme at Worbarrow Bay from October 1985 to May 1987. The instrumentation and sampling locations were grouped into six sub-sites (for each unit in Figures 3.10 and 3.11) within the mudslide and back-cliff for future correlation and to maximize the variability of the parameters being assessed. At Manor Lane, the periodic measurement of movement and pore water pressure took place between October 1985 to May 1986.

Data were collected at four temporal scales:

1. monthly;
2. weekly;
3. daily, and;
4. every 5 minutes.

At Manor Lane and Worbarrow Bay, manual measurements taken during site visits between October 1985 and May 1986 were only sufficient to establish a monthly average; site visits within this period were approximately every fortnight. Throughout November 1986 and May 1987 site visits to Worbarrow Bay were increased to weekly intervals. The data loggers further enabled the resolution of recordings to be taken every 5 minutes and thus provided a detailed daily summary.

With reference to Table 3.8, the field parameters measured at Worbarrow are detailed with a summary of the record interval and the total number of readings taken during the field work. Data were lost during the study for a number of reasons. The most common was through loss of battery power. On other occasions a data logger recorder motor malfunctioned, and some movement sensors seized, giving unreliable readings. However, the total loss of data when compared to the overall record amounted to only 7 per cent.

The choice of an appropriate logger scan rate was influenced by a number of considerations: the ideal scan rate maximizes the flexibility of data recordings, but minimizes the number of site visits, ensures the maintenance of a continuous data record, and remains within the data logger storage capacity. For such reasons, it is standard practice to operate the automatic weather station on a 5 minute scan rate, which typically functions for two weeks, or at a stretch three weeks with good batteries and a C60 capacity audio cassette.

The data logger network was thus set on a 5 minute scan rate to allow for the acquisition of a data set that could be subsequently compared on the same time-base, and would provide a sufficient level of detail or

Table 3.8. Summary of parameters, record interval and total length of data-set established from field-monitoring at Worbarrow.

MEASURE	#	SENSORS	RECORD INTERVAL	TOTAL RECORD OCT 1985+	PARAMETERS
Automatic Weather Station	1	8	5 minutes	1,342,976	Rain, Temp, Wind, Sun Rad ¹ , Evap
Event Recorder	1	1	5 minutes	163,840	Rain
Salt Gauges	6	1	Site visits*	3,024	Rain, Na, K Ca, Mg, Cl SO ₄ , HCO ₃
Slope Movement	1 20	8 1	5 minutes Site visits	1,305,232 1,260	Movement (cm)
Pore water pressure	2 2	1 1	5 minutes Site visits	283,520 126	Phreatic surface (cm head)
Soil water profiles	6	14	Site visits	882	MVF, %water
Pore water chemistry	6	1	Site visits	3,780	Na, K, Ca, Mg SO ₄ , Cl, Al, Fe, HCO ₃ , Si

TOTALS:					
Actual	45	36		3,104,640	
Expected	45	36		3,336,048	
Automatic	5	18		3,095,568	
Manual	40	18		9,072	

* Site visits at least every 2 weeks; during winter period every week.

¹ Rad: net radiation.

MVF: moisture volume fraction.

resolution of the parameters being assessed. Brunsden and Thornes (1978) have noted the need for more attention to experimental design and temporal sampling frameworks, stating:

"continuous observation is the only real way to catch the rare but sometimes important event."

The monitoring and temporal framework was thus considered to be the most extensive and comprehensive achieved in mass movement studies.

During site visits a small amount of maintenance was required for a number of reasons:

1. to maintain the operation of the data loggers and electronic sensors;
2. to ensure the security and cleanliness of the salt gauges, and;
3. to replace or re-locate lost pore water samplers and access tubes following major slope movements.

The viability of the logger network was maintained every site visit with a change of batteries and magnetic tapes using standard procedures. The GMT start and finish times were noted during the replacement of each cassette. Checks were routinely made to the logger mechanism and recording heads.

In addition, the movement sensors were frequently greased to prevent seizure and the loss of wire from the pulley through buffeting by the wind. The water depth sensors required occasional cleaning following clay blockage of the transducer pores and thus subsequent re-location. All the data loggers were housed in a 'black box' secured with two

padlocks which required frequent greasing to prevent rusting. Likewise, the padlocks securing each salt gauge required frequent greasing to reduce seizure, although these had to be replaced on several occasions. Following sampling, the gauges were also thoroughly cleaned with a 10 per cent nitric acid solution.

After major slope movements, it was necessary to replace some access tubes and pore water samplers. The location of each equipment site was re-established and new equipment installed. It was inevitable that during relocation, the exact positioning of the equipment may have resulted in some error. Moreover, the sub-sites chosen for the network would have moved slightly from their original positions following movement. This was assessed as a matter of course in the survey of the site.

It was found that with a small amount of continuous maintenance, the number of field-visits requiring major maintenance and relocation of equipment was kept to a minimum, with a resultant preservation of the data record.

3.4 Laboratory methods.

A wide range of analytical techniques was used in this study for the assessment of the physico-chemical properties of clay soils, the identification of clay minerals, and the routine determination of rain and pore water chemistry. Although it is preferable to carry out as many tests as possible *in situ*, constraints on some techniques such as the conditions at the time of sampling and the lack of recognised and available *in situ* methods, meant that the majority of the description and analysis of soil samples was undertaken in the laboratory.

The accurate analysis and description of soils is fundamental to both soil science and soil mechanics, and due to the dual nature of this research, standard laboratory methods have been used from both disciplines. Many textbooks describe methods typically used in soil analysis, such as Black (1965), Stuckl and Banwart (1980), Klute (1986), Smith (1983), Loveday (1974), Richards (1954) and Avery and Bascombe (1974). Standard techniques used in soil mechanics are detailed in British Standards (1975), Vickers (1983), Lee *et al* (1983) and Head (1984).

Problems exist in selecting representative samples for testing both in the field and laboratory due to the likelihood of disturbance and deterioration as a result of extraction and transportation. While efforts can be made to reduce these effects, the degree of 'representativeness' of any sample and associated tests remains the most critical in characterizing soil materials.

This is accentuated by the natural variability of materials forming slopes. No soil material is truly homogeneous, because the intrinsic properties themselves have small differences. The sophistication of laboratory techniques has reached a level that enables the detection of such small variations. Thus, it is important to distinguish the difference between accuracy and precision. Accuracy is the degree to which a measurement represents the variable in the field; precision is the 'exactness' of the measurement in the laboratory.

An important aspect of the laboratory analysis was the assessment of weathering upon the properties and behaviour of mudslide materials. Three approaches to such study were recognised by Duchaufour (1982):

1. the determination of geochemical and mineralogical balances;
2. laboratory experiments on parent materials to simulate the effects of drainage and climatic conditions of the natural environment, and;
3. the use of thermodynamic calculations.

In this study, emphasis was given to methods one and two. Laboratory tests were used to establish the nature, composition, and chemistry of the weathered profiles preserved in the core-samples (section 3.41), in addition to chemical analyses of rain and pore water (section 3.42) to establish predominant weathering reactions, saturation indices, ion activity products and mineral stability, and their probable effects upon slope instability. The effects of pore water chemistry and chemical weathering processes upon the shear strength behaviour of mudslide materials were established by laboratory simulations using an adapted Bromhead ring-shear apparatus (section 3.43). In this manner, seasonal

changes in pore water chemistry and residual strength could be applied to models of the stability of slopes. But before describing the methods used in the laboratory assessment of clay mineralogy and solution chemistry it is felt necessary to introduce some basic concepts of inorganic chemistry, for these will be subsequently used in the description, analysis and modelling stages of this work.

The concept of thermodynamic equilibrium is common to geochemistry and physical chemistry. The equilibrium approach is used because:

1. it often provides good approximations of the real world;
2. it indicates the direction where geochemical changes may take place: in the absence of an input of energy, systems can only move toward equilibrium;
3. it is the basis for calculations of rates of natural processes.

Several different conventions are used to define standard or 'steady' states. For example, if a hypothetical reaction is considered:



at equilibrium:

$$\frac{a_{d/D} \cdot a_{e/E}}{a_{b/B} \cdot a_{c/C}} = K_{eq}$$

where b moles of B and c moles of C, both in their standard states, are converted to d moles of D and e moles of E, with 'a' equal to the activity and 'K_{eq}' the equilibrium constant.

If the system is in disequilibrium, the expression on the left-hand side is termed the '*activity product*' (AP) or the '*ion-activity product*' (IAP) which will not be equal to K_{eq} providing the species involved are ions. If $IAP/K_{eq} > 1$ the reaction will tend to the left; if the $IAP/K_{eq} < 1$ the reaction will tend to the right. In this manner expressions may be derived to indicate how far a system deviates from equilibrium, such as IAP/K_{eq} which equals unity at equilibrium, $\log (IAP/K_{eq})$ which equals zero at equilibrium, and $RT \ln(IAP/K_{eq})$ which represents the change in free-energy by converting one mole of reactant to products under steady state (where R is the gas constant 1.987×10^{-3} kcal/°/mol, and T the temperature). The concept and expressions are of considerable importance when describing the extent to which a particular solution is chemically super-saturated or under-saturated with respect to a particular mineral.

In a solution containing two ionic species it may be shown by statistical arguments that providing the energy of interaction between molecules may be considered ideal, the activities of each species will equal their concentrations (Berner, 1971). In natural solutions, such as ionic species in water, these conditions are not met. Electrostatic forces exist between charged ions, and hydration shells may form around each ion in which water molecules are ordered in a structure different from that of pure water. In practice, for aqueous solutions less concentrated than sea water, the activity of water is very close to unity in contrast to sea water which equals 0.98. The ratio of the activity of a species to its concentration is called the '*activity coefficient*', which tends to be unity for uncharged species in dilute solutions rising above unity in concentrated solutions, largely because much of the water is associated with hydration shells with less water available to solvate uncharged species (Stumm and Morgan, 1981).

Geochemical models have been formulated to calculate ion activities of a variety of systems (Brownlow, 1979; Garrels and Christ, 1965) and Plummer and MacKenzie (1974) suggested an equation to calculate the activity coefficients of uncharged species. The Debye-Hückle theorem, however, allows coefficients to be calculated for single ion species for ionic strengths less than 10^{-2} . 'Ionic strength' refers to the concentration of the solution but takes into account the greater electrostatic effects of multivalent ions. Such models are usually applied with analytical data from chemical tests to establish chemical equilibria and mineral reactions in natural environments.

3.41 Physico-chemical analyses of core-samples:

3.411 Core sample processing.

Following transportation of the core samples to the laboratory, they were temporarily stored at a temperature of around 5°C. Every effort was made to extrude the core, catalogue the materials, and sub-sample for future analysis as quickly as possible. It was inevitable, however, that some delay would be incurred at this stage due to the number of cores awaiting processing and the length of time needed in the description and sub-sampling stages. On average each core took 3 hours to fully investigate, so that the maximum length of time between field sampling and processing of each core was 16 days.

To assist in the adequate description of each core, a log-sheet was designed to record site details, a description of the core materials, sub-sampling locations, and a summary of the laboratory analyses. On

reception at the laboratory, each core sample was assigned a log-sheet (Appendix 10). Every effort was made to complete the preliminary description and identification of discontinuities and sub-sampling sites as quickly as possible to prevent desiccation and contamination of the core materials. All sub-samples were catalogued, labelled and stored in sealed polyethylene bags to prevent further deterioration during the analysis phase.

To expose the core sample, an industrial circular saw was used to cut two grooves down opposite sides of the tube. The depth of each cut was not sufficient to break the seal, but adequate to allow a sharp knife to split the tube in two. The use of a knife ensured that damage and exposure of the sample would be minimized. Once exposed, the sample was placed on a glass plate, measured and processed. The location of shear surfaces and other discontinuities were noted.

3.412 Soil description and sub-sampling.

For the purposes of adequately and quickly recording a description of the soil core a procedure was adopted in which a number of characteristics could be tested rapidly. The primary characteristics such as particle size and plasticity were assessed by standard laboratory tests (see section 3.413). The secondary characteristics, soil colour, the shape, texture and composition of the particles were assessed using standard procedures (Craig, 1983) and were recorded on the log-sheets. The arrangement of discontinuities, weathering and minor lithological details, referred to as the soil macro-fabric, have been carefully described as these can significantly influence the engineering behaviour of the soil.

Four sub-samples were separated from each core. The number and location of the sub-samples was predetermined on the basis of the time and resources available for subsequent analysis. To enable the selection of sub-samples the core was divided into four zones (Plate 13), which were identified and sampled in the following order:

Zone 3 the basal shear surface (at 56 cm in example Plate 13);

Zone 4 the *in situ* clay below the shear surface (at 27 cm);

Zone 1 the surface 20-30 cm layer (at 76 cm), and;

Zone 2 the transition zone between 1 and 3 (at 64 cm).

It was thus possible to include maximum soil variability contained within the material, whilst ensuring that the sub-samples were extracted from the same position within each core for future correlation. Thus, from the 19 core samples, a total of 76 sub-samples were obtained for further soil analyses. At each sub-sampling zone material was preserved for a number of different tests. The nature and size of each sample was determined by the requirements of each testing programme and included:

1. the determination of moisture content;
2. the assessment of residual shear strength, plasticity and particle size;
3. the assessment of soil properties such as cation exchange capacity and the identification of clay minerals, and;
4. the observation of micro-fabric and individual particles.

Plate 13.

**Exposed core sample (W5) revealing shear surfaces
and the location of sub-sampling sites.**



Using cheese-wire cutters the sampling zones were separated and sub-sampled. At zone three, the slice contained the shear surface intact. The sample was cut in such a way to maintain the *in situ* isotropic alignment that existed in the field. The sample was sealed in a labelled plastic bag, recorded on the logging sheet, and set aside for testing (programme 2). Immediately adjacent to this section a larger slice was isolated. Using a palate knife the slice was cut into cubes, of which ≈ 30 grammes were immediately sealed and labelled for programme 1, the determination of moisture content. Two cubes were set aside for programme 4, and the remaining ≈ 400 g of sample was allowed to air-dry for programme 3, soil chemical analyses.

A number of additional samples were noted on the core log-sheets. These included the field bulk density samples (see Appendix 1) and free-water (FW) samples. The latter samples of clay, obtained from the cores, were used to obtain extracts of the interstitial free water for chemical analyses. Additionally, some unsampled material from each core was recorded and set aside for future posterity.

The procedures adopted for the description and sub-sampling of the cores were considered to be the most practical in view of the time and resources available, although an element of desiccation was unavoidable. The latter was minimized by the procedure and is thought to be negligible (p.289). The description stage achieved accurate and quick assessments of both structural and fabric characteristics with particular reference to their location within the core profile. The use of log-sheets substantially reduced processing time and provided a quick and easy way of comparing the core samples. The techniques adopted in locating and sub-sampling material for further testing were also standardized for this

reason. The time taken between field sampling and core-processing was reduced as a result of considerable planning and the use of the procedures outlined.

3.413 Physical analyses.

Eight physical properties of the mudslide materials were assessed for all of the sub-samples, except where otherwise stated. The total number of tests and sources of the methods are summarised in Table 3.9, and further detailed below:

1. particle size distribution: this involved a two stage analysis, following the pre-treatment of a ~200 g air-dried sample to disperse soil aggregates and colloids (Black, 1965; Vickers, 1983; BS 1377, 1975). The procedure used is described in Appendix 2. The coarse component was passed through a nest of BS sieves down to 500 μm . Particles passing the 500 μm sieve were analysed by a Malvern Particle Sizer. The weight retained on each mesh was recorded and the percentage of the total sample passing each sieve calculated.
2. moisture content: the natural, saturated and air-dry moisture contents (%) were measured using standard procedures given in Methods A-C in Appendix 3. The results were used for two reasons: in calculations of the phase relationships and for volume adjustments in the chemical analyses of the samples.
3. field bulk density: this was assessed from the density tubes extracted during field sampling. The method of analysis is given in Method D in Appendix 3. The bulk density was calculated as the ratio of the total wet-weight to the volume of sample, and the unit weight was calculated as the ratio of the dry-weight to the volume of sample. Field moisture content was also calculated

Table 3.9. Summary of parameters, techniques and total tests performed in the laboratory analysis of materials from both sites.

TEST	SAMPLE #	TEST #	PARAMETERS	TECHNIQUE
Shear strength (Peak)	2	6	τ_{cv}' , c_p' , ϕ_p'	Drained Triax. comp
(Residual Std.)	19	38	τ_r' , c_r' , ϕ_r'	Ring shear Bromhead (1979b)
(Residual Sim.)	8	36	[cation] τ_r' , c_r' , ϕ_r'	Steward ¹ (1983)
Atterberg Limits	18	36	LL, PL, Ip	BS 1377 (1975)
Phase relations	76	456	Wn, Ws, SG, VR P, γ , ρ , Sr	Head (1985)
Particle size	76	152	% particle size	Vickers (1983)
Clay mineral Anal.	38	380	% mineral (<2 μ m)	XRD, CEC
Observation SEM	38	38	Visual	Brindley & Brown (1980)
Clay chemistry	76	76	% bulk chem.	ICP Walsh (1982)
Soil chemistry	76	228	pH, % LOI Conductivity	Soil Survey Methods
Organic carbon	76	76	% organic	Loveday (1974)
Cation exchange capacity	76	76	CEC (Meq/100g)	Bascombe (1964)
Exchangeable cations	76	532	Na, K, Ca, Mg, Cl SO ₄ , Fe, HCO ₃ (Meq l ⁻¹)	Hendershot (1986) ²
Water soluble cations	76	380	Same as above	Soil Survey Methods
Rain and pore water chemistry			see Table 3.8	
TOTAL	731	2662		

¹ Steward and Cripps (1983), Steward (1983)

² Hendershot and Duquette (1986)

4. specific gravity of solids: this was measured using the standard density bottle technique (BS 1377, 1975; Vickers, 1983), given in Appendix 4. In knowing the moisture relationships measured above, the specific gravity was used to calculate the void ratio, porosity, unit weight and bulk density establishing the phase relationships of the soil materials. These results were compared with field measurements and their accuracy compared.
5. liquid limit: this was measured by the standard cone penetrometer test (BS 1377, 1975) outlined in Appendix 5.
6. Plastic limit: this was determined by the standard glass plate test (BS 1377, 1975) outlined in Appendix 5.
7. drained peak shear strength: triaxial compression tests were used to determine the peak strength parameters (Method A in Appendix 6) for the undisturbed core samples from both sites.
8. drained residual shear strength: using a Bromhead ring-shear apparatus the drained residual strength parameters were measured for all zone 3 sub-samples using the method of Bromhead (1979b). The procedure and test specifications are given in Method B in Appendix 6. The results of the tests were traced on a chart recorder via two sensitive load cells.

BASIC computer programmes were written to assist in data processing for many of these tests: results for 1,4 and 7 were processed in this manner.

3.414 Mineralogical and chemical analyses.

Ten tests were undertaken in analyses of the mineralogical and chemical properties of mudslide materials. The total number of tests and sources of the methods are summarised in Table 3.9, and detailed below:

1. clay mineral identification: using the technique of Bullock and Loveland (1974) and the procedure outlined in Method A in Appendix 7, semi-quantitative estimates of the proportion of clay minerals

from zones 3 and 4 were calculated from X-ray diffraction traces. Reference was also made to the cation exchange capacity and K_2O contents (see below) as supplementary indices of expandable-layer content and mica content, respectively.

2. micro-fabric observation: using a scanning electron microscope and microprobe, samples from zones 2 and 4 were analysed to assess differences in fabric and clay surface and fissure chemistry. The preparation and procedures used are given in Method B in Appendix 7.
3. pH: this was determined using standard procedures (Avery and Bascombe, 1974). 1:2.5 soil-water pastes were used to calculate an average from three pH measurements. In a similar manner, 1:2.5 soil pastes treated with calcium chloride were also measured for pH.
4. soil conductivity: this was measured from a 1:5 soil-water extract after Richards (1954). Two readings of conductivity were recorded (where 1 dS/m = 1 mhos or reciprocal ohm) and an average calculated.
5. organic matter: this was assessed using two standard methods. Their procedures are outlined in Methods A and B of Appendix 8. Method A describes the procedure for assessing the per cent loss on ignition (LOI). This method results in the loss of a small proportion of bonded water, and is not an accurate estimation of the total organic matter. Organic combustion (Method B) enables the assessment of organic matter or carbon (%), and by difference with the per cent LOI, the proportion of bonded soil moisture.
6. interstitial free water cations: within the core samples saturated clay extracts were preserved for the assessment of pore water chemistry. Solutions for analysis were obtained using a centrifuge technique described by Kinniburgh and Miles (1983) and detailed in Appendix 9A. Analytical procedures, described in Appendix 9F, were used in the assessment of solution chemistry.

7. water soluble cations: the soil-water extracts used in the determination of conductivity were also used to assess the concentration and types of soluble salts after Richards (1954). The procedure and test equipment is detailed in Appendix 9B. The solution extracts were measured using the analytical procedures described in Appendix 9F.
8. exchangeable cations: the procedure for the extraction of exchangeable cations is given in Appendix 9C after Bascombe (1964) and Henderson and Duquette (1986). Analytical procedures were the same as for the assessment of the soluble cations and are outlined in Appendix 9F.
9. cation exchange capacity: using the technique of Bascombe (1964) and Henderson and Duquette (1986) in Appendix 9D, the CEC was measured by creating a compulsive reaction between a soil-barium exchanger and the introduction of a magnesium reagent. The initial and final concentration of magnesium was measured by atomic adsorption spectrometry (Appendix 9F) and the CEC calculated.
10. clay chemistry: the chemical constitution of the clay minerals were assessed by the methods given in Appendix 9E. An inductively coupled plasma source spectrometer (ICP) was used to give a bulk analysis of the major cationic oxides, such as K_2O .

The range of cations measured in the solutions obtained from these methods, other than by clay breakdown, include: sodium, potassium, magnesium, calcium, chloride, sulphate, ferrous and total iron, aluminium, silica and bicarbonate. Five analytical techniques were used in the determination of the concentrations of these species, which are described in Appendix 9F in addition to the analysis procedure of the ICP, outlined in Appendix 9E.

Figure 3.20. Typical flame photometer calibrations for sodium and potassium.

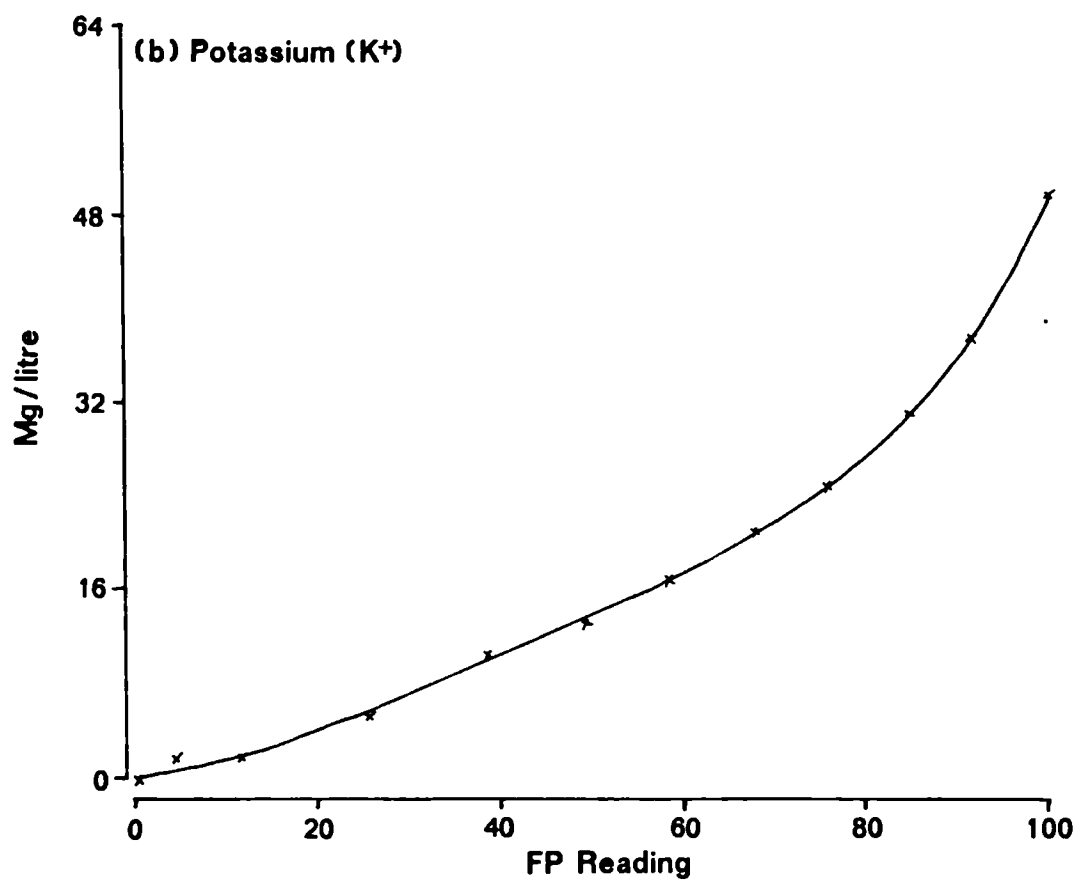
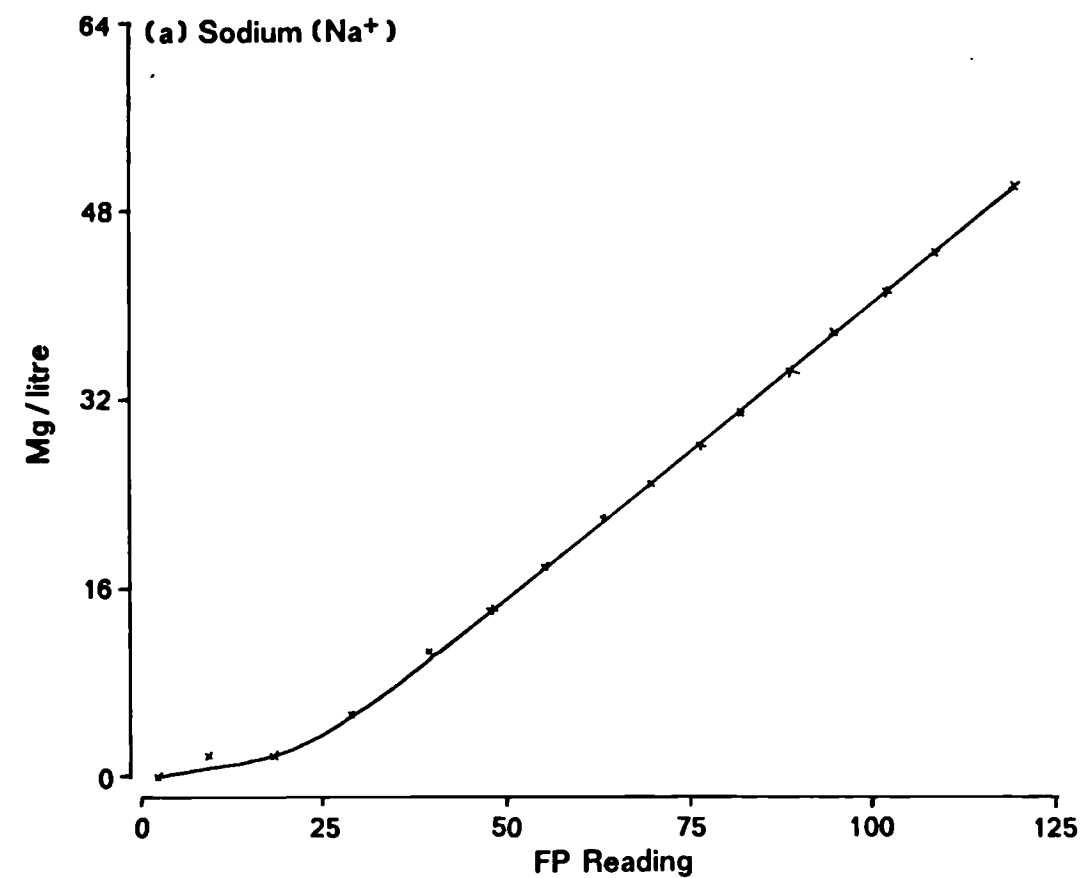


Figure 3.21. Typical atomic adsorption spectrometer calibrations for magnesium and calcium.

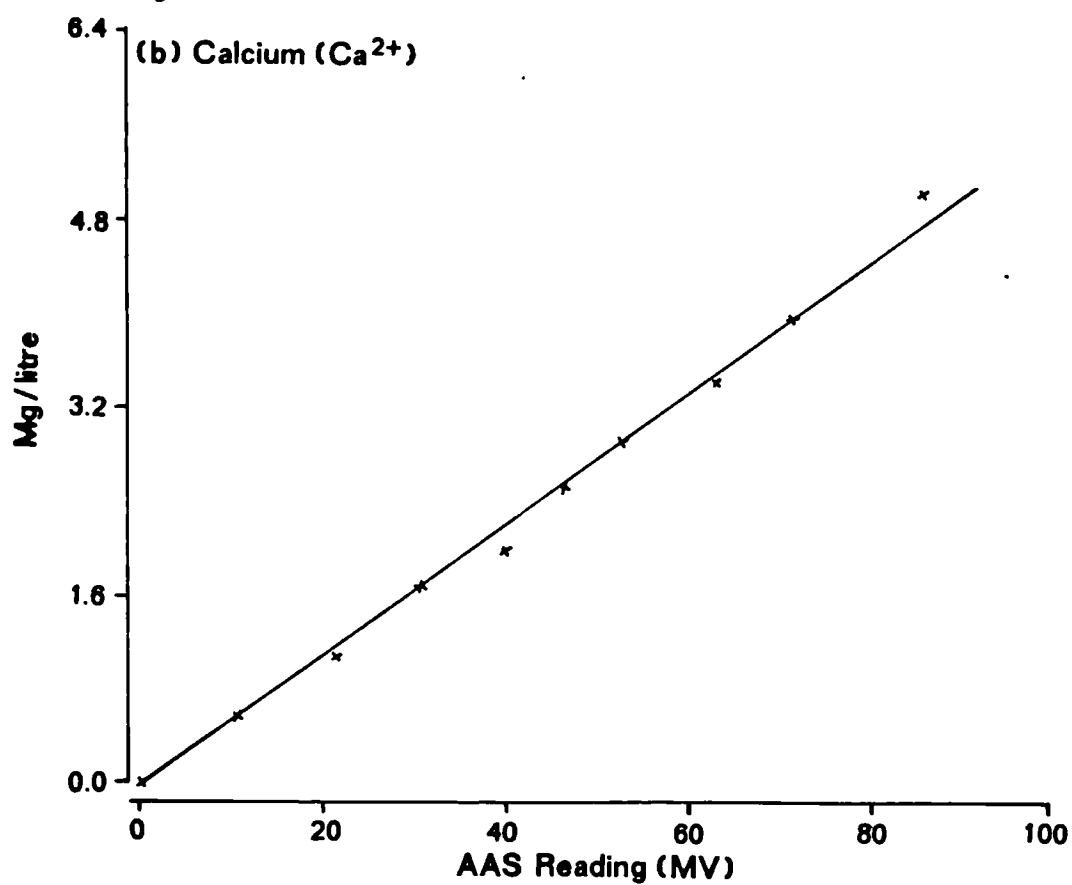
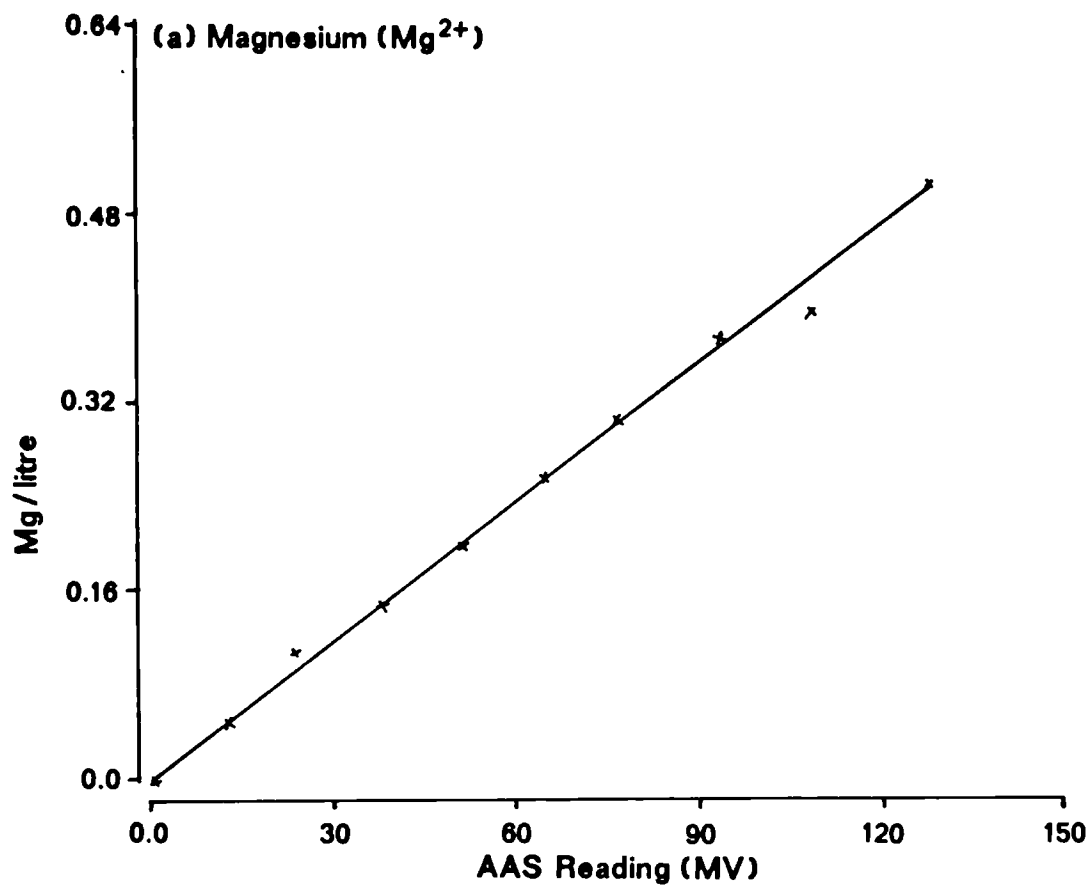
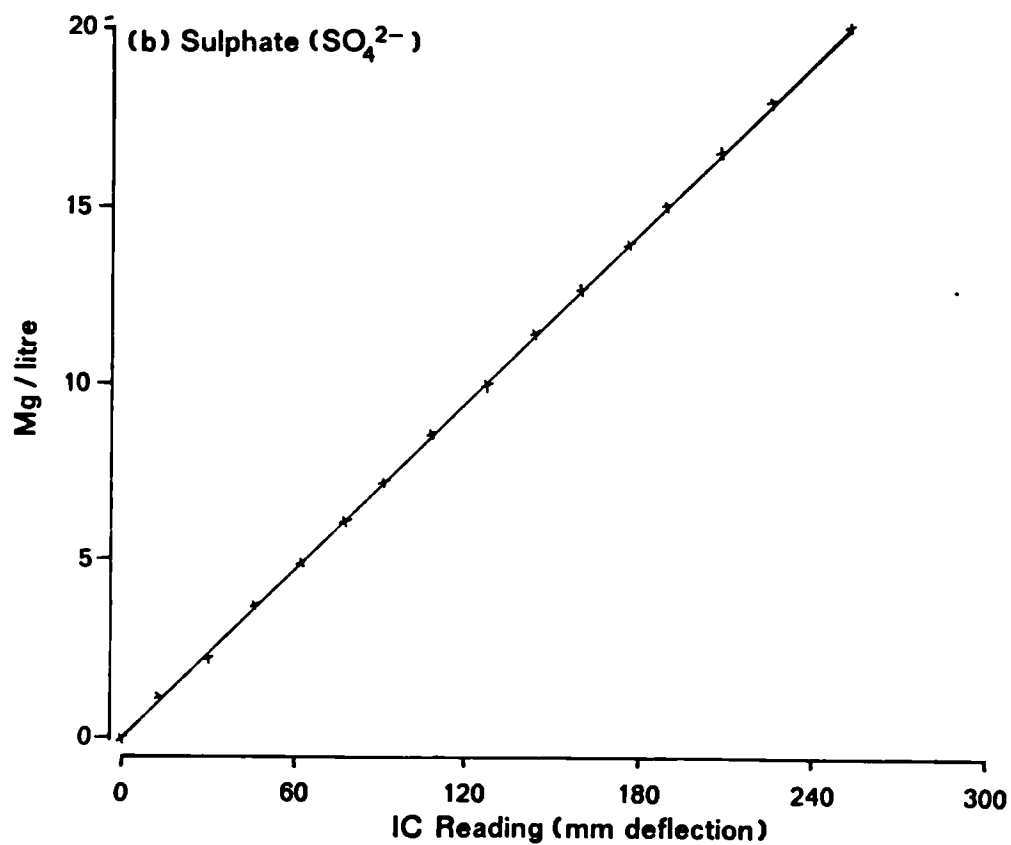
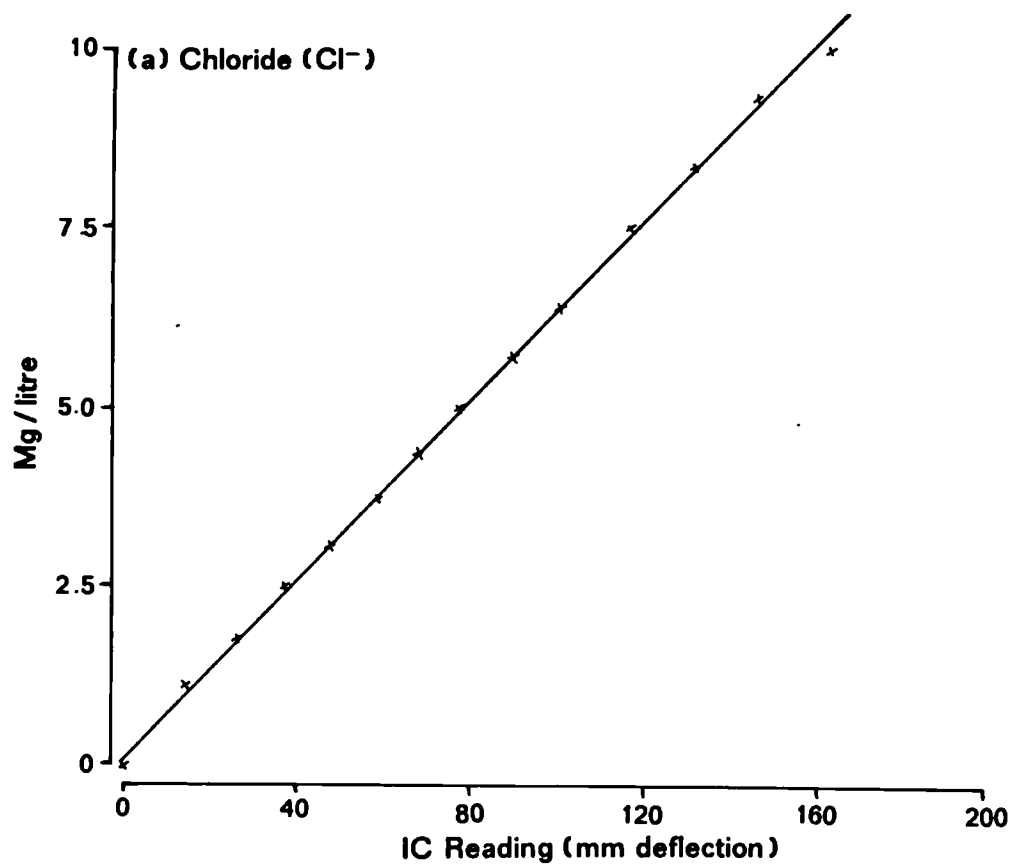


Figure 3.22. Typical ion chromatograph calibrations for chloride and sulphate.



Sodium and potassium were measured by standard flame photometry and the equipment was calibrated with solutions of known concentration. Typical calibration curves are shown in Figure 3.20. An atomic adsorption spectrometer was used in the calibration of readings for magnesium and calcium, shown in Figure 3.21, and a Dionex ion-chromatograph measuring the major anion species. The calibrations for chloride and sulphate are shown in Figure 3.22.

Ferrous iron, total iron, aluminium, and bicarbonate were determined using chemical procedures detailed in Appendix 9F. The determination of iron involved the use of a continuous flow technique described by Allen (1974). An auto-analyser linked to a colorimeter and chart recorder was used to obtain the measurements. Aluminium was similarly assessed using a continuous flow technique, while bicarbonate was determined by standard titration.

Control solutions were included in each run to assess the accuracy of the determinations, particularly where samples had to be diluted into the optimum calibration range of the analytical equipment. Computer programmes converted the readings to concentrations from the least squares best solution of the calibrations. Concentrations were reported in milligrammes per litre (mg/l or ppm) to the nearest whole number.

3.42 Routine analysis of rain and pore water samples.

The samples brought to the laboratory for analysis were of two forms (sections 3.325-326 and 3.412):

1. rain and pore-water, and;
2. clay samples.

Solutions were required for chemical analysis which meant that the interstitial water contained within the clay samples had to be extracted. Two methods may be used for this purpose which involve either the squeezing out of soil water under pressure or centrifuging the sample with immiscible fluids of greater density than pure water.

The latter technique was described by Kinniburgh and Miles (1983) and Barber *et al* (1977), and was adopted in this study. The procedure is given in Appendix 9A, and varies from those referred to in that a standard laboratory centrifuge was used in place of the recommended refrigerated high-speed centrifuge; the latter was unavailable for the purposes of routine analysis. Although a high-speed centrifuge is preferable, it was found that sufficient solution for chemical analyses could be obtained from a bench centrifuge. Table 3.10 presents results from control experiments on several samples to assess the performance of the centrifuge technique against solutions obtained directly from the field. Because the variability between methods was less than 7 mg/litre they were considered equally effective at obtaining accurate estimations of pore water chemistry. Estimations were also unaffected by the use of Arklone (see Appendix 9A) and independent of the yield of solution.

Table 3.10. Chemical compositions of solutions derived from different pre-treatments.

SAMPLE	% YIELD	Na	K	Mg	Ca	Cl	SO ₄
<hr/>							
(Pore water solution direct from field ¹)							
W0	-	546	16	58	86	952	318
W3	-	682	13	99	135	1330	318
W4	-	688	27	117	125	1354	304
WU	-	406	8	57	66	819	267
.....							
(Saturation extract from centrifuge method ² with arklone)							
W0	29.05	536	16	57	80	951	316
W3	27.53	680	16	94	129	1332	318
W4	22.97	688	32	115	126	1368	315
WU	14.16	404	8	54	65	817	270
.....							
(Saturation extract from centrifuge method ² without arklone)							
W0	19.23	545	16	57	81	948	321
W3	18.71	675	15	96	131	1341	319
W4	15.98	687	31	117	124	1365	306
WU	9.06	411	8	53	63	810	272

¹ Refer to section 3.326.

² Refer to Appendix 9.

Following this pre-treatment both rain water and pore-water samples were analysed using standard techniques. The chemical analysis of the solutions was divided into two stages: in the first stage, the following cations and anions were measured for both rain and pore water samples:

1. sodium (Na^+);
2. potassium (K^+);
3. magnesium (Mg^{2+});
4. calcium (Ca^{2+});
5. chloride (Cl^-), and;
6. sulphate (SO_4^{2-}).

In stage two, pore water samples were also tested for:

7. ferrous and total iron (Fe^{3+} , Fe^{2+});
8. aluminium (Al^{3+});
9. silica (Si^{4+})
10. and bicarbonate (HCO_3^-).

The procedures used in stage one and two are outlined in Appendix 9F. Except for the determination of potassium, most solutions were diluted into the optimum calibration range of the analytical equipment being used, with a consequent possibility of error. Thus, standard solutions were incorporated for two reasons: to calibrate the instrument readings with solutions of known concentration, and to control for operator and instrumental drift during and between the routine batch analyses.

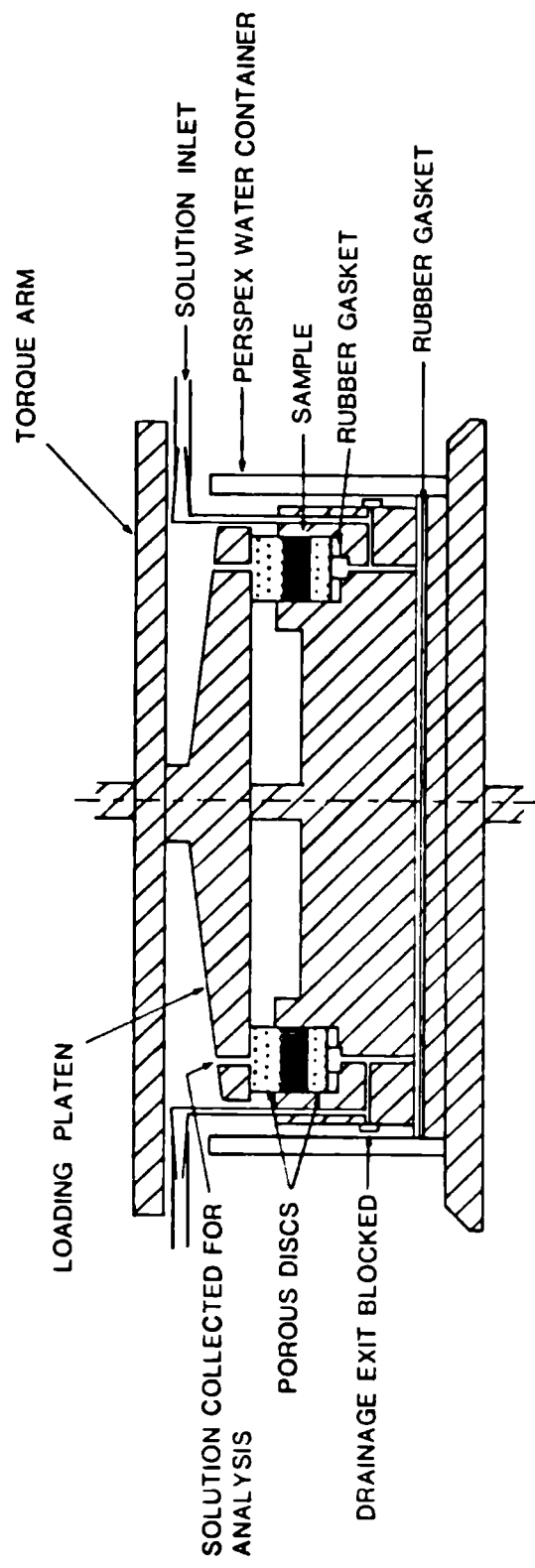
Purpose written computer programmes were used to calculate the final concentrations of the ionic species. This was achieved by adjusting the result of the linear least squares solution from the test calibration with the dilution factor of the sample. The concentrations in milligrammes per litre (mg/l or ppm) were reported to the nearest whole number.

3.43 Residual strength simulation.

A Bromhead ring-shear apparatus (Bromhead, 1979b) was adapted to allow the introduction and collection of solutions from clay samples during test as reported by Steward (1983) and Steward and Cripps (1983). The adaptations to the sample cell are shown in Figure 3.23. The alterations to the ring-shear were reversible.

The incorporation of a composite flow-system enables solution of known concentration to be placed in a constant head tank of varying height. Using a three-way stopcock valve, air could be evacuated from the hosing linking the tank to the sample cell. A four-way connector was used to link the valve to the lower section of the sample cell via four brass-nippled solution inlets. The four drainage holes were plugged and a rubber gasket placed under the cell to ensure the flow of solution up through the lower porous-bronze disc into and through the sample. An air outlet in the upper loading platen was sealed with a tube and valve to allow de-airing of the sample cell. Tubes from four solution outlets were linked to a four-way connector allowing the collection of post-flow solutions. The tubing and connectors were made of polyethylene to avoid contamination of the solutions.

Figure 3.23. Modified Bromhead ring-shear apparatus.



Source. Steward and Cripps (1983).

Steward and Cripps (1983) found a head pressure of one metre to be sufficient to maintain a steady flow of solution through the sample, and with a shear displacement rate of 0.032° per minute, drained conditions were attained. In this study, a series of tests were designed to establish control of the technique and to assess the effects of pore water composition upon the residual shear strength of pure and natural clays. The tests considered the effects of varying:

1. the head pressure;
2. the shearing rate;
3. the normal load;
4. mineral type and quantity;
5. the type of cation, and;
6. the concentration of cations.

Following these initial tests the most practical head pressure (1 metre), shearing rate (0.032°) and normal load (100N x 10 lever ratio) were held constant, with the type and quantity of clay minerals and ionic solutions being the only variables between tests.

The test procedure is detailed in Appendix 6C, and is not dissimilar to conventional tests. The technique enabled the addition of different chemical solutions during test, eliminating errors imposed by sample pre-treatments and the lithological variability between test samples.

Table 3.11. Solutions used in laboratory simulations of residual shear strength based on natural ionic concentrations.

CATION TYPE	RAIN WATER		PORE WATER		TEST RANGE	
	MAX	MIN	MAX	MIN	MAX	MIN
	mg/l		mg/l		Molarity ¹	
Na	1048	10	710	171	2	0.02
Mg	185	2	160	27	1	0.02
Ca	85	1	400	90	0.5	0.02
Cl	2168	20	2314	450	2	0.05

Chloride salts of each cation used as test solutions.

¹ Molar solutions = 1000 mg/litre.

Pure and natural clay specimens were used in the test programme under a variety of realistic chemical conditions and weathering states established from the field-monitoring programme. Chloride salts were used throughout the simulation tests since they were found in reality to dominate the rain and pore water samples at the field-sites (see Table 5.2). The species and concentrations of salts used in the tests are shown in Table 3.11. Analyses of the initial and post-flow solutions were achieved by using the procedures outlined in Appendix 9F.

Each test began by developing a shear surface by rapidly rotating the sample through a minimum of 720°. The sample was left to consolidate and establish drained conditions for the applied increment of load (1000N). Once at equilibrium, the sample was sheared at 0.032° per minute until the stress transmitted to the proving rings reached a constant value. From shear stress, values of residual shear strength were calculated; by assuming cohesion to be zero the residual friction angle was obtained. A computer programme was used to convert the displacement of the proving rings to stress, and to calculate the residual strength and effective residual friction angle (ϕ_r' ; see Appendix 6B).

3.5 Conclusions.

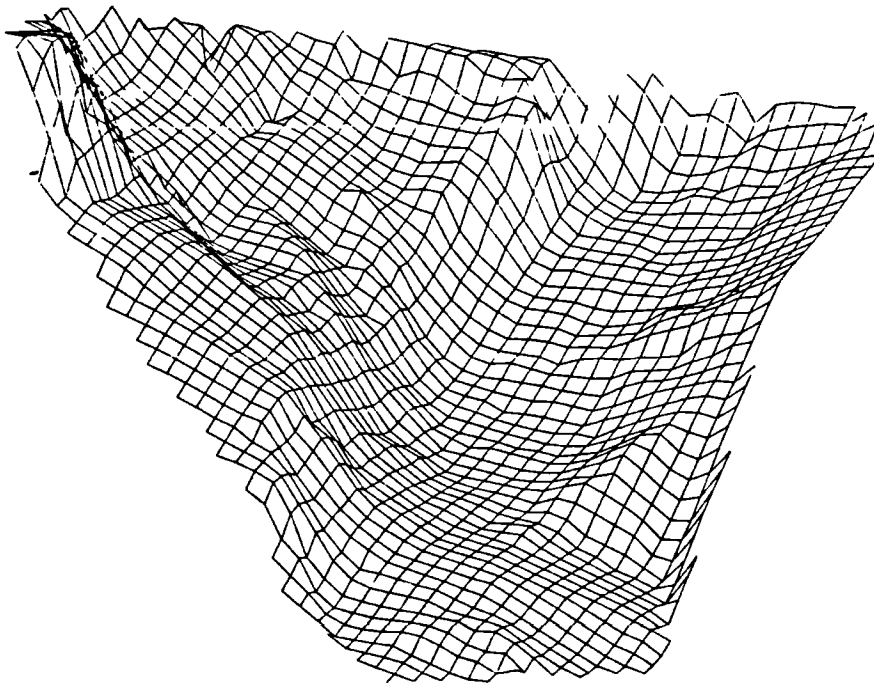
The methodology described in this chapter encompasses a wide range of techniques used by geomorphologists, field-surveyors, geotechnical engineers and soil chemists in the characterization of soil properties and the nature and behaviour of slope materials. New methods of surveying, monitoring and sampling have been employed to improve the accuracy of field mapping, data acquisition and the analysis and interpretation of weathered soil profiles.

Two coastal sites were studied based on their lithology and susceptibility to landsliding; one in uniform London Clay on the north Kent coast and the other in the heterogeneous Wealden Beds of the Hampshire Basin. A comprehensive programme of laboratory testing was undertaken to analyse materials extracted from 19 core samples taken from both sites to characterize the physico-chemical variability of mudslide materials.

The methodology was broadly split into firstly assessing the 'static' variability of the physico-chemical properties of mudslides, and secondly to monitor the 'dynamic' responses of soil behaviour to fluctuations in environmental and weathering conditions and the chemistry of soil water. The results are similarly presented in this manner, beginning in Chapter Four with the laboratory characterization of the weathered profiles of both mudslides; in Chapter Five the results of field monitoring and laboratory simulations are presented with reference to the dynamic nature of seasonal mudslide behaviour.

Chapter Four

PROPERTIES OF MUDSLIDES WITH RESPECT TO WEATHERING AND SLOPE MORPHOLOGY



4.1 Introduction.

The purpose of this chapter is to present the results of analyses undertaken in the laboratory to isolate the nature and distribution of the physico-chemical properties of mudslides. Because these analyses were based on a network of core-samples (section 3.31) the results are comparable within and between the weathered profiles obtained from Manor Lane and Worbarrow Bay.

The results represent a once only sample obtained during the most active period of mudsliding and thus only concern the spatial variability of soil properties at each site. No attempt was made to assess any temporal changes in such properties, except for pore water chemistry (section 5.323), owing to shortage of time. The accuracy of the samples were considered to represent the distribution of physico-chemical properties most closely associated with the seasonal instability of mudslides, or the 'worst-case' condition.

To facilitate the comparison and interpretation of the results every attempt was made to standardize the form of presentation which inevitably gave an impression of repetition owing to the volume of data. Thus, Appendix 10 contains all the core log-sheets and soil descriptions for each borehole along with a condensed summary of the main soil properties in order to ameliorate such repetition.

For each parameter analysed a detailed table summary is presented for discussion and wherever it was felt necessary to clarify the spatial distribution of properties, simple scatter plots are provided with respect to profile depth and the distribution along the basal shear

surface of each mudslide. In this manner it was aimed to establish the variability of the inherent and mechanical properties of mudslides with respect to weathering and slope morphology from clear empirical information. This enabled the isolation of those properties most closely associated with soil behaviour for further discussion and analysis (section 6.21). The association of soil behaviour with slope instability was reconsidered on the basis of these findings.

In section 4.21, the characterization of each site begins with a more detailed account of the surface and sub-surface morphology established during survey and sampling stages. For each slope unit the mudslide volume and sampling resolution was calculated. The soil materials preserved in the core samples are recorded with the aid of a core-log and description, discussed in section 4.22. Results of particle-size analyses are given in section 4.23 and those of the phase relationships in section 4.24. Moisture content and bulk density results obtained from direct field measurements are combined with calculated estimates from laboratory tests and their precision and accuracy compared.

Geotechnical test results are presented in section 4.3 and include the results of plasticity index tests, the determination of activity ratios and drained shear strength tests. The effective residual strength parameters are reported for each weathered profile from the shear surface, while the results of drained triaxial compression tests are reported for *in situ* undisturbed materials.

In section 4.4 soil chemical analyses are introduced by assessing the chemical characteristics of materials by determining soil pH, conductivity, organic matter content, chemical equilibria, the bulk

chemistry of clay-size materials, the determination of cation exchange capacity and the exchange reactions. The anisotropic nature of the soil fabric and solute chemistry was assessed in section 4.45 based on results from SEM observation and microprobe analyses.

The results of chemical and fabric tests were used in conjunction with X-ray diffraction data to derive a semi-quantitative determination of the properties of clay mineral species present within the clay-size fraction (section 4.46). The association of clay mineralogy with landslide susceptibility was further tested at a regional scale for southern and south-eastern England (section 4.61) and in more detail by using the London Clay Basin as a separate region, the results of which are discussed in section 4.62.

In the conclusions, section 4.5, the variability of properties between *in situ* and weathered states was clarified and the parameters showing the strongest associations with mudslide and weathering processes isolated for further discussion.

4.2 Characterization of mudslide materials:

4.21 Site morphology and sampling resolution.

By using accurate ground-survey and photogrammetric techniques it was possible to calculate the surface area of each site using the computed width and length of each mudslide unit (see Figures 3.10 and 3.11). Table 4.1 summarizes the dimensions and morphological indices for each

Table 4.1. Morphological indices and sampling resolution.

UNIT #	LENGTH m	WIDTH m	DEPTH m	SURFACE AREA m ²	X-SECTIONAL AREA m ²	VOLUME m ³	SAMPLING* RES x 10 ⁻⁴
<u>MANOR LANE</u>							
1	11.5	14.5	0.990	180.00	21.00	241.50	1.073
2	18.5	18.0	0.687	322.75	12.023	222.43	0.587
3	12.0	26.0	0.512	258.75	13.056	156.67	0.621
4	11.0	30.5	0.606	315.00	18.180	199.98	0.576
5	26.5	25.0	0.528	546.00	12.936	342.80	0.439
.....							
\bar{x}	-	22.8	0.665	-	15.439	-	-
Total	79.5	-	-	1622.50	-	1163.38	-

<u>WORBARROW BAY</u>							
0	12.0	(9.25) 15.75	1.257	(73.8) 147.75	(17.5) 30.5	(210.0) 366.0	0.519
1	7.25	4.0	1.204	30.80	4.214	30.550	3.732
2	7.25	4.75	0.696	31.50	2.958	21.446	3.082
3	5.75	4.0	0.491	23.00	1.719	9.880	4.727
4	6.25	8.0	0.605	43.13	4.538	10.788	5.33
5	10.0	9.0	0.682	67.50	5.797	50.797	1.276
.....							
\bar{x}	-	7.58	0.823	-	8.288	-	-
Total	48.5	-	-	343.68	-	489.461	18.666

Units may be identified from Figures 3.10 and 3.11 :

Unit 5 = source : unit 1 = base of feeder track

() : active portion of accumulation lobe

Surface areas are measured directly from survey data

Depth of mudslide is taken as the mean depth to the basal shear plane (Table 3.6)

Sampling resolution is calculated as the ratio of volume sampled to total volume

section, dividing the Manor Lane mudslide into 5 units and the Worbarrow system into 6. The position of the shear surface was established during the field sampling programme (Table 3.6) so that it was possible to calculate an approximate cross-sectional area and volume for each slope unit. In these calculations it was assumed that the mean depth of mudslide was constant for the sectional area and that the lateral shear plane attained this depth at an angle of 45° from within 0.5 m of the sides of the mudslide. These assumptions probably hold for translational mudslides under study here.

With reference to Table 4.1, both sites show a deepening of the mudslide in the source region and on the lower slopes, while there is a shallowing of the slides about mid slope (unit 3), the translational zone. The latter may in part be caused by both systems overriding resistant bands of bedrock or due to the more rapid translation of material down an increased slope gradient. This is better emphasised by the reduced volumes of material calculated for these slope sections.

Apart from the obvious size difference between the two sites there are a number of similarities, such as an increase in volume in units 1 and 2 at the base of the feeder track and rear of the accumulation lobe, and in unit 5 the source area. At Manor Lane an accumulation lobe (unit 0) was absent in comparison with the pronounced lobe at Worbarrow; only the central section of this lobe was currently active (shown in Figure 3.8) which is separated in the calculations of Table 4.1.

With reference to Table 4.1 it may be shown that a greater sampling resolution was achieved at Worbarrow amounting to one core every 57.28 m^2 of mudslide, and although a greater number of cores were taken at Manor

Lane each core accounted for approximately 147.5 m². A better estimation of the resolution achieved in the sampling programme was obtained from the volume sampled in each core in relation to the volume in each slope unit. The results are shown in Table 4.1 where it may be seen that the best resolution was achieved at Worbarrow, equivalent to 0.0019 per cent of the total volume of mudslide. The temporal aspects of the sampling resolution were stressed earlier in the introduction and consisted of a once-only sample representative of the 'worst-case' condition for slope instability.

With these forethoughts in mind it was considered that the optimum resolution of core samples was obtained at the sites given the limitations of resources and time. These samples are representative of the mudslide units from which they were extracted and were so distributed to include the maximum variability of materials, weathering and slope morphology.

4.22 Core sample descriptions.

Appendix 10 contains the completed core catalogues for each sampling location at both field sites. Each log-sheet provides full site details including core number, date of extraction, surveyed coordinates, levelled height, and the depth of tube penetration. Two further sets of information included a core description and visual log and sub-sample location with a condensed data summary. It is not intended to discuss each catalogue for this would be unnecessarily repetitive but instead to describe in detail a representative core sample of each site.

Table 4.2. Soil catalogue and description for core sample 2B.

SITE : Manor Lane CORE NUMBER : 2B
 CORING METHOD : Thin walled open drive GROUND LEVEL : 15.480 m OD
 TUBE DIAMETER : 110 mm COORDINATES (x,y) : 1018.61,
 1045.06
 TUBE PENETRATION : 0.773m DATE : 14 March 86

CORE PROFILE				SUMMARY OF PROPERTIES				
DESCRIPTION	LEGEND	LEVEL	SAMPLES	PARAMETER	S1	S2	S3	S4
saturated brown CLAY with some peds of blue CLAY		15.429	S1	FD1	Wn%	49	41	36
					Ws%	73	83	86
					Gs	2.63	2.65	2.68
					VR	1.9	2.2	2.3
					P	0.66	0.69	0.7
fissured brown CLAY		15.249	FW		UW KN/m ²	13.2	11.5	10.8
saturated active	15.179	RS1		BD Kg/m ³	1341	1174	1100
shear plane					Ø _r '			9.0
slickensided shear	15.102	S3		LL %			80
in brown/blue CLAY			RS2		PL %			30
					PSA%			
highly fissured		15.049	S4		<500µ	100	100	100
stiff blue CLAY					<100µ	100	100	100
		14.930			<20µ	75	87	75
sample end	-----	14.879			<4µ	32	38	32
					Org %	2.9	2.5	2.7
					pH	7.3	7.3	7.3
depth of hole	---	14.707	FD2		Cond. mS/cm	2.5	2.5	2.3
					mg/ltr			
					FW.cations			2047
					FW.anions			5560
					S.cations	371	440	360
					S.anions	1143	1296	1085
					Ex.cations	829	839	818
					CEC	56	61	56
					Minerals %			
					mica/illite	41	42	42
					Kaolinite	23	25	25
					swelling	35	33	34

KEY

S1 : sample zone
 FW : saturated extract for free water
 RS : residual strength sample
 F/BD: field & bulk density assessments
 ... : sample shear plane(s)
 --- : sample extent
 -- : field levels and shear surfaces

Gs : specific gravity
 VR : void ratio
 P : porosity
 Org : organic matter content
 CEC : cation exchange capacity
 in Meq/100g
 Cond : conductivity

With reference to Table 4.2, the log-sheet for core 2B is reproduced, which will be discussed as an example of the cores extracted from the Manor Lane site. The location of the core may be seen on the site plan (Figure 3.10) and has the coordinates x:1018.61, y:1045.06, and z:15.480 m O.D. The total depth of penetration was 0.773 m and the levelled height of the basal shear surface was 14.930 m.

The compression of the core during sampling can be gauged from the visual log and amounted to 22 per cent of the total sample (Table 3.6). This was unavoidably large because of the highly saturated materials above the basal shear surface although it was noted that only 3 per cent compression affected *in situ* clay.

Two shear surfaces were identified during the preliminary description. A basal shear surface was characterized by slickensided surfaces and underlain by stiff blue clay; approximately 10 cm above, a saturated and probably more active zone of shear was recognised. Materials in the latter zone were highly fissured and saturated forming a brown and sometimes brown-yellow weathered matrix containing smaller peds of blue London Clay. The *in situ* blue clay was encountered during sampling by a marked density change and resistance to tube penetration and was highly fissured and over-consolidated.

Four sample zones are indicated in Table 4.2 with the respective levels from which they were extracted. The purpose and nature of each sample was described in section 3.41 with an outline of the methods used in their analysis. A summary of the properties is included in the core catalogue although a more detailed description occurs with the discussion of results given later in this chapter.

Broadly the summary shows that the core materials contain 32-40 per cent clay-size particles of which 42 per cent are micaceous minerals, 35 per cent montmorillonite and approximately 24 per cent kaolinite. At the time of sampling the maximum natural moisture content was 49 per cent above the shear surface and 30 per cent below. The phase relationships were calculated from the specific gravity of the particles, which averaged 2.65, and the saturated moisture content of each zone. The results show little variation, the mean void ratio equalled 2.1, the porosity 0.67, the unit weight 11.7 kN/m^3 and the bulk density 1194 kg/m^3 . The liquid limit for zone 3 was 80 per cent which was close to the saturated moisture content of 86 per cent; the plastic limit equalled 30 per cent. The drained residual strength envelope was determined at the zone of shear and the internal residual friction angle (ϕ_r') was found to be 9.0° .

The chemical nature of the soil medium may be gauged by the pH of the soil solution which was almost neutral at 7.3, while the conductivity (2.3 mS/cm) indicated an inherently high electrolyte salt concentration. This was supported by the total soluble and exchangeable salt contents. The high cation exchange capacity was most likely the result of the presence of montmorillonite and mica clay minerals.

Notable variations in the values of these properties may be seen in the weathered profile and include:

1. a decrease in natural moisture content with depth;
2. a peak saturated moisture content at the basal shear surface;
3. a high void ratio and porosity at the shear surface;
4. a low unit weight and density at the zone of shear;
5. a low proportion of organic matter below the shear surface;
6. a high pH for *in situ* clay;

7. a decrease in soluble and exchangeable ions with depth, and;
8. a lower CEC for *in situ* material.

The variability of these properties within and between each core sample is further discussed in detail under the respective section headings for each parameter.

Table 4.3 is the log-sheet for core sample W2 from Worbarrow Bay. The Worbarrow site was referenced to a local datum so that the levelled heights are not fixed to O.D., and therefore only relative measurements between locations may be assumed. The survey station height on the back-cliff was set at a realistic 30.0 m L.D. At core sampling site W2, the depth of penetration was 0.871 m and the levelled height of the basal shear surface was 19.907 m. The overall compression of the core was only 4 per cent in comparison with the previous example; the difference in compression was partly due to the heterogeneous nature and greater density of the materials at Worbarrow Bay and the less saturated conditions at the time of sampling than experienced at Manor Lane.

Two shear surfaces were again identified. The basal shear surface was underlain by predominantly grey clay with red and yellow mottling, highly fractured and over-consolidated, with evidence of anisotropic particle and solute movement and deposition along silt-lined fissures. Approximately 35 cm above, a saturated shear surface was noted between a purple to red clay with dark grey and blue mottling overlain by a saturated grey, green and yellow clay with red mottling. The zone above was highly saturated and contained some coarse sand deposited on the surface from the bordering beds of sandstone (see section 3.232). The variability of material is more prevalent than experienced at Manor Lane as indicated by the range of colours noted in the visual core-log.

Table 4.3. Soil catalogue and description for core sample W2.

SITE : Worbarrow Bay CORE NUMBER : W2
 CORING METHOD : Thin walled open drive GROUND LEVEL : 20.603 m LD
 TUBE DIAMETER : 110 mm COORDINATES (x,y) : 86.3,
 145.64
 TUBE PENETRATION : 0.871 m DATE : 20 April 86

CORE PROFILE				SUMMARY OF PROPERTIES				
DESCRIPTION	LEGEND	LEVEL	SAMPLES	PARAMETER	S1	S2	S3	S4
coarse SAND in sat.			FD1	Wn%	17	20	22	17
red CLAY matrix		20.521	S0	Ws%	43	49	61	51
				Gs	2.66	2.66	2.60	2.65
saturated red CLAY/				VR	1.2	1.3	1.6	1.4
SAND				P	0.53	0.56	0.61	0.58
saturated pale grey			S1 FW	UW KN/m ²	14.2	13.6	12.0	13.0
green and yellow	20.341	RS1	BD Kg/m ³	1447	1389	1227	1324
mottled CLAY under				Ø _r '			5.7	
active shear plane				LL %			62	
				PL %			19	
softened dark grey		20.161	S2	PSA%				
blue mottled CLAY				<500µ	98	100	100	100
stiff dark grey				<100µ	98	100	100	100
CLAY - purple/red			S3	<20µ	88	83	94	93
& grey mottled CLAY	20.021	RS2	<4µ	41	39	50	50
lower-consolidated								
with silt lined	---	19.907		Org %	0.8	1.9	2.5	2.4
fissures				pH	5.0	5.5	5.1	6.3
dark grey stiff		19.841	S4	Cond. mS/cm	0.5	0.59	0.65	0.53
plastic clay with				mg/ltr				
slight mottling	-----	19.771		FW.cations			812	
sample end	---	19.732	FD2	FW.anions			1634	
depth of hole				S.cations	38	37	51	38
				S.anions	77	75	106	71
				Ex.cations	802	812	899	926
				CEC	48	54	57	56
				Minerals %				
				mica/illite	22	17	23	18
				Kaolinite	12	9	23	13
				swelling	66	74	55	70

KEY

S1 : sample zone
 FW : saturated extract for free water
 RS : residual strength sample
 F/BD: field & bulk density assessments
 ... : sample shear surface(s)
 --- : sample extent
 -- : field levels and shear surfaces

Gs : specific gravity
 VR : void ratio
 P : porosity
 Org : organic matter content
 CEC : cation exchange capacity
 in Meq/100g
 Cond : conductivity

The summary of material properties contained within the weathered profile revealed a number of differences between the two sites. When compared there appeared to be a greater proportion of clay-size material at Worbarrow, 40 per cent at the surface increasing with depth to 50 per cent. Approximately 20 per cent of the clay contained micaceous minerals, 14 per cent kaolinite and 66 per cent montmorillonite, the latter accounting for the fairly high cation exchange capacity of 54 Meq/100g. The material was more susceptible to saturation requiring only 50 per cent equivalent dry weight of water for full saturation. The specific gravity of the particles was 2.65, and as a consequence both the void ratio and porosity were low, averaging 1.4 and 0.57, while the unit weight and bulk density were greater, averaging 13.2 kN/m³ and 1347 kg/m³ respectively.

The liquid limit at the shear surface equalled 62 per cent which was equivalent to the saturated moisture content of the zone; the plastic limit was 19 per cent. The residual friction angle was surprisingly low at 5.7° which suggested very unstable conditions for mudsliding (section 4.321).

The pH of the soil solution was approximately 5.5, while the conductivity (0.6 mS/cm) was much lower than at Manor Lane indicating lower inherent salt concentrations in the more acidic pore water solution. This was validated by the total soluble and exchangeable salt contents.

In a similar manner to core 2B variations may be noted within the weathered profile and when compared it was found that the following trends exist in both core samples:

1. a peak saturated moisture content at the basal shear surface;
2. a high void ratio and porosity at the basal shear surface;
3. a low unit weight and density at the zone of shear, and;
4. a high pH for *in situ* clay solution.

In addition it may be seen that in sample W2 there was:

5. an increase in the proportion of clay with depth;
6. an increase in the per cent organic matter with depth;
7. an increase in exchangeable cations with depth, and;
8. an increase in the cation exchange capacity with depth.

The core descriptions of each site show a high degree of similarity throughout each mudslide (Appendix 10), although only 'physical' properties have been found here to show similar associations with weathering and slope morphology. The chemical properties were highly site-specific. The variability in the core descriptions for Manor Lane amounted to occasional deposits of pebbles and organic matter and to amorphous staining along fissures. Pebbles were found near the surface in the source (units 5 and 4), and near the shear surface in the lobe (unit 1). At Worbarrow the majority of variability was due to lithology, the presence of sandy deposits and some buried soil with occasional organic matter.

The detailed descriptions given in this section and Appendix 10 provides a basis to present the results of analyses of soil properties within and between each core profile and between the Manor Lane and Worbarrow sites.

4.23 Particle-size distributions.

The analytical procedures for determining the particle-size distributions of 76 sub-samples are discussed in section 3.413 and outlined in Appendix 2. The aim of the analysis was to determine the proportion of material contained within five particle-size ranges as classified by the International Society of Soil Science:

Classification	Size (μm)	Size (mm)
1. clay	<2	<0.002
2. silt	2 - 20	0.002 - 0.02
3. fine sand	20 - 200	0.02 - 0.2
4. coarse sand	200 - 2000	0.2 - 2.0
5. gravel	>2000	>2.0

The calculation of each distribution was based on the printout data provided by the Malvern Particle Sizer, shown in Table 4.4. The proportion of particles retained on the nearest size band to 2, 4, 10, 20, 50, 100 and 200 μm were extracted from the printout and used with the results of the coarse analysis to back-calculate the particle-size distribution of each sample.

Table 4.5, shows an example of the completed calculation. The core code is given along with a subscript (3) indicating the sub-sample zone (section 3.412), and the initial weight of sample. The mass retained on each coarse mesh was directly measured by sieve analysis whereas the proportion of the fine component retained on each mesh size was determined by laser diffraction. The latter were recorded as the 'laser' per cent retained and combined with the proportion of coarse particles to back-calculate the total per cent retained and finally the particle-size distribution from the original weight of sample.

Table 4.4. Computer output from laser particle-size analysis.

Malvern Instruments EASY Particle Sizer M1.2					Date 05—09—86 Time 11—55	
Size microns	under	Percentage in band	Size microns	under	Percentage in band	Result source =Sample Record No =1 Focal length =63mm Presentation = wet beam length =2.0mm Obscuration =0.23 Volume Conc. =0.08 % Log. Diff. = 3.48 Model indep
118.4	100.0	0.0	11.1	67.9	4.2	D(v,0.5) =6.1um
102.1	100.0	0.0	9.6	63.7	4.2	D(v,0.9) =25.0um
88.1	100.0	0.0	8.3	59.5	4.8	D(v,0.1) =1.3um
76.0	100.0	0.1	7.2	54.7	4.6	Span =3.9
65.6	99.9	0.0	6.2	50.1	3.8	D(4,3) =9.7um
56.6	99.9	0.0	5.3	46.3	3.1	S.M.D. =3.2um
48.8	99.9	0.0	4.6	43.3	3.7	
42.1	99.9	1.1	4.0	39.5	6.3	
36.3	98.9	2.7	3.4	33.3	7.5	
31.3	96.2	4.0	3.0	25.8	6.5	
27.0	92.2	4.1	2.6	19.3	3.8	
23.3	88.0	3.5	2.2	15.5	1.6	
20.1	84.5	3.4	1.9	13.9	1.3	
17.4	81.1	4.0	1.6	12.6	1.6	
15.0	77.1	4.5	1.4	11.0	1.6	
12.9	72.6	4.7	1.2	9.4	1.9	

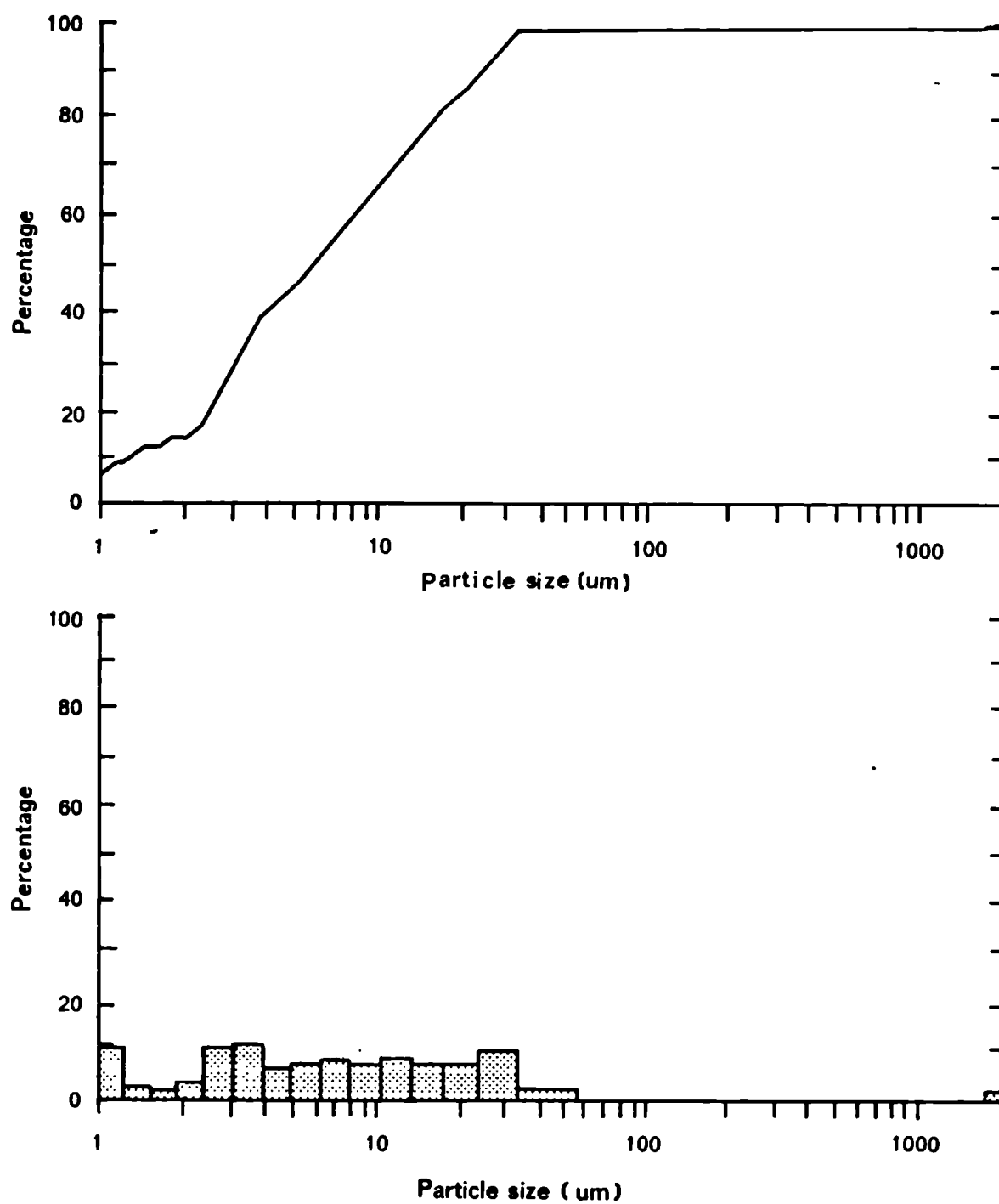
Sample details:- WARDEN CORE 5A, SAMPLE 3

Table 4.5. Particle size distribution back-calculation.

SAMPLE # AND WEIGHT : 5A₃ 250.905 g

SIEVE SIZE (mm)	MASS RET (g)	SUM RET (g)	LASER % RET	TOTAL % RET	% PASSING
2	.153	.153	-	.06	99.94
1	0	.153	-	0	99.94
.5	0	.153	-	0	99.94
.2	0	.153	0	0	99.94
.1	0	.153	0	0	99.94
.05	.251	.404	.1	.1	99.84
.02	47.145	47.549	18.8	18.79	81.05
.01	54.17	101.719	21.6	21.59	59.46
.004	65.687	167.406	26.2	26.18	33.28
.002	51.912	219.318	20.7	20.69	12.59
<.002	-	-	12.6	12.6	-

Figure 4.1. Particle-size distribution and frequency histogram for sample 5A₃



The results of all 76 analyses showed that the majority of particles were smaller than 100 μm and where a coarse component was present a bimodal distribution was evident (Figure 4.1). For this reason it was possible to maximize the detail of the size grades below 100 μm (0.1 mm). However, the International Soil Science Society system does not specify the sub-division of the silt band so that the size ranges used in this analysis were chosen partly for continuity, and on the basis of the US Department of Agriculture and British Standards systems. The final gradings were:

	This study	BS	USDA
1. clay	<4 μm	<2 μm	-
2. fine silt	4 - 9.6	2 - 6	-
3. medium silt	9.6 - 20.1	6 - 20	-
4. coarse silt	20.1 - 56.6	20 - 60	-
5. very fine sand	56.6 - 102.1	-	50 - 100

A small discrepancy may be noticed between the silt and clay divisions used in this study in comparison with the British Standards system. This was introduced as a result of errors arising from the Malvern Sizer which was believed to underestimate the clay fraction for fine silt (E. Derbyshire 1987, pers.com.). By increasing the upper size limit for clay particles to 3 μm a more realistic estimate of the proportion of clay size material was obtained. Other discrepancies result from the size ranges used by the Malvern Particle Sizer (Table 4.4).

Tables 4.6a, 4.6b, and 4.7 summarize the results for both sites. Table 4.6 contains the core samples from Manor Lane and Table 4.7 those from Worbarrow Bay. The format of each table includes the core number and particle-size grades, and for each zone in the weathered profile, results are reported for the per cent of sample passing each grade.

Table 4.6a. Manor Lane particle-size data summary of cores 1A - 4A.

CORE #	PARTICLE* SIZE mm	ZONE ONE % UNDER	ZONE TWO % UNDER	ZONE THREE % UNDER	ZONE FOUR % UNDER	MEAN %
1A	0.1	98.08	96.43	99.74	99.87	
	0.05	95.63	91.22	92.65	94.47	
	0.02	78.37	70.95	68.49	77.27	
	0.01	59.73	52.9	50.52	61.47	
	0.004	33.25	24.23	25.36	29.08	27.98
1B	0.1	99.81	99.83	99.88	99.9	
	0.05	93.12	96.23	99.68	94.8	
	0.02	70.14	77.64	84.1	78.8	
	0.01	52.76	58.75	64.12	63.9	
	0.004	25.58	32.57	35.75	34.8	32.18
2A	0.1	99.7	100.0	100.0	100.0	
	0.05	92.91	98.6	100.0	100.0	
	0.02	70.06	82.3	87.6	90.5	
	0.01	52.79	63.1	67.6	72.0	
	0.004	25.94	34.3	36.8	41.4	34.61
2B	0.1	99.9	100.0	99.9	100.0	
	0.05	93.8	100.0	93.9	100.0	
	0.02	74.6	86.6	75.0	88.5	
	0.01	57.9	67.4	57.7	68.4	
	0.004	32.3	38.3	32.4	39.8	35.70
3A	0.1	100.0	100.0	99.8	100.0	
	0.05	98.7	100.0	91.71	99.9	
	0.02	85.9	90.0	72.23	86.5	
	0.01	68.5	72.2	56.05	67.8	
	0.004	38.2	43.3	31.07	38.6	37.79
3B	0.1	98.66	99.72	99.9	100.0	
	0.05	96.09	97.43	96.2	97.9	
	0.02	81.88	83.17	80.0	85.6	
	0.01	64.91	65.02	63.6	68.2	
	0.004	35.41	34.42	34.0	33.4	34.31
4A	0.1	94.08	99.34	99.84	100.0	
	0.05	93.99	93.67	97.64	99.9	
	0.02	82.32	76.17	85.96	89.1	
	0.01	65.1	61.15	68.79	70.1	
	0.004	37.06	31.62	28.95	37.1	33.68

0.1 - 0.05 very fine sand
0.05 - 0.02 coarse silt
0.02 - 0.01 medium silt
0.01 - 0.004 medium - fine silt
{ 0.004* clay size

* See text for choice of size range

Continued in Table 4.6b

Table 4.6b. Manor Lane particle-size data summary of cores 4B - 7U.

CORE #	PARTICLE* SIZE mm	ZONE ONE % UNDER	ZONE TWO % UNDER	ZONE THREE % UNDER	ZONE FOUR % UNDER	MEAN %
4B	0.1	91.1	77.48	91.87	100.0	
	0.05	89.55	77.4	89.11	99.9	
	0.02	75.34	67.71	72.46	88.5	
	0.01	58.3	52.52	54.62	69.0	
	0.004	28.97	24.94	27.77	40.7	30.60
5A	0.1	99.87	96.08	99.94	99.97	
	0.05	99.87	95.79	99.84	99.87	
	0.02	90.48	81.57	81.05	84.07	
	0.01	69.81	63.7	59.46	63.78	
	0.004	38.05	32.28	33.28	34.09	34.43
5B	0.1	99.49	100.0	100.0	99.98	
	0.05	98.59	99.5	99.9	99.98	
	0.02	84.16	87.8	88.3	93.48	
	0.01	65.16	70.2	66.1	73.68	
	0.004	35.21	32.6	27.9	34.79	32.63
6	0.1	100.0	100.0	98.27	100.0	
	0.05	99.9	99.9	97.78	100.0	
	0.02	86.7	85.9	84.71	91.0	
	0.01	69.3	67.7	66.53	72.7	
	0.004	36.6	38.0	31.15	36.1	35.46
7U	0.1	99.93	100.0	100.0	100.0	
	0.05	99.73	99.9	100.0	99.6	
	0.02	83.14	89.2	94.4	91.4	
	0.01	62.85	70.6	75.8	71.5	
	0.004	31.07	36.2	30.2	25.3	30.69
X	0.004	33.14	33.56	31.22	35.43	33.34

0.1 - 0.05 very fine sand
0.05 - 0.02 coarse silt
0.02 - 0.01 medium silt
0.01 - 0.004 medium - fine silt
{ 0.004* clay size

* See text for choice of size range

Table 4.7. Worbarrow particle-size data summary for all core samples.

CORE #	PARTICLE* SIZE mm	ZONE ONE % UNDER	ZONE TWO % UNDER	ZONE THREE % UNDER	ZONE FOUR % UNDER	MEAN %
W0	0.1	96.57	97.22	93.31	97.07	
	0.05	94.35	94.79	92.84	96.49	
	0.02	80.44	81.37	81.18	87.66	
	0.01	63.83	64.84	62.61	71.35	
	0.004	37.08	38.1	33.5	41.65	37.58
W1	0.1	98.48	91.19	85.77	99.9	
	0.05	95.92	90.28	85.68	93.2	
	0.02	79.67	78.79	76.59	80.4	
	0.01	60.27	61.37	59.78	66.6	
	0.004	33.19	34.19	33.28	38.9	34.89
W2	0.1	98.21	100.0	100.0	100.0	
	0.05	98.11	97.6	100.0	100.0	
	0.02	88.19	82.5	93.9	93.0	
	0.01	69.82	64.6	80.0	79.0	
	0.004	41.24	39.2	50.4	50.2	45.26
W3	0.1	90.43	96.2	97.87	100.0	
	0.05	90.43	96.01	96.6	99.7	
	0.02	83.1	85.43	83.58	86.0	
	0.01	64.47	66.19	68.21	68.9	
	0.004	34.99	36.46	39.44	42.1	38.25
W4	0.1	98.74	87.0	99.99	100.0	
	0.05	97.26	85.06	99.99	100.0	
	0.02	82.45	71.82	94.99	96.2	
	0.01	60.13	55.6	80.59	82.4	
	0.004	29.82	29.47	49.5	50.9	39.92
W5	0.1	100.0	100.0	100.0	100.0	
	0.05	99.6	99.6	100.0	99.3	
	0.02	90.3	91.3	93.3	92.4	
	0.01	76.6	78.3	81.6	80.7	
	0.004	48.6	50.9	54.7	53.9	52.03
WU	0.1	100.0	100.0	100.0	100.0	
	0.05	99.9	99.76	100.0	100.0	
	0.02	93.45	97.21	98.4	96.74	
	0.01	74.08	75.82	81.3	80.02	
	0.004	45.2	43.34	44.6	46.53	44.92
X	0.004	38.59	38.81	43.63	46.31	41.84

0.1 - 0.05 very fine sand
0.05 - 0.02 coarse silt
0.02 - 0.01 medium silt
0.01 - 0.004 medium - fine silt
< 0.004* clay size

* See text for choice of size range

The nature of the particle size distribution at the zone of shear was considered to be of major importance in this discussion. To facilitate the interpretation of this analysis the proportion of clay-size particles was used as an index of the size distribution. A mean value was computed for each core zone and for each slope unit within the mudslide. The following associations were noted:

1. the Wealden Clay samples contained a greater proportion of clay-size particles (42% in the slipped zones) when compared with the London Clay (33%).
2. both mudslides show an increase in the proportion of clay with depth (Figure 4.2), although at Manor Lane the sample mean showed a small 2 per cent depletion at zone 3, the basal shear surface.
3. when plotted with respect to the mudslide section (Figure 4.3) the association with morphology seems quite distinct at Worbarrow, with a marked increase in the proportion of fines in the source unit probably as a consequence of weathering and erosion when compared with the undisturbed profile, followed by a gradual decrease downslope towards the High Water Mark (HWM; Figure 4.3b). This trend was clearest at the basal shear surface although the sample mean also validates the finding.
4. similarly at Manor Lane, where an increase in clay-size material was measured in the source unit followed by a rapid reduction on transportation down to the lower slopes (Figure 4.3a).

By using the clay fraction as an 'index' of particle size it was possible to relate particle size characteristics to the morphology of both systems. At Worbarrow this association seemed reasonably clear whereas the complexity of the source unit at Manor Lane to some extent confused this trend. Assuming the Manor Lane mudslide to have two retrogressive source inputs (units 6 and 3), both mudslides showed an increase in clay-

Figure 4.2. Percent clay profiles for selected core samples.

* Please note: for absolute distributions downslope please refer to appending plots throughout Chapter Four.

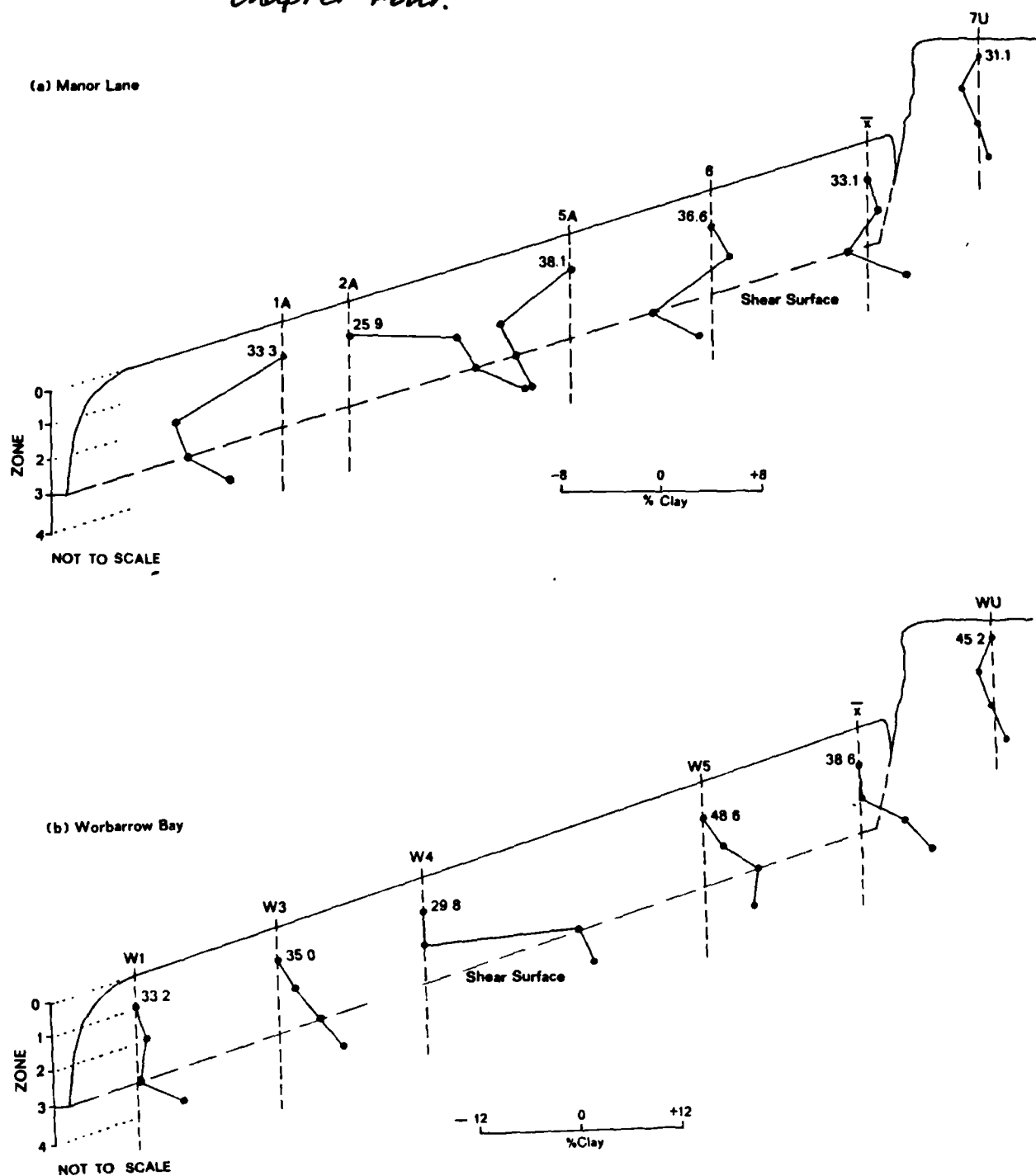
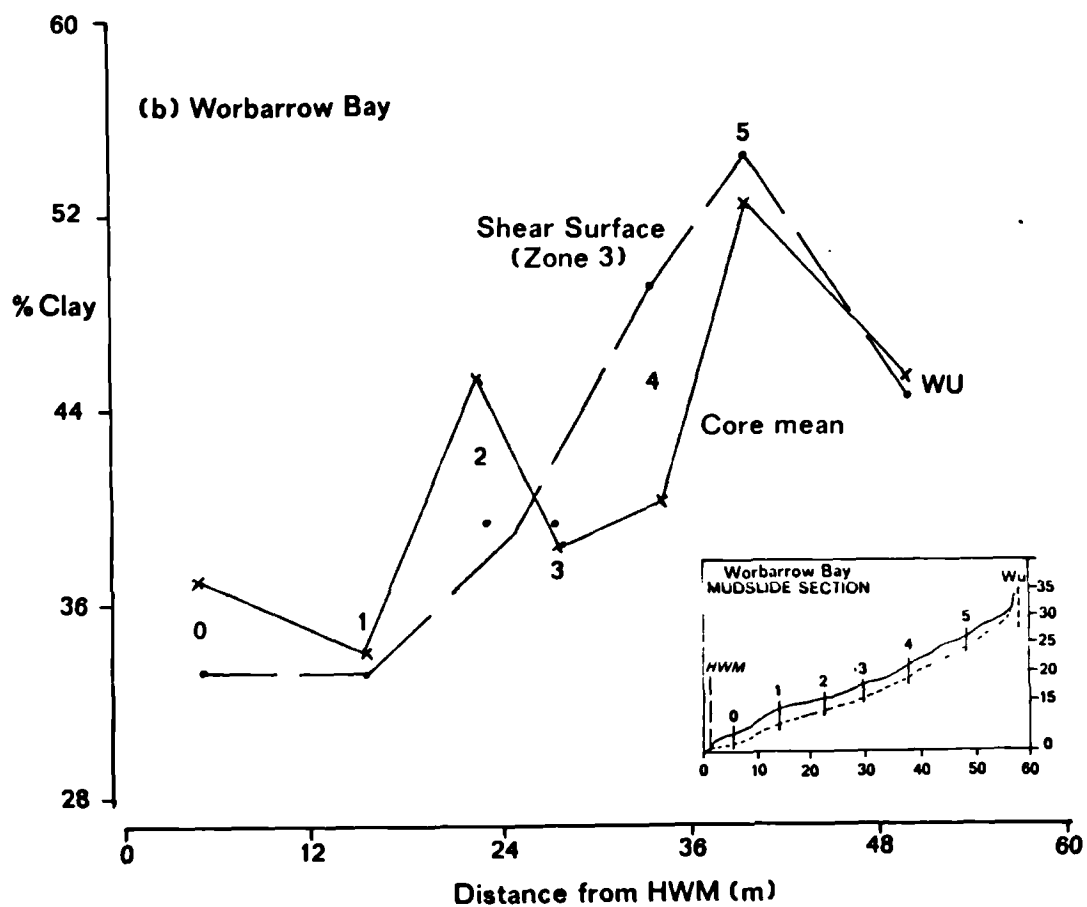
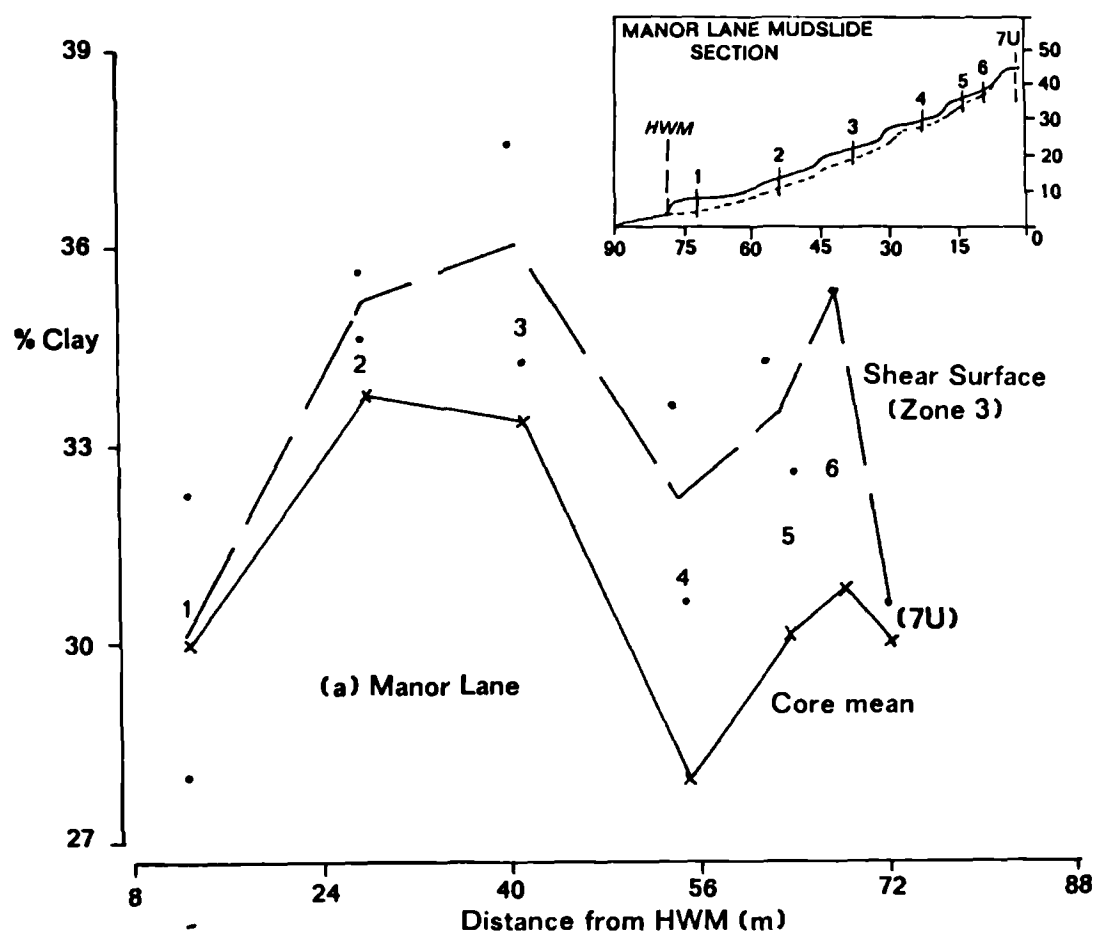


Figure 4.3. The distribution of clay at the shear surface.



size material directly on erosion and weathering, and a gradual reduction at the shear surface following the transportation of material downslope to the HWM. Both mudslides show an increase in clay immediately below the shear surface.

4.24 The phase relationships:

4.241 Moisture content.

The accurate determination of the natural (W_n), saturated (W_s), and air-dry (W_a) moisture contents of materials contained within the weathered profiles was required for the subsequent calculation of the phase relationships, and for volume adjustments in determinations of soil chemistry.

In assessing the natural moisture content sample errors can arise as a consequence of evaporation of moisture following the extraction from the ground, transportation to the laboratory and the length of time to analysis. Even though the core samples were completely sealed, it was felt necessary to control for such errors by directly assessing moisture content in the field. This was made possible by taking tube samples at the surface and base of each borehole for bulk density evaluations (see Appendix 1).

The pre-weighed tubes were immediately cleaned and weighed in the field following sampling, sealed and taken to the laboratory along with the core samples. Each tube was re-weighed in the laboratory and compared with the field measurement before placing in a drying oven to determine

the dry weight and moisture content. As an example of the errors experienced in the sampling phase the standard deviations for the first few cores from Manor Lane are listed below:

CORE	FIELD WEIGHT (g)	LAB. WEIGHT (g)	STANDARD ERROR (%)
1A	207.14	207.04	0.048
1B	304.10	304.07	0.015
2A	380.04	379.70	0.170
2B	280.57	280.49	0.040
3A	465.34	465.20	0.070
3B	286.56	286.47	0.045
4A	505.39	505.33	0.030
4B	222.90	222.83	0.035
5A	504.60	504.56	0.020
			=====
		\bar{x}	0.053
			=====

The example error of 0.053 per cent differs little from the total sample error of 0.051 per cent. It was thus considered that the transfer of samples to the laboratory was successful.

During the laboratory analysis every effort was made to reduce the time taken between extracting each sub-sample from the cores and the initial 'wet' weight measurements. Such precautions were discussed in section 3.411 and the methods used in the analyses of moisture content are detailed in Appendix 3. For each core zone three independent samples were analysed to establish a mean value for each parameter provided that the variation between each result did not exceed one per cent.

The results for Manor Lane are presented in Table 4.8 and those for Worbarrow in Table 4.9. The parameters of most importance in this

Table 4.8. Moisture content relations for all Manor Lane core samples.

CORE #	% MOISTURE CONTENT n=3	ZONE ONE	ZONE TWO	ZONE THREE	ZONE FOUR	MEAN %
1A	Wn	38.51	37.33	44.11	37.1	39.3
	Ws	70.22	70.83	74.75	70.03	71.5
	Wa	5.57	4.83	5.24	5.13	
1B	Wn	44.35	40.99	41.32	31.56	39.6
	Ws	76.79	68.12	79.44	86.6	77.7
	Wa	5.72	5.62	6.0	5.58	
2A	Wn	44.78	38.5	45.78	30.99	40.0
	Ws	76.01	78.6	80.43	82.94	79.5
	Wa	5.29	5.08	5.83	6.97	
2B	Wn	49.2	41.35	35.78	29.81	39.0
	Ws	73.21	82.64	86.09	74.02	79.0
	Wa	5.56	6.38	11.69	5.32	
3A	Wn	31.76	35.33	41.36	32.53	35.3
	Ws	78.9	76.38	79.64	83.88	79.7
	Wa	5.99	5.87	5.91	5.83	
3B	Wn	46.5	39.4	43.11	33.22	40.6
	Ws	76.57	84.57	84.64	80.68	81.6
	Wa	7.49	14.2	7.53	6.25	.
4A	Wn	40.2	36.85	34.68	31.66	35.9
	Ws	74.55	72.62	80.63	91.96	79.9
	Wa	5.96	5.93	6.88	5.87	
4B	Wn	36.73	37.39	33.61	29.43	34.3
	Ws	59.77	75.37	61.4	101.26	74.5
	Wa	4.86	5.48	5.66	6.29	
5A	Wn	34.32	35.16	28.56	24.96	30.8
	Ws	82.24	76.99	89.93	91.72	85.2
	Wa	8.47	6.99	6.46	7.51	
5B	Wn	29.79	31.49	34.91	34.37	32.6
	Ws	70.92	86.17	82.5	84.29	81.0
	Wa	5.39	15.43	16.2	6.81	
6	Wn	32.01	34.33	32.76	25.29	31.1
	Ws	87.92	85.14	76.28	90.94	85.1
	Wa	7.78	8.1	6.53	8.81	
7U	Wn	33.34	35.02	29.36	25.54	30.8
	Ws	78.08	97.2	80.69	60.62	79.2
	Wa	8.03	16.47	6.79	5.63	
X	Wn	38.5	36.9	37.1	30.5	35.8
	Ws	75.4	79.6	79.7	83.3	79.5
	Wa					

=====

Wn : natural moisture content
 Ws : saturated moisture content
 Wa : air-dry moisture content

Table 4.9. Moisture content relations for all Worbarrow core samples.

CORE #	% MOISTURE CONTENT n=3	ZONE ONE	ZONE TWO	ZONE THREE	ZONE FOUR	MEAN %
W0	Wn	22.63	28.78	27.82	31.01	27.6
	Ws	46.23	58.75	42.34	58.57	51.5
	Wa	3.91	7.59	4.06	3.74	
W1	Wn	20.28	17.99	21.21	13.7	18.3
	Ws	47.82	37.06	47.52	40.22	43.2
	Wa	2.57	1.41	4.7	2.42	
W2	Wn	16.87	19.82	22.14	17.44	19.1
	Ws	43.16	48.66	61.06	50.96	51.0
	Wa	2.59	4.62	4.66	5.27	
W3	Wn	25.85	25.06	20.93	18.78	22.7
	Ws	61.02	49.03	51.34	51.35	53.2
	Wa	5.48	4.62	4.92	4.29	
W4	Wn	17.79	25.9	30.01	23.43	24.3
	Ws	42.12	42.14	75.43	64.99	56.2
	Wa	2.44	1.44	5.12	6.25	
W5	Wn	25.07	27.16	21.42	20.39	23.5
	Ws	59.03	77.11	62.78	56.94	64.0
	Wa	5.17	9.95	6.47	3.77	*
Wu	Wn	15.0	17.4	14.73	23.66	17.7
	Ws	74.04	88.92	81.05	83.38	81.9
	Wa	7.35	8.38	7.29	7.29	
X	Wn	20.5	23.2	22.6	19.8	21.5
	Ws	53.4	57.4	60.2	58.1	57.3
	Wa					

Wn : natural moisture content
 Ws : saturated moisture content
 Wa : air-dry moisture content

discussion are the natural and saturated moisture contents for these are fundamental to soil behaviour and are required for the determination of the phase relationships. With respect to the morphology of each mudslide the following associations were recognised:

1. in comparison, the Manor Lane mudslide had a greater natural and saturated water content (Wn 36% : Ws 80%) at the time of sampling than found at Worbarrow (Wn 22% : Ws 57%).
2. with reference to Figure 4.4b, the weathered profiles at Worbarrow show a 6 per cent increase in mean natural moisture content in comparison with the 'unweathered' core profile (sample WU), with maximum values at sub-zones 2 and 3. The peak moisture content within each profile coincides with the depth of the basal or most active shear surface; such as zone 2 for the uppermost slope unit (5), and zone 3 in core 4 where the basal shear surface is known to have deepened (section 4.21). The results suggest a 'saturated' zone above the shear surface and that moisture content could be used as a diagnostic feature in their location (see section 5.321).
3. in relation to the Worbarrow mudslide section (Figure 4.6a) there was a maximum Wn in the source and upper slope units (5 and 4) with lower moisture levels downslope to the rear of the accumulation lobe (unit 2). The moisture content of the mudslide toe showed a dramatic increase when compared with the other slope units which was considered to be the result of moisture accumulation from upslope and the proximity of the sea. The mean profile corresponded with the shear zone measurements with a less pronounced peak in the source unit. Figure 4.6b shows a uniform decrease in saturated moisture content at the basal shear surface downslope from the source unit.
4. the natural moisture content of weathered materials at Manor Lane showed a 10 per cent increase in comparison with the undisturbed profile (Figure 4.4a), but differs in profile from the Worbarrow site. In the source unit the moisture profiles are similar in

Figure 4.4. Natural moisture content profiles of selected core samples.

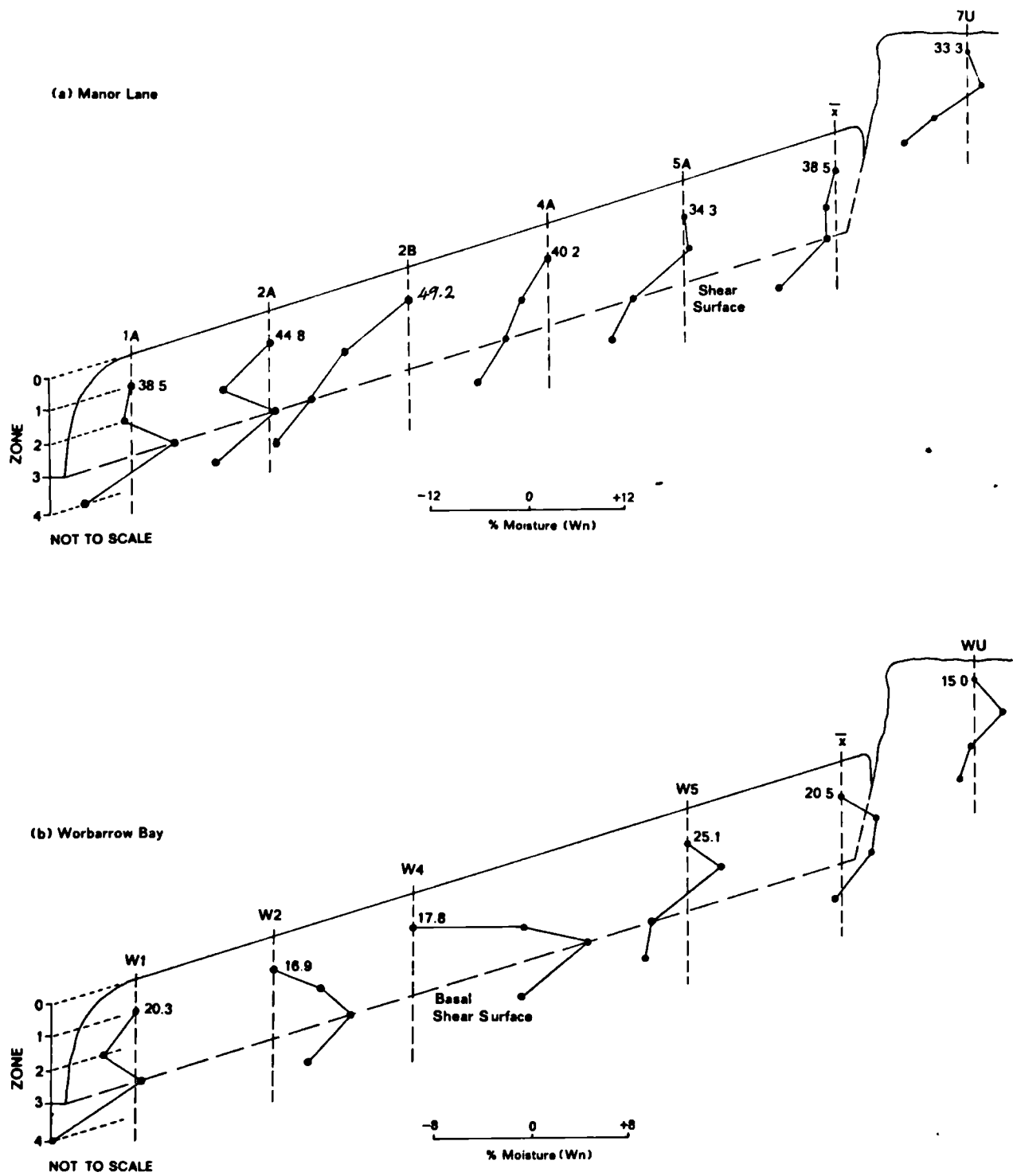


Figure 4.5. The distribution of moisture content at Manor Lane.

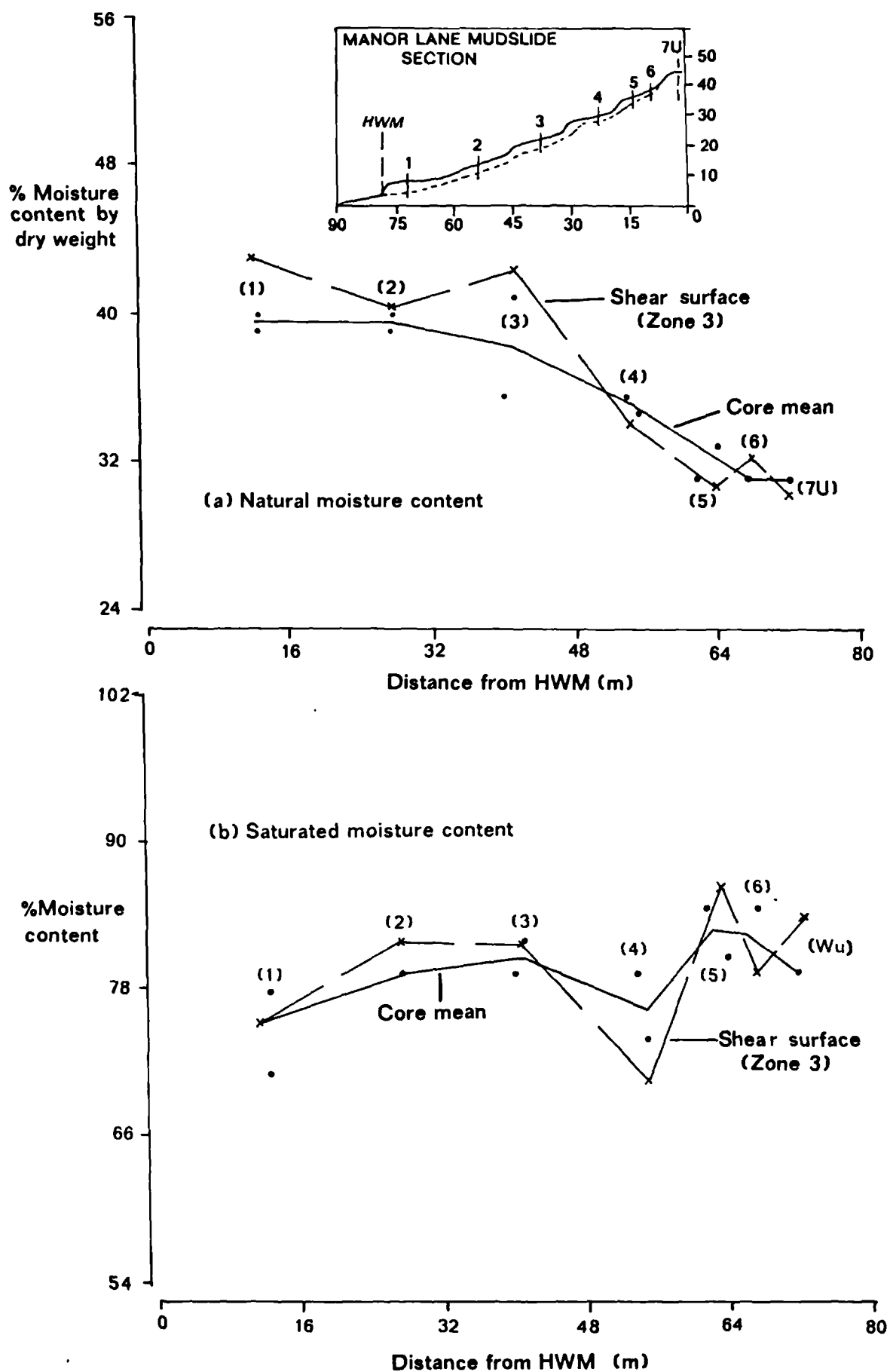
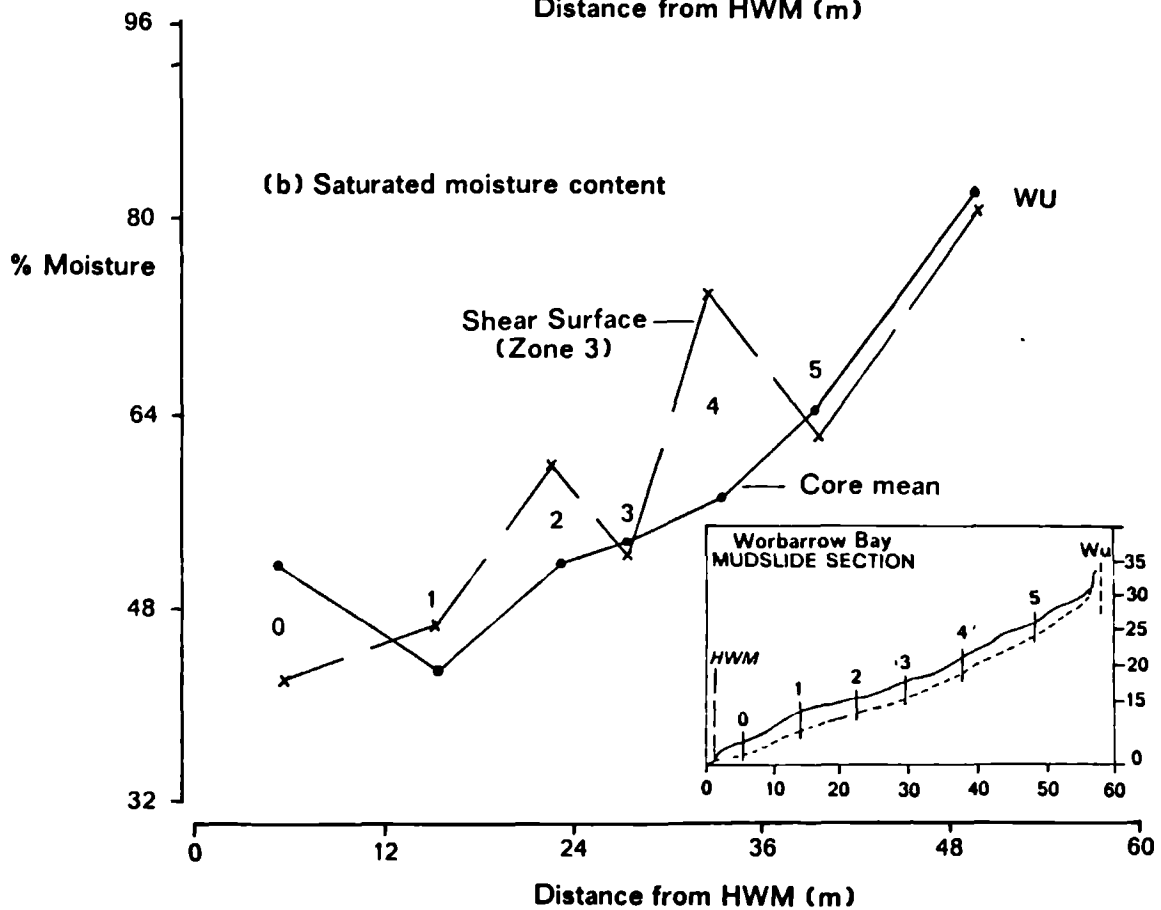
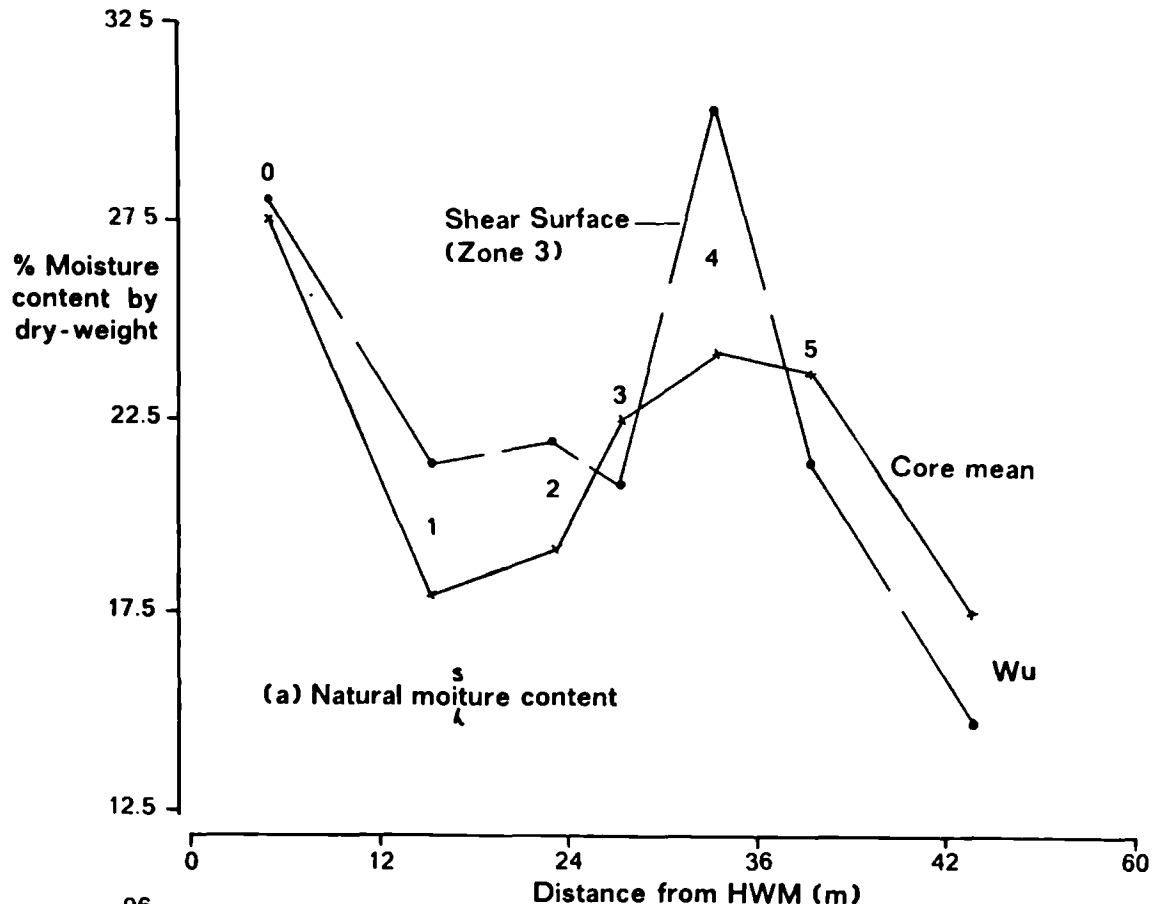


Figure 4.6. The distribution of moisture content at Worbarrow Bay.



nature to the undisturbed sample (7U) with a decrease in W_n with depth. There was a gradual increase in natural soil moisture in the surface layers until about midslope (unit 3) where there was a dramatic increase in moisture content at the basal shear surface. This change coincided with the secondary source input recognised in the previous section. This suggested the presence of a basal aquifer and the input of considerable amounts of groundwater. Downslope of this region the surface layers became progressively more saturated.

5. The latter association is better emphasised in Figure 4.5a where the mean moisture content is plotted with respect to the mudslide section. The diagram clearly indicates the accumulation of soil moisture at the base of the feeder track before overflowing onto the beach. As for Worbarrow there was a decrease in the saturated moisture content (Figure 4.5b), the materials becoming more susceptible to saturation after weathering and movement downslope.

Although moisture content is an important factor in slope instability the nature of the interaction of water with soil particles enables a better understanding of soil behaviour under natural soil water regimes.

4.242 Specific gravity, void ratio and porosity.

To enable the calculation of the void ratio and porosity of materials the specific gravity of the particles were measured according to the methods described in Appendix 4. An average value of the specific gravity was computed from three determinations, providing that the variation between each result did not exceed 0.05 per cent.

The void ratio and porosity were calculated for a two-phase system from established equations (Appendix 4) using the saturated moisture content

Table 4.10. Data summary of the phase relationships at Manor Lane.

CORE #	PARAMETER n = 3	ZONE ONE	ZONE TWO	ZONE THREE	ZONE FOUR	\bar{X}
1A	Gs	2.66	2.57	2.72	2.63	2.65
	e	1.87	1.82	2.03	1.84	1.89
	n	0.65	0.65	0.67	0.65	0.655
1B	Gs	2.62	2.62	2.64	2.64	2.63
	e	2.01	1.79	2.1	2.29	2.05
	n	0.67	0.64	0.68	0.7	0.673
2A	Gs	2.63	2.63	2.68	2.63	2.64
	e	1.99	2.07	2.16	2.18	2.1
	n	0.68	0.67	0.68	0.69	0.680
2B	Gs	2.63	2.65	2.68	2.65	2.65
	e	1.93	2.19	2.31	1.96	2.1
	n	0.66	0.69	0.7	0.66	0.678
3A	Gs	2.73	2.63	2.73	2.62	2.68
	e	2.15	2.01	2.17	2.2	2.13
	n	0.68	0.67	0.69	0.69	0.680
3B	Gs	2.6	2.61	2.63	2.62	2.62
	e	1.99	2.21	2.23	2.11	2.14
	n	0.67	0.69	0.69	0.68	0.683
4A	Gs	2.6	2.58	2.72	2.59	2.62
	e	1.94	1.87	2.19	2.38	2.1
	n	0.66	0.65	0.69	0.7	0.675
4B	Gs	2.67	2.55	2.65	2.6	2.62
	e	1.6	1.92	1.63	2.63	1.95
	n	0.62	0.66	0.62	0.73	0.658
5A	Gs	2.58	2.59	2.6	2.58	2.59
	e	2.12	1.99	2.34	2.37	2.21
	n	0.68	0.67	0.7	0.7	0.688
5B	Gs	2.72	2.63	2.66	2.64	2.66
	e	1.93	2.27	2.2	2.23	2.16
	n	0.66	0.69	0.69	0.69	0.683
6	Gs	2.63	2.59	2.68	2.61	2.63
	e	2.31	2.21	2.04	2.37	2.23
	n	0.7	0.69	0.67	0.7	0.690
7U	Gs	2.62	2.61	2.62	2.62	2.62
	e	2.05	2.54	2.11	1.59	2.07
	n	0.67	0.72	0.68	0.61	0.670
\bar{X}	Gs	2.64	2.61	2.67	2.62	2.64
	e	1.99	2.07	2.13	2.18	2.09
	n	0.666	0.674	0.680	0.683	0.676

Gs : specific gravity of particles

e : void ratio n : porosity

Table 4.11. Data summary of the phase-relationships at Worbarrow Bay.

CORE #	PARAMETER n = 3	SURFACE LAYER	ZONE ONE	ZONE TWO	ZONE THREE	ZONE FOUR	IN-SITU CLAY	- X
W0	Gs		2.68	2.68	2.64	2.63		2.66
	e		1.24	1.58	1.12	1.54		1.37
	n		0.55	0.61	0.53	0.61		0.575
	UW kN/m ³		14.39	13.14	15.62	13.29		14.11
	BD kg/m ³	1809.9	1467.9	1340.6	1593.4	1356.3	-	1624.7
W1	Gs		2.66	2.64	2.65	2.61		2.64
	e		1.27	0.98	1.26	1.05		1.14
	n		0.56	0.5	0.56	0.51		0.533
	UW		13.80	15.43	13.93	14.19		14.34
	BD	1301.3	1408.2	1574.5	1421.7	1447.8	-	1382.2
W2	Gs		2.66	2.66	2.6	2.65		2.64
	e		1.15	1.29	1.59	1.35		1.35
	n		0.53	0.56	0.61	0.58		0.57
	UW		14.18	13.61	12.03	12.97		13.2
	BD	1543.3	1447.2	1389.2	1227.3	1324.1	1833.4	1574.6
W3	Gs		2.72	2.62	2.63	2.65		2.66
	e		1.66	1.29	1.35	1.36		1.42
	n		0.62	0.56	0.58	0.58		0.585
	UW		12.61	14.06	13.26	13.07		13.25
	BD	1692.6	1287.0	1434.2	1353.3	1333.3	2228.1	1757.6
W4	Gs		2.67	2.63	2.61	2.58		2.62
	e		1.13	1.11	1.97	1.68		1.47
	n		0.53	0.53	0.66	0.63		0.588
	UW		14.51	15.39	11.20	11.66		13.19
	BD	2080.4	1480.3	1570.6	1143.0	1189.7	2056.7	1827.7
W5	Gs		2.68	2.62	2.66	2.63		2.65
	e		1.24	2.02	1.67	1.5		1.608
	n		0.55	0.67	0.63	0.6		0.613
	UW		14.39	10.81	11.86	12.42		12.37
	BD	1751.8	1467.9	1103.1	1209.7	1267.8	2257.5	1757.1
Wu	Gs		2.69	2.68	2.65	2.69		2.68
	e		1.99	2.25	2.36	2.24		2.21
	n		0.67	0.69	0.70	0.69		0.688
	UW		10.14	9.29	9.07	10.06		9.64
	BD	2068.3	1034.6	947.7	925.9	1026.7	2393.1	1815.0
- X	Gs		2.68	2.65	2.63	2.63		2.65
	e		1.38	1.50	1.62	1.53		1.51
	n		0.573	0.589	0.61	0.60		0.593
	UW		13.43	13.10	12.42	12.52		12.87
	BD	1749.6	1370.4	1337.1	1267.8	1278.0	2153.8	1526.1

Gs : specific gravity of particles

e : void ratio

n : porosity

UW : unit weight

BD : bulk density

and the specific gravity of the particles. Errors of calculation were related to the precision of laboratory assessments of both the soil moisture and specific gravity. Since the former results were constrained to a standard error of 1 per cent, and the latter to 0.05 per cent for three independent samples, the derivations were considered an accurate estimate of field conditions.

Tables 4.10 and 4.11 present the results for Manor Lane and Worbarrow Bay, respectively. The following associations were noted:

1. the specific gravity of soil particles from both sites showed little variation about the mean of 2.65 Gs. The main differences between the phase relationships of the London and Wealden Clay sites were a greater void ratio ($e = 2.09$) and porosity ($n = 0.68$) at Manor Lane than found at Worbarrow ($e = 1.51$; $n = 0.59$).
2. the weathered profiles of Worbarrow Bay and Manor Lane show an apparent increase in void ratio with depth (Figure 4.7). This amounts to an average increase with depth of 9 per cent at Manor Lane and 15 per cent at Worbarrow. The void ratio was greatest at the basal shear surface at Worbarrow, but for *in situ* clay at Manor Lane. The undisturbed core profile corresponded with the weathered profiles at Worbarrow. In contrast, the unweathered core sample from Manor Lane (7U) showed an increase in void ratio of 19 per cent to sub-zone 2, followed by a 37 per cent reduction with depth to zone 4, contrary to the weathered mudslide profiles.
3. at both Worbarrow and Manor Lane the void ratio decreases downslope towards the HWM (Figure 4.8). At Manor Lane there was an initial increase in void ratio to 2.2 in the source unit (6) and in the secondary source area (unit 3), presumably as a consequence of weathering and erosion of materials from these regions before decreasing to a value of 2.0 at the base of the feeder track. At Worbarrow there was a greater reduction in void ratio on weathering from 2.3 to 1.1. These consistent findings

Figure 4.7. Void ratio depth profiles for selected core samples.

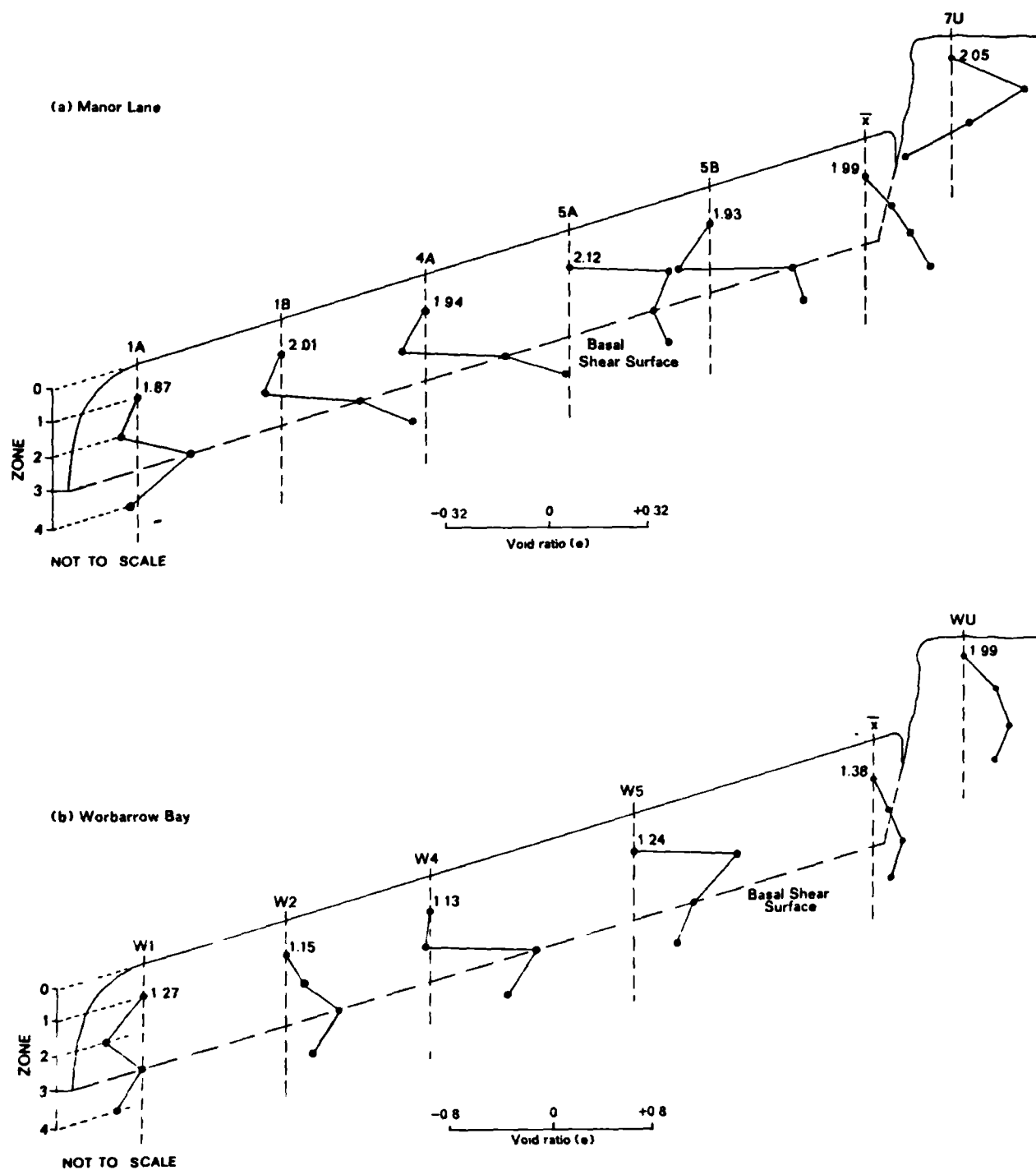


Figure 4.8. The distribution of the void ratio at the shear surface.

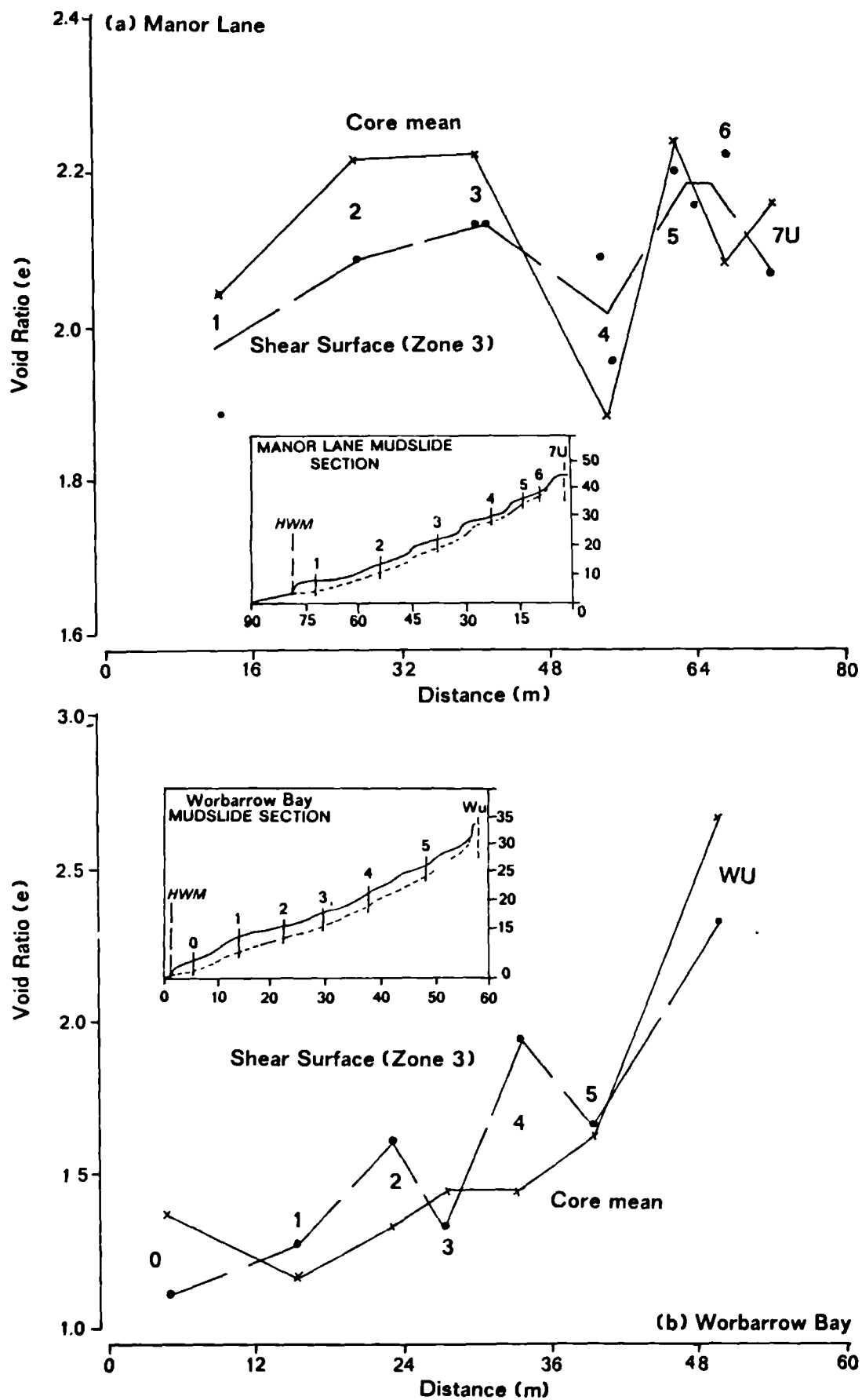
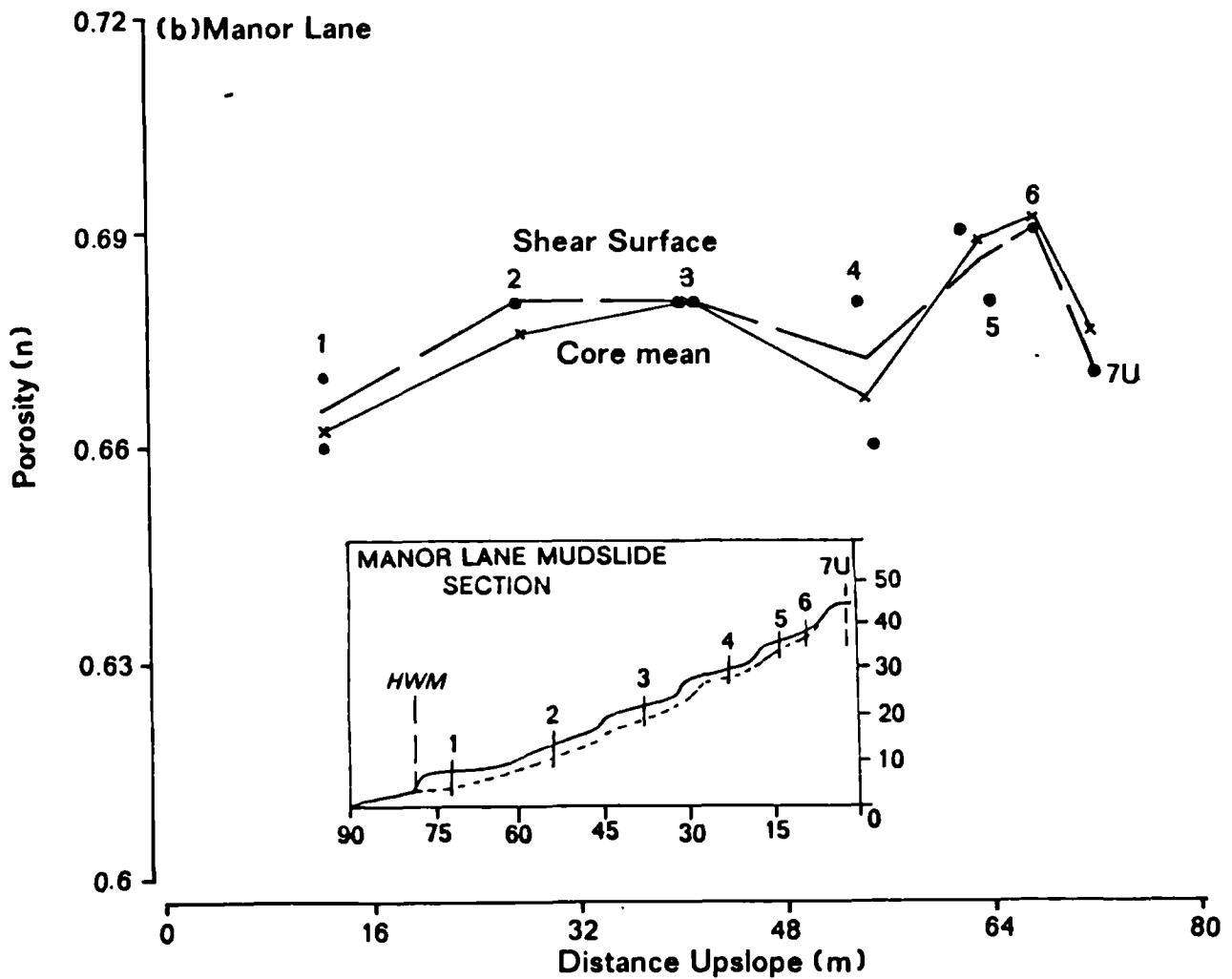
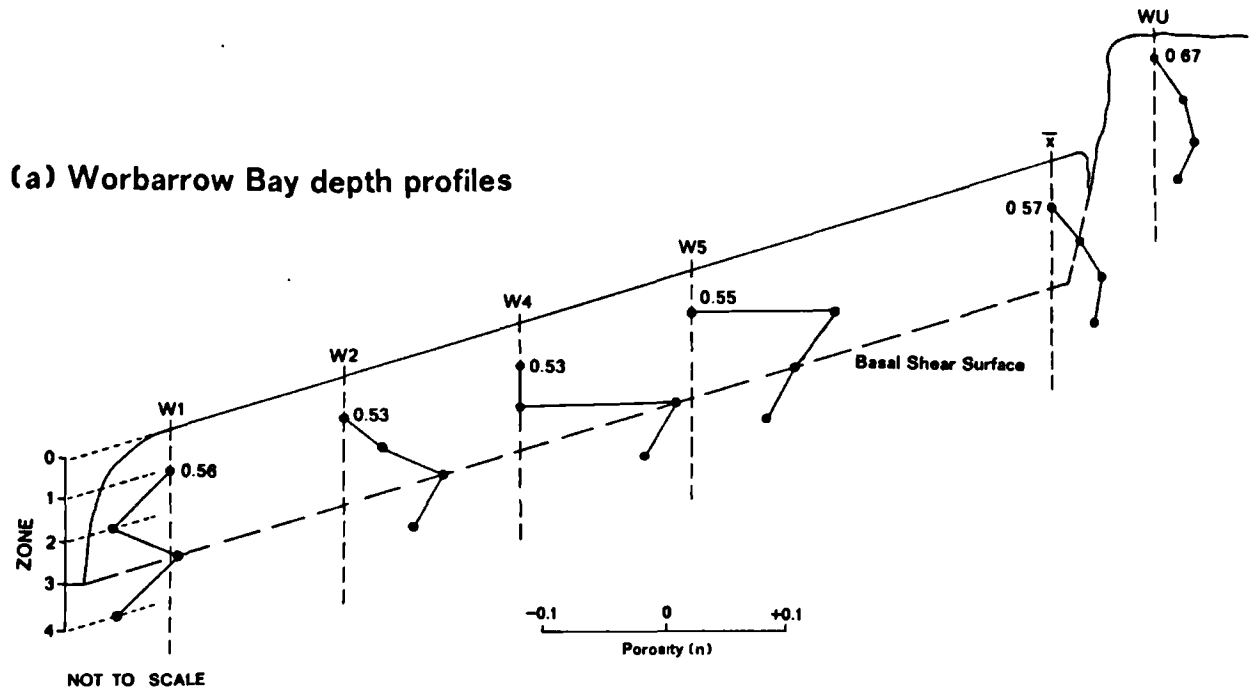


Figure 4.9. The distribution of porosity with depth and along the shear surface.



might suggest the gradual compression of particles on the lower slopes in comparison with tension experienced in the source units.

4. Since porosity is directly related to void ratio the same associations were found at both sites as indicated in Figure 4.9. For example at Worbarrow there was a reduction in porosity from 0.7 to 0.5 on weathering and transportation of materials downslope (Figure 4.9b); at Manor Lane there was a reduction from 0.69 to 0.66 downslope. The highest porosity was found at the shear surface relative to the mean distribution.

4.243 Unit weight and particle density.

The unit weight and bulk density were determined from field and laboratory tests. Laboratory calculations were based on the specific gravity and void ratio of the particles, the natural moisture content and the unit weight and density of water. The accuracy of the calculations were based on the precision of laboratory tests as previously mentioned, and since the errors of these tests were kept to within stringent limits the derivations were considered an accurate measure of field conditions.

In situ field bulk density tests were undertaken at the surface and below the base of each core sample (section 3.31 and Appendix 1) the findings of which are included as supplementary results and further serve to substantiate the mathematical derivations. However, the two sets of results cannot be directly compared for accuracy since they represent materials from different locations within the weathered profile.

The results of the density tests are shown in Table 4.11 for Worbarrow and Table 4.12 for Manor Lane. The following associations were noted:

Table 4.12. Unit weight and bulk density results for Manor Lane.

CORE #	PARAMETER n = 3	SURFACE LAYER	ZONE ONE	ZONE TWO	ZONE THREE	ZONE FOUR	IN-SITU CLAY	- X
1A	UW KN/m ³	-	12.59	12.26	12.67	12.44	-	12.5
	BD Kg/m ³	912.5	1284.7	1251.4	1292.3	1268.8	-	1093.4
1B	UW	-	12.31	13.0	11.81	10.36	-	11.9
	BD	1330.7	1255.7	1326.5	1204.6	1056.9	1691.8	1411.1
2A	UW	-	12.44	11.64	12.13	10.61	-	11.7
	BD	1236.0	1269.6	1187.6	1238.1	1082.9	2050.0	1493.5
2B	UW	-	13.15	11.51	10.78	11.38	-	11.7
	BD	1262.4	1341.3	1174.2	1100.3	1161.6	2226.4	1561.1
3A	UW	-	11.18	11.59	11.92	10.64	-	11.3
	BD	981.6	1140.5	1182.9	1215.8	1085.9	2222.9	1453.6
3B	UW	-	12.48	11.12	11.43	10.99	-	11.5
	BD	1091.2	1273.6	1134.4	1166.7	1120.9	1998.2	1421.1
4A	UW	-	12.16	12.04	11.24	9.88	-	11.3
	BD	970.8	1240.6	1228.7	1147.2	1008.4	1863.6	1330.2
4B	UW	-	13.78	11.75	13.21	9.07	-	12.0
	BD	1175.5	1406.4	1199.0	1347.8	926.3	1767.8	1387.7
5A	UW	-	10.88	11.46	9.81	9.39	-	10.4
	BD	1467.3	1110.1	1169.2	1001.3	957.7	1584.6	1370.5
5B	UW	-	11.81	10.38	11.01	10.78	-	11.0
	BD	1026.7	1205.3	1058.8	1123.4	1099.9	1443.0	1197.2
6	UW	-	10.27	10.64	11.45	9.50	-	10.5
	BD	1145.7	1048.2	1085.5	1168.7	969.3	1830.1	1347.9
7U	UW	-	11.24	9.76	10.67	12.45	-	11.0
	BD	1338.0	1147.0	996.3	1088.4	1270.8	1954.0	1472.5
-	UW	-	12.0	11.4	11.5	10.6	-	11.4
X	BD	1161.5	1226.9	1166.2	1174.6	1084.1	1875.7	1281.5

UW : unit weight
BD : bulk density

1. the mean unit weight profiles of both sites (Figure 4.10) were inversely related to the void ratio and porosity. The mean profile for Manor Lane showed a 12 per cent reduction with depth, mostly beneath the shear surface, in comparison with 8 per cent for the weathered mudslide profiles at Worbarrow. These varied in nature from the unweathered sample profiles at both sites where the unit weight increased with depth, particularly between sub-zones 3 and 4. This was quite considerable at Manor Lane amounting to 22 per cent in comparison with an 8 per cent change at Worbarrow.
2. when plotted in relation to the slope section in Figure 4.11, the unit weight increases uniformly downslope at both sites. At Manor Lane the unit weight increased 16 per cent from 10.5 kN/m³ directly upon weathering and erosion increasing to 12.5 kN/m³ at the toe of the slope. This feature was even more marked at Worbarrow where the unit weight increased 33 per cent from 9.64 kN/m³ to 14.34 kN/m³ upon weathering and movement downslope to the accumulation lobe.
3. the bulk density profiles at both sites, presented in Figure 4.12, demonstrate a two-fold increase in density below the basal shear surface. This sharp density change was experienced during the penetration of the sampling tubes (Appendix 1). At Worbarrow the surface layers showed a greater particle density than found in the 'body' of the mudslide, whereas at Manor Lane a slight reduction was noted. The density of the weathered mudslide profiles were generally consistent between sub-zones 2 and 3.
4. the distribution of density throughout both mudslide sections is presented in Figure 4.13. At Worbarrow the results indicate a small reduction in the mean bulk density downslope and similarly for Manor Lane. In contrast, the bulk density at the shear surface of both mudslides showed an inverse relationship with the core mean suggesting that the bulk density at the shear surface was independent of the weathered profiles. The density increased uniformly downslope amounting to 16 per cent at Manor Lane and 42 per cent at Worbarrow. This probably occurred as a consequence of an increase in overburden compression or volume of material.

Figure 4.10. Unit weight profiles for selected core samples.

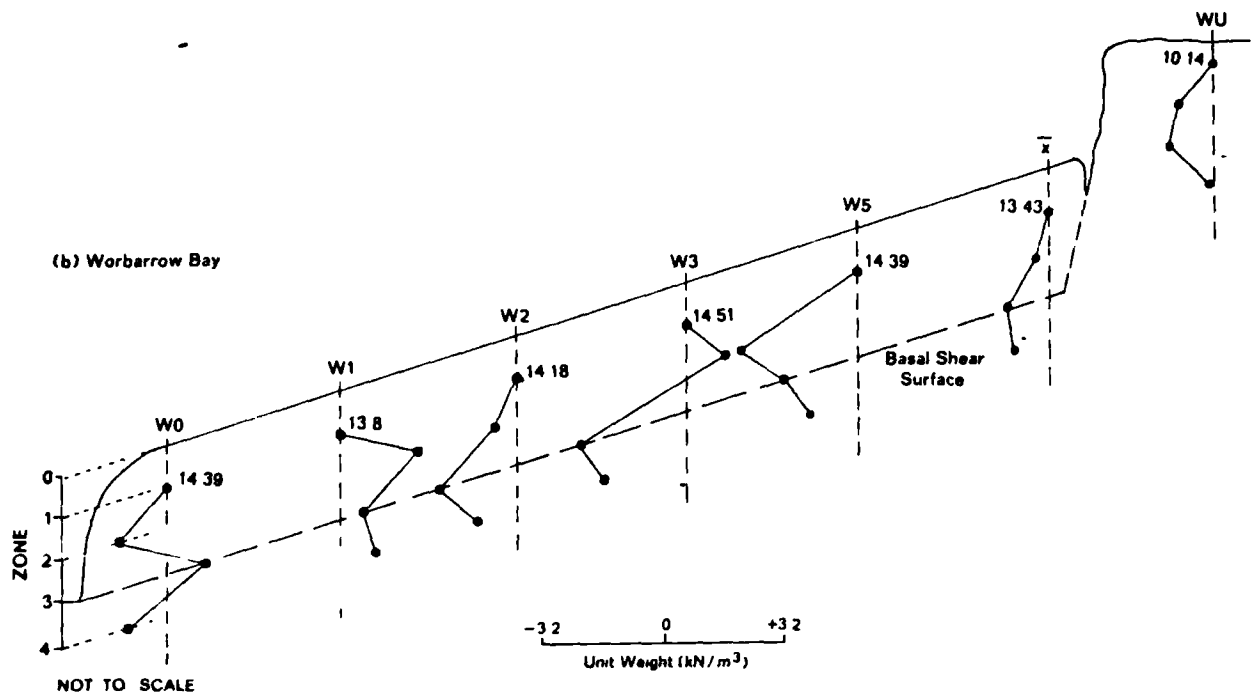
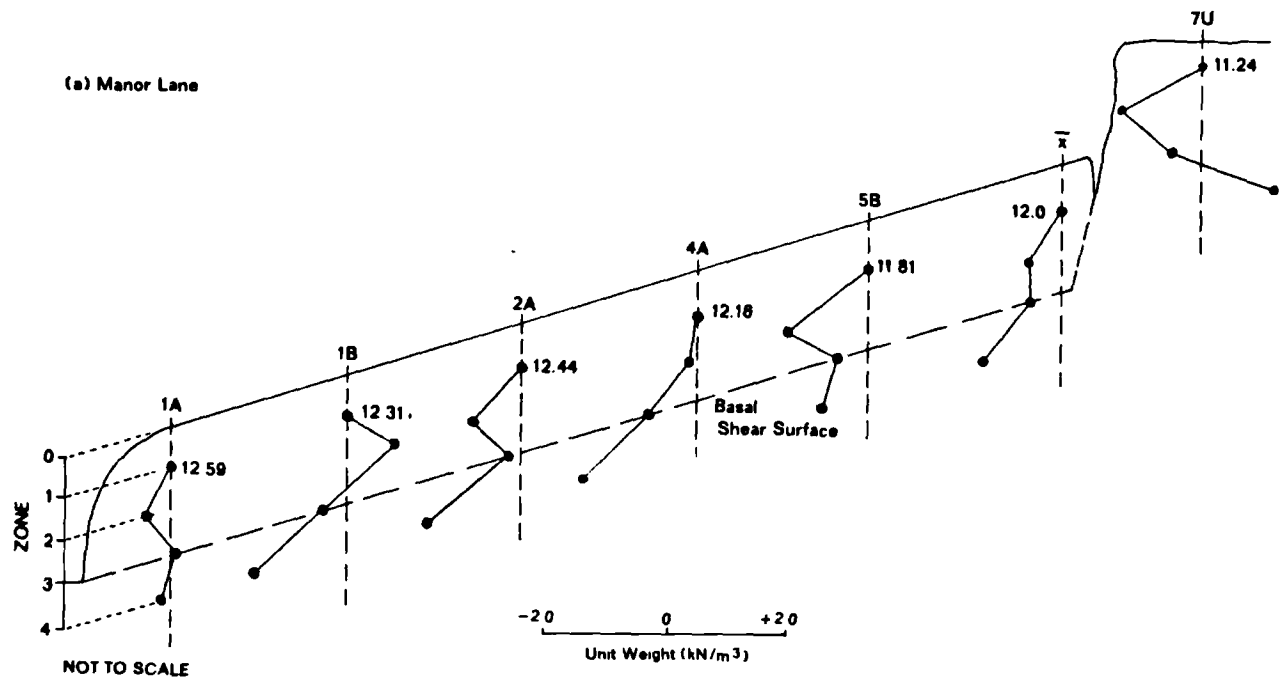


Figure 4.11. Distribution of unit weight at the shear surface.

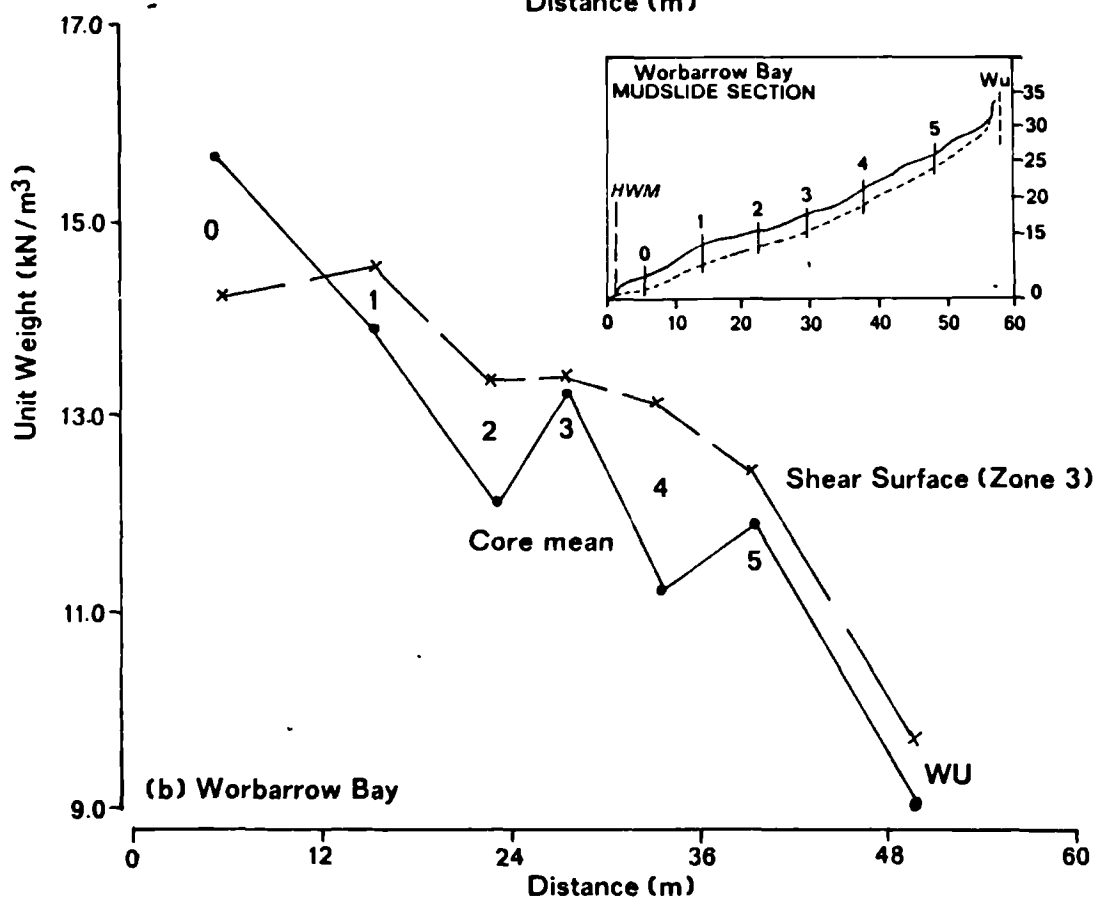
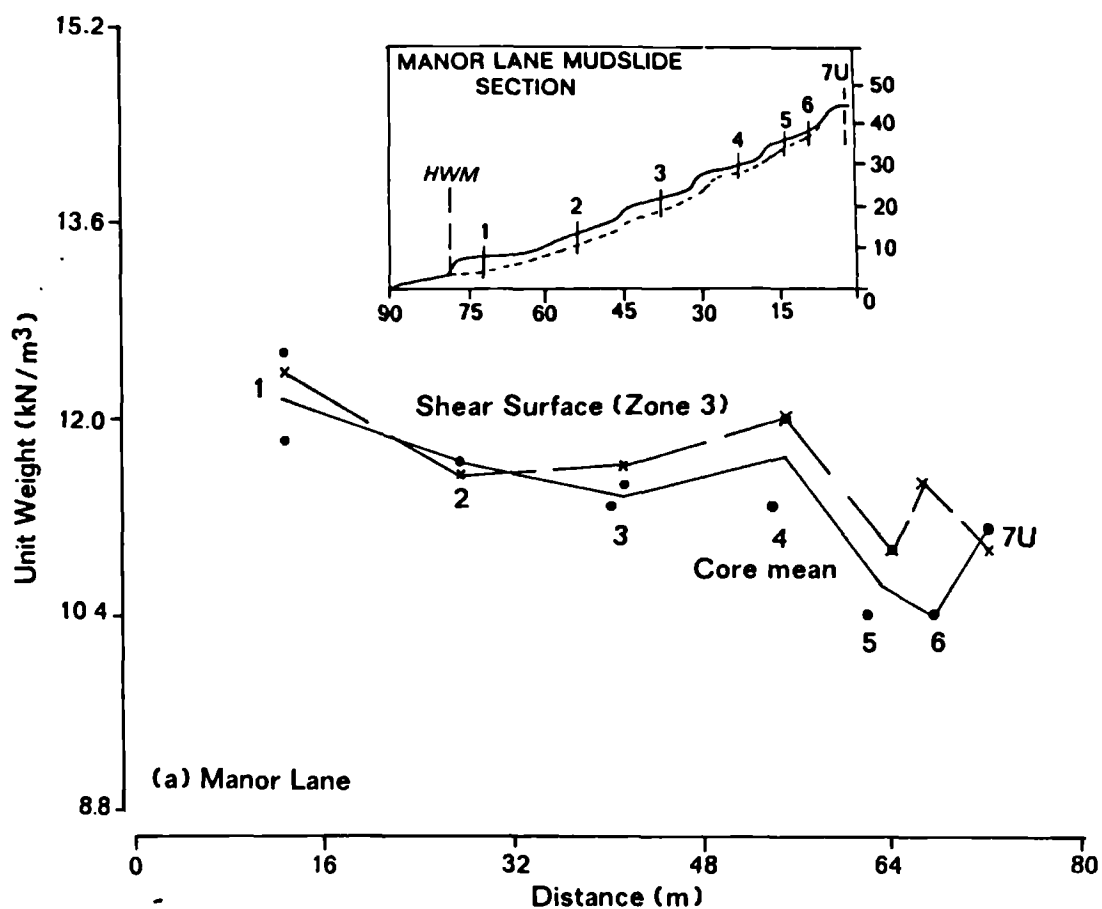


Figure 4.12. Bulk density profiles of selected core samples.

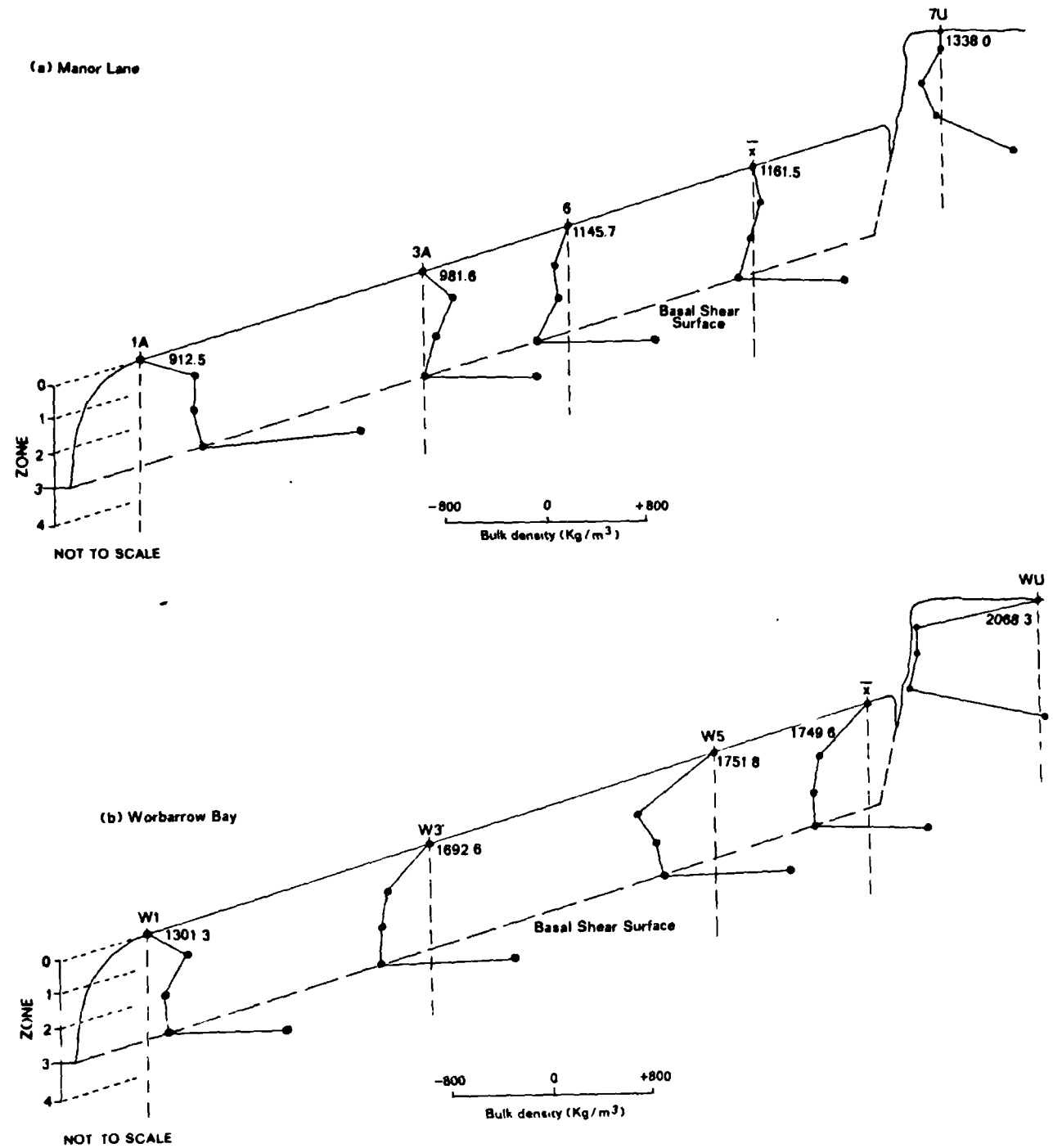
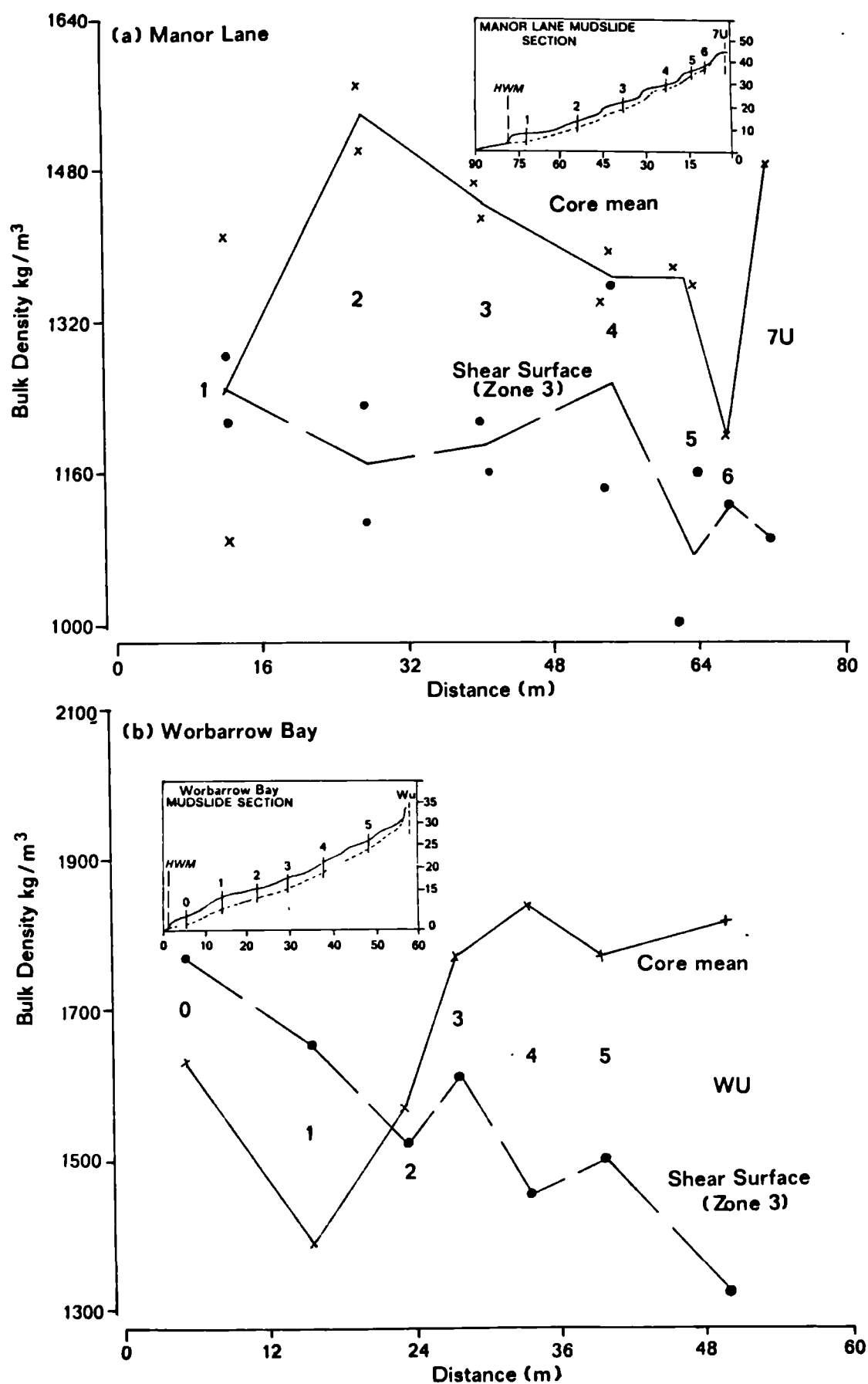


Figure 4.13. Distribution of bulk density at the shear surface.



The association of the phase relationships with weathering and slope morphology has shown an increase in the unit weight following weathering and erosion corresponding with an inverse relationship with void ratio and porosity. The unit weight and bulk density at the basal shear surface increased downslope with respect to the mudslide sections in contrast to reductions in the profile means. There were very marked two-fold increases in bulk density below the basal shear surface separating the over-consolidated *in situ* clay from the unconsolidated mudslide debris. The development of this density change may be either a direct or indirect cause of shear surface formation.

4.3 Geotechnical properties:

The geotechnical properties of both mudslides were only assessed at the basal shear surface and for *in situ* clay, since the plasticity and shear strength behaviour exhibited in these zones are the most critical for the stability of the slope. The determination of the residual shear strength parameters was an important aspect of this study because shear surfaces pre-existed in all weathered core profiles from Manor Lane and Worbarrow Bay, whereas the parameters measured for *in situ* undisturbed clays corresponded to the peak condition (section 2.32).

Standard consistency tests were undertaken to determine the liquid and plastic limits from which the plasticity index and activity ratios were calculated (section 2.24). The results of these tests are presented in section 4.31. Two types of strength test were conducted to assess the drained peak and residual parameters (section 4.32). A Bromhead ring-shear was used to determine the effective residual parameters for each

weathered profile (4.321), and two series of triaxial compression tests (4.322) were undertaken to determine the effective peak parameters at zone 3 of the undisturbed core samples 7U and WU.

4.31 Plasticity and activity.

A series of tests were performed to establish the consistence limits of the materials extracted from the basal shear surface. The methods used to determine the liquid and plastic limits are outlined in Appendix 5, along with the calculation of the results and the computation of the plasticity index and activity ratio.

Using the cone-penetrometer technique the linear least squares regression curve of penetration against moisture content was computed; the liquid limit was interpolated as the moisture content allowing a standard penetration of 20 mm. The correlation coefficients of the regressions provided an estimation of the accuracy of the results, and since these were mostly 0.99 the errors of test were considered negligible. The samples from Worbarrow showed a small degree of scatter around the linear regression which was thought to have been imposed by the inherent heterogeneity of material, but at worst these returned a correlation coefficient of 0.97.

The plastic limit was established from 4 independent threads of material for each sample. The mean moisture content was calculated at the point where the threads of 3 mm diameter began to fracture and crumble. Although the accuracy of these tests was less rigorous than the liquid limit, reproducible results were obtained by constraining the variability

Table 4.13. Geotechnical properties at the basal shear surface for all Manor Lane core samples.

CORE #	ZONE n=5	LL %	PL %	Ip %	ACTIVITY RATIO	RESIDUAL MOHR ENVELOPE ϕ_r' (°) C_r' (kN/m ²)	
1A	4	73.3	22.2	51.1	1.76	9.54	2.4
1B	3	75.6	28.3	47.3	1.32	6.76	2.25
2A	3	75.0	27.7	47.3	1.29	7.96	2.64
2B	3	80.1	29.9	50.2	1.55	8.98	2.17
3A	3	76.3	28.1	48.2	1.55	7.84	1.67
3B	3	69.9	26.9	43.0	1.27	7.91	3.93
4A	3	68.3	26.1	42.2	1.46	11.36	2.31
4B	3	74.9	24.2	50.7	1.83	11.42	4.17
5A	2	41.1	21.4	19.7	0.61	11.0	2.8
5B	3	42.9	20.3	22.6	0.81	11.06	1.98
6	3	43.0	22.1	20.9	0.67	11.30	1.27
\bar{X}	3	65.5	25.2	40.3	1.28	9.56	2.51
						(ϕ_p')	(c_p')
7U	3	74.5	23.8	50.7	1.68	15.52	13.0

LL : liquid limit

PL : plastic limit

Ip : plasticity index

C' : effective cohesion

ϕ_r' : residual friction angle (p refers to the peak condition)

Table 4.14. Geotechnical properties at the basal shear surface for all Worbarrow core samples.

CORE #	ZONE n=5	LL %	PL %	Ip %	ACTIVITY RATIO	RESIDUAL MOHR ENVELOPE	
						ϕ_r' (°)	C_r' (kN/m ²)
W0	4	51.2	17.0	34.2	0.82	7.86	2.87
W1	4	42.0	15.5	26.5	0.68	10.38	3.63
W2	3	61.5	18.9	42.6	0.85	5.73	1.9
W3	2	52.9	15.3	37.6	1.03	12.5	2.35
W4	3	51.8	15.2	36.6	0.73	7.38	2.83
W5	3	54.6	17.8	36.8	0.67	6.85	5.27
X	3	52.3	16.6	35.7	0.80	8.45	3.14
						(ϕ_p')	(c_p')
WU	3	39.0	22.7	16.3	0.37	23.20	12.31

LL : liquid limit

Ip : plasticity index

ϕ_r' : residual friction angle

PL : plastic limit

C' : effective cohesion

ϕ_p' : peak friction angle

of moisture content between tests to within 1 per cent. Further tests were undertaken when this limit was exceeded.

The plasticity index (I_p) was calculated by subtracting the plastic limit from the liquid limit, and the activity ratio determined by dividing the plasticity index by the per cent clay-size particles in the sample, shown in section 4.23. The results of the plasticity tests are presented in Tables 4.13 and 4.14 for Manor Lane and Worbarrow, respectively. The following associations were recognised:

1. at Manor Lane the mean liquid limit was 65.5 per cent; the mean plastic limit was 25.2 per cent and the average range in which the weathered London Clay exhibited plasticity was 40.3 per cent. These compare favourably with reported values in the literature (see Table 2.6). The corresponding values for Worbarrow were 52.3 per cent for the liquid limit, 16.6 per cent for the plastic limit, and 35.7 per cent for the plasticity index. This broadly suggested that the disturbed Wealden materials were more susceptible to plastic behaviour at 9 per cent lower moisture contents than found for the weathered London Clay. The presence of fine sands and the lower values of porosity and void ratio discussed in the previous sections were thought to account for this fact. The larger porosity and void ratio at Manor Lane enables a greater adsorption of water before particles are able to slide across thin films of water separating the grains and exhibit plastic behaviour (section 2.24). This was also emphasised by the larger plasticity index of the London Clay, in addition to the higher moisture contents required by the latter to reach the plastic and liquid limits.
2. in comparison with the undisturbed materials at Manor Lane it was noted that upon weathering there was a average reduction of 10 per cent in the liquid limit and plasticity index. In contrast, there was an increase of 13 per cent in the liquid limit and 19 per cent in the plasticity index at Worbarrow. The undisturbed London Clay

Figure 4.14. Distribution of the liquid limit at the shear surface.

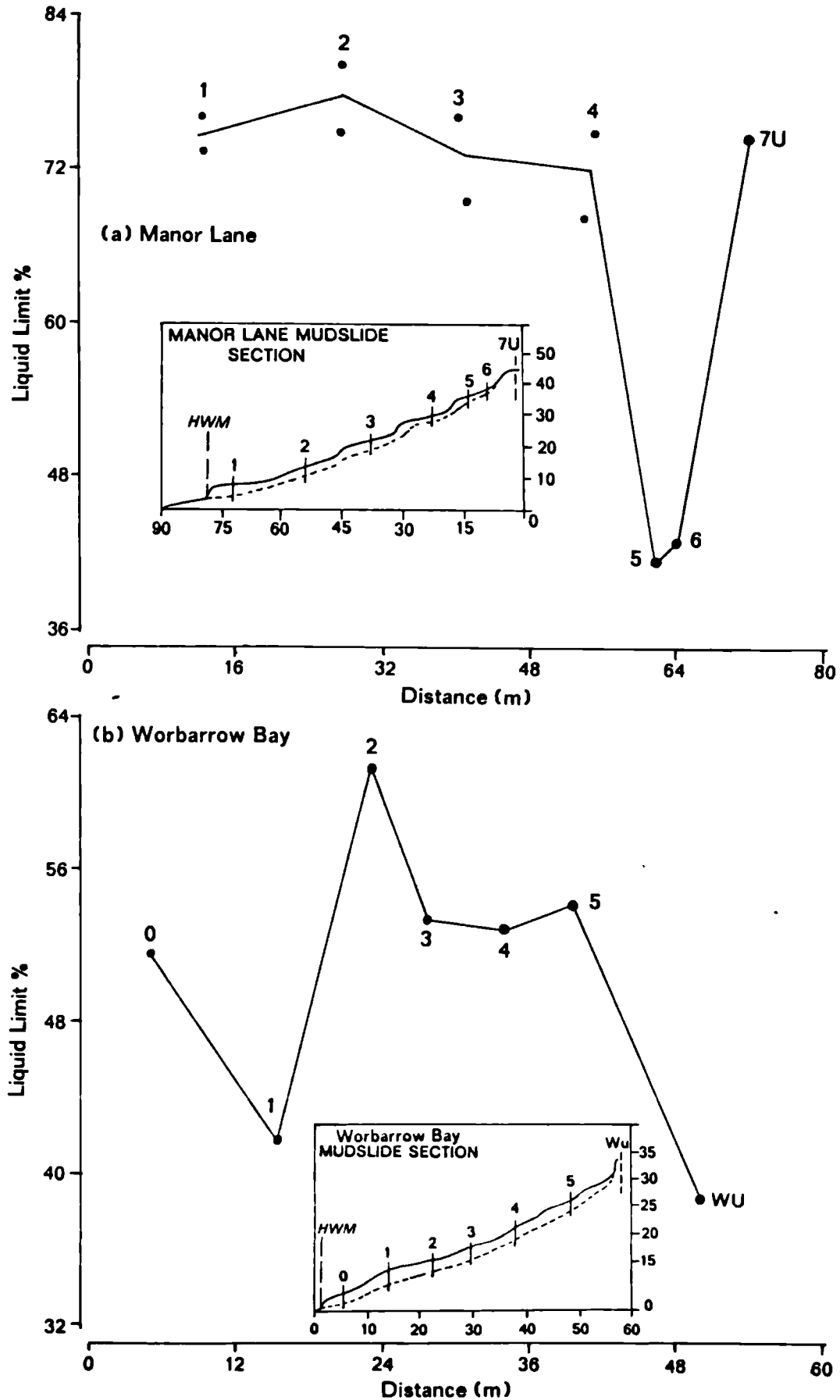
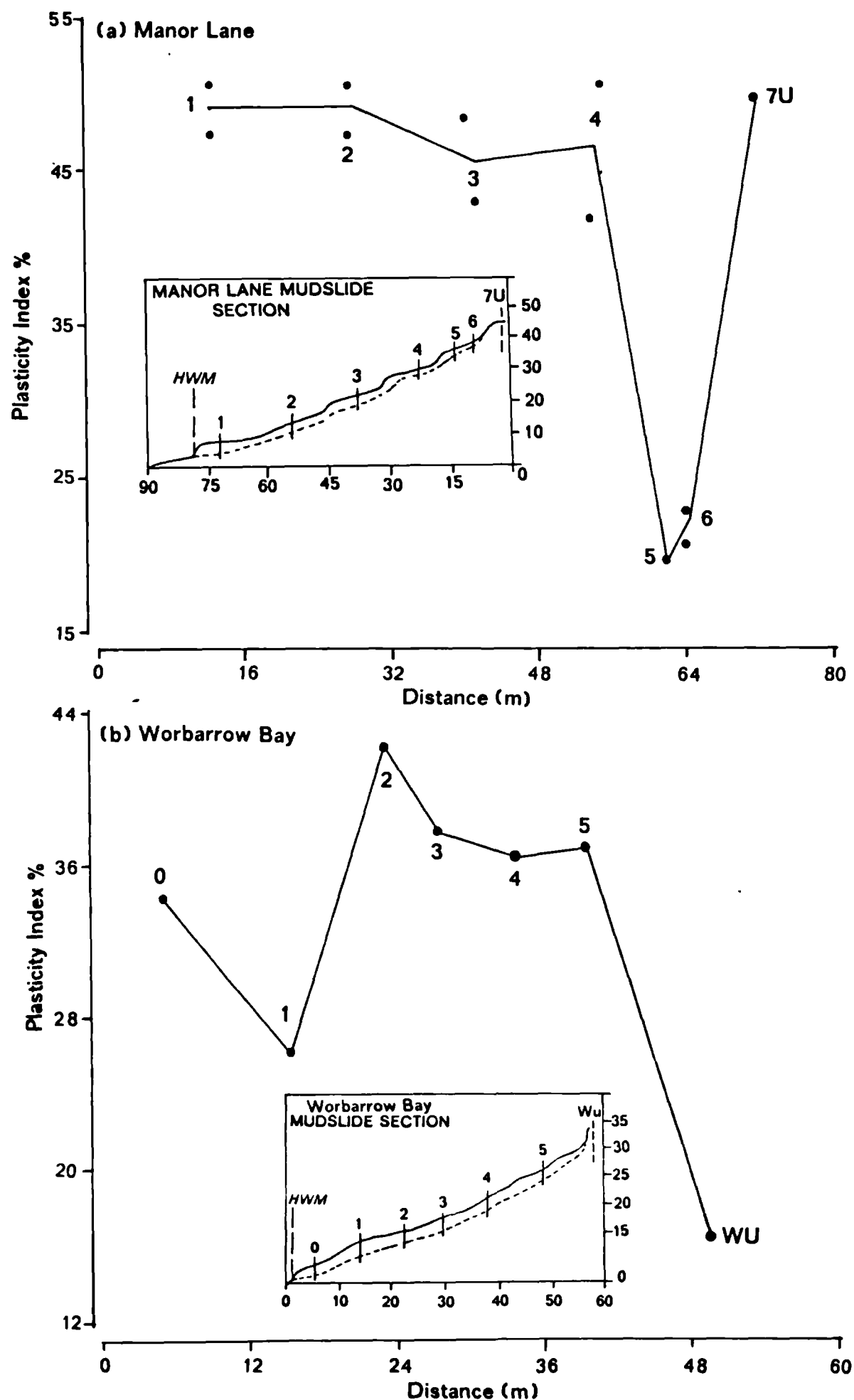


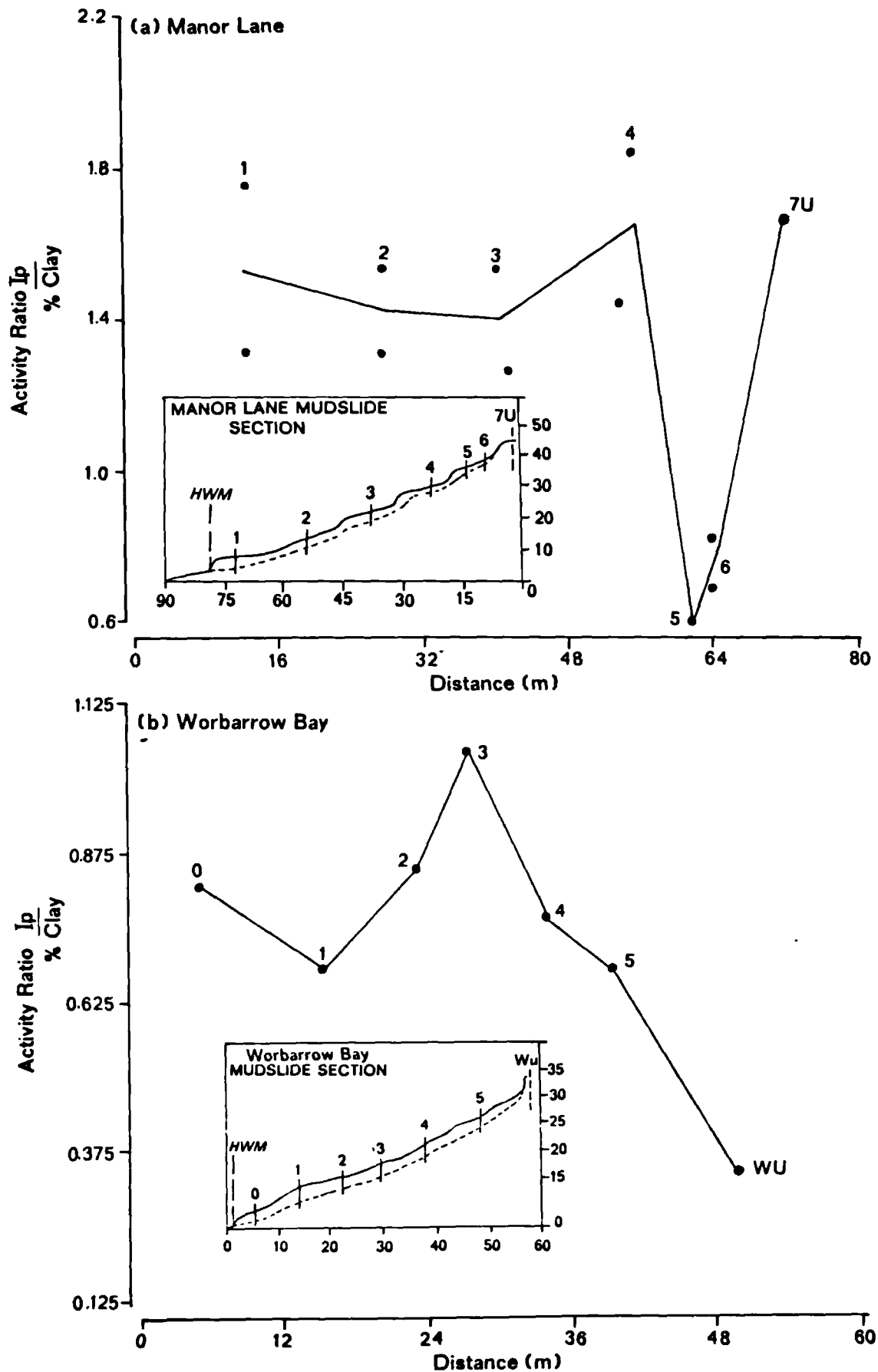
Figure 4.15. Distribution of the plasticity index at the shear surface.



exhibited greater plasticity than the weathered material, whereas the disturbed material at Worbarrow was more susceptible to plastic behaviour, although a change in lithology between *in situ* Wealden Clay and the greater proportion of sands and clays in the mudslide matrix may account for this anomaly.

3. with reference to the Manor Lane section Figure 4.14a the distribution of the liquid limit is plotted at the shear surface revealing that the materials within the source units were generally more susceptible to plastic and liquid deformation than both undisturbed and the fully weathered materials in the feeder track downslope. The plot for Worbarrow (Figure 4.14b) was more variable showing an increase in the liquid limit towards the base of the feeder track, decreasing in the lobe, suggesting that the materials were more susceptible to saturation after weathering and movement downslope. Upon drainage in the lobe the materials exhibit lower liquid limits. The distribution of the plasticity indexes for both sites (Figure 4.15) was found to be influenced by the liquid limit and showed similar distributions.
4. the mean activity ratio at Manor Lane was 1.28 in comparison to 0.8 at Worbarrow. Both contrast with the undisturbed sample as for the plasticity results. Broadly there was a two-fold increase in the activity ratio upon weathering at Worbarrow, whereas the activity decreased by 24 per cent at Manor Lane. With reference to Figure 4.16 the activity of the materials is plotted at the shear surface. At Manor Lane the activity ratio in the source unit was roughly half that attained by the undisturbed and fully weathered clays. A similar trend was found at Worbarrow (Figure 4.16b): following weathering and an initial rise in the source there was markedly lower activity in unit 4, the lower section of the source unit. The activity at both sites showed an overall increase in value towards the toe of each mudslide.

Figure 4.16. Distribution of the activity ratio at the shear surface.



4.32 Shear strength:

4.321 Drained residual shear strength.

The methods of establishing the residual shear strength parameters are detailed in Appendix 6. Remoulded samples were tested at five normal effective stresses (25, 50, 100, 150, 200 kPa) and for each increment of load (100N, 200N etc.) the residual shear stress was recorded via two sensitive load cells. The effective normal stresses were chosen to be as realistic to the field condition as possible, although the ring shear apparatus was unable to test at the low normal loads experienced in shallow mudslides (7 - 19 kPa).

Initially the sample was allowed to consolidate at the lowest effective stress following 720° of rotation to create a well developed shear surface. The sample was sheared at a constant rate of strain (0.032° per minute), sufficiently low to maintain fully drained conditions and prevent pore water pressures. Once constant residual shear stress was established and recorded the second increment of load was applied.

The residual strength was computed using the equations outlined in Appendix 6. For each increment of normal effective stress the shear strength envelope was established (Figure 4.17). The effective residual parameters were determined from the gradient and y-axis intercept of the linear regression, respectively. An important issue in soil mechanics concerns whether the cohesion term may be considered to equal zero for the residual condition (section 2.32). It is common practice to assume that cohesion approximates to zero, the Mohr envelope intercepting the origin of the y-axis; the assumption is usually adopted because current

Figure 4.17. Residual strength Mohr envelopes at the shear surface.

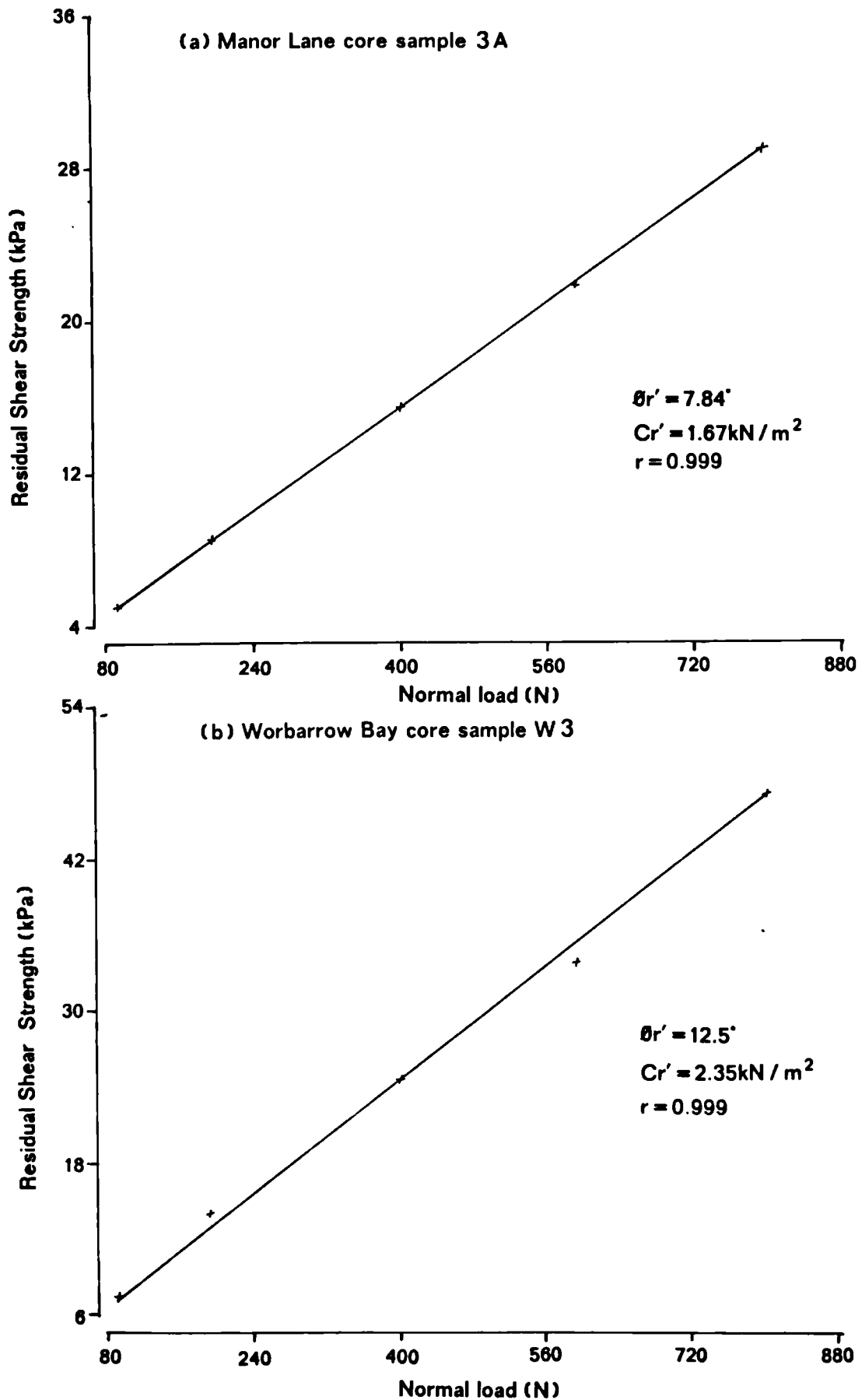
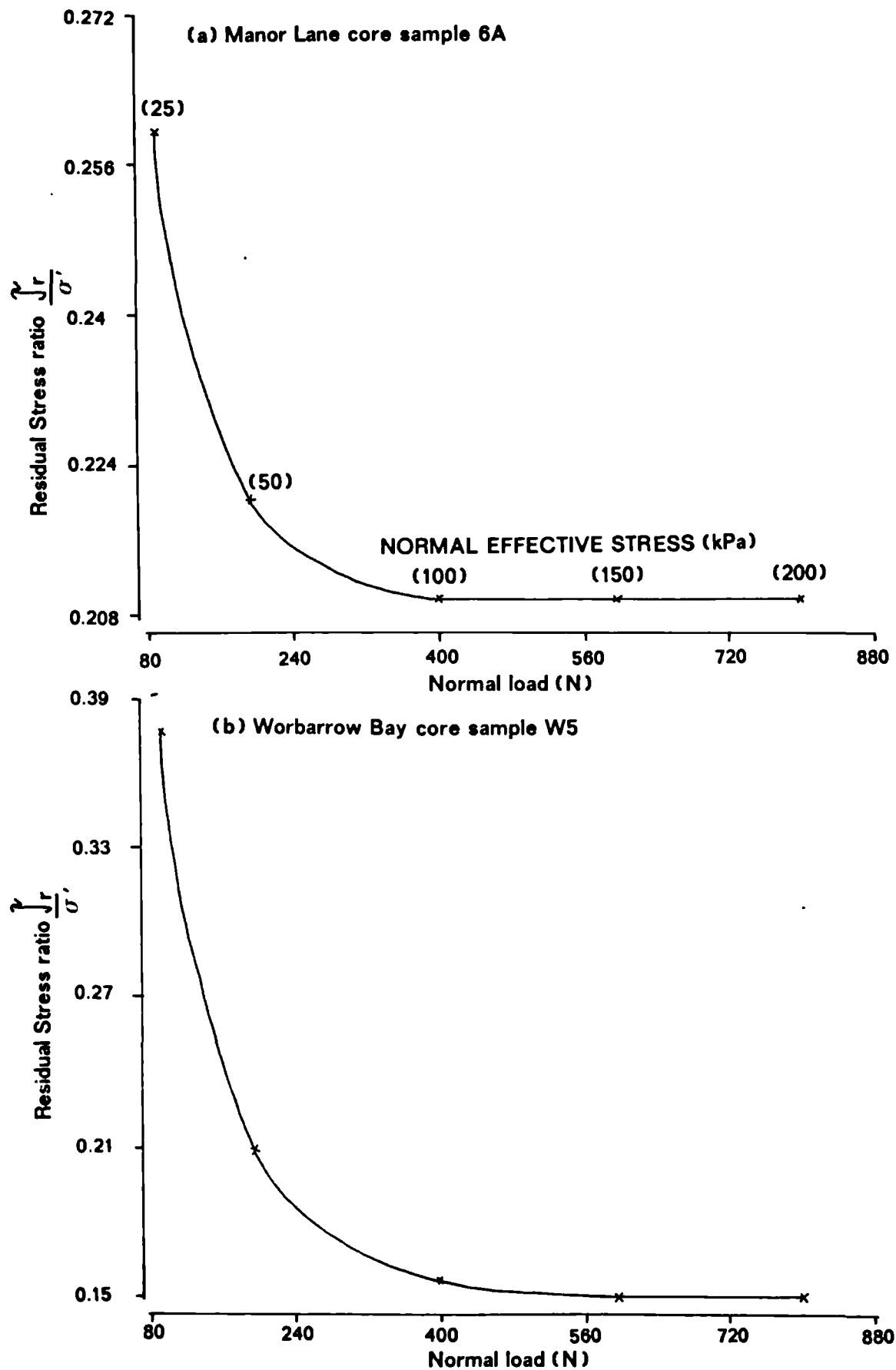


Figure 4.18. Residual stress ratio at the basal shear surface.



laboratory techniques are unable to measure cohesion at low effective stresses. The regression results of this study indicated small values of cohesion in the range 1.3 to 5.3 kPa; perfect regression coefficients ($r = 0.999$) were obtained for most Mohr envelopes so that it was statistically unreasonable to assume an intercept at the origin or zero cohesion.

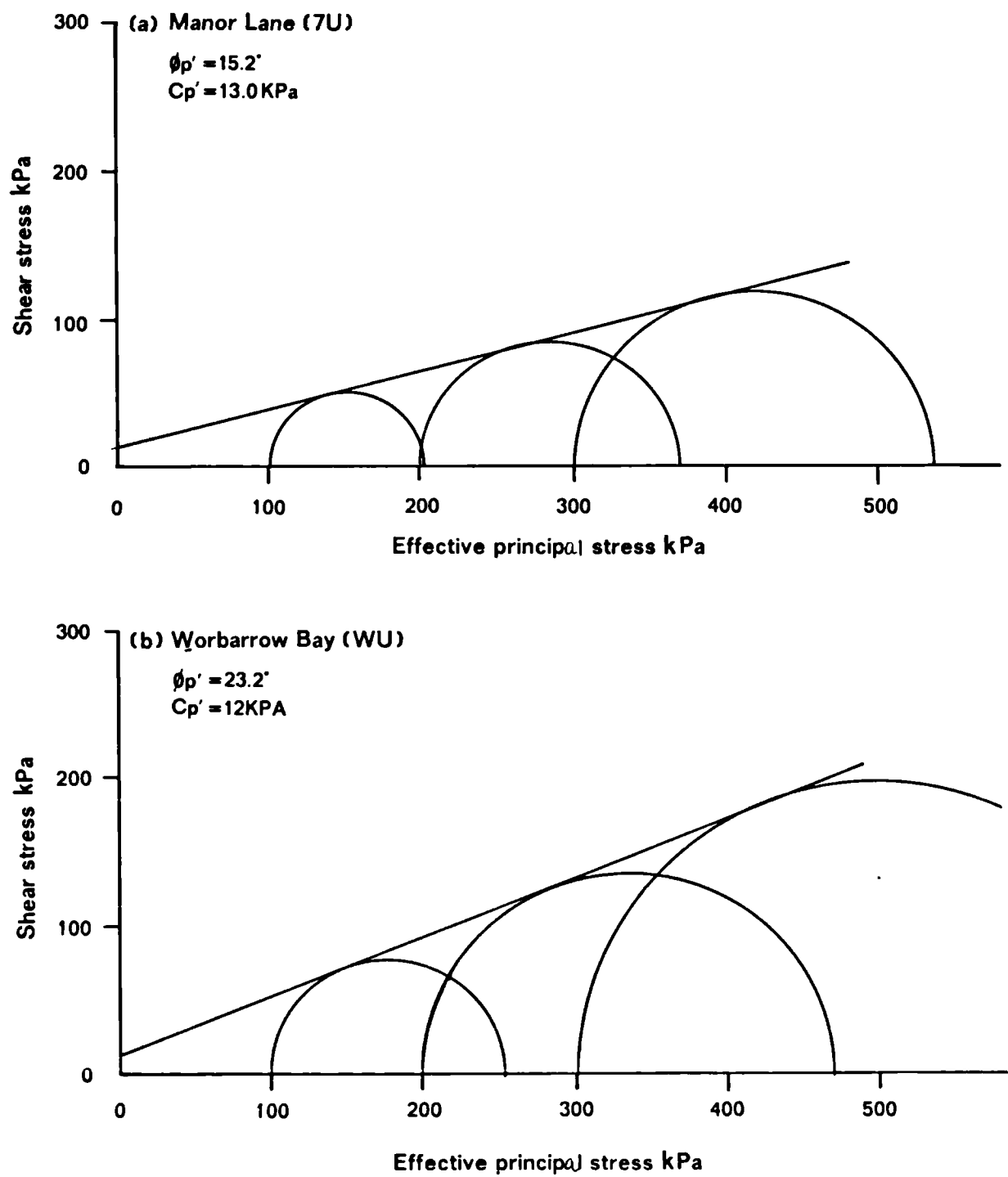
The ratio of strength to effective stress is plotted in Figure 4.18 and shows that the residual condition was directly proportional to the applied load above 400 N. Below this stress level the strength of material was greater and disproportional to the applied load. The results of these tests are presented with the peak shear strength results in the next section.

4.322 Drained peak shear strength.

For each site *in situ* undisturbed samples were used in drained triaxial compression tests to determine the peak shear strength parameters. The method of test is fully described in Appendix 6. Broadly two series of three tests were conducted for each sample under varying effective principal stresses.

Vertical loads were applied at a constant rate of strain ($0.0076 \text{ mm/hr} \approx 6\% \text{ compression per day}$) until the sample sheared. The total vertical or principal stress σ_1 , and the confining stress σ_3 , were used to calculate the deviatoric stress (or additional load applied to the proving ring to initiate sample failure) and since the pore water pressures were monitored throughout effective stress conditions applied. Moreover, since

Figure 4.19. Peak strength Mohr envelopes for *in situ* materials.



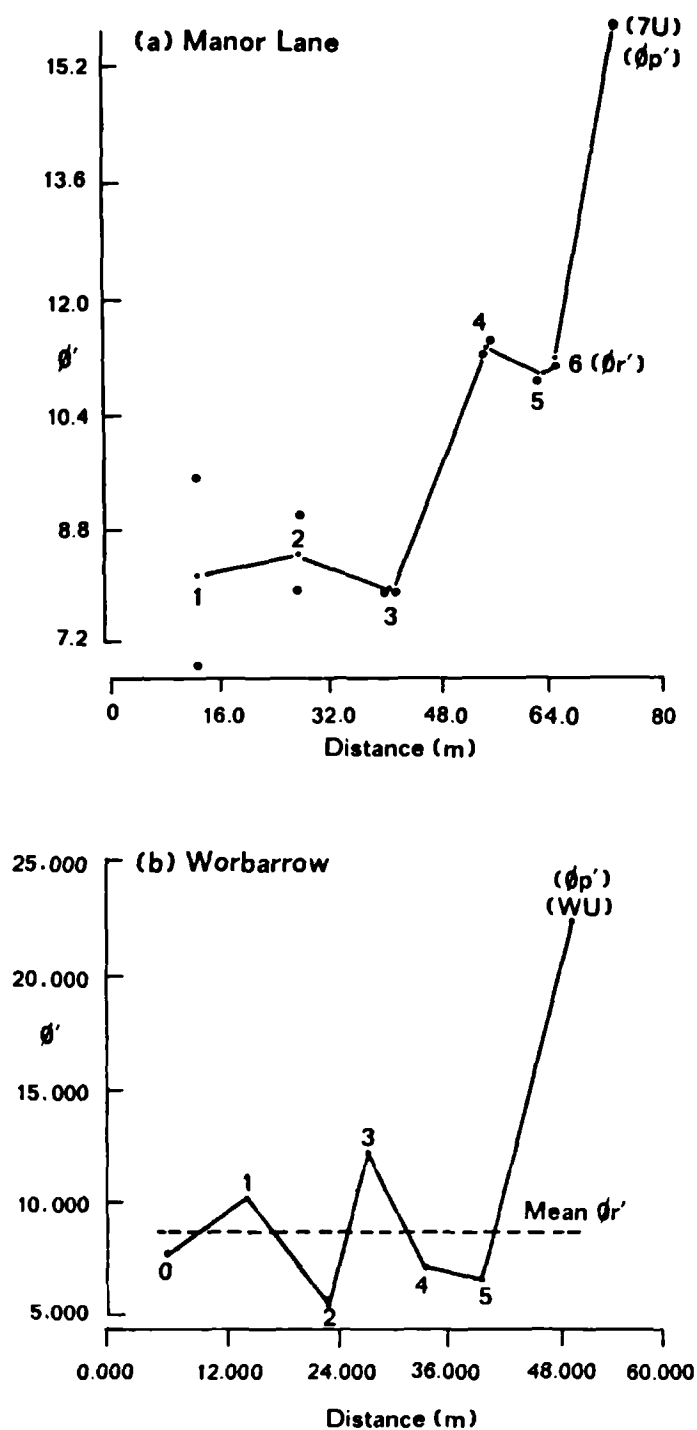
the low rate of strain ensured that excess pore pressures did not develop, each test was fully drained.

For each increment of effective stress, Mohr circles of stress were plotted for each test series, and a line tangential to all circles drawn to represent the shear strength envelope (Figure 4.19). Values of ϕ_p' and c_p' were determined from the gradient and intercept of the fitted line.

The results from both the residual and peak strength analyses are presented in Tables 4.13 and 4.14 for Manor Lane and Worbarrow Bay respectively. The following associations with weathering and slope morphology were noted:

1. the peak internal friction angles for *in situ* undisturbed materials equalled 15.5° at Manor Lane and 23.2° at Worbarrow. The difference between these values could not be explained by variations in the particle-size distributions of core samples 7U and WU (see Tables 4.6b and 4.7). The peak strength envelopes for both sites showed a cohesive force equal to 12 - 13 kPa.
2. the mean residual friction angle within the Manor Lane mudslide was equal to 9.6° which was equivalent to a 38 per cent reduction from the peak condition. Similarly, the mean residual friction angle at Worbarrow was 8.45° , equivalent to a 64 per cent drop from the peak value. As might be expected there was a considerable reduction in cohesion from peak to residual amounting to 81 and 75 per cent for Manor Lane and Worbarrow, respectively. Mean values of residual cohesion measured at both sites varied from 2.51-3.14 kPa.
3. although there was a consistent drop in strength from peak to residual values, the residual strength at the basal shear surface was found to decrease downslope towards the HWM. With reference

Figure 4.20. Distributions of the peak and residual friction angles in relation to the Manor Lane and Worbarrow mudslide sections.



to Figure 4.20a this association was clearest at Manor Lane, where the residual friction angle decreased from 11° to 8°. The transition between these extremes was not necessarily smooth, and involved a substantial reduction between slope units 4 and 3.

4. the plot for Worbarrow (Figure 4.20b) showed an immediate reduction in the residual friction angle to 7.1° upon weathering and erosion in the source (unit 5). The variability of results was quite marked, the values in slope units 2, 3 and 1 fluctuating from 5.7°, 12.5° and 10.4°, respectively. This was explained by a high proportion of coarse and fine sands in core sample W3 in comparison with the dominance of clay in W2. The variability may also reflect the influence of the input of materials from the perched mudslides; debris from the perched system overflows onto the main track at slope units 1, 2 and 3. Even with such variability it was recognised that the lowest residual shear strengths were most critical to soil behaviour.

4.4 Soil Chemistry:

4.41 Chemical Characterization of mudslide materials:

4.411 pH and conductivity of soil solution.

In soil science it is standard practice to undertake a series of tests as a preliminary study to the analysis of the chemical constitution of soil materials to establish the acidity and nature of soil reactions. Thus, the pH and electrical conductivity (EC) of soil-water suspensions were measured as indices of the concentration of salts and the reactivity of soil particles.

The techniques used in their measurement have been outlined in section 3.414). In assessing the pH of 1 : 2.5 soil-water suspensions two treatments were used; one natural sample, and another treated with CaCl_2 . For each sample, 3 readings were recorded and provided the variability in measurements did not exceed 0.1 pH, and those of conductivity 0.05 mS/cm, a mean value was calculated. If the variability in readings exceeded these limits further measurements were taken.

The results of pH and EC tests are presented in Tables 4.15a and 4.15b and 4.16 for Manor Lane and Worbarrow Bay, respectively. The following associations were noted:

1. at Manor Lane the pH averaged 7.29 for the untreated samples and 7.17 for the CaCl_2 treated solutions. These compared with an average pH of 5.69 and 5.21 at Worbarrow Bay, respectively. The larger discrepancy existing between the natural and treated samples at the latter site suggested a dominance of adsorbed hydrogen and aluminium ions on particle surfaces giving rise to

Table 4.15a. Chemical characteristics and percent organic matter for Manor Lane cores 1A - 4A.

CORE #	PARAMETER n = 3	ZONE ONE	ZONE TWO	ZONE THREE	ZONE FOUR	\bar{X}
1A	pH1	7.23	7.27	7.27	7.25	7.26
	pH2	7.13	7.12	7.2	7.21	7.17
	C mS	2.0	1.47	2.21	2.28	1.99
	LOI %	7.85	6.98	8.91	8.5	8.06
	Org %	2.39	1.27	2.26	2.43	2.09
1B	pH1	7.34	7.3	7.3	7.96	7.48
	pH2	7.27	7.25	7.2	7.74	7.37
	C mS	1.89	2.32	2.06	1.52	1.95
	LOI %	8.99	8.82	9.44	8.67	8.98
	Org %	2.33	2.1	2.84	2.58	2.46
2A	pH1	7.36	7.26	7.2	7.67	7.37
	pH2	7.32	7.21	7.21	7.57	7.33
	C mS	2.39	2.63	2.98	1.83	2.46
	LOI %	8.98	9.02	11.10	9.31	9.60
	Org %	3.15	2.64	2.44	3.2	2.86
2B	pH1	7.33	7.26	7.31	7.51	7.35
	pH2	7.3	7.32	7.29	7.39	7.33
	C mS	2.54	2.5	2.25	1.74	2.26
	LOI %	9.58	9.32	9.57	8.68	9.29
	Org %	2.88	2.49	2.68	1.99	2.51
3A	pH1	7.09	7.1	7.18	7.14	7.13
	pH2	7.1	7.15	7.11	7.16	7.13
	C mS	3.17	2.79	3.05	3.15	3.04
	LOI %	9.15	10.03	9.65	9.38	9.55
	Org %	3.01	2.96	2.16	2.71	2.71
3B	pH1	7.3	7.43	7.41	7.25	7.35
	pH2	7.09	7.34	7.31	7.17	7.23
	C mS	0.981	1.62	2.23	2.61	1.86
	LOI %	9.68	9.31	9.45	9.63	9.52
	Org %	3.34	2.69	2.33	2.67	2.76
4A	pH1	6.07	7.46	7.15	7.25	6.98
	pH2	5.57	7.07	6.92	7.2	6.69
	C mS	0.348	0.485	0.778	1.57	0.795
	LOI %	8.77	8.75	10.55	11.15	9.81
	Org %	3.35	2.76	3.62	2.91	3.16

pH1 - 1:2% soil water paste

pH2 - 1:2% soil water paste treated with 0.125M $\text{CaCl}_2 \cdot 6\text{H}_2\text{O}$

C - soil conductivity of 1:5 soil water solution (millisiemens/cm)

LOI - loss on ignition

Org - % organic from wet combustion with 30% H_2O_2

Continued in Table 4.15b

Table 4.15b. Chemical characteristics and percent organic matter for Manor Lane cores 4A - 7U.

CORE #	PARAMETER n = 3	ZONE ONE	ZONE TWO	ZONE THREE	ZONE FOUR	\bar{X}
4B	pH1	7.21	7.36	6.97	7.8	7.34
	pH2	7.0	7.03	6.78	7.75	7.14
	C mS	0.947	0.726	0.965	1.55	1.05
	LOI %	8.0	9.61	8.07	10.06	8.94
	Org %	2.62	3.3	1.88	2.17	2.49
5A	pH1	7.71	7.67	7.26	7.42	7.52
	pH2	7.52	7.59	7.3	7.46	7.47
	C mS	0.642	0.864	2.59	2.32	1.60
	LOI %	9.27	9.56	10.85	11.54	10.31
	Org %	2.71	3.05	2.93	2.71	2.85
5B	pH1	7.4	7.38	7.61	6.74	7.28
	pH2	7.38	7.36	7.51	6.88	7.28
	C mS	1.58	2.79	2.09	3.65	2.53
	LOI %	9.51	9.02	9.39	11.15	9.77
	Org %	2.9	3.07	3.03	3.66	3.17
6	pH1	7.6	7.66	7.53	7.21	7.50
	pH2	7.28	7.34	7.38	7.24	7.31
	C mS	0.582	0.591	0.810	2.61	1.15
	LOI %	9.27	8.6	10.12	10.95	9.74
	Org %	3.49	2.64	2.92	2.95	3.00
7U	pH1	5.13	7.96	7.4	7.28	6.94
	pH2	4.63	7.56	7.11	7.15	6.61
	C mS	1.98	3.57	4.88	6.42	4.21
	LOI %	9.22	8.83	8.23	6.97	8.31
	Org %	3.81	3.14	2.59	1.37	2.73
\bar{X}	pH1	7.06	7.43	7.3	7.37	7.29
	pH2	6.88	7.28	7.19	7.33	7.17
	C mS	1.59	1.86	2.24	2.60	2.07
	LOI %	8.94	8.99	9.61	9.67	9.30
	Org %	3.08	2.68	2.72	2.61	2.77

pH1 - 1:2% soil water paste

pH2 - 1:2% soil water paste treated with 0.125M $\text{CaCl}_2 \cdot 6\text{H}_2\text{O}$

C - soil conductivity of a 1:5 soil water solution, measured in millisiemens

LOI - loss on ignition

Org - % organic from wet combustion with 30% H_2O_2

Table 4.16. Chemical characteristics and percent organic matter for all core samples from Worbarrow Bay.

CORE #	PARAMETER n = 3	ZONE ONE	ZONE TWO	ZONE THREE	ZONE FOUR	\bar{X}
W0	pH1	7.32	6.63	5.96	5.37	6.32
	pH2	6.96	6.14	5.4	4.93	5.80
	C mS	0.818	0.639	0.558	0.614	0.66
	LOI %	6.54	5.79	6.06	7.12	6.38
	Org %	2.46	1.16	1.23	2.5	1.84
W1	pH1	5.2	5.44	5.37	6.42	5.61
	pH2	4.77	4.83	4.80	5.95	5.09
	C mS	0.579	0.592	0.527	0.519	0.554
	LOI %	5.94	4.23	4.77	4.18	4.78
	Org %	1.86	0.83	1.04	1.04	1.19
W2	pH1	4.96	5.46	5.11	6.25	5.45
	pH2	4.37	4.97	4.75	5.74	4.96
	C mS	0.502	0.587	0.654	0.529	0.568
	LOI %	5.4	6.31	8.33	7.2	6.81
	Org %	0.79	1.85	2.46	2.38	1.87
W3	pH1	5.37	5.19	4.67	4.98	5.05
	pH2	4.89	4.76	4.29	4.54	4.62
	C mS	0.576	0.672	0.593	0.64	0.62
	LOI %	6.44	7.12	6.59	6.98	6.78
	Org %	1.22	1.42	1.66	2.13	1.61
W4	pH1	5.99	5.47	5.12	5.99	5.64
	pH2	4.93	5.46	4.74	5.6	5.18
	C mS	0.582	0.65	0.733	0.632	0.649
	LOI %	6.66	4.83	8.69	8.43	6.65
	Org %	2.18	1.69	2.86	3.07	2.08
W5	pH1	4.94	4.99	6.28	6.42	5.66
	pH2	4.38	4.54	5.86	5.94	5.18
	C mS	0.554	0.593	0.685	0.621	0.61
	LOI %	7.01	7.04	7.09	7.31	7.11
	Org %	2.66	2.80	2.69	2.51	2.67
WU	pH1	5.91	5.87	6.15	6.39	5.90
	pH2	5.20	5.46	5.79	5.73	5.55
	C mS	0.592	0.619	0.656	0.688	0.639
	LOI %	6.14	6.41	7.16	7.04	6.69
	Org %	1.59	1.96	2.23	2.81	2.15
\bar{X}	pH1	5.67	5.58	5.52	5.97	5.69
	pH2	5.07	5.17	5.09	5.49	5.21
	C mS	0.60	0.62	0.63	0.61	0.62
	LOI %	6.30	5.96	6.96	6.89	6.53
	Org %	1.82	1.67	2.02	2.35	1.97

pH1 - 1:2% soil water paste

pH2 - 1:2% soil water paste treated with 0.125M $\text{CaCl}_2 \cdot 6\text{H}_2\text{O}$

C - soil conductivity of 1:5 soil water solution (millisiemens/cm)

LOI - loss on ignition

Org - % organic from wet combustion with 30% H_2O_2

acidic conditions. Excess base cations cause alkalinity, but when balanced the pH of the soil solution equals 7.0.

2. with reference to Figure 4.21a, the weathered core samples at Manor Lane showed pH profiles with a high degree of uniformity. The mean profile indicated a slight increase with depth, particularly for sub-zone 2. In contrast, the undisturbed core profile was relatively acidic at the surface (5.13) increasing 36% to 7.96 in zone 2, and further decreasing 9% to 7.28 in zone 4.
3. the weathered profiles at Worbarrow (Figure 4.21b) show a slight reduction (3%) in the mean and undisturbed pH profiles in the surface layers, increasing 8% beneath the basal shear surface of the mean profile. The pH for sub-zone 2 of the undisturbed profile was 5.87 increasing 8% with depth to 6.39. Upon weathering and erosion the materials of the source unit were characterized by very acidic surface layers (4.94 for core W5) increasing 23% with depth, particularly between sub-zones 2 and 3. This effect was probably caused by the leaching of base cations from the surface layers consequent upon weathering. On the lower slopes the pH of the surface layers was greater (7.32 for core W0) decreasing considerably (26%) with depth to 5.37. The latter was considered to result from an increase in base saturation from the accumulation of cations and the intrusion of sea salts in the surface layers.
4. the distributions of pH in relation to the mudslide section of each site is presented in Figure 4.22. These show an increase of 8% pH at Manor Lane and 2% at the shear surface at Worbarrow Bay in the source units. This might be expected as a result of the release of base cations upon weathering. Both sites showed a reduction in pH immediately downslope of the source towards slope units 3 and 4. The degree of change was much greater at Worbarrow and included an increase in pH towards the toe of the slope. This feature was not observed at Manor Lane probably due to the absence of a lobe although a slight increase in pH was seen towards the base of the feeder track where salts were probably accumulating. The mean pH was generally higher than values recorded at the shear surface for both sites.

Figure 4.21. Hydrogen ion activity profiles of selected core samples.

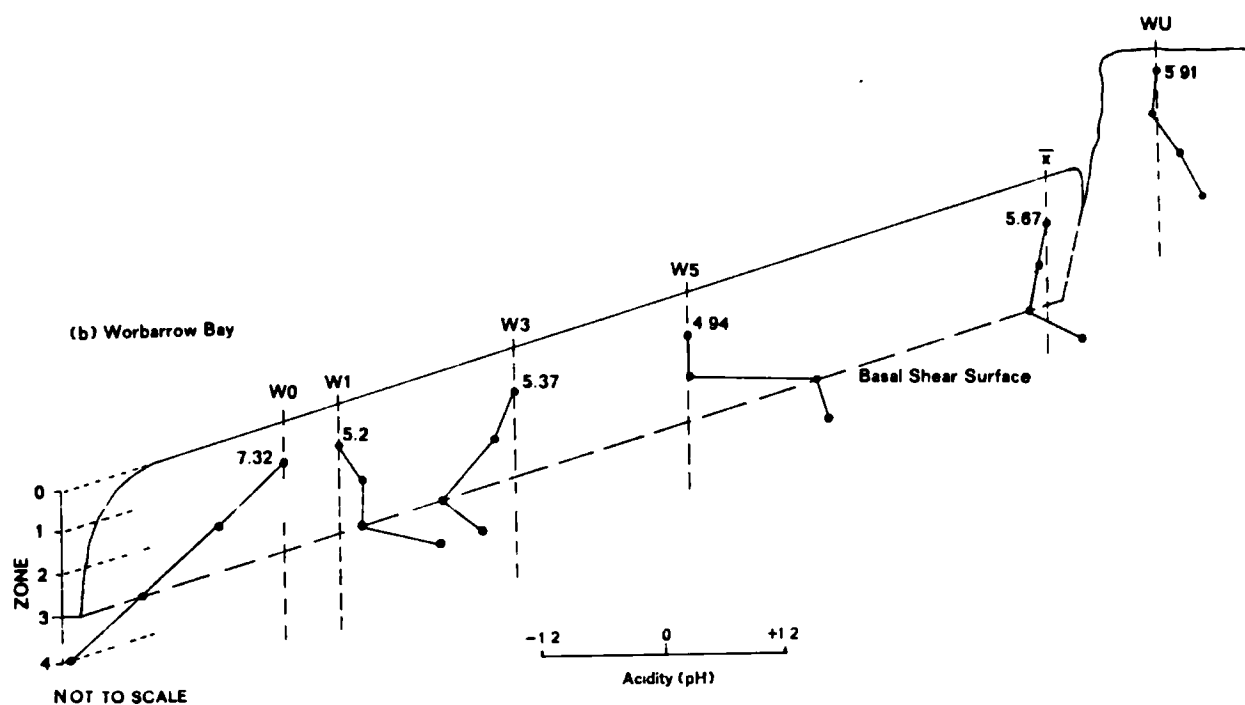
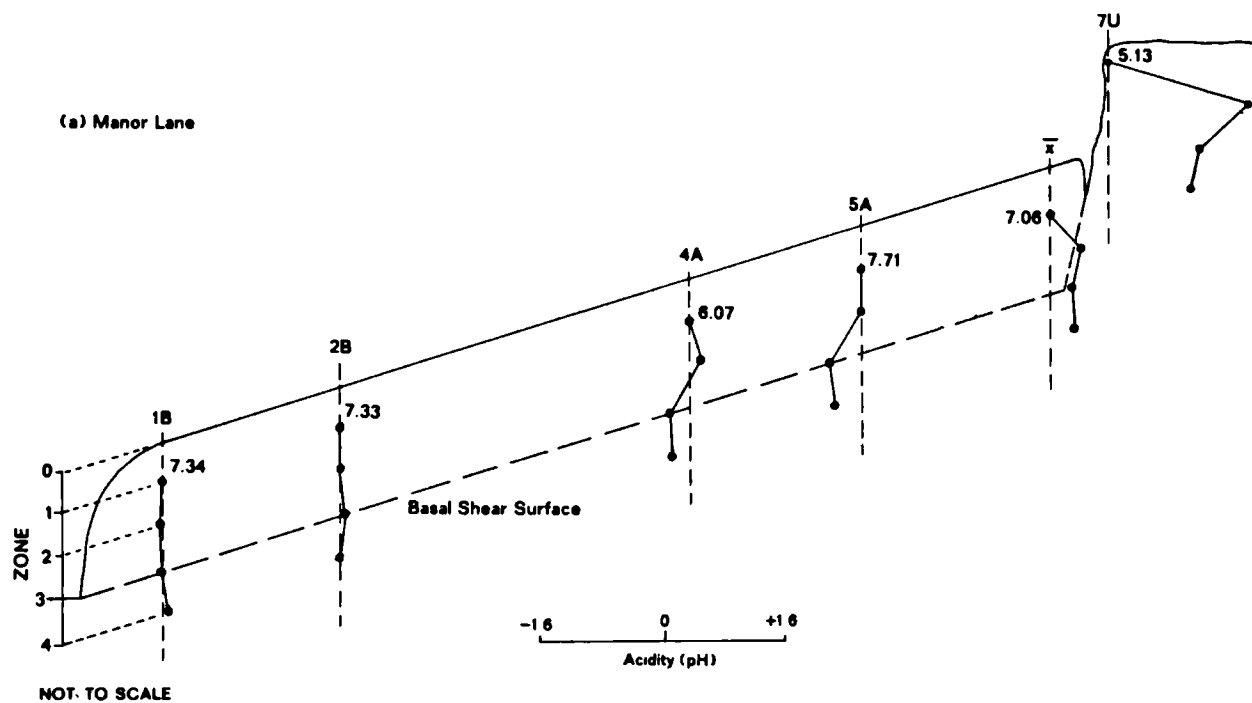
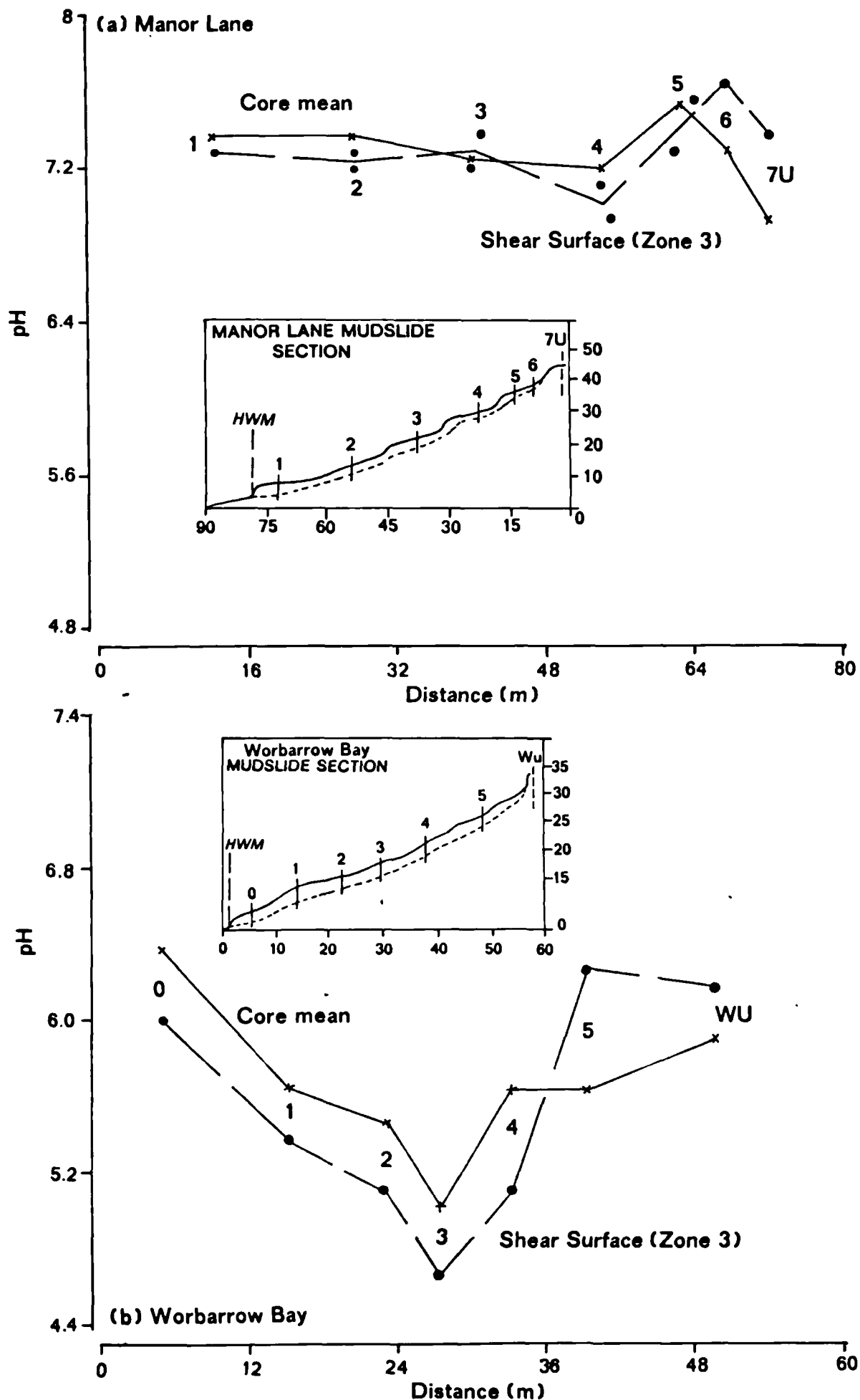


Figure 4.22. Distribution of pH at the shear surface.



5. the EC at Manor Lane averaged 2.07 mS/cm in comparison to 0.62 mS/cm at Worbarrow, suggesting that the London Clay site contains a much greater proportion of neutral salts in comparison to the Wealden system.
6. with reference to Figure 4.23a the *in situ* conductivity profile for Manor Lane shows a uniform increase with depth from 1.98 mS/cm to 6.42 mS/cm and was significantly greater than the mean. The weathered profiles of the source units had lower values although they still showed an increase with depth. With reference to Figure 4.24a the distribution of conductivity with respect to the Manor Lane section shows an initial reduction in EC from 4.21 to 0.78 mS/cm consequent upon weathering and erosion. This subsequently increased to 3.0 mS/cm in the secondary source unit 3 but further decreased towards the HWM. The reduction in EC from 4 mS/cm to 2 mS/cm within the mudslide was considered to reflect a net dilution of salts in comparison with the undisturbed particles. EC was generally greatest at the shear surface.
7. at Worbarrow (Figure 4.23b) there was a lower mean EC in relation to the unweathered profile but a similar increase with depth as found at Manor Lane. With respect to the Worbarrow section (section 4.24b) the distributions of EC were found to decrease towards the HWM. However, upon weathering and erosion in the source unit an increase in conductivity was noted at the basal shear surface relative to the reduction in the core mean. EC decreased towards the lobe where a slight increase was noted. The greater variability of the feeder track may be explained by the input of debris from the perched mudslide system. However, the net reduction from 0.64 mS/cm to 0.56 mS/cm within the mudslide was considered to represent an overall dilution of salts in comparison with the unweathered sediments.

The results of these tests show that there are significant differences in the chemical characteristics of each site. The London Clay contains a high proportion of neutral salts. The conductivity of this solution following weathering was intrinsically less than found for unweathered

Figure 4.23. Electrical conductivity with depth of selected profiles.

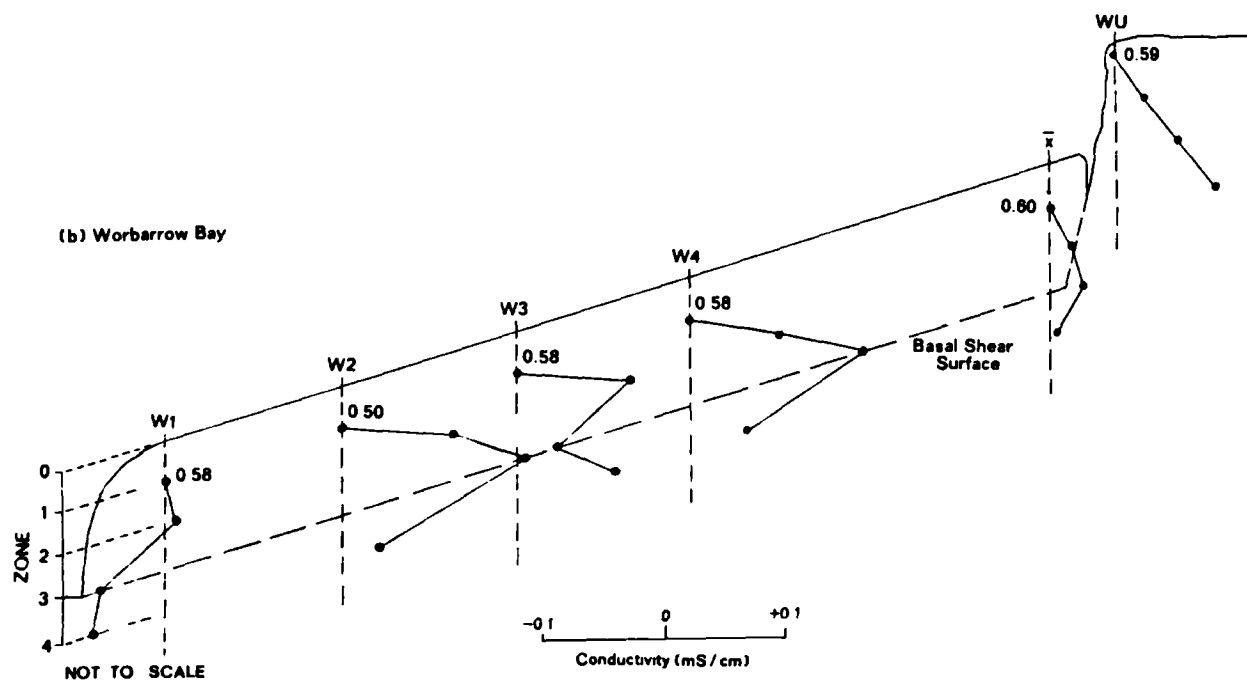
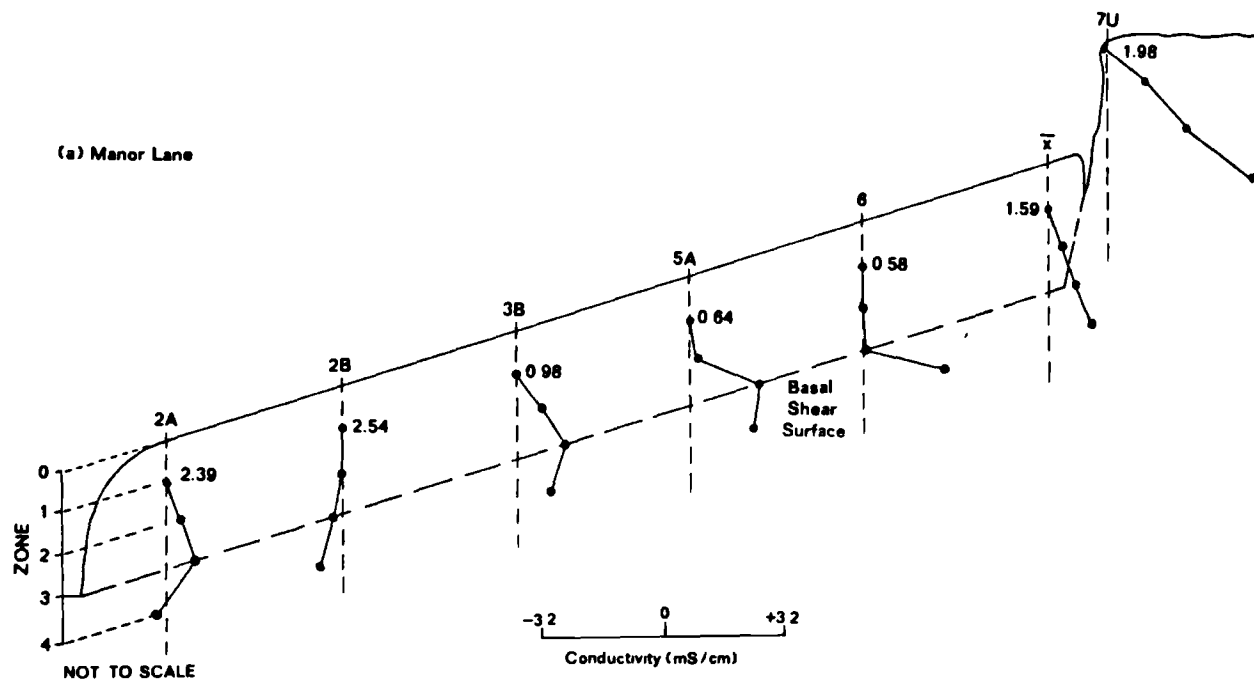
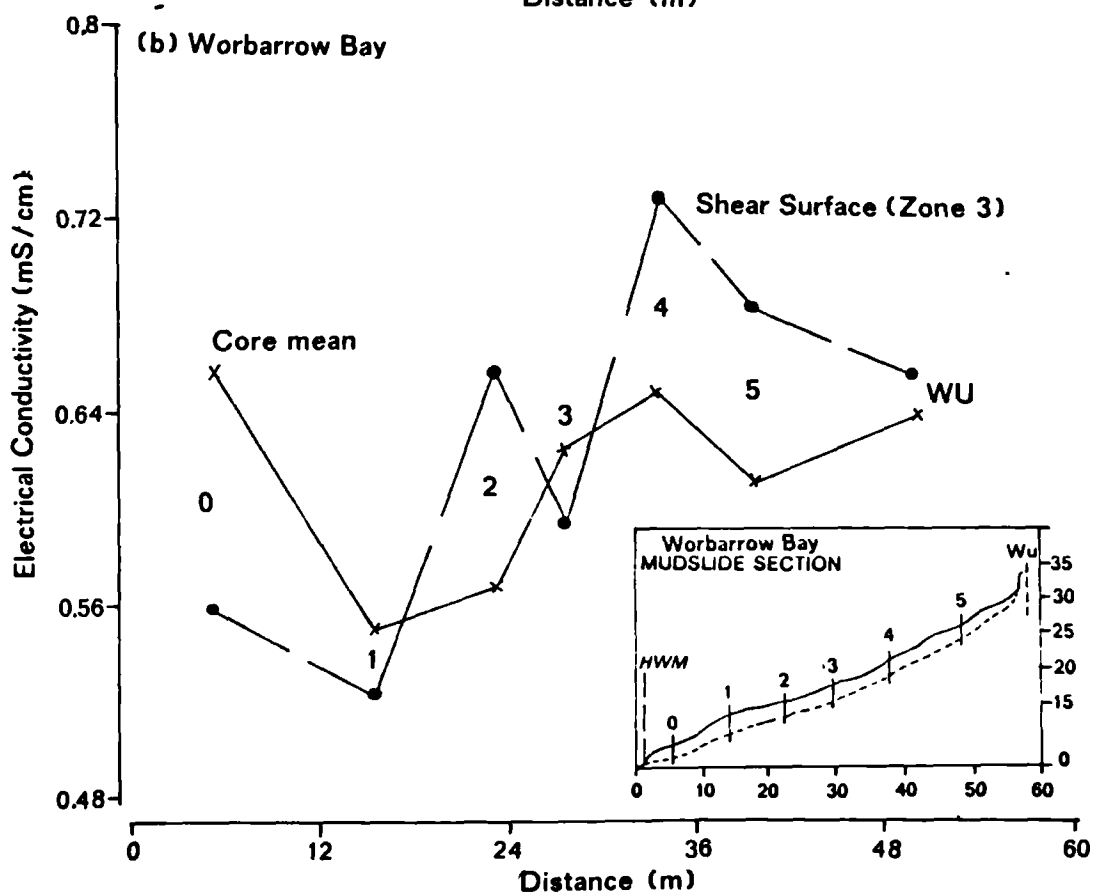
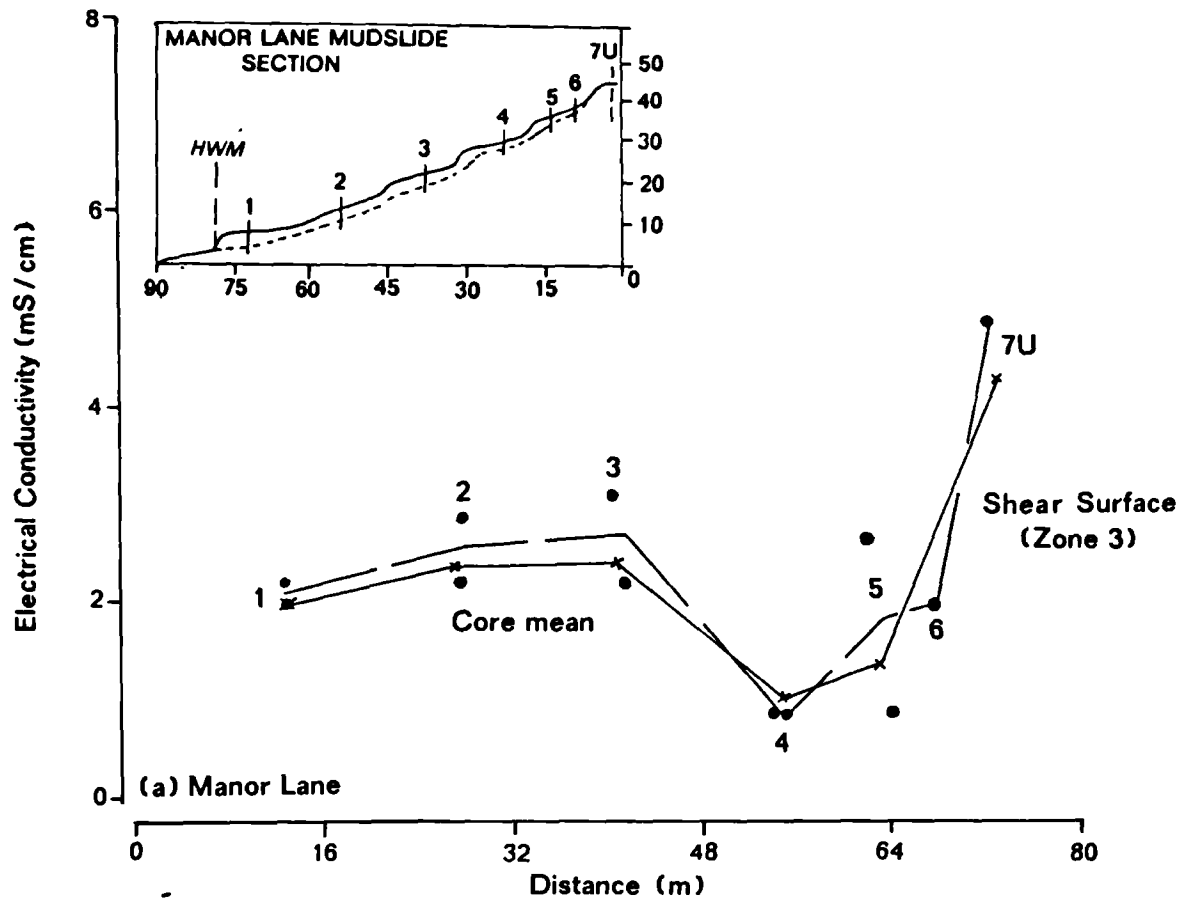


Figure 4.24. Distribution of conductivity at the basal shear surface.



sediments. At Worbarrow the clays contain few soluble salts and are mildly acidic. They show an increase in conductivity following erosion and weathering probably as a result of the breakdown of aggregates and the release of base cations to the pore water solution but a net dilution downslope as for Manor Lane.

4.412 Organic matter content and loss-on-ignition.

The presence of organic matter in soils can significantly affect soil reactions and the cation exchange capacity. It was thus essential to know the proportion of organic material present within the soil to assess the degree to which this might account for the nature of soil-water reactions.

The per cent organic matter was determined directly by wet combustion and indirectly by the weight loss-on-ignition (LOI) when heated to 800°C; the methods of analysis are detailed in Appendix 8. A mean value of the per cent LOI was calculated from two independent determinations to within an error of 0.2 per cent; the per cent organic matter by wet combustion could only be reported for one test owing to the number of analyses undertaken. The difference between LOI and organic matter content was assumed to be the per cent loss of bonded water released between 150-800°C. This information was used in the determination of the proportion of certain clay minerals (section 4.46).

The results of both tests are presented in Table 4.15a, 4.15b for Manor Lane and Table 4.16 for Worbarrow Bay. The following associations were recognised:

1. at Manor Lane the mean per cent organic matter was equal to 2.8% in comparison to 2% at Worbarrow. With such small values it was considered that the effects of organic content on soil reactions in mudslides was negligible. The corresponding results for the LOI were 9.3% and 6.5% respectively, suggesting that the larger part of the weight loss-on-ignition was due to bonded water and not due to the presence of organic materials.
2. the LOI profile for the undisturbed London Clay, plotted in Figure 4.25a, showed a relatively large weight loss in comparison with the profile mean, with a significant (0.68%) reduction below the shear surface (zone 4). The mean profile increased with depth, in contrast to the undisturbed condition. This consisted of an increase in LOI with depth for the weathered cores in the source units but a converse reduction in LOI for weathered profiles on the lower slopes.
3. this was supported by the mean LOI when plotted with respect to the mudslide section (Figure 4.26a). The relationship plotted for the mean at Manor Lane shows a distinctive peak of 10% LOI immediately upon weathering and erosion with a smaller reduction downslope. The plot at the shear surface broadly shows the same result except that the LOI was often greater than the core means showing larger extremes such as the peak noted in the source unit.
4. at Worbarrow the LOI mudslide profiles (Figure 4.25b) showed a slight reduction in the mean surface values in comparison with the undisturbed sample. Core profile 4 shows a dramatic variation between zones 2 and 3 implying depleted values of LOI in the highly disturbed and weathered materials overlying the shear surface. As the mudslide deepened there was a general decrease downslope particularly in the surface layers, but also with depth. This was emphasised by the plot in Figure 4.26b which indicates a sharp peak LOI in the source (unit 4) with reduced values downslope akin with the Manor Lane site. At Worbarrow this relationship was clearest at the basal shear surface.

Figure 4.25. Loss-on-ignition with depth of selected profiles.

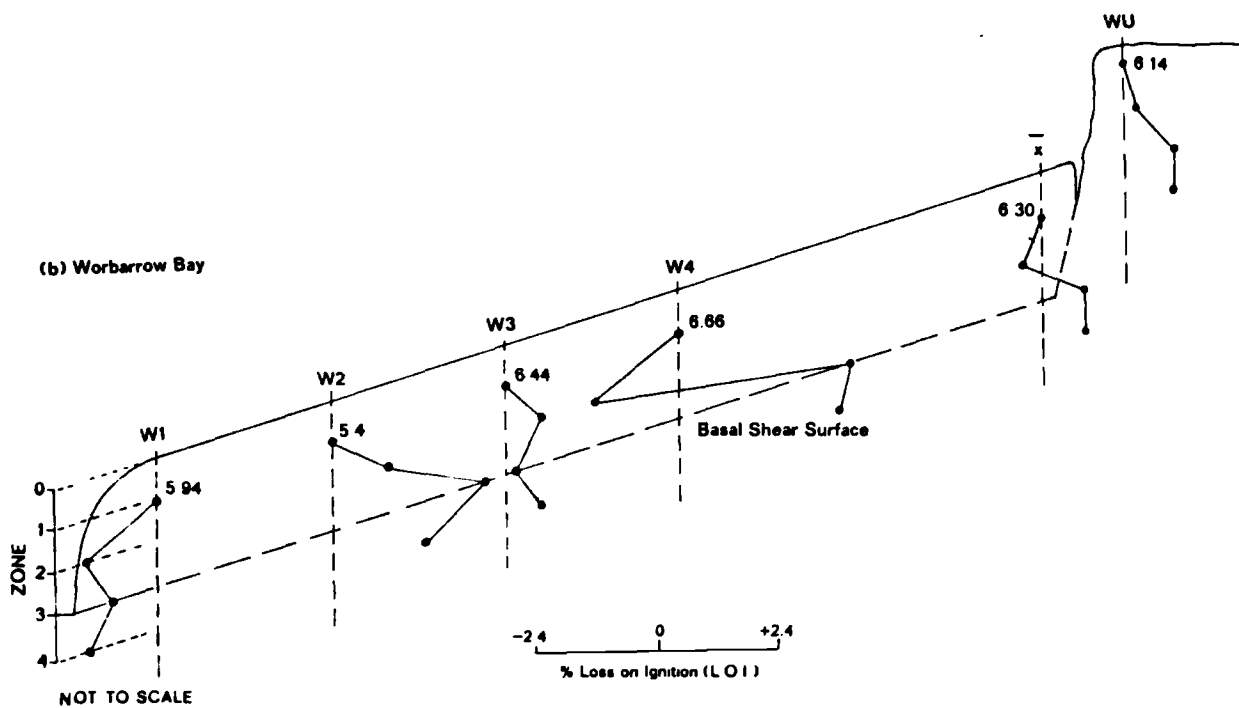
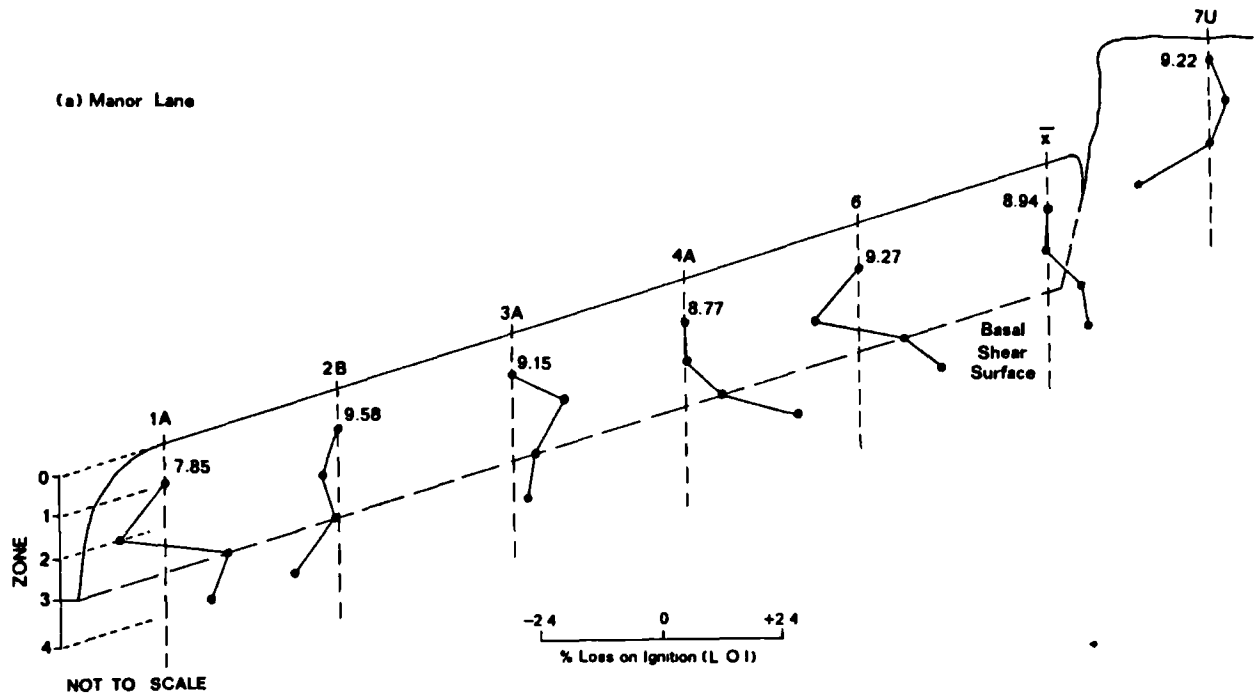
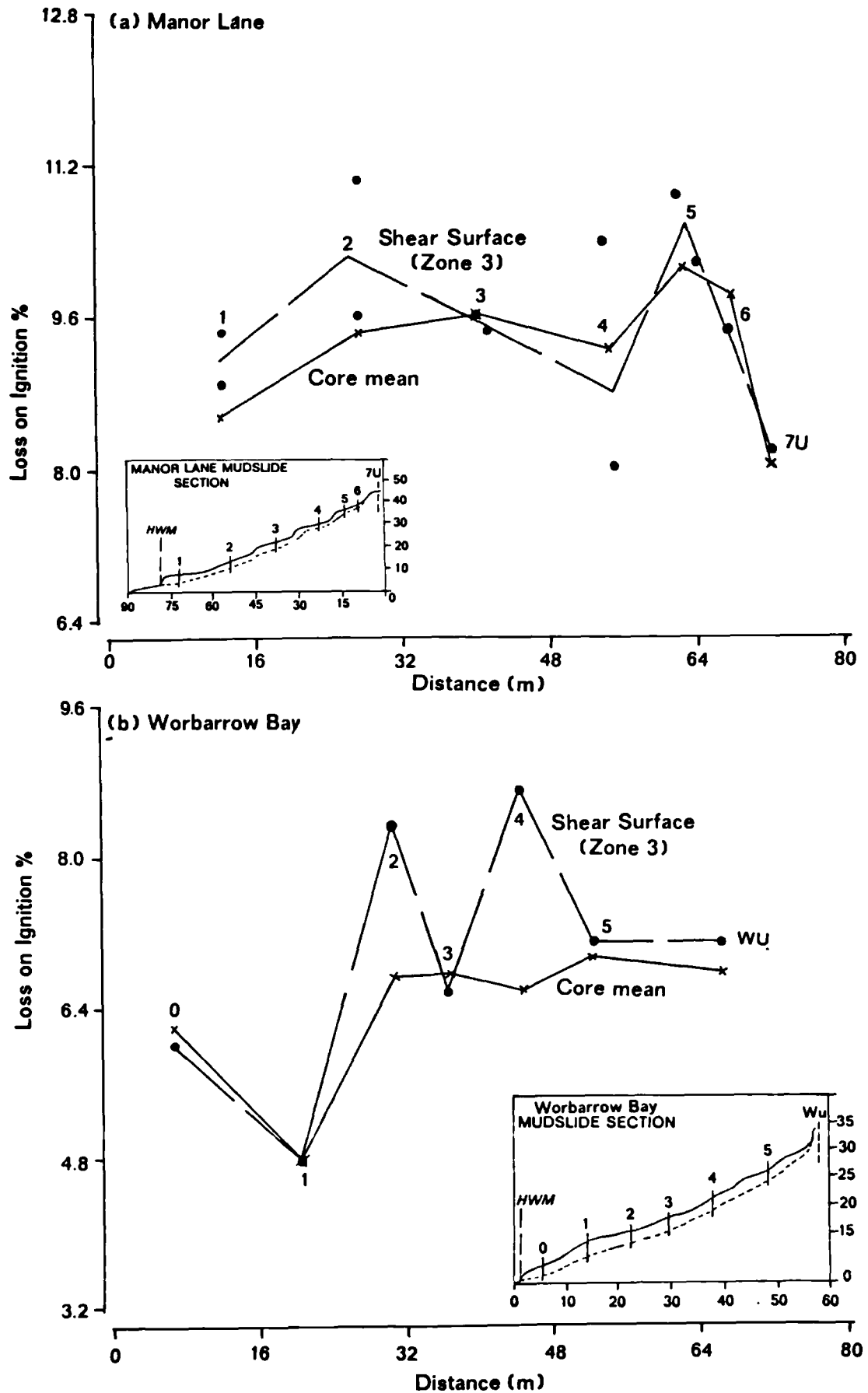


Figure 4.26. Distribution of LOI at the basal shear surface.



4.42 Cation balance:

4.421 Interstitial free water.

Zones of saturation found above the basal shear surface were recognised in all core samples during the description and sub-sampling stages (section 3.41). A sufficient quantity of this clay slurry was set aside for chemical analysis. The method by which the interstitial free-water (unbound to clay surfaces) was extracted is given in Appendix 9A along with the calculation of the sample solution yield. To enhance the yield of water an immiscible fluid of greater density than water was used under centrifugal force (4000 r.p.m.) to separate the pore water from the clay. Since the high-density fluid used was a hydrocarbon the interstitial water sample obtained was not contaminated by the extraction procedure (see section 3.42).

The extracts were temporarily refrigerated in polyethylene bottles prior to analysis for Na^+ , K^+ , Mg^{2+} , Ca^{2+} , total Fe^{3+} , Al^{3+} , Si^{4+} , Cl^- , SO_4^{2-} , and HCO_3^- , by the analytical procedures outlined in Appendix 9F. Standard solutions were used (section 3.414) against which each sample was calibrated with two independent readings, and providing the results were within a standard 5% error, a mean value was recorded. Further readings were taken when the variability exceeded this limit. The results of the major cations and anions were recorded to the nearest mg/litre, whereas iron, aluminium and silica, also in mg/l, were reported to one decimal place.

The results are presented in Tables 4.17 and 4.18 for Manor Lane and Worbarrow, respectively. Data are presented for the concentration of

Table 4.17. Interstitial free water chemistry at the basal shear surface for all Manor Lane core samples.

CORE #	YIELD %	Na	K	Mg	Ca	Fe	Al	Si	TOTAL (+)	Cl	SO ₄	HCO ₃	TOTAL (-)
1A	22.06 mg/l me/l	552 24.0	80 2.1	575 47.4	648 31.6	1.7	.38	13.8	1871 105.1	570 16.1	4130 86.0	14.6 0.50	4715 102.6
1B	19.16 mg/l me/l	576 25.0	64 1.6	477 39.8	575 28.0	1.4	.42	13.5	1707 94.4	462 13.0	3682 76.8	15.9 0.55	4160 90.4
2A	22.44 mg/l me/l	720 31.3	152 3.9	713 59.4	543 26.4	1.1	.27	8.4	2138 121.0	589 16.6	4802 100	11.3 0.39	5402 117.0
2B	22.65 mg/l me/l	624 27.0	136 3.5	700 58.4	566 27.6	1.2	.53	13.3	2041 116.5	534 15.0	5026 104.7	18.1 0.62	5578 120.3
3A	22.41 mg/l me/l	688 30.0	176 4.5	775 64.6	595 29.0	0.4	.33	9.0	2244 128.1	806 22.7	5138 107.0	11.2 0.39	5955 130.1
3B	21.54 mg/l me/l	688 30.0	128 3.3	674 56.2	657 32.0	1.0	.31	7.6	2156 121.5	552 15.6	4690 97.7	18.6 0.64	5261 113.9
4A	15.73 mg/l me/l	360 15.7	16 0.4	290 24.2	300 14.6	0.8	.28	7.8	975 54.9	389 11.0	1553 32.4	9.30 0.32	1951 43.7
4B	25.57 mg/l me/l	624 27	80 2.1	583 48.6	825 40.2	1.0	.39	9.3	2123 117.9	516 14.5	4466 93.0	6.80 0.23	4989 107.7
5A	16.62 mg/l me/l	344 15.0	2 0.1	144 12.0	251 12.2	1.0	.47	9.9	1752 139.3	534 15.0	993 20.7	13.8 0.48	1541 36.2
5B	19.55 mg/l me/l	560 24.4	88 2.3	870 72.6	644 31.4	1.0	.42	9.5	2173 130.7	552 15.6	5362 111.7	30.7 1.06	5945 128.4
6	26.39 mg/l me/l	256 11.1	8 0.2	258 21.6	431 21.0	0.9	.41	11.1	1965 153.9	353 9.9	2113 44.0	24.0 0.82	2490 54.7
7U	10.78 mg/l me/l	200 8.7	8 0.2	68 2.8	97 2.4	0.8	.46	11.5	1386 114.1	425 12.0	432 9.0	18.0 0.62	875 21.6

% yield : weight of water extracted divided by the total weight of water in sample
 mg/l : milligrammes per litre (or parts per million, ppm)
 me/l : milliequivalents per litre (ppm divided by the atomic weight of ion)
 (+) : total cations
 (-) : total anions

Table 4.18. Interstitial free water chemistry at the basal shear surface for all Worbarrow Bay core samples.

CORE #	YIELD %	Na	K	Mg	Ca	Fe	Al	Si	TOTAL (+)	Cl	SO ₄	HCO ₃	TOTAL (-)
W0	29.05	536	16	57	80	0.2	.17	7.4	1697	951	320	0.41	1271
	me/l	23.3	0.4	4.8	3.9				32.4	26.8	6.7	.014	33.5
W1	28.75	456	8	57	70	0.3	.27	18.0	1610	915	320	0.11	1235
	me/l	19.8	0.2	4.8	3.4				28.2	25.8	6.7	.004	32.4
W2	24.23	536	16	92	136	0.3	.41	26.6	1807	1314	320	.06	1634
	me/l	23.3	0.4	7.7	6.6				38.0	37.0	6.7	.002	43.7
W3	27.53	680	16	94	129	0.04	.19	17.0	1936	1332	320	.023	1652
	me/l	29.6	0.4	7.8	6.3				44.1	37.5	6.7	.001	44.2
W4	22.97	688	32	115	126	0.9	.52	21.4	1984	1368	320	.06	1688
	me/l	29.9	0.8	9.6	6.2				46.5	38.5	6.7	.002	45.2
W5	26.64	640	8	89	97	0.7	.47	22.4	1858	1242	320	.89	1562
	me/l	27.8	0.2	4.5	3.2				40.2	35.0	6.7	.03	41.7
WU	14.16	204	8	54	65	0.8	.46	18.2	1351	1017	275	.64	1292
		8.9	0.2	4.5	3.2				16.8	28.7	5.7	.022	34.4

=====

% yield : weight of water extracted divided by the total weight of water in sample
mg/l : milligrammes per litre (or parts per million, ppm)
me/l : milliequivalents per litre (ppm divided by the atomic weight of ion)
(+) : total cations
(-) : total anions

each ion and their milliequivalents per litre (meq/l). In calculating the meq/l the concentration of each ion was directly comparable enabling the summation of the cations and anions and the derivation of any imbalance of charge. The difference between the totals may be considered the error of analysis. The following associations were noted:

1. the maximum concentration of salt (cations + anions) amounts to 8.19 g/l at Manor Lane (core 3A) compared with 2.68 g/l at Worbarrow (W4). The corresponding minimums were found for both undisturbed samples and were equal to 1.25 g/l and 1.65 g/l respectively.
2. by far the most dominating ions in the free water extracted from the London Clay site were magnesium and sulphate with subordinate but high concentrations of calcium and sodium. At Worbarrow the dominating ions were sodium and chloride suggesting a different chemical system to that found at Manor Lane which probably reflects their original depositional environment: marine at Manor Lane and lacustrine at Worbarrow (section 3.23).
3. of particular interest was the balance of the major ions. It was found that both undisturbed saturation extracts have greater proportions of anions in solution giving rise to an imbalance of charge equivalent to 7.52 meq/l at Manor Lane and 17.62 meq/l at Worbarrow. At Manor Lane a positive charge was found following the weathering of materials in slope units 6 to 3 and from units 2 to 1 equivalent to approximately 6.14 meq/l which was assumed to be balanced by unmeasured ions or due to errors of analysis. In contrast to this feature a net negative charge was found for cores 3A and 2B averaging 2.9 meq/l implying an excess of anions in solution.
4. at Worbarrow the chemical balance for the mudslide cores showed a predominant excess negative charge averaging 2.52 meq/l. Only in core W4 was there an apparent excess positive charge amounting to 1.3 meq/l. The latter may well reflect the dominant weathering processes in the source releasing base cations to the pore water.

Figure 4.27. Distribution of dominant free-water anions at the basal shear surface.

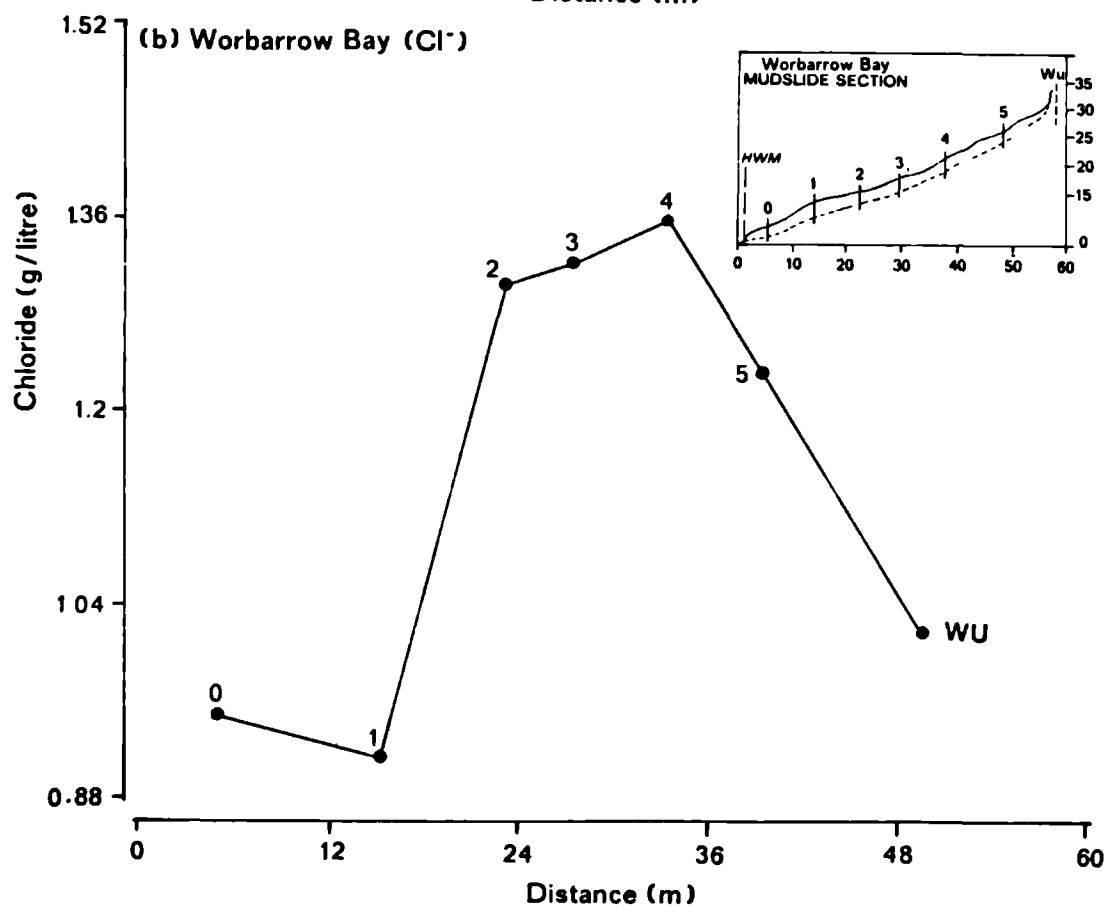
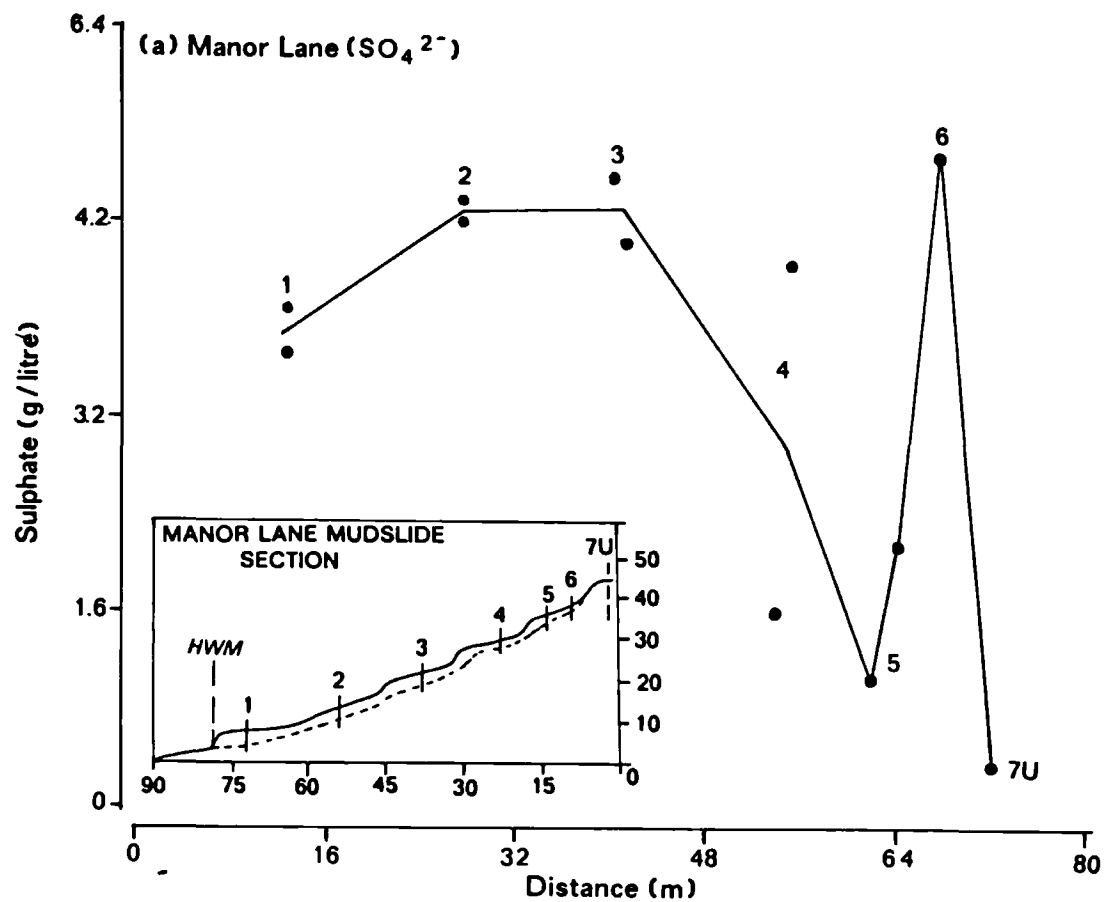
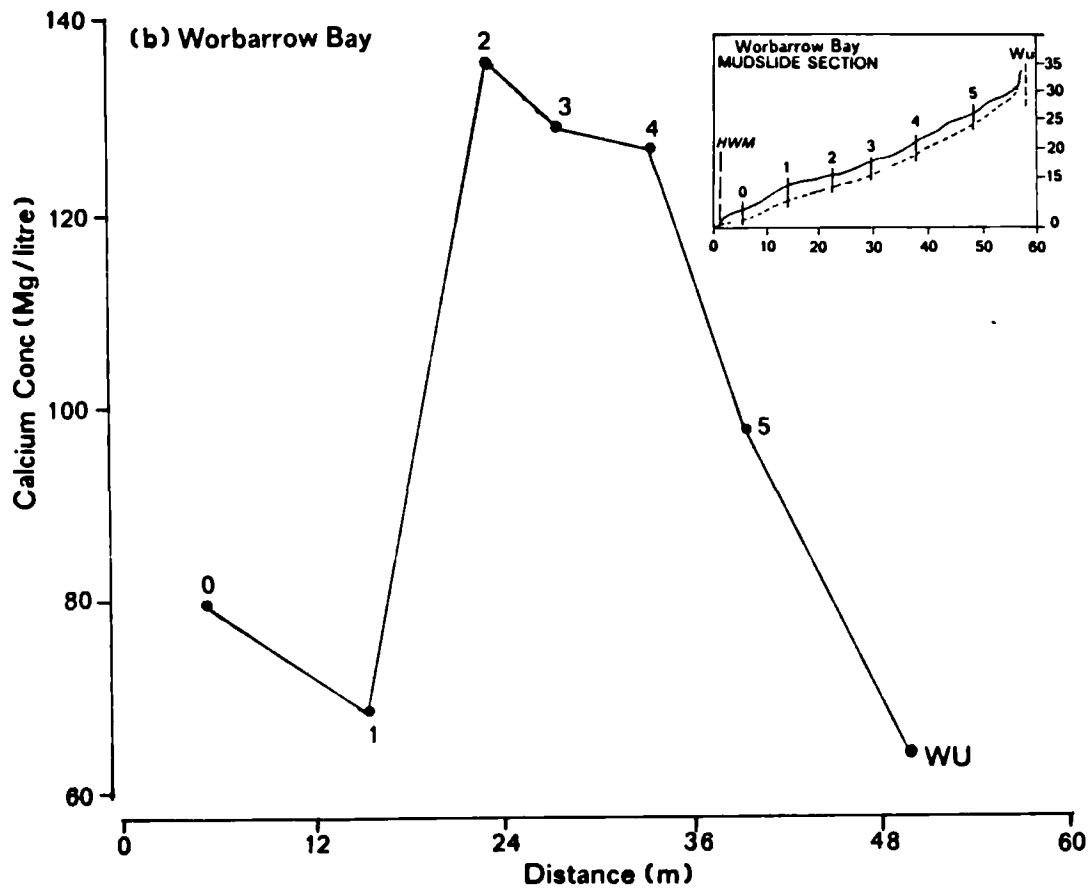
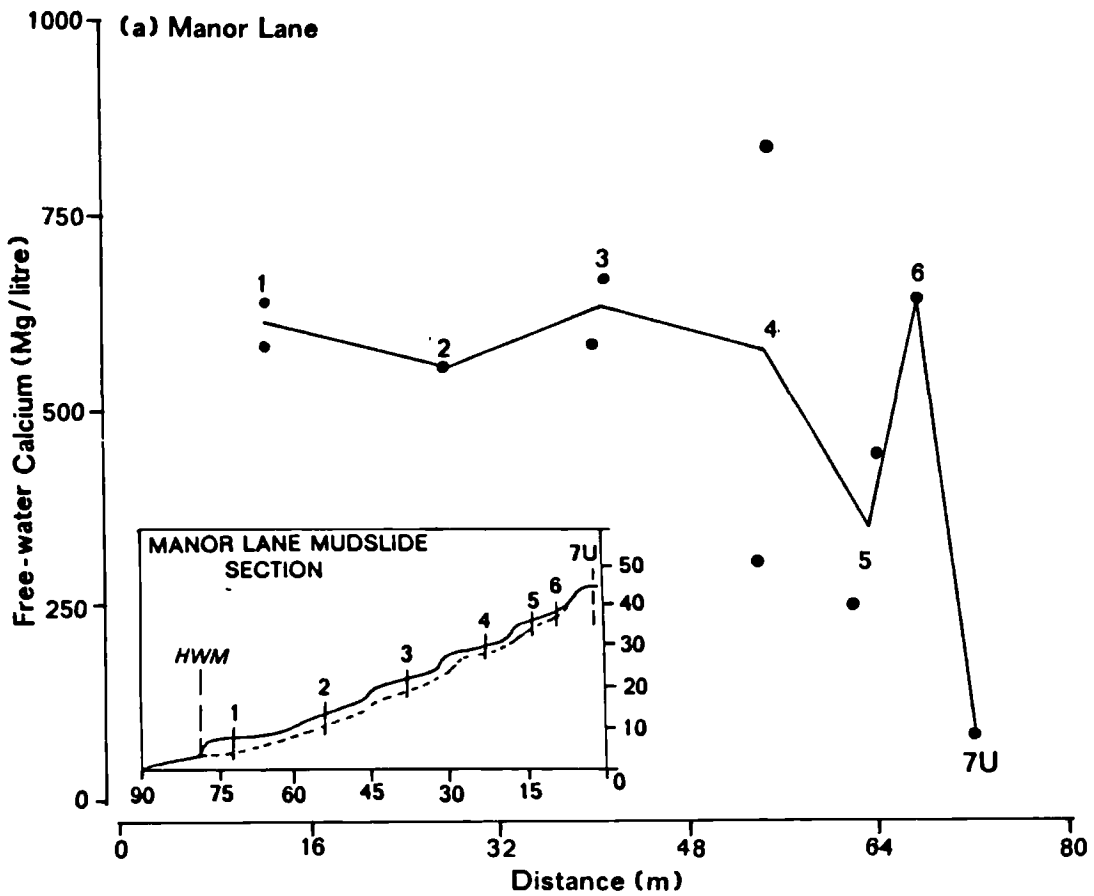


Figure 4.28. Distribution of free-water calcium at the shear surface.



5. with reference to Figure 4.27 the dominant anions at both sites are plotted with respect to the mudslide sections. These were sulphate at Manor Lane and chloride at Worbarrow. Both showed a rapid rise in concentration (80% at Manor Lane; 26% at Worbarrow Bay) following weathering and erosion in the source unit with subsequent marked reductions towards the base of the feeder track (unit 2), 21 per cent at Manor Lane and 33 per cent at Worbarrow. The secondary source unit at Manor Lane was again evident causing an increase in concentration in slope units 3 and 4B. It was considered that the dominant anions were related to the dominant cations in the form of NaCl at Worbarrow, and MgSO_4 or Na_2SO_4 at Manor Lane.
6. with reference to Figure 4.29 similar trends were recognised for the sodium cation at both sites; there was a rapid increase in sodium upon weathering in the source and upper feeder track followed by a reduction downslope. There was a net increase in concentration of the sodium cation equivalent to 65 per cent at Manor Lane and 62 per cent at Worbarrow in comparison with undisturbed sediments.
7. there was a large increase in the concentration of calcium from source to toe at Manor Lane (Figure 4.28) from approximately 100 mg/l to 600 mg/l. At Worbarrow a similar increase was found (60 mg/l to 130 mg/l), but the concentration was noted to decrease to 80 mg/l in the accumulation lobe as for the chloride ions. Thus there was a notable increase in calcium on the lower slopes at Manor Lane.
8. the concentration of iron at both sites contrasts markedly showing an increase downslope at Manor Lane but a decrease at Worbarrow (Figure 4.30). The proportion of iron at Manor Lane was fairly uniform and increased from 1.0 mg/l in the source and translational units to 1.5 mg/l at the base of the slope in cores 2 and 1. The origin of iron on the lower slopes was attributed to the secondary source (unit 3). In contrast, the concentration of iron at Worbarrow decreased from approximately 0.75 mg/l to 0.25 mg/l, particularly down the feeder track.

Figure 4.29. Distribution of free-water sodium at the shear surface.

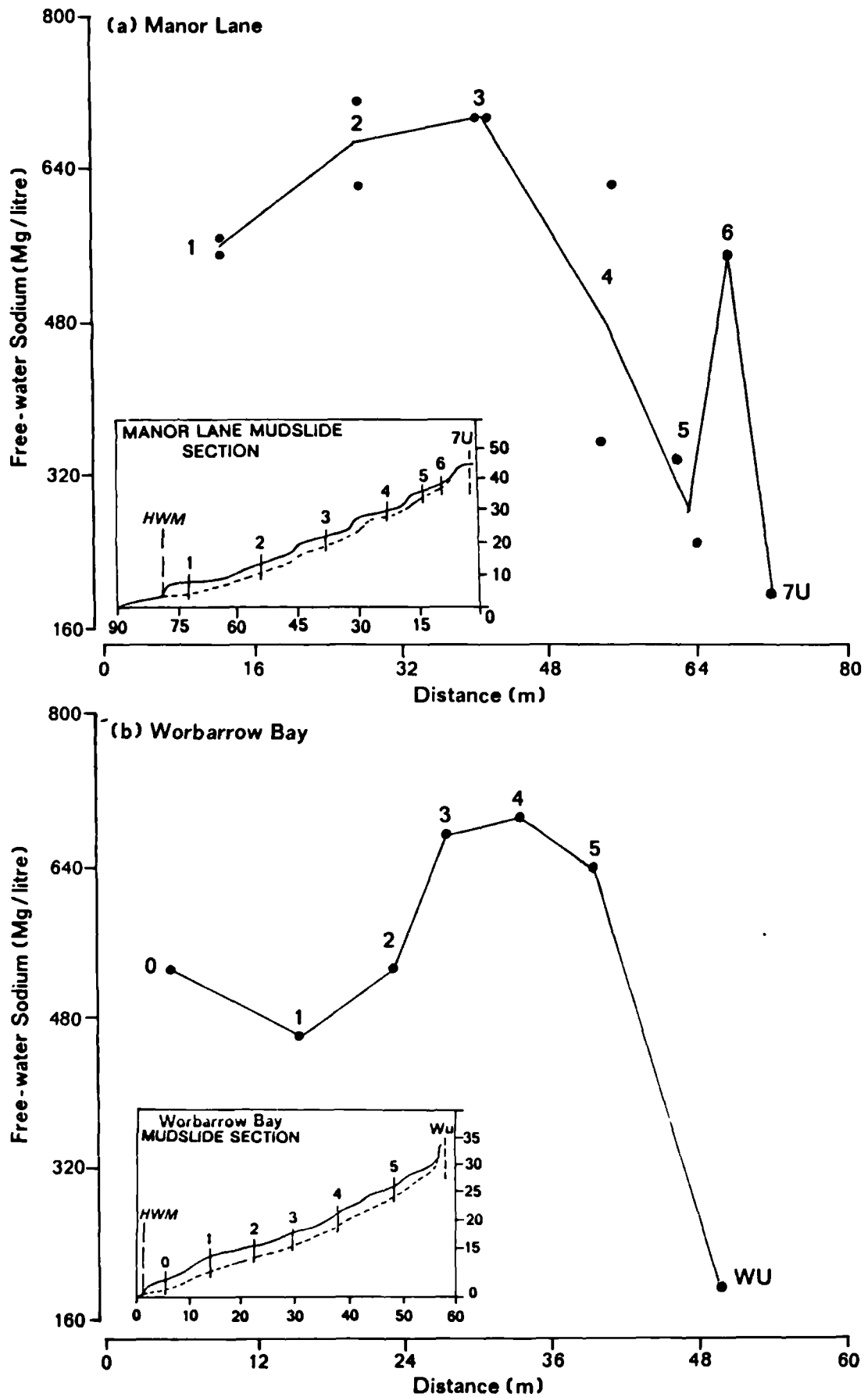


Figure 4.30. Distribution of free-water iron at the shear surface.

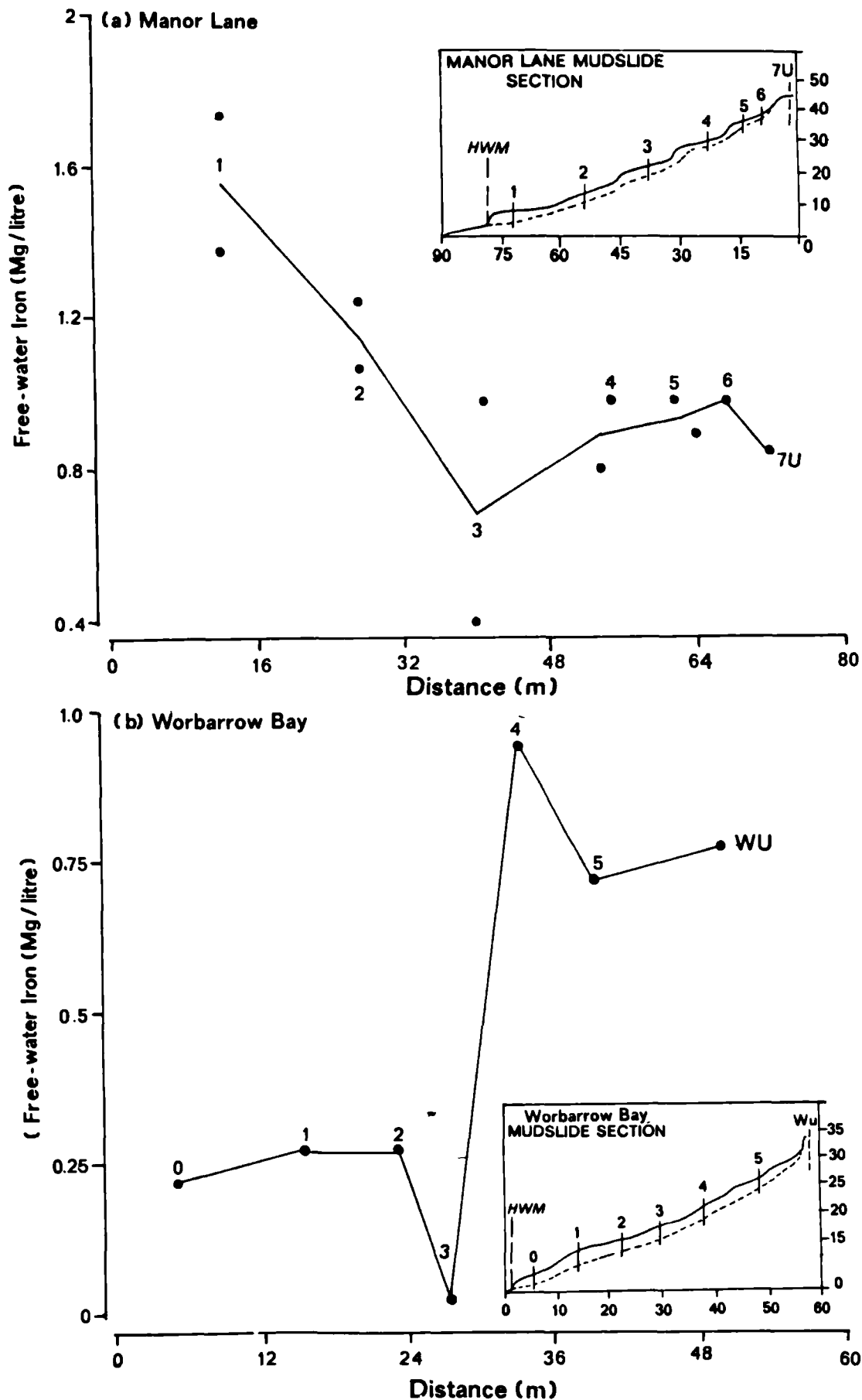
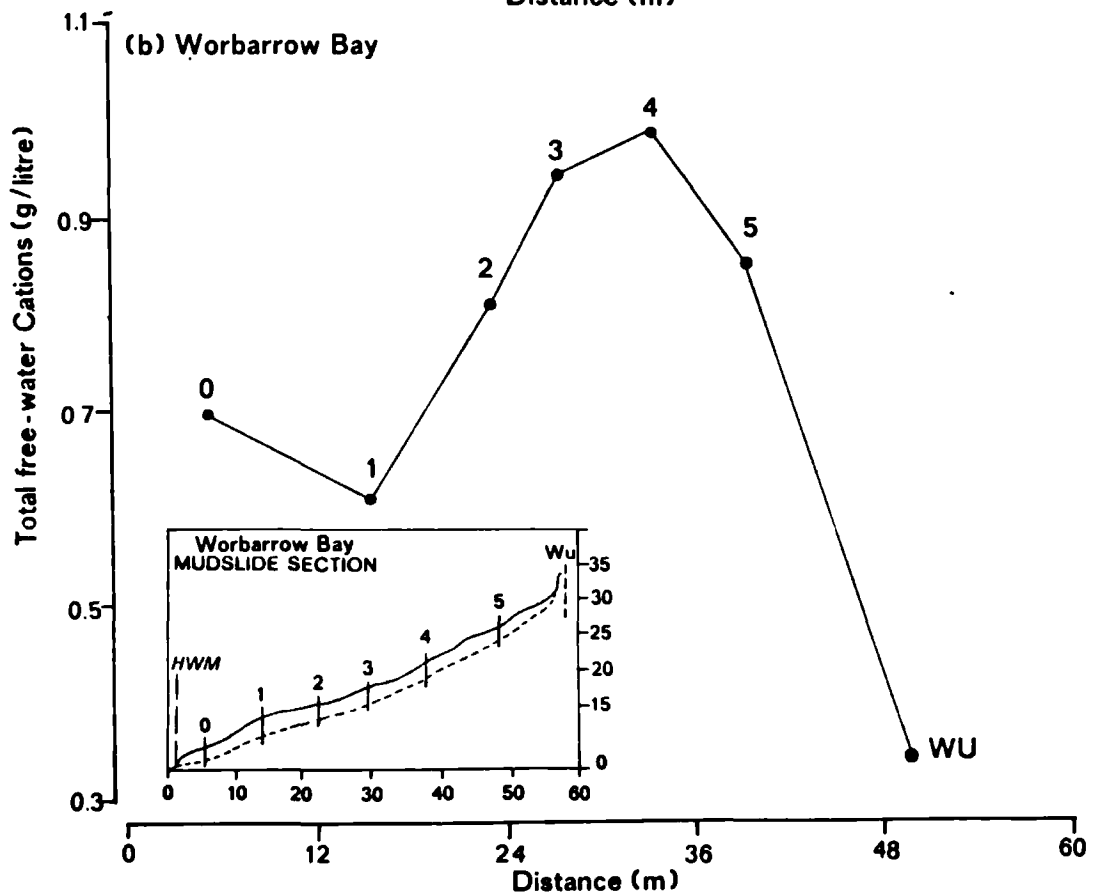
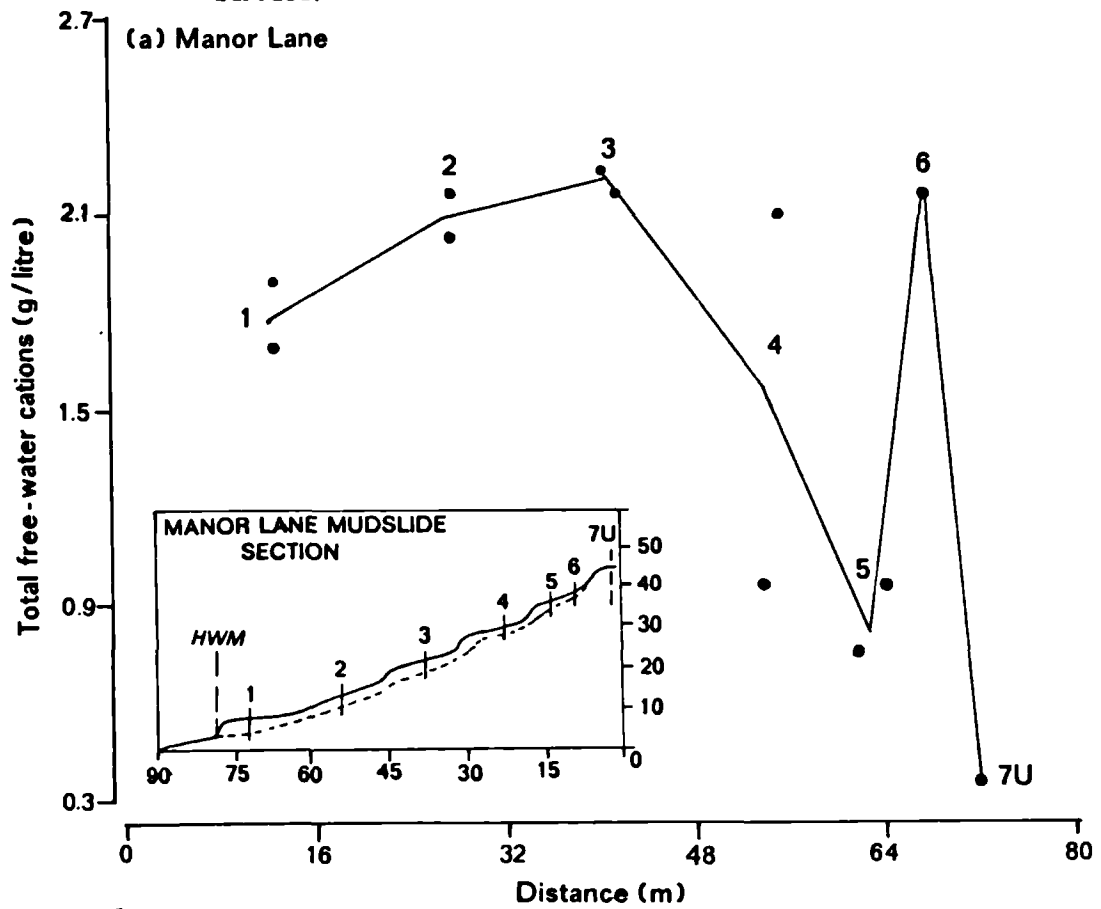


Figure 4.31. Distribution of the total free-water cations at the shear surface.



9. finally it was noted that there was a three-fold increase in the total concentration of cations and salts in the pore water at both sites from the undisturbed to the highly weathered states (Figure 4.31). The concentration reached a maximum in the central section of the feeder track with a subsequent reduction towards the rear of the accumulation lobe. The release of base cations to the pore solution upon weathering resulted in this distribution.

4.422 Soluble ions and exchangeable bases.

For the purpose of establishing a chemical balance of the clay materials in relation to the interstitial pore water, standard soil chemical pre-treatments were used to measure the concentrations of water soluble and exchangeable ions. The methods are outlined in Appendix 9B and 9C, respectively. Control samples were included in all pre-treatment procedures to assess the margin of error incorporated into the test results. Since high-grade analytical reagents were used along with the strict adherence to standard procedures the errors of pre-treatment were found to be negligible for the water soluble analyses.

The chemical exchange procedures were found to be slightly sensitive to the reaction environment and laboratory conditions, such as temperature, pH and the time allowed for the pre-treatment. As a consequence the control samples showed a standard error of up to 5 per cent for the exchangeable cation analysis.

Analyses of the water-soluble supernatant solutions included Na^+ , K^+ , Mg^{2+} , Ca^{2+} , Cl^- , and SO_4^{2-} , and the spectrographic techniques used are outlined in Appendix 9F. The exchangeable Na^+ , K^+ , Mg^{2+} , and Ca^{2+} were also measured using the same procedures.

Table 4.19a. Water soluble and exchangeable cations for Manor Lane core samples 1A - 3B from Manor Lane.

CORE #	ION n = 2	ZONE ONE		ZONE TWO		ZONE THREE		ZONE FOUR		SQL X
		S	E	S	E	S	E	S	E	
1A	Na	54	86	65	97	80	106	90	114	72
	K	21	20	15	15	24	19	27	20	22
	Mg	52	325	47	303	82	348	81	342	66
	Ca	75	379	67	346	118	336	134	348	99
	Cl	34	-	45	-	45	-	44	-	42
	SO ₄	501	-	462	-	802	-	813	-	645
	Total salt	737		701		1151		1189		945
1B	Na	46	74	71	91	76	131	86	205	70
	K	23	19	24	18	27	23	29	39	26
	Mg	65	349	94	386	59	373	17	310	59
	Ca	106	441	131	362	76	352	19	331	83
	Cl	24	-	30	-	35	-	23	-	28
	SO ₄	651	-	936	-	643	-	339	-	642
	Total salt	915		1286		916		513		908
2A	Na	64	97	67	111	93	120	110	177	84
	K	30	21	28	20	35	25	37	35	33
	Mg	101	381	96	371	99	419	42	344	85
	Ca	135	342	112	297	110	325	51	353	102
	Cl	45	-	48	-	55	-	29	-	44
	SO ₄	975	-	873	-	968	-	580	-	849
	Total salt	1350		1224		1360		849		1196
2B	Na	96	134	127	143	100	145	130	174	113
	K	44	26	50	26	39	28	45	32	45
	Mg	120	368	121	395	106	367	48	294	99
	Ca	111	301	142	275	115	278	64	298	108
	Cl	49	-	60	-	62	-	35	-	52
	SO ₄	1094	-	1236	-	1023	-	659	-	1003
	Total salt	1514		1736		1445		981		1419
3A	Na	89	145	93	165	103	157	165	180	113
	K	43	31	44	35	48	29	46	29	45
	Mg	97	416	114	477	83	426	150	412	111
	Ca	118	275	136	340	100	307	212	296	142
	Cl	45	-	45	-	31	-	49	-	43
	SO ₄	983	-	1133	-	912	-	1711	-	1185
	Total salt	1375		1565		1277		2333		1638
3B	Na	51	97	71	94	61	123	93	165	69
	K	5	10	21	17	42	29	35	32	26
	Mg	16	373	65	297	90	316	59	394	58
	Ca	27	481	103	361	116	316	64	307	78
	Cl	28	-	29	-	38	-	42	-	34
	SO ₄	205	-	659	-	881	-	659	-	601
	Total salt	332		948		1228		952		865

All values in mg/litre S : soluble ions E : exchangeable ions T : trace
Total salt content based on the sum of soluble ions

Continued in Table 4.19b

Table 4.19b. Water soluble and exchangeable cations for Manor Lane core samples 4A - 7U.

CORE #	ION n = 2	ZONE ONE		ZONE TWO		ZONE THREE		ZONE FOUR		SOL X
		S	E	S	E	S	E	S	E	
4A	Na	11	60	14	66	31	83	68	94	31
	K	31	9	47	11	5	12	22	20	26
	Mg	15	361	21	281	10	260	55	323	25
	Ca	T	435	T	457	9	489	111	446	30
	Cl	13	-	13	-	18	-	31	-	19
	SO ₄	31	-	19	-	129	-	827	-	252
	Total salt	101		114		202		1114		383
4B	Na	45	80	36	71	44	77	104	145	57
	K	6	10	7	10	5	9	34	32	13
	Mg	21	299	13	288	13	401	32	293	20
	Ca	36	467	12	470	23	458	43	387	29
	Cl	20	-	18	-	18	-	47	-	26
	SO ₄	224	-	111	-	158	-	404	-	224
	Total salt	352		197		261		664		369
5A	Na	43	100	47	97	72	94	77	97	60
	K	2	5	2	6	18	16	20	18	8
	Mg	6	243	15	264	15	363	51	399	22
	Ca	16	590	28	607	134	533	100	458	70
	Cl	29	-	32	-	41	-	46	-	37
	SO ₄	61	-	123	-	837	-	649	-	418
	Total salt	157		247		1117		943		616
5B	Na	34	57	77	91	66	86	106	123	71
	K	32	22	34	20	35	23	51	27	38
	Mg	59	335	59	375	74	356	198	504	98
	Ca	69	388	128	235	80	292	200	325	119
	Cl	7	-	26	-	32	-	44	-	27
	SO ₄	519	-	502	-	666	-	166	-	463
	Total salt	720		826		953		765		816
6	Na	23	86	35	89	42	83	87	100	47
	K	56	12	14	13	7	13	36	21	28
	Mg	40	277	7	256	10	259	110	404	42
	Ca	T	508	1	483	19	470	111	324	33
	Cl	16	-	17	-	34	-	41	-	27
	SO ₄	33	-	43	-	109	-	879	-	266
	Total salt	168		117		221		1264		443
7U	Na	11	54	31	86	32	117	70	134	36
	K	37	16	8	11	1	12	18	12	16
	Mg	20	200	6	217	28	242	9	261	16
	Ca	T	528	1	606	T	562	2	502	1
	Cl	15	-	13	-	24	-	79	-	33
	SO ₄	36	-	36	-	36	-	58	-	42
	Total salt	119		95		121		236		143
X	Total salt	654		755		855		984		812

All values in mg/litre S : soluble ions E : exchangeable ions T : trace
Total salt content based on the sum of soluble ions

Table 4.20. Water soluble and exchangeable cations at Worbarrow Bay.

CORE #	ION n = 2	ZONE ONE		ZONE TWO		ZONE THREE		ZONE FOUR		SOL X
		S	E	S	E	S	E	S	E	
W0	Na	241	154	127	111	124	91	44	114	134
	K	128	17	164	18	70	19	4	20	92
	Mg	18	110	15	102	15	98	3	131	13
	Ca	T	297	T	233	0	219	1	314	T
	Cl	67	-	59	-	50	-	62	-	60
	SO ₄	58	-	38	-	23	-	38	-	39
	Total salt	512		403		282		152		338
W1	Na	94	248	90	265	84	256	76	245	86
	K	14	12	13	10	28	13	44	17	25
	Mg	12	194	12	141	13	189	16	147	13
	Ca	T	219	T	99	0	177	0	219	T
	Cl	74	-	73	-	63	-	44	-	64
	SO ₄	35	-	19	-	27	-	35	-	29
	Total salt	229		207		215		215		217
W2	Na	63	265	62	245	74	276	61	293	65
	K	13	20	13	20	14	24	15	25	14
	Mg	12	207	12	199	12	200	12	201	12
	Ca	T	310	T	348	1	399	T	407	T
	Cl	64	-	58	-	70	-	54	-	62
	SO ₄	23	-	27	-	46	-	27	-	31
	Total salt	175		172		217		169		184
W3	Na	52	271	62	254	48	242	54	293	54
	K	9	19	9	19	9	23	9	22	9
	Mg	7	205	7	174	7	210	7	174	7
	Ca	T	211	1	265	1	352	1	322	1
	Cl	35	-	81	-	57	-	60	-	58
	SO ₄	15	-	35	-	35	-	42	-	32
	Total salt	118		196		157		173		161
W4	Na	38	276	24	225	40	145	50	248	38
	K	4	16	120	16	6	20	5	24	34
	Mg	2	172	12	138	3	237	3	251	5
	Ca	T	192	0	120	2	491	2	281	1
	Cl	56	-	55	-	77	-	54	-	61
	SO ₄	27	-	15	-	46	-	58	-	37
	Total salt	127		226		174		172		176
W5	Na	37	125	41	125	49	131	38	106	41
	K	3	27	2	13	4	20	4	20	3
	Mg	2	177	2	154	2	161	2	147	2
	Ca	T	307	1	382	1	382	T	383	1
	Cl	59	-	64	-	79	-	63	-	66
	SO ₄	27	-	27	-	27	-	27	-	27
	Total salt	128		137		162		134		140
WU	Na	87	179	90	177	79	166	76	170	83
	K	9	19	7	13	9	18	11	14	9
	Mg	8	213	7	220	8	247	7	261	8
	Ca	3	205	4	217	4	225	5	218	4
	Cl	166	-	170	-	206	-	203	-	186
	SO ₄	83	-	71	-	72	-	79	-	76
	Total salt	356		349		378		381		366
X	Total salt	234		241		226		199		226

All values in mg/litre S : soluble ions E : exchangeable ions T : trace
 Total salt content based on the sum of soluble ions

The results of these analyses are presented in two forms. Firstly, Tables 4.19a, 4.19b and 4.20 present the concentrations of the cations and anions and total salt contents in mg/l, whereas Appendix 11 presents the ionic balance and speciation of ions in terms of equivalent weights (meq/l). The following associations were noted:

1. the total soluble salt content at Manor Lane averages 0.81 g/l in comparison to 0.23 g/l at Worbarrow. This accounts for the higher values of electrical conductivity measured at the former site.
2. at Manor Lane the total concentration of soluble salt cations in the mean profile (0.81 g/l) showed a six-fold increase in concentration in comparison to the undisturbed sample (0.14 g/l). There was an increase in concentration of soluble cations (Figure 4.32a) with depth particularly below the basal shear surface. In the source unit profiles, there were substantial increases (472% in core 6) in the concentration of soluble salts for *in situ* clay at zone 4, whereas there was a converse depletion (23% in core 3B) below the shear surface along the feeder track. The profiles located in the body of the mudslide (Figure 4.32a) show a large increase in concentration downslope predominantly at the surface of the profile. This implied that the increase in concentration of soluble salts downslope was related to the surface conveyance and weathering of landslipped materials and due to the development of diffuse double layers and the addition of sea-salts.
3. the weathered profile plots for Worbarrow (Figure 4.32b) showed a decrease in the mean concentration of water soluble cations with depth in comparison with the uniform undisturbed sample. The weathered profiles also showed a high degree of uniformity. However, two profiles deviate from this trend. Core profile 4, at the uppermost region of the feeder track, showed a two-fold increase in soluble salt concentration from 0.13 g/l to 0.23 g/l at zone 2, probably a consequence of weathering and erosion in the source unit. Additionally, profile 0 at the toe of the mudslide shows a marked five-fold increase in soluble cation concentration at the surface (sub-zone 1) decreasing uniformly from 0.51 g/l to

Figure 4.32. Concentration of water-soluble cations of selected core profiles.

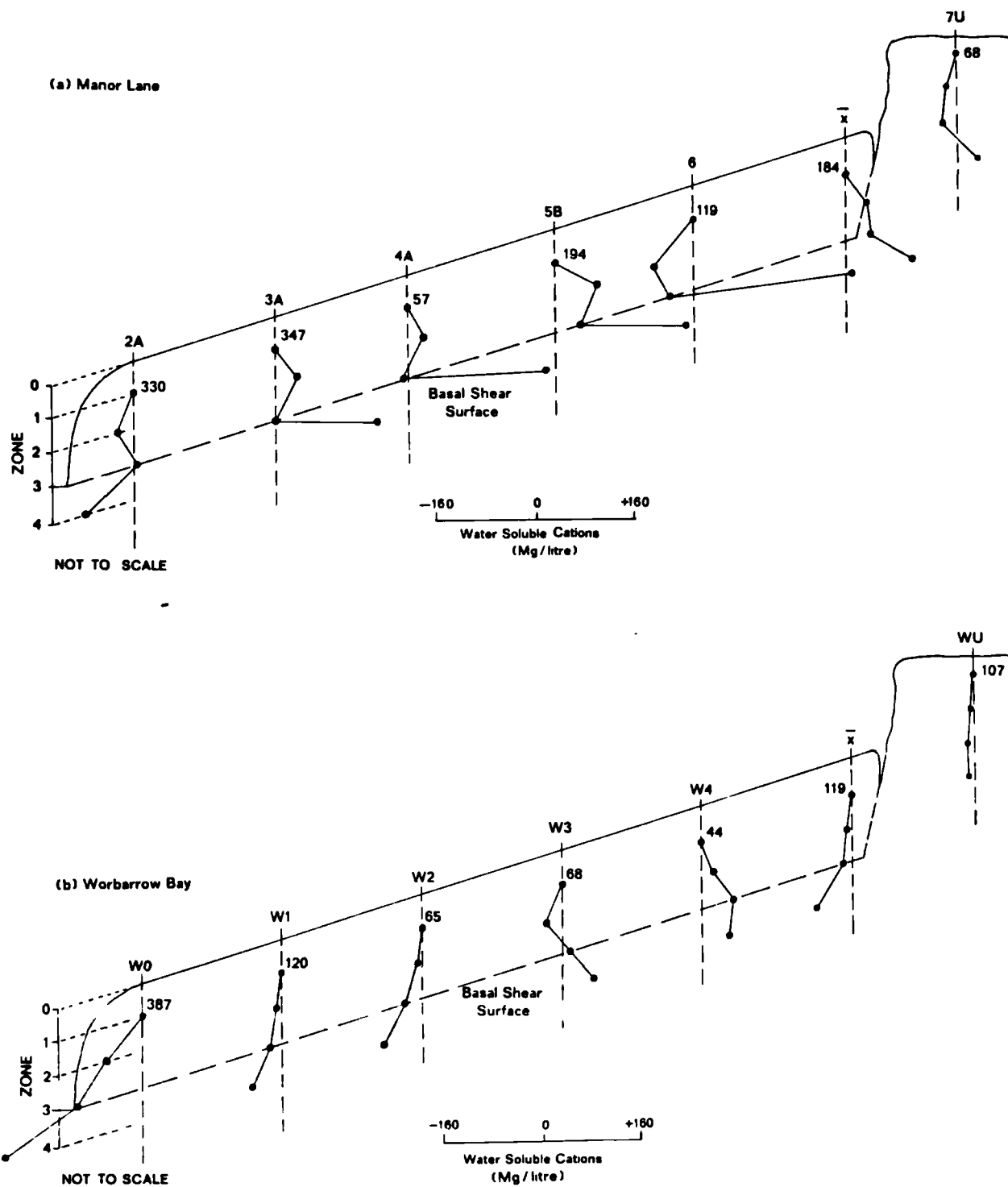
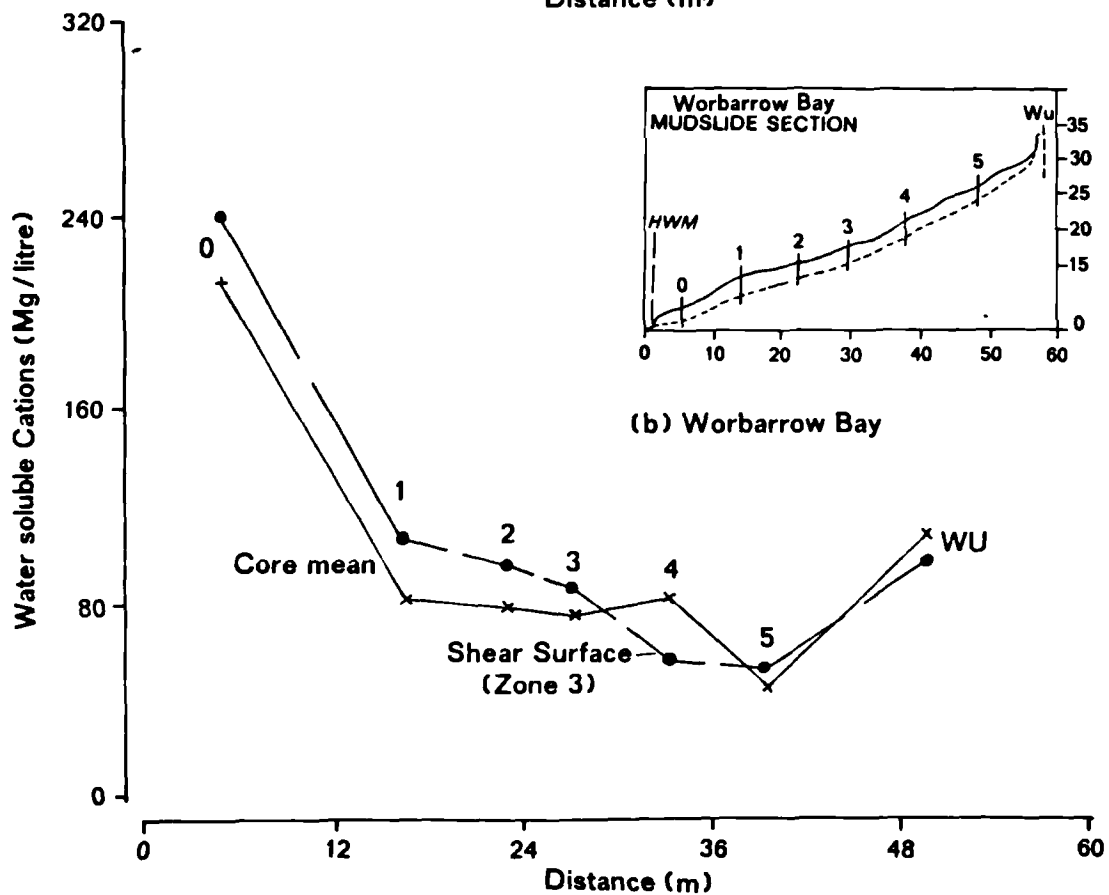
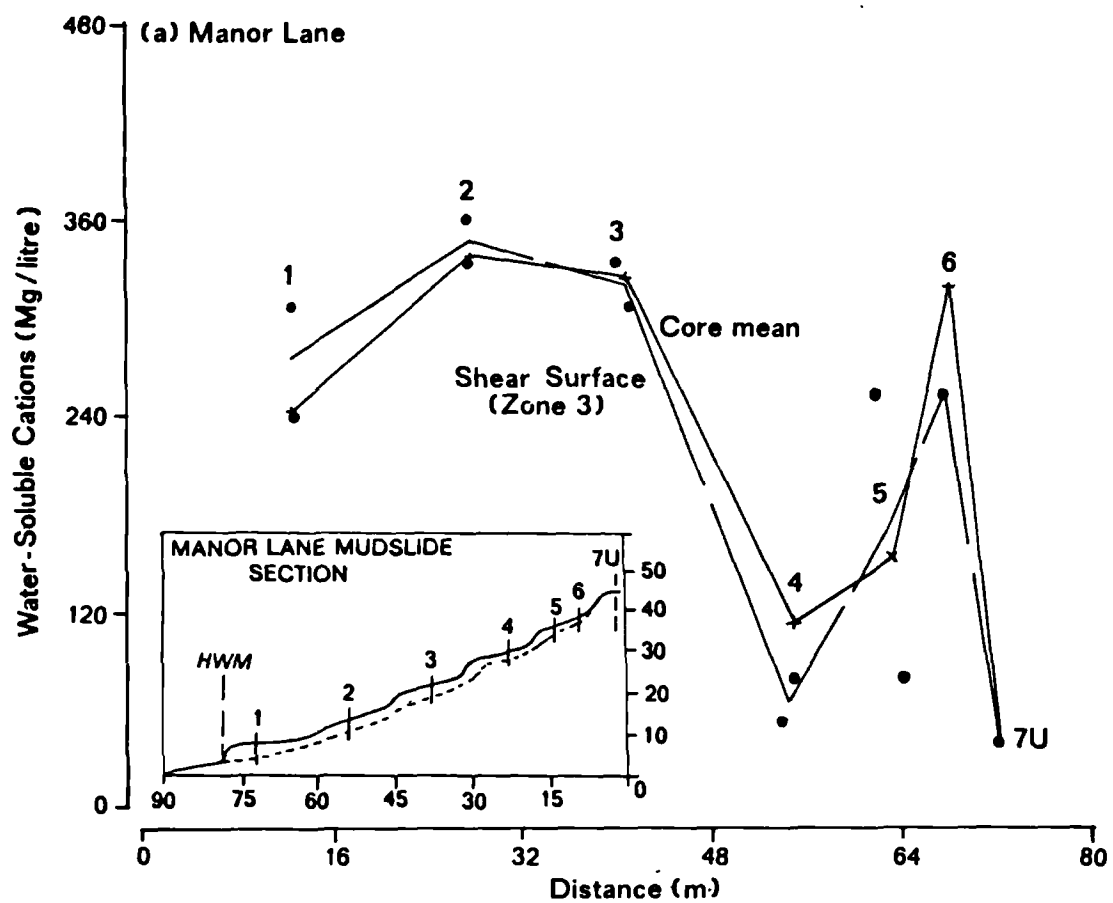


Figure 4.33. Distribution of water-soluble cations at the shear surface.



- 0.15 g/l with depth. The increase in soluble salt was considered to result from the development of double layers and from the inundation of the clay materials with sea spray and water.
4. the concentrations of soluble cations are plotted in relation to the mudslide sections (Figure 4.33). The plot for Manor Lane showed a five-fold increase in soluble salt concentration at the shear surface from 0.12 g/l for the undisturbed condition to 1.15 g/l at the toe of the slope. The influence of the secondary source unit was again evident (unit 3). In comparison, the Worbarrow plot showed a similar increase in concentration at the basal shear surface of the weathered materials from 0.16 g/l (unit 5) to 0.28 g/l (unit 0). The undisturbed materials at Worbarrow had a relatively high soluble salt content (0.36 g/l) in contrast to Manor Lane. However, there was a net increase in the solubility of cations as a result of mudsliding at Manor Lane and Worbarrow.
 5. with reference to Appendix 11 it was clear that the soluble and exchangeable cations at Manor Lane were dominated by magnesium, calcium and sodium, averaging 4.86 and 28.21 meq/l (Mg^{2+}), 3.64 and 19.38 meq/l (Ca^{2+}) and 2.98 and 4.79 meq/l (Na^{+}), respectively. Sulphate soluble anions almost entirely balanced the soluble cations with a total equivalent charge of 11.44 meq/l. The exchangeable cations were approximately five times more concentrated than the soluble cations.
 6. at Worbarrow sodium dominated the water soluble cations averaging 3.11 meq/l from a total of 4.69 meq/l, with the highest concentrations of soluble salts occurring on the lower slopes (5.83 meq/l for unit 0). The dominant balancing anion was chloride with an average of 2.24 meq/l. However, the exchanger was dominated in order of magnesium, calcium and sodium, in a similar fashion to Manor Lane although less concentrated with equivalent weights of 15.06, 13.59, and 8.85 meq/l, respectively. The low concentrations of soluble salts suggested that the majority of cations are held by the exchanger which could explain both the lower conductivity readings and interstitial pore water salt concentrations at Worbarrow Bay. The mean totals of soluble and exchangeable ions at Worbarrow showed a ten-fold difference in concentration.

Figure 4.34. Concentration of exchangeable cations for selected core profiles.

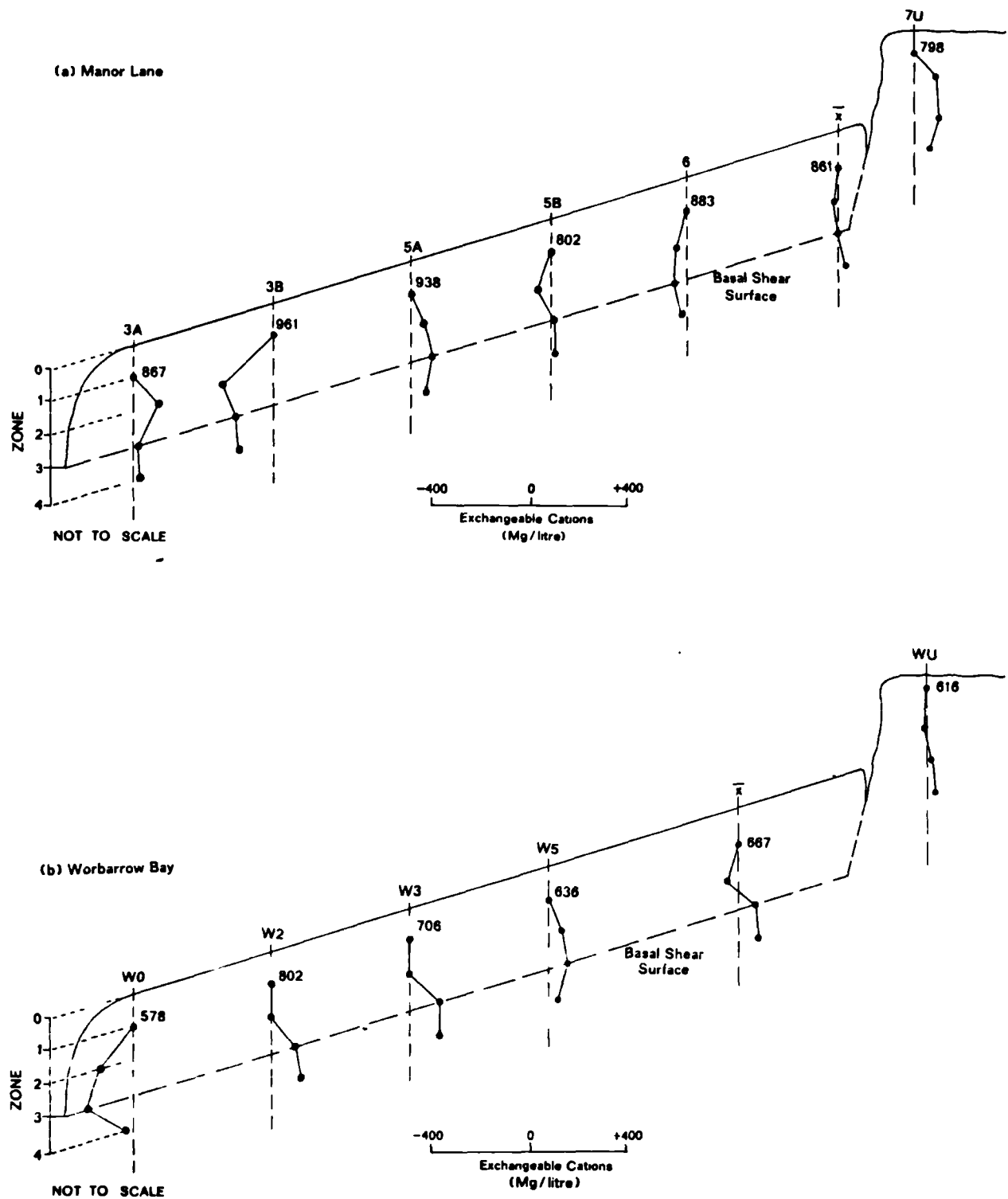
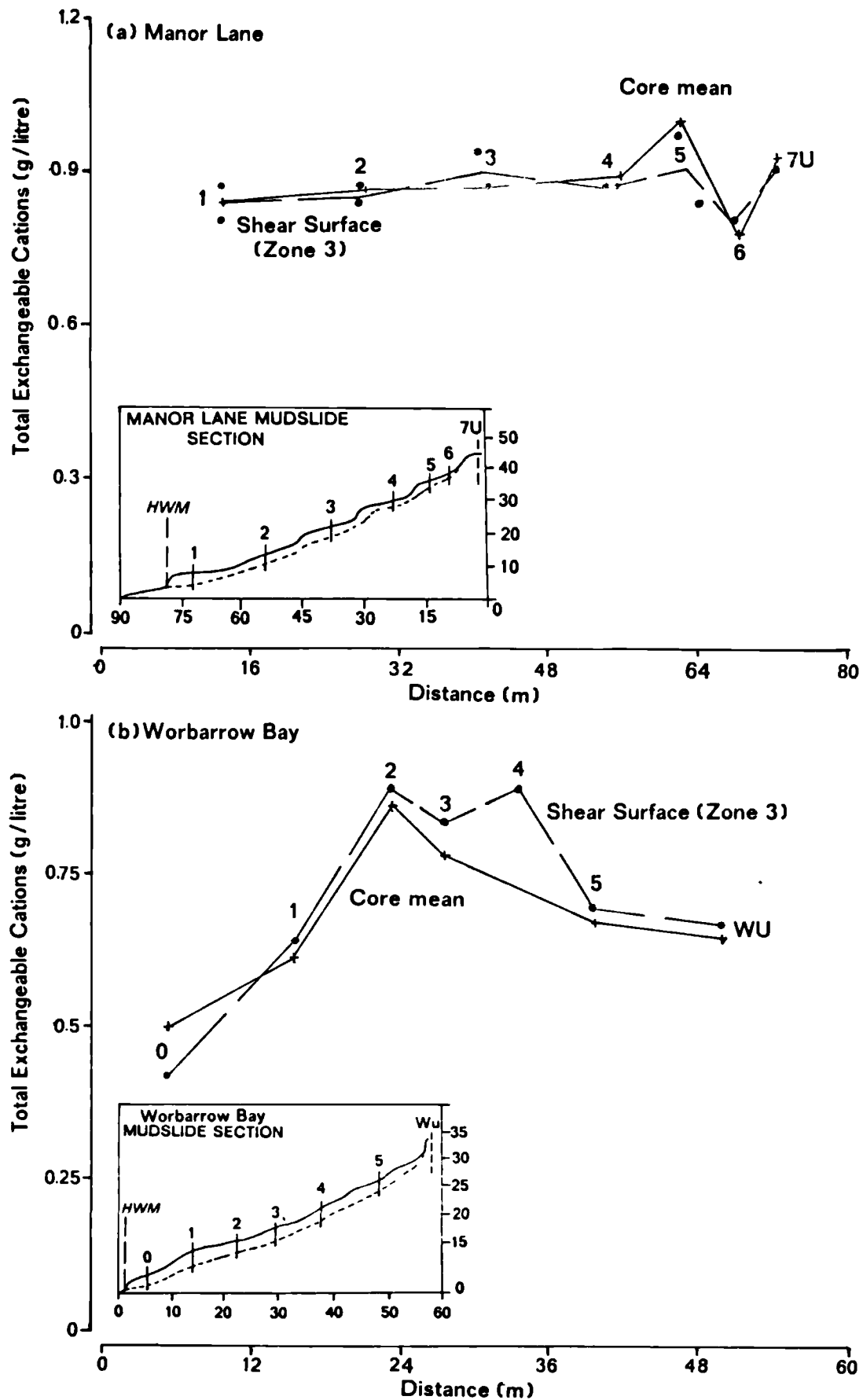


Figure 4.35. Distribution of exchangeable cations at the shear surface.



7. when compared with the undisturbed sample, the mean profile at Manor Lane (Figure 4.34a) showed an overall reduction in concentration of exchangeable cations from 0.92 to 0.84 g/l (sub-zone 2) attributable to weathering. The results of the weathered profiles were fairly uniform and showed little variation with depth or location within the slope section, although the mean indicated a slight increase in exchangeable ions with depth.
8. the corresponding plot for Worbarrow (Figure 4.34b) shows an increase in the mean concentration of exchangeable cations in relation to the unweathered profile. Profile 4 however, showed a marked reduction in concentration in sub-zone 2, decreasing from 0.67 to 0.499 g/l, which was thought to reflect the leaching of ions experienced in the source unit.
9. with reference to the Manor Lane section in Figure 4.35a the concentration of exchangeable cations is plotted at the shear surface. Overall, the mean concentration decreased from 933 to 800 mg/l downslope, closely mirrored by the values at the shear surface. There was a peak exchangeable ion content of 1.0 g/l in the source (unit 5). The Worbarrow plot Figure 4.35b contrasts to some extent indicating an increase in concentration from the undisturbed sample value of 656 to 900 mg/l in slope unit 2 before rapidly reducing to 400 mg/l at the toe of the mudslide. These distributions suggest a release of bonded cations at Manor Lane in contrast to an increase in exchangeable ions at Worbarrow.

4.43 Cation exchange capacity and the exchange reactions.

In order to calculate indices of the nature of exchange reactions using the chemical data presented in the previous section, the cation exchange capacity (CEC) was determined analytically using the method detailed in Appendix 9D. The errors of determination were broadly similar to those measured in the pre-treatment of the exchangeable cations and the control samples revealed an error of estimation equivalent to 4.8 per cent.

Table 4.21a. Cation exchange capacity and ion-exchange relations for Manor Lane core samples 1A - 4B.

CORE #	PARAMETER n = 2	ZONE ONE	ZONE TWO	ZONE THREE	ZONE FOUR	\bar{X}
1A	CEC	54	56	57	55	56
	BS %	78.56	71.45	89.3	93.4	83.2
	ESP %	5.84	6.39	8.09	9.02	7.3
	SAR	0.55	0.65	0.68	0.73	0.65
1B	CEC	58	59	51	57	56
	BS %	54.84	54.69	54.97	52.29	54.2
	ESP %	5.55	5.74	8.38	15.63	8.8
	SAR	0.45	0.56	0.82	1.37	0.8
2A	CEC	58	55	54	57	56
	BS %	53.61	51.11	57.03	54.92	54.2
	ESP %	7.28	8.78	8.7	13.51	9.6
	SAR	0.6	0.71	0.73	1.13	0.8
2B	CEC	56	61	56	53	57
	BS %	52.22	53.56	51.5	47.79	51.3
	ESP %	10.41	10.2	10.33	14.28	11.3
	SAR	0.86	0.91	0.95	1.21	0.98
3A	CEC	57	73	63	58	63
	BS %	55.52	64.82	58.42	57.67	59.1
	ESP %	11.05	9.82	10.84	13.5	11.3
	SAR	0.91	1.03	0.96	1.12	1.01
3B	CEC	64	57	51	57	57
	BS %	59.61	47.33	48.22	56.17	52.8
	ESP %	6.59	7.18	10.49	12.58	9.21
	SAR	0.57	0.63	0.82	1.03	0.76
4A	CEC	59	53	58	54	56
	BS %	54.67	49.42	50.04	53.82	52.0
	ESP %	4.42	5.42	6.22	7.57	5.91
	SAR	0.36	0.42	0.53	0.58	0.47
4B	CEC	54	55	61	54	56
	BS %	52.01	50.85	59.94	50.89	53.4
	ESP %	6.44	5.62	5.49	11.67	7.31
	SAR	0.5	0.45	0.45	0.95	0.59

CEC : cation exchange capacity (Meq/100g)

SAR : sodium adsorption ratio (Meq/litre)

ESP : exchangeable sodium percentage

BS : base saturation (%)

Continued in Table 4.21b

Table 4.21b. Cation exchange capacity and ion-exchange relations for Manor Lane cores 5A - 7U.

CORE #	PARAMETER n = 2	ZONE ONE	ZONE TWO	ZONE THREE	ZONE FOUR	\bar{X}
5A	CEC	57	63	64	62	62
	BS %	95.14	90.03	95.94	98.11	94.8
	ESP %	7.63	6.7	6.39	6.81	6.88
	SAR	0.62	0.58	0.54	0.56	0.58
5B	CEC	55	55	54	69	58
	BS %	91.56	86.31	90.0	93.17	90.3
	ESP %	4.51	7.2	6.93	7.75	6.60
	SAR	0.36	0.6	0.56	0.7	0.56
6	CEC	56	67	67	61	63
	BS %	93.8	74.15	73.16	89.77	82.7
	ESP %	6.68	5.78	5.39	7.13	6.25
	SAR	0.54	0.56	0.54	0.62	0.57
7U	CEC	52	67	57	61	59
	BS %	88.14	78.2	94.16	86.87	86.8
	ESP %	4.52	5.58	8.93	9.56	7.15
	SAR	0.36	0.54	0.73	0.85	0.62
\bar{X}	CEC	58	60	59	58	58
	BS %	69.14	64.33	68.56	69.57	67.9
	ESP %	6.74	7.03	8.02	10.75	8.14
	SAR	0.56	0.64	0.69	0.90	0.70

CEC : cation exchange capacity (Meq/100g)

SAR : sodium adsorption ratio (Meq/litre)

ESP : exchangeable sodium percentage

BS : base saturation (%)

Table 4.22. Cation exchange capacity and ion-exchange relations for all cores from Worbarrow Bay.

CORE #	PARAMETER n = 2	ZONE ONE	ZONE TWO	ZONE THREE	ZONE FOUR	\bar{X}
W0	CEC	61	58	64	62	61
	BS %	72.47	66.95	56.12	76.68	68.1
	ESP %	20.3	12.71	9.43	12.4	13.7
	SAR	1.36	1.08	0.91	0.99	1.09
W1	CEC	54	65	62	47	57
	BS %	86.84	51.78	85.86	92.68	79.3
	ESP %	24.5	20.95	26.5	28.78	25.2
	SAR	2.07	2.82	2.24	2.21	2.34
W2	CEC	48	54	57	56	54
	BS %	93.29	83.59	86.39	90.14	88.4
	ESP %	24.0	19.72	21.05	22.75	21.9
	SAR	2.01	1.83	2.06	2.09	2.00
W3	CEC	61	48	54	48	53
	BS %	65.41	81.83	85.57	91.46	81.1
	ESP %	19.31	23.0	19.48	26.54	22.1
	SAR	2.24	2.1	1.78	2.3	2.11
W4	CEC	42	46	57	49	48.5
	BS %	86.45	60.2	89.67	94.63	82.7
	ESP %	28.57	21.26	11.05	22.0	20.7
	SAR	2.46	2.34	0.95	1.82	1.89
W5	CEC	61	47	44	43	49
	BS %	59.38	80.19	88.02	84.93	78.1
	ESP %	8.9	11.55	12.96	10.72	11.0
	SAR	0.99	0.96	1.0	0.82	0.94
WU	CEC	63	67	49	59	60
	BS %	57.57	55.54	80.63	68.48	65.6
	ESP %	12.35	11.49	14.74	12.53	12.8
	SAR	1.47	1.43	1.28	1.29	1.37
\bar{X}	CEC	53	52	50	48	51
	BS %	74.49	68.58	81.75	85.57	77.6
	ESP %	19.70	17.24	16.46	19.39	18.2
	SAR	1.80	1.79	1.46	1.65	1.68

CEC : cation exchange capacity (Meq/100g)

SAR : sodium adsorption ratio (Meq/litre)

ESP : exchangeable sodium percentage

BS : base saturation (%)

The results are presented in Tables 4.21 and 4.22; the CEC was reported in units of milliequivalents per 100 grammes of soil, along with the calculation of the per cent base saturation (%BS), the exchangeable sodium percentage (ESP) and the sodium adsorption ratio (SAR), introduced in section 2.232. The following associations were recognised:

1. the mean CEC at Manor Lane was 58 meq/100g compared with 51 meq/100g at Worbarrow Bay. The CEC at both sites tended to reduce with depth although this may equally be due to the surface layers supporting higher values, particularly in sub-zone 2.
2. with reference to Figure 4.36 the CEC weathered profiles were variable at both sites, although at Manor Lane there was a tendency for the CEC to increase downslope in the surface layers (sub-zone 1) but decrease below the basal shear surface (sub-zone 4) for *in situ* clay. With reference to the Manor Lane section Figure 4.37a, the CEC at the shear surface shows a rise from 57 to 67 meq/100g immediately following weathering and a reduction downslope to 56 meq/100g. The CEC at the shear surface was also greater than the mean throughout the mudslide. The distribution reflects the clay mineralogy of the soil (see section 4.46).
3. the profile plots for Worbarrow in Figure 4.36b showed that there was a net reduction in the mean cation exchange capacity of weathered sediments in comparison with the undisturbed profile. Profiles 4, 3 and 2 showed an increase in CEC with depth, reaching a maximum of 57 meq/100g at the shear surface. The CEC was low in the surface layers (sub-zones 1 and 0) of cores 4, 2 and 1 but very high at the surface of the feeder track. In contrast there was generally a reduction in CEC below the shear surface, suggesting that the materials within the mudslide are chemically more active. When plotted in relation to the mudslide section Figure 4.37b there was an apparent reduction in CEC from 60 to 49 meq/100g immediately upon weathering in relation to the undisturbed sample. There was however an increase in CEC at the shear surface from 44 (unit 5) to 64 meq/100g (unit 0) downslope.

Figure 4.36. Cation exchange capacity profiles of selected core samples.

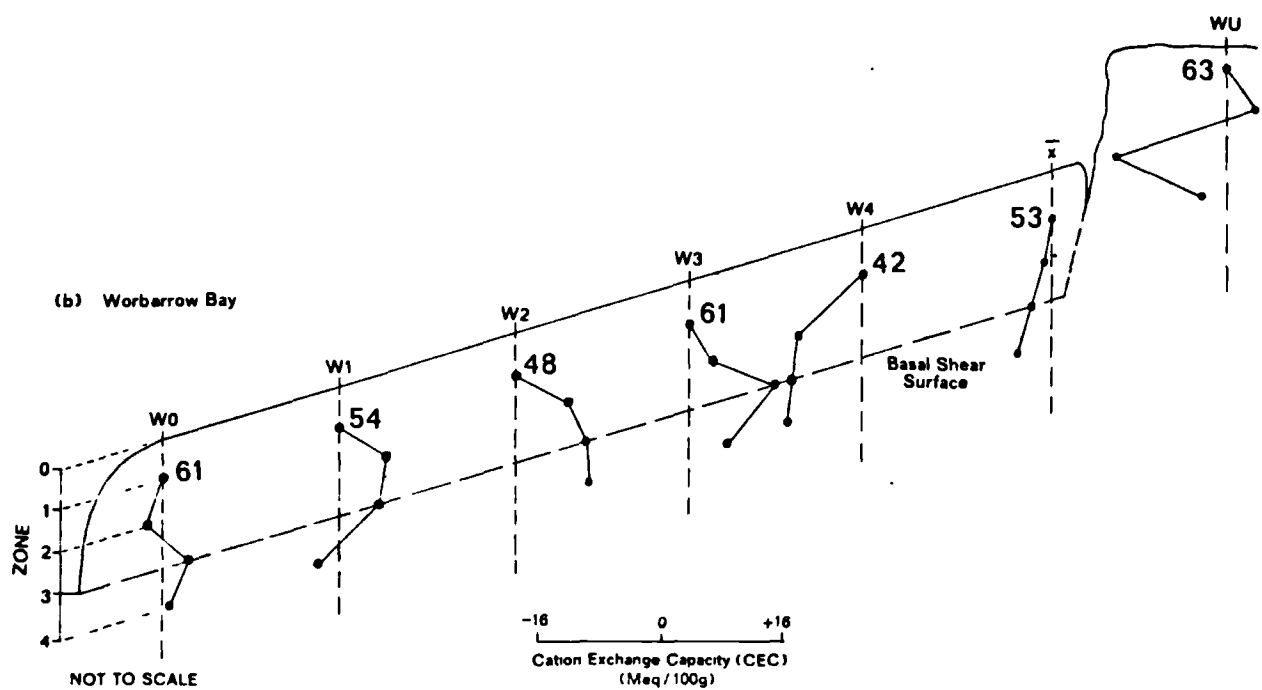
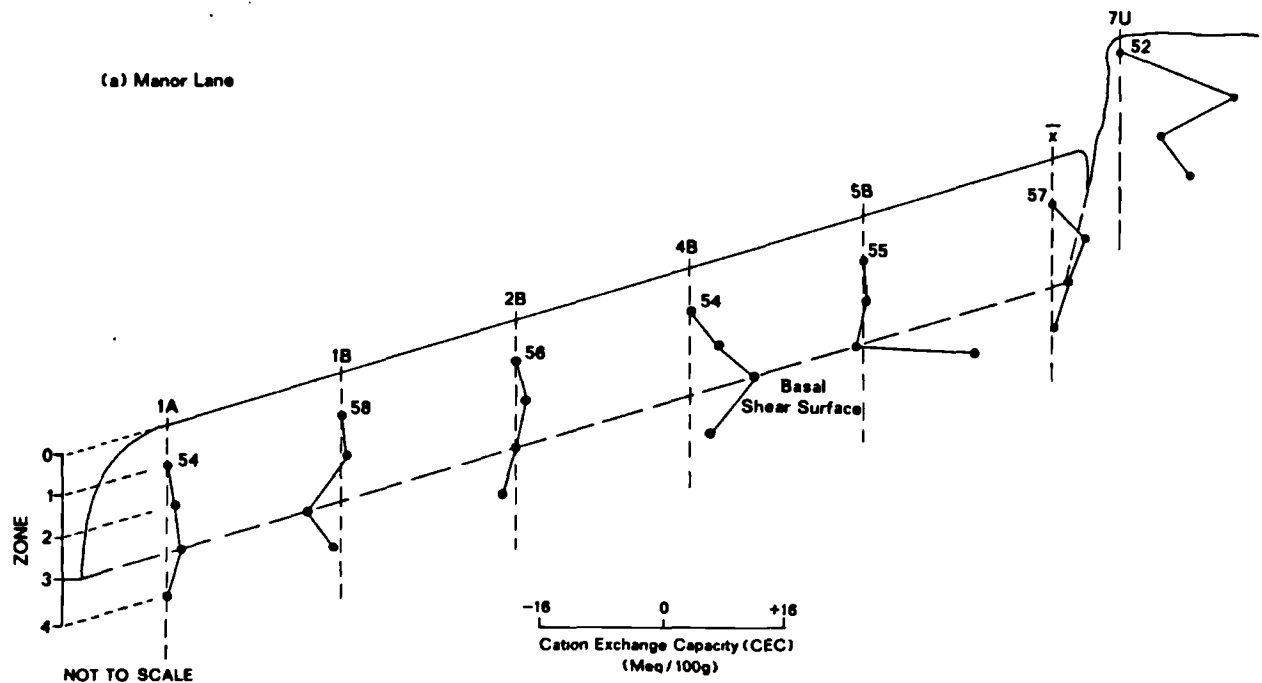
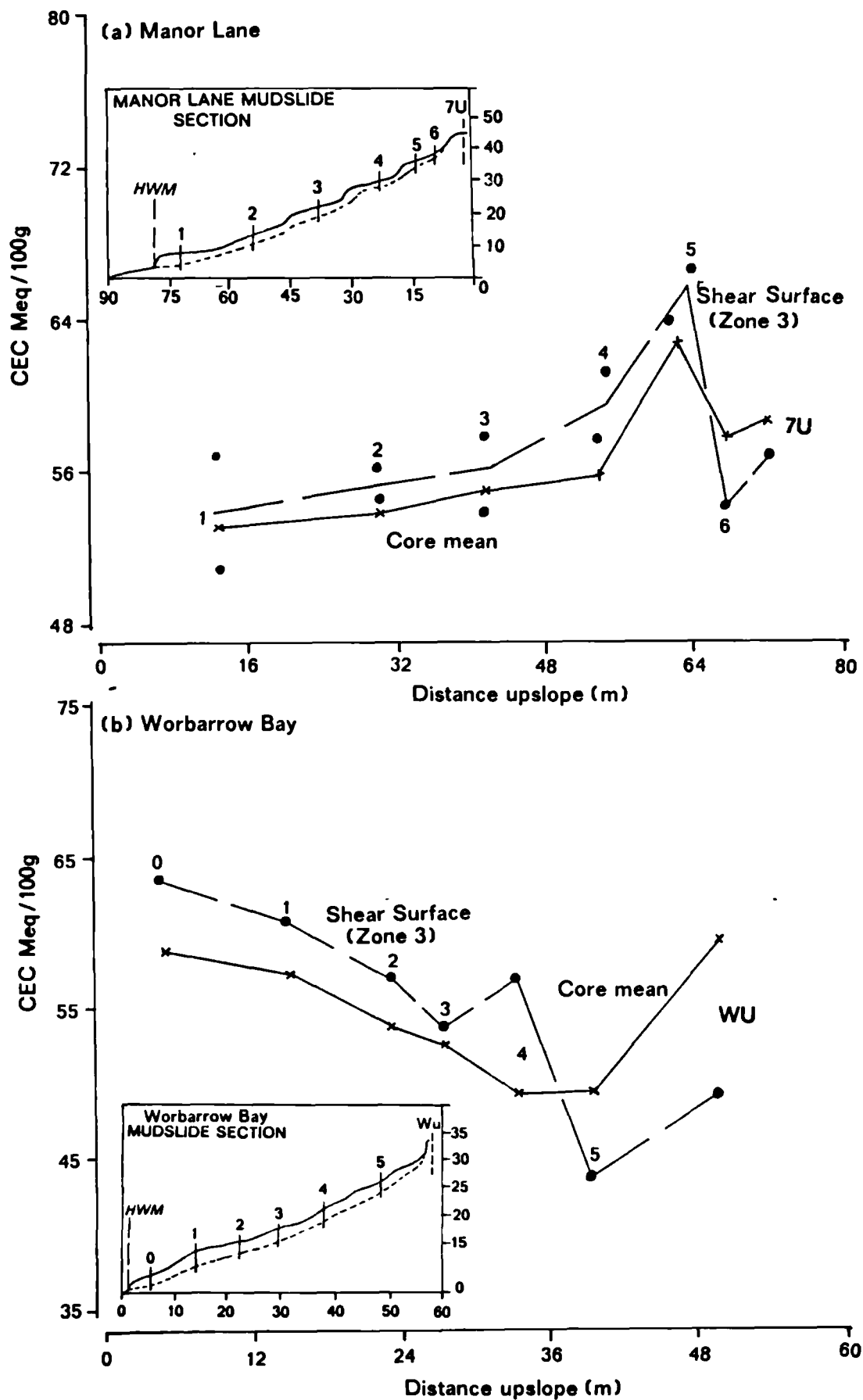


Figure 4.37. Distribution of CEC at the basal shear surface.



As for Manor Lane the distribution corresponds with the mineralogy of the soil.

4. the mean base saturation profile, or proportion of bases occupying the available exchangeable positions, averaged 67.9 and 77.6 per cent at Manor Lane and Worbarrow, respectively. At Manor Lane there was a reduction in the mean base saturation profile in comparison with the undisturbed sample, whereas at Worbarrow there was an increase in the proportion of base cations on the exchanger. This is shown in Figure 4.38 where at Manor Lane an almost bimodal base saturation exists between the core profiles of the source unit and those of the upper feeder track and toe of the slope. Between the two modes there was a jump equivalent to 40 per cent base saturation which was thought to reflect a considerable release of base cations from the exchanger following the weathering and movement of materials away from the source unit. The weathered profiles for Worbarrow Bay (Figure 4.38b) showed an increase in base saturation with depth, although clearly this amounted to a net loss of base cations (26% unit 3) in the surface layers.
5. the release of bases from the exchange sites is clearer in relation to the mudslide sections (Figure 4.39) where the base saturation is plotted at the shear surface. There was a reduction in base saturation from approximately 95% to 52% between the source units and the feeder track at Manor Lane. This remained constant for much of the feeder track, increasing to 83% at the toe of the slope probably as a consequence of the accumulation and addition of salts from sea-water. The distribution plot for Worbarrow Bay (Figure 4.39b) showed an increase in base saturation upon weathering reaching a maximum of 88% about midslope (units 3 and 2), followed by a reduction to 56% towards the accumulation lobe. These distributions demonstrate a net dispersion of cations on the exchanger relative to an increase in pore water salt concentration downslope (see section 4.422).
6. the proportion of sodium cations in the total exchangeable bases is represented by the exchangeable sodium percentage (ESP). The

Figure 4.38. Percent base-saturation profiles of selected core samples.

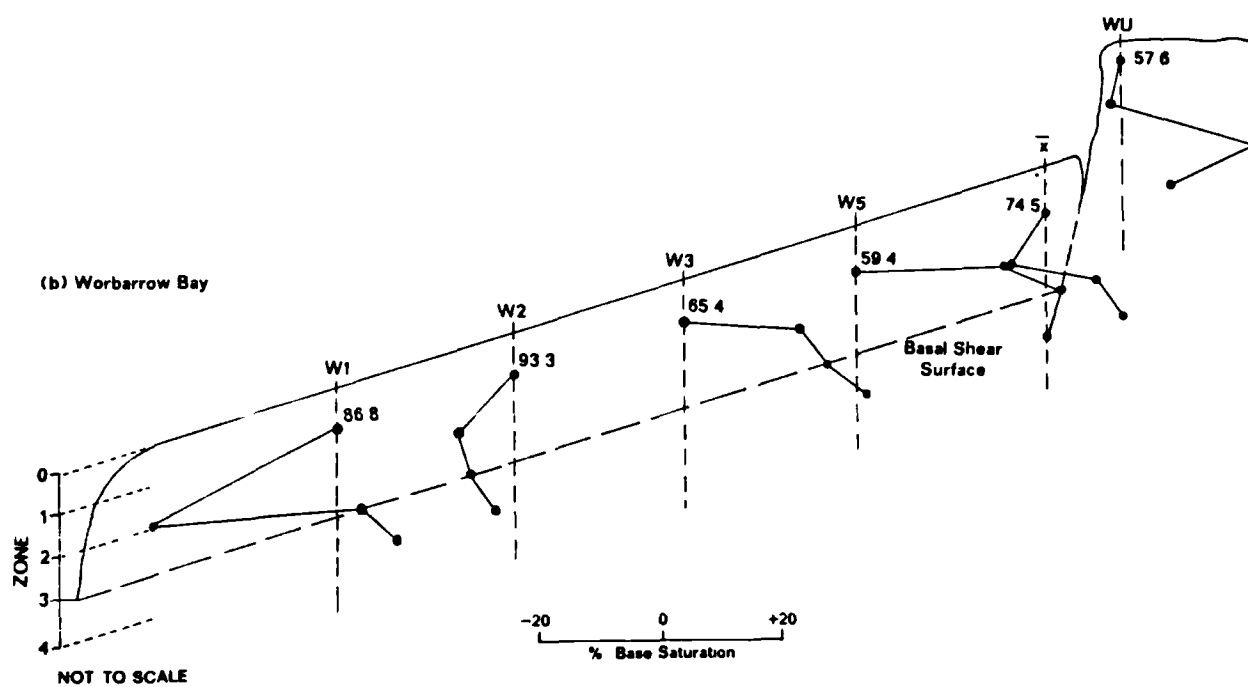
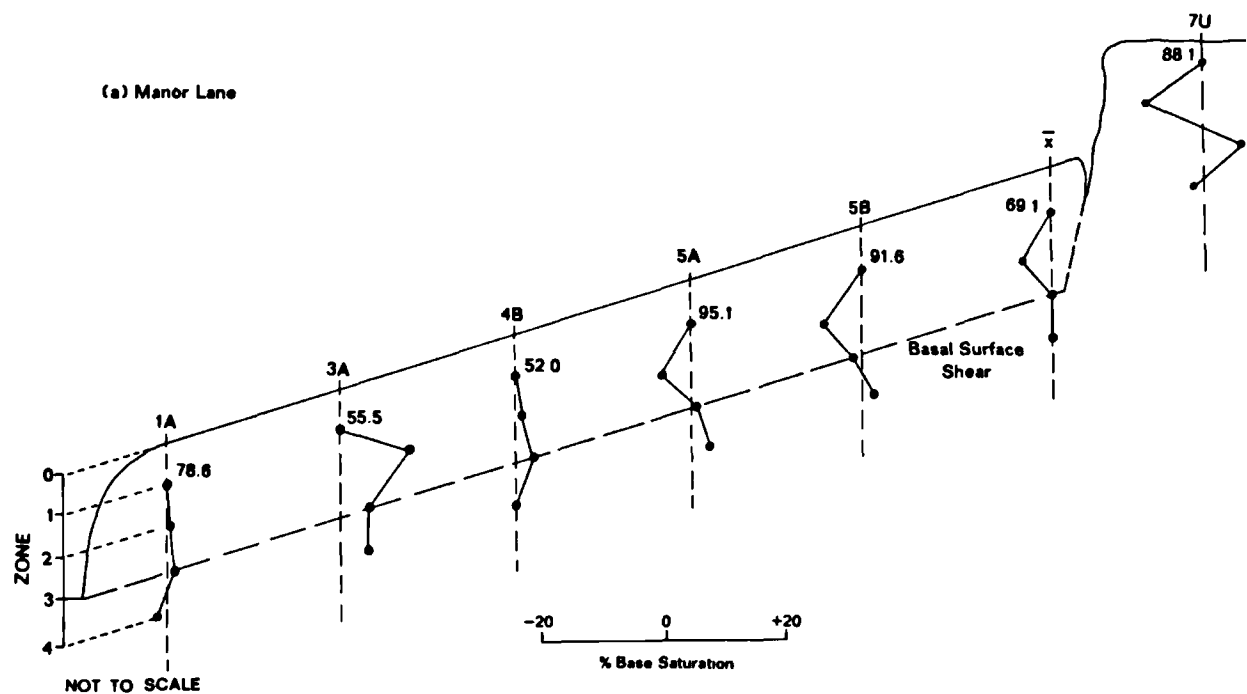
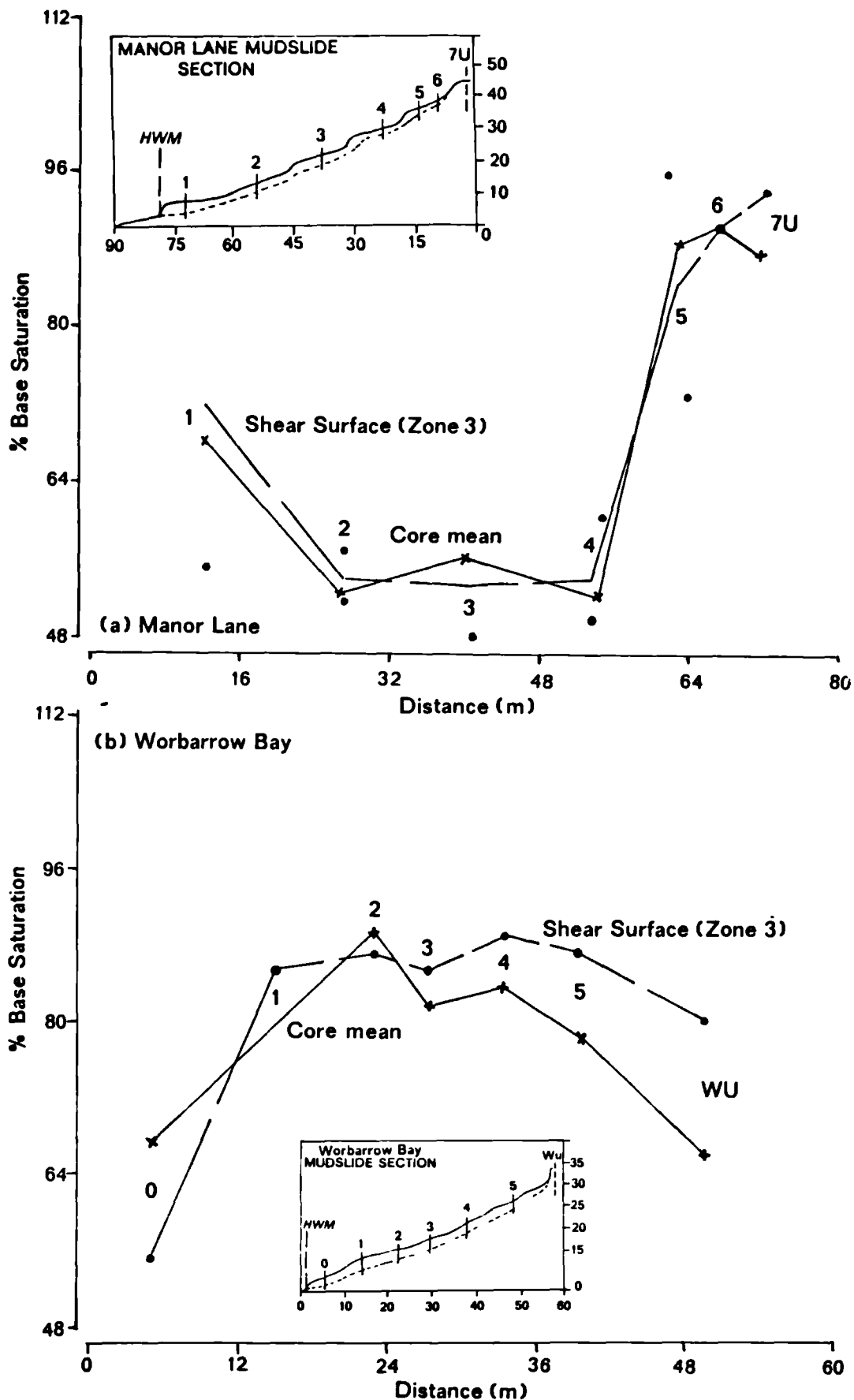


Figure 4.39. Distribution of base-saturation at the basal shear surface.



mean ESP for Manor Lane was 7.3% compared with 18.2% at Worbarrow. This accounted for the findings of the previous section where sodium was found to dominate the water soluble cations at Worbarrow Bay. The ESP increased downslope at both sites from 12 to 25 % at Worbarrow and from 6.6 to 10 % at Manor Lane. This was due to an increasing deposition and intrusion of sea-water salts.

7. the sodium adsorption ratio (SAR) represents the proportion of monovalent sodium occupying the ion-exchanger in comparison to the divalent cations (see section 2.232). This was found to equal 0.7 at Manor Lane and 1.68 at Worbarrow, emphasising the fundamental difference between each site: the London Clay at Manor Lane was predominantly divalent, whereas the Wealden system was dominated by monovalent cations. The SAR for undisturbed material at Worbarrow was 1.4, reducing upon weathering to 0.9 in the source units followed by an increase to 2.34 in the accumulation zone. A similar increase downslope was found at Manor Lane, where the corresponding values were 0.62 (7U) decreasing to 0.57 (unit 6) upon weathering and increasing to 1.01 (unit 3A) downslope. There was, however, a slight reduction to 0.65 at the toe of the slope. The latter probably reflects the increase of calcium on the ion-exchanger on the lower slopes (see section 4.422).

4.44 Bulk chemistry of the clay-size fraction.

The chemical constitution of the clay fraction was analysed to assess the inherent variability of clay mineral chemistry, to facilitate the semi-quantitative estimation of clay mineralogy and to account for the nature of the exchange reactions. Although the results are not directly associated with soil behaviour they do provide a quantitative index of mineral variability with respect to weathering processes.

Clay-size materials were decomposed into solution using concentrated perchloric and hydrofluoric acids using the methods outlined in Appendix

9E. The resultant test solutions were left for several weeks to allow the total release of aluminium and decomposition of mineral particles. The bulk chemistry of each solution was measured analytically by an Inductively Coupled Plasma Source Spectrometer (ICP) interfaced with a Pet computer. The ICP was automatically calibrated using an established programme routine, although it was necessary to monitor the drift for the large batches of samples analysed. By including standard solutions within the batch the standard error of analysis was 0.38%. The results of the bulk analyses may be split in two: the percentage of major oxides and the trace elements. Only the former concern this study.

The results are presented in Tables 4.23a, 4.23b and 4.24 for Manor Lane and Worbarrow, respectively. The following features were noted:

1. the oxides of aluminium, iron and silicon accounted for 90 per cent of the major elements within the clay fraction of both sites typical of sediments dominated by alumino-silicate clay minerals. The mean results for Manor Lane were 17.03% Al^{3+} , 8.11% Fe^{3+} , and 69.95% Si^{4+} in comparison with 15.77% Al^{3+} , 4.73% Fe^{3+} , and 75.45% Si^{4+} for Worbarrow. Thus the variability between the two sites amounted to approximately 4 per cent less iron and 7 per cent more silica in the crystal lattice clays at Worbarrow.
2. in relation to the undisturbed sample at Manor Lane the weathered profiles showed an increase of approximately 1.2 per cent aluminium oxide upon weathering, particularly in the surface layers (Figure 4.40a. The mean profile for Worbarrow was variable but showed an overall decrease in aluminium oxide in relation to the undisturbed sample (Figure 4.40b). The mean profiles at both sites show a small increase with depth; the profiles at Manor Lane, however, are more uniform. At Worbarrow the increase in the per cent aluminium was particularly marked at the ground surface and at the basal shear surface.

Table 4.23a. Bulk chemistry of clay-size material from Manor Lane core samples 1A - 3B.

CORE #	MAJORS Wt %	ZONE ONE	ZONE TWO	ZONE THREE	ZONE FOUR	\bar{X}
1A	Na ₂ O	0.52	0.5	0.57	0.61	0.55
	K ₂ O	3.03	2.6	3.26	3.15	3.01
	MgO	2.93	2.31	3.14	2.98	2.84
	CaO	1.48	1.15	1.58	1.55	1.44
	Al ₂ O ₃	16.51	14.29	17.26	16.06	16.03
	Fe ₂ O ₃	7.9	7.09	8.47	7.64	7.78
	SiO ₂	66.57	71.15	64.63	66.96	67.33
1B	Na ₂ O	0.54	0.56	0.5	0.56	0.54
	K ₂ O	3.25	3.2	3.2	3.43	3.27
	MgO	3.04	3.03	3.21	3.42	3.18
	CaO	1.53	1.44	1.46	1.17	1.40
	Al ₂ O ₃	17.16	16.96	17.81	18.6	17.63
	Fe ₂ O ₃	8.14	8.02	8.27	8.26	8.17
	SiO ₂	65.23	65.7	64.44	63.45	64.71
2A	Na ₂ O	0.58	0.58	0.51	0.52	0.55
	K ₂ O	3.28	3.21	3.25	3.46	3.30
	MgO	3.22	3.15	3.56	3.48	3.35
	CaO	1.64	1.62	1.75	1.21	1.56
	Al ₂ O ₃	17.14	16.93	18.16	19.52	17.94
	Fe ₂ O ₃	8.24	8.74	9.14	8.95	8.77
	SiO ₂	64.79	64.68	62.47	61.72	63.42
2B	Na ₂ O	0.52	0.54	0.51	0.56	0.53
	K ₂ O	3.31	3.36	3.32	3.34	3.33
	MgO	3.55	3.38	3.35	3.28	3.39
	CaO	1.6	1.31	1.12	1.21	1.31
	Al ₂ O ₃	18.19	18.65	18.89	18.54	18.57
	Fe ₂ O ₃	8.45	8.82	8.63	8.49	8.60
	SiO ₂	63.24	62.82	63.07	63.46	63.15
3A	Na ₂ O	0.55	0.49	0.46	0.53	0.51
	K ₂ O	3.26	3.4	2.88	3.08	3.16
	MgO	3.23	3.73	3.26	3.4	3.41
	CaO	1.4	1.58	1.51	1.73	1.56
	Al ₂ O ₃	17.99	19.47	16.69	17.23	17.85
	Fe ₂ O ₃	7.92	8.43	7.59	8.0	7.99
	SiO ₂	64.58	61.77	66.65	64.99	64.5
3B	Na ₂ O	0.49	0.51	0.58	0.56	0.54
	K ₂ O	2.78	3.1	3.29	3.45	3.16
	MgO	2.03	3.08	3.36	3.65	3.03
	CaO	0.86	1.46	1.55	1.64	1.38
	Al ₂ O ₃	16.61	17.49	17.36	18.76	17.56
	Fe ₂ O ₃	7.92	8.18	8.0	8.51	8.15
	SiO ₂	68.3	65.07	64.75	62.25	65.09

To convert to mg/litre multiply readings by 1000 and divide by the following factors
for Na - 1.35 : K - 1.21 : Mg - 1.66 : Ca - 1.4 : Al - 1.89 : Fe - 1.43 : Si - 2.14

Continued in Table 4.23b

Table 4.23b. Bulk chemistry of clay sized material for Manor Lane cores
4A - 7U.

CORE #	MAJORS Wt %	ZONE ONE	ZONE TWO	ZONE THREE	ZONE FOUR	- X
4A	Na ₂ O	0.42	0.57	0.52	0.43	0.49
	K ₂ O	2.25	3.02	3.03	3.46	2.94
	MgO	1.36	2.13	2.04	3.77	2.33
	CaO	0.58	0.9	0.74	1.8	1.01
	Al ₂ O ₃	14.18	16.11	17.14	19.97	16.85
	Fe ₂ O ₃	7.57	7.64	8.72	8.22	8.04
	SiO ₂	72.77	68.6	66.72	61.09	67.30
4B	Na ₂ O	0.43	0.42	0.45	0.43	0.43
	K ₂ O	2.33	2.1	2.37	3.14	2.49
	MgO	1.68	1.41	1.64	3.68	2.10
	CaO	0.76	0.63	0.67	1.69	0.94
	Al ₂ O ₃	13.81	12.63	14.05	17.93	14.61
	Fe ₂ O ₃	6.76	6.43	6.89	7.88	6.99
	SiO ₂	73.34	75.63	73.08	64.16	71.55
5A	Na ₂ O	0.47	0.47	0.49	0.48	0.48
	K ₂ O	2.42	2.51	3.05	3.41	2.85
	MgO	1.75	1.87	3.06	3.33	2.50
	CaO	1.21	1.62	2.88	2.0	1.93
	Al ₂ O ₃	15.33	15.81	17.3	19.21	16.91
	Fe ₂ O ₃	8.46	8.47	7.67	7.93	8.13
	SiO ₂	69.42	68.38	64.45	62.43	66.17
5B	Na ₂ O	0.51	0.56	0.53	0.4	0.50
	K ₂ O	3.05	3.08	2.9	3.28	3.08
	MgO	3.01	3.05	3.01	4.08	3.29
	CaO	1.44	1.49	1.76	2.2	1.72
	Al ₂ O ₃	16.3	16.03	15.48	19.01	16.71
	Fe ₂ O ₃	7.5	7.65	7.31	9.14	7.90
	SiO ₂	67.12	67.12	68.04	60.76	65.76
6	Na ₂ O	0.54	0.64	0.49	0.46	0.53
	K ₂ O	3.34	3.17	2.77	3.45	3.18
	MgO	2.53	2.24	2.27	3.94	2.75
	CaO	0.88	1.04	1.17	1.89	1.25
	Al ₂ O ₃	18.72	16.08	15.37	19.38	17.39
	Fe ₂ O ₃	9.32	7.8	8.02	7.74	8.22
	SiO ₂	63.51	67.99	68.93	61.95	65.60
7U	Na ₂ O	0.47	0.48	0.47	0.52	0.49
	K ₂ O	2.36	2.42	2.86	3.03	2.67
	MgO	1.41	1.45	2.06	2.18	1.78
	CaO	0.68	0.67	2.77	0.76	1.22
	Al ₂ O ₃	15.27	15.54	16.97	17.47	16.31
	Fe ₂ O ₃	7.8	7.39	9.89	9.18	8.57
	SiO ₂	71.13	71.15	63.98	65.84	68.03
-	Al ₂ O ₃	16.43	16.33	16.87	18.47	17.03
X	Fe ₂ O ₃	8.0	7.89	8.22	8.33	8.11
	SiO ₂	67.5	67.09	65.93	63.26	65.95

To convert to mg/litre multiply readings by 1000 and divide by the following factors
for Na - 1.35 : K - 1.21 : Mg - 1.66 : Ca - 1.4 : Al - 1.89 : Fe - 1.43 : Si - 2.14

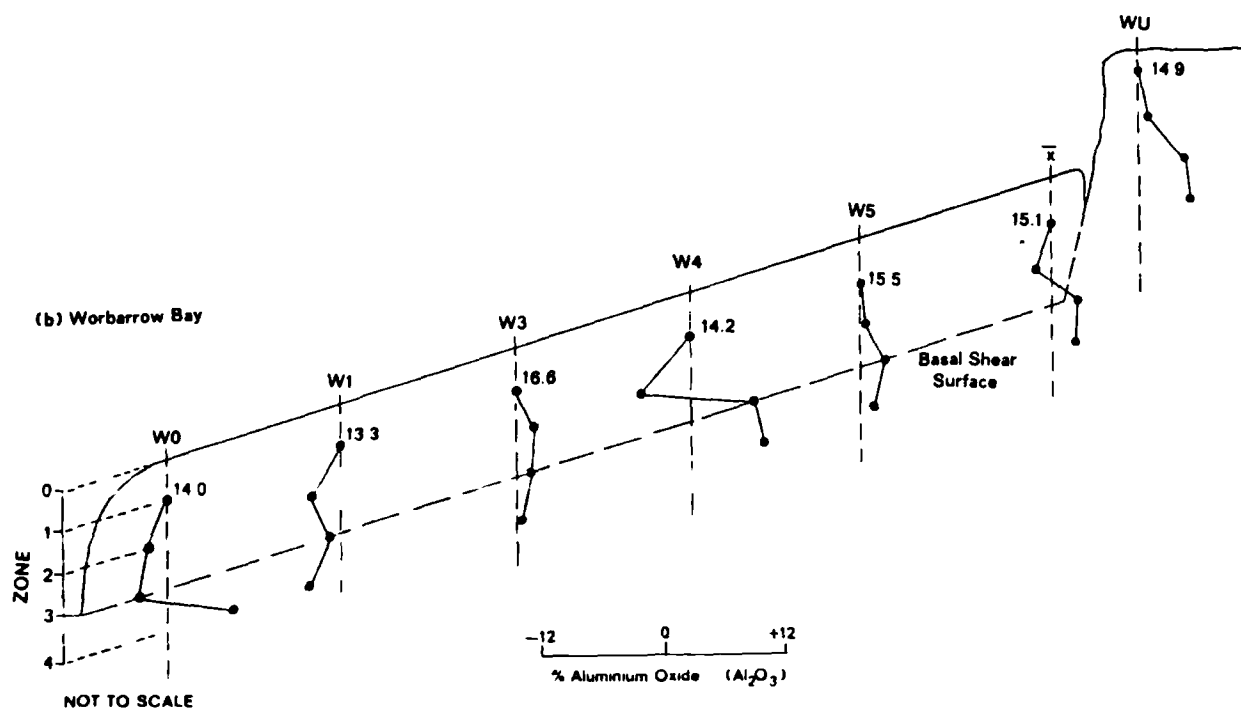
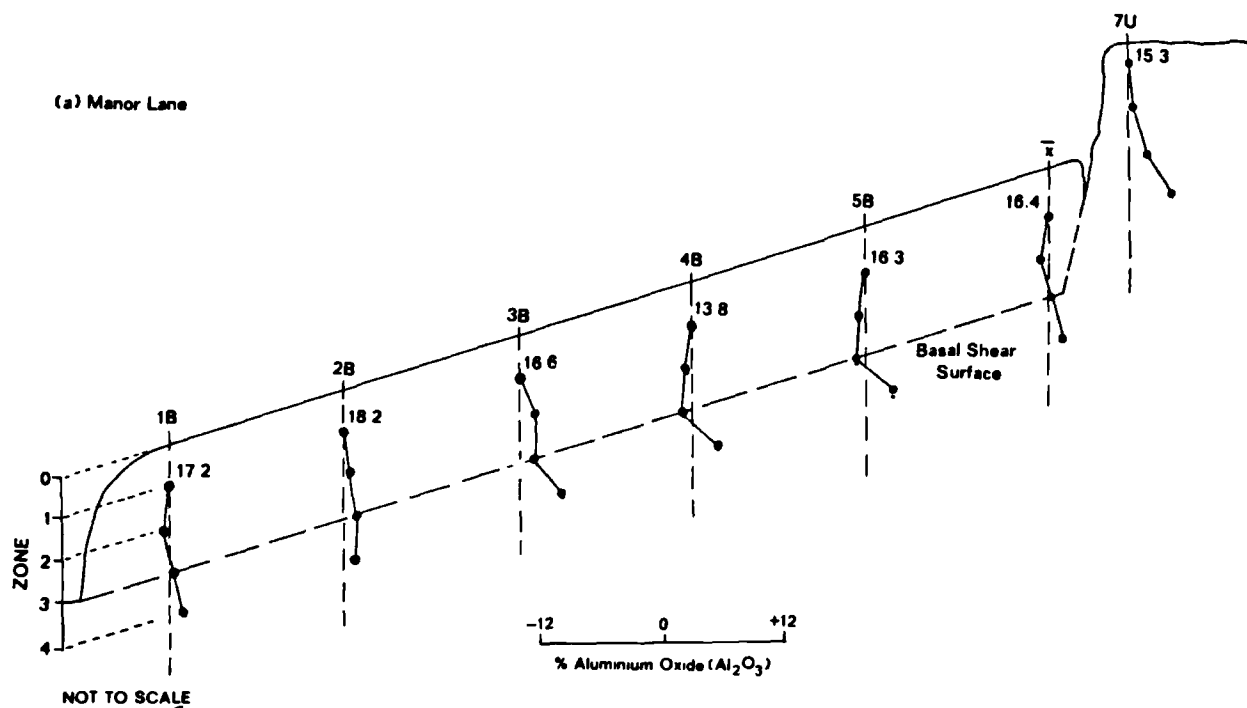
Table 4.24. Bulk chemistry of clay size material for all Worbarrow Bay cores.

CORE #	MAJORS Wt. %	ZONE ONE	ZONE TWO	ZONE THREE	ZONE FOUR	- X
W0	Na ₂ O	0.23	0.2	0.16	0.2	0.20
	K ₂ O	1.87	1.68	1.38	1.85	1.70
	MgO	0.8	0.7	0.6	0.86	0.74
	CaO	0.41	0.32	0.29	0.41	0.36
	Al ₂ O ₃	14.0	13.43	12.68	17.08	14.30
	Fe ₂ O ₃	8.15	6.39	4.55	5.53	6.16
	SiO ₂	73.62	76.43	79.58	73.09	75.68
W1	Na ₂ O	0.16	0.12	0.14	0.12	0.14
	K ₂ O	1.49	0.99	1.35	1.07	1.23
	MgO	0.61	0.4	0.57	0.47	0.52
	CaO	0.27	0.16	0.23	0.25	0.23
	Al ₂ O ₃	13.28	9.95	12.48	10.12	11.46
	Fe ₂ O ₃	3.99	2.33	3.19	1.64	2.79
	SiO ₂	79.42	85.54	81.4	85.74	83.03
W2	Na ₂ O	0.21	0.18	0.21	0.2	0.20
	K ₂ O	1.78	1.32	1.81	1.43	1.59
	MgO	0.86	0.68	0.93	0.78	0.81
	CaO	0.43	0.45	0.54	0.56	0.50
	Al ₂ O ₃	17.32	15.88	20.3	19.44	18.24
	Fe ₂ O ₃	5.07	4.69	7.47	3.38	5.15
	SiO ₂	73.31	75.84	67.59	73.08	72.46
W3	Na ₂ O	0.2	0.21	0.18	0.19	0.20
	K ₂ O	1.91	2.05	1.53	1.67	1.79
	MgO	0.83	0.96	0.79	0.86	0.86
	CaO	0.32	0.38	0.49	0.41	0.40
	Al ₂ O ₃	16.58	17.6	17.47	16.0	16.91
	Fe ₂ O ₃	4.5	4.99	3.1	6.05	4.66
	SiO ₂	74.71	72.84	75.34	73.92	74.20
W4	Na ₂ O	0.16	0.12	0.22	0.2	0.18
	K ₂ O	1.74	0.88	1.88	1.9	1.60
	MgO	0.8	0.38	1.02	1.02	0.81
	CaO	0.29	0.18	0.52	0.56	0.39
	Al ₂ O ₃	14.16	9.10	19.83	19.91	15.75
	Fe ₂ O ₃	3.35	3.19	5.58	4.14	4.07
	SiO ₂	78.71	85.64	69.97	71.24	76.39
W5	Na ₂ O	0.18	0.18	0.2	0.17	0.18
	K ₂ O	1.09	1.08	1.24	1.13	1.14
	MgO	0.63	0.62	0.7	0.61	0.64
	CaO	0.36	0.4	0.47	0.49	0.43
	Al ₂ O ₃	15.46	15.61	17.84	16.41	16.33
	Fe ₂ O ₃	3.94	4.23	4.32	3.92	4.10
	SiO ₂	77.46	76.88	74.31	76.35	76.25
WU	Na ₂ O	0.56	0.64	0.48	0.47	0.54
	K ₂ O	2.28	2.98	2.43	2.75	2.61
	MgO	1.04	2.0	1.66	1.94	1.66
	CaO	0.65	0.79	0.85	0.84	0.78
	Al ₂ O ₃	14.85	15.53	19.6	19.73	17.43
	Fe ₂ O ₃	5.73	6.46	6.33	6.21	6.18
	SiO ₂	73.84	70.59	67.59	68.06	70.02
- X	Al ₂ O ₃	15.09	13.87	17.17	16.96	15.77
	Fe ₂ O ₃	4.96	4.61	4.93	4.41	4.73
	SiO ₂	75.87	77.68	73.73	74.5	75.45

=====

To convert to mg/litre multiply readings by 1000 and divide by the following factors
for Na - 1.35 : K - 1.21 : Mg - 1.66 : Ca - 1.4 : Al - 1.89 : Fe - 1.43 : Si - 2.14

Figure 4.40. Crystal lattice aluminium profiles for selected samples.



3. in Figure 4.41 the distribution of aluminium oxide is plotted with respect to the mudslide sections. Both plots show relatively constant proportions of aluminium ($\approx 16\%$) increasing slightly in the feeder track. At Worbarrow there was more aluminium oxide in the source and feeder track (18.24%) in comparison with the undisturbed sample (17.43%), decreasing 7% from slope unit 2 towards the lobe. The proportion of aluminium at the shear surface of weathered profiles was greater (upto 4.1% in unit 4) than the core means. This feature was not apparent at Manor Lane, but would suggest considerable leaching and removal of aluminium from the weathered zone.
4. the per cent iron oxide in the crystal lattice clays for all weathered profiles showed a slight increase of 1% towards sub-zone 4 at Manor Lane, and 2% at the basal shear surface at Worbarrow, in comparison with the mean (8.1% and 4.7% , respectively). The variability was greater at Worbarrow probably due to the influence of secondary inputs from the perched mudslides. No clear associations within the weathered profiles could be seen. With respect to the mudslide sections (Figure 4.42) both sites showed an apparent reduction in the proportion of iron oxide upon erosion and weathering particularly at the shear surface, followed by an increase downslope to the base of the feeder track. Both sites showed slight reductions (1% at Manor Lane; 2% at Worbarrow) between slope units 1 and 2, although at Worbarrow there was a further increase of 3.4% iron oxide at the toe of the lobe.
5. the mean per cent silicon dioxide at Manor Lane reduced from 68% to 66% upon weathering in relation to the undisturbed profile. There was also a slight reduction with depth from 67.5% to 63.3% . In contrast the results for the weathered profiles at Worbarrow showed a gradual increase in the proportion of silica following erosion, from 70% to 75.5% , but an overall reduction with depth in the mean profile from 75.9% to 73.7% .
6. with respect to the mudslide sections in Figure 4.43, the distribution of silica at the basal shear surface at Manor Lane showed a peak 72% silica (unit 4) consequent upon weathering in

Figure 4.41. Distribution of aluminium oxide at the shear surface.

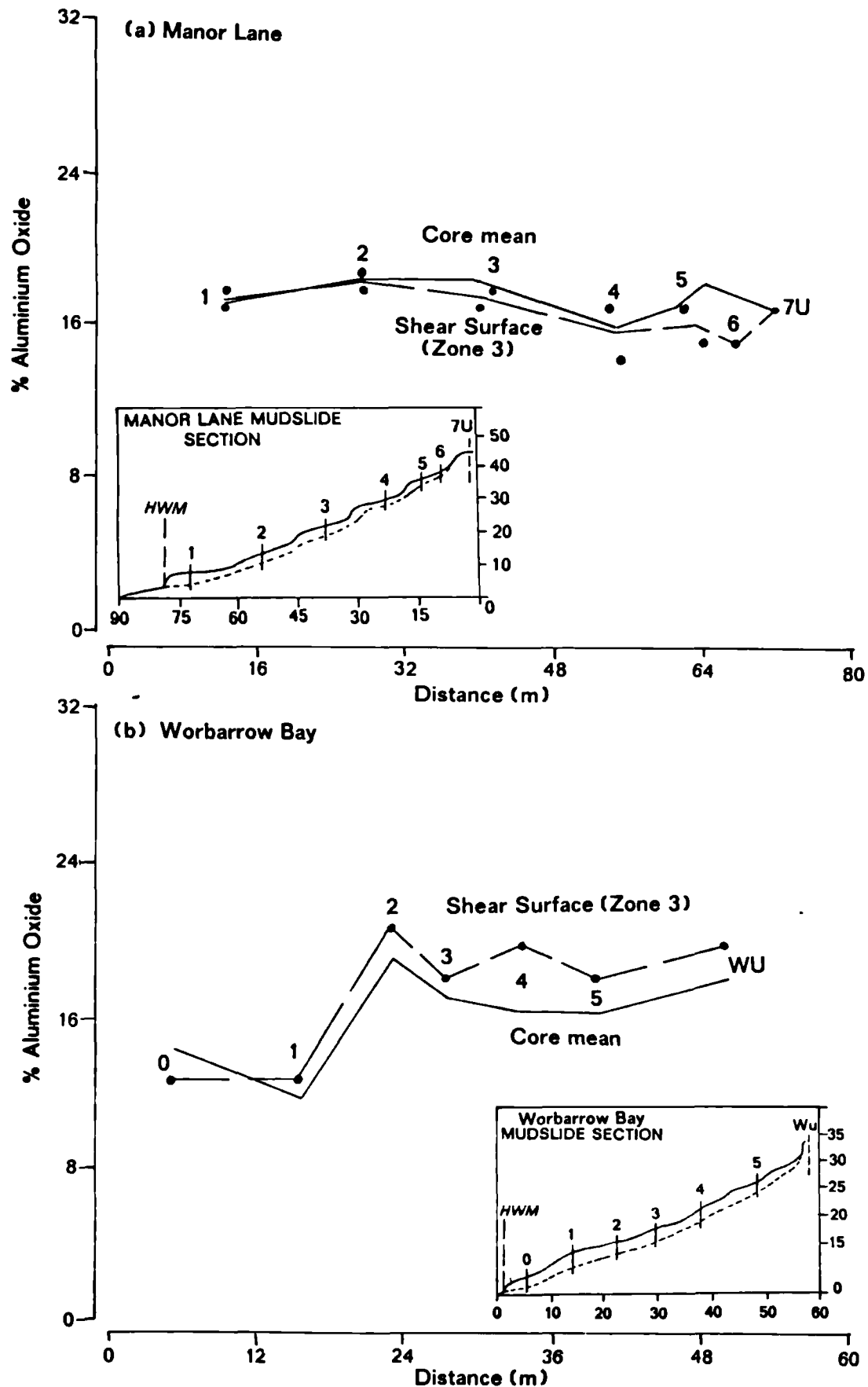


Figure 4.42. Distribution of crystal lattice iron at the shear surface.

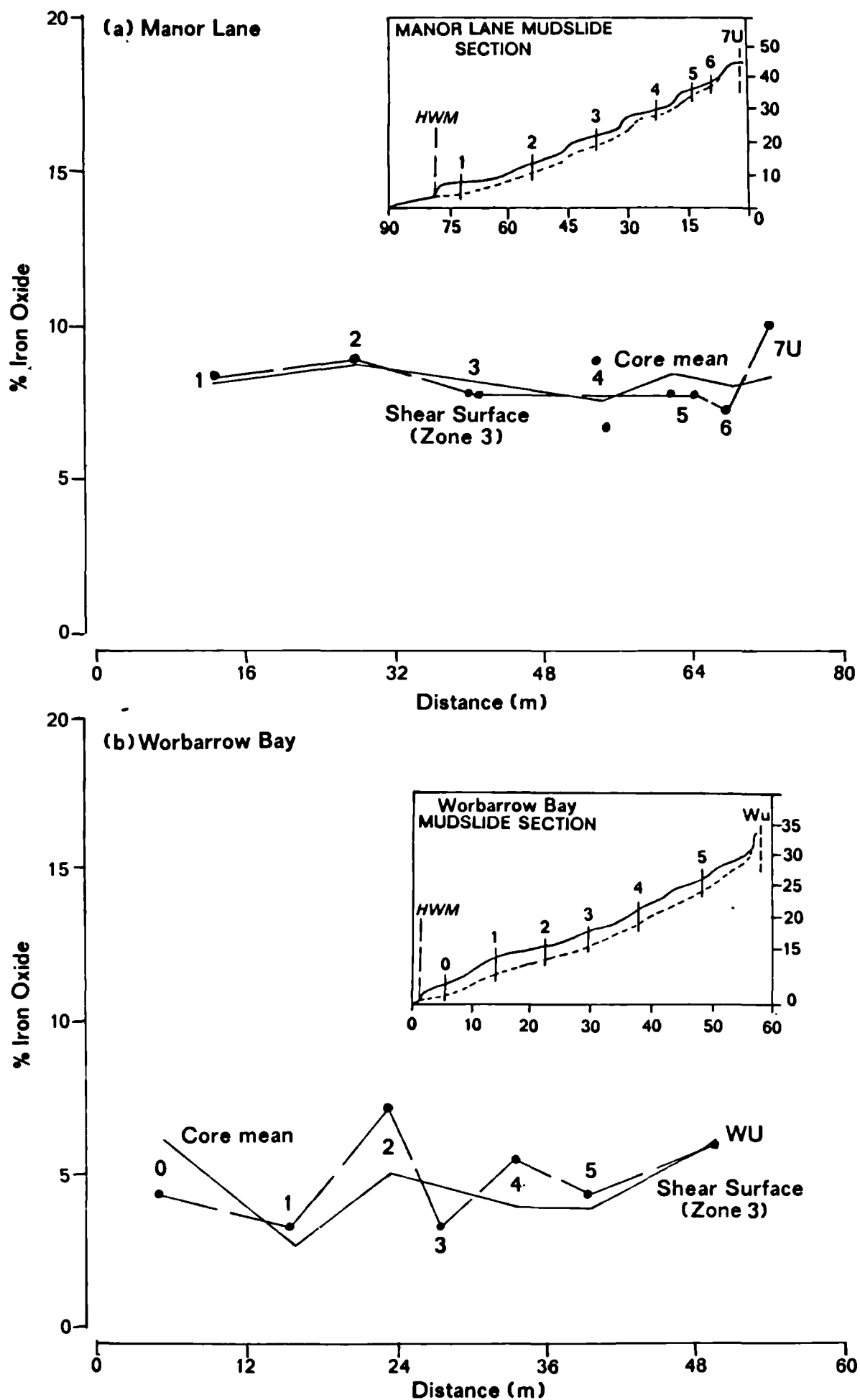
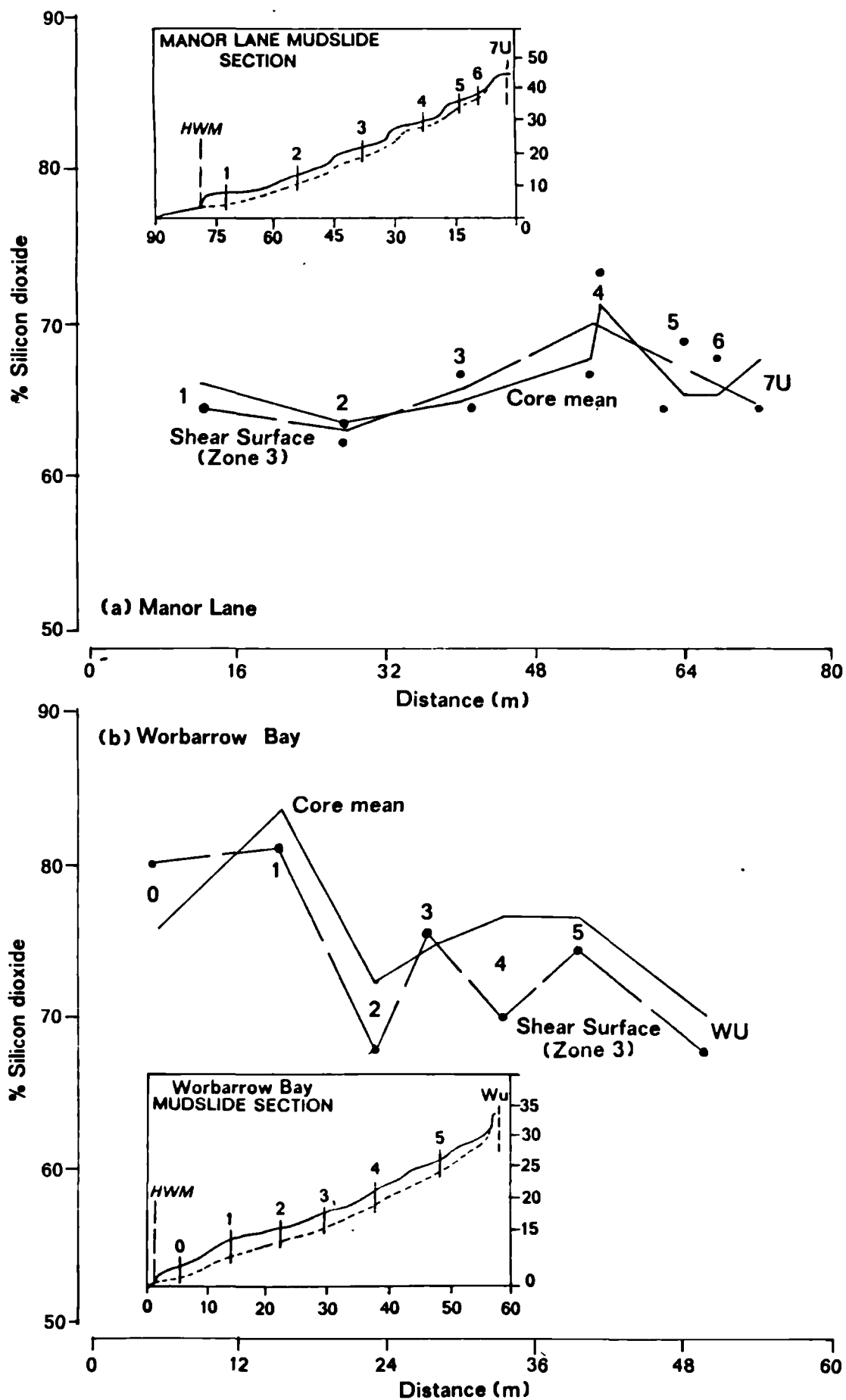


Figure 4.43. Distribution of lattice silica at the basal shear surface.



the source, followed by a reduction to 63% downslope. The plot for Worbarrow shows a similar increase in the source from 70% to 76.3%, but a further increase downslope to 83% (unit 1) in contrast to Manor Lane. Both plots were inversely related to the distribution of aluminium with respect to weathering and the morphology of the slope section.

4.45 Anisotropic particle and solute chemistry.

The importance of micromorphology in studies of slope instability was introduced in section 2.21, where it was considered that the orientation of fabric and particles and the movement and deposition of amorphous oxides along discontinuities was an area poorly understood with respect to shear strength behaviour (section 2.21) and thus requires detailed study. To meet these requirements observations and analytical measurements were undertaken for samples from above (sub-zone 2) and below (sub-zone 4) the basal shear surface using an Hitachi S-450 Scanning Electron Microscope with a Links Systems 860 computer and micro-probe facility.

Air-dried samples were analysed following the methods of preparation outlined in Appendix 7B. Since intact samples were specially set aside for this analysis the disturbance encountered during sample splitting and pre-treatment were kept to a minimum. For each sample there were three stages of analysis:

1. a general observation of the sample, noting the presence of major discontinuities, any preferential orientation and areas of oxide deposition. Photographs were taken of surface and fissure detail and close images of individual mineral grains.

Plate 14.

Platy and wave-like form of mixed clays.

- (a) 33393 Manor Lane core sub-sample 7A₄.
- (b) 33395 Manor Lane core sub-sample 7A₄.
- (c) 00292 Manor Lane core sub-sample 4A₂.
- (d) 41358 Worbarrow Bay core sub-sample W3₂.

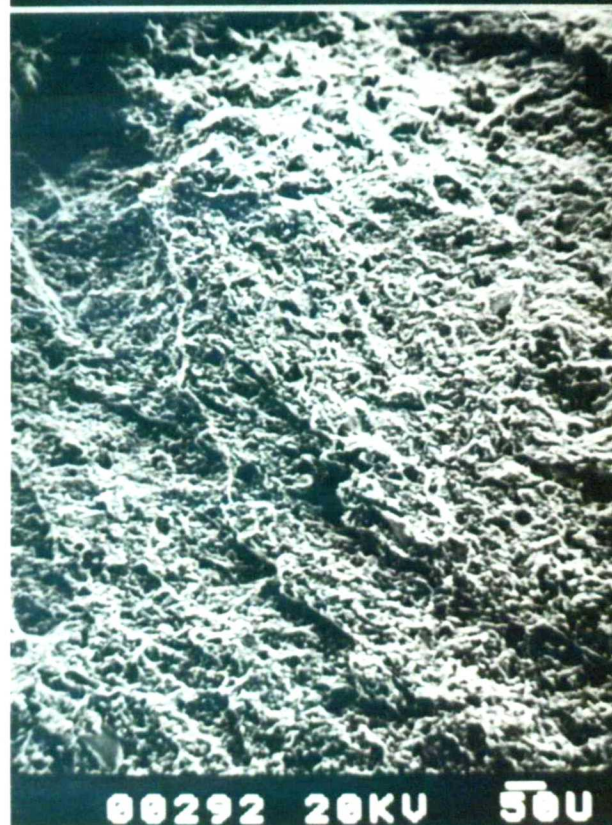
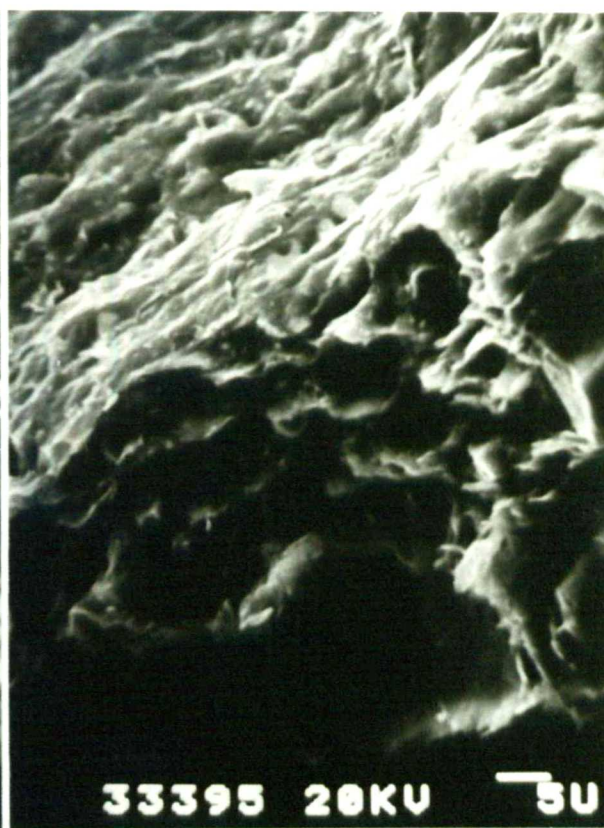
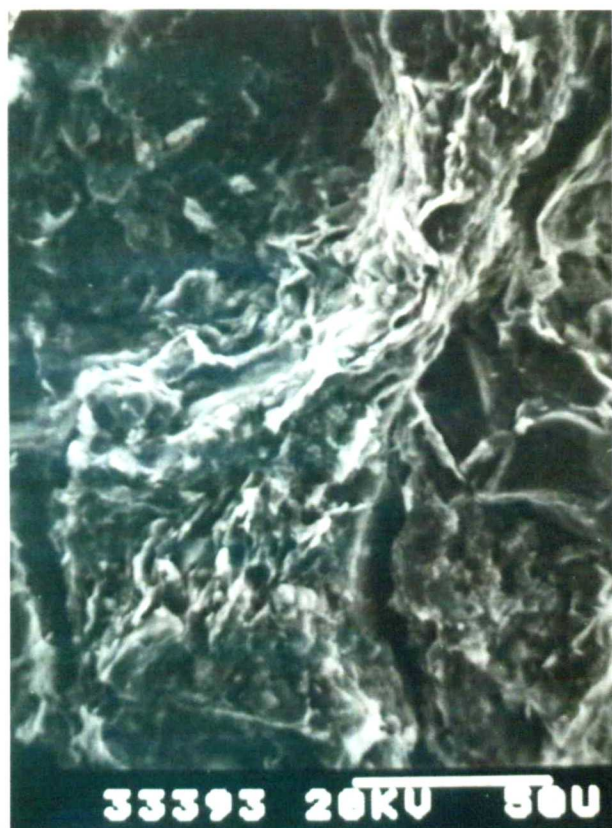
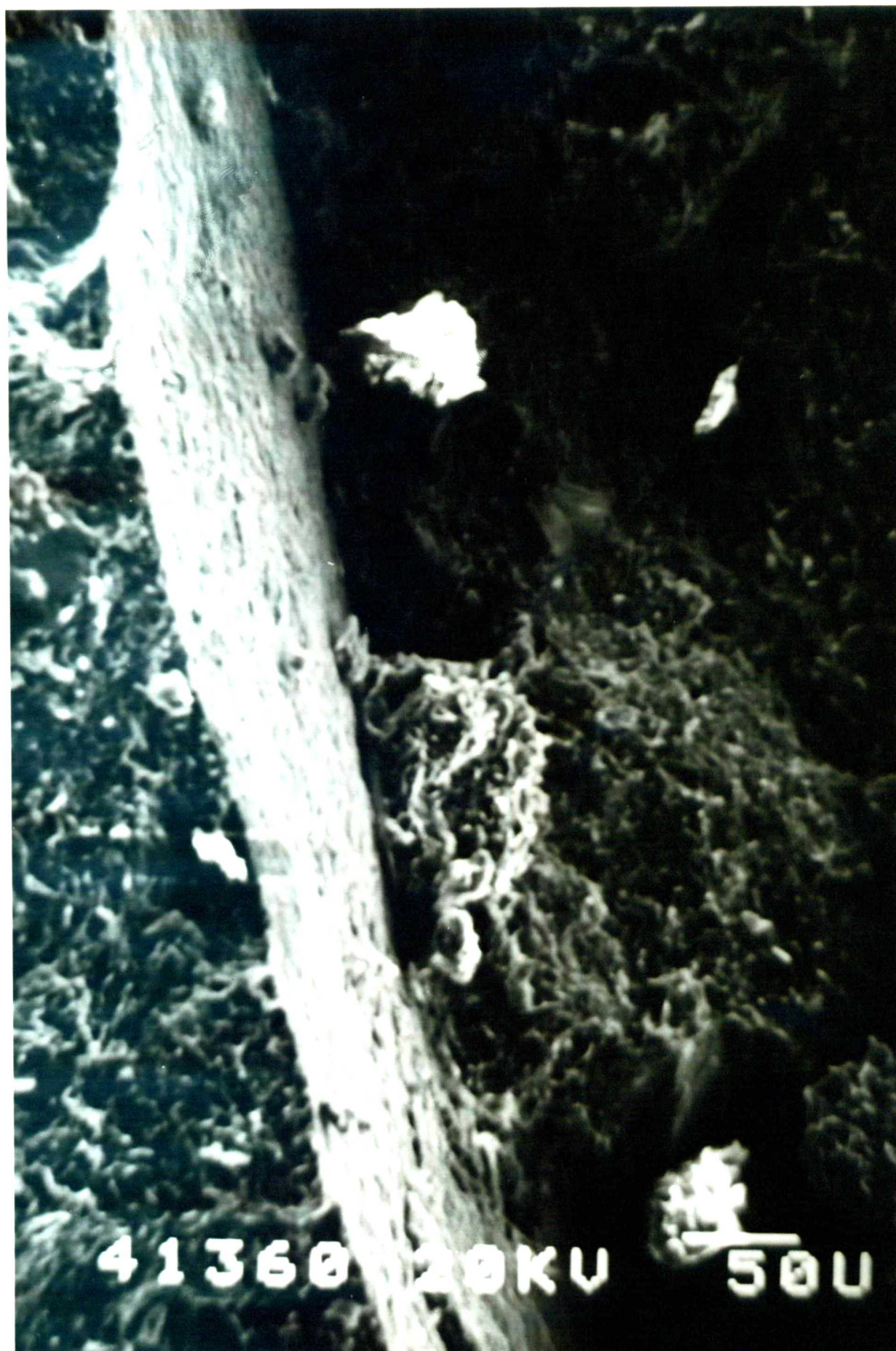


Plate 15.

**SEM print illustrating the nature of fissures and slickensides
and the preferential orientation of clays.**

(a) Manor Lane core sub-sample 5A₃.



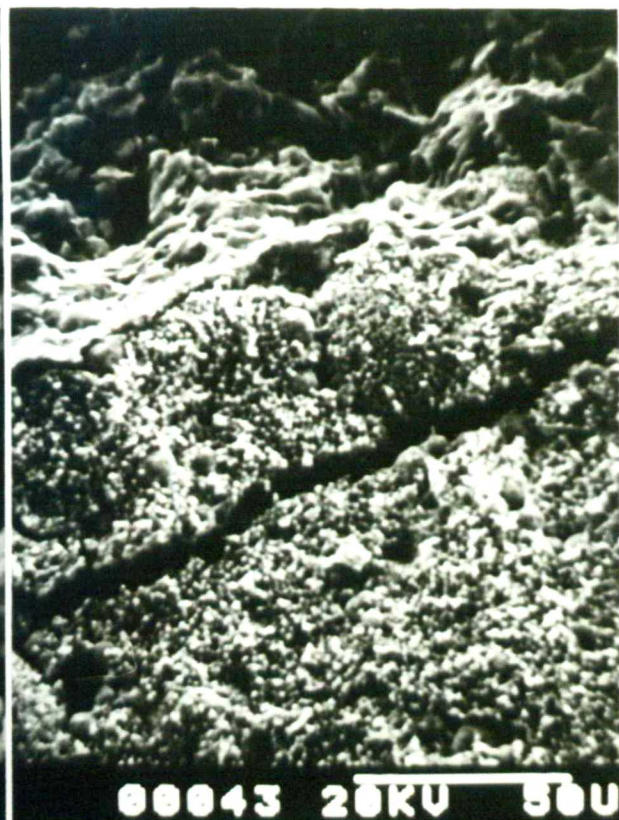
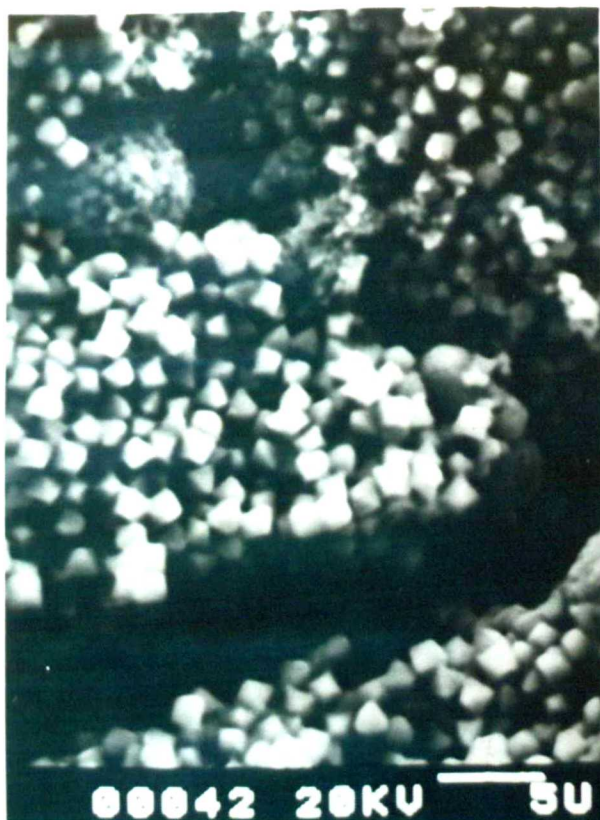
41360 20KV

50U

Plate 16.

SEM prints showing the anisotropic deposition of iron.

- (a) 00042 Worbarrow Bay core sub-sample W5₄.
- (b) 00043 Worbarrow Bay core sub-sample W5₄.
- (c) 00293 Manor Lane core sub-sample 6A₄.
- (d) 00296 Manor Lane core sub-sample 6A₄.



2. The chemistry of the sample surface was measured analytically by the micro-probe. Since small variations in chemistry would be expected an average of three analyses were taken from different fields of view at a magnification of 140K.
3. Where fissures were present a microprobe point analysis was taken at a magnification of 550K for comparison with the surface analyses. All photographs and analyses were catalogued on data-sheets.

The photographs obtained from the SEM highlighted a number of characteristics of the sediments present in each mudslide:

1. the sediments observed at Manor Lane and Worbarrow Bay were comprised of predominantly silt and clay-size particles and were practically identical in nature.
2. the presence of clay was recognised in platy and wave-like forms. The clay-matrix consisted of mixed minerals of various sizes, shapes and forms (Plate 14 and d in Plate 16).
3. the plate-like particles were often stacked together typical of an open 'house of cards' type structure (b in Plate 14).
4. within both sub-zones of each mudslide the arrangement of particles showed a high degree of preferred orientation along slickensided and fissured surfaces (d in Plate 16 and Plate 15).
5. in sub-zones 3 and 4, particularly below the basal shear surface, fissures were often clearly defined and planar (Plate 15).
6. amorphous oxides, particularly of iron, were found deposited along fissures and slickensided surfaces at both sites above and below the shear surface (a-c in Plate 16).
7. amorphous deposits were also noted on the surfaces of particles for *in situ* clay material below the basal shear surface (c in Plate 16).

Table 4.25a. Anisotropic surface and fissure chemistry for Manor Lane core samples 1A - 4A.

CORE #	ZONE n=3	Si	Al	Fe	Mg	Ca	K	S
% oxide								
1A	3 S	56.09	19.29	13.98	3.36	0.98	3.52	0.8
	F	51.8	18.33	19.91	3.18	0.6	2.31	0.27
	4 S	54.35	19.79	9.99	3.91	2.73	3.05	4.14
	F	57.12	25.85	7.4	4.67	0.46	3.1	0.22
1B	3 S	60.35	20.12	9.44	3.7	1.05	3.57	0.37
	F	57.72	23.81	8.46	4.22	0.64	3.25	0.53
	4 S	61.01	20.9	7.66	4.17	0.72	3.27	0.55
	F	65.09	22.05	5.87	3.77	0.31	1.91	0.36
2A	3 S	57.98	20.93	10.1	3.9	0.98	3.59	0.69
	F	56.14	25.9	7.69	5.06	0.42	3.43	0.34
	4 S	54.91	20.70	13.18	3.92	0.97	3.85	0.36
	F	16.56	7.21	63.23	1.37	0.86	4.7	0.06
2B	3 S	60.36	21.76	8.13	3.94	0.52	3.42	0.24
	F	56.43	27.22	7.04	4.88	0.38	2.79	0.24
	4 S	65.75	23.17	6.05	1.25	0.4	1.55	0.11
	F	61.69	28.91	2.8	1.33	0.44	1.71	0.06
3A	3 S	56.01	19.74	11.73	3.48	1.2	3.61	2.74
	F	27.37	14.03	49.91	3.6	0.29	1.96	0.4
	4 S	57.73	20.33	10.23	3.67	1.23	3.47	1.5
	F	32.8	21.0	34.3	1.4	0.8	0.6	8.9
3B	3 S	70.26	21.3	3.45	1.17	0.43	1.52	0.11
	F	58.46	27.5	4.93	1.45	0.62	2.91	0.19
	4 S	58.53	21.59	9.19	3.90	0.87	3.51	0.23
	F	39.28	12.08	31.55	1.33	1.3	6.77	0.31
4A	3 S	61.53	19.32	10.15	2.83	0.68	3.41	0.24
	F	15.84	6.63	66.86	0.38	1.49	6.12	0.36
	4 S	55.49	20.42	12.45	3.67	1.56	4.03	0.54
	F	85.42	8.73	2.35	1.76	0.17	0.9	0.14

S : % major oxides of sample surface area

F : % major oxides along fissures

Continued in Table 4.25b

Table 4.25b. Anisotropic surface and fissure chemistry for Manor Lane core samples 4B-7U.

CORE #	ZONE	n=3	Si	Al	Fe	Mg	Ca	K	S
% oxide									
4B	3	S	51.03	25.95	8.17	4.18	1.15	3.78	2.05
		F	50.79	28.90	4.08	3.0	0.43	2.09	0.24
	4	S	43.63	17.3	7.37	3.33	9.13	2.83	14.9
		F	54.8	27.4	6.5	3.4	1.0	4.7	1.4
5A	3	S	64.58	24.56	5.03	1.44	0.37	2.29	0.07
		F	64.97	27.44	2.35	1.57	0.32	1.92	0.07
	4	S	60.07	22.08	7.51	3.68	1.05	3.77	0.2
		F	64.45	18.91	7.03	3.97	0.73	3.0	0.17
5B	3	S	60.59	20.2	8.7	4.03	0.92	3.4	0.64
		F	63.90	22.91	6.19	3.52	0.17	2.01	0.14
	4	S	59.86	16.41	6.1	3.84	1.52	3.63	1.5
		F	54.9	17.52	5.24	3.05	5.19	4.62	0.54
6	3	S	57.8	20.93	10.33	3.1	1.83	3.03	1.7
		F	52.1	21.3	10.0	3.1	3.8	5.0	1.4
	4	S	48.6	18.47	7.77	3.77	6.9	2.9	10.17*
		F	52.0	22.2	5.9	4.6	3.7	3.2	7.0
7U	3	S	58.17	20.67	12.71	2.87	0.72	3.29	0.29
		F	57.11	24.03	8.31	3.67	0.83	3.92	0.05
	4	S	61.41	19.34	9.97	3.0	0.81	3.27	0.14
		F	46.56	19.07	19.18	5.08	1.27	3.09	0.01
X	3	S	59.56	21.23	9.33	3.17	0.90	3.20	0.83
		F	51.05	22.33	16.31	3.14	0.83	3.14	0.35
	4	S	56.78	20.04	8.96	3.51	2.32	3.26	2.86
		F	52.56	19.24	15.95	2.98	1.35	3.19	1.60

S : % major oxides of surface area

F : % major oxides along fissures

Table 4.26. *Anisotropic surface and fissure chemistry at Worbarrow Bay.*

CORE #	ZONE n=3	Si	Al	Fe	Mg	Ca	K	S
% oxide								
W0	3 S	56.56	20.08	12.31	3.57	1.35	3.41	0.46
	F	55.62	24.87	9.56	3.46	0.99	4.29	0.17
	4 S	57.64	19.64	9.13	4.07	1.71	3.45	2.28
	F	55.58	30.29	3.93	2.63	2.1	4.64	0.18
W1	3 S	69.48	21.19	4.34	1.18	0.17	2.3	0.04
	F	77.56	16.85	2.15	0.64	0.15	1.64	0.1
	4 S	72.86	19.31	3.08	0.99	0.3	2.09	0.14
	F	No fissures						
W2	3 S	68.12	21.35	5.55	0.89	0.47	2.01	0
	F	60.73	31.7	2.41	1.51	0.36	1.93	0.11
	5 S	70.11	22.87	2.28	1.2	0.36	1.75	0.09
	F	84.72	10.53	2.54	0.15	0.15	1.51	0.15
W3	3 S	71.82	18.54	2.37	1.47	0.42	1.82	0.44
	F	60.16	29.24	2.84	1.34	0.38	2.16	0
	4 S	67.44	21.83	4.88	1.35	0.3	2.29	0.1
	F	56.73	30.98	5.14	1.89	0.35	2.98	0.05
W4	3 S	65.85	23.38	4.37	1.10	0.61	2.74	0.18
	F	81.04	14.73	1.2	1.01	0.13	1.04	0.1
	4 S	57.44	20.53	10.7	3.91	0.95	3.75	0.6
	F	61.23	25.94	4.2	4.03	0.26	3.19	0.17
W5	3 S	56.56	20.08	12.31	3.57	1.35	3.41	0.46
	F	55.62	24.87	9.56	3.46	0.99	4.29	0.17
	4 S	57.64	19.64	9.13	4.07	1.71	3.45	2.28
	F	55.58	30.29	3.93	2.63	2.1	4.64	0.18
WU	3 S	59.7	20.72	13.77	4.07	1.68	3.98	0.53
	F	57.68	22.9	6.71	3.45	2.34	4.21	0.25
	4 S	52.2	23.1	17.6	5.93	.59	3.96	0.2
	F	47.4	29.86	18.1	3.89	1.88	4.39	0.15
X	3 S	64.01	20.76	7.86	2.26	0.86	2.81	0.30
	F	64.06	23.59	4.92	2.12	0.76	2.79	0.11
	4 S	62.19	20.99	8.11	3.07	0.85	2.96	0.81
	F	60.21	26.32	6.31	2.54	1.14	3.56	0.15

S : % major oxides of surface area

F : % major oxides along fissures

The results of quantitative analyses of mineral surface and fissure chemistry are presented in Tables 4.25 and 4.26 for Manor Lane and Worbarrow respectively. The following associations with slope morphology were recognised:

1. silica: at Manor Lane the mean per cent silicon dioxide on weathered clay surfaces above the basal shear plane was 59.6% in comparison with 64.0% at Worbarrow. Corresponding values for the proportion of silica along fissures above the shear surface were 51.1% and 64.0%. At Manor Lane this suggested a loss 8.5% silica along fissures above the basal shear surfaces. There was no apparent leaching of silica from similar fissures at Worbarrow. For *in situ* material beneath the basal shear surface the mean proportion of silica on the surface of clays was 56.8% at Manor Lane and 62.2% at Worbarrow in comparison with 52.6% and 60.2% along fissures. Thus, there was generally less silica on unweathered clay surfaces below the shear plane. The results also show a greater proportion of silica along *in situ* fissures, in contrast to a reduction at Worbarrow, when compared with weathered materials. These results demonstrate significant redistributions of solutes within the mudslide matrix when compared with *in situ* clay.
2. when plotted with respect to the mudslide sections Figure 4.44, the deposition of silica on the surface of clays at Manor Lane showed a more uniform association than found along fissures above and below the shear zone. The plot for Manor Lane indicates an increase in silica above the shear surface from 59% to 62% in the source unit upon weathering, a depletion in unit 4 to 55%, rising to 68 % towards the toe of the mudslide. Deposition along fissures was variable within the section particularly for *in situ* clay, increasing 34% in the source area. This might suggest that the weathering residues of silica are leached from above the shear surface to the clay below. The distribution plotted for Worbarrow showed a similar increase in silica from approximately 55 % to 70%.

Figure 4.44. Anisotropic silica deposition across the shear surface.

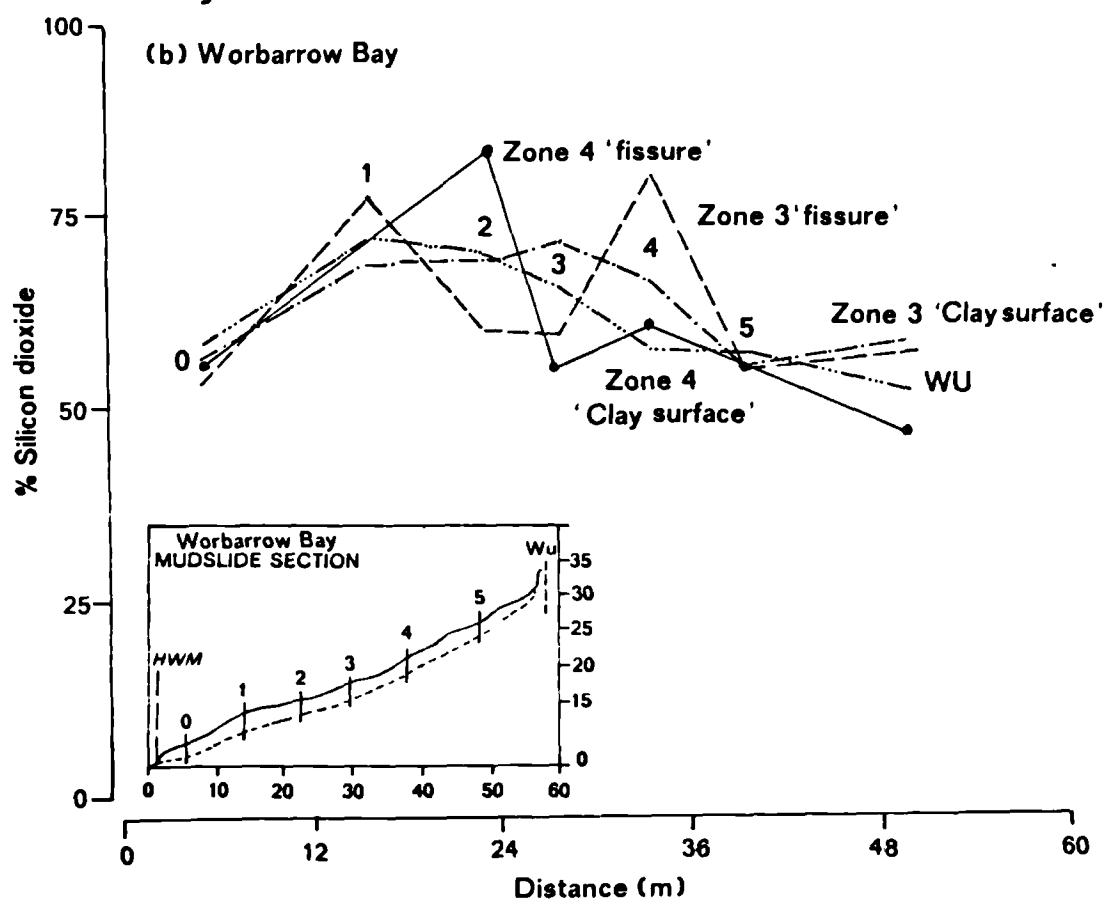
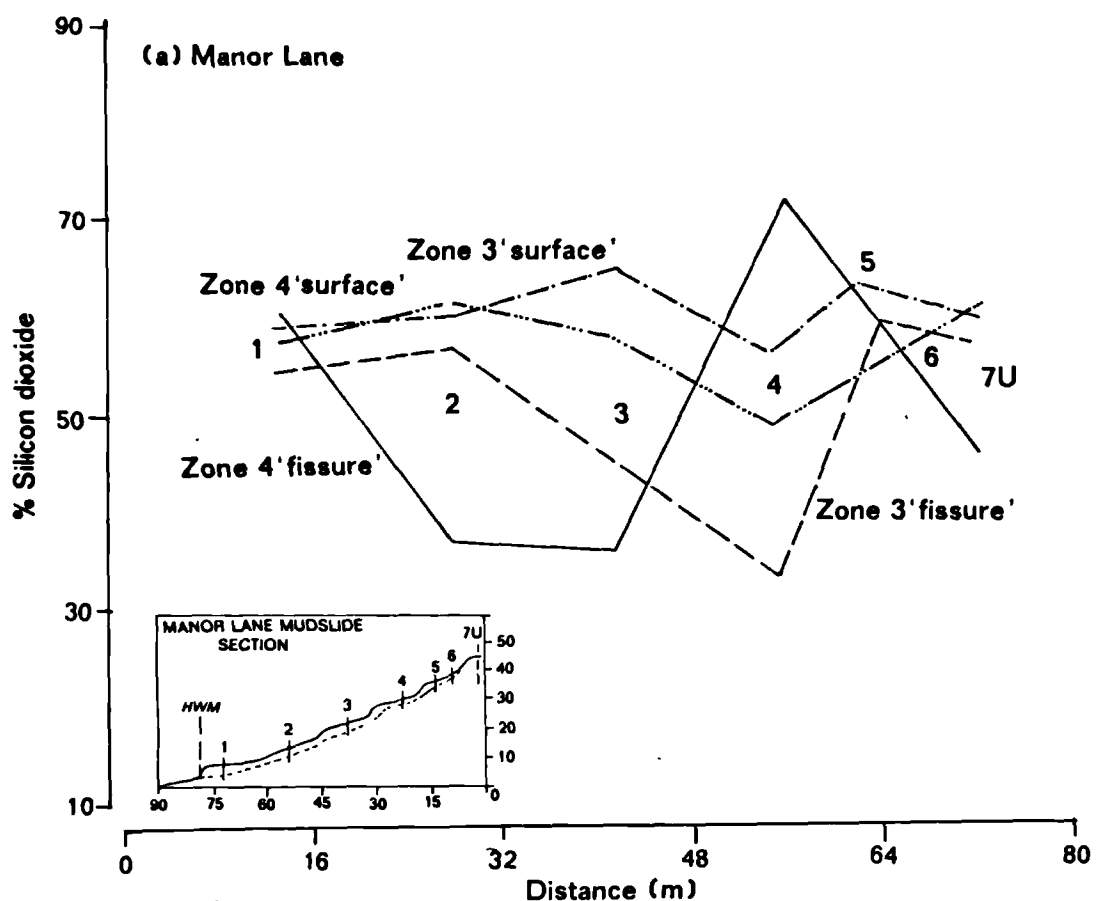
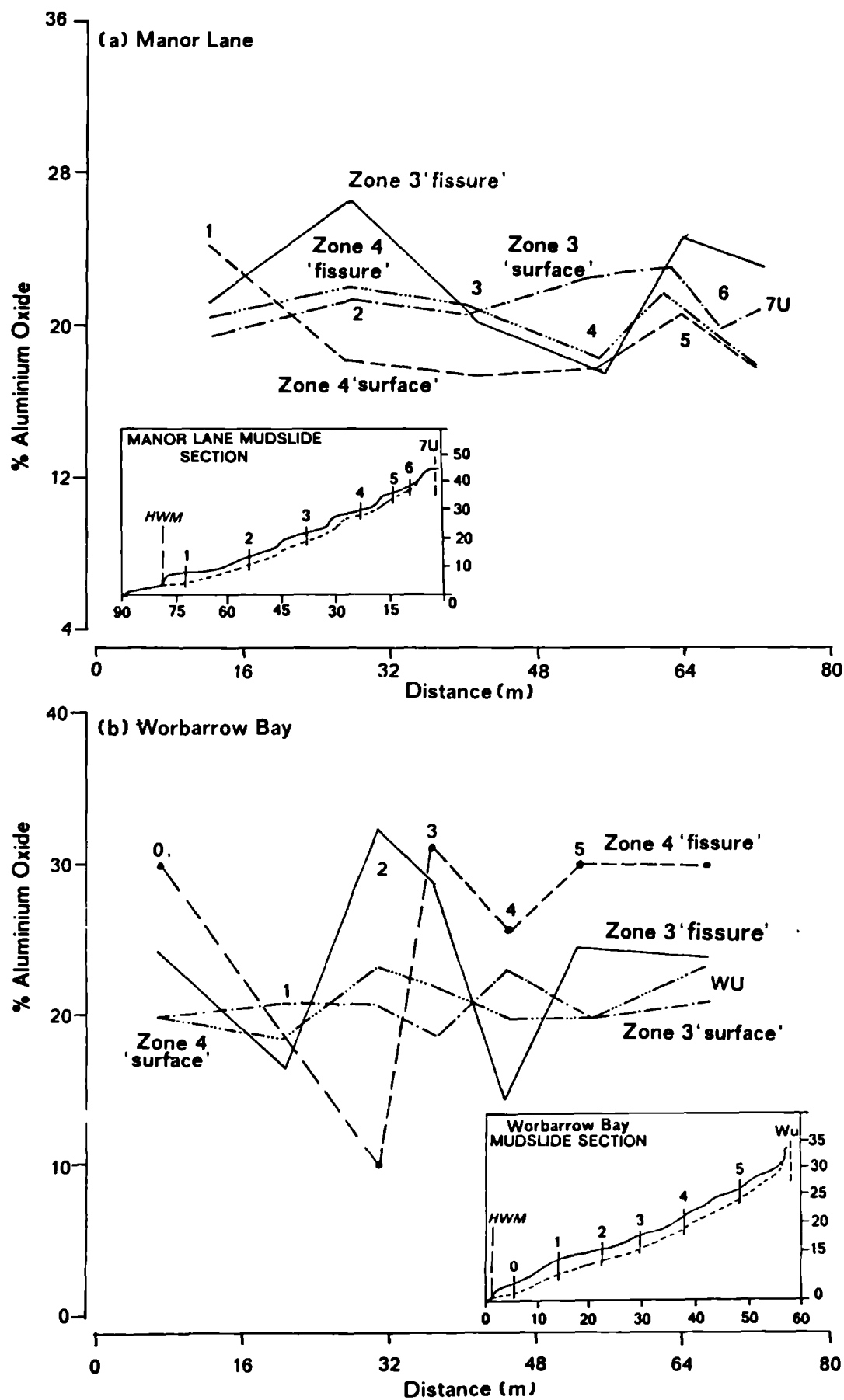
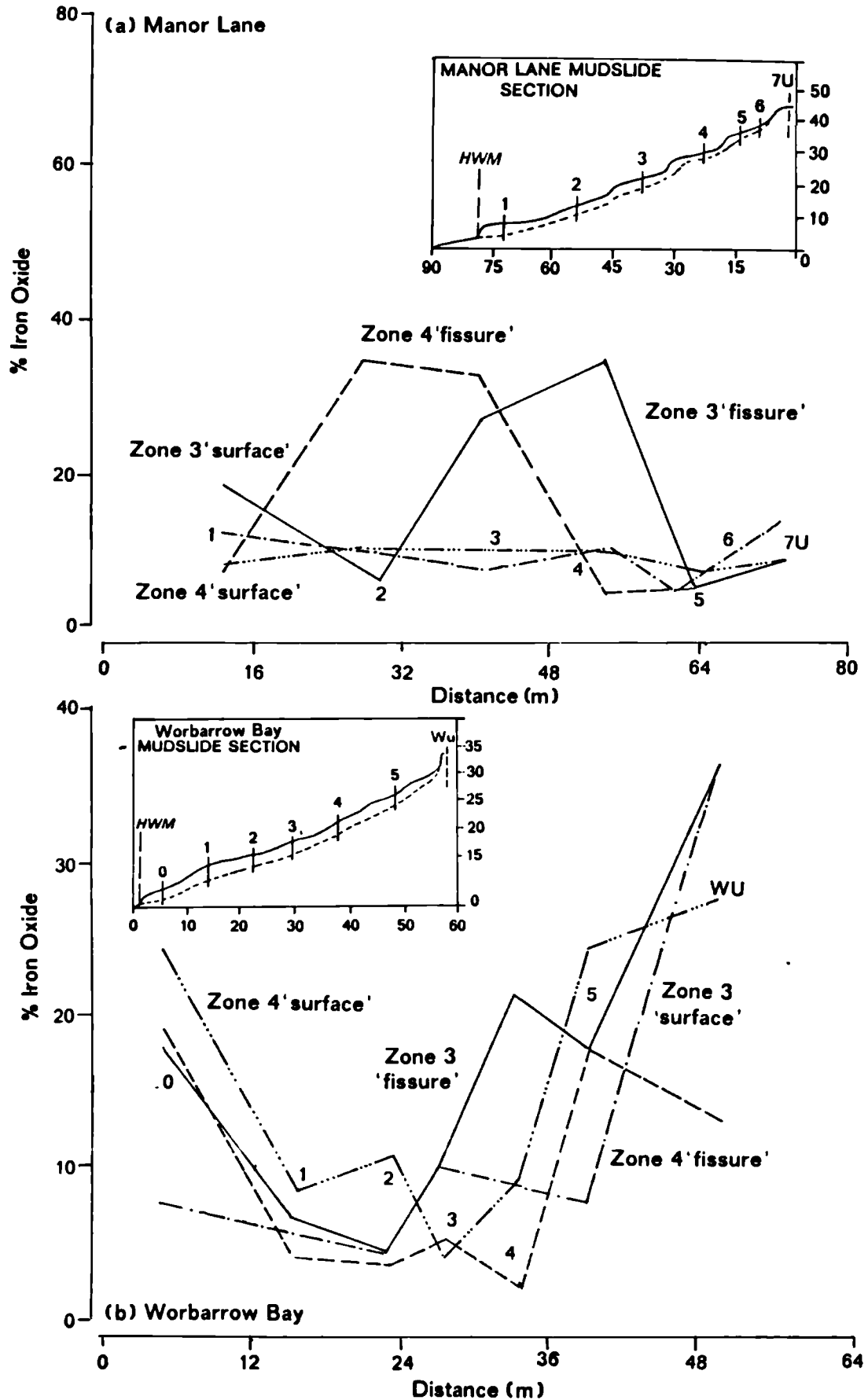


Figure 4.45. Anisotropic aluminium deposition across the shear surface.



3. aluminium: at Manor Lane the percentage aluminium oxide present on clay surfaces above the basal shear plane was 21.2% in comparison with 22.3% along fissures, although below the shear surface (sub-zone 4) the corresponding values were 20.0% and 19.2%. The variation was quite small but did indicate the deposition of aluminium along fissures in the weathered zone above the shear surface, lower proportions below the shear surface and generally less aluminium along fissures in comparison with the surface of clays. In contrast, there was a greater proportion of aluminium deposited along fissures at Worbarrow Bay, especially below the shear surface. Approximately 21.0% aluminium oxide coated the surface of the clays above and below the shear zone with 24% along fissures in the weathered zone and 26.3% along *in situ* fissures. This suggested that aluminium was leached from the weathered zone similar to silica.
4. Figure 4.45 plots the distribution of aluminium with respect to the mudslide sections. As for silica there was a relatively uniform distribution of aluminium upon clay surfaces above and below the shear surface at both sites. In contrast, the deposition along fissures was highly variable, although at Worbarrow there was a greater proportion of aluminium oxide along fissures above and below the shear surface, suggesting a high degree of mobility and redistribution within the weathered profile. This feature was particularly prevalent in the source and upper slope units of the mudslide (Figure 4.45b). The distribution was broken at the base of the feeder track (unit 2), probably as a consequence of the input of material from the perched mudslides. The distribution also showed a high degree of association between the fissures and clay surfaces such that an increase in aluminium oxide along fissures typically corresponded with a depletion on clay surfaces.
5. iron: the preferential deposition of iron along fissures was clearly illustrated at Manor Lane. From the mean results in Table 4.25b there was little differentiation between the weathered and undisturbed states since 9.0% iron oxide was found deposited upon the surface of the clays above and below the shear plane whereas

Figure 4.46. Anisotropic iron deposition across the shear surface.



16.0% was found along the fissures. Worbarrow was an exception to this trend, the mean showing a difference between the clay surfaces and fissures of 2.9% above and 1.8% below the shear surface, amounting to an overall loss of iron along fissures. The presence of iron was thus more concentrated at Manor Lane than Worbarrow.

6. with reference to the mudslide sections Figure 4.46b, there was a loss of iron from a maximum 18% to 3% upon weathering and movement down the Worbarrow mudslide, but an increase to 9% at the toe of the slope. The corresponding plot for Manor Lane (Figure 4.46a) showed that the proportion of iron upon the surface of clays was fairly uniform. Along the fissures however, in zones 2, 3 and 4 both above and below the shear surface, there was a marked increase in the deposition of iron oxide from approximately 9% to a maximum of 66.9%. Although the mean isolated this difference it was clear that in reality the preferential solution and deposition of amorphous iron can vary by as much as 700%.

4.46 Semi-quantitative analysis of the clay minerals.

In the conclusions of Chapter Two, it was noted that the clay mineralogy and proportion of clay-size particles were fundamental to soil behaviour, and should therefore be an important property influencing the stability of slopes. Research objectives were designed to assess the variability of clay mineralogy within and between individual mudslides in addition to a regional analysis of the distribution of landslides and clay minerals. Thus this section presents the results of clay mineral analyses for the two field sites, while in section 4.6 the findings of the regional study are discussed.

To meet the requirements of the 'field-site' objectives (section 2.5), semi-quantitative analyses of the clay minerals were undertaken using the methods outlined in Appendix 7. The adoption of these methods enabled a large throughput of samples for mineral identification using X-ray diffraction techniques. Additional quantitative data were used to supplement the diffraction results during the calculation of the proportion of the various types of mineral species. These included the bulk chemistry of the clay material, the CEC, and the loss-on-ignition results.

It is well known that clay mineral analysis is fraught with errors and that truly accurate estimations of mineral species requires a wide variety of chemical and observational tests and considerable investment of time. Quantitative determinations of clay mineral species are normally based on detailed knowledge of the chemistry and physico-chemical properties of soils. The approach used in this study was considered semi-quantitative but of a higher order of accuracy than usual following the incorporation of the chemical and loss-on-ignition results. The calculation of the proportion of clay mineral species within each core sample followed a series of stages:

1. X-ray diffraction traces were studied to identify the type and range of clay minerals present with reference to 'standard' mineral species;
2. the per cent non-exchangeable potassium was used to calculate the total proportion of mica-illite clay minerals;
3. the per cent loss-on-ignition between 150-800°C was used to calculate the proportion of kaolinite clays;

4. the cation exchange capacity was used with respect to the proportion of montmorillonite and vermiculite clay minerals, and;
5. areas beneath the principal peaks of identifiable mineral species from X-ray traces were weighted according to the Soil Survey Methods (Avery and Bascombe, 1974).

In order to control for the accuracy of the techniques and calculations of the results two 'standard' kaolinite and montmorillonite samples were included in the analyses, from which an error of estimation of 4.6% was established.

Although this procedure was able to identify and accurately estimate a wide range of clay minerals, such as biotite and illite, this form of speciation was not considered to be of any additional benefit to the objectives of the study, and the results reported are classified under the three major groups of minerals: micaceous, kaolinite and smectite since in most case these were found to form more than 98 per cent of the clay fraction.

The results are presented in Tables 4.27 and 4.28 for Manor Lane and Worbarrow, respectively. The following associations were noted:

1. at Manor Lane the clay-size material consisted of a mean 38.0% micaceous clay minerals, 20.6% kaolinite and 41.5% smectite. In comparison, the clay mineralogy at Worbarrow consisted of 20.8% micaceous, 11.0% kaolinite and 68.3% smectite. Thus it was noted that both sites were dominated by 2:1 layered montmorillonite clays and that there was a low proportion of 1:1 layered kaolinite; additionally the London Clay was characterised by a high percentage of mica and illite clay minerals.

Table 4.27. Clay mineralogy of weathered materials at Manor Lane.

CORE #	% CLAY MINERAL	ZONE ONE	ZONE TWO	ZONE THREE	ZONE FOUR	- X
1A	Micaceous	37.9	32.5	40.8	39.4	37.7
	Kaolinite	12.1	12.3	22.8	17.6	16.2
	Smectite	50.1	55.2	36.5	43.1	46.2
1B	Micaceous	40.6	40.0	40.0	42.9	40.9
	Kaolinite	22.8	23.1	22.1	18.9	21.7
	Smectite	36.5	36.9	37.9	38.2	37.1
2A	Micaceous	41.0	40.1	40.6	43.3	41.3
	Kaolinite	16.1	20.3	26.9	19.2	20.6
	Smectite	42.9	39.5	32.2	37.6	38.1
2B	Micaceous	41.4	42.0	41.5	41.8	41.7
	Kaolinite	23.4	24.7	25.0	23.4	24.1
	Smectite	35.2	33.4	33.5	34.9	34.3
3A	Micaceous	40.8	42.5	36.0	38.5	39.5
	Kaolinite	10.4	26.8	28.1	22.2	21.9
	Smectite	48.9	30.7	35.9	39.4	38.7
3B	Micaceous	34.8	38.8	41.1	43.1	39.5
	Kaolinite	18.2	21.9	26.7	26.1	23.2
	Smectite	47.0	39.4	32.1	30.8	37.3
4A	Micaceous	28.1	37.8	37.9	43.3	36.8
	Kaolinite	8.5	16.4	24.1	28.4	19.4
	Smectite	63.4	45.9	38.0	28.3	43.9
4B	Micaceous	29.1	26.3	29.6	39.3	31.1
	Kaolinite	8.5	15.2	15.3	32.4	17.9
	Smectite	62.4	58.6	55.1	28.3	51.1
5A	Micaceous	30.3	31.4	38.1	42.6	35.6
	Kaolinite	18.6	18.5	32.3	41.3	27.7
	Smectite	51.2	50.2	29.6	16.1	36.8
5B	Micaceous	38.5	38.5	36.3	41.0	38.6
	Kaolinite	21.6	16.3	18.9	29.7	21.6
	Smectite	40.4	45.2	44.9	31.4	40.5
6	Micaceous	41.8	39.6	34.6	43.1	39.8
	Kaolinite	15.9	16.7	17.1	34.6	21.1
	Smectite	42.3	43.6	48.3	22.3	39.1
7U	Micaceous	29.5	30.3	35.8	37.9	33.4
	Kaolinite	8.9	11.4	12.8	13.2	11.6
	Smectite	61.6	58.3	51.4	48.9	55.1
- X	Micaceous	36.2	36.7	37.7	41.4	38.0
	Kaolinite	15.4	18.6	22.7	25.6	20.6
	Smectite	48.5	44.7	39.6	33.3	41.5

Micaceous group contains mica and illite clay minerals

Smectite group contains montmorillonite and vermiculite expansible clays

Table 4.28. Clay mineralogy of weathered materials at Worbarrow Bay.

CORE #	% CLAY MINERAL	ZONE ONE	ZONE TWO	ZONE THREE	ZONE FOUR	- X
W0	Micaceous	23.4	21.0	17.3	23.1	21.2
	Kaolinite	8.3	12.0	12.4	12.6	11.3
	Smectite	68.4	67.0	70.4	64.3	67.5
W1	Micaceous	18.6	12.4	16.8	13.4	15.3
	Kaolinite	6.7	T	3.3	T	2.5
	Smectite	74.7	87.6	79.9	86.6	82.2
W2	Micaceous	22.3	16.5	22.6	17.9	19.8
	Kaolinite	12.2	9.1	22.7	12.5	14.1
	Smectite	65.5	74.4	54.7	69.6	66.1
W3	Micaceous	23.9	25.6	19.1	20.9	22.4
	Kaolinite	9.6	14.1	13.8	13.8	12.8
	Smectite	66.6	60.3	67.0	65.4	64.8
W4	Micaceous	21.8	11.0	23.5	23.8	20.0
	Kaolinite	11.01	T	22.7	18.9	13.2
	Smectite	67.24	89.0	53.8	57.4	66.9
W5	Micaceous	13.6	13.5	15.5	14.1	14.2
	Kaolinite	7.3	7.1	8.3	7.9	7.7
	Smectite	79.1	79.4	76.2	78.0	78.2
WU	Micaceous	28.5	37.2	30.4	34.4	32.6
	Kaolinite	13.8	15.9	17.5	13.1	15.1
	Smectite	57.7	46.9	52.1	52.5	52.3
X	Micaceous	21.7	19.6	20.7	21.1	20.8
	Kaolinite	9.8	8.3	14.4	11.3	11.0
	Smectite	68.5	72.1	64.9	67.7	68.3

Micaceous group contains mica and illite clay minerals

Smectite group contains montmorillonite and vermiculite expansible clays

T : trace

Figure 4.47. Distribution of micaceous clay minerals at Manor Lane.

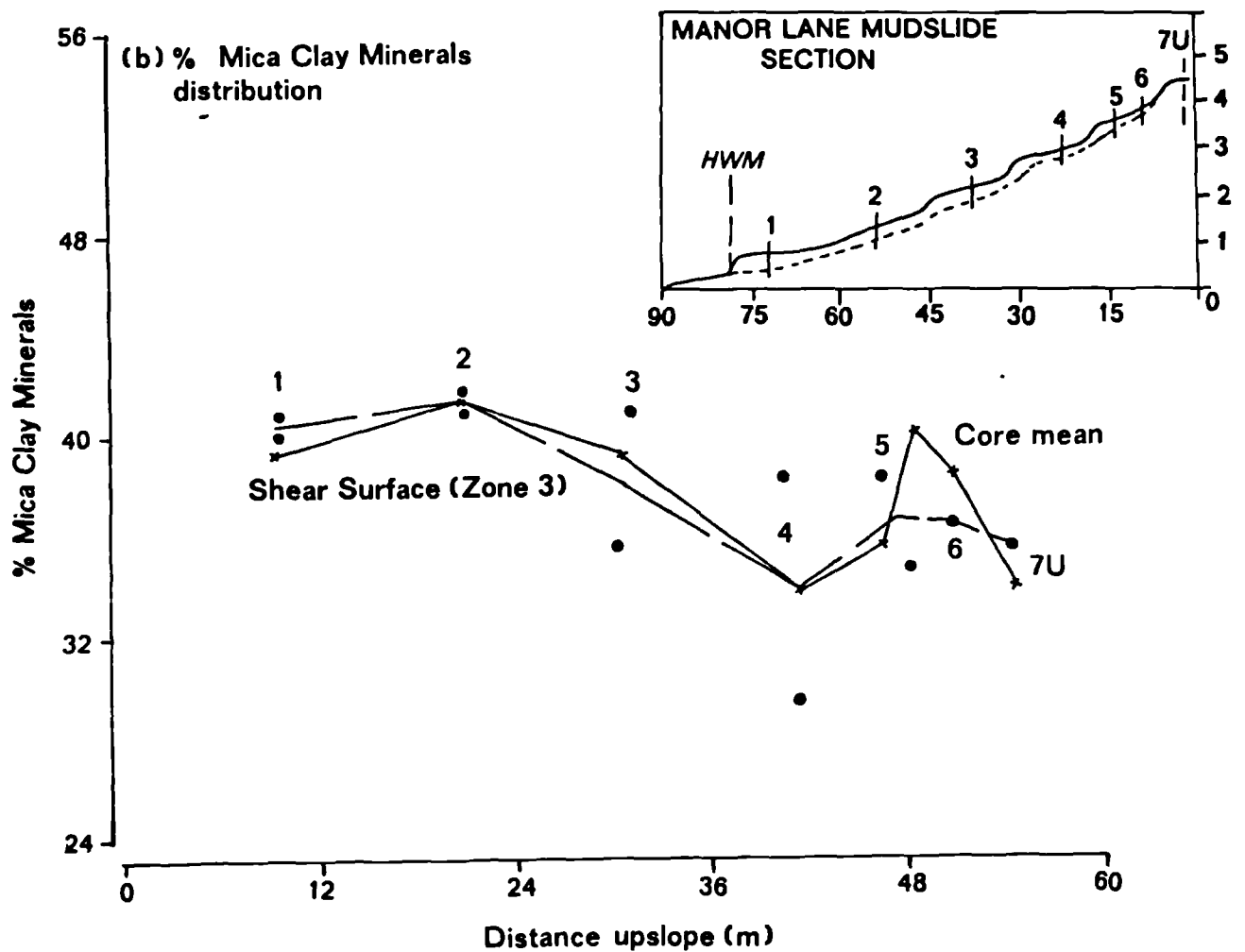
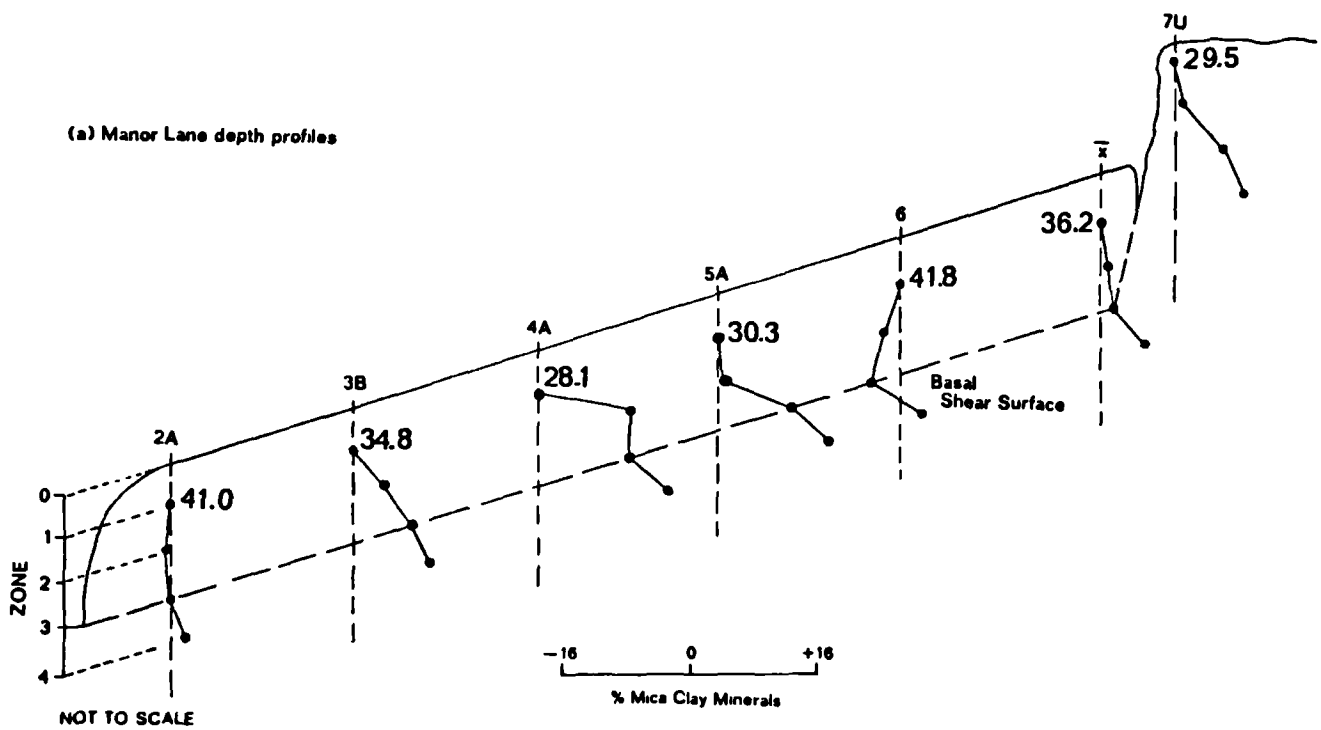
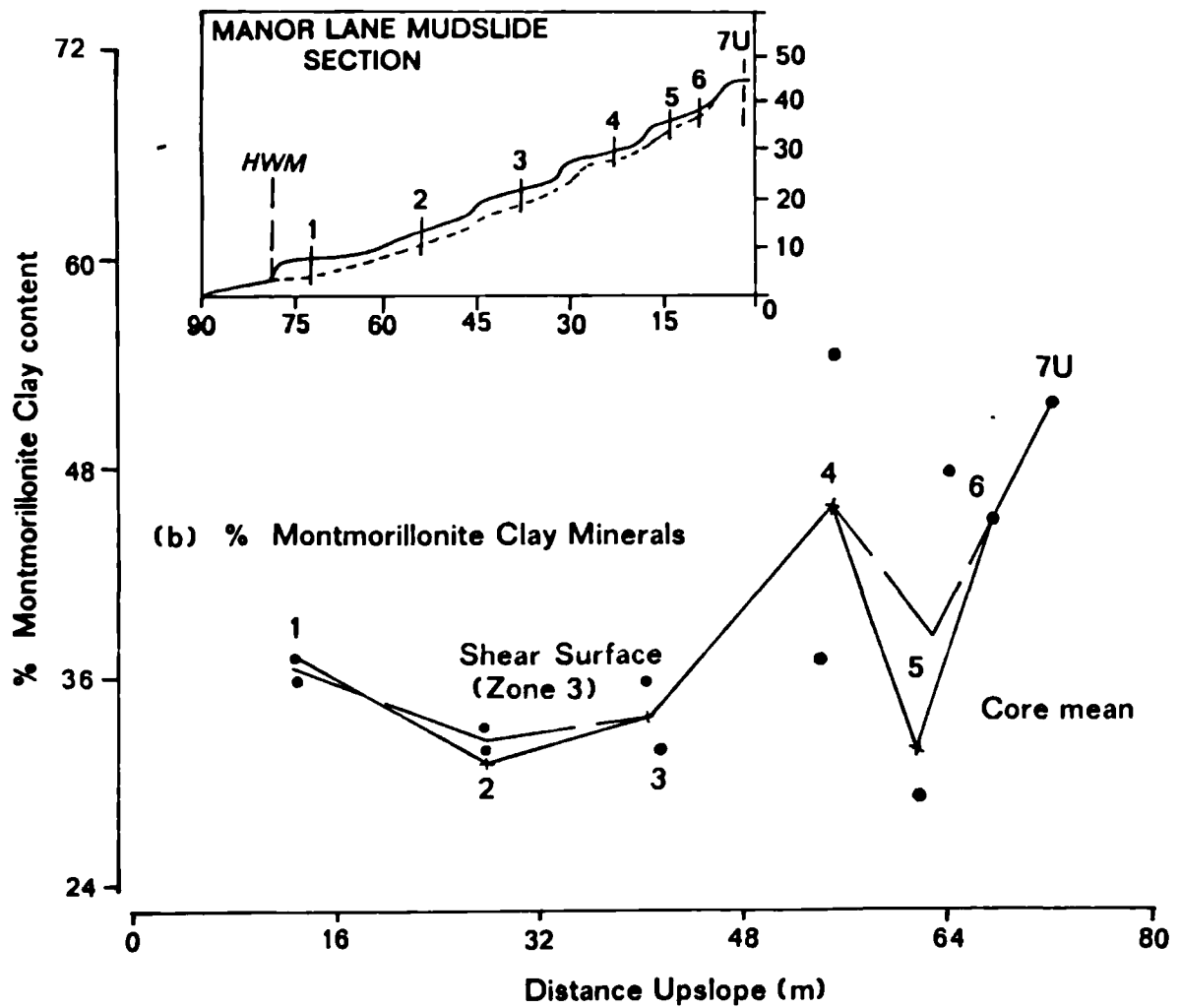
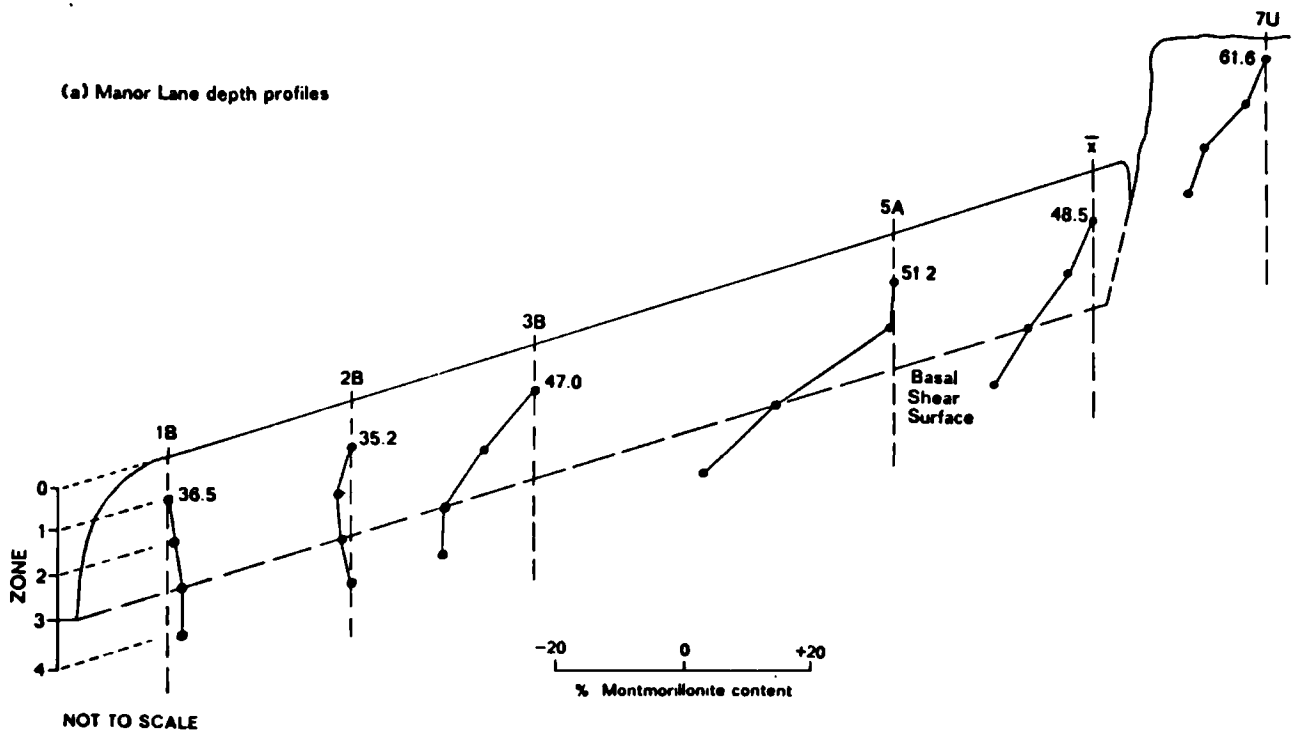


Figure 4.48. Distribution of montmorillonite clays at Manor Lane.



2. the Manor Lane mean profile showed an increase in the proportion of mica from 36.2% to 41.4% with depth (Figure 4.47a), and similarly for kaolinite increasing from 15.4% to 25.6% (Table 4.27). The proportion of smectite compensated for this gain, decreasing 15.2% with depth from 48.5% to 33.3% (Figure 4.48a), and it was noted that 6% of this reduction occurred across the shear surface. The weathered profiles in the source unit contained significant amounts of smectite (63.4% in unit 4A) in the surface layers decreasing quite sharply with depth (28.3%). The profiles on the lower slopes were more uniform, the proportion of smectite in the weathered profile varying only 5% (42.9% in zone 1; 37.6% in zone 4 of core 2A). The proportion of smectite within the weathered profiles of the source unit were more variable ranging from 16.1% (zone 4 in unit 5A) to 61.6% (zone 1 in unit 7U) in contrast to an 11.3% variation in mica content. Montmorillonite was thus considered to have a greater influence upon the properties and behaviour of the Manor Lane mudslide.
3. when plotted with respect to the mudslide section Figure 4.48b the proportion of smectite at the shear surface was found to decrease uniformly downslope from 51.4% to 36.5%. Similarly for the mean distribution of montmorillonite which decreased 18.3% upon erosion in the source unit (6 and 5), increasing 11% (to \approx 48%) in the feeder track coincident with the secondary source unit, followed by a consistent reduction to 34.3% towards the HWM. An increase to 46.2% at the toe of the slope was found to reflect the proximity and incorporation of salts originating from sea-water (section 6.312). With reference to the distribution of mica (Figure 4.47b) an inverse distribution to montmorillonite was noted with an increase in the proportion of mica corresponding with the reduction in montmorillonite downslope.
4. the mean profile at Worbarrow Figure 4.49a showed a reduction of 11.8% in the micaceous mineral content in relation to the undisturbed profile. The mean profile was uniform varying only 2.1% from the mean value (20.8%). The undisturbed profile was more variable increasing with depth from 28.5% to 34.4%. As found

Figure 4.49. Distribution of micaceous clay minerals at Worbarrow Bay.

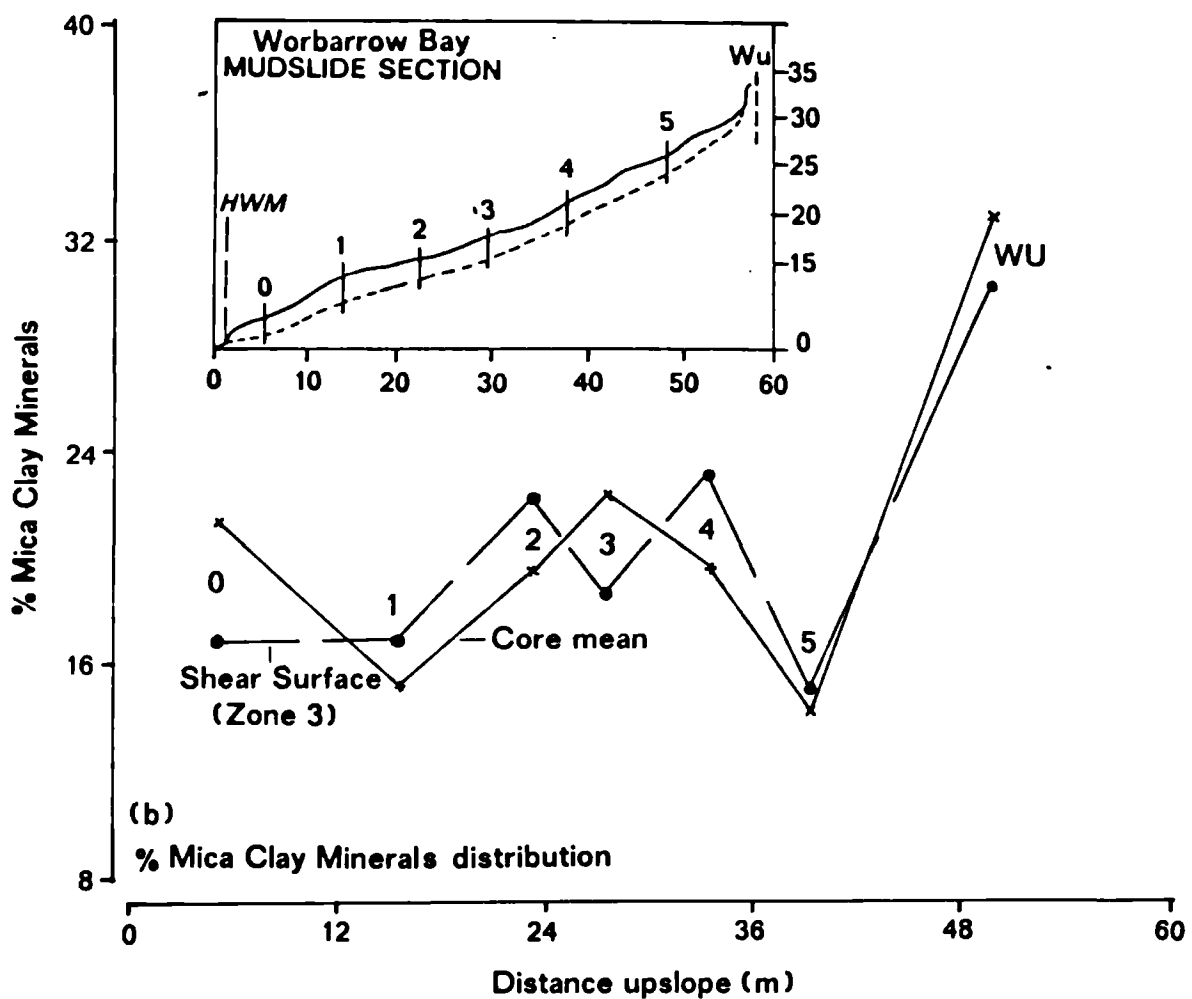
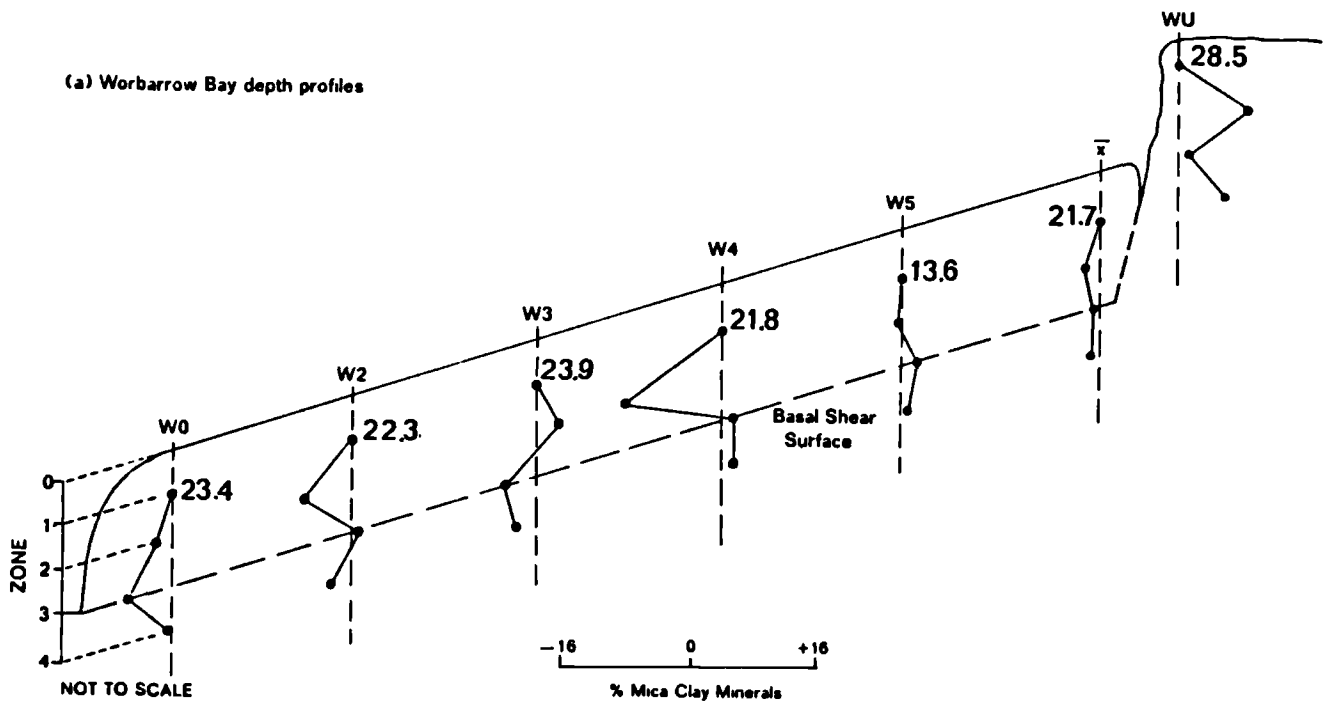
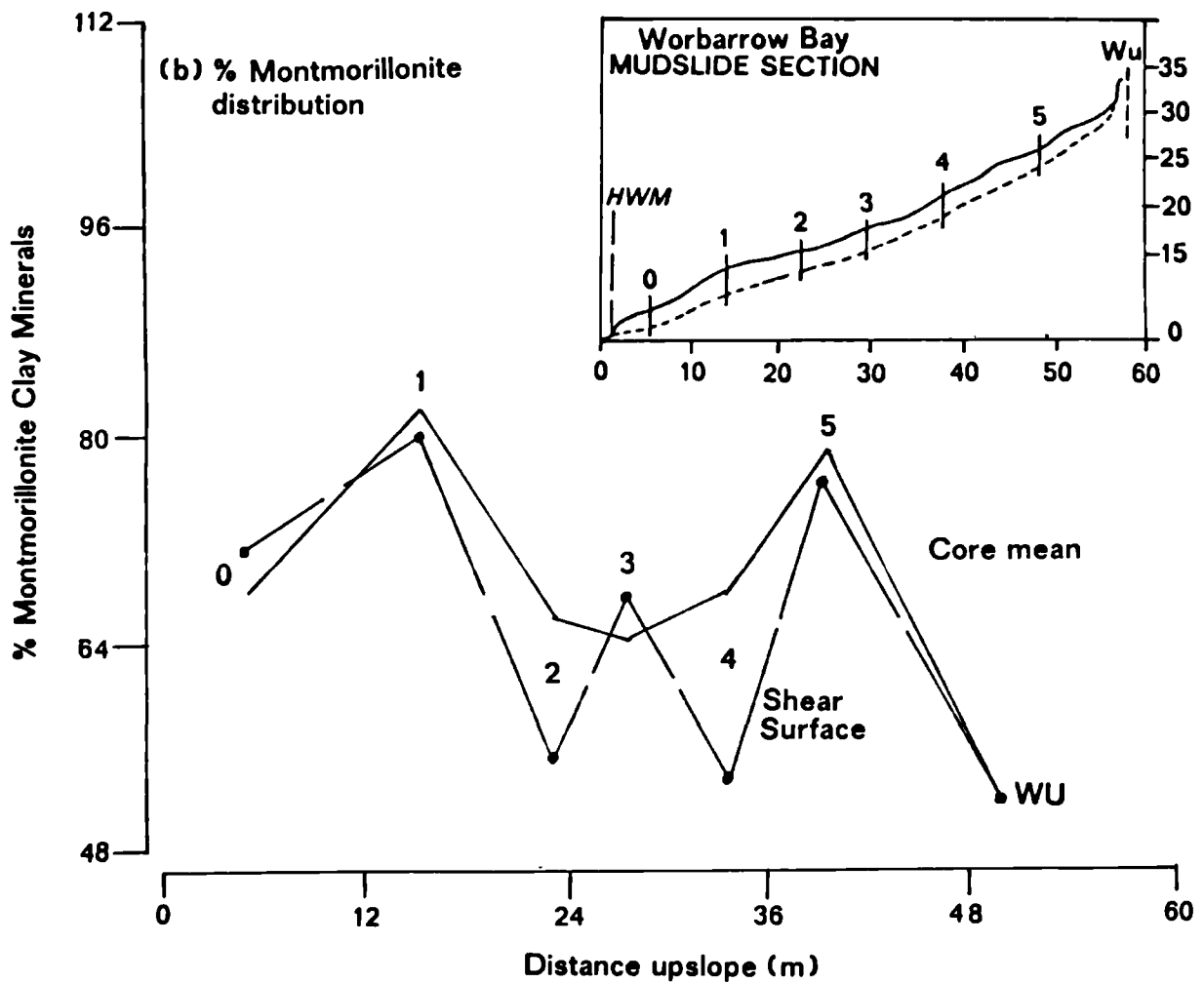
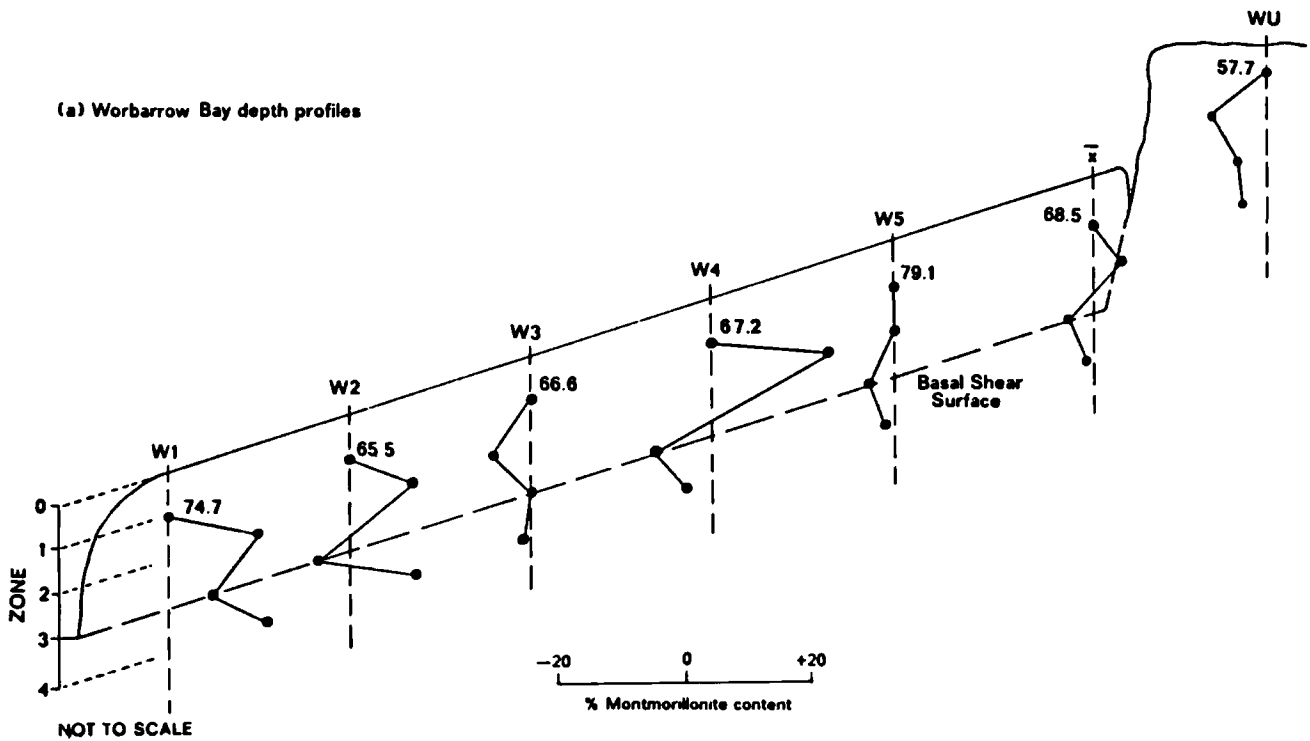


Figure 4.50. Distribution of montmorillonite clays at Worbarrow Bay.



at Manor Lane montmorillonite was closely related to the mica content (Figure 4.50a). Maximum montmorillonite contents were found in the surface layers (sub-zone 1) of the undisturbed and weathered profiles in contrast to beneath the basal shear surface (zone 4). Profile W4, for example increased from 67.2% (zone 1) to 89% (zone 2), decreasing 35% to the basal shear surface and *in situ* clay. The profile demonstrated that the materials within the mudslide contained greater proportions of montmorillonite clay minerals than beneath the basal shear surface and up to 42.1% greater than in the undisturbed profile.

5. with respect to the mudslide section Figure 4.50b there was an increase in the mean proportion of montmorillonite from 52.1% to 76.2% upon weathering and erosion in the source (unit 5), followed by a gradual reduction to 66% down the feeder track, increasing once more in the accumulation lobe to 79.9%. The latter peak was considered to reflect the accumulation of materials from upslope and from the perched mudslides bordering the main track. There appeared to be less montmorillonite at the shear surface in comparison with the core means. With reference to the section in Figure 4.49b. there was a corresponding net reduction of 18.4% in the proportion of mica from the undisturbed state (32.6%) to the weathered state (14.2%) in contrast to the increase in smectite.
6. although kaolinite was subordinate to mica and smectite it was found to increase from 11.6% to 20.6% upon weathering and erosion at Manor Lane, whereas at Worbarrow there was a small reduction from 15.1 to 11 % downslope.

The results indicate that relatively high proportions of expansive 2:1 layered montmorillonite minerals were involved in active translational mudsliding at the two sites under study. Both sites showed high proportions of montmorillonite in surface layers of undisturbed samples and following weathering in the source units. Montmorillonite contents within the mudslide mass were greater than found below the shear surface. At Worbarrow Bay there was an increase in the amount of montmorillonite

downslope. There was also an increase in the proportion of exchangeable sodium (section 4.422) which suggested that the Wealden materials at Worbarrow may become progressively more unstable upon translation down the mudslide and are, thus, potentially more unstable than the London Clay. In contrast, montmorillonite was found to decrease towards the HWM at Manor Lane relative to an increase in micaceous minerals. However, the dominance of montmorillonite in the source units was an important reason for the instability of the site. Slight variations to these trends were found at both sites but were accounted for by morphological and external influences.

4.5 Conclusions of the laboratory analysis.

The 'static' analysis of the physico-chemical variability of properties within mudslides has isolated a number of associations with respect to weathering behaviour and slope morphology. Both the physical and chemical properties were distinctly related within both sites; differences in the character of these properties were noted when comparing highly weathered materials with undisturbed samples. Further differences were found to occur depending on the location within the mudslide section emphasising the characteristic morphology of mudslides; spatial variability in the distribution and nature of soil properties was intrinsically associated with the source unit, feeder track and accumulation zone. These may be summarized as follows:

1. the proportion of clay size particles was found to increase with depth, particularly across the shear surface, but decreased downslope contrary to theory.

2. the saturated moisture content of the mudslide materials was found to decrease downslope suggesting an increased susceptibility to saturation. Correspondingly there was a slight reduction in plasticity following the weathering and remoulding of material.
3. the phase relationships were highly dependent; there was a reduction in the void ratio and porosity below the basal shear surface and upon movement downslope. The unit weight and bulk density showed an inverse relationship to the void ratio and porosity indicating a two fold increase in density below the shear surface and downslope.
4. the peak shear strength condition of the London Clay at Manor Lane consisted of an effective friction angle of 15.5° , compared with 23.2° for the Wealden Clay at Worbarrow, and an effective cohesion for both of 12-13 kPa. The greater friction angle was related to the sandy Wealden Beds lithology. The reduction in shear strength from undisturbed to weathered states was found to result in a 30-50 per cent reduction in the peak friction angle and a 70-80 per cent reduction in peak cohesion. The effective residual friction angle at the shear surface was further found to decrease from 11° to 8° upon remoulding downslope at Manor Lane. The strength of weathered materials at Worbarrow was inherently more variable, the residual friction angle ranging from 12.5° to 5.73° , averaging 8.45° . A small 2-4 kPa residual cohesion was noted at both sites. The reduction in residual strength within the mudslide was considered to reflect either an incomplete fall in strength from peak to residual upon disturbance or an effect of the physico-chemical processes of weathering leading to further degradation of residual strength.
5. the chemistry of each system was very different and the London Clay was noted to be highly saturated with neutral divalent base cations in association with sulphate balancing anions. The chemical system at Worbarrow was mildly acidic and was dominated by monovalent sodium cations in association with chloride balancing anions. Since the exchangeable cations of undisturbed materials at Manor Lane were highly concentrated there was an

apparent dilution of salts on the exchanger following weathering, evidenced by a reduction in the per cent base saturation. The opposite was found at Worbarrow, where there was an increase in concentration of cations adsorbed to the exchanger. The chemistry was found to be particularly sensitive to morphological and external influences such as the location of secondary source units at Manor Lane, and the input of materials from perched mudslides at Worbarrow Bay.

6. the chemistry of the alumino-silicate clays showed only small variations upon weathering although there was a slight increase in the proportion of iron oxide within the crystal lattice downslope. The results of the analyses of micromorphology revealed clear differences between particle and solute movements along discontinuities above and below the shear surface. The oxides of silica and aluminium were found to be preferentially deposited along fissures and upon the surfaces of mineral particles below the shear surface suggesting leaching from the overlying mudslide materials. There was also an increase in the proportion of aluminium above the shear surface which was assumed to result from the disruption and weathering of the materials, especially in the source units. The movement and deposition of iron oxides was highly variable and although 9.0 per cent was generally found on the surfaces of clays at both sites, the concentration was found to vary by as much as 700 per cent along fissures at Manor Lane.
7. substantial proportions of expansive 2:1 layered montmorillonite clay minerals were involved in active translational mudsliding at Manor Lane and Worbarrow. High proportions of montmorillonite occurred in the surface layers of undisturbed samples and following weathering in the source units. Montmorillonite clay contents within the mudslides were greater than found below the shear surface. The presence and formation of montmorillonite within mudslides was considered an important reason for the instability of the weathered mass. Slight variations to these trends were explained by morphological and external influences.

The physical and chemical properties have shown similar associations with weathering and the morphology of mudslides and have important implications for soil behaviour. The importance of these findings with respect to slope instability is discussed in section 6.21. The application of these results can best be illustrated by digressing from the main theme to place the detailed studies of Manor Lane and Worbarrow Bay into a more general regional and scientific context. Thus, before presenting the results of the 'dynamic' behaviour of mudslides (Chapter Five) the following regional appraisal (section 4.6) attempts to establish the association of landsliding with the occurrence of clay minerals in order to demonstrate that the site specific studies may have much wider application.

4.6 Regional variations in clay and landslide distribution:

4.61 *Southern and south-eastern England.*

The area of study incorporated into the regional analysis included the counties of south-east England (as defined by the DOE, 1987) in addition to the counties of Wiltshire and Dorset, shown in Figure 4.51. The aim of this exercise was to assess the susceptibility of the outcropping geological formations to landsliding with respect to lithology and specifically to the proportion and type of clay-size particles.

A report prepared by Geomorphological Services Limited for the DOE (1987) catalogues the number of reported landslides from the literature for each county, region and geological formation or BGS code. For a fuller state-of-the-art review of the distribution of landslides within this region the reader is referred to this report. The total number of landslides known to exist on the outcropping bedrock strata in the region are listed in Table 4.29, along with the total number of youthful (originating over the last century) inland and coastal landslides, the outcrop area and the density of youthful inland landsliding. The DOE review further classifies the types of landslide and assesses the distribution with lithology (ie, with clay, sand, etc). However, there were no reports of the quantity and types of clay involved in active landsliding.

Mineralogical data were collated for each geological code from four main sources in order of importance: (a) Perrin's (1971) *Mineralogy of British Sediments*, (b) Avery and Bullock's (1977) *Mineralogy of Clayey Soils in Relation to Soil Classification*, (c) Laboratory assessments, (d) Loveland's (1984) *Soil Clays of England and Wales*, and several additional

Figure 4.51. The geological formations of the study area.

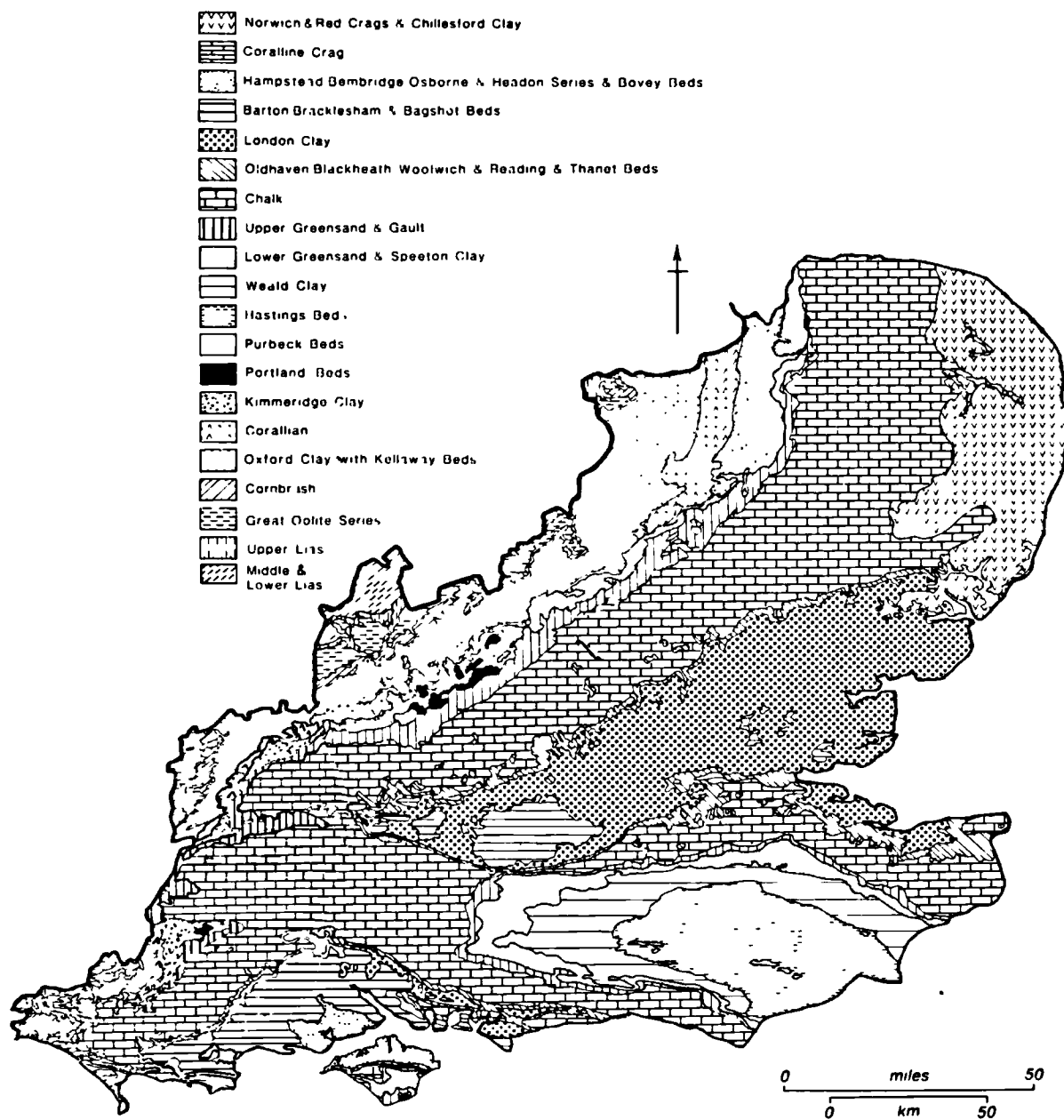


Table 4.29. Reported number of landslides occurring on the geological formations of southern and south-east England.

FORMATION AND BGS CODE	LANDSLIP TOTAL	TOTAL YOUTHFUL	COASTAL YOUTHFUL	OUTCROP AREA *	DENSITY YOUTHFUL	INLAND DENSITY	SLIDES /FLOWS	S & M ROTAT	OTHER
91 L.Lias	48	33	32	104	0.317	.010	11	3	18
92 M.Lias	63	18	17	295	0.061	0.003	2	0	15
93 U.Lias	22	6	0	108	0.056	0.056	2	2	2
94/95 Oolite	77	9	1	529	0.017	0.015	3	1	5
97 Oxford Clay	42	13	1	1698	0.008	0.007	2	6	4
98 Corallian	30	5	2	685	0.007	0.004	1	2	0
99 Kimmeridge	29	15	11	588	0.026	0.007	2	3	9
100 Portland	16	13	12	4.2	3.095	0.238	0	1	11
101 Purbeck	7	2	2	19	0.105	0	0	0	2
102 <i>Hastings Beds</i> <i>Fairlight Clay</i> <i>Wadhurst Clay</i> <i>Grinstead Clay</i>	98	18	9	1873	0.010	0.005	3	1	14
103 Weald Clay Atherfield Clay	127	35	8	1700	0.021	0.016	5	7	23
104 Lower Greensand	161	39	16	1358	0.029	0.017	7	10	22
105 Gault Upper Greensand	184	51	25	1029	0.05	0.025	3	7	36
106 Chalk	69	52	36	8023	0.007	0.002	8	1	41
107 Thanet Beds Woolwich Beds Reading Beds	17	12	5	728	0.017	0.01	3	5	4
108 London Clay	343	206	91	5013	0.041	0.023	42	84	80
109 Bagshot Beds	42	10	8	1202	0.008	0.002	0	3	6
111 Hampstead Beds	24	18	16	344	0.0523	0.006	6	2	10

* Outcrop area x 10 Km² : density indices over-estimated by a factor of 10

All values are for the 'youthful' category of landslides : age < 100 years

S & M Rotat : the sum of single and multiple rotational failures in the GSL data-base

Slides/flows : assumed to be the sum of translational mudslides

sources. With reference to Table 4.30, the reported clay mineralogy for each geological formation is presented to the nearest ten per cent, along with the number of determinations, and where available the mean proportion of clay within the samples, the CEC and the non-exchangeable K_2O .

There are major limitations of both data sets which must be borne in mind with any subsequent analysis:

1. the distribution and density of landslides are governed by the caveats stated in the DOE (1987) review which warn of the sparsity of our current knowledge and survey of the distribution of landslides.
2. both data sets are based on reports available in the literature and do not necessarily reflect the true distribution of clay minerals or the number of landslides.
3. the reported clay mineralogy is not necessarily estimated for *in situ* bedrock as might be noted by the high proportions of clay-size material within certain non-clayey lithologies. In such cases these are taken from surface soils considered indigenous of the underlying bedrock and are therefore assumed to be related.
4. the 308 reported analyses of mineralogy within the region are not equally distributed and vary in the methods of determination. They are mostly semi-quantitative estimates provided by the Soil Survey of England and Wales.
5. additional data of varying quality has been used to supplement the data set. These are of limited use and often fail to report basic information such as the per cent clay-size material and other chemical indexes of mineralogy.

Table 4.30. Reported clay mineralogy of landslide prone geological formations.

FORMATION AND BGS CODE	n	%	%	CEC	LAYER SILICATE SPECIES							CLASS
					Ka	Mi	Mi-Sm	Chl	Mi-Chl	Vm		
91 L.Lias *	17	60	2.7	50	3	2	4	1	-	-	S	
92 M.Lias *	6	51	2.2	46	3	3	1	1	-	2	M & S	
93 U.Lias *	6	61	2.3	38	3	2	4	-	1	-	S	
94/95 Oolite	1	47	3.4	48	1	4	5	-	-	-	S	
97 Oxford Clay	10	63	2.8	55	1	3	6	-	-	-	S	
98 Corallian	14	-	-	-	1	2	6	-	-	-	S	
99 Kimmeridge	6	63	2.9	48	2	2	5	-	-	-	S	
101 Purbeck	1	-	-	-	1	4	5				M & S	
102 <u>Hastings Beds</u>												
Fairlight Clay	2	48	2.7	59	1	3	6	-	-	p	S .	
Wadhurst Clay	3	-	-	-	2	3	5	-	-	p		
Grinstead Clay	1	-	-	-	2	4	-	4	-	-		
103 Weald Clay	35	-	-	-	2	1	7	-	-	-	S	
Atherfield Clay	NA											
104 Lower Greensand	4	-	-	-	1	5	3			1	M	
105 Gault	8	57	2.3	53	1	2	7	p	-	-	S	
Upper Greensand	1	-	-	-	2	8	p	-	-	-		
106 Chalk	44	-	-	-	1	4	5	-	-	-	M & S	
107 Thanet Beds	NA											
Woolwich Beds	NA											
Reading Beds	6	58	2.3	54	1	2	6	1	-	-	S	
108 London Clay	62	60	2.6	56	2	4	4	p	-	-	M & S	
109 Bagshot Beds	43	-	-	-	3	4	3	-	-	-	M	
111 Hampstead Beds	14	-	-	-	2	5	2	-	-	-	M	

* Estimates established outside southern and south-eastern England

Values of the layer silicates estimated to the nearest 10%

M : micaceous S : smectitic p : present

With these limitations in mind an attempt was made to correlate the distribution of landslides with the mineralogy of clayey lithologies. It was realised from the outset that in order to assess the degree of lithological susceptibility to slope instability the density of slope failures would provide a more realistic estimation than just the total number of landslides. Moreover, the density of 'youthful' landslips are of most interest to this study as well as bearing a more accurate association with the more recent mineralogical assessments and thus the weathering and source environments of the sediments.

The geological formations outcropping on the coasts are found to have relatively large numbers of landslides which may be considered to bias the distribution against those formations that do not form coastlines. Thus the number of inland youthful landslides were included in the analysis.

With reference to Figure 4.52 the total and youthful number of landslides occurring within the region are plotted with respect to the geological codes. Both plots show that the London Clay has the largest number of landslides followed by the Gault Clay-Upper Greensand unit, the Weald Clay-Lower Greensand unit, Chalk, the Hastings Beds, the Lias and Oxford Clays and the Bagshot and Reading Beds. When plotted in relation to outcrop area (minus superficial deposits) the total outcrop density clearly indicated the Lias, Cretaceous and Tertiary Beds were the most prone to landsliding over the past 100 years (Figure 4.53). When the inland density was considered the Lias formation was the most susceptible to landsliding, although it was noted that the small outcrop area may have resulted in a spurious density function since few landslides need be recorded in relation to other outcrops to obtain this result.

Figure 4.52. Frequency histograms of the total and youthful number of landslides reported for each geological formation.

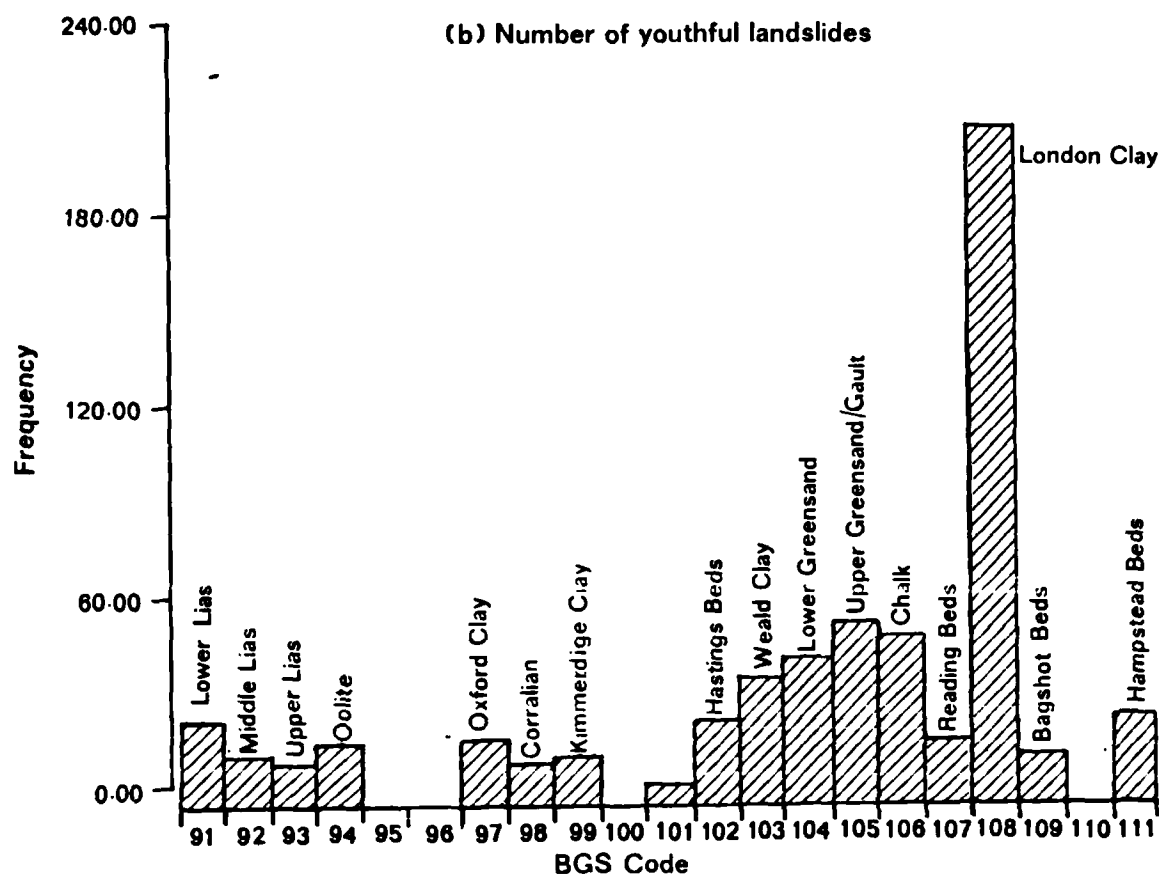
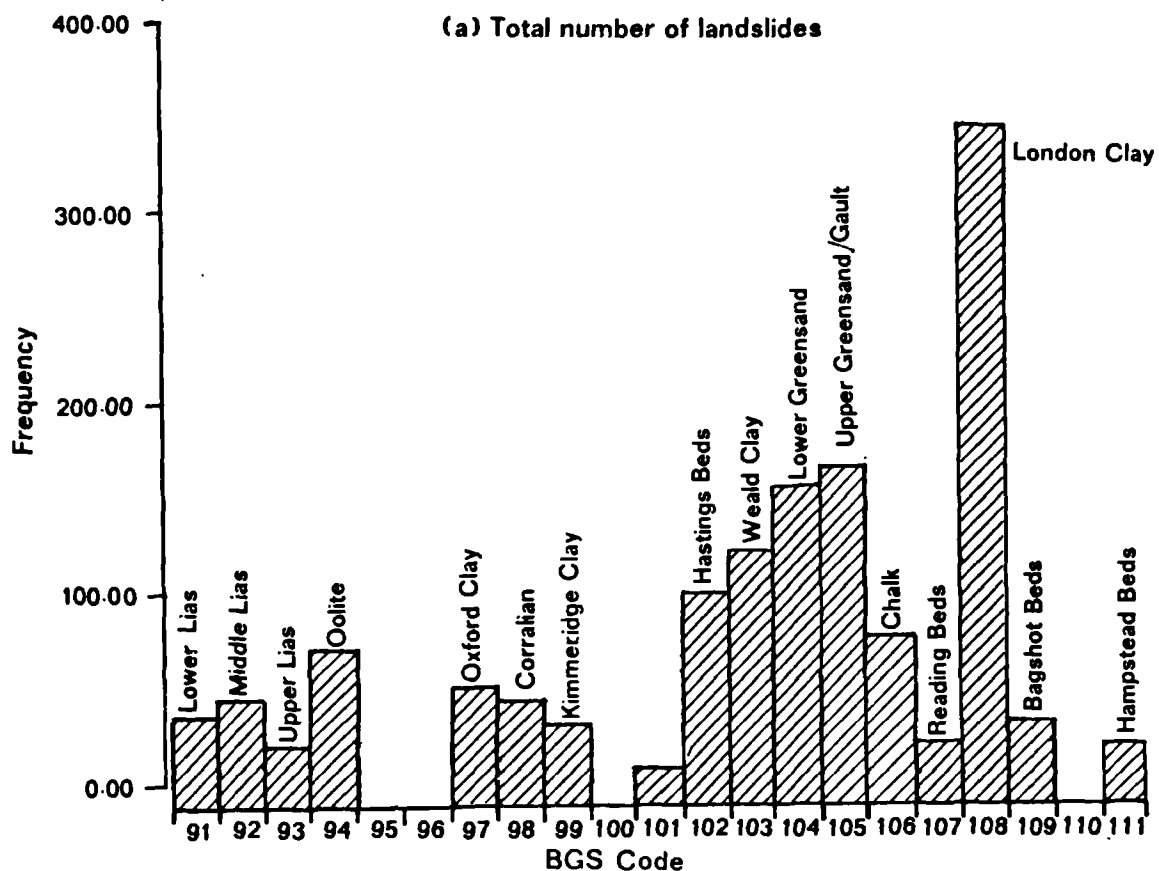
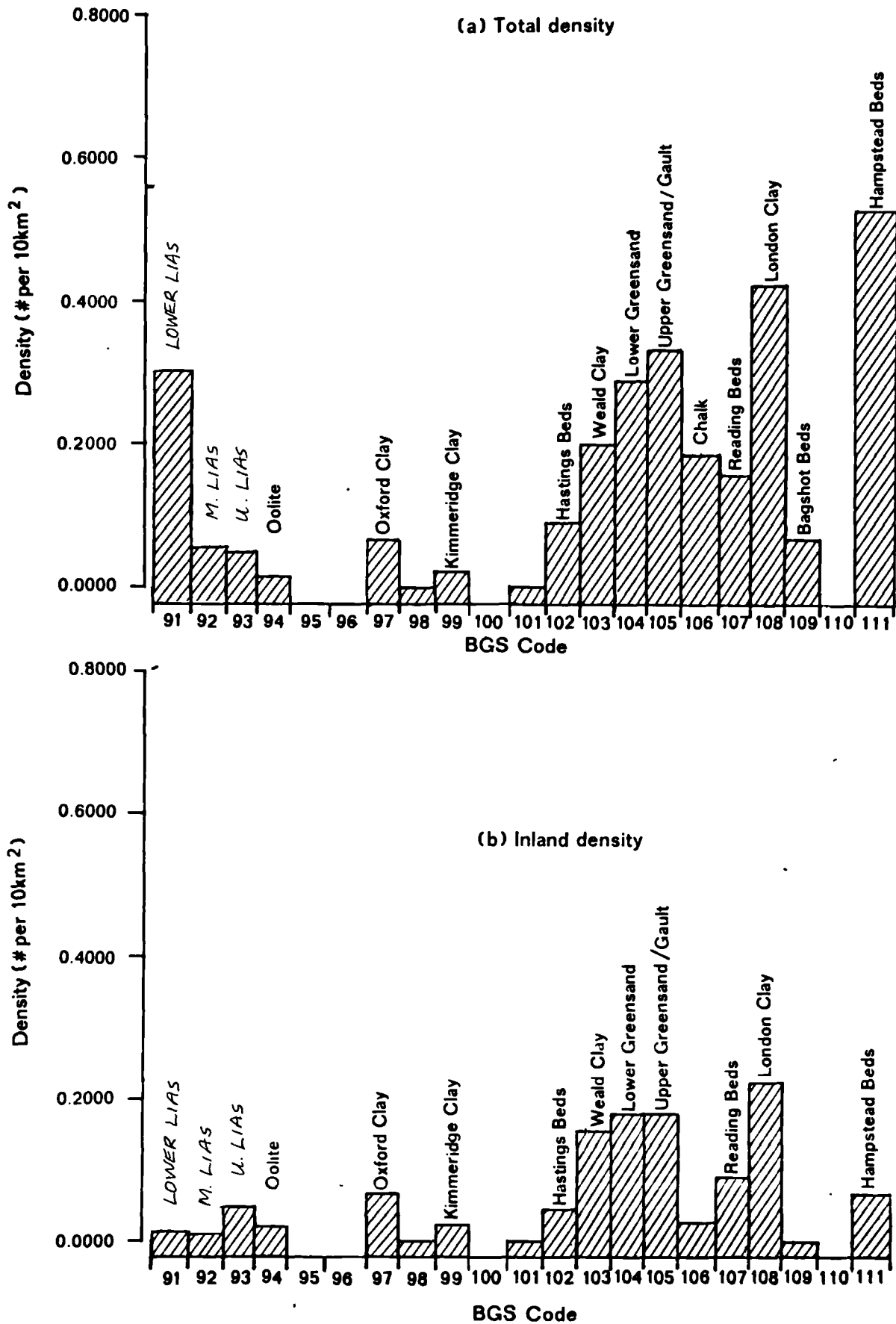


Figure 4.53. The total and inland density of youthful landslides reported for each geological formation.



Treating the Lias formation with caution the London Clay was found to have the greatest density of inland slips followed closely by the Gault-Upper Greensand unit, the Weald-Lower Greensand unit, with significant densities on the Reading Beds, Great and Inferior Oolite, Oxford Clay and Hastings Beds.

With reference to Figure 4.54b, the number of mudslides (slides and flows) indicates that the beds most susceptible to translational mudslide behaviour were the London Clay, Lower Lias, the Weald and Lower Greensand association, Chalk, the Hampstead Beds, the Reading Beds, the Hastings Beds, the Gault and Upper Greensand unit, Oxford Clay and Upper Lias. However, the proportion of unclassified landslides, shown in Figure 4.54a, suggests that the London Clay, Chalk, Upper Greensand, Lower Greensand, Lower and Middle Lias, and the Hastings Beds are the most susceptible lithologies to landsliding.

Figure 4.55, plots the per cent mica and montmorillonite content for each geological formation and showed an interesting feature in that the proportion of mica broadly decreases with the age of the sediment, whereas the amount of montmorillonite shows an inverse trend indicating that the more recent Tertiary Beds contain relatively low proportions of expansible minerals (Figure 4.55b). This trend could well be a function of distance from the source environment or a consequence of reworking.

When the density of the total number of landslides was plotted in relation to the proportion of mica (Figure 4.56a) there appeared to be a general association between lithologies with large densities of landslides with an increased proportion of mica. The Upper Lias was an exception to this rule, but was considered a spurious result for the

Figure 4.54. The number of translational mudslides and unclassified landslides reported for each geological formation.

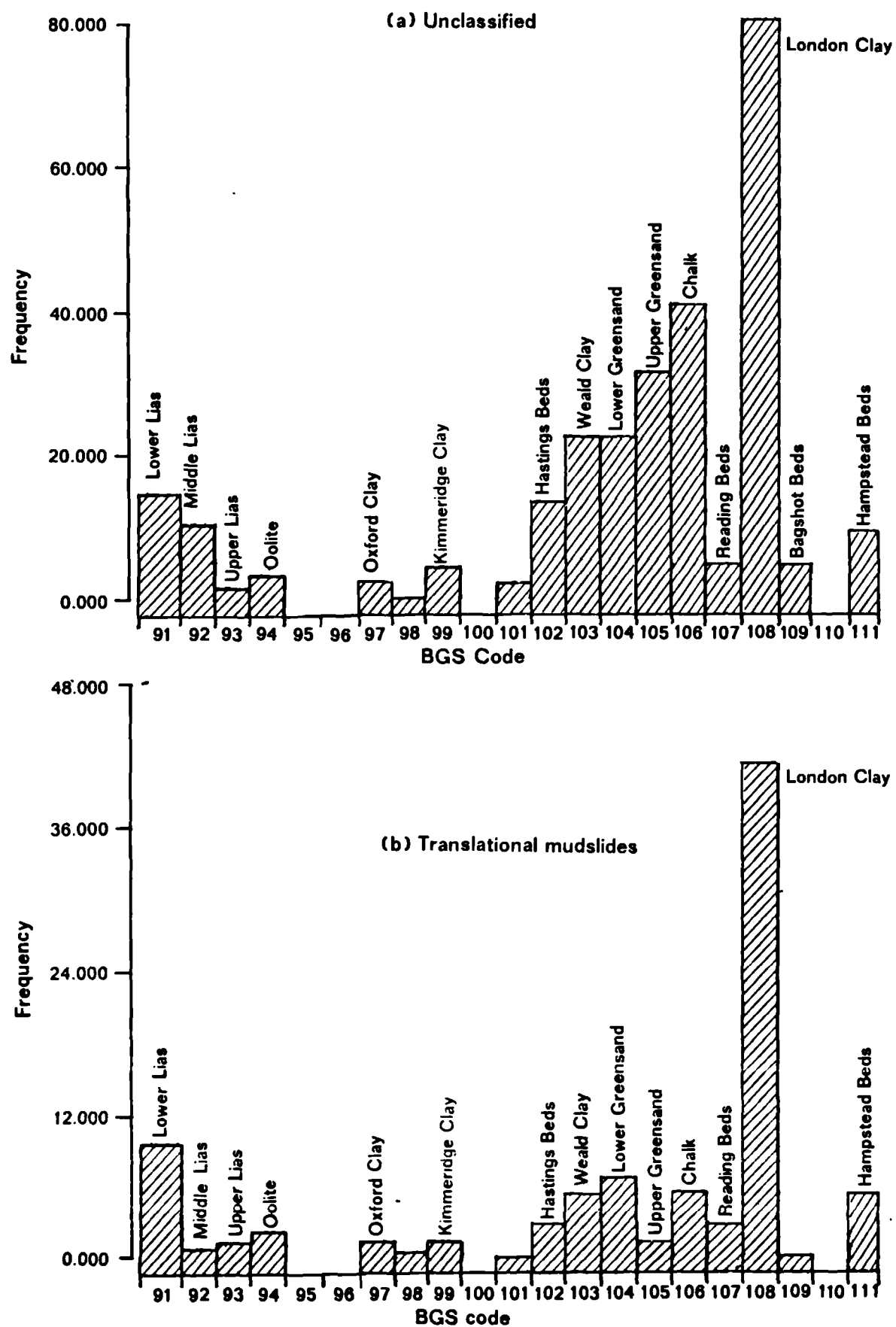
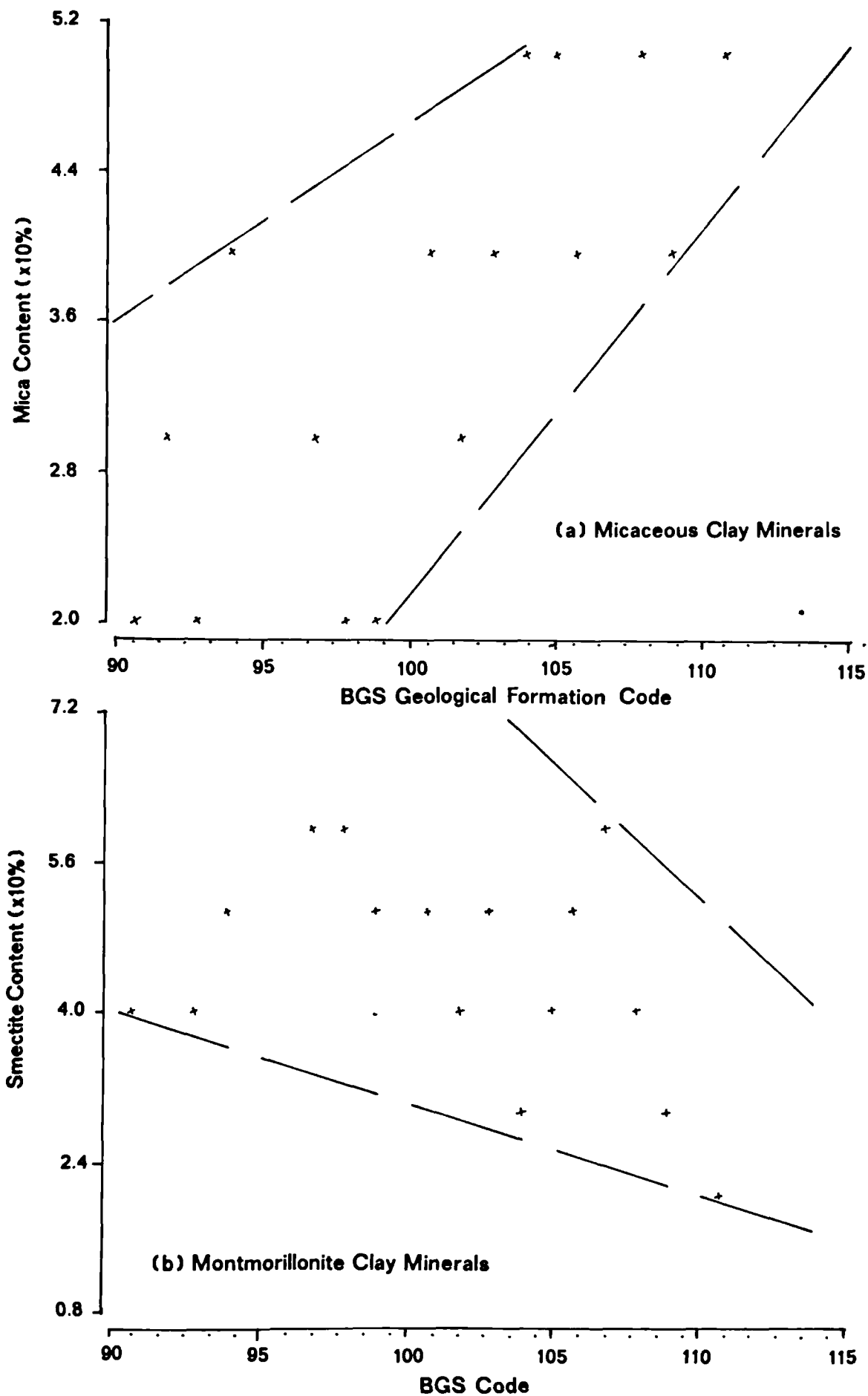


Figure 4.55. The distribution of mica and montmorillonite clay minerals associated with each geological formation.



reasons mentioned earlier. In relation to the inland density of youthful landslides (Figure 4.57a) a similar relationship was noted with the proportion of mica with the highest densities associated with a minimum content of 40 to 50 per cent micaceous clay minerals.

With reference to Figure 4.56b the total density of youthful slides was plotted with the proportion of montmorillonite and does suggest that the greatest densities are associated with relatively low proportions of montmorillonite. The finding contrasts with theory and comes as a surprise. However, when the inland density was considered (Figure 4.57b) the data showed a 'normal' distribution; at about 40 per cent montmorillonite content the greatest densities of landslides were found.

The associations of mineralogy with the type of landslip are not included due to the limited number of classified types and to the vagaries of the literature discovered by the review. However, it was found that the density of mudslides were broadly similar to the total and inland densities of the youthful category of landslides and thus showed similar associations with mineralogy as described above.

The associations discussed between the density and mineralogy of landslide-prone geological formations were not considered to be highly significant because the inadequate data-bases do not permit such conclusions. It does seem, however, that the most susceptible formations contain 40 to 50 per cent expansive smectitic minerals and that there was an increase in the proportion of 2:1 layered mica illite clay minerals in relation to an increase in the density of youthful landslides.

Figure 4.56. The density of youthful landslides in association with the proportion of micaceous and montmorillonite clay minerals.

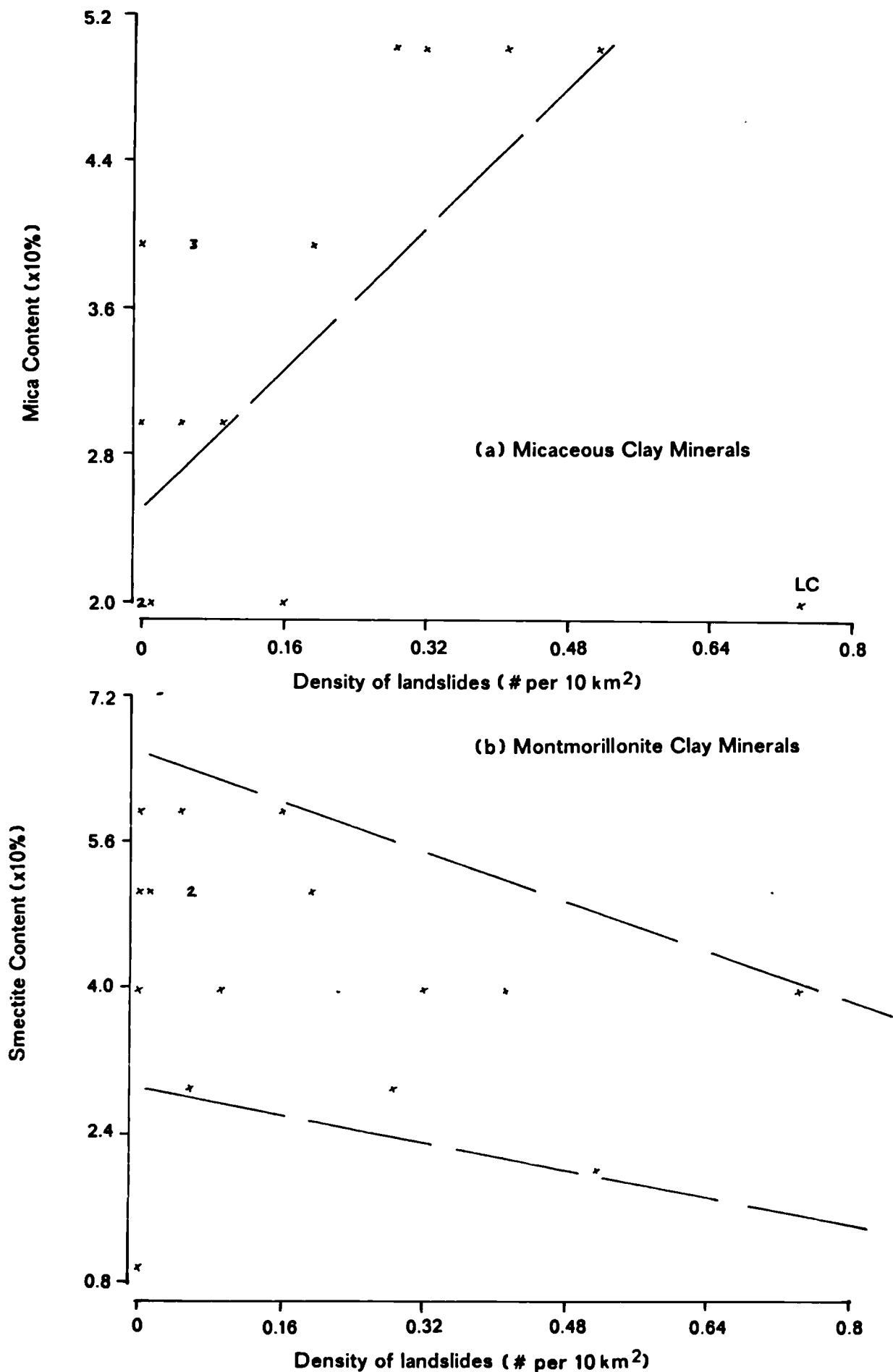
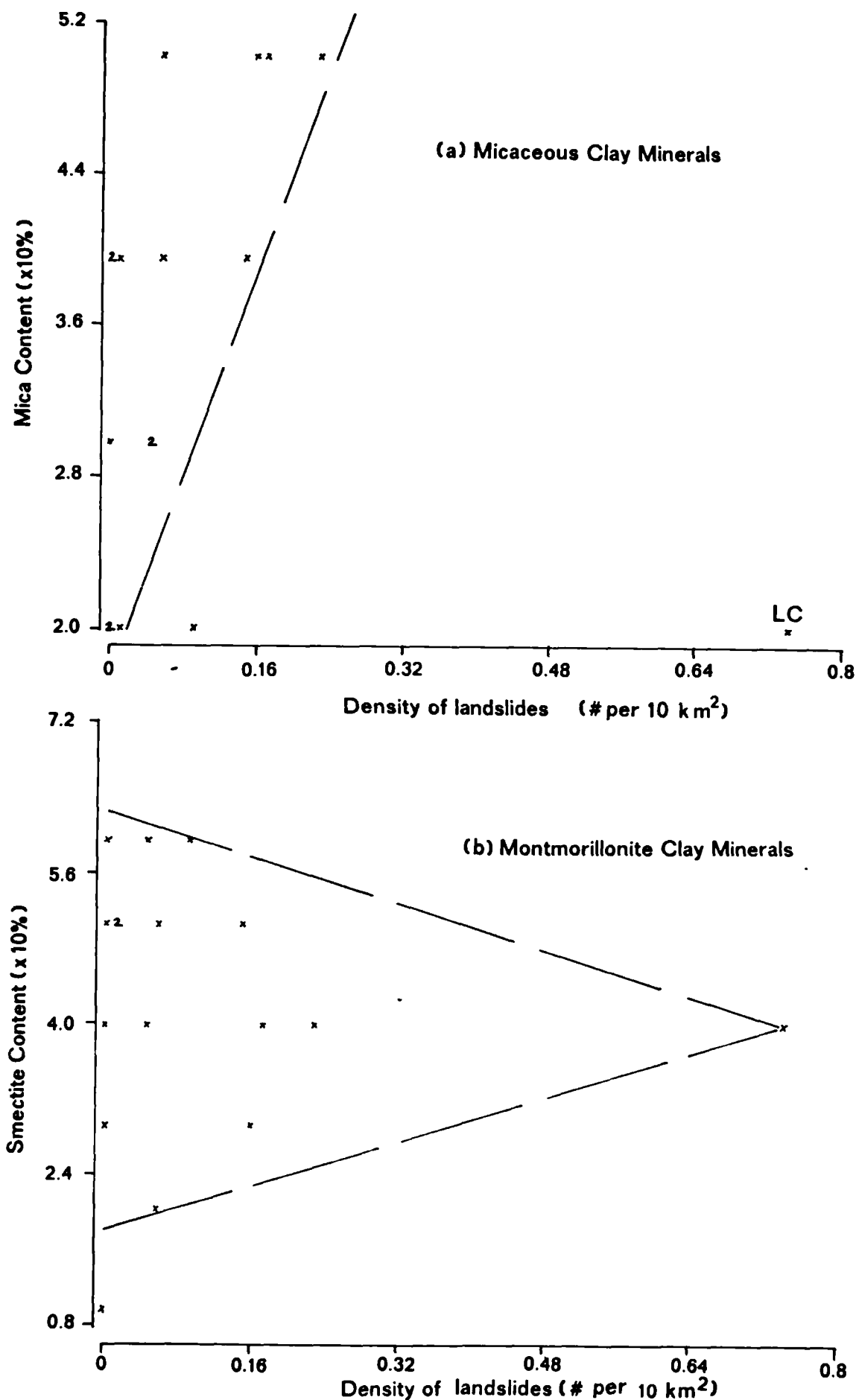


Figure 4.57. The inland density of youthful landslides in association with the proportion of mica and montmorillonite clays.



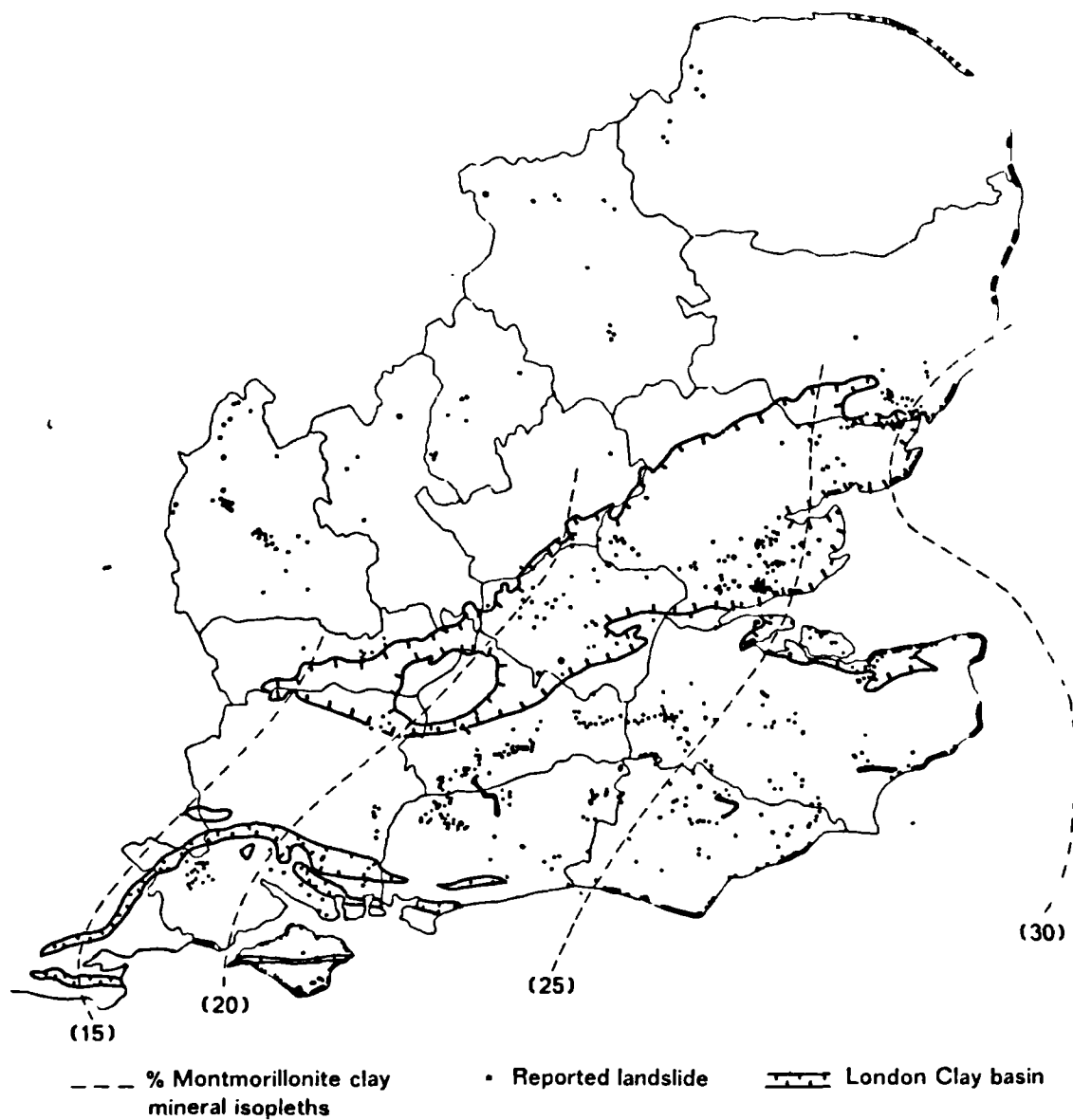
Although this section has considered the distribution of landslides on independent geological formations it was also expected that the variability in lithology and mineralogy within formations may give rise to a correspondingly variable distribution of landslides. Few geological formations have been studied more extensively than the London Clay, which provides an ideal opportunity to relate the distribution of landslides with the regional variability in lithology of this deposit.

4.62 *The London Clay Basin.*

With reference to section 3.231 the London Clay may be found in the London and Hampshire Basins contained within the region specified in the previous section. The extent of the outcrop is shown in Figure 4.51. The engineering geomorphology of the London clay has been well studied in recent years and since the DOE (1987) review was commissioned the distribution of reported landsliding within the region is known. The regional variability in lithology of the deposit was studied by Burnett (1972) and published by Burnett and Fookes (1974) from which the change in the proportion of clay, and the type of clay minerals across the Basin formed a major part of this survey. Here it is intended to combine the known distribution of landslides with the regional variation in lithology and mineralogy across the London Clay Basin to assess whether there is any association between lithology and the degree of susceptibility to landsliding.

The distribution of landslides within the London Clay Basin is shown in Figure 4.58, which broadly indicated an increase in the number of landslides to the eastern extremity of the outcrop where it forms a

Figure 4.58. The distribution of landslides in the London Clay Basin with respect to the proportion of montmorillonite clays.



coastline. Along this coastal fringe the number of reported landslides was comparatively high which reflects both the direct influence of wave action promoting landsliding through the undermining of the cliffs and also due to the extensive interest and research shown in this coastline, particularly along the north-Kent coast. These factors may well result in a small bias in landslide distribution to the east of the formation.

With reference to the findings of Burnett and Fookes (1974) they found an increase from west to east across the Basin in the total proportion of clay-size particles from approximately 50-74 per cent, and an increase in the per cent montmorillonite from 10-35 per cent. The proportion of illite was relatively constant and its distribution ubiquitous. The proportions of kaolinite and quartz were found to decrease towards the east. The CEC showed a similar increase similar to montmorillonite content. Additionally, calcium was distinguished as the major exchangeable cation and the montmorillonite clay minerals were thus assumed to be the less active variety. Burnett and Fookes (1974) related these findings with the engineering index properties and showed consistent increases in plasticity across the Basin from 45 per cent in the west and 60 per cent in the east. Similarly, there was a decrease in the undrained shear strength in the surface horizons and towards the east of the deposit.

With reference to Figure 4.58, isopleths of the proportion of montmorillonite are superimposed on the distribution of landslides. This clearly shows an increase in the number of landslides across the Basin particularly between the 20 and 30 per cent contour intervals. The current research has demonstrated that in coastal environments, and as a result of weathering processes, the proportion of montmorillonite in the

London Clay may reach as much as 63 per cent of the clay fraction. The average content for the entire coastal mudslide was 41.5 per cent and the dominant cation was magnesium.

The *in situ* unweathered values reported by Burnett in combination with the distribution of landslides in the GSL data-base, and the findings of this study, suggests a considerable increase in the susceptibility of London Clay to landsliding in the east of the formation which was best accounted for by an increase in the proportion of clay-size particles and montmorillonite clay minerals, and by an increase in the activity of chemical weathering processes on coastal cliffs.

4.63 Conclusions.

The findings of the last section revealed more expectable results than for the regional appraisal in section 4.61 which did not establish a direct increase in landslide susceptibility with montmorillonite content. The variability in results, however, could be explained as a function of montmorillonite type. Smectite clays saturated with divalent salts such as calcium will be more stable than the same clay saturated with monovalent ions (see section 2.312). Such physico-chemical processes contribute to the increased susceptibility of the London Clay to landsliding on coasts. Because the exchanged form of montmorillonite was not differentiated in the regional assessment of clay mineralogy such direct relationships with increased landsliding may not materialise, particularly when the true distribution of landslides is unknown.

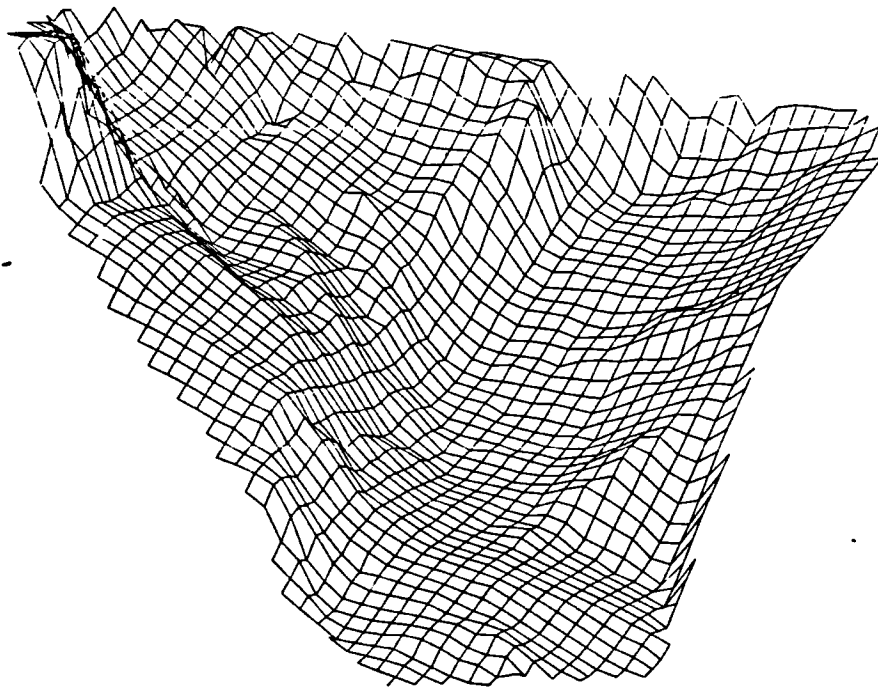
The results of the regional analysis was limited to the accuracies of two incomprehensive data-bases although it was concluded that the formations most susceptible to landsliding in southern and south-eastern England contained significant proportions of smectite clay minerals. The geological formations showing the highest densities of landsliding were associated with the highest per centages of micaceous minerals, and were normally distributed around a 40 per cent montmorillonite clay content.

A more detailed analysis of the distribution of landslides with respect to the lithology of London Clay revealed clear associations with the spatial variability of soil properties. There was an increase in landslide susceptibility with an increase in the proportion of clay-size particles and montmorillonite content towards the east of the Basin. Unfortunately, similar data were not available for the Wealden Beds and it was therefore impossible to draw regional conclusions of relevance to the Worbarrow site.

However, the results of this chapter have shown that the mudslides considered by this study contained significant proportions of montmorillonite clays within the weathered materials in comparison with values below the basal shear surface and for undisturbed samples. In principal, these findings demonstrated that the spatial distribution of physico-chemical properties within mudslides are fundamental to soil behaviour. Therefore, such properties should be considered a causal factor of the instability of shallow translational mudslides.

Chapter Five

THE DYNAMICS OF SEASONAL MUDSLIDE BEHAVIOUR



5.1 Introduction.

This chapter presents results from the field-monitoring programme and considers the dynamic nature of mudsliding. Although related to the static interpretation given in Chapter Four, the results presented here differ with respect to the variability of mudslide properties and processes in both space and time, while the former chapter was only concerned with the spatial distribution of the physico-chemical properties of materials. Thus, both chapters complement one another in the final interpretation of the physico-chemical behaviour of mudslides, fully discussed and presented in Chapter Six.

The Manor Lane and Worbarrow sites were used in the 'static' model, but only Worbarrow was fully monitored for the 'dynamic' assessment of mudsliding. However, periodic measurements of movement and pore water pressures were undertaken at Manor Lane for the purposes of stability calculations. These are summarized in Appendix 12 so that attention may be focused here on the Worbarrow site.

This chapter has three distinct parts. Firstly, Section 5.2, presents the results of the photogrammetric programme for the quantification of changes in mudslide form and extent throughout the study period. The properties and processes underlying such change were monitored at a greater temporal frequency with electronic sensors and automatic recorders. These results are given in the second part (section 5.3), and include the assessment of weather and climate (5.31), the soil water relations (5.32) and surface movement (5.33). Also considered in the former sub-sections are the results of chemical analyses of rainfall and pore water solutions.

Thirdly, section 5.4 contains the results of laboratory simulation tests which attempt to relate the measured fluctuations in atmospheric and groundwater chemistry to slope instability. Since the method of simulation is new to geomorphology and engineering geology, control tests were performed on pure clay mineral systems (5.41). The effects of monovalent and divalent chemical states upon the shear strength of pure clays are assessed in section 5.412. Natural samples from Manor Lane and Worbarrow Bay were then used in test under a range of sea-water concentrations (section 5.42), simulating actual fluctuations in pore water chemistry measured in the monitoring programme. Changes in shear strength were found to be dependent on pore water chemistry.

In conclusion the properties most important in explaining seasonal mudslide behaviour are isolated for further discussion in Chapter Six.

5.2 Morphological change and mudslide development:

5.21 Photogrammetric analyses:

During this study three photogrammetric surveys (epochs) were undertaken on the 7th March 1986, the 5th September 1986 and the 27th May 1987. Detailed planimetric, profile and contour analyses were used to assess the degree of change in mudslide form and extent.

In section 3.22 the importance of the conditions and quality of survey in maintaining the optimum accuracy of the analyses was discussed in detail. In this study it was found that sufficient quality was achieved for all surveys with the exception of the September 1986 epoch; conditions for

photography on this date were not ideal, which meant that the resultant exposures were grainy with little contrast. However, sufficient information was extracted for use in locating equipment and in defining the morphology of the mudslide, but the quality proved too poor to extract points for profile and digital terrain modelling (DTM).

The photogrammetric results discussed in this section are divided into a planimetric comparison (section 5.211), surface profile change (5.212), contours and DTM of difference (5.213), and the assessment of instrument and target locations between epochs (5.214). The majority of the findings are presented visually, with accurately determined measurements to aid the discussion of results.

5.211 Planimetric comparison.

With reference to Figure 5.1, the morphology of the mudslide is plotted for each epoch. Areas of change were noted for the two periods encompassed by the surveys. Between March and September 1986 little change was recorded, but during September to May 1987 significant alterations to the source and toe-slope extents were measured.

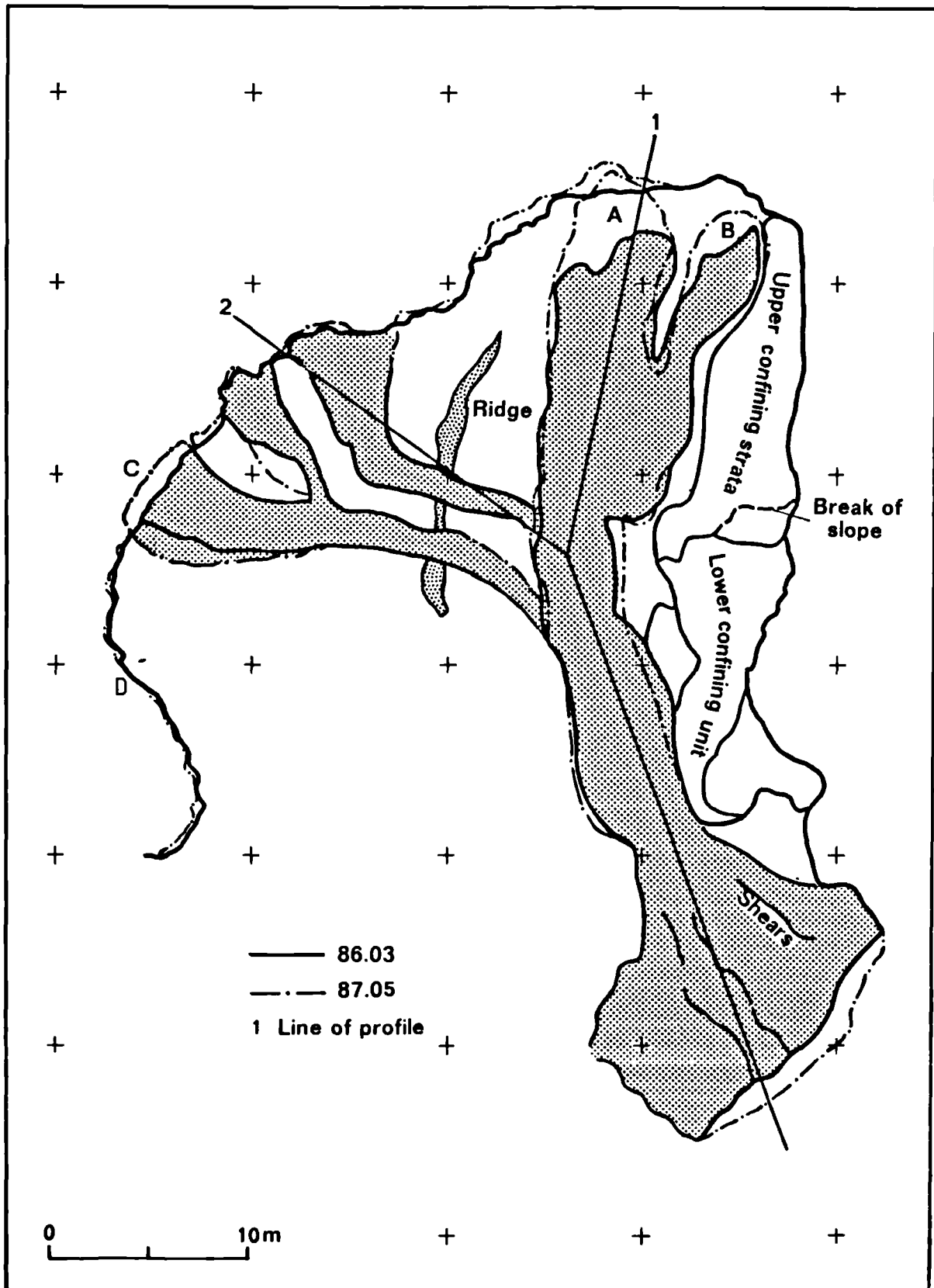
During the first period, only a small element of weathering and erosion of the back-cliff was assumed to have occurred. The boundaries of the mudslide plotted for the first two epochs corresponded to a high degree, especially in the source and accumulation zones. The limited change in form might have been expected since the dry summer months are known to be less active (see section 1.4).

Between September 1986 and May 1987, the form of the mudslide changed as a result of the recession of the back-cliff, the advance of the toe and also slight alterations in the position of the lateral shear surfaces. Both mudslide source units extended inland amounting to a maximum of 4.76 metres ± 5 cm for the most active unit (see A in Figure 5.1), and 2.25 m ± 5 cm for source unit marked 'B'. Much of this change occurred in single events (see section 5.33) rather than uniformly in time, and would have exposed the cliff-top to critical pre-failure conditions. The extension inland may not necessarily be permanent since the debris which loaded the back of the mudslide following cliff-failure increased the length of the source area. After settlement and mudslide movement the size of the source unit may decrease slightly from the overall net-gain.

Two areas of back-cliff showed recessions of greater than 1 m between the latter epochs 8-month winter period. The cliff-edge to the rear of the main source unit (A in Figure 5.1) receded a maximum of 1.38 m ± 5 cm and the cliff towards the rear of the perched mudslide system by 1.13 m ± 5 cm (C in Figure 5.1). Such development was rapid but by no means extreme, and it was considered that the cliff-top recession generally occurs by a series of jumps of up to several metres or more following cliff-failures triggered by the undermining of the slope through mudsliding. Other areas of cliff-top showed very little or no change such as at 'D' in Figure 5.1, areas dominated by the resistant beds of sandstone that enclose the mudslide 'corrie-like' complex.

Coincident with the recession of the back-cliff, the accumulation lobe was found to have advanced seaward by a corresponding distance of 1.38 m ± 5 cm. This coincidence was not considered to be of any great significance because the position of the toe may have been greater or

Figure 5.1. Morphological change at Worbarrow Bay revealed in plan by photogrammetric analyses between March 1986 and May 1987.



less at the time of survey dependent on the severity of toe erosion. This does however suggest that the response of the system to change was not only sensitive but in dynamic equilibrium. There was no apparent widening of the lobe during the study period since the most active area was confined to the central zone.

The lateral shear surfaces showed a greater degree of change between the second and third epochs which was thought to be a direct reflection of the greater activity of mudsliding during the winter months. Apart from the extension of the lateral shears in the source units there was an apparent widening of the mudslide in this zone probably arising from the greater abrasion and attrition of rocks and particles at the shearing surfaces. The most significant extension of the lateral shear surface occurred about mid-slope where the mudslide was constricted. The feeder track measurably widened by a maximum of $0.88 \text{ m} \pm 5 \text{ cm}$.

In other areas, a change in the position of the lateral shear surface resulted in the narrowing of the mudslide track. Below the area in which the lateral shear was noted to have widened, the same active shear surface was found to have retreated into the mudslide by $0.75 \text{ m} \pm 5 \text{ cm}$. The latter change was associated with the confluence of the perched mudslides with the main track.

The changes in width were confined to the seaward side of the mudslide with the opposite lateral shear surface showing little or no change. This was due to the resistant *in situ* rocks confining this edge of the mudslide. The seaward side was inherently more unstable and subject to change although overall the form of the mudslide would appear to be in steady state, the changes being limited to the straightening of the feeder track with some widening.

5.212 Profile change.

Two pre-defined skew profiles were accurately measured using the techniques discussed in section 3.222. With reference to Figure 5.1, the plan of both profiles was dog-legged owing to the non-linear shape of the mudslide tracks. A point of inflexion was defined between slope units 2 and 3 towards the base of the translational zone. One profile was measured down the entire length of the main mudslide and another down the perched system intersecting the former at the point of inflexion. Both profiles were compared at two epochs in March 1986 and May 1987 to assess the degree of change in surface elevation or mudslide volume.

Figure 5.2, contains the main surface profiles for each epoch. As was identified in the planimetric comparison relatively little change in elevation was assumed to have occurred over the summer months. During the winter period changes in profile were noted in response to the recession of the back-cliff and advance of the mudslide toe. Values of these changes were given in the previous section. The plot shows additional information not revealed in plan, such as an increase in volume below the cliff-top, a reduction in volume of the upper feeder track and a marked loss at the rear of the accumulation zone.

The source unit level had risen by 0.61 m \pm 5 cm in the third epoch probably as a consequence of loading and expansion of the disturbed materials. About mid-slope a reduction of 0.9 m \pm 5 cm in the level of the mudslide was noted for the same epoch which was thought to have arisen following the 'unloading' of the lower slope significantly advancing the toe across the beach. The surface profiles of the perched mudslides (Figure 5.3) show similar relationships with an increase in

Figure 5.2. Change in surface profile of the main mudslide at Worbarrow Bay between March 1986 and May 1987.

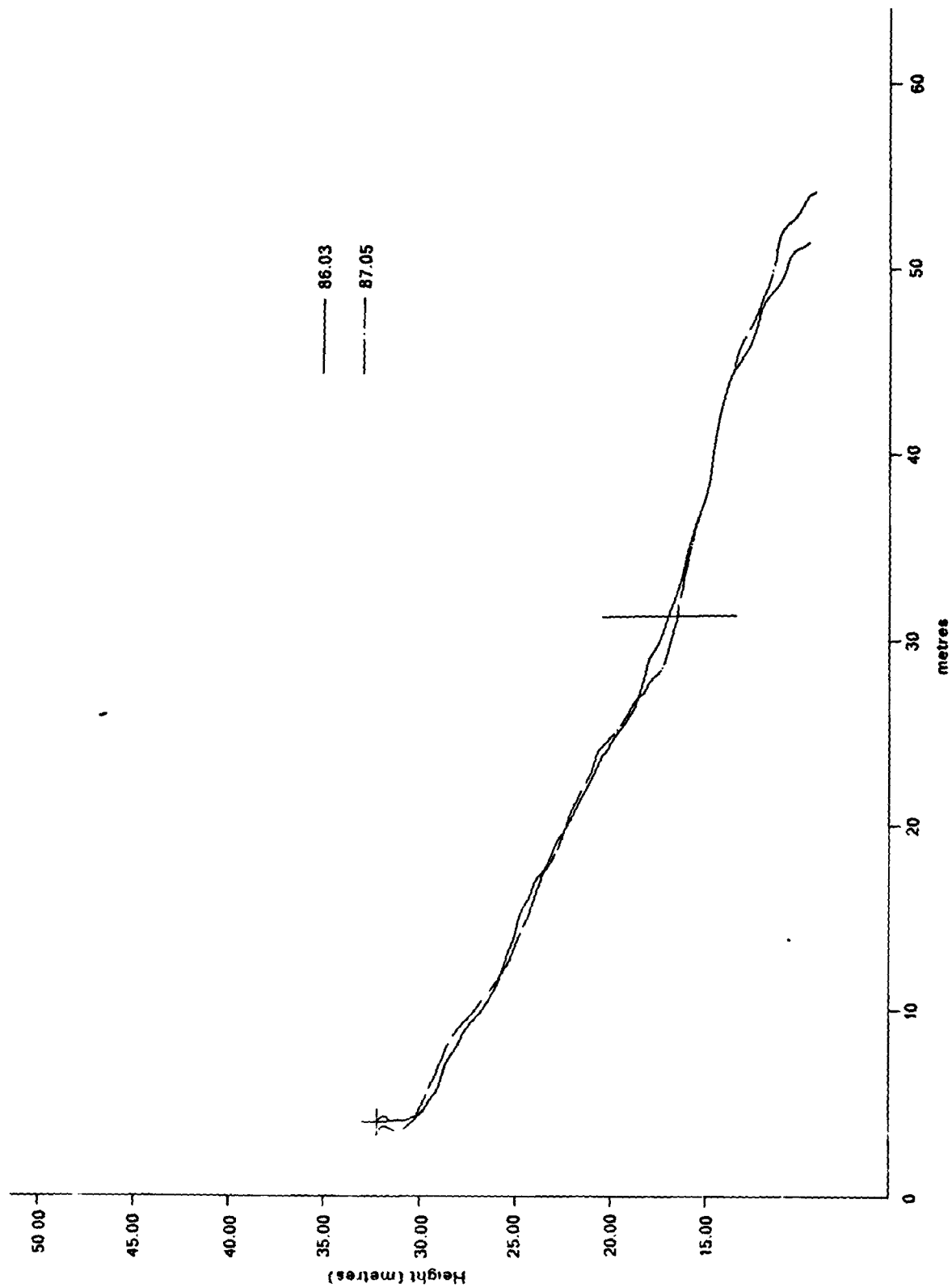
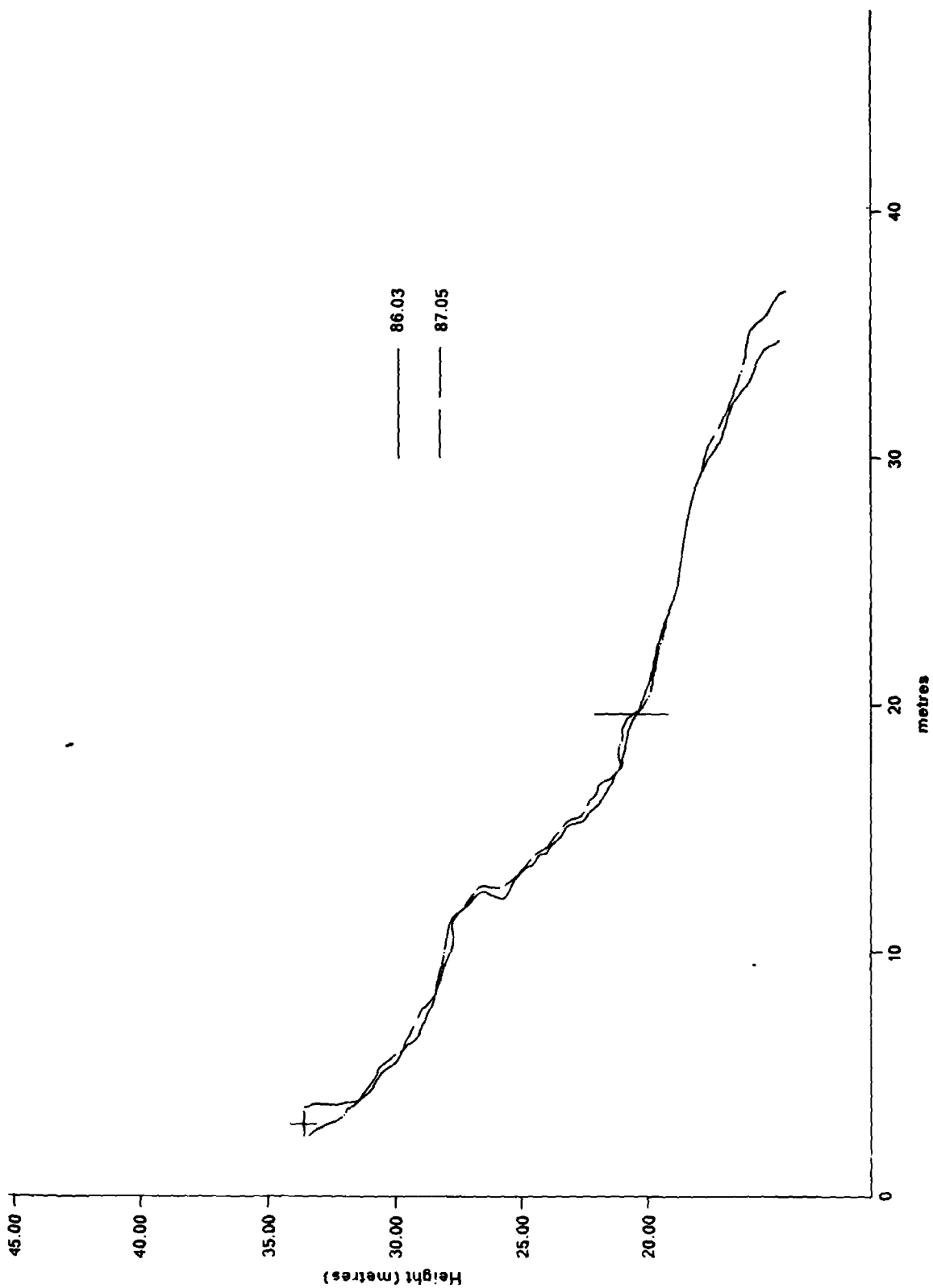


Figure 5.3. Change in surface profile of the perched mudslide system at Worbarrow Bay between March 1986 and May 1987.



level at the base of the back-cliff indicative of loading, a depleted zone towards the resistant sandstone strata and an increase downslope to the point of inflexion indicating a second zone of loading below the perched system.

The surface profiles suggest that the Worbarrow mudslide has two critical areas from which movements may be generated: a lower slope sector incorporating the accumulation lobe and a zone of loading at the base of the feeder track, and secondly an upper slope sector incorporating the source units and the translational zone. It was not possible on the basis of this information to conclude whether failure was normally generated by the unloading of the lower slope or by loading in the source region or both, for this requires continuous field monitoring.

5.213 Contours and DTM of difference.

Point and string data were used to create a DTM for the March 1986 and May 1987 epochs using software discussed earlier in section 3.222. A DTM surface was established from which contours could be computed. A typical DTM surface is shown in the isometric plot reproduced on the frontispiece of this chapter, clearly indicating variations in elevation, mudslide form and locating breaks of slope. Contours were plotted from the surface at a variety of scales but it was found that little additional information was gained by using a contour interval smaller than 0.5 m. The contour plot for the 1986 survey shown in Figure 5.4 gives a reasonable representation of site morphology. The dominance of the main mudslide is clearly shown, along with the closely spaced contours of the sandstone strata separating the perched system on the landward side to

Figure 5.4. Contour map of the Worbarrow site from the March 1986 DTM.

MARCH 1986
CONTOUR INT. = 0.5M

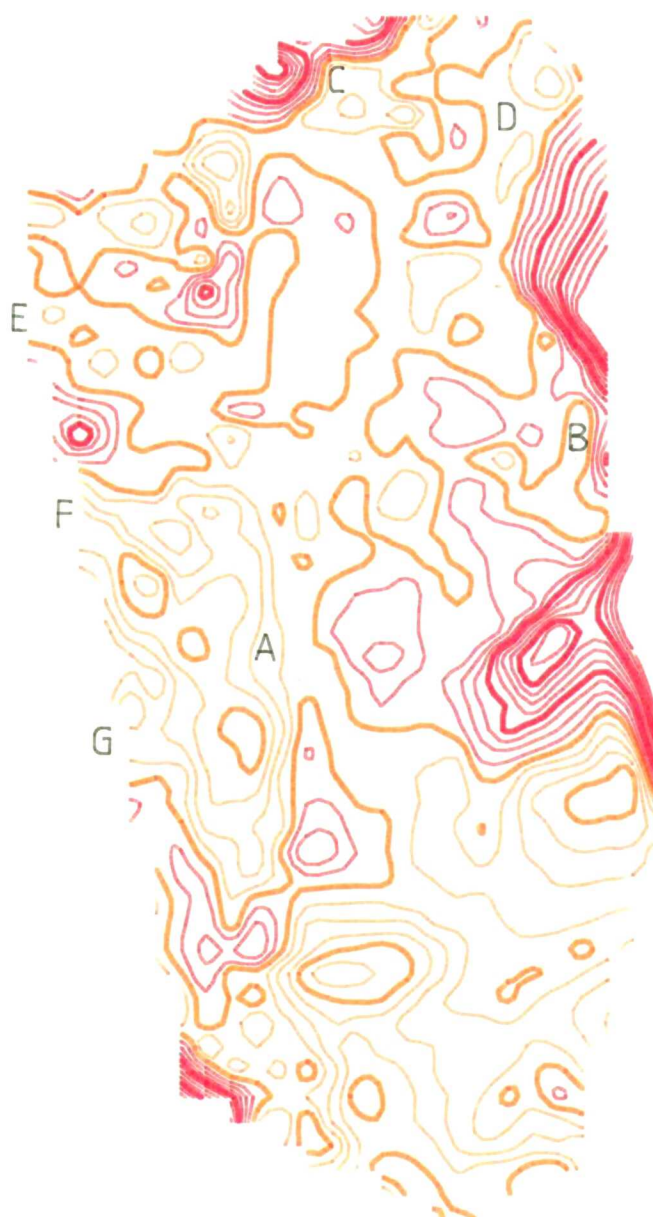


the north-west. The mudslides may be seen to have smoother, well-spaced contours with concave and convex forms, suggesting areas of translation or erosion and deposition or toe-bulging, respectively. By comparing the two epochs it was possible to identify areas of erosion and deposition with respect to the form of each contour. However, this is more accurately achieved by computing a DTM of difference.

Recent advances in photogrammetric hardware and modelling procedures allows for the subtraction of DTM surfaces. The resultant DTM of difference (Figure 5.5) represents a direct change in surface form equivalent to the magnitude of surface process or erosion, within the tolerance of the model. The change plotted in Figure 5.5 is directional the contours representing the total change in surface volume between epochs: the red contours represent negative changes in elevation while the brown contours positive volume changes. The first bold brown contour between these limits represents zero change.

The plot clearly delimits the mudslide which shows an increase in volume ranging from 0 - 1.25m; the majority of the feeder track showed only small increases in volume in comparison with the bulging of the lobe by up to 1.25m. The negative volume changes at the edges should be treated with caution because spurious points seen in the contour plot will also give rise to biased changes in volume. Areas within the complex illustrate locations where mudslides are confined by the underlying geology, such as at 'A' (Figure 5.5), and by the near-vertical coastal cliff to the south at 'B'. The former example is less clear because mudslides overflow the resistant sandstone strata onto the main mudslide.

'DTM OF DIFFERENCE' OF
WORBARROW MUDSLIDE
-MARCH 1986 AND MAY 1987



CONTOUR INT. 0.25M

10.0 METRES

FIGURE 5.5

The two main sources (marked C and D) are separated by an area of zero change, and those of the perched system may be recognised (E, F and G). The cliffs behind these regions similarly show significant change but mainly due to the recession of the cliff-edge. The active feeder tracks (1, 2 and 3) are characterized by uniform volume change and are generally uninterrupted by contour lines. The contours of the accumulation lobe (4) are also uniform in nature and show an increase in the spacing between lines. In contrast, the edges and confined areas of the system have non-uniform and closely spaced contours.

5.214 Target and instrument fix.

The potential for using analytical photogrammetry in monitoring landslips was realised in target analysis. Bentley (1985) has expressed the usefulness of the measurement of surface displacement rates in the investigation, prediction, management and control of slope instability. The accurate survey of targets, peglines or ground stations are easily achieved by this technique. The cartesian components of movement were determined to plot the resultant horizontal displacement.

Targets were installed over the entire Worbarrow mudslide and along with the location of equipment clusters in each slope unit, their positions were initially fixed and compared at different epochs. Unfortunately, at the time of processing software had not been sufficiently developed to enable the direct computation of movement vectors, hodographs of velocity or strain rates. However, the calculation of changes in the location of designated targets and instrumentation can be made from the plan-projection of the slope and hand calculations of the cartesian coordinates. This was undertaken for the second survey period from September 1986 to May 1987 to assess the cumulative displacement of the

mudslide and to account for the shift in positions of monitoring and sampling equipment.

With reference to Figure 5.6, the initial positions of the targets are plotted for the 5th September 1986; the equipment clusters are shown in Figure 3.11. By the 27th May 1987 the majority of the targets had moved considerably from their original positions and some were even lost. The identification of the remaining targets was found to be easiest in the field, rather than from the photographs. The loss of targets meant that the subsequent analysis could not be as detailed as hoped. Additionally, since the rates of movement encountered between surveys were relatively high, equipment had to be relocated to remain representative of each slope unit, so that they could no longer be used in the analysis of surface movements. An increase in the frequency of survey would have averted this loss of detail, but was not possible due to limited resources and time.

Figure 5.6, shows the final locations of the targets at the end of the field-monitoring programme, and Table 5.1 summarizes the total displacements of each target in comparison with the continuous recordings (section 5.331) where available. It was noted that the fixed points of reference, used as control targets, showed no change. In addition, the clusters of sampling and monitoring equipment within each slope unit were kept within a 4 m sphere of influence of their original positions. In actively moving sections of slope the equipment required relocation 2 or 3 times between December and April, but in other areas their position remained within the pre-defined limit.

Figure 5.6. Movement trajectories of targets installed at Worbarrow.

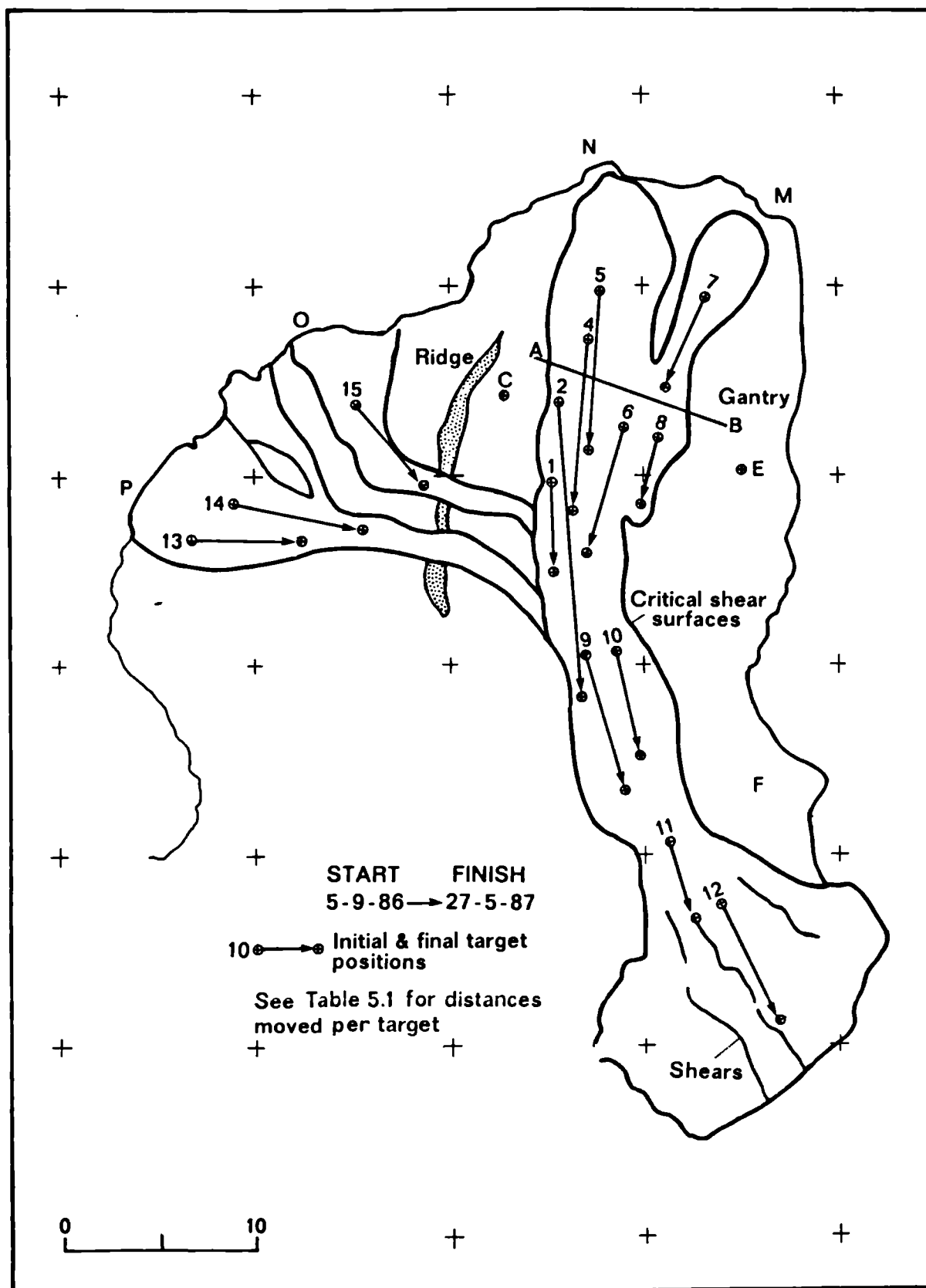


Table 5.1. Summary of target movements between September 1986 and May 1987.

PHOTOGRAMMETRIC ANALYSIS		CONTINUOUS DATA RECORD	
Target # ¹	Distance (m \pm 5 cm)	Pin # ¹	Distance (m \pm 1 cm)
1	4.87	A	0.00
2	15.90	2	16.08
3	*	3	19.98
4	9.23	4	9.88
5	8.72	5	7.21
6	7.18	6	6.21
7	5.13	7	3.95
8	3.59	B	0.00
9	7.69		
10	5.90		
11	4.36		
12	6.92		
13	5.64		
14	6.91		
15	5.65		
C, E, F, M, N, O, P	0.00		
D	*		

* Lost or Buried target : refer to Figure 5.6 for target locations

¹ Target and pin numbers are comparable for area of mudslide only

Convention: letters- control targets; digits- designated movement targets

The movement of targets from different areas of the mudslide revealed that the cumulative surface movement was far from uniform. The maximum displacement recorded was 15.90 m \pm 5 cm by target 2 down the central part of the feeder track. On either side movements equalled 4.87 m and 7.18 m (\pm 5 cm) for targets 1 and 6, respectively. Similar values were recorded for the base of the feeder track and the active portion of the accumulation lobe amounting to 7.69 m and 6.92 m (\pm 5 cm), respectively. Target 5, located in the main source unit, recorded 8.72 m \pm 5 cm of movement between both epochs, while 5.65 m \pm 5 cm of movement occurred in the feeder tracks of the perched mudslides.

These values are likely to have underestimated the true totals since they are measured horizontal distances and do not take into account the gradient of the mudslide. Although they reflect the location and activity of slope instability this was not sufficient to identify the mechanisms responsible for slope movements for this requires the use of electronic sensors and recorders to improve the temporal sampling framework. The non-contact photogrammetric results corresponded to within 10 per cent of movement estimates from the continuous electronic recordings.

From a total of three surveys it was possible to derive a wide variety of accurate planimetric, profile and contour data to assess morphological change consequent upon seasonal mudslide behaviour. The computation of a DTM of difference represented the magnitude of process or erosion throughout the study period. Additionally, it was possible to measure surface movements from installed targets. The necessary field-work and data processing was usually completed within 5 days for each epoch, but this will normally depend on the scale and purpose of the analysis required.

It is emphasised that the application of this new technique to monitoring mudslides holds considerable promise for locations where accessibility, scale or vandalism present a problem. It avoids the need for regular maintenance or electronic recording equipment and extensive field surveying time, and records a permanent computerized record for future consultation. With further improvements to the models and software used in data processing, analytical photogrammetry could provide accurate estimations of the stability of landslides using velocity and strain-rate vectors which would be of considerable benefit to the geomorphologist and geotechnician for the interpretation, prediction and management of slope instability, especially for large landslides.

5.3 Field monitoring.

The findings of the field investigations are presented at three time-scales: a monthly summary for the purpose of isolating broad cycles of change, a daily summary, and the continuous record used to monitor the critical parameters promoting seasonal mudsliding. With reference to the monitoring design outlined in section 3.33, it was not possible to measure all parameters at each time-scale. A complete monthly summary, is however, provided for comparison between all parameters. Both soil moisture and the chemistry of rainfall and ground water were only monitored at weekly intervals, sufficient to return a monthly average, although the greater resolution of data was included to clarify the discussion of results.

As a consequence of the shorter sampling interval there was a vast increase in the size of the resultant data-base and the record is too large to warrant inclusion here. Thus, the form of analysis adopted in

this chapter includes the broad inspection of the monthly summary to isolate seasonal cycles of change, with reference to the daily summary for the recognition of individual events. For selected parameters, the events identified from the daily summary are studied in greater detail from the continuous data-base when considering the sensitivity of the causal factors of mudsliding. Wherever possible the results are related to a previous study of the site (Allison, 1986) although most of these data were unavailable, nor presentable at the same time-scales, at the time of writing.

5.31 Weather and climate:

5.311 Rainfall.

The climatic parameters of most importance in this study were isolated and discussed in section 3.321. The total monthly rainfall throughout the study period from October 1985 to May 1987, is presented in Figure 5.7. The 20 month record shows a clear seasonal climatic trend with maximum rainfall occurring in the months of November and December, and minima in February, June and July. There are slight fluctuations to this trend. The 1985 winter maximum of 144 mm occurred in December, but in 1986 the peak winter rainfall occurred in November with a total of 123 mm. There are sharp minima following each winter maximum which coincided with cold spells. Values of rainfall during this period are unreliable since snow overfilled the gauges. Attention is also drawn to the large rain total recorded in August 1986 the events of which are considered in greater detail in section 5.322. The climatic cycles revealed in this survey vary little from those measured at the same site by Allison (1986) during 1983 and 1984, but the latter could not be included because the data were not presented as a monthly summary.

Figure 5.7. Total monthly rainfall throughout the study.

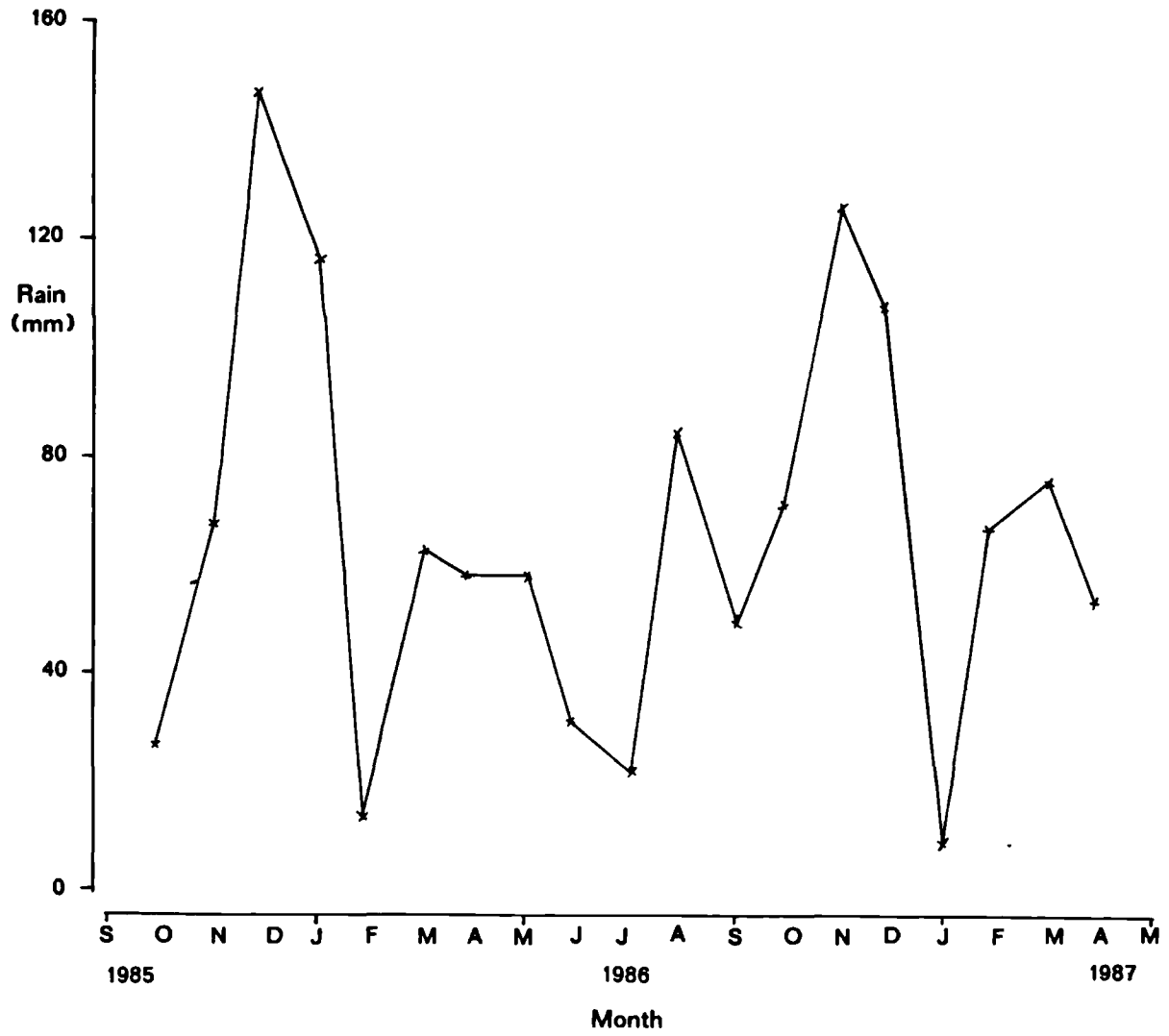
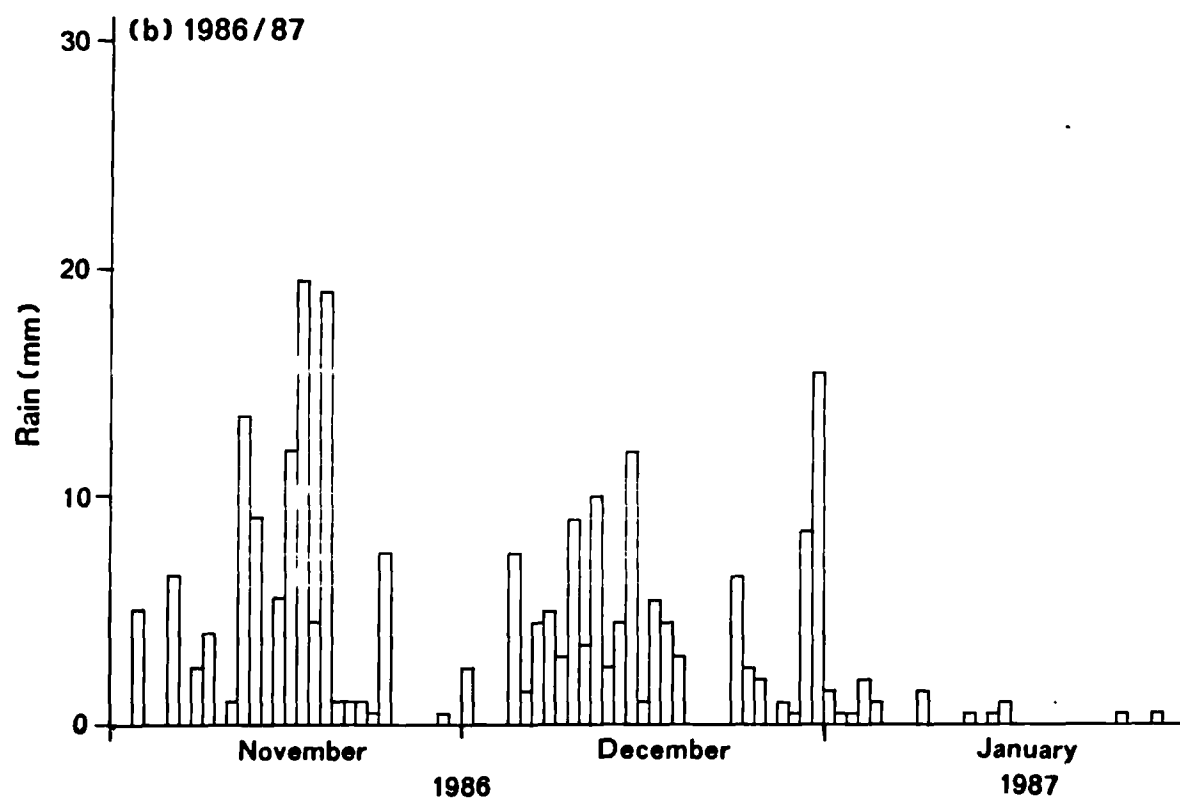
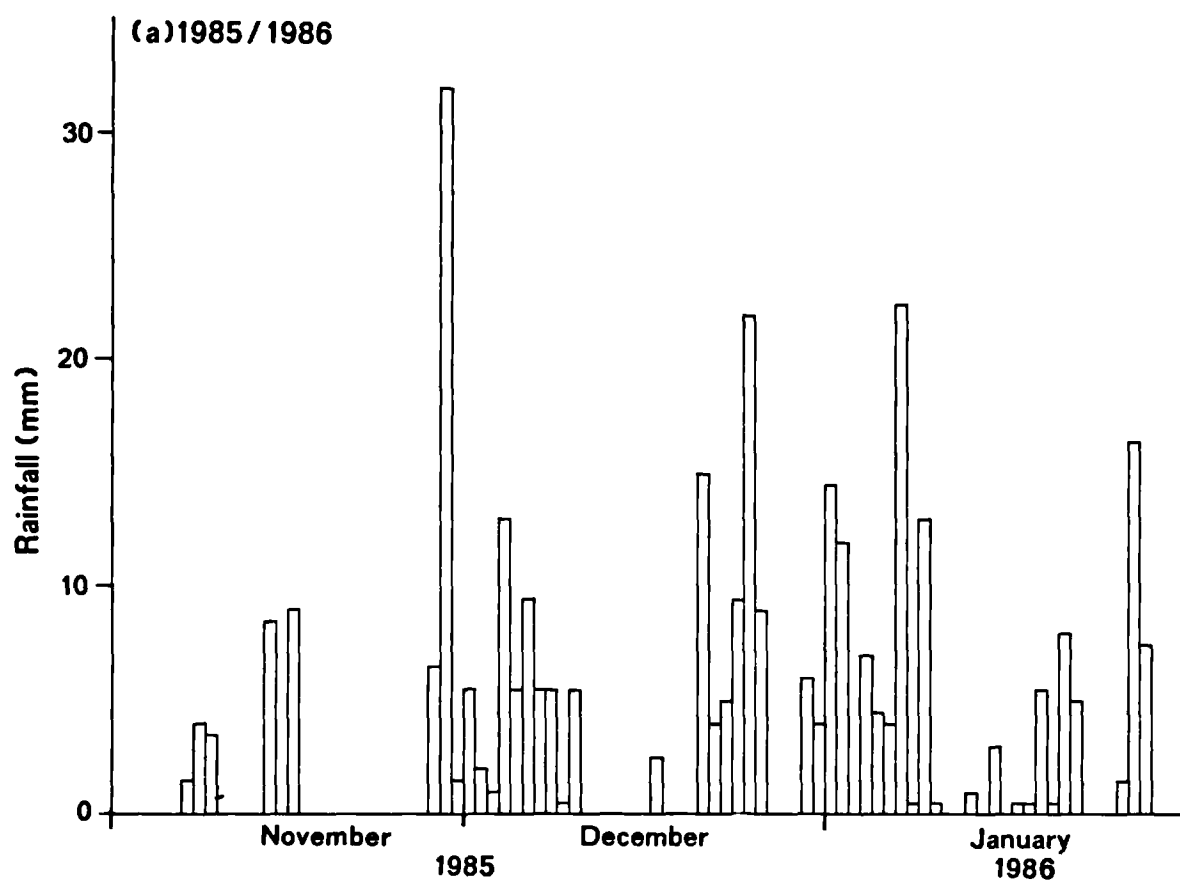


Figure 5.8. Daily rainfall histograms of peak winter rainfall in the 1985/86 and 1986/87 seasons.

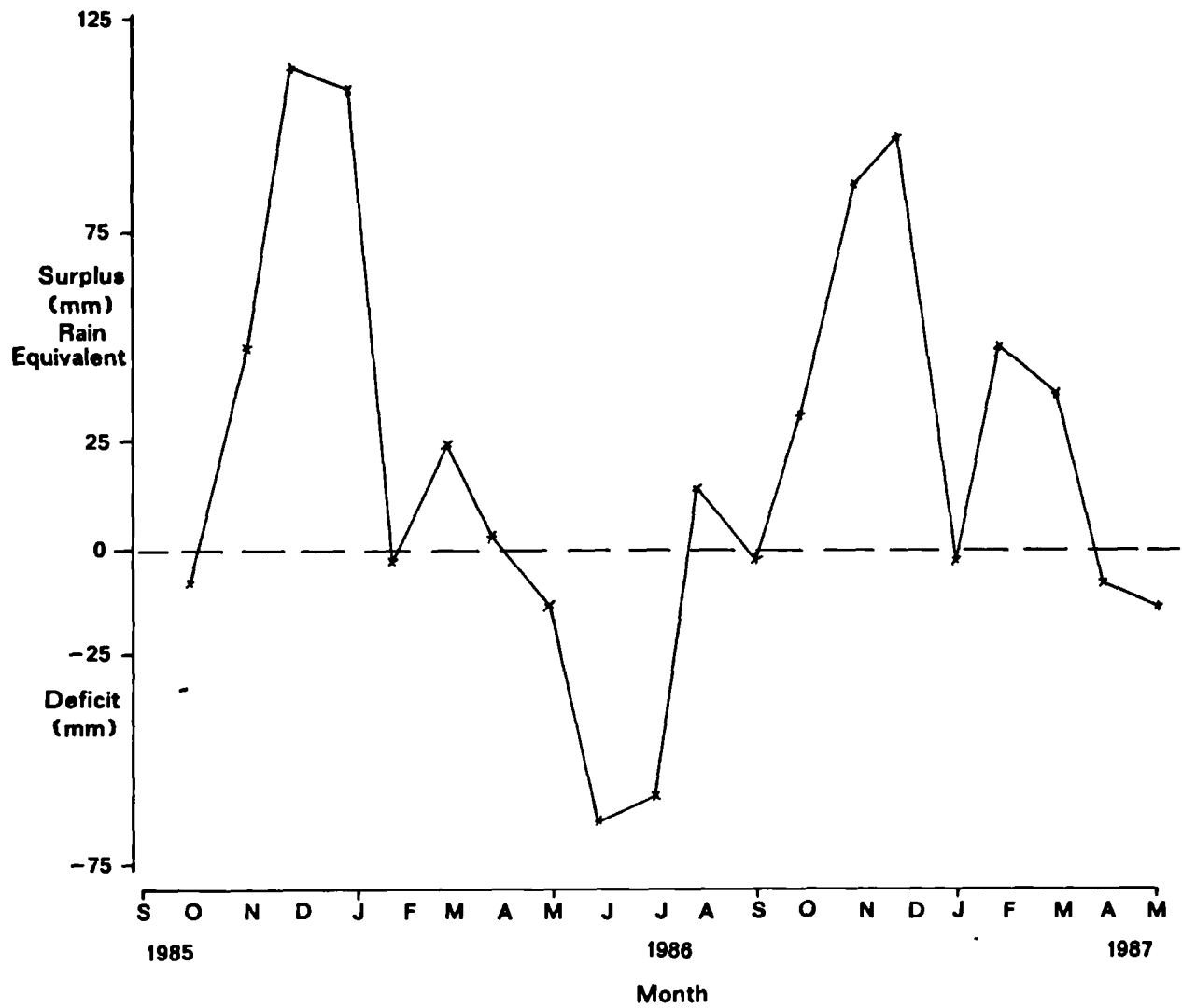


With reference to Figure 5.8, daily rainfall histograms are presented for the two winter maximums. The plot for November 1985 to January 1986 was characterised by three major rainfall events, each containing a daily maximum in excess of 20 mm. The first event began on the 28th of November and lasted for 13 days reaching a peak intensity of 6 mm per hour on the second day. The duration of the second event was 6 days and attained a peak intensity of 7 mm per hour on the 25th December. The third principal rain period lasted 12 days with a peak intensity of 5mm per hour. These three events accounted for 249 mm of rain in 44 days, 30 per cent of the annual total. The plot for November 1986 to January 1987 contrasts with the previous winter because the highest daily maximum was only 19.5 mm. Three major events are again recognised which accounted for 235 mm of rain in 66 days. The duration of the latter events were 14, 15 and 12 days respectively, which suggested that the duration of rainfall as well as the intensity should be considered in the analysis of seasonal mudsliding in temperate climates.

5.312 Net hydrological flux.

The difference between rainfall and evapotranspiration, termed 'effective rainfall' (ER) or the net hydrological flux, provides a more useful parameter than rainfall when relating climatic events to slope movement because it is closely related to the soil water relations. The net hydrological flux is calculated as the difference between the rainfall and the Penman estimate of evaporation based on the heat budget and aerodynamic parameters. The resultant total monthly surplus and deficits further emphasises the seasonal climatic cycle.

Figure 5.9. Net monthly hydrological flux during the study.



With reference to Figure 5.9, a very marked water deficit occurred from April to August 1986 amounting to -64.1 mm, surrounded by two winter surpluses. The magnitudes of the latter peaks show that there was a greater surplus of 113.3 mm in December 1985 compared with 98.2 mm in December 1986. It was important to realise, however, that these results were not calculated for the soil and that time-lags probably exist before the corresponding peaks affect the ground water regime of the mudslide; but as far as atmospheric conditions prevail, December was clearly the most significant contributor to the seasonal instability of mudslides. Indeed, mudslide displacements were found to be greatest for the larger winter surplus recorded in December 1985 than for the lower positive flux in December 1986. Thus, the likely effects of water surpluses and deficits upon movement suggests that more than just the rainfall parameter ought to be considered in studies of this nature.

5.313 Wind speed and direction.

The wind directions recorded at Worbarrow show a marked bi-directional form (Figure 5.10) prevailing south-south-westerly with less frequent winds from the north-north-east. The axis of the Tyneham valley backing the landslip was responsible for funnelling the northern winds towards the site; the latter winds are thus site-specific whereas the south-westerly winds are a well known feature of the southern coasts of Britain. They are responsible for many storms causing severe marine erosion and the shaping of the coastal cliffs, and the deposition of considerable amounts of sea-spray.

Figure 5.10. Prevailing wind directions at the coastal cliffs of Worbarrow Bay.

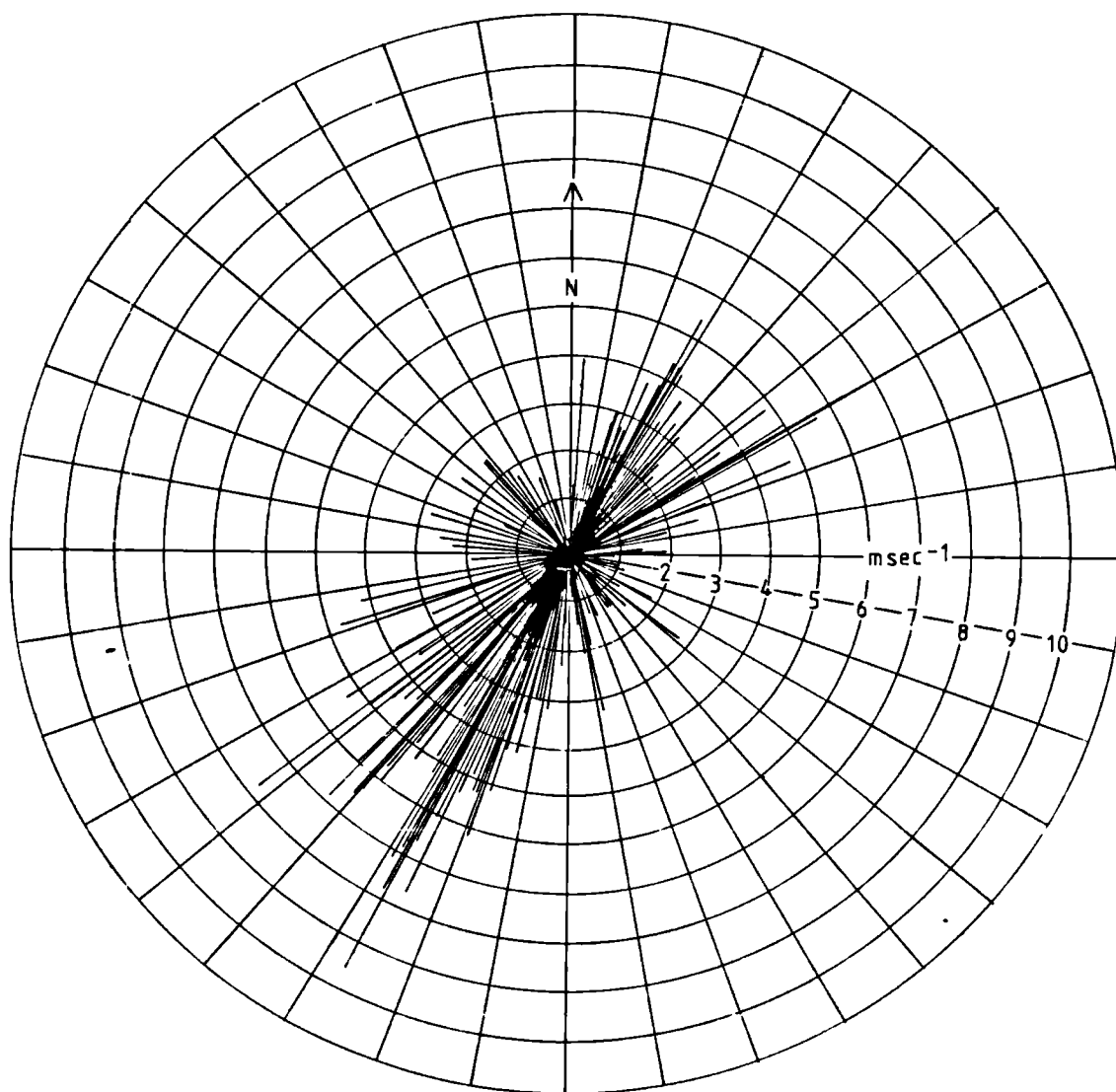
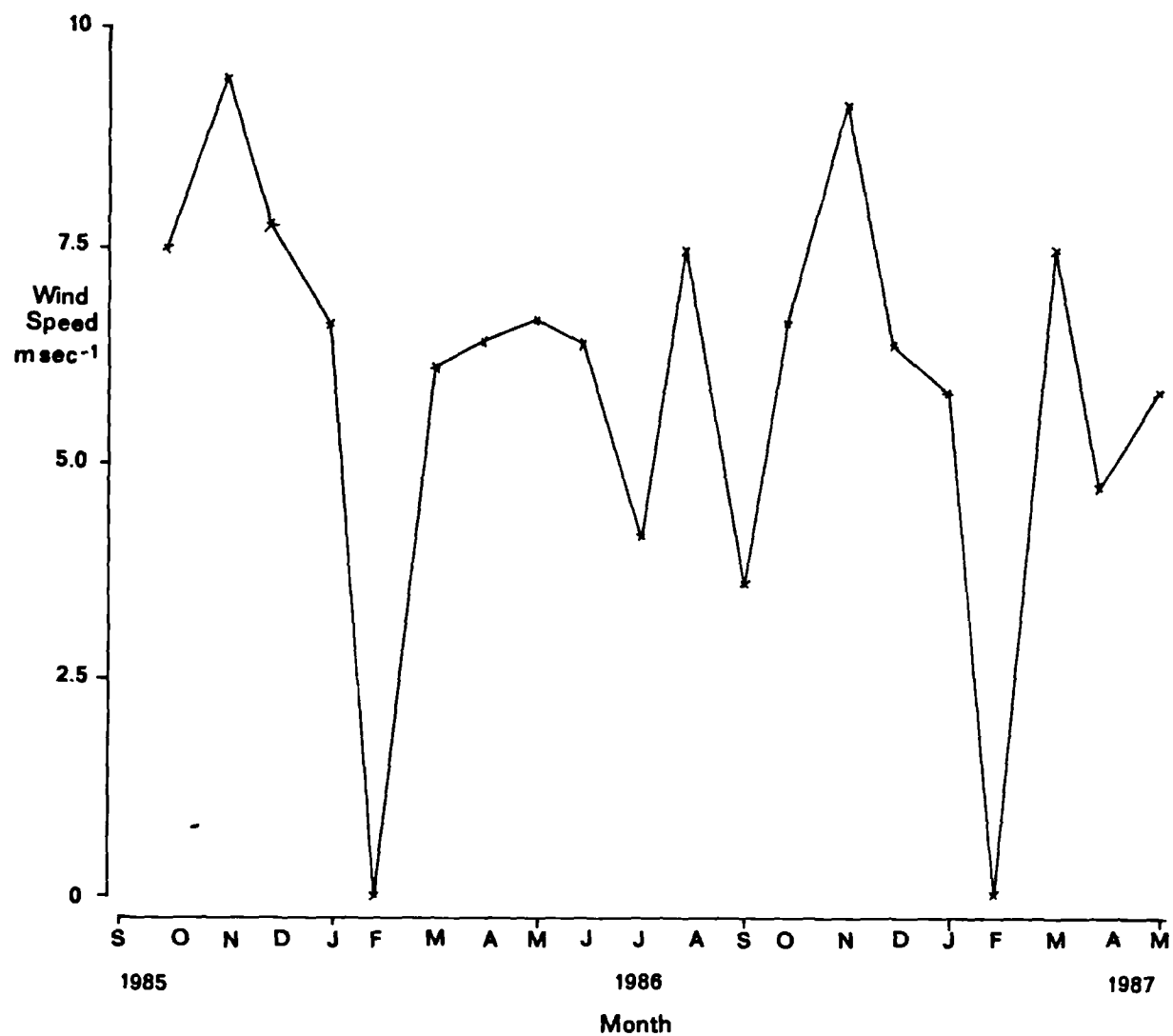


Figure 5.11. Maximum monthly wind speed during the study.



The maximum monthly wind speed during the study is plotted in Figure 5.11. There was a high degree of correspondence between the peaks and the seasonal climatic cycle, with maximum south-westerly wind speeds occurring in November, equalling 9.4 and 9.1 msec^{-1} in 1985 and 1986, respectively. The mean wind speed in the summer months was 5.9 msec^{-1} , which suggested that the cliffs were more susceptible to weathering and erosion during November and December from the combined effects of both rainfall and strong south-westerly winds. Rather surprisingly, no wind was recorded throughout either February 1986 or February 1987. Both coincided with cold spells and it was not possible to discount the possibility that the wind vane became frozen during these periods.

5.314 Salt deposition.

The deposition of salts on the coastal cliffs might be expected to show a similar seasonal climatic cycle to rainfall and wind speed. With reference to Figure 5.12, the total monthly concentration of salt deposited on the Worbarrow cliffs is plotted from data collected throughout the study period. The plot shows clearly defined peaks of 36 and 32 g/m^2 in December 1985 and November 1986, respectively, in contrast to the summer average where less than 5 g/m^2 was deposited on the coastal slopes. The composition of salt deposited on the cliffs is detailed in Table 5.2 along with the composition measured for pore water (section 5.323) and sea-water. Each solution was dominated by chloride salts and because the proportion of the constituents closely corresponds to that of sea-water it was assumed that the chemistry of rain and pore water derived from the latter.

Figure 5.12. Monthly weight of salt deposited on the coastal cliffs at Worbarrow Bay.

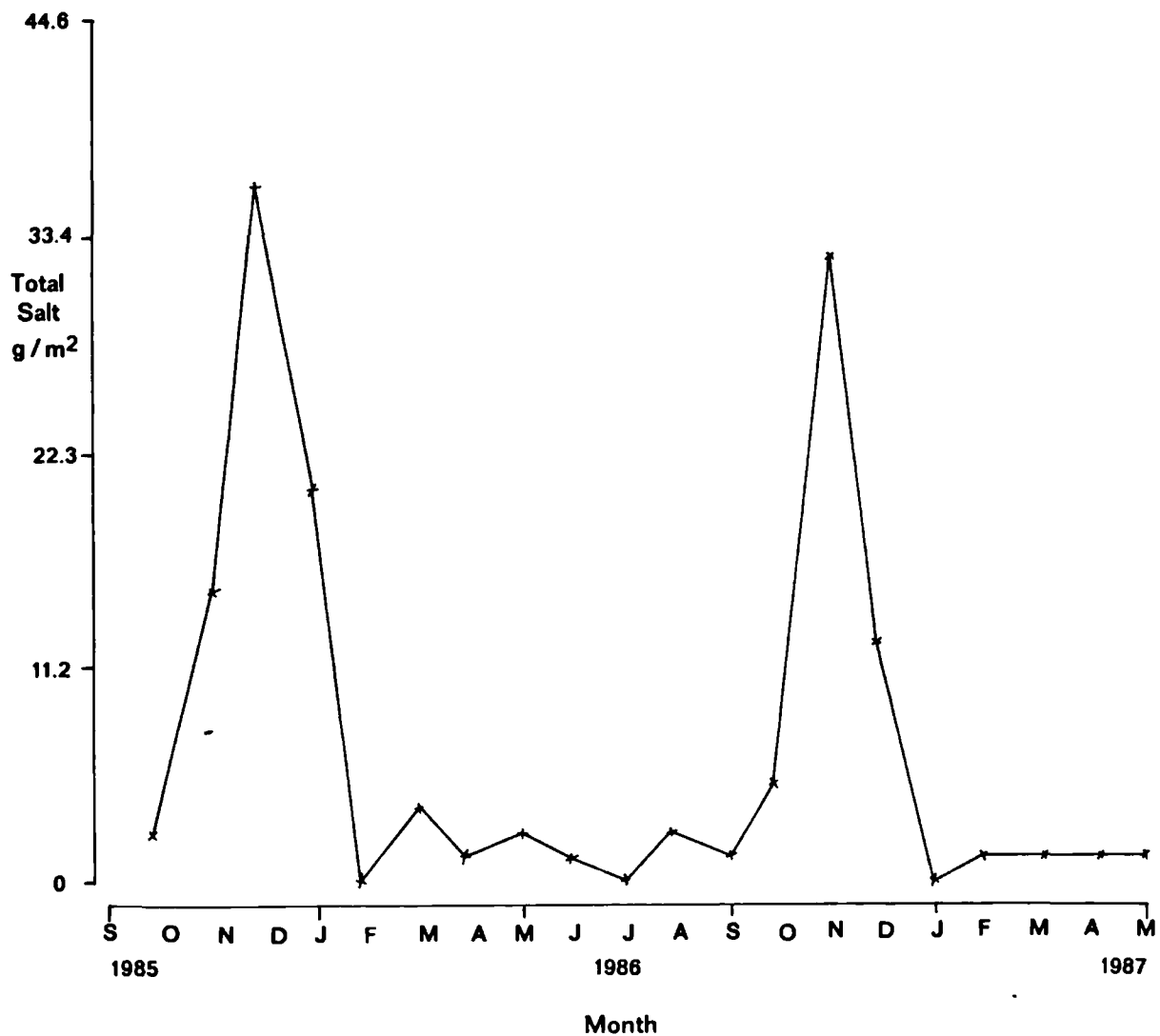


Table 5.2. Chemical composition of rainfall, interstitial pore water and sea-water measured at Worbarrow Bay.

Ion species	Rain water ¹		Pore water ²		Sea-water ³	
	mg/litre	%	mg/litre	%	mg/litre	%
Na ⁺	938	29.1	585	14.4	9617	28.9
K ⁺	35	1.1	20	0.5	399	1.2
Mg ²⁺	130	4.0	110	2.7	1272	3.8
Ca ²⁺	48	1.5	157	3.9	403	1.2
Cl ⁻	1734	53.8	2973	73.1	18980	57.0
SO ₄ ²⁻	338	10.5	222	5.5	2649	8.0
TOTAL	3223	100.0	4067	100.0	33320	100.0

Compositions based on the principal dissolved substances in sea-water

¹Rainfall composition in salt gauge #1 on the 28th November 1986

²Pore water composition collected in pore water sampler #5 on 9-1-1987

³Sea-water sample obtained from offshore at Worbarrow Bay on 29-8-1986

As might be expected peak salt deposition coincided with the winter maximum rainfall and wind speeds. Although the incorporation and concentration of salt entrained in precipitation was directly related to the occurrence of strong winds, the total amount deposited on the cliffs will also be influenced by the amount of rainfall. Thus an index of the 'effectiveness' of salt-laden south-westerly precipitation was derived based on the following calculation:

$$E = \frac{WD * WS * V}{D}$$

where: E = the 'effective' south-westerly salt precipitation in units of millimetres of rain per msec⁻¹ per month⁻¹

WD = the number of south-westerly windy days

WS = mean monthly south-westerly wind speed (msec⁻¹)

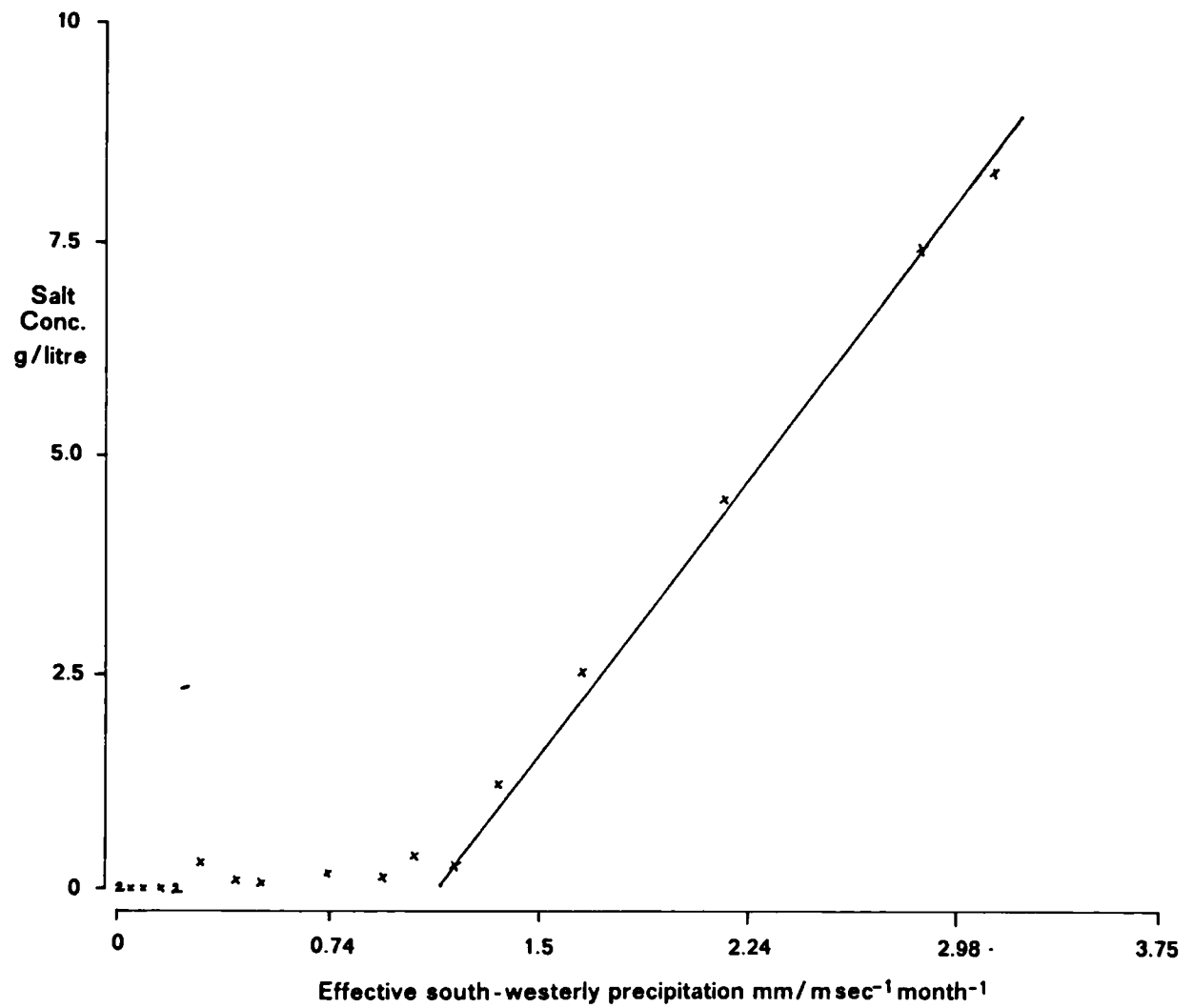
V = the total monthly rainfall (mm), and;

D = the number of days in the month.

The index was correlated with the concentration of salt deposited on the cliffs (Figure 5.13). Above an intensity of 1.35 mm/msec⁻¹month⁻¹ the plot revealed a direct linear relationship between the deposition of salt and effective salt precipitation. The latter value would confirm the operation of a threshold below which sea-spray was not entrained in precipitation nor deposited on the coastal cliffs; this was defined by a wind speed of less than 7.5 msec⁻¹ (see Figure 5.11).

This discussion has so far only considered climatic data at the on-site weather station and the salt-deposition on the coastal cliffs. This has assumed a uniform distribution over the whole site area. It was considered important to establish the effects of micro-climate when

Figure 5.13. Relationship between effective south-westerly precipitation and salt deposition.



assessing the variability of rain and salt deposition upon the coastal cliffs in comparison to the inland station. This was facilitated by a series of specially designed salt gauges (section 3.325), which were used to directly measure rainfall and to collect samples for chemical analysis. The effects of micro-relief upon winds were not directly measured although by inference any difference between the rainfall totals could be considered to result from localised wind effects; for instance, winds funnelling up the coastal slope may cause a depletion of rainfall on the cliff-top with an equivalent gain inland of the cliff-edge where the winds are less strong.

The effects of micro-climate were assessed every site visit, but the results presented here are for the most active winter periods. In Figure 5.14 the total monthly rainfall was plotted as a function of distance inland for December 1985 and January, November and December 1986. The two winters contrast considerably but both indicate an increase in precipitation inland from the cliff-edge. Figure 5.14a shows a decrease in rainfall upslope towards the rear-scarp of the mudslide, with a substantial increase in precipitation inland of the cliff-edge. In Figure 5.14c this effect is even more dramatic with an 80 per cent increase in the total monthly rainfall 50 m inland of the cliff-edge which was considered to be due directly to the effects of wind. It has already been established that maximum rainfall and wind speeds were recorded in November 1986 so this would seem likely. Errors would have arisen in assessing the concentration of salts deposited as sea-spray if these discrepancies had not been considered.

Figures 5.15a and c show that the deposition of salts decreased exponentially by as much as 80 per cent upslope from the mudslide toe.

Figure 5.14. Total monthly rainfall with respect to micro-climate.

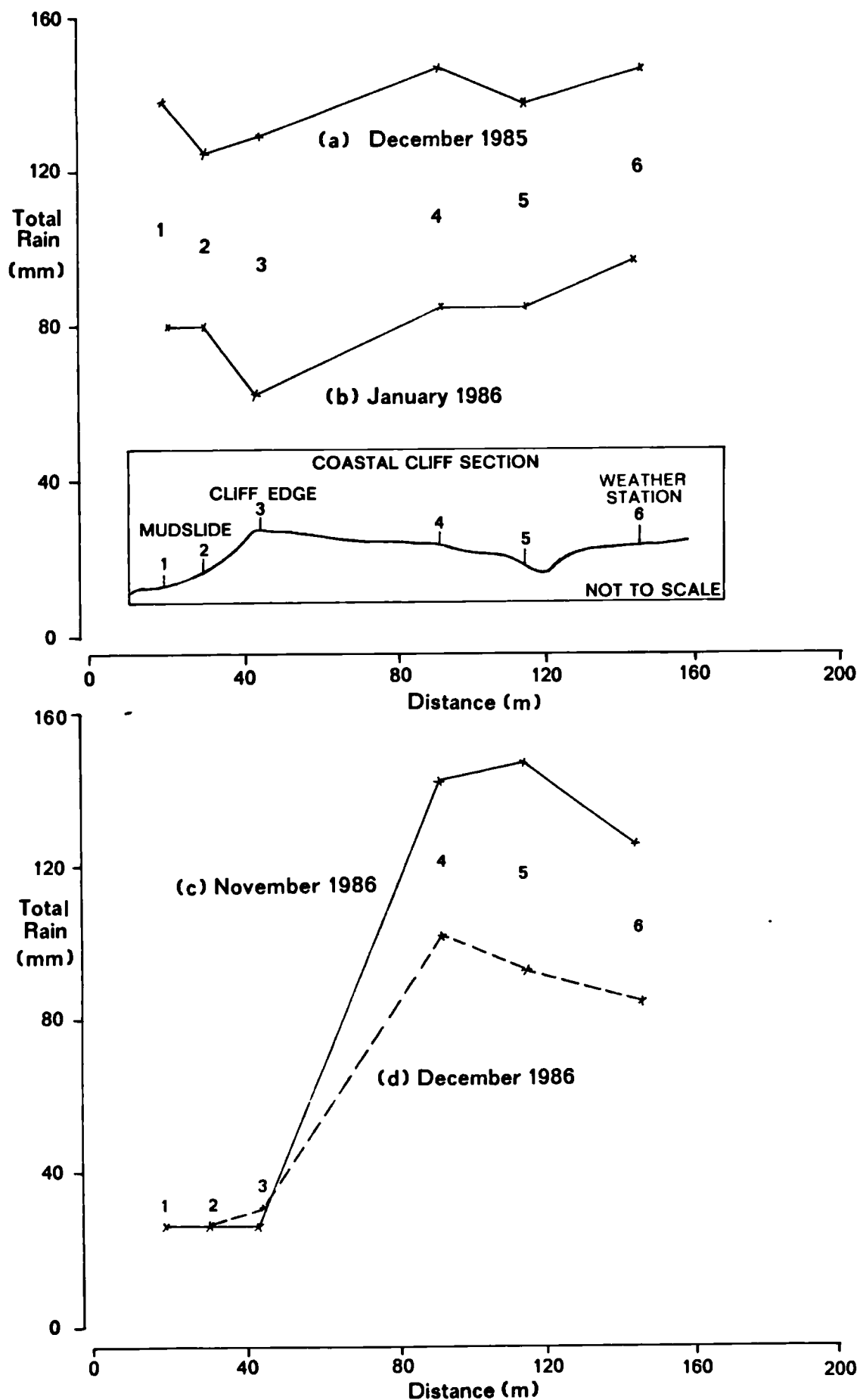
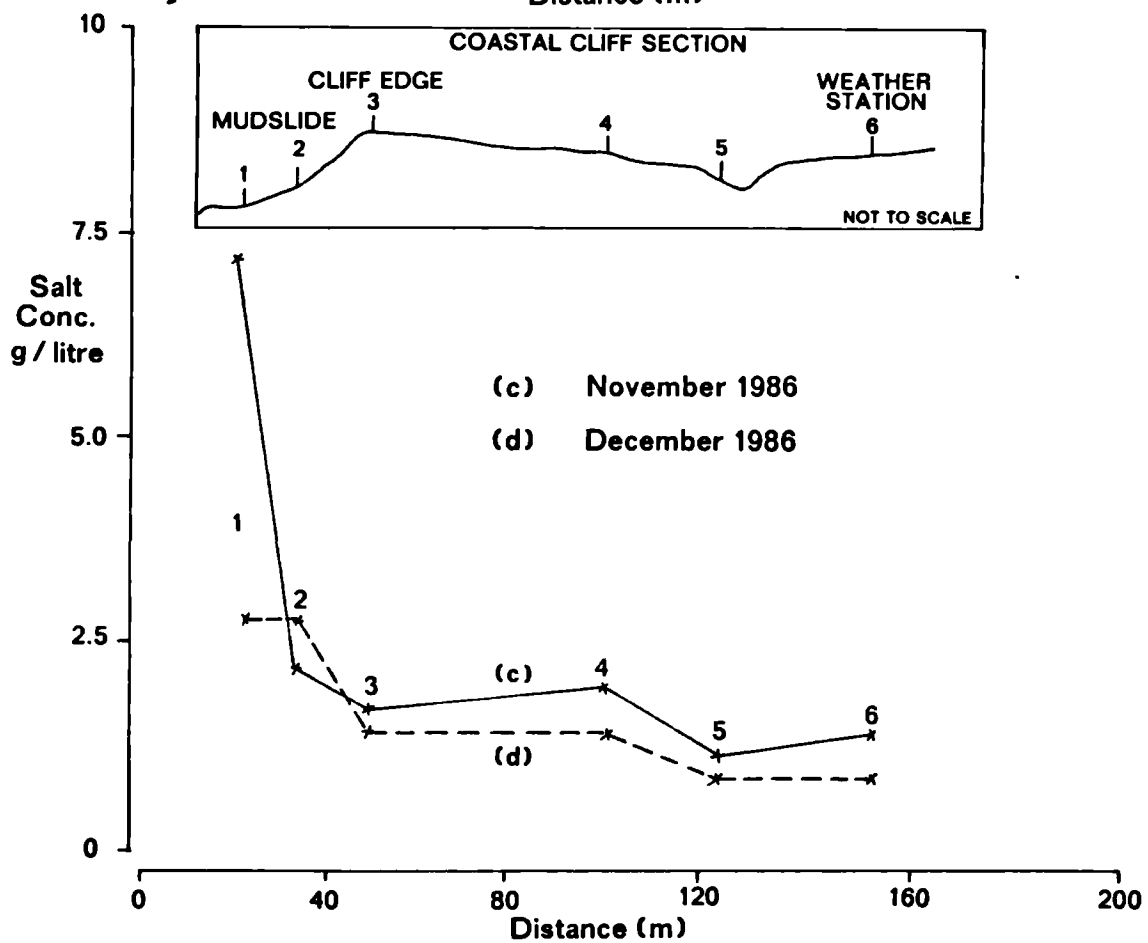
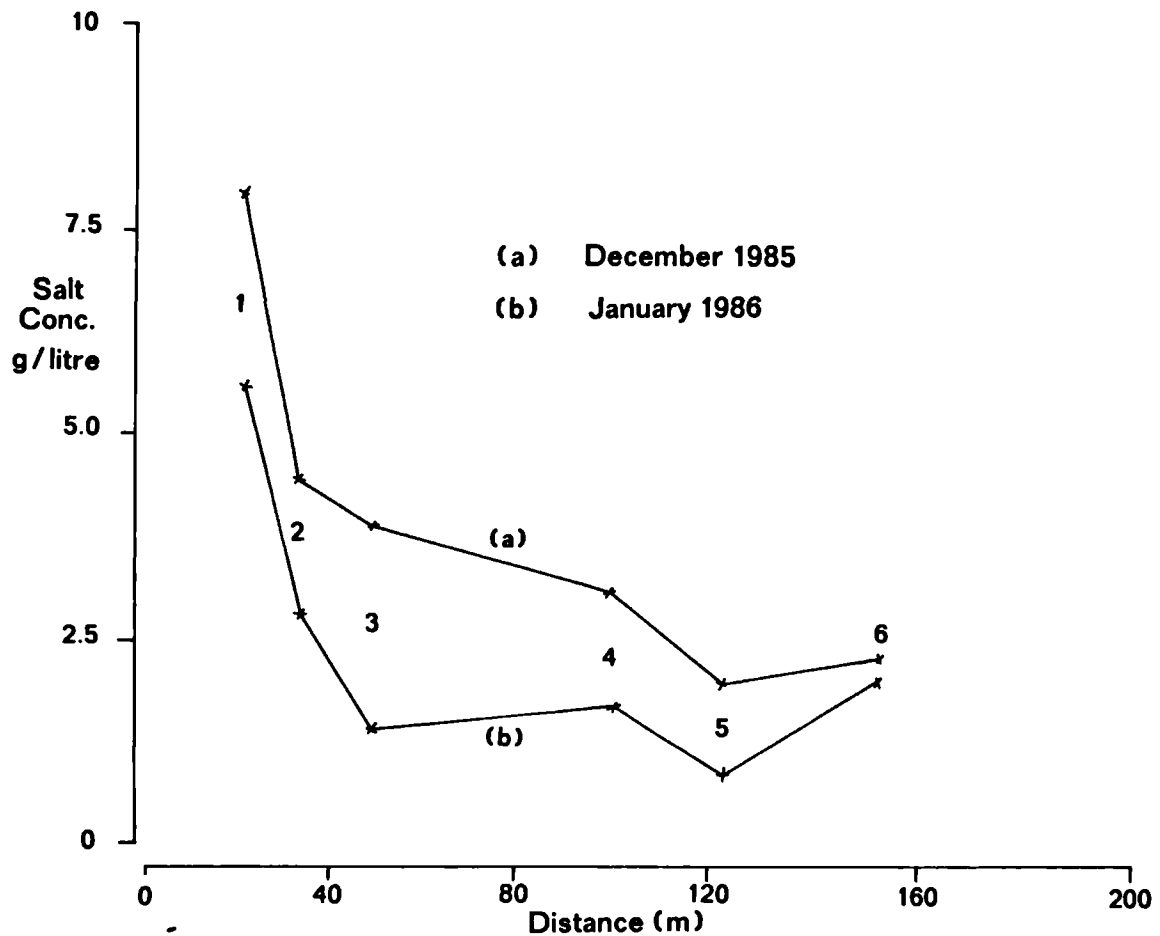


Figure 5.15. Deposition of sea-salts with respect to micro-climate.



There was a further reduction inland from the cliff-edge although the low values are partly due to the dilution caused by increased rainfall. The greater proportion of salt deposited in December 1985 arises from the higher rainfall reaching the lower slopes of the mudslide than in November 1986. However, the stronger winds in November 1986 ensured that the small volume of precipitation reaching the mudslide was highly saturated with sea-salts. When the winds abated in December 1986 a lower concentration of salts was deposited at the toe of the slope.

5.32 Soil water relations:

5.321 Soil moisture.

The results of the neutron probe soil moisture surveys are best presented as plots of moisture volume fraction (m.v.f.) against profile depth. Additionally, the variation in the soil moisture estimate throughout the study period is presented in Table 5.3. This was included to illustrate the accuracy of the measurements and to identify zones of greatest moisture fluctuation. It was found that the greatest variation in the soil water estimate occurred in the surface layers which might be expected as a result of the constant wetting and drying caused directly from atmospheric conditions. In comparison with *in situ* clay the body of the mudslide shows a high degree of variation, particularly above the basal shear surface. Below the shear surface the soil moisture readings were relatively constant, suggesting that the measurement of moisture profiles in this manner could be used to locate shear surfaces and the depth of mudslides.

Table 5.3. Profile variations in moisture volume fraction throughout the study.

Depth m	CLIFF 6	SOURCE 5	4	FEEDER TRACK 3	2	LOBE 1	0
0.2	.02	.042	.051	.045	.039	.057	.043
0.3	.019	.025	.034	.011	.022	.029	.023
0.4	.015	.008	.019	.005	.01	.008	.035
0.5	.013	.008	.013	.016	.007	.023	.045
0.6	.011	.006	.023	.027	.013	.025	.076
0.7	.013	.016	.017	.019	.024	.015	.039
0.8	.007	.004	.01	.018	.009	.016	.019
0.9	.005	.005		.018	.006	.006	.016
1.0	.005	.006		.005	.008	.018	.015
1.1	.003	.01		.007	.008	.016	.015
1.2	.004	.005		.014	.005	.015	.017
1.3	.004			.012	.004		
1.4	.005			.005	.006		
1.5	.01			.005	.007		
1.6	.014						
1.7	.026						
1.8	.022						
1.9	.009						
2.0	.022						
2.1	.018						
2.2	.024						
2.3	.004						

=====
All values in % moisture variation

— : *in situ* wetted zone

--- : secondary shear surface

→ : surveyed depth of basal shear surface

Figure 5.16. Moisture volume fraction depth profile within the backcliff at Worbarrow Bay.

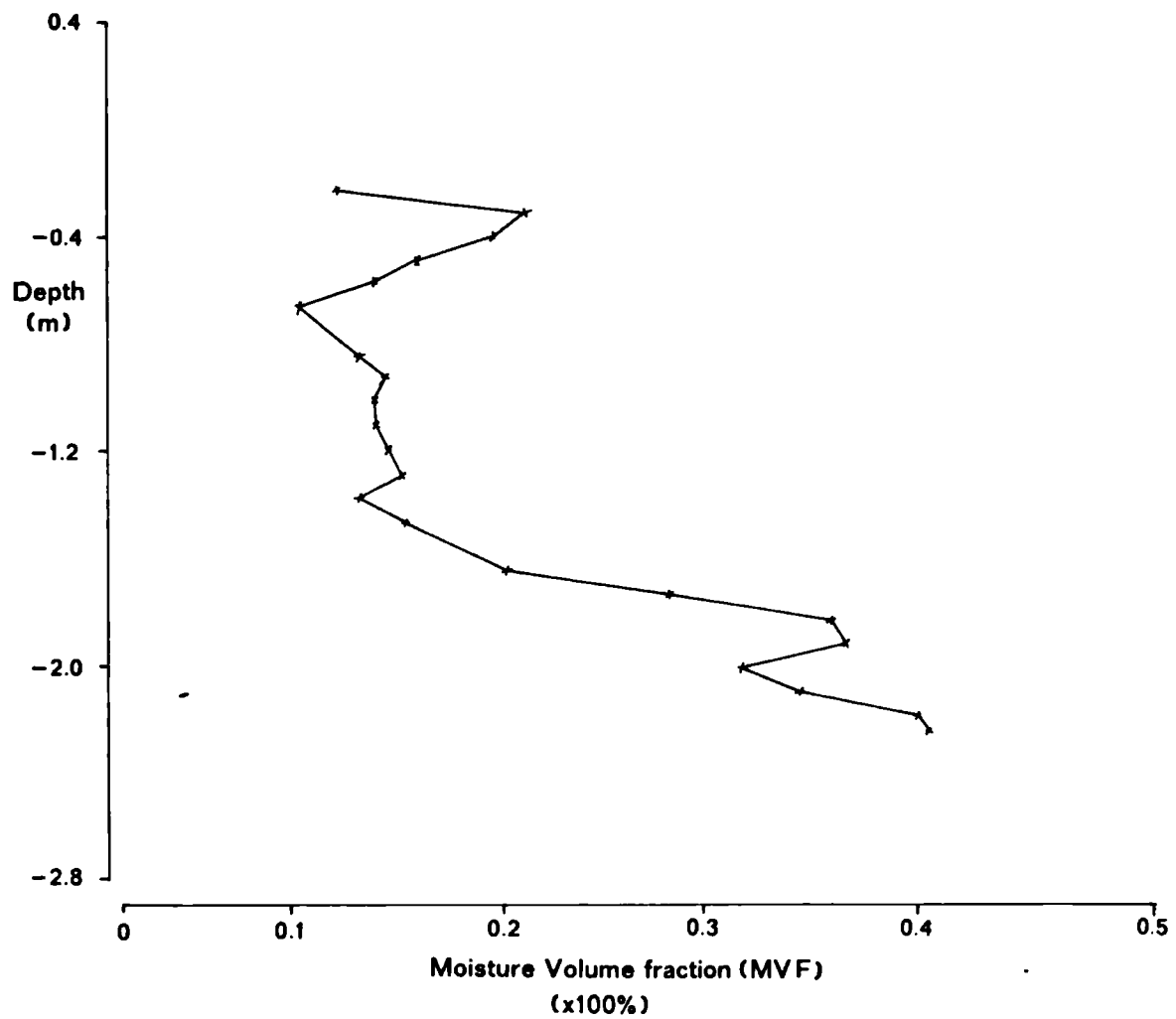
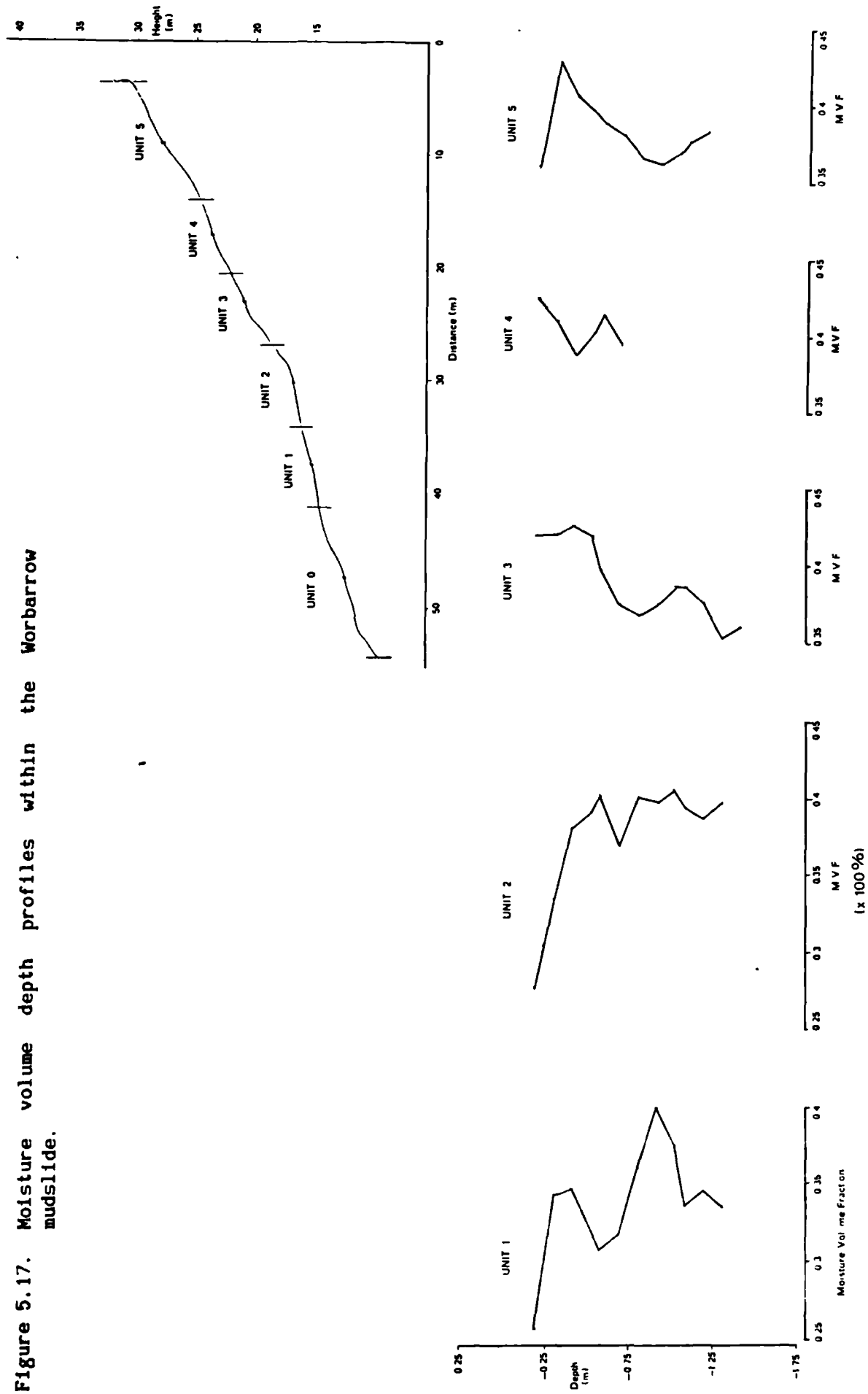


Figure 5.16 shows the moisture profile of the back-cliff of the mudslide and clearly indicates a marked four-fold increase in moisture content at a depth of -1.7 m. This sharp division was characterised by a change of texture from a sandy loam above -1.7 m to stiff plastic clay below forming an impermeable boundary, along which moisture accumulated and instability may be generated. Ground water seeps from this zone into the source unit. It is likely that other similar bedding planes exist below the depth to which this profile was taken and may similarly affect the mudslide further downslope from the source. Slope unit 3 (Table 5.3) may be a case in point since the per cent moisture variation beneath the shear surface was quite high throughout the study suggesting a basal source input of ground water, or an aquifer.

In Figure 5.17 a further series of profiles were plotted to represent each slope unit of the mudslide section. In units 5, 4 and 3, the shallow upper slope sections, the maximum moisture contents were found above the shear surface as a saturated surface mass. Towards the base of the feeder track, at unit 2, there was significantly less moisture in the surface horizons although a sharply defined saturated zone at -0.6 m occurred above the active shear surface (-0.7 m). This wetted horizon deepened with the shear surface in unit 1. Hence, it was noted that in the source unit the total thickness of mudslide material tended to be highly saturated, draining upon movement to the basal shear surface and as the mudslide deepened downslope, indicated by a sharply defined maximum moisture content. The accumulation of moisture at the basal shear surface may result in the preferential movement and piping of throughflow.

Figure 5.17. Moisture volume depth profiles within the Worbarrow mudslide.



To assess the cyclical change in the soil moisture status throughout the study period, the m.v.f. at specific depths were plotted for the back-cliff and accumulation lobe for comparison (Figure 5.18). A profile depth of -1.7 m was chosen for the back-cliff because this was considered to be the most sensitive zone to seasonal fluctuations in both moisture content and the water table; there were no active shear zones in the back-cliff. The plot for the accumulation lobe was taken from the basal shear surface.

Figure 5.18 shows that there was an increase in the natural moisture content from 29 to 45 per cent between the *in situ* state of the back-cliff and the highly weathered materials of the accumulation lobe. Additionally, the climatic cycle was recognised as a smooth curve in the latter case, whereas the undisturbed moisture content of the back-cliff showed a high degree of variability and sensitivity to change. For instance, the August storm noted in section 5.311, was represented by a sharp peak in the back-cliff which accounted for an increase in soil moisture of 9 per cent. This is discussed later in an attempt to establish the response times between the storm and the soil water relations. The accumulation lobe plot shows winter maxima of 48.3 and 49.5 per cent in January 1986 and February 1987, respectively, and a summer minimum of 36.6 per cent from May to July. The back-cliff shows less of a summer minimum, with a sharp drop to 24.6 per cent in July, but similar winter maxima in January 1986 and March 1987 equalling 34.2 and 34.4 per cent, respectively.

The winter maximum of 1987 was plotted at a greater resolution for both the source and accumulation lobe in Figure 5.19. Both plots show relatively smooth increases in soil moisture, although there was an

Figure 5.18. Mean monthly soil moisture in the backcliff and accumulation lobe at Worbarrow Bay.

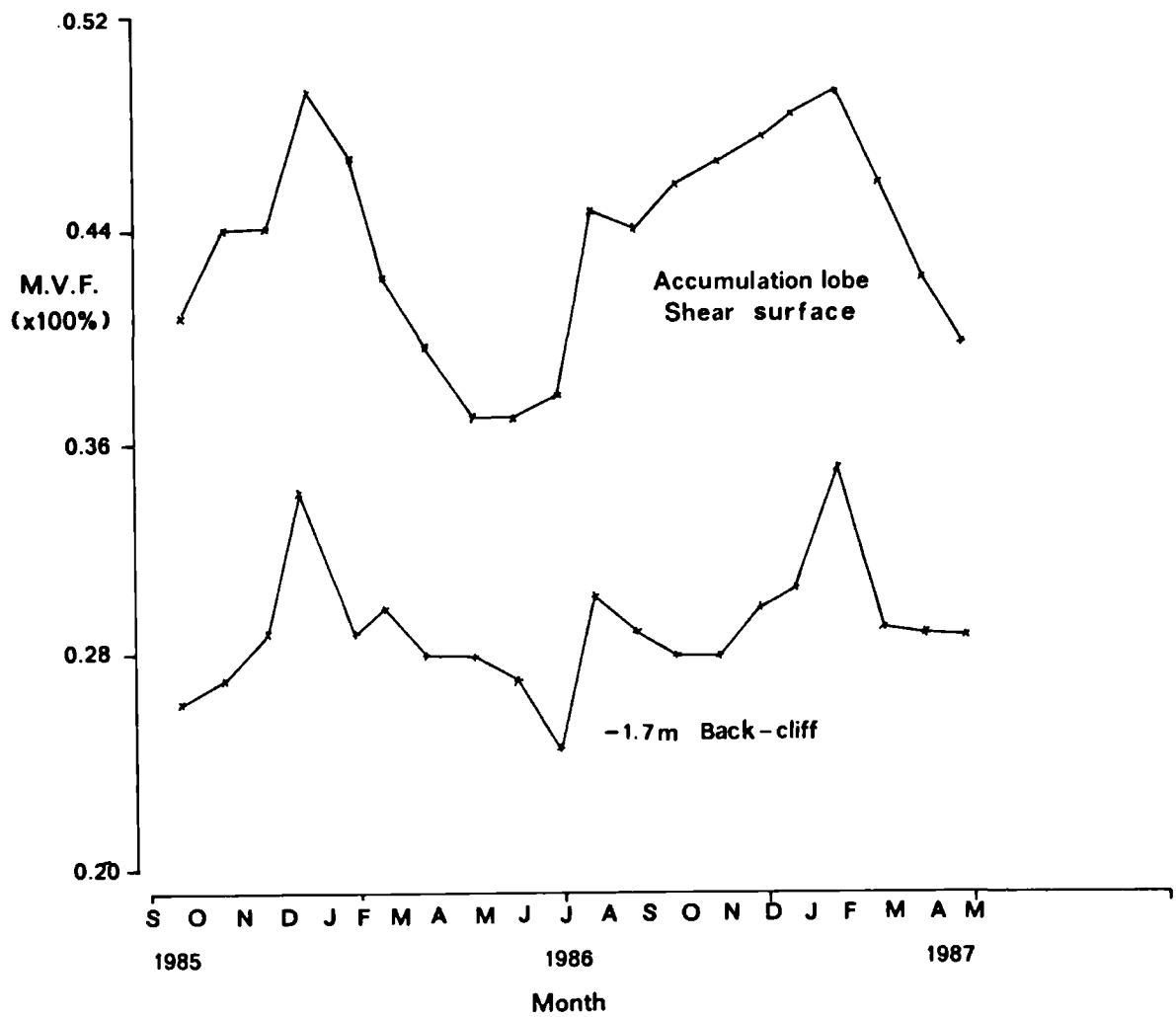
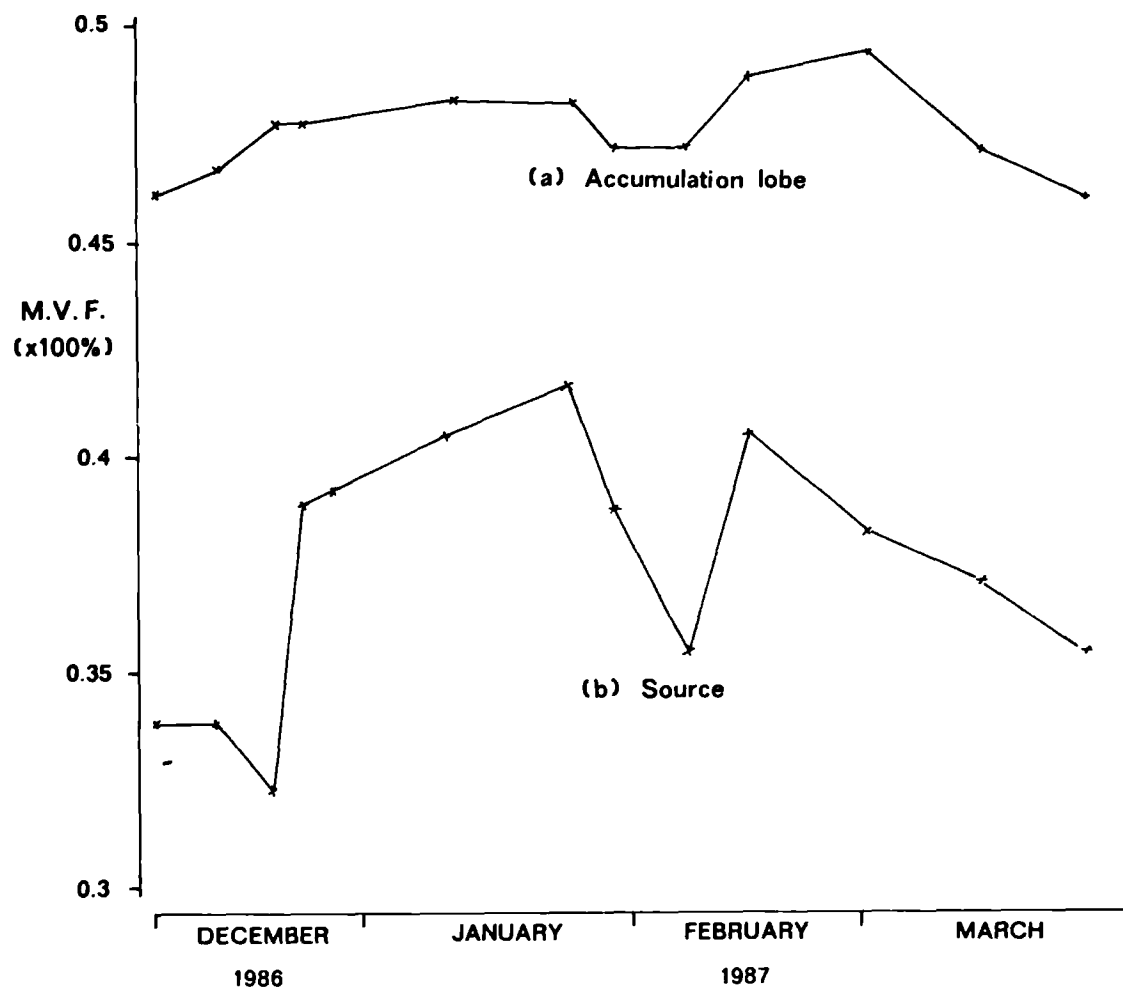


Figure 5.19. Soil moisture at the shear surface in the source and lobe between December 1986 and March 1987.



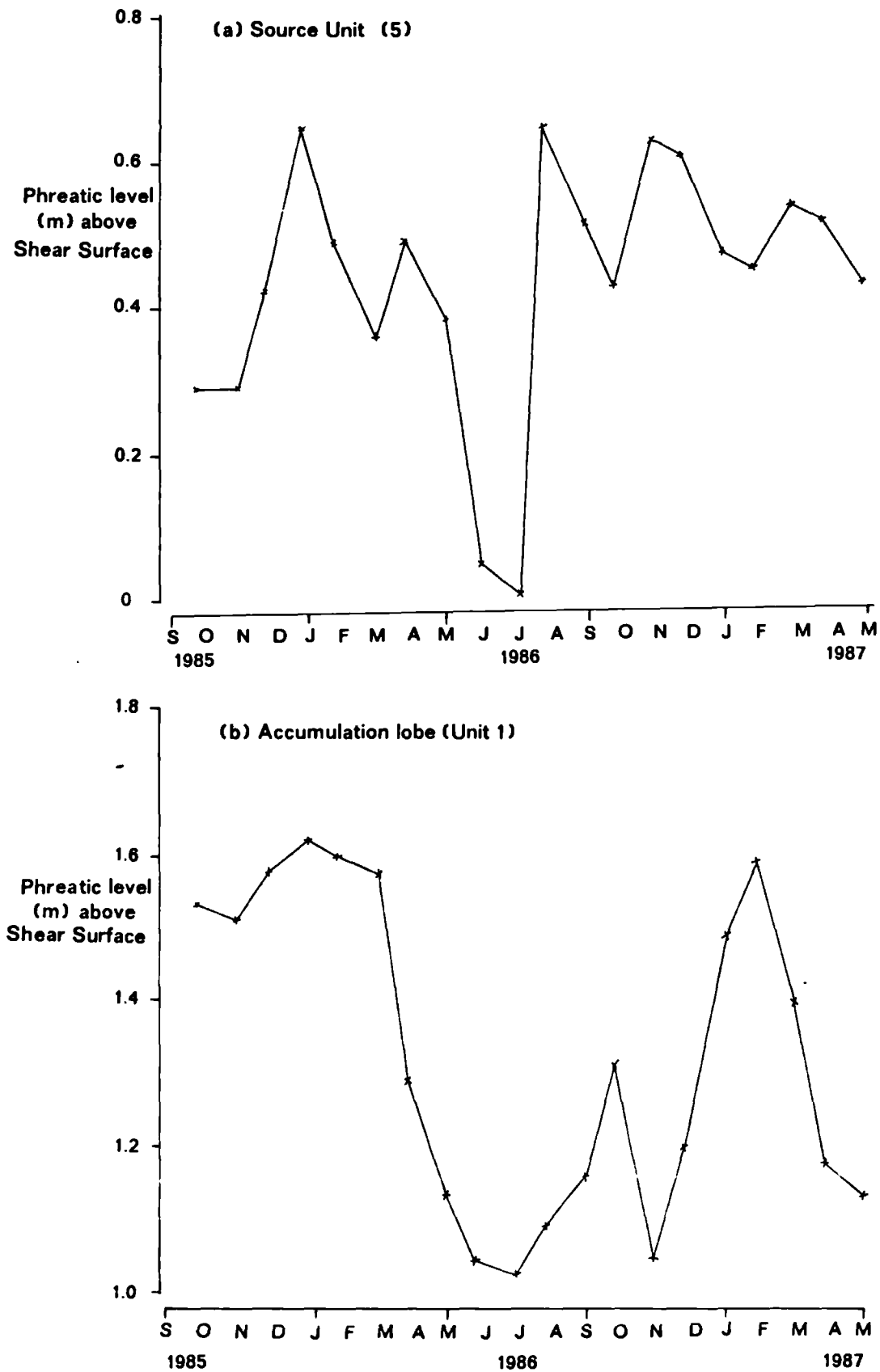
inherently greater rise from 34 to 42 per cent in the source unit. However, this trend was broken in both plots towards the end of January and beginning of February which was considered to have resulted from the long cold spell experienced at that time. The effect was more severe in the source unit since the shear surface was closer to the *frozen* layer.

In the source unit the maximum moisture content of 41.4 per cent was attained by the 23 January 1987, whereas in the lobe the maximum of 49.5 per cent was achieved one month later by the 27 February. This would suggest that there was not only a time-lag between the maximum hydrological flux, in this case December, and the highest recorded moisture content in the source, but also a time-lag downslope from the source to the accumulation lobe (see section 6.22).

5.322 *Pore water pressure.*

Changes in the phreatic level were monitored at 4 locations within the mudslide and in the back-cliff using pressure transducers and conventional standpipe piezometers. The pore water pressure may be calculated from a knowledge of the phreatic level and the unit weight of water. A Casagrande piezometer (see section 3.322) inserted 3.15 m into the cliff-top showed no pore pressure response throughout the period of study except for a recorded level of -3.1 m on the 10th April 1987. It was not clear whether this was a *bona fide* reading or an anomaly. Even so the absence of pressures in the back-cliff would suggest that artesian conditions may be operating in strata at greater depths.

Figure 5.20. Mean monthly phreatic levels in the source and accumulation lobe throughout the study.



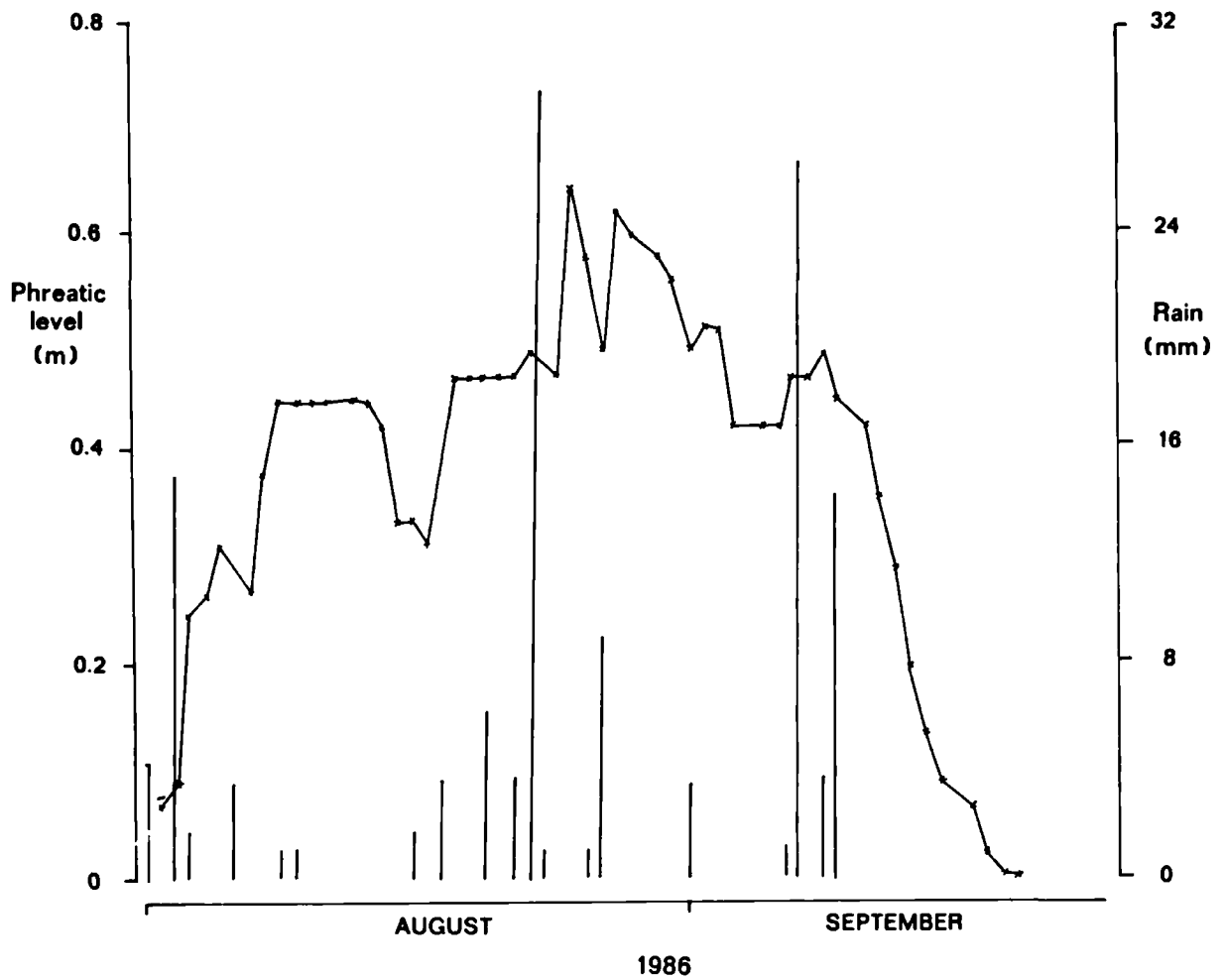
Figures 5.20a and 5.20b summarize the piezometric levels measured in the source unit and accumulation lobe. The seasonal cycle is apparent in both plots, and it may be seen that pore water pressures in excess of 1 m head of water prevailed throughout the year in the accumulation lobe. This adds support to the contention that artesian pressures exist on the lower slopes. The lobe showed a much clearer seasonal cycle than in the source, showing sharp winter maxima of 1.63 m and 1.6 m in January 1986 and February 1987, respectively. The summer minima were equal to 1.03 m or a 40 per cent reduction in the pressure head.

The phreatic levels in the source unit throughout the study were much more variable, although peaks occurred in January 1986 (0.65 m), April (0.48 m), August (0.64 m), November (0.62 m) and March 1987 (0.53 m). Apart from the peak recorded in August, shown later to be related to the freak storm in that month, two seasonal maxima may be recognised. There was a major peak in either November, December or January, and a further secondary peak in March or April. During June and July there was no recorded pressure head in the source unit.

As for the soil moisture analysis, it was of interest to note differences in the temporal sequence of fluctuations in pore water pressure within the mudslide. The clearest event that allowed such correlation was the unusual freak storm in August 1986. Figure 5.20a shows the peak in phreatic level in the source unit and it was assumed that the peak in the accumulation lobe recorded in October may also be a response to this event.

Figure 5.21 is a daily summary of the phreatic level in the source unit during August and September, and indicates that daily records were

Figure 5.21. Daily rainfall and phreatic level during August 1986 illustrating associated time-lagged responses.



sufficiently detailed to allow the identification of individual events. The superimposed rainfall histogram suggests that peak pore water pressures in the source unit were attained within days of the storm event, in this case 3 days after the peak rainfall. Within a further 20 days the piezometric level had reduced to zero following drainage. The findings confirm that the source region of the mudslide was very sensitive to changes in the soil moisture status. If the corresponding less-intense peak in the lobe recorded in October was related to the earlier event, then a further time-lag exists between the source and toe of the mudslide as found for soil moisture (sections 5.321 and 6.222).

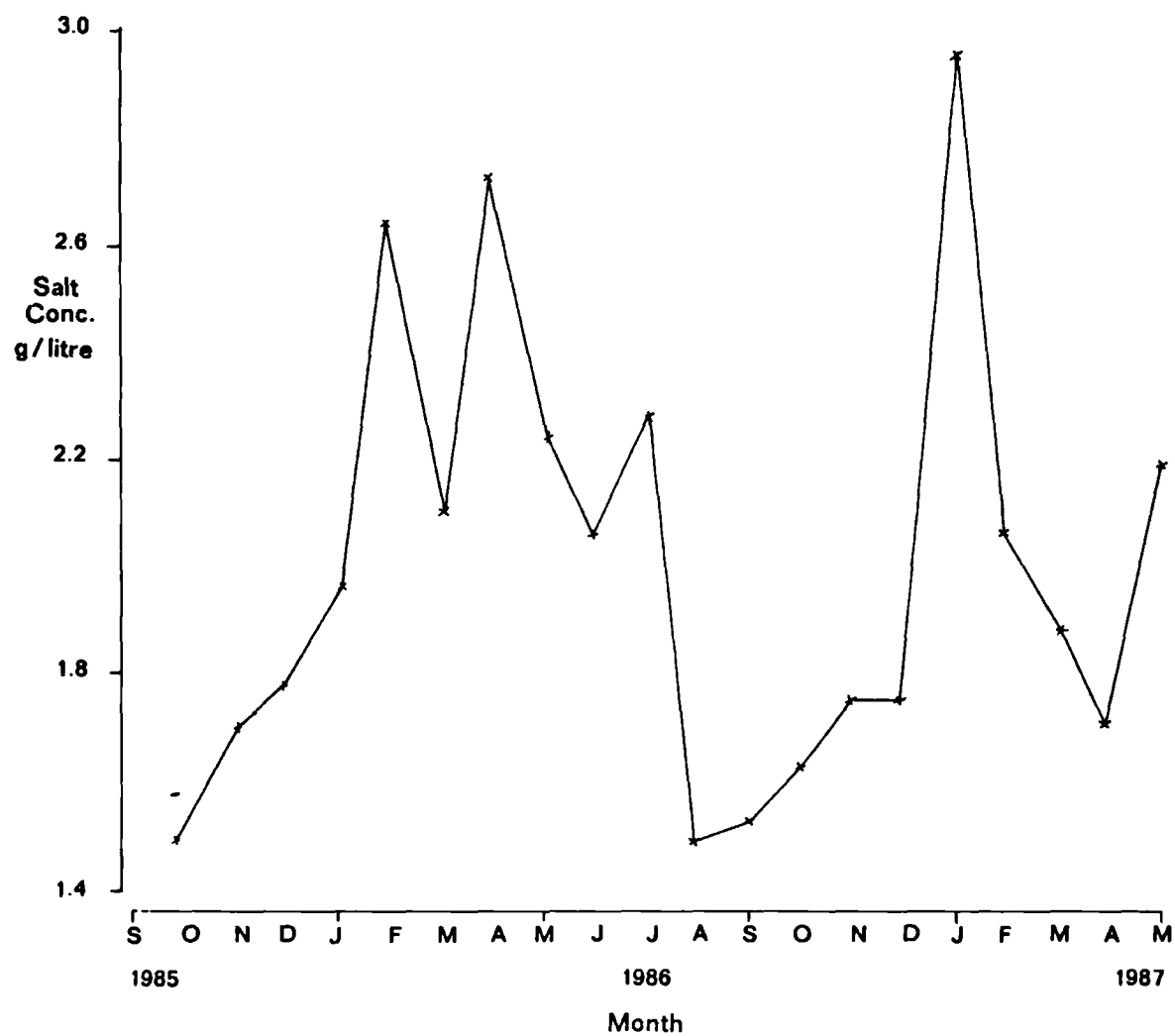
Pore water pressures are further presented at a much greater resolution in relation to the measurement of slope movements in section 5.33.

5.323 Pore water chemistry.

The chemistry of the pore water was monitored throughout the study to assess whether there was any association between weathering behaviour and mudslide instability. Pore water samples were extracted from the shear surface at 5 locations within the mudslide and from *in situ* ground water from the back-cliff, using the techniques described in sections 3.326 and 3.42.

The pore water chemistry of the site was dominated by chloride salts (see Table 5.2) typical of coastal environments: the speciation measured in pore water from the source unit consisted predominantly of 14 per cent sodium, 73 per cent chloride, 6 per cent sulphate, 4 per cent calcium and 3 per cent magnesium with other constituents occurring in proportions

Figure 5.22. Pore water salt concentration at the shear surface of the accumulation lobe throughout the study.

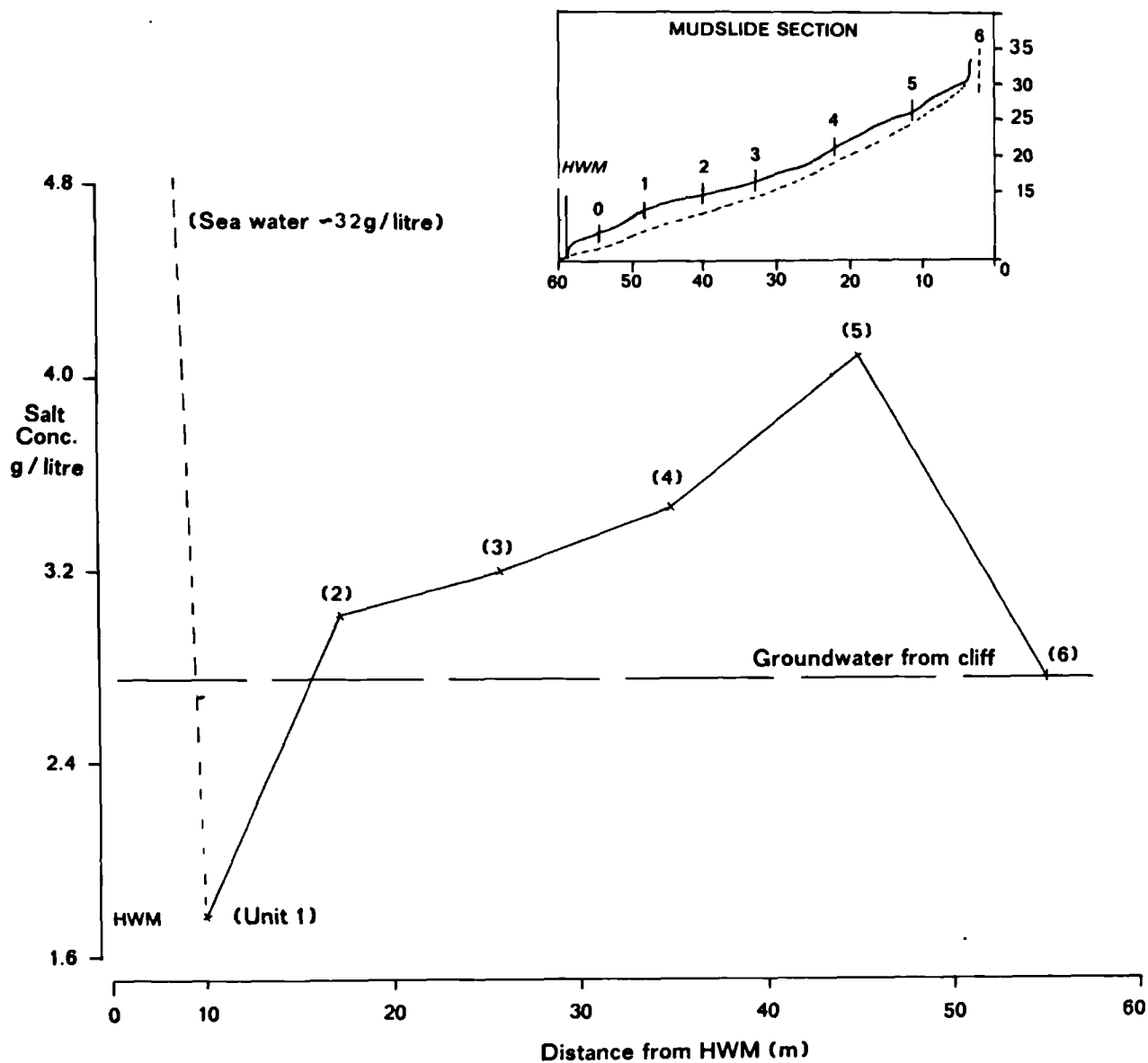


less than 1 per cent. Figure 5.22 summarises the concentration of total salt content in the accumulation lobe (unit 1) throughout the study period. Three major peaks are apparent in February and April 1986, and January 1987, with values of 2.66, 2.73 and 2.94 g/l, respectively. There was also a summer minimum of 1.49 g/l in October 1985 and August 1986, pore water concentration gradually rising until the sudden winter maxima.

The variable nature (peaks) of pore water chemistry was expected because salt concentration is dependent on a number of factors such as the moisture content, the origin of salts, chemical reactions and weathering conditions. This is clearly illustrated in Figure 5.23, where the peak concentration during January 1987 is plotted with respect to the mudslide section. The plot shows an increase in salt concentration upslope, reaching a maximum of 4.11 g/litre in the source unit. In relation to the maximum, there were significant differences of 33 and 56 per cent between the concentrations of ground water in the backcliff (2.75 g/l) and the pore water at the snout of the slide (1.8 g/l), respectively. Otherwise there was a uniform decrease in salt concentration down the mudslide. Pore water concentrations within the source and feeder track were always greater than the regional ground water entering the mudslide.

This indicates a substantial increase in salt content in the source unit which was assumed to originate from either sea-spray or weathering processes. Because the maximum concentration of salt input to the source at this time of year was 2 g/l (section 5.314) it was considered that weathering and erosion processes must contribute significantly to the peak concentration. The temporal relationships between pore water chemistry and major erosive and weathering events were thus considered.

Figure 5.23. Distribution of pore water salt concentrations at the shear surface of the Worbarrow mudslide on the 30th January 1987.



The oxides of iron, aluminium and silica may be used as indicators of weathering processes (see section 6.3; Ruxton, 1968; Statham, 1979; Brady, 1984) because their solubility and mobility is naturally low and only occurs under relatively intense weathering conditions. In Table 5.4 the concentrations of these elements in the pore water solution are presented from October 1986 to May 1987. It may be recognised that there were marked peaks at regular intervals throughout the period. For illustration aluminium will be considered in greater detail since in the unweathered state the proportion of aluminium in undisturbed bedrock is relatively low at 0.01-1 μ m (Drever, 1982). However, weathering processes may mobilise significant quantities of amorphous aluminium (see section 4.45). This form of behaviour is clearly demonstrated in Table 5.4, although better portrayed in Figure 5.24 where the concentrations of aluminium in the ground water, source unit and accumulation lobe, are plotted over the winter period.

Significant peaks of aluminium were first recognised in the back-cliff groundwater on the 12th December 1986 (2.73 mg/l) and the 9th January 1987 (3.39 mg/l). A further maximum had occurred by the 13th March 1987 (4.23 mg/l). These were thought to reflect severe phases of weathering, erosion and failures of the back-cliff of the mudslide, releasing the oxides of aluminium, iron and silica after the disruption and attrition of *in situ* clayey sediments. Corresponding peaks were measured in the source, with associated time-lags, by the 23rd January 1987 (2.17 mg/l), the 13th February (4.073 mg/l) and the 13th of March (3.44 mg/l). The results indicate three main erosive events which were mirrored closely by the weathering and movement of materials in the source of the mudslide. The concentration of aluminium in the lobe remained negligible all year, although two-fold increases were recorded on the 23 January (.109 mg/l),

Table 5.4. Release of iron, aluminium and silica upon weathering of the backcliff, source and mudslide accumulation lobe.

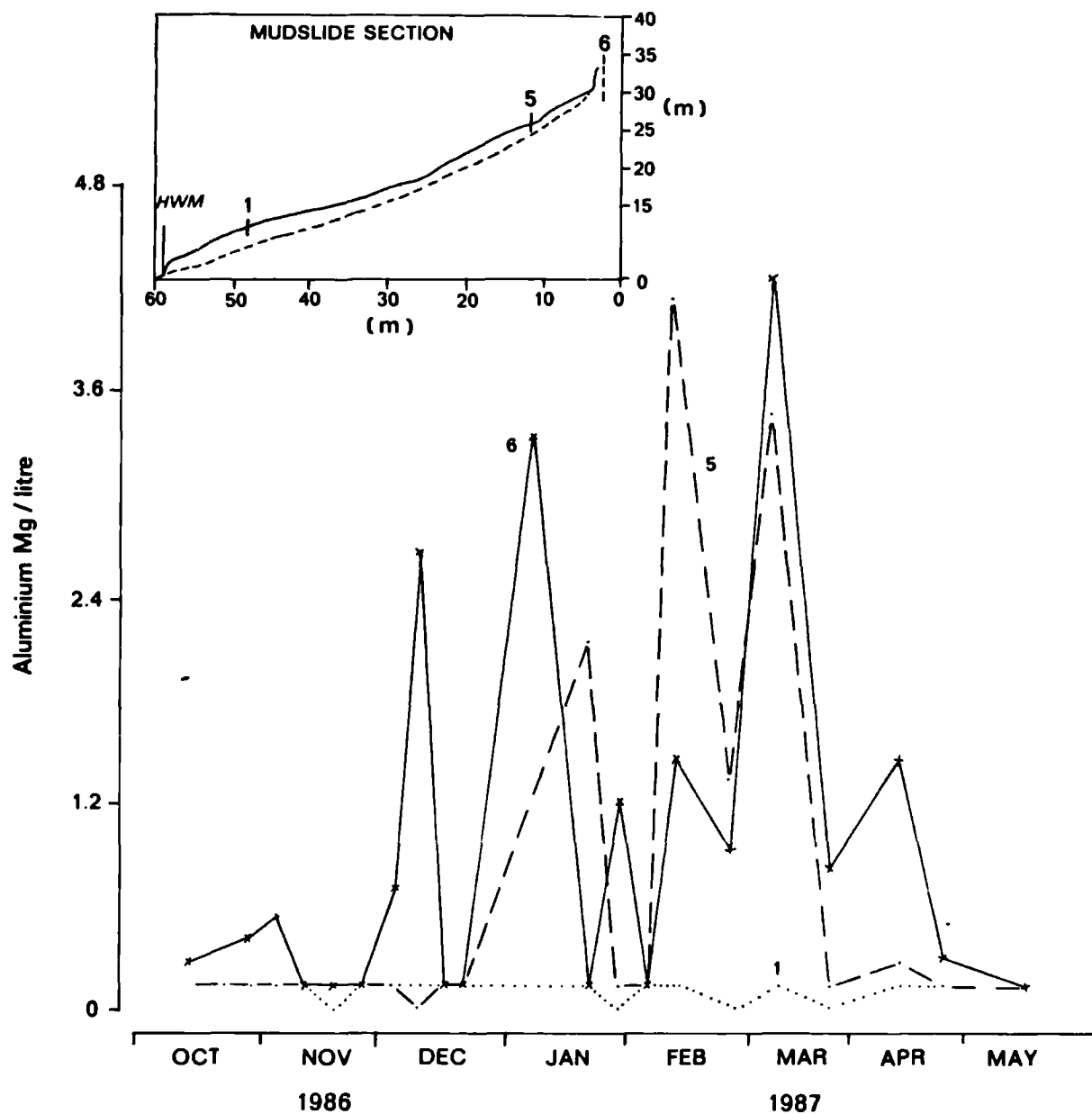
Date	Backcliff			Source unit			Accumulation lobe		
	Al	Fe	Si	Al	Fe	Si	Al	Fe	Si
17.10.86	.237	0.26	7.93	.154	0	5.2	.079	0	14.62
31.10.86	.443	1.13	14.49	.150	0	4.69	.092	0	12.76
7.11.86	.555	1.08	14.63	.174	0	4.8	.089	0	12.31
14.11.86	.103	0	7.02	.164	0	4.29	.089	0	12.17
21.11.86	.166	0	6.68	.147	0	3.91	.065	0	10.42
28.11.86	.338	0.58	14.97	.157	0	4.44	.075	0	9.91
5.12.86	.665	1.35	16.64	.133	0	3.64	.069	0	6.73
12.12.86	<u>2.729</u>	<u>4.95</u>	<u>53.87</u>	.021	0	0.22	.072	0	6.91
19.12.86	.143	0	8.66	.147	0	3.38	.075	0	9.56
20.12.86	.147	0	8.12	.163	0	4.18	.072	0	12.14
21.12.86	.140	0	8.32	.167	0	3.88	.072	0	11.94
22.12.86	.099	0	6.34	.157	0	3.83	.086	0	10.64
9.1.87	<u>3.391</u>	<u>8.43</u>	<u>66.17</u>	<u>1.225</u>	<u>3.95</u>	<u>27.51</u>	.069	0	10.29
23.1.87	.164	0.02	10.53	<u>2.170</u>	<u>7.68</u>	<u>46.02</u>	<u>.109</u>	0	11.54
30.1.87	<u>1.177</u>	<u>2.31</u>	<u>30.06</u>	.198	1.35	9.68	.065	0	8.53
6.2.87	.171	0.31	6.13	.086	0	8.6	<u>.144</u>	0	7.82
13.2.87	<u>.467</u>	<u>3.14</u>	<u>33.19</u>	<u>4.073</u>	<u>14.34</u>	<u>72.75</u>	.079	0	8.1
27.2.87	.908	2.33	25.92	<u>1.317</u>	<u>3.52</u>	<u>30.09</u>	.065	0	6.99
13.3.87	<u>4.23</u>	<u>11.45</u>	<u>76.11</u>	<u>3.442</u>	<u>9.93</u>	<u>62.13</u>	.086	0	6.23
27.3.87	.768	<u>33.03</u>	9.84	.181	0.58	10.22	.065	0	10.1
13.4.87	<u>1.525</u>	2.83	<u>41.86</u>	.236	0.62	<u>11.55</u>	.092	0.06	8.93
24.4.87	.204	1.2	9.26	.163	0.53	8.73	<u>.198</u>	<u>0.42</u>	10.36
15.5.87	.169	0.44	5.12	.156	0.48	5.39	<u>.159</u>	<u>0.55</u>	12.57

=====

All values in mg/litre

Significant releases of ions highlighted: bold referring to global events, and underline to localised releases in each mudslide unit.

Figure 5.24. Release of aluminium oxide during 1986/7 in relation to the seasonal intensity of weathering and erosion of the cliff and source units of the Worbarrow mudslide.



6th February (.144 mg/l), the 24th April (.198 mg/l) and 15th May (.159 mg/l).

The time-lag decreased with each event until in March the peak concentrations of aluminium in the rear-scarp and source unit corresponded. This suggested that the initial events were primarily responsible for loading the mudslide, whereas the latter may have resulted from the unloading of the source unit and the direct triggering of cliff-failure. When compared with the movement of the mudslide (see Figure 5.27) significant slope movements in mid-December, early and late January, early February and late March correspond with the peak concentrations of aluminium, silica and iron oxides. The first and last events would appear to have slight time-lags, increases in amorphous oxides occurring before slope movement; the intermediary events correspond very closely. The former association was considered to reflect the loading of the source from small-scale weathering and cliff-failure, whereas the latter peaks of amorphous oxide were the direct result of slope movement and the unloading of the source unit.

If the doubling of the concentration in the lobe towards the end of April was a response of the earlier events in the source, a minimum time-lag of 36 days operated between these slope units. The findings do show that aluminium, and similarly iron and silica, can be used to establish phases of erosion and weathering, particularly in the rear-scarp where the extent of loading may be monitored chemically.

5.33 Surface movement:

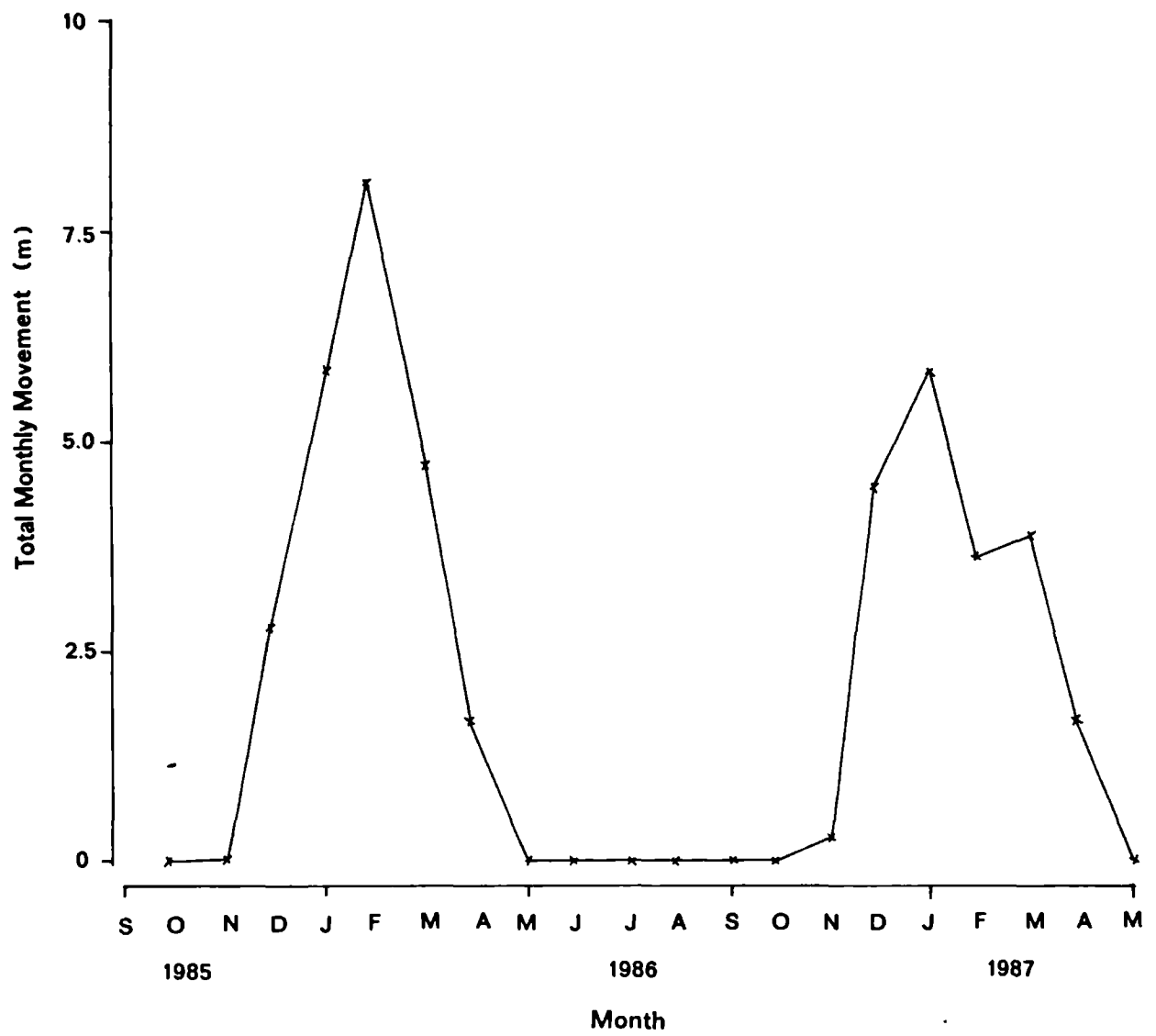
5.331 Automatic movement sensors.

A modified automatically recording technique developed by Allison (1986) was used at Worbarrow to monitor surface displacement rates. The method was described in section 3.324 and broadly consisted of eight movement sensors attached to a gantry spanning the mudslide. The sensors were connected to the surface of the mudslide by pins and wire such that when displacement occurred wire was withdrawn from the sensor pulley. The rotation of the pulley was automatically recorded every 5 minutes, and directly calibrated to determine the rate of movement. Each pulley had a wire capacity of 5 m, so that the sensors needed constant resetting during active periods. Hence, the results presented here are more an assessment of the translation of material beneath the gantry, rather than the total movement of individual targets (see section 5.214).

The continuous movement record spans from January 1986 to May 1987 which accumulated over 1 million individual recordings (Table 3.8). Large sections of the data-set showed no change which allowed significant reductions in the volume required for data storage although it remains too voluminous to warrant reproduction here. The high frequency recordings were used to calculate a daily total, from which the monthly summary was derived. The monthly movement summary was supplemented by target measurements during October, November and December 1985 when the continuous record was unavailable.

The total monthly maximum movement throughout the period of study is presented in Figure 5.25. The plot shows the very marked seasonal

Figure 5.25. Maximum monthly movement throughout the study.

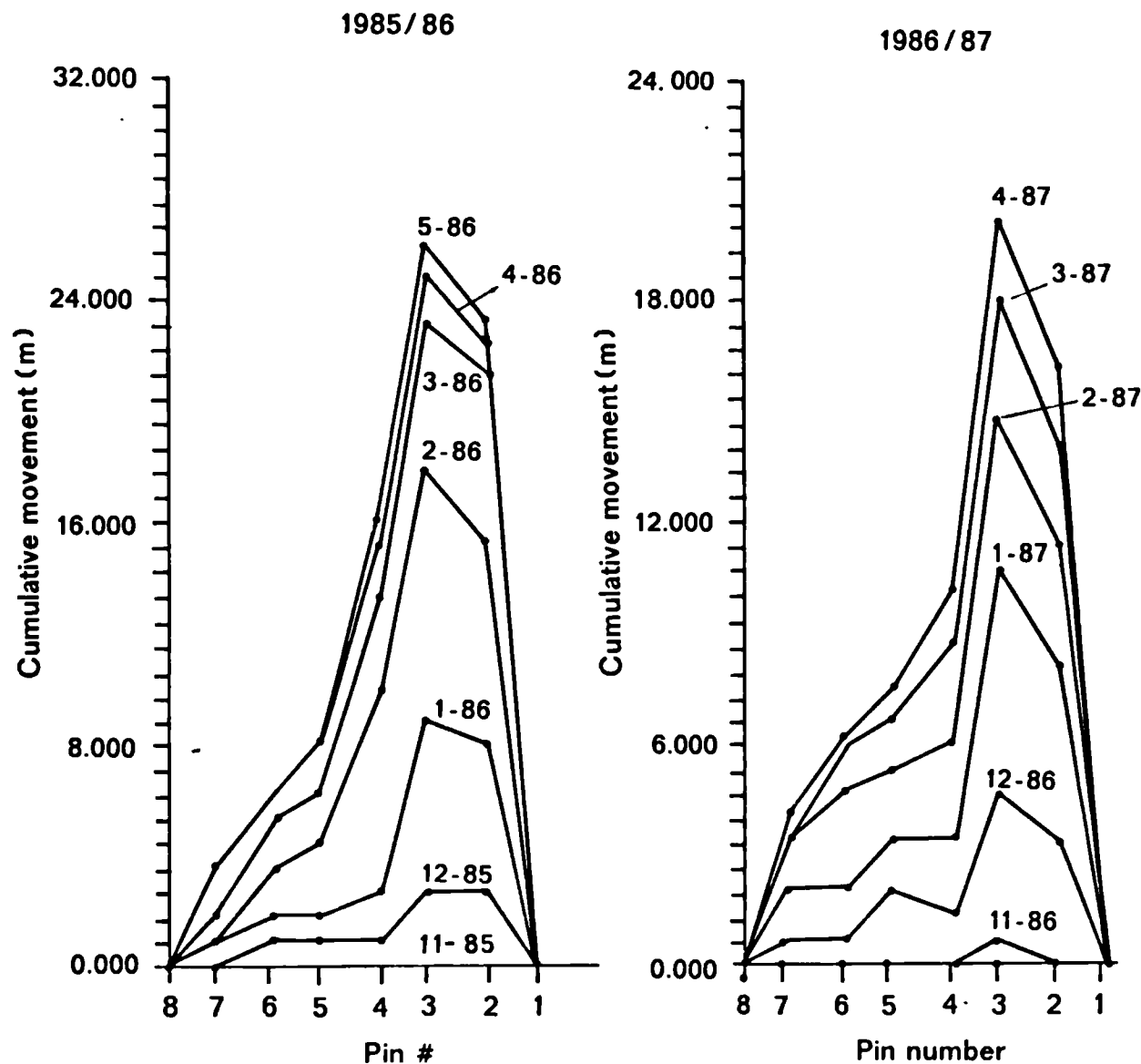


movements exhibited by mudslides beginning in December with the cessation of displacement by May. Two peaks of maximum monthly movement were recorded in February 1986 (7.53 m) and January 1987 (5.86 m), indicating a greater degree of displacement in the former winter. Movement started earlier in the latter year as for the net hydrological flux (section 5.312).

In section 5.214, photogrammetric analyses of target vectors showed that the greatest movement was confined to the western extremity of the mudslide. This was confirmed by the pattern of the cumulative translation of material beneath the gantry, plotted for each winter period in Figure 5.26. The maximum surface displacement in the 85/86 winter was 25.65 m compared to 19.98 m in 86/87, recorded by pin 3. These totals were slightly less than the maximum 30 m recorded by Allison (1986; see Table 1.5) in previous years. The movement pattern reflects the dominance of the main source unit with smaller movements recorded in the secondary source unit. The latter were partly limited due to the constriction of the mudslide at mid-slope where the secondary system was diverted into the main feeder track. The plot for 1987 emphasised this fact because the pattern of movement was initially bimodal suggesting more stable ground between each source unit. This was also recognised by the DTM of difference (section 5.213).

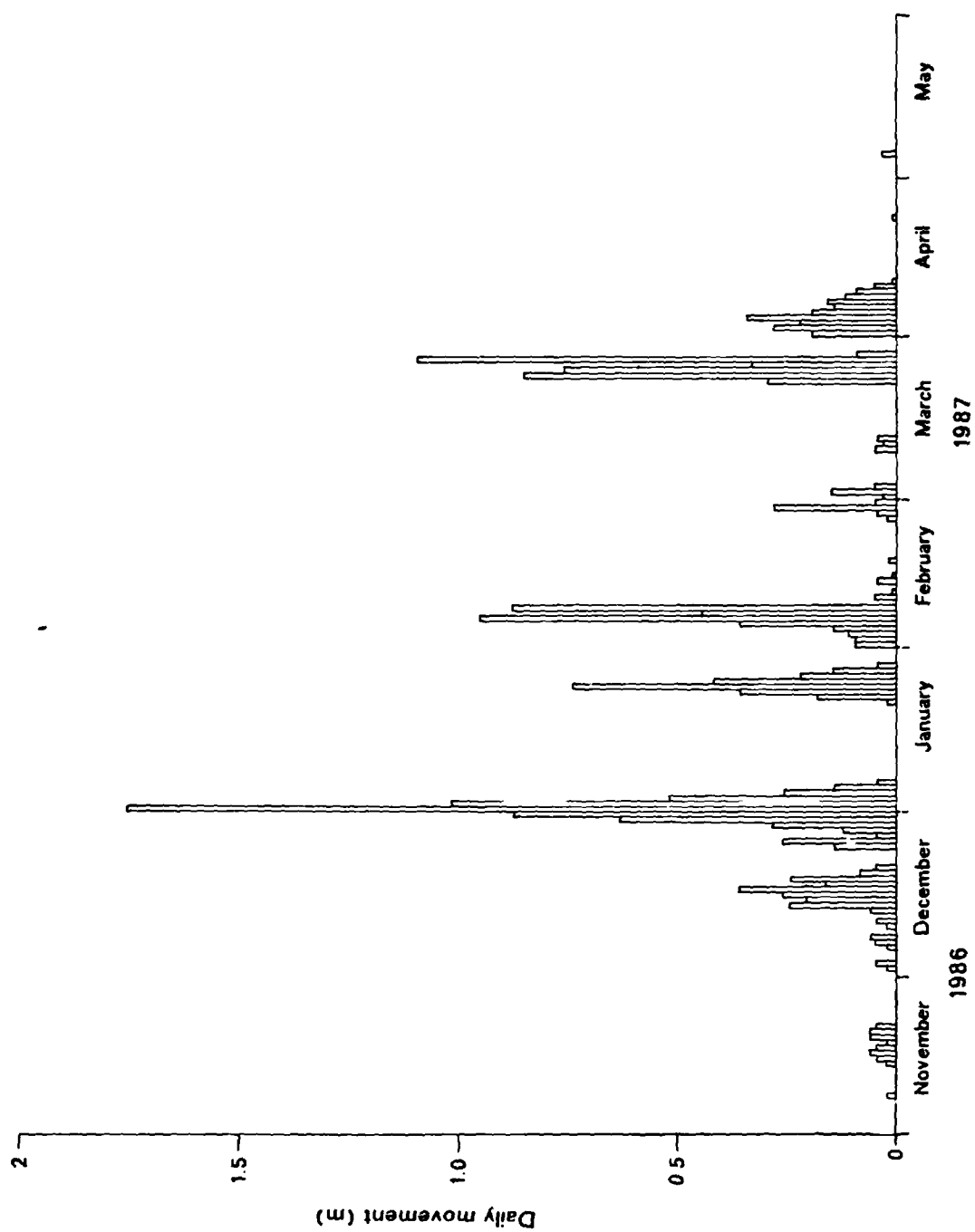
Allison (1986) identified three mechanisms of displacement from a continuous record of movement from the same site in 1983/4. These were classified as multiple, graded and surge events (section 1.4). It was of interest to validate these findings with the current record obtained with the newer and improved design of equipment. As found in the previous

Figure 5.26. Cumulative pattern of movements during the winters of 1985/86 and 1986/87.



See Fig.3.11 for pin location on gantry

Figure 5.27. Daily movement of pin 3 from November 1986 to May 1987.

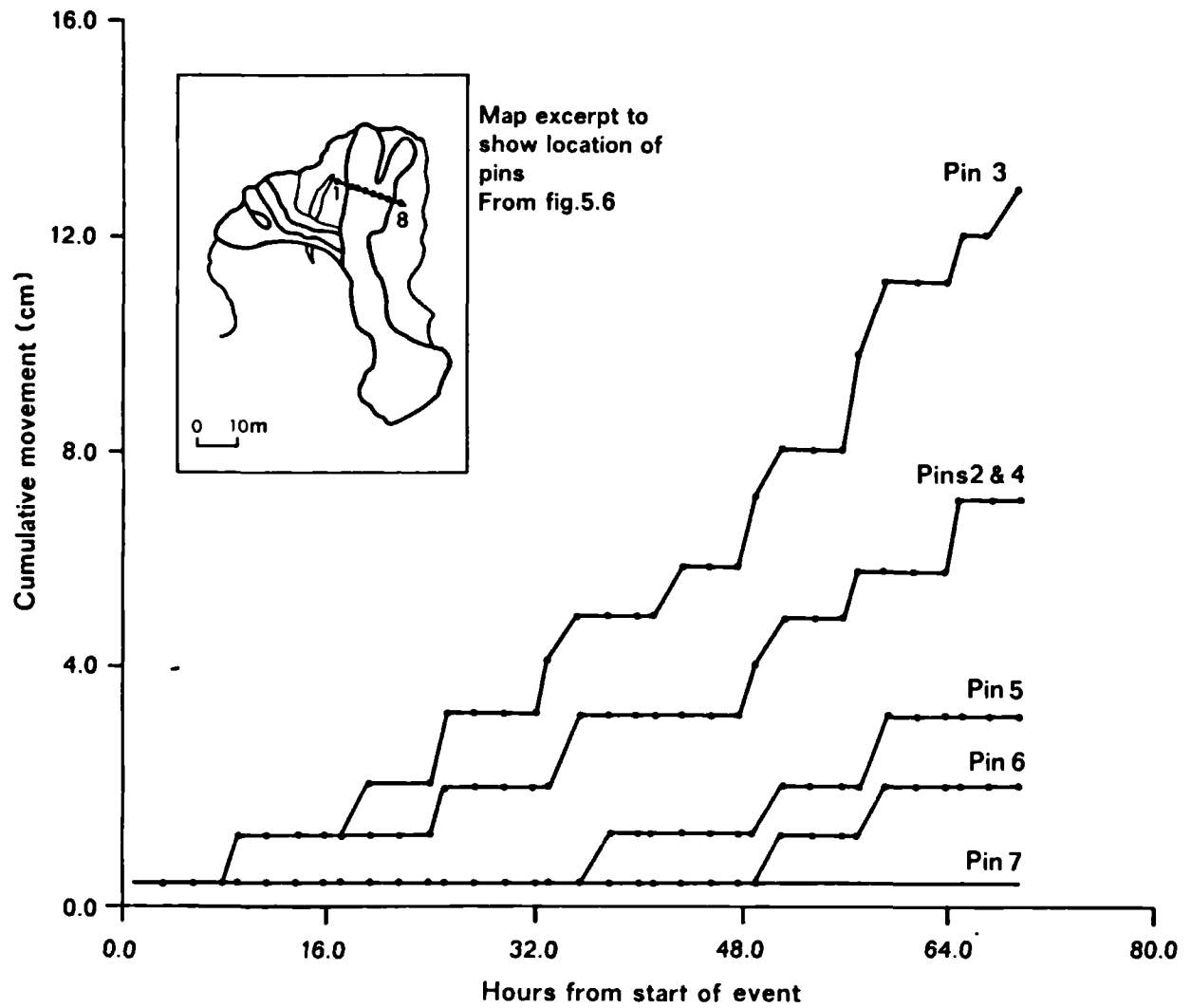


work three intensities of movement were recognised: a low-intensity 'multiple' displacement, a medium-intensity 'graded' movement, and a high-intensity infrequent 'surge'. For example the daily summary of pin 3 for the 86/87 winter period is plotted in Figure 5.27, from which the magnitude of these movements may be identified. The first category involved movements of less than 10 cm per day, while graded displacements may be classified as those between 0.1 to 1.0 m per day. Surge events were considered to be individual events involving displacements in excess of 1.0 m per day.

The plot also showed that the temporal sequence of movements involved phases of activity interspaced with no displacement. The phases of activity may include a single category or a combination of movement mechanisms which usually operate over a series of days. Two phases of low-intensity multiple movements were first measured in November 1986, followed by 6 days of graded movements in mid-December before the first major surge on January 1st 1987. Three subsequent phases of graded displacements were recorded before a further surge on the 27th March. Some graded events during this period contained daily averages close to the arbitrary division of 1.0 m, which may be considered small-magnitude surges. Major movement ceased on the 11th April 1987 although two further displacements were recorded for the low-intensity multiple category of movement.

The daily summary implies that the duration of each phase of movement may range from one day to several weeks, but it was not clear whether displacements during these periods are uniform. The continuous record enables the identification of the intensity and duration of such events

Figure 5.28. An example of a low-intensity 'multiple' mechanism of movement from 0900 hours on the 14th November 1986.



which have until recent years been unobtainable in studies of mass movement. Thus an example of each category of movement will be described, followed in the next section by a discussion of the influence of other factors upon seasonal mudslide behaviour.

With reference to Figure 5.28, the first sequence of multiple movements in November 1986 was plotted for each movement sensor with respect to time. The plot is similar to the findings of Allison (1986) but it is further noted that there was a tendency for the intensity, frequency and extent of displacements to increase from the start of movement. Multiple events were limited to individual displacements of one or two centimetres per hour. Pins 1 and 8, connected to stable ground either side of the lateral shear surface, recorded zero movement throughout the study and were not included in these plots. Pins 5, 6 and 7 only recorded movement during the most intensive phases of displacement.

Figure 5.29, is an example of the graded style of movement from the 22-24 of January 1987. Movement was characterised by an increase in the intensity of displacement to approximately 10 cm per hour, although there was an apparent reduction in the duration and frequency of event in comparison to multiple movements. However, care was required in assuming this change since the displacements of the multiple events were smaller than the recording capabilities of the data-logger: a rotation of the pulley through 14.4° arc was required to register one millivolt or logger step, so that a uniform creep or stick-slip type movement could result in the same plot as Figure 5.28.

Figure 5.29. An example of a 'graded' mechanism of movement from 0600 hours on the 22nd January 1987.

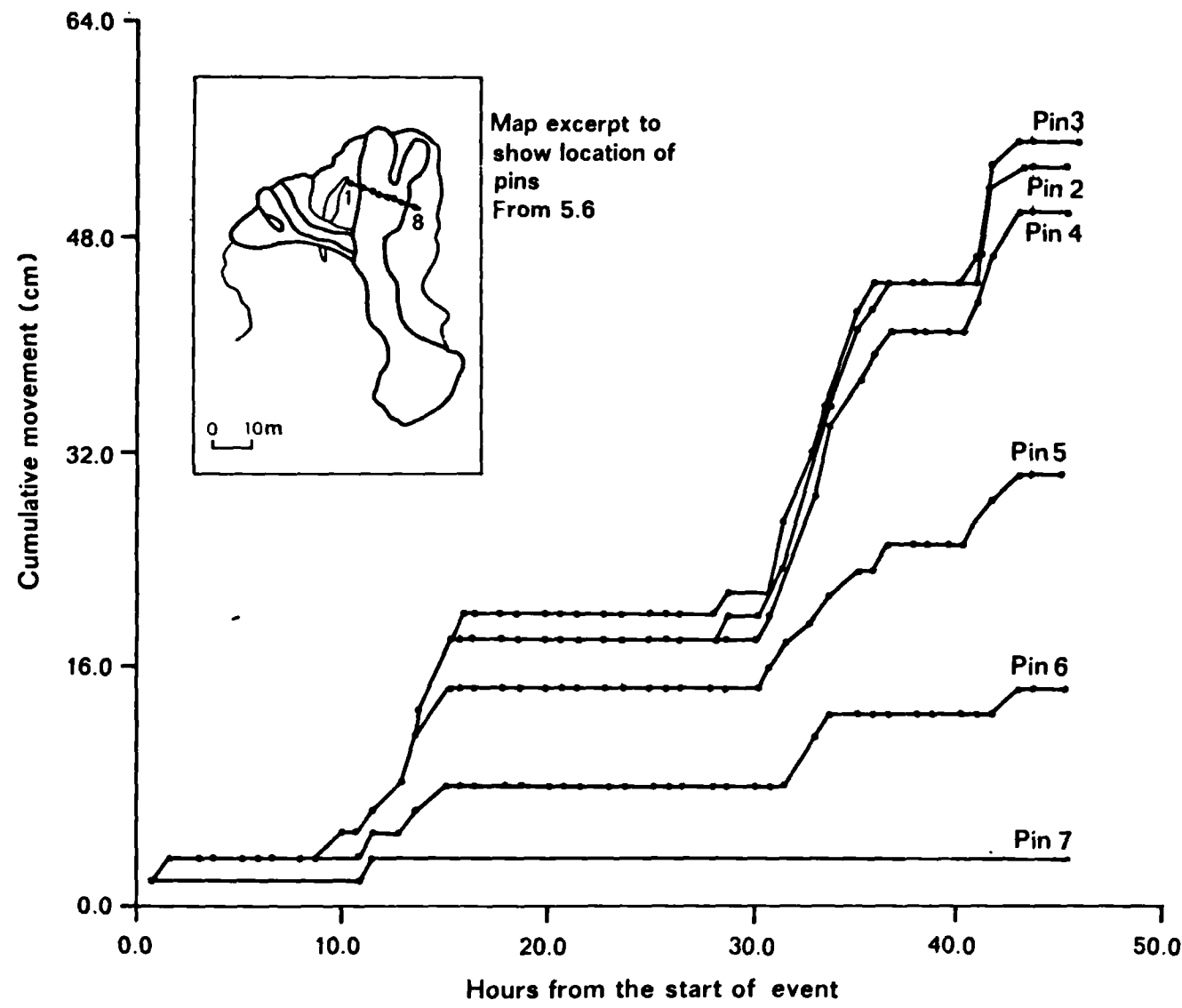
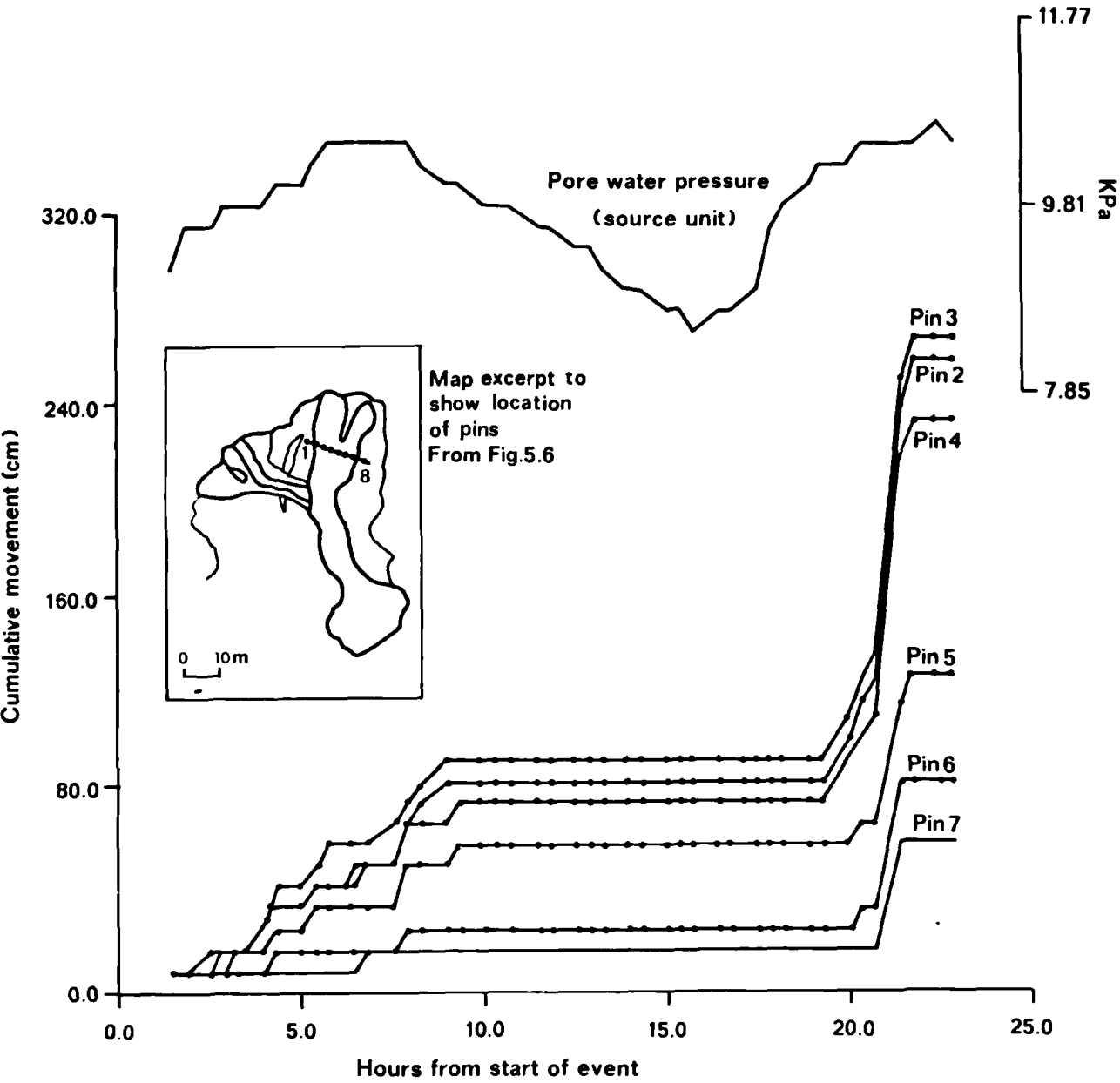


Figure 5.30. An example of a high-intensity 'surge' mechanism of movement from 0300 hours on the 1st January 1987.



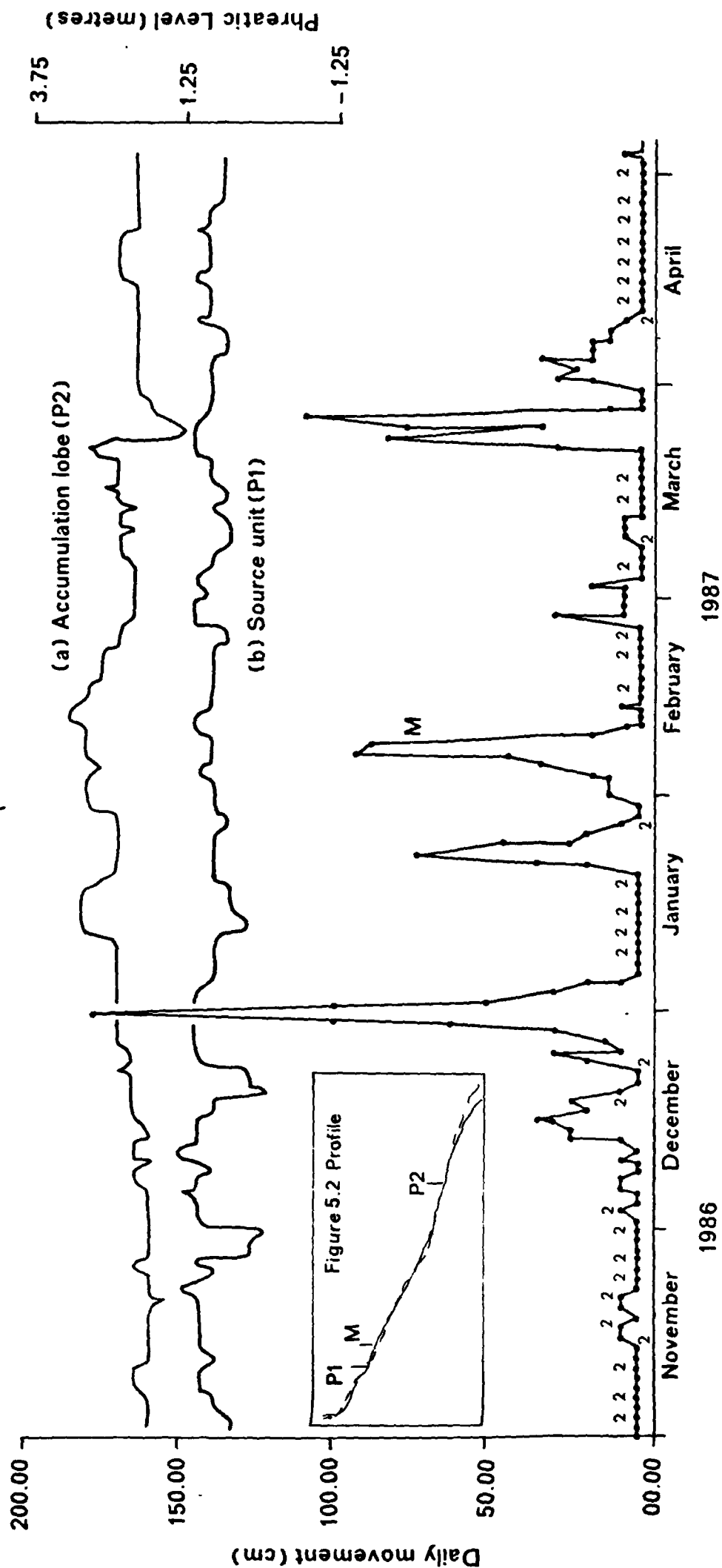
The frequency and duration of graded movements surrounding surge events were considered to be the same as found above, although the intensity was found to increase slightly to 20 cm per hour (Figure 5.30). The phase of movement in which the surge occurred involved a sequence of graded events over 90 minutes culminating in a rapid displacement of 1.2 m in 10 minutes. The higher intensity graded and surge events were clearly separated by periods of no movement emphasising the cyclical nature of mudslide behaviour. The pore water pressures in the source were found to coincide with each phase of movement, with a characteristic rise before each event, reaching a maximum during displacement and subsequent reduction following the cessation of movement.

Two interesting facts may be isolated from Figure 5.30: firstly, the pore water pressures required for the start of movement were lower than at the finish; secondly, the intensity of pore water pressures required for the second movement event was greater than for the first. Thus, the temporal distribution of each category of movement was considered to reflect the influence of pore water pressures and other de-stabilizing factors (see section 6.22).

5.332 Association of movement with other factors.

The category or intensity of movement was directly influenced by the soil water relations. Both pore water pressure and soil moisture increased during the winter months in response to the positive net hydrological flux which attained a maximum in December 1985. Soil moisture potentials or pressures are by nature more sensitive to change and are normally associated with slope instability. With reference to Figure

Figure 5.31. Daily summary of maximum movement (pin 3) and pore water pressure throughout the 1986/87 winter period.



5.31, pore water pressures were superimposed upon the daily summary of movement from November 1986 to May 1987. The plot revealed a close relationship between movement events and large fluctuations in pore water pressures in the source unit, and a gradual rise in pressure in the lobe.

It was therefore considered unlikely that the pore pressures in the accumulation lobe were directly related to movement generation, except under the most extreme conditions: it was noted that the pore water pressures of the lobe increased in response to major movements from upslope as a consequence of secondary loading at the base of the track.

The seasonal activation of the mudslide occurred following a rise in the water table above the shear surface in the source units during November and December. The magnitude and frequency of pressure fluctuations during this period, initially resulted in multiple 'creep' movements, followed by more rapid graded displacements. Changes in pressure associated with movements were not very sensitive in the first instance, but maximum values were recorded within several hours before the onset of the graded displacements, after a total rise in pressure equivalent to 5 kPa. Following reactivation, lower pore water pressures were associated with the graded category of movement, although a rise in pressure of 5 kPa was generally found, suggesting that an element of 'strain-softening', bond-breaking or mobilization of the shear surface may have taken place during the reactivation process.

Towards the end of December there was a rapid rise in pressure in the source unit, from 0 to 10 kPa in 4 days, which was considered responsible for the major surge. A similar response was attributed to the second surge on March the 27th. Elevated pressures remained for several days

reaching a maximum within an hour before the surge occurred (Figure 5.30). Pore pressures in the source decreased substantially following movement, but as a result of the surge a large increase in pressure was subsequently recorded in the accumulation lobe (Figure 5.31).

It was not possible to associate pore water chemistry or salt deposition directly with movement since the sampling framework was inadequate for this purpose. However, it was shown that the deposition of salt was greatest in November and most severe on the lower slopes. Peak pore water salt concentrations were measured in January 1987 although these would have partly been due to weathering and slope movements themselves. The release of aluminium from the rear-scarp suggested at least one phase of major erosion and weathering before the major failure, which may have been associated with the primary undrained loading of the mudslide source. Subsequent releases of aluminium in the source were considered to arise from movement events with variable time-lags (section 5.323). The effects of variations in the type and concentration of salts upon the shear strength of the slope materials was simulated in the laboratory to establish to what extent this might affect the stability of the slope.

5.4 Shear strength simulation.

The methods used in the shear strength simulation are fully described in section 3.43 and Appendix 6C. Because this form of test has only recently been developed it was felt prudent to rigorously control for the effects of head pressure, strain rate and normal load. Additionally, since the aims of the simulation were to assess the role of chemistry upon the residual shear strength of a single sample, a pre-

defined effective stress had to be chosen for use in all tests to allow for the comparison of each chemical treatment within and between test samples. A normal load of 1000 Newtons was found to be ideal since this significantly reduced the seepage of solution and loss of clay from the sides of the sample cell (section 3.43). However, it was noted that the corresponding normal effective stress of 249.7 kPa was twelve times greater than the respective stresses measured in reality for shallow mudslides 7-19 kPa (see section 4.321); the ring-shear was unable to test at these low effective stresses.

Drained conditions were maintained throughout the tests using a head pressure of 1.0 m and a rate of strain of 0.032 min^{-1} , which resulted in a minimum flow of solution of $3 \text{ cm}^3/\text{hr}$. This set-up was held constant for each test series, the only variables being the sample and pore water chemistry.

Preliminary tests showed that a minimum of 48 hours were required for full residual conditions to develop following each chemical treatment, which meant that the length of time for each test-sample was approximately 14 days. This constrained the number of samples to be tested considerably. Eight series were thus designed (see section 3.43), in each of which two independent samples were simulated. Thus each series took on average one month to complete.

In every series one test specimen was treated with an increasing concentration of chemicals, whereas the second was treated with a decreasing concentration of salt. This was considered necessary to account for the inevitable variation in strength caused through physical effects, softening and alignment, so that variability unaccounted for by

these could be considered to be chemical effects. The results of the two simulations were combined and an average calculated. Although the same material was used for both samples slight variations in sample lithology were unavoidable, but the residual shear strength was calculated to within a 5 per cent error.

5.41 Pure clay minerals:

5.411 Effect of mineral type and quantity.

With reference to Table 5.5, the effect of different types of clay minerals upon shear strength was assessed. Pure montmorillonite and kaolinite clay minerals were used in two proportions: one third montmorillonite with two thirds kaolinite and vice versa. Each proportion was leached with a range of solution concentrations of sodium and calcium chloride salts in separate test-series.

The residual shear strength of all four series showed differences in strength dependent on the proportion and type of clay mineral, and the dominant exchangeable cation (Figure 5.32). Where kaolinite dominated, relatively high mean strengths were recorded (60-75 kPa) equivalent to a residual friction angle of 14-16°. The range of values were attributed to the chemical status of the clays, with sodium monovalent cations supporting the lowest strengths.

Where montmorillonite clays dominated lower residual shear strengths were measured, decreasing 50 per cent to 33.1 kPa for sodium exchanged clay, and by 25 per cent to 54.5 kPa for calcium exchanged clay. The range of

Table 5.5. Relationship between residual strength and solution chemistry from simulation tests on pure clay minerals.

Conc.	τ_r' (kPa)	ϕ_r' (°)	$\frac{\tau_r'}{\sigma'}$	pH	Cond. mS/cm	Na	K	Mg (mg/l)	Ca	Fe
<u>Series 1.</u>										
0.3	72.11	16.1	0.29	6.57	1.85	642	2	1	8	0
0.5	56.29	12.7	0.23	6.64	2.02	809	3	T	8	0
0.75	59.48	13.4	0.24	6.69	2.36	1167	5	0	8	0
1.0	60.85	13.7	0.24	6.72	2.8	1402	7	0	8	0
\bar{X}	62.18	14.0	0.25	6.66	2.26	1005	4	T	8	0
<u>Series 2.</u>										
0.3	80.71	17.9	0.32	6.81	2.31	84	4	2	856	3.4
0.5	70.51	15.8	0.28	6.94	2.73	76	9	4	1030	4.31
0.75	69.81	15.6	0.28	7.1	2.94	14	8	3	1327	5.24
1.0	70.78	15.8	0.28	7.15	3.1	5	8	3	1567	6.54
\bar{X}	72.95	16.3	0.29	7.0	2.77	45	7	3	1195	4.87
<u>Series 3.</u>										
0.3	32.09	7.3	0.13	6.46	2.31	604	4	3	149	0
0.5	28.94	6.6	0.12	6.56	2.66	968	5	1	64	0
0.75	34.88	7.9	0.14	6.8	2.76	1203	4	T	20	0
1.0	36.52	8.3	0.15	6.83	2.97	1537	4	0	16	0
\bar{X}	33.11	7.5	0.14	6.66	2.68	1078	4	1	62	0
<u>Series 4.</u>										
0.3	48.27	13.1	0.19	6.84	2.1	55	6	3	869	3.21
0.5	49.95	11.3	0.2	6.85	2.64	19	7	4	1049	5.33
0.75	58.28	13.1	0.23	6.94	2.76	10	10	5	1350	8.55
1.0	61.47	13.8	0.25	7.15	2.97	7	9	5	1945	8.67
\bar{X}	54.49	12.8	0.22	6.95	2.62	23	8	4	1303	6.44

Series 1 : 33 % montmorillonite with 66 % kaolinite, Na-saturated clay

Series 2 : 33 % montmorillonite with 66 % kaolinite, Ca-saturated clay

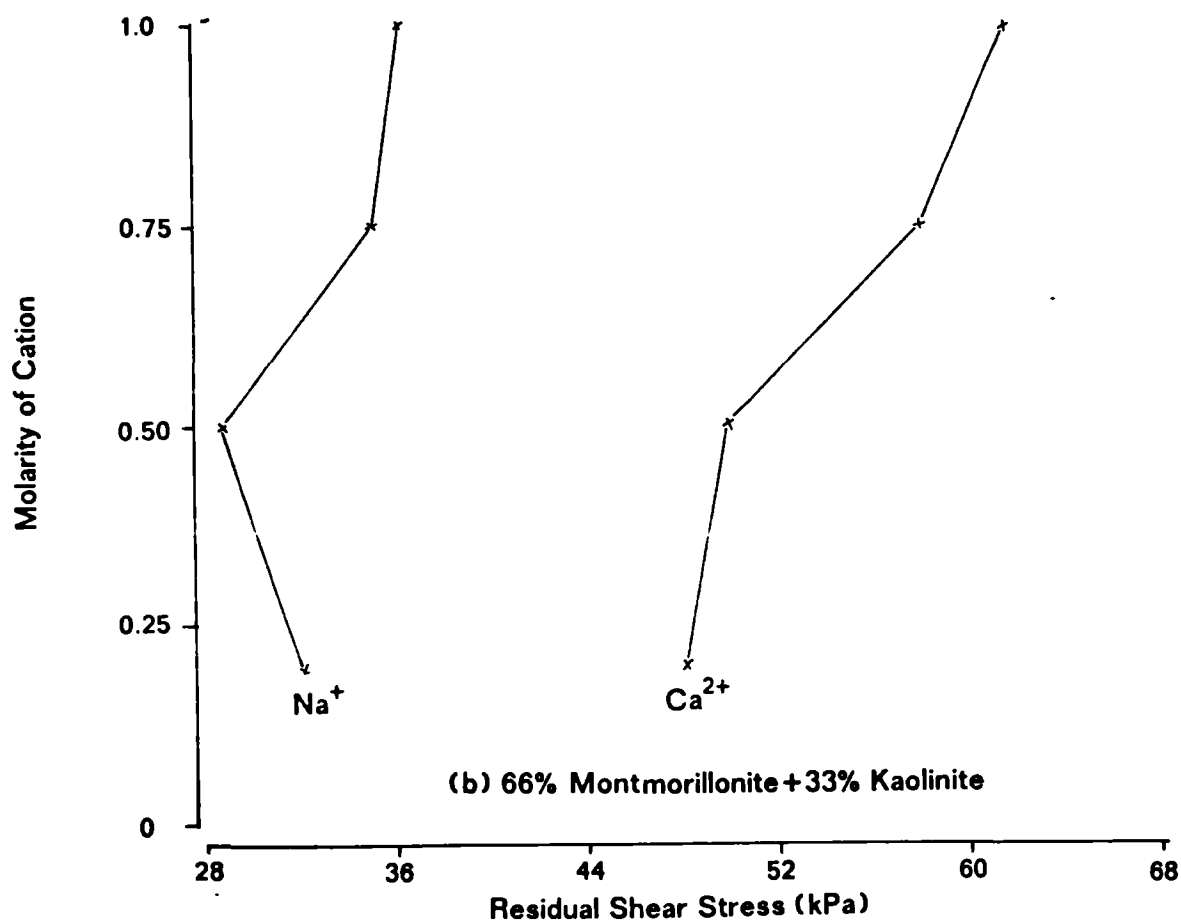
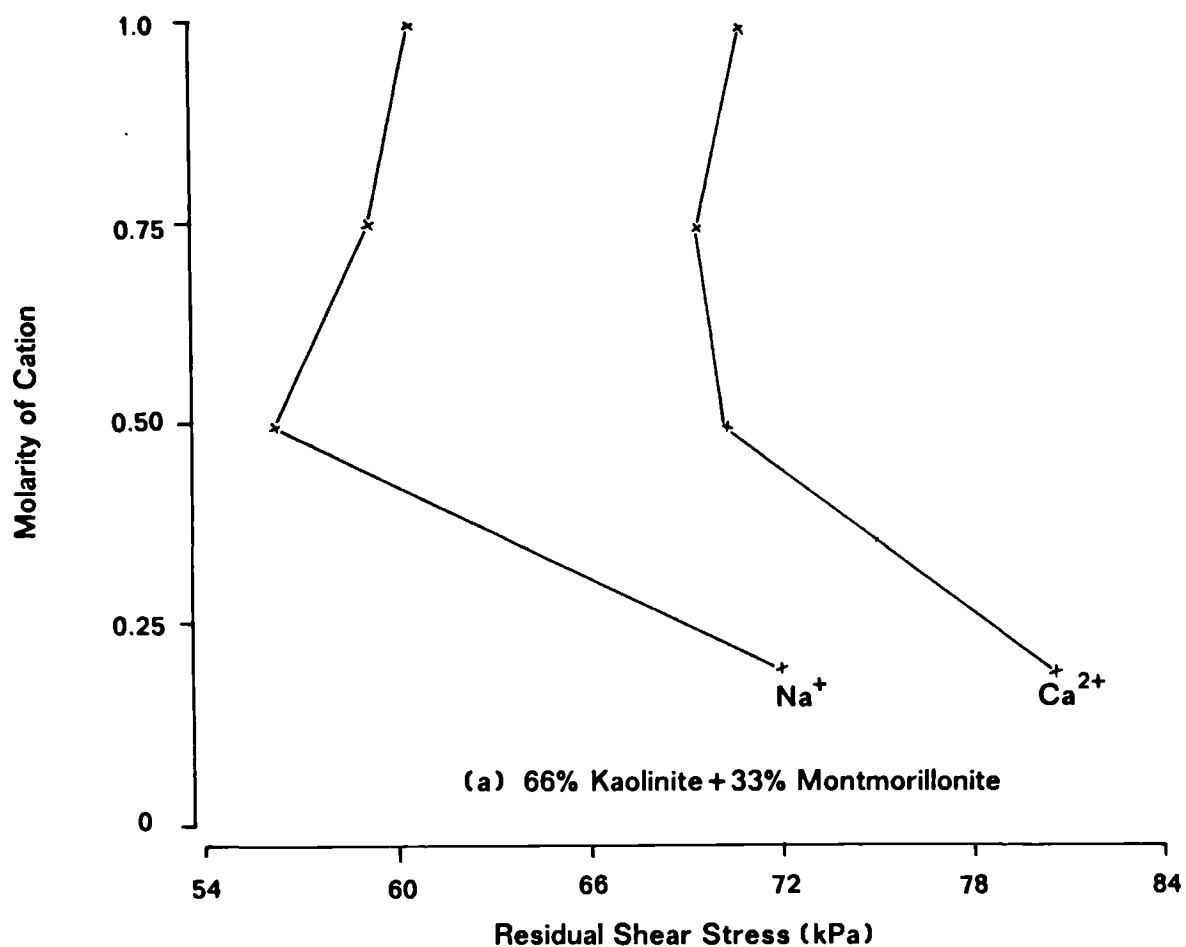
Series 3 : 66 % montmorillonite with 33 % kaolinite, Na-saturated clay

Series 4 : 66 % montmorillonite with 33 % kaolinite, Ca-saturated clay

Conc. : Molarity where 1 M equals 1000 mg/litre

T : trace <1 mg/l

Figure 5.32. Relationship between clay mineral content, the type and concentration of pore water cations and residual strength.



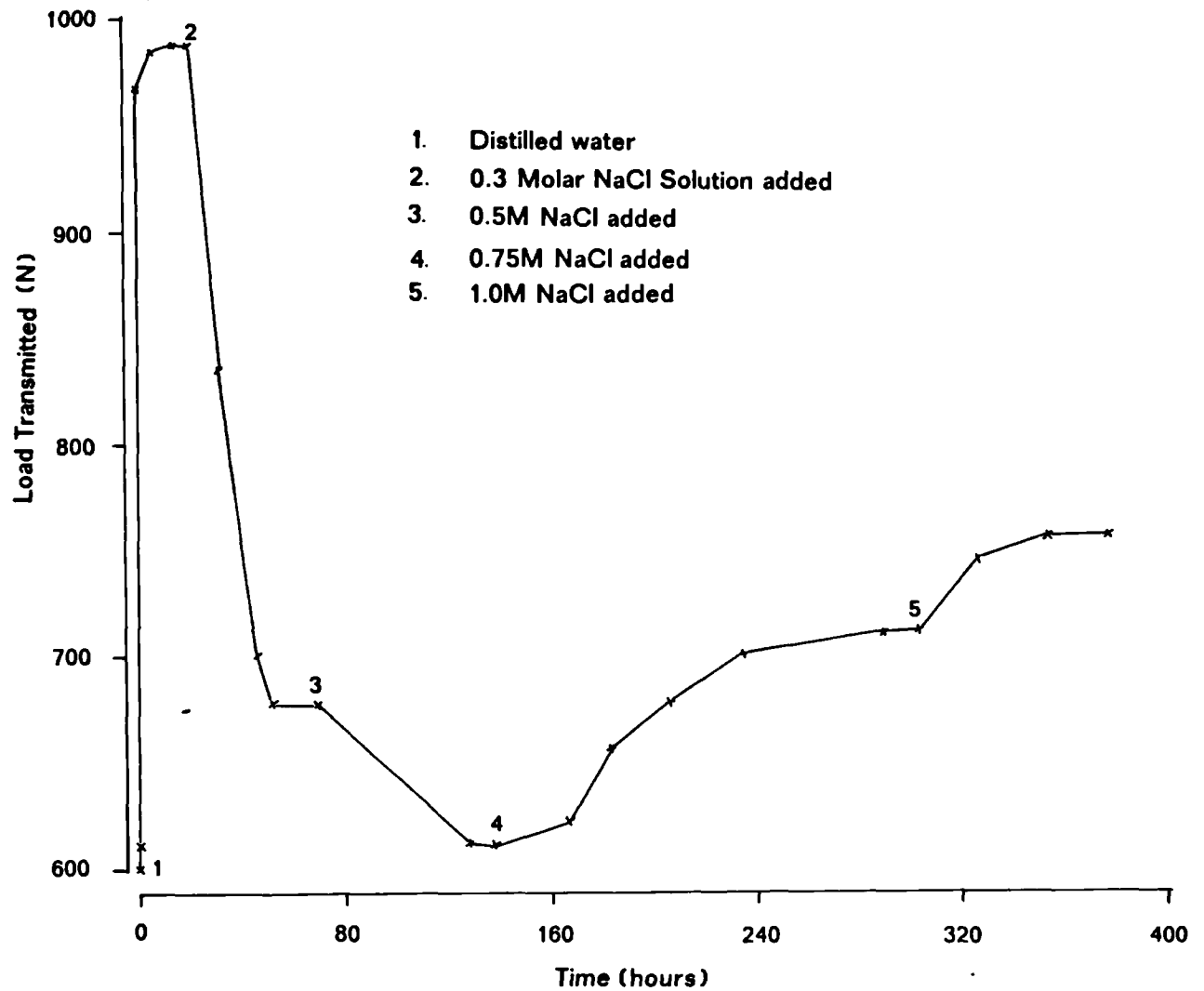
strength attributable to clay chemistry doubled to 20 kPa or 36 per cent of the residual strength term. The findings of these pure clay mineral tests confirmed the theoretical conclusions of section 2.32, and suggested that montmorillonite clay minerals and the chemistry of clay surfaces can account for changes in residual shear strength of upto 50 per cent.

5.412 Effect of exchangeable cations.

With reference to Figure 5.32 monovalent sodium cations consistently supported lower residual strengths than calcium divalent cations. For kaolinite dominated systems a 15 per cent difference in strength occurred with respect to the valency state of the exchangeable cation, increasing to 39 per cent with montmorillonite clay minerals. The concentration of each ion was also found to result in changes in shear strength of up to 15.82 kPa. This effect was greatest for kaolinite dominated clay at low solution concentrations (Figure 5.32a), where residual shear strength was found to decrease with an increase in concentration to 0.5 M. This would suggest that the effect of the small percentage of montmorillonite was suppressed by the dominant kaolinite at low concentrations. Once saturated with salts, the more reactive montmorillonite minerals have an overriding effect upon the shear strength of the kaolinite dominated system.

This is partly supported by the fact that such an effect was absent from the montmorillonite dominated clay samples. These not only showed a reduction in strength as a result of mineral type, but also a reduction in residual strength from salt concentration effects by up to 13.2 kPa or 22 per cent of the strength term. Figure 5.32b shows a clear reduction

Figure 5.33. Residual stress transmitted in relation to pore water chemistry and time.



in shear strength with concentration. For calcium exchanged clay this results in a decrease in strength of 13.2 kPa, whereas for sodium saturated clay the corresponding value was 7.58 kPa. The latter clays showed that a salt concentration of 0.5 M supported the lowest residual shear strengths.

This is clearly shown in Figure 5.33 where the stress transmitted throughout the sodium test simulation is plotted with time. Following the initial rapid rise in strength, residual conditions were attained for the first solution increment of 0.3 M concentration. The stress transmitted was seen to drop further with the second increment of 0.5 M sodium solution. Subsequently, the transmitted stress increased uniformly and predictably with further increases in salt concentration.

The findings show that the type and concentration of cations can account for changes of up to 46 per cent of the residual strength of montmorillonite dominated clays (Table 5.5). This was reduced to 15 per cent where kaolinite was the dominant clay mineral. The concentration of pore solutions consistently accounted for up to 22 per cent of the strength term for all simulations except for the calcium saturated kaolinite dominated clay where this effect was reduced to 14 per cent.

5.42 Natural samples:

5.421 Effect of sea-salts on residual strength.

Undisturbed and weathered mudslide samples from both Manor Lane and Worbarrow Bay were used in simulation to assess the effects of sea-salts upon residual shear strength. Filtered sea-water was diluted into four concentrations of 10, 30, 50 and 75 per cent and along with normal (100%) sea-water each were used as test solutions in each simulation. The residual strength results are presented in Table 5.6, in addition to the pre- and post-flow solution chemistry. The results may be compared with the standard ring-shear tests reported in section 4.32. The simulated residual friction angles for both the disturbed and undisturbed London Clay were found to vary between 9.6 and 11.9° respectively, which compare favourably with the standard residual strength results (see Table 4.13). The corresponding range measured for the Weald Clay was 17.6 to 22.2, which again were in reasonable agreement with earlier findings (Table 4.14) although it was noted that significantly lower residual friction angles were found for the weathered materials in the standard determinations.

With reference to Figure 5.34 the weathered and undisturbed residual strength of the London and Weald Clay are plotted with respect to sea-water concentration. The plots show the inherently lower shear strengths exhibited by weathered materials, and also an increase in strength with sea-water concentration. This was most marked with the weathered Weald Clay series where a reduction in residual strength of 18.07 kPa or 19 per cent, was accountable by pore-water concentration. In the undisturbed condition only 3.67 kPa or a 4% reduction of the residual term could be accounted for in this manner.

Table 5.6. Relationship between residual shear strength and solution chemistry from simulations on weathered and unweathered London and Weald Clay.

Conc. %	τ_r' (kPa)	ϕ_r' (°)	$\frac{\tau_r'}{\sigma'}$	pH	Cond. mS/cm	Na	K	Mg (mg/l)	Ca	Fe
<u>100 % sea-water chemistry</u>				6.98	48.2	9617	399	1272	403	1.79
<u>Series 5.</u>										
10	42.46	9.6	0.17	7.01	5.67	941	70	185	404	0.47
30	45.12	10.2	0.18	7.03	14.74	2527	105	408	261	0.62
50	46.63	10.6	0.19	7.08	25.85	4642	184	633	315	1.05
75	48.31	10.9	0.19	7.14	36.73	6879	262	950	378	1.24
100	49.33	11.2	0.2	7.19	49.77	10179	389	1297	463	1.82
\bar{X}	46.37	10.5	0.16	7.09	26.55	5034	202	695	364	1.04
<u>Series 6.</u>										
10	79.25	17.6	0.32	6.97	4.91	960	60	156	114	0
30	80.89	17.9	0.32	7.00	14.20	2511	121	374	187	0.41
50	91.92	20.2	0.37	7.02	24.97	4680	179	650	259	0.77
75	96.09	21.0	0.39	7.06	36.36	6817	253	961	331	0.99
100	97.32	21.3	0.39	7.07	47.88	9850	333	1234	394	1.3
\bar{X}	89.09	19.6	0.36	7.02	25.66	4964	189	675	257	0.69
<u>Series 7.</u>										
10	49.33	11.2	0.2	7.02	5.09	959	56	159	123	0.03
30	50.44	11.4	0.2	7.04	13.82	2538	143	412	208	0.45
50	51.15	11.6	0.21	7.07	25.3	4689	213	687	282	0.83
75	52.48	11.9	0.21	7.11	37.18	6891	286	978	353	1.27
100	54.79	11.9	0.22	7.17	50.06	10244	403	1339	410	1.41
\bar{X}	51.64	11.6	0.21	7.08	26.29	5064	220	715	275	0.8
<u>Series 8.</u>										
10	98.13	21.4	0.39	6.94	4.9	943	55	148	73	0
30	96.93	21.2	0.39	6.96	13.66	2500	125	377	152	0.43
50	101.45	22.1	0.41	7.05	24.54	4664	229	659	231	0.77
75	101.67	22.1	0.41	7.05	36.33	6806	278	952	326	1.16
100	101.8	22.2	0.41	7.06	46.96	9407	313	1214	389	1.57
\bar{X}	100.0	21.8	0.4	7.01	25.28	4864	200	670	234	0.79

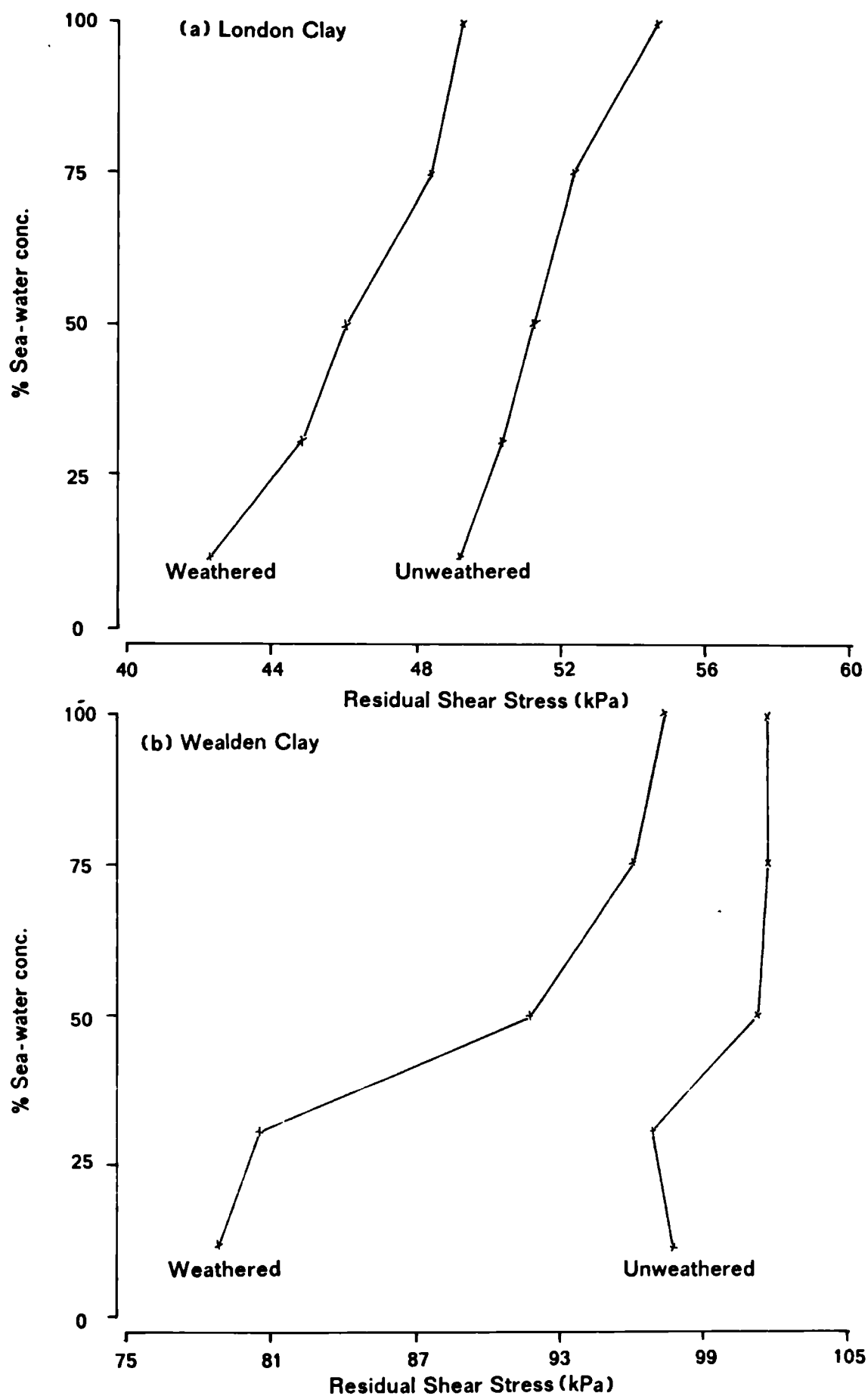
Series 5 : weathered London Clay

Series 6 : weathered Weald Clay

Series 7 : undisturbed London Clay

Series 8 : undisturbed Weald Clay

Figure 5.34. The effect of sea water concentration upon the residual strength of weathered and unweathered London and Wealden Clay.



The London Clay showed a similar association between residual strength and sea-water concentration. The strength of weathered clay was found to decrease by 6.87 kPa or 14 per cent with a reduction in concentration; the undisturbed strength decreased by 5.46 kPa or 10 per cent with concentration. Throughout the test-series of simulations the post-flow chemistry remained relatively constant, suggesting equilibrium within the clay-water system and the pre-flow solution chemistry. However, it was noted that at low concentrations (10%) a large proportion of divalent cations were released to the pore water from the weathered clays, which were assumed to have been replaced by monovalent cations. The conversion from a divalent to a monovalent system would have significant effects upon the stability of the clays (see section 2.312) and may well account for the greater fluctuation or sensitivity of residual strength at these low salt concentrations.

These findings show that the residual strength of fully weathered clay may fluctuate by up to 20 per cent through the effects of pore water concentration. The type of clay minerals and dominant cation have already been shown to produce even greater effects. The leaching of undisturbed clay samples resulted in less pronounced effects on shear strength suggesting that an element of physical erosion and weathering is required to promote the physico-chemical behaviour of mudslipped clays.

5.5 Conclusions.

The findings of this chapter have shown that the dynamics of mudslide behaviour are intrinsically related to weather and climatic conditions. This association was emphasised in the isolation of seasonal cycles of change in both weather conditions and mudslide displacement rates. Although an increase in the duration and intensity of rainfall was typically associated with an increase in mudsliding, as observed in this study, the net hydrological flux was found to provide a closer estimation of the likely effects of rainfall upon the soil moisture status. Maximum surpluses occurred in December and were primarily responsible for the re-activation of mudslide movements. Moisture deficits from May to September coincided with the cessation of mudsliding.

The per cent soil moisture and phreatic levels showed corresponding seasonal cycles. Differences were recognised between the source and lobe slope units for both parameters, amounting to 16 per cent for the moisture volume fraction and a pore water pressure equivalent to a 1 m head of water above the shear surface. The maximum soil moisture content and pore water pressure recorded in the source unit and accumulation lobe were 34.4 and 49.5 per cent and 6.33 kPa and 15.94 kPa, respectively. Artesian conditions prevailed on the lower slopes all year with a minimum phreatic level of 1 m, and the presence of large soil moisture variations below the shear surface at the base of the feeder track located the presence of an *in situ* basal-aquifer.

The soil water relations of the source unit were highly sensitive to change with respect to climatic conditions, and time-lags were identified such as several days, in the case of pore pressures. Changes in the soil

moisture status of the lobe were more uniform and only occurred under the severest of climatic conditions or slope movements. Time-lags were also identified between the source and lobe slope units.

The seasonal movement and morphological change of the mudslide were assessed by photogrammetry and by automatic movement sensors. Photographic analyses showed the back-cliff had receded in several places by up to a maximum of 1.38 m. Other areas of cliff-top showed little change, any recession ^{being} limited to the surface weathering and erosion of individual particles. The extent of the mudslide revealed greater differences between September 1986 and May 1987, with both source units extending towards the rear-scarp by up to 4.76 m and the toe of the slope advancing seaward by 1.38 m. Changes in the position of the lateral shear surfaces were noted but these were found to be in steady-state and along with the overall form of the landslip the mudslide was considered to be in dynamic equilibrium.

Maximum cumulative movements equalled 25.65 m in 1985/86 compared with 19.98 m in 1986/87. The pattern of movement revealed large differences in surface displacement across and down the mudslide. Three intensities of movement were identified which were termed multiple, graded and surge events after Allison (1986). Each mechanism was closely associated with a different intensity and duration of pore water pressure and other destabilizing factors, although lower intensities were recorded immediately following the seasonal re-activation process.

The deposition of sea-salts showed very marked peaks in November 1985 and 1986 as a result of maximum south-westerly wind speeds. An index of the effectiveness of south-westerly precipitation and salt deposition showed

that for rainfall and wind speeds in excess of $1.35 \text{ mm/msec}^{-1} \text{ month}^{-1}$, the concentration of salts deposited on the coastal cliffs was linearly related to monthly rainfall in excess of 42 mm and mean monthly wind speeds above a threshold 7.5 msec^{-1} .

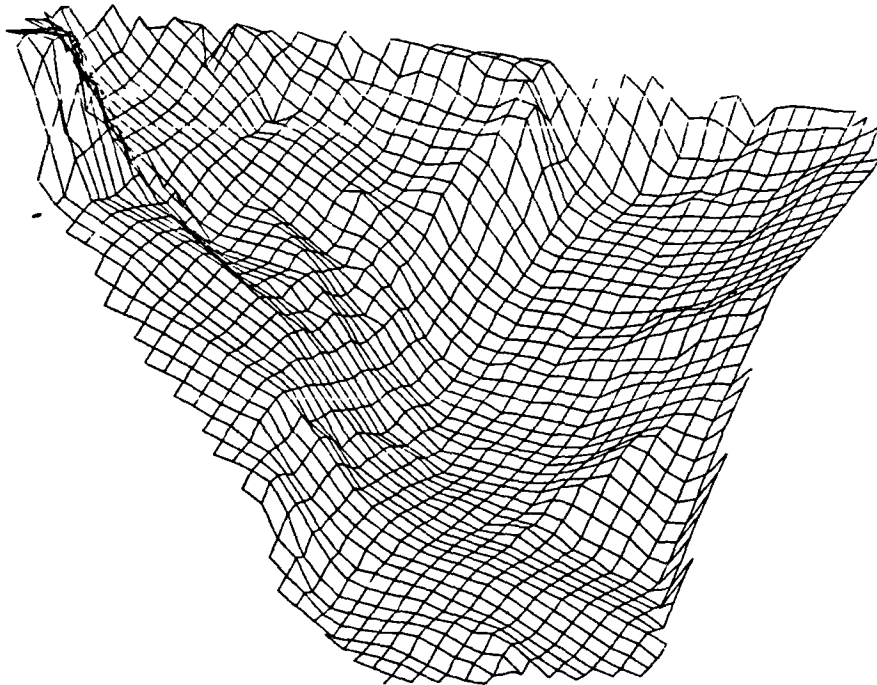
Local topography was found to have quite large effects upon micro-climate. During periods of high wind rainfall was considerably reduced on the mudslide as a result of the funnelling of winds up the coastal slope, resulting in an increased deposition inland towards the weather station. Additionally, salt deposition was found to decrease exponentially up the mudslide away from the sea, the cliffs acting as a 'salt-trap', and only in the most intense storms were salts carried inland decreasing in concentration with distance.

The deposition of salts on the coastal slopes has a direct influence upon the intensity of surface weathering and erosion of material from the cliff, loading the source region before the onset of movement. At least two phases of loading were recognised from chemical analyses of pore water from the mudslide and ground water input to the source unit from the back-cliff. The release of aluminium, iron and silica into solution were found to be highly sensitive to erosion and movement events. The concentration of salts in the pore water showed maxima of 2.94 g/litre from January to April and always remained more concentrated than the dilute groundwater (2.1 g/l). Peak concentrations were considered to have arisen from both the diffusion of surface sea-salts to the zone of shear and from the release of salts from the weathering and erosion of material following cliff failures and mudslide movements.

Simulation tests found that the residual strength of the clays was extremely sensitive to the mineralogy and chemistry of the system. The findings have implications to the seasonal instability of mudslides because where montmorillonite minerals are present in excess of 30 per cent, fluctuations in the valency and concentration of cations can cause changes in residual strength of up to 39 per cent. The lowest strengths coincided with low pore water concentrations. Conversely, residual shear strength was found to increase by as much as 20 per cent with an increase in sea-water concentration. These effects may be of considerable importance when modelling the stability of coastal slopes with respect to fluctuations in pore water pressure, soil moisture, pore water chemistry and the physico-chemical properties of clays (see sections 6.223 and 6.4).

Chapter Six

SOLUTE GEOCHEMISTRY AND SLOPE STABILITY ANALYSIS



6.1 Introduction.

Although the results of the 'static' and 'dynamic' properties of mudslides have been considered separately (Chapters Four and Five), the purpose of this chapter is to combine these findings to evaluate the importance of the physico-chemical variability of clays upon the seasonal behaviour of mudslides; this was undertaken in three parts.

Firstly (section 6.21), the most important soil chemical, mineralogical and mechanical properties were cross-correlated to identify the properties most closely associated with the residual strength parameters. A correlation matrix was provided for values measured at the shear surface (sub-zone 3) and for the mean computed from all four sub-sample zones (section 6.412). In section 6.22, the field results are correlated in a similar manner. A correlation matrix of all the parameters in the 20-month summary was produced to identify which variables were most closely associated with mudslide movement. Although adequate for this purpose the monthly summary was not sufficiently resolute to identify time-lags operating between the variables. Thus, for those parameters measured continuously a correlation matrix was also computed for the daily summary. Time-lags of 1, 2, 4, 7, 14, 21 and 28 days were assumed and applied to the matrix in an attempt to quantify the antecedent lags operating between the parameters such as slope movement, climatic and soil water variables.

Secondly (section 6.3), the chemical properties of each site were verified using established geochemical programmes of the US Geological Survey. Programmes WATEQF and PHREEQE were used to clarify and simulate the likely changes to chemical equilibria through the dilution and

addition of salts to the pore water, and from varying intensities of weathering. From these results a geochemical model was proposed to complement the physical process-response system of Brunsden (1973).

Thirdly (section 6.4), the observed fluctuations in shear strength were related to the seasonal instability of mudslides. From laboratory simulation tests changes in residual strength were directly measured and calibrated for known fluctuations in pore water concentration measured on-site at Worbarrow Bay. The resultant change in residual shear strength was applied to the cohesion term and used in a custom-designed slope stability model to enable the input of a higher resolution of data than conventionally used. The factor of safety was assessed throughout the study period where it was found that in combination with pore water pressure and undrained loading, the model provided very realistic estimations of the seasonal instability of each site with respect to field observations.

6.2 The physico-chemical variability and behaviour of mudslides.

6.21 Static properties and residual strength:

The static properties of two independent mudslide systems were presented in Chapter Four. In conclusion to this chapter a number of associations between parameters were recognised and considered to be common to both landslides. Others were assumed to reflect local variations in lithology and morphology. Although the variability in soil properties was established, it was necessary to obtain a quantitative expression of the degree of association between respective parameters, and in

particular to account for the observed distribution of residual shear strength.

The sampling and laboratory design was such that a regular and comparative data-set was produced for all parameters suitable for statistical analysis. Because the purpose of this exercise was to assess the degree of association between properties the coefficient of correlation was chosen in preference to more complex analyses such as trend-surface or factor analysis. The latter tests are appropriate for large data-sets with at least 20-30 sampling points. The current data-set is limited to a maximum of 12 sampling locations at Manor Lane and 7 at Worbarrow Bay, each location consisting of four sub-sampled zones (section 3.412).

In principle a correlation matrix could be computed for each sub-zone, although it has been made clear that the properties at the basal shear surface (zone 3) are the most critical in controlling the behaviour of mudslides (section 1.5). In Chapter Four mean values were computed for most parameters for each zonal horizon and for each slope unit. Thus, the values used in the subsequent analyses were based on the core means and those measured directly at the active shear surface.

Using the statistical package SPSS-X on the University of London Amdahl computer, a correlation matrix was obtained for 13 selected parameters. The results are summarized in Tables 6.1 and 6.2 for Manor Lane and Worbarrow, respectively. Tables suffixed with 'a' represent the correlation of values from the shear surface with others from the same zone and the core means. Tables suffixed with 'b' refer to correlations based on the core mean with other means and values from the shear

surface. The significance levels of each coefficient were dependent on the sample size, n , and the critical values for all of the following matrices in this chapter were as follows:

Degrees of freedom	Level of significance (%/100 for two-tailed test)			
($n-2$)	.05	.02	.01	
18	.433	.503	.549	Source : Fisher (1970)
33	.325	.381	.418	
58	.250	.295	.325	
185	.141	.167	.184	

The parameters used in the correlation of the static properties may be divided into three parts: the particle and density characteristics, the geotechnical properties, and the mineralogical and chemical properties. The former and latter characteristics are discussed with respect to the geotechnical properties since these ultimately control slope instability.

6.211 Particle and density characteristics.

The proportion of clay was used to represent the compositional character of each mudslide. The total clay content, the type of clay minerals and the structure and orientation of clay particles were isolated as the most important attributes of the composition of mudslides (section 2.21). Thus, this section (6.211) will concern itself with the effect of clay upon the phase relationships, particle density and micro-structural characteristics and their associations with residual shear strength.

The succeeding section (6.212) discusses the mineralogical and chemical controls upon residual shear strength.

With reference to Table 6.1a for Manor Lane, the proportion of clay at the basal shear surface was found to correlate positively with both the saturated moisture content ($r=.61$) and the void ratio (.71). Both parameters showed a reduction downslope especially for the saturated moisture content (see sections 4.23-4.24). When the proportion of clay at the shear surface was compared with the core sample means a reduced degree of correlation was noted, although the coefficient of correlation with the mean void ratio (.41) remained significant at the 1 per cent confidence level. However, when the mean clay percentage was compared with other variables (Table 6.1b) stronger associations were found between the mean saturated moisture content (.69), mean void ratio (.74), and mean unit weight (-.39). The negative coefficient arises from an increase in unit weight downslope, noted in Figure 4.11, in relation to the slight reduction in clay content. Generally, these results do support the known descriptions of the uniformity of the London Clay, suggesting that the values at the shear surface are inherently more variable within an overall uniform mudslide profile.

At Worbarrow Bay (Table 6.2a), the proportion of clay at the shear surface also correlates strongly with a decrease in saturated moisture content (.68) and void ratio (.59) downslope, and negatively with the unit weight (-.66) as a consequence of an increase in particle density downslope. The coefficients obtained with the means were significant at the 1 per cent level although of lower value. When the mean proportion of clay within the profile was correlated with other variable means (Table 6.2b) such as for saturated moisture content (.59), void ratio

Table 6.2a. Correlation matrix of soil properties from the shear surface at Worbarrow Bay.

PROPI	%C	Ws	e	Y	Ør'	Cr'	Ip	pH	mS/cm	IW	SS	CEC	CM	SP = Value at shear surface M = Mean value								
n=33	SP	M	SP	M	SP	SP	SP	SP	SP	SP	SP	SP	SP	M								
%C	1.0	.86	.68	.43	.59	.35	-.66	-.43	-.19	.13	.03	.15	-.21	.90	.03	.52	-.08	-.27	.49	.47	-.42	-.10
Ws	.68	.51	1.0	.77	.99	.76	-.97	-.80	.45	.63	-.62	.20	.02	.84	.28	.05	.41	.22	.49	.73	-.74	-.55
e	.59	.50	.99	.84	1.0	.84	-.97	-.88	.58	.74	-.65	.28	.08	.75	.29	-.10	.52	.33	.40	.76	-.72	-.61
Y	-.66	-.57	-.97	-.80	-.97	-.79	1.0	.87	-.55	-.70	.51	-.19	.11	-.74	-.11	-.45	-.15	-.26	-.18	.28	.67	.54
Ør'	-.19	-.02	.45	.73	.58	.79	-.55	-.78	1.0	.87	-.52	.25	.11	-.05	.23	-.63	-.69	-.60	-.06	.64	-.32	-.66
Cr'	.13	.36	.63	.90	.74	.92	-.70	-.91	.87	1.0	-.54	.64	.37	-.42	-.25	-.66	-.77	-.64	-.21	.60	-.29	-.53
Ip	.03	.21	-.63	-.44	-.65	-.46	.51	.42	-.52	-.54	1.0	-.16	-.33	.32	.38	.31	.43	.41	-.05	-.18	.38	.32
pH	.15	.52	.20	.58	.28	.54	-.19	-.47	.25	.64	-.16	1.0	.77	.13	.28	-.58	.62	.58	-.67	-.06	.18	-.02
mS	.90	.67	.84	.53	.75	.48	-.74	-.50	-.05	-.42	.32	.13	-.06	1.0	.35	.49	.12	-.03	.56	.46	-.61	-.30
IW	.52	.18	.05	-.31	-.10	-.36	.02	.33	-.63	-.66	.31	-.58	-.62	.49	.06	1.0	.63	.63	.65	-.02	-.14	.16
SS	-.08	.16	.41	.76	.52	.80	-.38	-.70	-.69	-.77	.43	.62	.69	.12	.62	.63	1.0	.97	-.17	.33	.46	.75
CEC	.49	.09	.49	.05	.40	.07	-.46	-.15	-.06	-.21	-.05	-.67	-.57	.56	.07	.65	-.17	-.28	1.0	.56	.78	.47
CM	-.42	-.18	-.74	-.49	-.72	-.53	.67	.55	-.32	-.29	.38	.18	.01	-.61	-.36	-.14	.46	.33	.78	.68	1.0	.83

Percent clay

Saturated moisture content

Void ratio

Unit weight

Residual friction angle

Residual cohesion

Plasticity

Hydrogen ion activity

Conductivity

Free-water concentration

Soluble salt content

Cation exchange capacity

Percent montmorillonite

(.52) and unit weight (-.57) lower values were obtained, but all remained significant at the 1 per cent confidence level as for Manor Lane.

Thus the results from both Worbarrow and Manor Lane show a high degree of association between the proportion of clay and the phase relationships. At both sites there was a positive association between the proportion of clay, the saturated moisture content and void ratio (and therefore porosity), and a negative relationship with unit weight or particle density. As might be expected, there were even greater coefficients of correlation between the phase relationships or saturated moisture content, void ratio and unit weight. The findings support the theoretical considerations reviewed in section 2.2, on the inherent properties of landslide clays.

Slight differences in the nature and value of the coefficients seem to reflect the variability in soil properties noted at each site. At Manor Lane correlations between mean values showed the best associations whereas at Worbarrow the values obtained at the shear surface were more significant. This was considered very important because where soil variability is imposed by heterogeneous lithologies the association of clay with other properties along critical shear surfaces will control the stability of the overlying mass of debris.

In relation to the residual shear strength measured at the shear surface for Manor Lane (Table 6.1a), the proportion of clay shows a negative correlation with the residual friction angle (-.53;1%) and residual cohesion (-.25;5%). A better correlation with cohesion was found with the mean per cent clay (-.51;1%). This suggested that the residual strength was more closely related to friction than cohesion, as might be

expected, and that the reduction in friction and cohesion downslope was disproportionately related to the small reduction in clay content (see Figures 4.3 and 4.20).

With reference to Table 6.2a for Worbarrow, the association between the proportion of clay with residual friction at the shear surface was very poor, although the mean per cent clay correlated positively with cohesion (.36) at the 5 per cent significance level. Because the proportion of clay was weakly and negatively correlated with residual friction (-.19) this might suggest that the frictional strength of the mudslide was more closely related to the presence of other 'massive' minerals, originating from the Wealden Beds, which would also account for the variability in the standard residual shear strength test results (see section 2.21 and Table 4.14).

Both sites show a greater degree of association of clay with friction at the shear surface but when the mean proportion of clay was correlated with strength the most significant coefficients were found for residual cohesion. This suggested that the cohesive force established at the shear surface was better associated with the mean proportion of clay within the mudslide profile. The positive correlation existing at Worbarrow and the negative association at Manor Lane may be accounted for by the chemistry of the clays controlling the development of cohesive forces between clay particles (section 6.212). Generally, the findings show that for mudslides with clay particles in excess of 30%, the residual strength was negatively related to the proportion of clay, suggesting that both the internal friction angle and cohesion were associated with other mechanical or physico-chemical factors.

It was interesting to note that although the proportion of clay is important in determining the shear strength of soils, the unit weight or particle density at both sites showed strong negative correlations, implying that structure and micro-fabric may have important effects upon residual shear strength: the reduction in the residual strength parameters downslope coincided with an increase in particle density at the shear surface. At Manor Lane coefficients of correlation significant to 1 per cent were computed for the residual friction angle ($r = -.55$) and cohesion ($r = -.44$) in comparison with Worbarrow ($r = -.55$, $r = -.70$).

This might suggest that shear surfaces were underlain by highly compact *in situ* clay, probably highly orientated, the increase in density reflecting the degree of compaction (by translation) or particle orientation experienced by the basal shear surface particularly on the lower slopes. The development of this process may result in the self-preservation of mudsliding across such surfaces (section 4.243). The degree of alignment or remoulding experienced upon movement could also account for the observed reduction in residual friction angles due to micro-fabric and particle disruption.

Additionally, with reference to Table 6.2a for Worbarrow, the saturated moisture content and void ratio show significant associations with residual shear strength. The saturated moisture content decreased with strength ($r = .45$; $r = .63$) downslope along with the void ratio ($r = .58$; $r = .74$), although better coefficients were noted for the correlation of the profile means. The susceptibility of the materials to saturation will ultimately have a profound effect upon shear strength, especially where expansive minerals are present. Such correlations were not found

for the London Clay at Manor Lane which was thought to be due to mineralogical (and thus chemical) differences.

The association of the plasticity index with the particle and density characteristics of both sites broadly showed a poor correlation with the proportion of clay at the shear surface (.09; Table 6.1a), strong negative associations with the phase relationships (-.83; Table 6.1a: -.65; Table 6.2a), and strong positive correlations with the unit weight (.51; Table 6.2a, .78; Table 6.1a). The most significant correlations were found by correlating the plasticity index at the shear surface with the Manor Lane core means. In contrast with the values measured at the shear surface at Worbarrow. The results suggest that an increase in the plasticity index downslope coincides with a reduction in void ratio (see Figure 4.8) and the saturated moisture content (Figures 4.5 and 4.6).

This not only suggested that for a given volume of soil moisture the materials on the lower slopes would be more susceptible to saturation, but the range in which the material exhibited plastic behaviour increased principally due to an increase in the liquid limit (see Table 4.13). Such an effect would in principle be counteractive producing the negative correlation, but apart from an increase in clay content or a change in mineralogy and geochemistry, the only way in which the liquid limit could be increased is if soil water was progressively adsorbed onto clay surfaces following weathering and movement. However, because there was a small reduction in total clay content downslope the plasticity index was also negatively correlated with the proportion of clay above 30 per cent (-.41; Table 6.1a). Thus, although an increase in plasticity downslope counteracted an increase in susceptibility to saturation, a

reduction in total clay content towards the accumulation lobe will make the materials on the lower slopes extremely susceptible to liquefaction.

6.212 Mineralogical and chemical properties.

In sections 2.22 and 2.23 the importance of clay mineralogy and chemistry was reviewed. Broadly it was noted that the predominant type of clay mineral, the valency of the exchangeable cations, and the type and concentration of pore fluids, exert an important influence upon the forces of particle interaction and thus the mechanical properties of soil. This research has provided an opportunity to assess the degree of association between such parameters measured directly in the laboratory through soil chemical analyses (section 4.4 and 4.5). The parameters used in the correlation matrix included the pH, electrical conductivity, interstitial pore water concentration, water soluble salts, cation exchange capacity, and the proportion of smectite clay minerals. Before discussing the outcome of the statistical analysis it was necessary to understand the geochemical nature of each site, briefly summarised in section 4.5 but further discussed in greater detail in section 6.3. However, for clarity a brief account will be given here.

The mudslides monitored as part of this study contrast most significantly with respect to the soil and groundwater chemistry (section 4.42). In principle it will be assumed that the chemistry of both sites fluctuates about an equilibrium with respect to the solid-phase mineralogy of the system. At Manor Lane there was a distinctive reduction downslope in the proportion of montmorillonite clay minerals (see Figure 4.47b) in relation to the small decrease in clay content (-.67; 1%). In contrast,

there was an increase in micaceous clay minerals. The more heterogeneous Wealden Beds at Worbarrow Bay give rise to variable quantities of montmorillonite clays (Figure 4.48b), increasing upon weathering in the source and upon deposition downslope relative to a decrease in overall clay content (-.42).

One of the effective differences between the clays of both sites was the degree to which the clay mineral exchange sites were occupied with base cations. At Worbarrow, the per cent base saturation increased downslope to about 87 per cent, decreasing dramatically at the toe of the slope (see Figure 4.39b). In contrast, there was a large reduction in the percentage base saturation in the source unit and feeder track at Manor Lane, decreasing from approximately 90 to 50 per cent (Figure 4.39a). The loss of cations from the exchanger was most likely attributable to a reduction in pH and the prevention of drainage due to the lower permeability of the clays under saturated conditions. The fall in per cent base saturation could also represent the exchange of divalent cations as a consequence of weathering and clay mineral diagenesis, such as magnesium for calcium (see Appendix 11). At Worbarrow sodium monovalent cations were selectively adsorbed onto the exchanger following weathering and movement downslope (section 4.422). Such exchanges will affect the degree of attraction or repulsion between particles, and would account for the difference in association between the clay content and cohesion referred to earlier.

Because the chemistry of the pore water reflects the chemistry of the clay minerals in equilibrium, the concentration of water soluble cations was related to the type and quantity of exchangeable bases. At Worbarrow Bay the concentration of soluble cations was low because any

free cations were strongly adsorbed to the exchanger giving rise to a positive correlation (.75) between soluble salts and clay mineralogy. This contrasts with Manor Lane where the concentration of soluble cations was comparatively high due to the instability of the clay mineral exchange sites, accounting for the negative relationship with clay mineralogy (-.99). There was however an increase in the concentration of water soluble cations downslope at both sites (section 4.422).

As a consequence of these different chemical effects one would expect similar associations between other variables but occasionally of opposite sign. This was illustrated by the clay mineralogy of both systems where such relationships could be expected to have contrasting effects upon residual shear strength. This was confirmed with correlations of clay mineralogy with residual friction and cohesion, negatively associated at Worbarrow (-.32 and -.29), and positively associated at Manor Lane (.87 and .57), respectively. These associations were enhanced when correlated with the core means. In theory an increase in the proportion of montmorillonite clay minerals should result in a reduction in residual shear strength (section 2.32) explaining the negative correlation at Worbarrow, but the more significant correlations noted at Manor Lane would suggest the contrary. An answer to this anomaly was that the predominant clay mineral reaction at each site was probably more closely related to residual strength, in which case the latter association would be improved, and positively correlated, if the proportion of 2:1 mica/illite clay minerals were used, because these show an increase in proportion downslope (Figure 4.47). Only a few minerals, such as montmorillonite and swelling illite, are known to exert an influence upon the mechanical properties of soils in excess of their relative abundance.

The ability of 2:1 clay minerals to adsorb large quantities of cations and water was illustrated by correlations between clay mineralogy and the concentration of soluble salts released from the soil particles. At Manor Lane a perfect correlation ($-.99$) existed between the proportion of montmorillonite clays and the concentration of soluble salts, or alternatively, this suggested a strong positive relationship between the dominant 2:1 mica/illite minerals and water soluble cations. At Worbarrow, the distribution of montmorillonite was positively associated with the concentration of soluble salts ($.46$) which increased in value when the mean concentration of salts was considered ($.75$).

An increase in soluble salts downslope at both sites would result in a greater tendency for the development of large diffuse double layers containing many layers of water and loosely bound cations (following an effective dilution of mineral surface chemistry), confirming the greater affinity for cations and water exhibited by expansive clays. This appeared to be the case at Worbarrow where there was an increase in montmorillonite and soluble salts downslope, although at Manor Lane there was an increase in soil mica and illite clays although the latter, like montmorillonite, may have a tendency to swell and develop large diffuse double layers. Such an effect would also explain the increase in the liquid limit and plasticity index discussed earlier.

The importance of clay mineralogy in determining the chemical nature of clays was reflected in the cation exchange capacity of soils. At both Manor Lane and Worbarrow Bay positive coefficients of correlation were obtained at the 1 per cent confidence level ($.37$ and $.78$, respectively). The stronger coefficient recorded at Worbarrow probably reflects the dominance of montmorillonite at the site, in comparison to the

micaceous/montmorillonite suite at Manor Lane. Montmorillonite and vermiculite clay minerals have the greatest affinity for cations and water and thus CEC.

The chemistry of the clays and pore water were considered to have important effects upon residual strength (section 2.32). The pH or hydrogen ion activity of both the London and Wealden Clays showed clearly defined associations with the mean proportion of clay particles (.35 and .52) and negative associations with particle density (-.87 and -.47), respectively. These correlations support theoretical considerations in that the activity of clays would be expected to override the effects of other inert minerals. Such activity would result from an increase in particle disruption and saturation as a consequence of a change from an over-consolidated to a normally-consolidated condition.

The conductivity of the soil solution, a measure of the amount of salt in the pore water, was strongly correlated with the proportion of clay at Worbarrow (.90 ; 1%) but negatively related with clay content at Manor Lane (-.32 ; 2%). This would endorse the chemical differences between the sites outlined earlier in this section, since the concentration of salts associated with the clays was positive and in equilibrium at Worbarrow, but negative and in disequilibrium at Manor Lane. As for pH, the conductivity was negatively related to the density of particles (-.56) at Worbarrow and (-.74) at Manor Lane. The tendency for over-consolidated clays to develop a normally-consolidated condition was thus not only important from the physical or geotechnical point of view, but also a fundamental cause of the chemical activity of the system.

The pH and conductivity appeared from Tables 6.1a and 6.2a to be partially related to the residual strength parameters. Both sites showed strong negative associations between conductivity and cohesion ($-.84$) at Manor Lane and ($-.42$) at Worbarrow. This implied that a high electrolyte salt content in the hydration shell surrounding the clays corresponds with a reduction in the cohesive force operating between particles. The transference of salts from strong ionic bonds between particles to a soluble form would encourage the development of diffuse double layers and would result in a significant reduction in cohesion.

With reference to the chemistry of the pore water and clay particles, strong coefficients of correlation were obtained for both the concentration of water soluble cations and the interstitial water at both sites. The former variable represents cations held loosely in the outer hydration shell of clay minerals, whereas the latter is the salt concentration in the pore water solution (section 4.42). That both are in equilibrium was reflected by the positive coefficients between these parameters, 0.96 at Manor Lane and 0.63 at Worbarrow. Negative coefficients were computed at both sites when the water soluble cations were correlated with the residual strength parameters: at Manor Lane correlations with the internal friction angle equalled $-.90$ and cohesion $-.56$ in comparison with $-.69$ and $-.77$ at Worbarrow, respectively. These significant results suggest that a reduction in residual strength might coincide with an increase in double layer activity and the degradation of primary bonds between particles, with a transference of salts from an exchangeable to a soluble state downslope. This process would cause changes in the strength of bonding from strong ionic forms to weaker ionic or hydrogen bonds, and the separation of mineral layers through the

adsorption of water. The coefficients obtained between the conductivity and shear strength support these findings.

Additionally, the association was supported by negative correlations with the interstitial free-water concentration where an increase in pore water salt concentration downslope coincided with a reduction in residual shear strength: at Manor Lane correlations with friction (-.92) and cohesion (-.61) correspond with (-.63) and (-.66) at Worbarrow, respectively, all significant at the 1 per cent confidence level. This relationship appears contrary to that established from laboratory simulation tests (section 5.4) where pore water concentration was found to be positively associated with residual strength. However, it is pointed out that there was a net dilution of salts associated with clay mineral surfaces and thus an apparent disequilibrium between the exchange reactions (base saturation) and pore water salt concentration. Weathering processes resulted in a net dilution of salts on the exchanger at both sites. In the laboratory, solutions artificially introduced cause changes in strength consequent upon exchange reactions between soil and water. Under naturally occurring conditions disequilibrium prevails and both physical and chemical weathering processes promote the development of diffuse double layers causing a net reduction in strength. Such weathering reactions were not reproduced in the laboratory giving rise to this anomaly. But there can be little doubt that the mineralogical and chemical properties of mudslides show the most significant coefficients of correlation with the residual shear strength parameters.

6.22 Dynamic behaviour:

In section 1.4 it was concluded from a review of the mechanics of mudsliding that 'the onset of movement was generated by an increase in winter rainfall and water surplus, a decrease in evapotranspiration, a general rise in groundwater and soil moisture levels, material saturation, an increase in pore water pressure, and a decrease in shear strength'. Such relationships were monitored at Worbarrow Bay, the results of which were presented in Chapter Five.

The monitoring framework (section 3.33) was designed in such a way that data for each parameter could be processed at a number of time-scales. This vastly improved the versatility and ease of interpretation of the results and provided data-sets conducive to statistical analysis. Because all variables used in the dynamic analysis of mudslide behaviour were condensed to a monthly summary an opportunity arose to compute a global correlation between all field parameters throughout the monitoring programme; a total of 9 variables were correlated throughout the 20 month study period. Although much variability is lost in such a summary, the statistical analysis was used to provide a quantitative statement of the degree of association between the variables quoted at the beginning of this section.

The variables used in the analysis may be divided into four groups: the climatic controls upon slope instability, the soil water relations, residual shear strength and movement. The first three groups will be discussed with respect to movement for this is the ultimate expression of slope instability (section 5.33). The results of the monthly summary

are presented in Table 6.3 and the confidence levels of significance were given earlier in section 6.21.

For certain critical variables such as movement, pore water pressure and climate, the daily summary of the continuous data-set was statistically analysed to assess the degree of causal association or sensitivity between these parameters at a much increased resolution and accuracy. A total of 6 variables were used from the daily summary over a sample period of 187 days between the 1st of November 1986 and the 6th May 1987. With 185 degrees of freedom the significance levels are much lower in this test than those encountered in the other correlation matrices.

Because antecedent time-lags operate between individual events the correlation matrix was re-computed with the movement column weighted with assumed lags of 1, 2, 4, 7, 14, 21 and 28 days, to establish the most significant coefficients of correlation between the input variables. The results are summarised in Table 6.4.

Table 6.3. Correlation matrix of the monthly summary of dynamic mudslide variables at Worbarrow.

PROP n=18	ER	WS	SD	SMB	SMA	PWPS	PWPA	PWS	M
ER	1.0	.28	.84	.54	.75	.58	.44	.52	.48
WS	.28	1.0	.53	-.29	-.15	.04	-.19	.31	-.17
SD	.84	.53	1.0	.21	.40	.38	.24	.44	.27
SMB	.54	-.29	.21	1.0	.70	.41	.46	.16	.59
SMA	.75	-.15	.40	.70	1.0	.52	.54	.56	.54
PWPS	.58	.04	.38	.41	.52	1.0	.44	.46	.60
PWPA	.44	-.19	.24	.46	.54	.44	1.0	.26	.57
PWS	.52	.31	.44	.16	.56	.46	.26	1.0	.46
M	.48	-.17	.27	.59	.54	.60	.57	.46	1.0

=====

All coefficients computed from monthly averages.

Confidence intervals 5% = .433, 1% = .549

ER = Effective rainfall or hydrological flux
WS = Wind speed
SD = Weight of salt deposited
SMB = Backcliff soil moisture
SMA = Accumulation lobe soil moisture
PWPS = Source unit pore water pressure
PWPA = Accumulation lobe pore water pressure
PWS = Pore water salt concentration
M = Maximum movement

6.221 *Climatic controls upon slope instability.*

In temperate latitudes the seasonality of landsliding has long been recognised and associated with climatic cycles (section 1.4). This has led to many attempts to relate weather events with incidences of slope instability. The task is easier when extreme climatic events coincide with an increase in the magnitude and frequency of landslides. Attempts have also been made to correlate mudsliding with seasonal rainfall. Such work has proved less successful because antecedent time-lags exist, for various reasons, before the effects of an increase in the duration or intensity of rainfall finally promotes slope instability. However, recent studies (Craig, 1979; Brunsden, 1984; McConchie, 1986; Allison, 1986) have shown that the degree of association between rainfall and movement can be improved if evaporation is considered in calculating the net hydrological flux or effective rainfall (ER). This parameter is more closely related to the soil water relations, which are ultimately responsible for triggering slope movements.

This is demonstrated when ER is correlated with other variables monitored in the field (Table 6.3). Effective rainfall was significantly related to movement (.48) at the 5 per cent confidence interval. However, a much closer relationship was found between ER and the soil water relations. These include the soil moisture of the back-cliff (.54;1%) and the accumulation lobe (.75), and pore water pressure in the source (.58) and the lobe (.44;5%).

These coefficients confirm the belief that the net hydrological flux can only be indirectly related to mudslide movement because a greater degree of association is found with soil moisture and pore water pressure which

both show very significant direct relationships with slope instability (section 6.222). It was interesting to note that the best association between ER and the soil water relations was found with the soil moisture in the accumulation lobe. An explanation for this could be that the depositional zone remained saturated for much of the year, with only slight surface crusting during the summer months, and thus remains more sensitive to further inputs of moisture. The presence of a secondary basal aquifer (section 5.321) would also significantly reduce the antecedent time-lag associated with the flow of groundwater entering the source unit to the lobe. Effective rainfall was, however, positively related to the pore water pressures in the source unit and the soil moisture of the back-cliff. Significantly, pore water pressures in the source more closely reflected weather conditions than either pore pressures in the lobe and the soil moisture within the cliff.

The deposition of sea salts was considered in section 1.5 to have an important role in promoting the weathering and shear strength behaviour of mudslide clays. Subsequently, it was necessary to assess the amount of sea salt deposited on the coastal cliffs. The results are presented in Chapter Five (section 5.314) and broadly showed peak deposition in November as a direct consequence of maximum wind speeds and heavy rainfall. When the amount of salt deposited is correlated with ER (.84) and wind speed (.53) it may be seen that the increase in rainfall during the winter months is more closely associated with the atmospheric deposition of salts, but there is no doubt that the peaks measured in November (Figure 5.12) are also related to the occurrence of maximum wind speeds.

It was of interest to note that the atmospheric input of salts shows a positive association with the concentration of salts in the pore water (.44) significant at the 5 per cent confidence interval. This relationship is attributed to the peak deposition of salts in November with the corresponding large winter maxima in pore water salt concentration one to two months later. This explains the low coefficient of correlation and suggests that the groundwater chemistry attains an equilibrium with the atmospheric deposition of salts upon the coastal cliffs.

With reference to Table 6.4, climatic variables were taken from the continuous data-set to assess the antecedent time-lags operating between pore water pressure and movement. Mean daily rainfall, temperature and wind speed were correlated against pore water pressure in the source and accumulation lobe and with movement at the top of the feeder track, close to the source piezometer. The monitoring equipment and design was discussed in section 3.33.

Positive coefficients between the weather variables were found when correlating rainfall with temperature (.23) and wind speed (.29), and when correlating temperature with wind speed (.38) all significant at the 1 per cent confidence interval. It is noted that wind speed is the common factor behind the large coefficients with rainfall and especially temperature. This may well reflect the dominance of the south-westerly airstream (section 5.313) and associated cyclones experienced on the south coast of England, bringing generally mild, wet and windy weather during the winter months.

Table 6.4. Correlation of dynamic variables with slope movement with associated time-lags from continuous recordings between November 1986 and May 1987 at Worbarrow Bay.

PROP n=185	W	T	R	PWA	PWS	M	
W	1.0	.38	.29	-.33	.39	.16	Mean wind speed
T	.38	1.0	.23	-.58	.45	.08	Mean temperature
R	.29	.23	1.0	-.11	.16	.10	Total rainfall
PWA	-.33	-.58	-.11	1.0	-.31	.08	Max phreatic level in lobe
PWS	.39	.45	.16	-.31	1.0	.28	Max phreatic level in source
M1	.16	.08	.10	.08	.28	1.0	Total surface movement
M2	.20	.13	.32	.14	.29	1.0	Movement with assumed 1 day time-lag
M3	-.09	-.05	.19	.16	.03	1.0	Movement with assumed 2 day lag
M4	.08	.09	.16	.20	.24	1.0	Movement with assumed 4 day lag
M5	-.09	-.21	-.004	.09	-.23	1.0	Movement with assumed 7 day lag
M6	.01	-.17	.006	.009	.003	1.0	Movement with assumed 14 day lag
M7	.001	-.08	.08	.009	.09	1.0	Movement with assumed 21 day lag
M8	.204	.063	.01	-.08	.14	1.0	Movement with assumed 28 day lag

All coefficients computed from daily averages.

Confidence intervals 5% = .141, 1% = .184

Surprisingly large coefficients were obtained when correlating temperature and wind speed with pore water pressure, positively in the source unit (.45 and .39, respectively), but negatively in the accumulation lobe (-.58 and -.33) all significant at the 1 per cent confidence interval. Direct correlation with rainfall produced much lower coefficients although similar in nature, and the only significant value (.16;5%) was obtained between rainfall and the pore water pressures in the source. Extreme caution is required when interpreting such findings since there was no empirical evidence nor logical argument to suggest that movement is generated by strong winds. However, the association between temperature and pore water pressures is worthy of consideration since it would support the principle of Mitchell (1976) that soil deformation is a thermally activated process (see section 2.231).

The interaction between soil water and clay minerals, exchangeable cations and dissolved salts is a sensitive function of temperature and the relative vapour pressure of the soil water White (1979; see page 135). Hence, in principle one would expect a positive correlation between temperature and pore water pressure, although a direct response between these variables could only exist at the soil surface. This was the case in the source unit (evidenced by the positive coefficient) where the mudslide depth was only 0.5-0.6m (Table 3.6). In contrast, the shear surface of the lobe deepened to 1.81m and atmospheric temperature was in disequilibrium with soil temperature and the negative correlation was justified.

As for the monthly correlation matrix the association between the climatic events and the soil water relations are of much greater

significance than correlating weather parameters directly with slope movement. Although antecedent time-lags operate between all variables, with varying intensity, the greatest interval between events can be expected when correlating rainfall (the precursor) with slope movement (the consequence). It is not surprising, therefore, to note the poor correlation (.10) between the latter parameters. This value is less than those obtained when correlating rainfall with pore water pressure.

When time-lags are weighted on the movement column a dramatic improvement in the coefficients of correlation were found, increasing to (.32;1%) for a 1 day lag, (.19;2%) for a 2 day lag, and (.16;5%) for a 4 day lag. There is no correlation between rainfall and movement for time-lags of 7, 14, 21, and 28 days (-.004). Thus, throughout the study period from November to May, an increase in rainfall was most significantly associated with slope movement following a 24 hour time-lag. The association decreases with significance for at least 4 days after the initial event. This relationship is supported by similar time-lags associated with pore water pressures, discussed in the next section. The small size of the Worbarrow system in combination with highly permeable sandstone strata contribute significantly to this quick response.

6.222 Soil water relations.

With reference to Table 6.3, the monthly summary, both soil moisture and pore water pressure are highly related to one another. The best coefficient amongst these relations is obtained when correlating the soil moisture of the back-cliff with the soil moisture of the accumulation lobe (.70;1%). The corresponding relationship between pore water pressures (.44;5%) suggests that soil moisture is less variable within

the mudslide than the distribution of pore water pressures. It is interesting to note that the soil moisture of the back-cliff correlates significantly with the pore water pressures within the mudslide (.44 source; .46 lobe), although the greatest coefficients are obtained when correlating the soil moisture of the accumulation lobe with pore water pressure, again most significant in the lobe (.54;1%) than in the source (.52;2%). This suggests, as might be expected, that the pore water pressures required to trigger movements are more closely associated with the soil moisture within the mudslide than with the surrounding groundwater regime, so that the pressures are generated within rather than from external influences.

Before considering the role of the soil water relations in promoting slope movements, it is noted that the soil moisture of the accumulation lobe was positively related to the concentration of salts in the pore water (.56;1%). This implied that both attain an equilibrium and the positive coefficient is obtained as a result of the winter maximums observed for both parameters. The pore water pressure in the source was also related (.46) at the 5 per cent confidence level, which might suggest that pressure solution may be an important consideration at the site, or simply that increases in solute concentration coincide with phases of weathering and movement induced by high pore water pressures.

Both soil moisture and pore water pressure correlate significantly with slope movement at the 1 per cent confidence interval. The influence of the source over the accumulation lobe is readily apparent with pore water pressure (.60) and the soil moisture of the back-cliff (.59) in comparison with the pore water pressure (.57) and soil moisture (.54) of the lobe, respectively. This supports the contention that movements are

generated from the source region rather than within the lobe, which is only thought to fail only under the most severe conditions.

Of lesser significance, at the 5 per cent confidence interval, the pore water salt concentration correlates with movement (.46), but although this was not strongly related to individual movement events, the association represents a seasonal change in the shear strength of mudslide materials (see section 6.223), which in combination with climatic variables predisposes the slope mantle to seasonal instability, finally triggered by pore water pressure.

With reference to Table 6.4, the relationship between pore water pressures triggering slope movements is statistically tested using the daily summary of the continuous data-set. When the pore water pressure in the source is correlated with the lobe (-.31) a negative association was found. This probably results from the presence of artesian conditions on the lower slope throughout the year in contrast to zero pressures or suctions experienced in the source during the dry months of summer. Additionally, it would suggest that changes in pressure in the source are not necessarily associated with the magnitude and frequency of changes in the lobe (section 5.322).

Of greater interest is the relationship between pore water pressures in the source and lobe with individual movement events. The correlation matrix revealed a strong association with pore pressures in the source (.28;1%) but not in the lobe (.08). This strongly suggests that movement of the Worbarrow mudslide was triggered by pore water pressures in the source. As for rainfall, the presence of time-lags were assumed, and it was found that the correlation coefficient was improved (.29) for

a lag of 1 day and (.24) for 4 days. No significant association was noted for a time-lag of 2 days. The absence of a significant correlation between those for 1 and 4 days is strong evidence to suggest the operation of pulses or waves of movement: the build-up of pore pressures to a threshold and subsequent release, followed by another phase until the effects of individual events are nullified. This process would explain the mechanism of movement, termed stick-slip, where movement events are interspaced by periods of no movement. No associations were found after a time-lag of 7 days.

When time-lags were associated between movement and the pore water pressure in the accumulation lobe an increasing degree of correlation was found for up to 4 days (.20;1%), from (.16; 2%) for a 1 day lag, and (.14;5%) after 2 days. This would confirm the dominance of pore water pressures in the source unit over the lobe, and strongly implied a time-lag between the latter of around 3-4 days. It has been suggested that 'kinematic' waves of loading and movement (Brunsden pers.com. 1987) could be responsible for such observed behaviour, whereby movements from upslope transport materials to the lower sections causing secondary undrained loading.

6.223 Shear strength.

Little attempt has been made in past studies to relate seasonal fluctuations in shear strength with slope instability. It is a contention of this thesis that the shear strength of mudslides varies in relation to both an increase in soil moisture (as evidenced by the relations in the preceding section) and pore water chemistry. In section 5.4, laboratory simulation tests showed that the residual strength of

clay materials was extremely sensitive to clay mineralogy and the type and concentration of pore water salts. Moreover, under naturally occurring conditions, significant differences in shear strength behaviour were recognised for different weathered state of mudslide clays, and that the residual strength was considerably reduced at low pore-water salt concentrations, and enhanced at higher pore water salt contents.

These findings suggested that seasonal fluctuations in pore water concentration (section 5.323), could in effect control seasonal variations in the residual strength exhibited by mudslides. By testing Wealden and London Clay samples in the laboratory, natural fluctuations in pore water salt content were calibrated against the respective simulation curves (Figure 5.34) to produce an estimate of the corresponding change in residual strength in the field. In this manner, it was possible to obtain a quantitative expression of the seasonal fluctuation in shear strength attributable to pore water salt concentration.

Table 6.5 summarizes the calculations and results used in the analysis for Worbarrow Bay. Changes in strength were calculated relative to the pore water chemistry of the standard set of residual strength results (Table 4.18) and are plotted in Figure 6.1 as the variation in strength (kPa) for each month of the study period. Calculations were also undertaken for the London Clay, assuming the same fluctuations in pore water chemistry as measured at Worbarrow, to assess whether the fluctuations in strength are consistent between sites of contrasting mineralogy, geochemistry and residual shear strength properties. Figure 6.2 shows the likely fluctuations in strength at Manor Lane for the same study period.

The plots show two interesting facts. Firstly, from July to November 1986 there is an observable decrease in residual strength associated with the reduction in pore water concentration (Figure 5.22). Assuming equilibrium between the pore solution and mineral surfaces, a dilution of the diffuse double layers would occur encouraging dispersion between particles (see section 2.23), producing a significant fall in effective residual shear strength. However, because the soil moisture levels are generally low at this time of year slope movements do not materialise until December when the degree of saturation and pore water pressures are sufficient to trigger failure within the mudslide.

Secondly, following slope movements and surface weathering (loading) or as a consequence of the deposition of salts in November, there is an increase in the shear strength coincident with a dramatic increase in pore water salt concentration (Figure 5.22). An increase in concentration would cause a relative compression of the double layers enhancing the attractive force between particles (cohesion) and increasing residual shear strength. However, slope failure continues until April because of the high pore water pressures and degree of saturation of the materials. Stability is probably recovered as a result of a reduction in the triggering process and an increase in the strength of the materials brought about by an increase in pore water salt concentration.

Table 6.5. Calculation of the change in residual shear strength attributed to fluctuations in pore water concentration at Worbarrow Bay.

MONTH	PORE WATER (CONC g/l)	CHANGE (%)	CALCULATED CHANGE IN RESIDUAL STRENGTH kPa					
			0	1	2	3	4	5
Oct 1985	1.51	-23.43	-.239	-.224	-.296	-.313	-.324	-.293
Nov	1.698	-13.89	-.141	-.133	-.175	-.186	-.192	-.174
Dec	1.743	-11.61	-.118	-.111	-.147	-.155	-.161	-.145
Jan 1986	1.957	-.76	-.008	-.007	-.010	-.010	-.011	-.010
Feb	2.656	34.69	.3531	.3309	.4380	.4640	.4803	.4341
Mar	2.733	38.59	.3929	.3682	.4873	.5162	.5343	.4829
Apr	2.109	6.95	.0707	.0663	.0877	.0929	.0962	.0869
May	2.262	14.71	.1497	.1403	.1857	.1967	.2036	.1840
Jun	2.087	5.83	.0594	.0556	.0736	.0780	.0807	.0730
Jul	2.274	15.31	.1559	.1461	.1934	.2048	.2120	.1916
Aug	1.494	-24.24	-.247	-.231	-.306	-.324	-.336	-.303
Sep	1.537	-22.06	-.225	-.210	-.279	-.295	-.305	-.276
Oct	1.6	-18.86	-.192	-.180	-.238	-.252	-.261	-.236
Nov	1.71	-13.29	-.135	-.127	-.168	-.178	-.184	-.166
Dec	1.766	-10.45	-.106	-.100	-.132	-.140	-.145	-.131
Jan 1987	2.942	49.19	.5008	.4693	.6211	.6580	.6811	.6156
Feb	2.073	5.12	.0521	.0489	.0647	.0685	.0709	.0641
Mar	1.895	-3.90	-.040	-.037	-.049	-.052	-.054	-.049
Apr	1.704	-13.59	-.138	-.130	-.172	-.182	-.188	-.170
May	2.216	12.37	.1260	.1180	.1562	.1655	.1713	.1548
STATIC SALT CONCENTRATION g/l			1.972	1.848	2.446	2.591	2.682	2.424
See Table 4.18								
RANGE OF FLUCTUATIONS g/l			1.448	1.357	1.796	1.903	1.969	1.78
KPa			.7476	.7006	.9273	.9825	1.017	.9190

Calculation based on simulation for Wealden Clay where:

[100% change in sea water concentration] = 18.07 kPa
 [34.476 g/l] = 18.07 kPa
 [1 g/l] = 0.5163 kPa

Figure 6.1. Fluctuation in strength attributed to pore water chemistry at Worbarrow Bay.

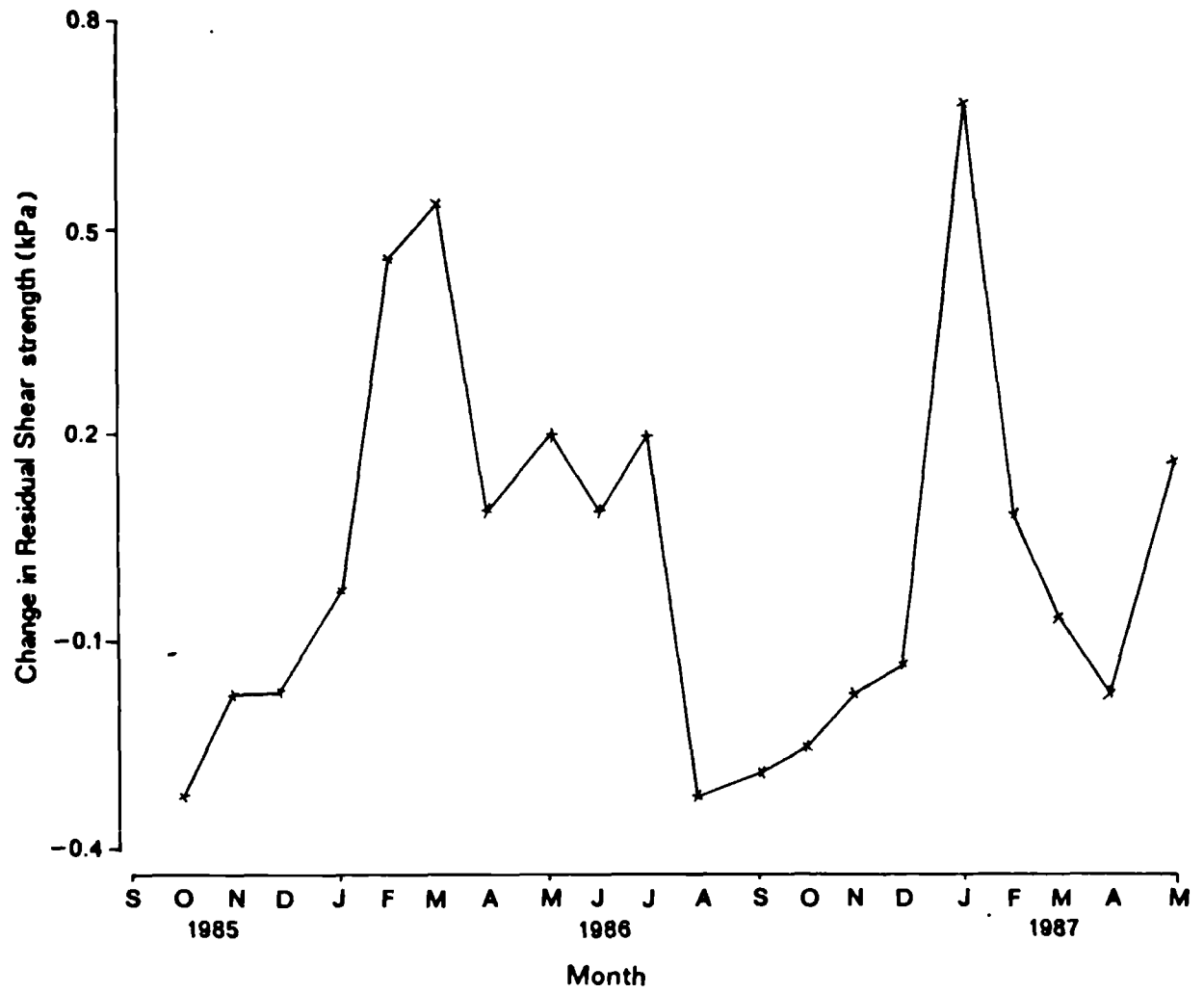
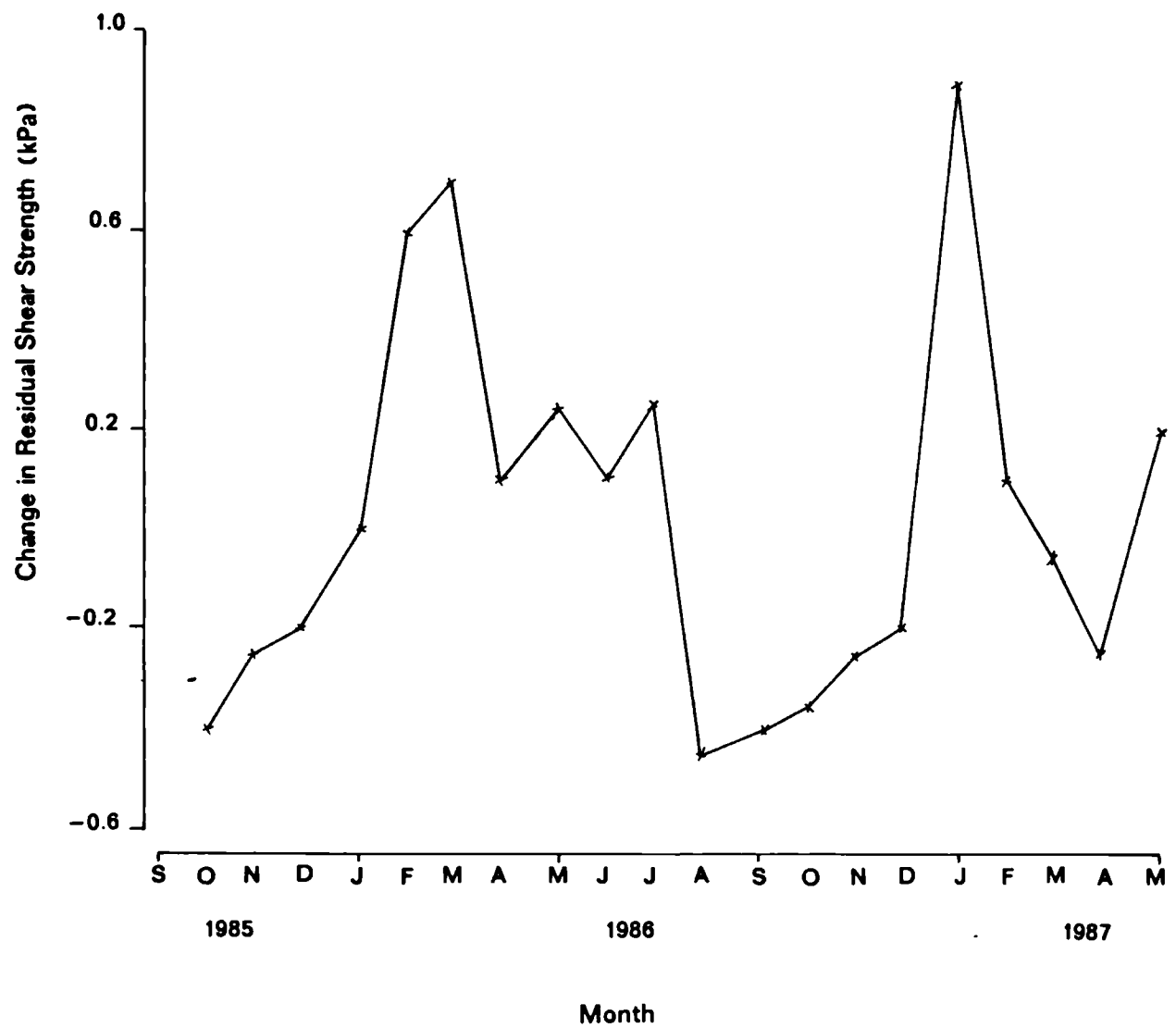


Figure 6.2. Fluctuation in strength attributed to pore water chemistry at Manor Lane.



The exact manner in which these processes interact is mathematically modelled in section 6.4. However, a number of considerations need to be borne in mind when associating the chemistry of clays to shear strength (and effective stress), and indeed to the methods used in the laboratory determinations.

1. The results from the ring-shear test represent a change in actual residual strength (kPa). Because the normal effective stress was held constant within and between test series, it was not possible to attribute the change to either friction or cohesion.
2. In theory, the fluctuations in strength associated with the chemical forces of particle interaction can affect both the cohesive force (or primary ionic bonds) directly between particles and also in terms of the repulsive and attractive forces (of the diffuse double layer) associated with effective and total stresses for inter- and intra-particle associations (see section 2.32).
3. Chemical properties are unlikely to change the inherent frictional component of shear strength, although the frictional interaction between opposing particles could be lessened by the expansion of the diffuse double layers separating the minerals. This effect is highly dependent on the clay minerals and chemistry within the system (see section 2.23), and especially important if montmorillonite minerals are present since the associated double layers are particularly dynamic.

Before considering the models of slope instability for both sites, the aqueous and solid phase geochemistry is discussed in relation to clay mineral activity, weathering processes, the dilution of the pore water, and the effects of the seasonal deposition of salts.

6.3 Geochemical modelling:

The effects of weathering upon the stability of clay minerals were reviewed in section 2.31, and the methods used in the field and laboratory investigations of this process are detailed in section 3.4. The purpose of this section is to consider the relationships between the measured solution chemistry and clay mineralogy at both sites, describe phase equilibria to identify predominant weathering reactions and to simulate the effects of additions of salts and dilute groundwater upon the stability and weathering behaviour of the clays. By way of conclusion a geochemical model is proposed to apply the physico-chemical properties of landslipped clays to the stability and weathering behaviour of coastal mudslides.

6.31 Phase equilibria:

The geochemical interactions between minerals and water are the interest of this section. A phase is defined as a region of uniformity such that a unit of soil may have uniform chemical composition and uniform physical properties (Castellan, 1971). The clay mineralogy and chemistry of mudslide materials have been described in sections 4.46 and 4.44, respectively. When in equilibrium with the soil solution (aqueous phase), the chemistry of the pore water will reflect the chemistry of the solid phase. This is rarely the case, however, since weathering disturbs the balance between the phases and alterations to the mineralogy and pore water chemistry occur through dissolution and precipitation processes to attain a new equilibrium; the changes are mostly irreversible. Thus in principle it is possible to model the state of equilibrium between the phases if either are known, and to predict

reaction paths of the mineral phase given certain environmental conditions. Because of the uncertainties of mineralogical analyses estimations of this sort are best achieved when based on analyses of the soil solution or the chemistry of the clay minerals.

Ion activity products (IAP) are used to identify the components that control the composition of the soil solution (section 3.4). They are calculated by assuming equilibrium between both phases although this assumption may be inaccurate when modelling geochemical processes in the natural environment. Nevertheless, for purposes of analysis equilibrium was assumed because the behaviour of most ions in solution may best be described in this manner (Nordstrom *et al*, 1979).

When the soil phase is in a state of equilibrium it follows that the concentration of salts in solution must be related to the solubility of salts from the mineral phase. The solubility of a given element is the sum of the stoichiometric concentrations of all dissolved species containing the element. Therefore, accurate calculations of solubility requires knowledge of all species contributing to the result of chemical analysis, plus a relation between the concentration of a given species and its activity (Garrells and Christ, 1965). Thus activity is a term used to quantify the effect of ionic concentration upon the solubility of salts in both phases (section 3.4). Where the ionic strength is low activity or solubility is high, and vice versa, such that long-range electrostatic forces may affect the activity of ions. This process is described by the Debye-Hückle theorem.

These theoretical considerations may be used to model the relationships between mineral and aqueous phases, but for accuracy and speed of

analysis this requires the use of a mainframe computer. The US Geological Survey has developed a series of programmes that enable the determination of ion activities and saturation indices, as well as identifying phase boundaries and modelling reaction paths (weathering), such that physico-chemical transformations may be predicted for known environmental conditions. The models used in this work are WATEQF and PHREEQE, and both are described by Plummer (1984). These routines will be discussed with respect to the aims of four models:

1. to assess the activity of the aqueous and mineral phases;
2. to identify predominant weathering reaction paths;
3. to model the effects of dilution upon mineral stability;
4. to model the effects of an increase in salt concentration upon clay mineral stability.

6.311 Weathering reactions.

To assess models 1 and 2, the programme WATEQF was executed on the University of London Amdahl computer. Because the initial source routine was written in FORTRAN 4, slight alterations were required to operate the programme on modern FORTRAN 7 compilers. The changes are listed in Appendix 13, and the updated version was checked using a standard analysis detailed by Plummer *et al* (1976). WATEQF calculates the activity coefficients and ratios of aqueous speciation from known concentrations of the major elements in solution, and then calculates the ion activity product ratios of the mineral phase identifying the saturated status of the associated clays.

Table 6.6. Description of aqueous and mineral phase geochemistry for each slope unit at Worbarrow Bay.

WATEQF INPUT AND RESULTS	SLOPE UNIT						
	0	1	2	3	4	5	WU
pH	5.96	5.37	5.11	4.67	5.12	6.28	6.15
T°C	5.00	5.00	7.80	7.80	6.60	5.50	5.50
LOG Pco ₂	-3.501	-3.500	-3.500	-3.499	-3.501	-3.501	-3.500
IONIC STRENGTH	3.88E-02	3.61E-02	4.90E-02	5.23E-02	5.47E-02	4.83E-02	3.23E-02
TOT. ALKALINITY	2.25E-02	1.33E-02	8.08E-03	-2.56E-02	3.02E-02	7.32E-02	6.96E-02
EPMCAT - ANAL	32.432	28.264	38.138	44.180	46.585	40.284	25.545
- COMP	31.518	27.400	36.917	42.988	45.329	39.171	24.771
EPMAN - ANAL	33.410	32.369	43.539	44.192	45.146	41.647	28.676
- COMP	32.512	31.513	42.319	42.974	43.901	40.584	27.950
<u>MOLE RATIOS</u>							
Cl/Ca	1.51E+01	1.67E+01	1.20E+01	1.28E+01	1.34E+01	1.60E+01	1.59E+01
Cl/Mg	1.23E+01	1.18E+01	1.04E+01	1.03E+01	8.636	1.02E+01	1.11E+01
Cl/Na	1.158	1.310	1.599	1.278	1.297	1.266	1.319
Cl/K	6.60E+01	1.27E+02	9.11E+01	9.24E+01	4.74E+01	1.72E+02	1.13E+02
Cl/Al	2.59E+04	4.62E+03	3.60E+03	6.88E+03	2.83E+03	4.05E+04	1.93E+04
Cl/Fe	6.63E+25	2.60E+24	1.00E+24	1.15E+24	4.15E+23	1.06E+26	3.72E+25
Cl/SO ₄	9.702	9.266	1.45E+01	1.44E+01	1.50E+01	1.30E+01	9.619
Cl/HCO ₃	4.08E+03	1.53E+04	4.03E+04	1.12E+05	4.03E+04	2.52E+03	2.29E+03
Ca/Mg	8.14E-01	7.11E-01	8.66E-01	8.05E-01	6.43E-01	6.36E-01	7.00E-01
Na/K	5.70E+01	9.70E+01	5.70E+01	7.23E+01	3.66E+01	1.36E+02	8.59E+01
<u>LOG ACT RATIOS</u>							
Ca/H ₂	8.882	7.650	7.395	6.485	7.372	9.589	9.193
Mg/H ₂	8.980	7.806	7.467	6.590	7.575	9.795	9.355
Na/H ₁	4.251	3.593	3.395	3.056	3.510	4.642	4.323
K/H ₁	2.491	1.602	1.633	1.191	1.941	2.503	2.386
Al/H ₃	10.215	9.196	8.600	6.986	8.723	11.040	10.892
Fe/H ₂	-15.775	-15.557	-15.543	-16.485	-15.134	-15.246	-15.190
Ca/Mg	-0.098	-0.156	-0.072	-0.105	-0.203	-0.207	-0.162
Na/K	1.760	1.991	1.761	1.865	1.569	2.139	1.938
LOG (H ₄ SiO ₄ . Aq)	-3.905	-3.519	-3.348	-3.542	-3.442	-3.423	-3.515
<u>LOG IAP/KT</u>							
Quartz	0.430	0.816	0.938	0.744	0.865	0.903	0.811
Kaolinite	1.697	2.430	1.857	-1.758	1.798	6.361	5.881
Ca-Mont	2.581	1.418	0.931	-3.691	0.736	6.447	5.697
Mont-AB	2.087	1.224	1.198	-2.916	0.997	5.988	5.155
Mont-BF	3.250	2.547	2.583	-1.438	2.310	7.077	6.295
Muscovite	1.436	-1.353	-2.135	-8.000	-1.936	5.453	4.614
Illite	1.060	-0.761	-1.265	-6.140	-1.240	4.917	4.073
Albite	-2.099	-2.620	-2.772	-5.306	-2.869	0.587	-0.157
Alunite	2.268	0.705	0.237	-3.285	0.684	3.470	3.420
Magnetite	18.369	17.843	17.911	14.204	18.924	20.692	20.601
Leonhardite	0.834	-2.621	-3.527	-13.354	-4.093	9.516	7.395
Hematite	13.653	12.910	12.811	10.046	13.480	15.421	15.273
Amor. Fe(OH) ₃	0.744	0.372	0.202	-1.181	0.588	1.606	1.532

All values computed in Molality

Pco₂ = Partial pressure of CO₂

Unit of ALKALINITY = MeqKg⁻¹ water

IAP = Ion activity product

KT = Equilibrium constant

EPMCAT/AN = Sum of cations and anions ; analytical and computed

Table 6.7a. Description of aqueous and mineral phase geochemistry for slope units 1A - 3B at Manor Lane.

WATEQF INPUT AND RESULTS	SLOPE UNIT					
	1A	1B	2A	2B	3A	3B
pH	7.27	7.30	7.20	7.31	7.18	7.41
T°C	7.30	7.30	7.30	7.00	4.60	5.50
LOG Pco ₂	-3.500	-3.500	-3.500	-3.500	-3.500	-3.500
IONIC STRENGTH	1.31E-01	1.17E-01	1.49E-01	1.49E-01	1.63E-01	1.48E-01
TOT. ALKALINITY	2.72E-01	2.74E-01	2.11E-01	2.90E-01	1.87E-01	3.09E-01
EPMCAT - ANAL	105.797	94.721	121.025	116.550	127.923	121.500
- COMP	77.938	71.116	89.806	84.379	94.781	90.255
EPMAN - ANAL	102.231	89.867	116.733	119.892	129.848	113.450
- COMP	75.042	66.796	86.238	88.454	97.488	82.957
<u>MOLE RATIOS</u>						
Cl/Ca	1.639	1.482	2.084	1.853	2.601	1.590
Cl/Mg	9.62E-01	9.32E-01	8.22E-01	7.70E-01	1.018	7.97E-01
Cl/Na	7.02E-01	5.44E-01	5.59E-01	5.87E-01	8.02E-01	5.47E-01
Cl/K	8.258	8.345	4.517	4.590	5.336	5.011
Cl/Al	3.44E+06	3.33E+06	2.86E+06	2.70E+06	1.51E+06	7.19E+06
Cl/Fe	1.98E+27	2.33E+27	2.16E+27	3.14E+27	7.26E+27	6.57E+27
Cl/SO ₄	5.58E-01	4.97E-01	4.91E-01	4.21E-01	6.24E-01	4.75E-01
Cl/HCO ₃	1.13E+02	8.58E+01	1.36E+02	9.51E+01	1.88E+02	7.70E+01
Ca/Mg	5.87E-01	6.29E-01	3.94E-01	4.16E-01	3.91E-01	5.01E-01
Na/K	1.18E+01	1.54E+01	8.077	7.823	6.653	9.154
<u>LOG ACT RATIOS</u>						
Ca/H ₂	12.104	12.130	11.859	12.088	11.850	12.370
Mg/H ₂	12.356	12.350	12.286	12.492	12.282	12.693
Na/H ₁	5.521	5.573	5.560	5.607	5.518	5.752
K/H ₁	4.437	4.376	4.638	4.699	4.679	4.776
Al/H ₃	11.472	11.513	11.324	11.636	11.660	11.530
Fe/H ₂	-14.997	-15.086	-15.176	-15.159	-15.613	-15.264
Ca/Mg	-0.252	-0.221	-0.427	-0.404	-0.432	-0.323
Na/K	1.084	1.198	0.922	0.908	0.839	0.976
LOG (H ₄ SiO ₄ . Aq)	-3.623	-3.635	-3.837	-3.637	-3.805	-3.881
<u>LOG IAP/KT</u>						
Quartz	0.672	0.661	0.459	0.664	0.538	0.446
Kaolinite	7.001	7.061	6.279	7.273	6.747	6.425
Ca-Mont	7.335	7.394	6.167	7.632	6.762	6.369
Mont-AB	8.068	8.072	6.898	8.234	6.855	6.994
Mont-BF	8.654	8.668	7.483	8.826	7.504	7.500
Muscovite	8.377	8.406	7.494	9.042	8.193	7.822
Illite	7.223	7.240	6.239	7.709	6.826	6.530
Albite	1.379	1.439	0.631	1.575	0.896	0.814
Gypsum	0.428	0.369	0.373	0.407	0.427	0.455
Alunite	4.786	4.679	4.924	5.489	5.713	4.563
Magnetite	23.770	23.564	23.094	23.305	21.214	22.899
Leonhardite	15.067	15.193	12.278	15.516	13.262	13.377
Hematite	18.151	18.034	17.654	17.865	16.359	17.645
Amor. Fe(OH) ₃	2.893	2.834	2.644	2.762	2.113	2.717

All values computed in Molality
Pco₂ = Partial pressure of CO₂
Unit of ALKALINITY = MeqKg⁻¹ water

IAP = Ion activity product KT = Equilibrium constant
EPMCAT/AN = Sum of cations and anions ; analytical and computed

Table 6.7b. Description of aqueous and mineral phase geochemistry for slope units 4A - 7U at Manor Lane.

WATEQF INPUT AND RESULTS	SLOPE UNIT					
	4A	4B	5A	5B	6A	7u
pH	7.15	6.97	7.26	7.61	7.53	7.40
T°C	5.50	4.60	4.20	3.60	4.60	4.60
LOG Pco ₂	-3.500	-3.501	-3.500	-3.500	-3.499	-3.500
IONIC STRENGTH	6.70E-02	1.41E-01	5.05E-02	1.64E-01	7.33E-02	2.71E-02
TOT. ALKALINITY	1.73E-01	1.54E-01	2.33E-01	4.82E-01	3.70E-01	2.74E-01
EPMCAT - ANAL	54.955	118.395	39.473	130.397	54.149	19.418
- COMP	45.998	87.335	34.551	94.152	41.923	17.909
EPMAN - ANAL	43.423	107.621	35.887	127.596	54.237	21.177
- COMP	34.528	77.325	31.035	92.270	42.110	19.732
<u>MOLE RATIOS</u>						
Cl/Ca	2.020	1.163	3.116	1.659	1.377	5.918
Cl/Mg	1.131	8.45E-01	2.986	6.21E-01	1.212	4.778
Cl/Na	7.17E-01	5.63E-01	1.024	6.76E-01	9.22E-01	1.391
Cl/K	2.75E+01	7.470	3.00E+02	7.312	5.02E+01	5.92E+01
Cl/Al	1.39E+06	2.55E+05	2.07E+06	1.58E+07	1.07E+07	6.96E+06
Cl/Fe	1.83E+27	6.86E+26	3.72E+27	1.57E+28	9.99E+27	8.69E+27
Cl/SO ₄	9.51E-01	4.75E-01	1.933	4.15E-01	6.31E-01	3.210
Cl/HCO ₃	1.04E+02	1.97E+02	1.12E+02	4.73E+01	3.88E+01	6.71E+01
Ca/Mg	5.60E-01	7.27E-01	9.58E-01	3.74E-01	8.80E-01	8.08E-01
Na/K	3.83E+01	1.33E+01	2.93E+02	1.08E+01	5.45E+01	4.25E+01
<u>LOG ACT RATIOS</u>						
Ca/H ₂	11.687	11.603	11.888	12.741	12.561	11.855
Mg/H ₂	11.951	11.763	11.917	13.192	12.630	11.954
Na/H ₁	5.245	5.272	5.347	5.858	5.472	5.271
K/H ₁	3.655	4.135	2.875	4.808	3.728	3.639
Al/H ₃	11.523	11.642	11.894	11.766	11.712	11.844
Fe/H ₂	-15.288	-15.186	-15.204	-15.340	-15.338	-15.323
Ca/Mg	-0.265	-0.161	-0.029	-0.451	-0.069	-0.099
Na/K	1.590	1.137	2.472	1.050	1.744	1.632
LOG (H ₄ SiO ₄ , Aq)	-3.879	-3.793	-3.777	-3.782	-3.725	-3.715
<u>LOG IAP/KT</u>						
Quartz	0.447	0.549	0.571	0.579	0.616	0.626
Kaolinite	6.414	6.735	7.230	6.906	7.010	7.294
Ca-Mont	6.243	6.724	7.368	7.129	7.291	7.517
Mont-AB	6.476	6.648	7.254	7.695	7.711	7.558
Mont-BF	7.131	7.356	7.933	8.126	8.250	8.234
Muscovite	6.684	7.632	7.107	8.544	7.636	7.973
Illite	5.660	6.370	6.237	7.335	6.738	6.854
Albite	0.303	0.667	1.021	1.365	1.139	1.099
Gypsum	-0.053	0.546	-0.205	0.471	0.187	-0.769
Alunite	3.775	5.849	3.215	4.322	3.017	2.825
Magnetite	22.306	22.073	22.522	22.692	22.740	22.525
Leonhardite	11.992	12.790	14.404	15.430	15.527	14.721
Hematite	17.077	16.792	17.280	17.621	17.610	17.380
Amor. Fe(OH) ₃	2.434	2.330	2.592	2.788	2.740	2.625

All values computed in Molality

Pco₂ = Partial pressure of CO₂

Unit of ALKALINITY = MeqKg⁻¹ water

IAP = Ion activity product

KT = Equilibrium constant

EPMCAT/AN = Sum of cations and anions : analytical and computed

For both Worbarrow Bay and Manor Lane the analytical results of the interstitial water chemistry (Tables 4.17 and 18) were used to define the ionic concentrations of specified elements in the pore water of each slope unit. Because space does not permit the computed distribution of the aqueous species has been omitted. However, the description of the solution, the calculated molal and activity ratios of the aqueous phase, and the ion activity product ratios of the mineral phase are summarized in Tables 6.6 and 6.7 for Worbarrow and Manor Lane, respectively.

To obtain as realistic a model as possible the temperature at the time of sampling was included, and the partial pressure of carbon dioxide was assumed to be atmospheric owing to the proximity of the ground surface. The only other input variables were the pH and measured ionic concentrations of known elements obtained analytically in the laboratory. The accuracies of chemical analyses may be gauged by the balance of cations and anions. The model will work providing the accuracy of the balance is to within an error of 5 per cent (Plummer, 1984). The balance error of this study was less than 3 per cent (section 4.42).

When the data are applied to the model, WATEQF undergoes a series of iterations to obtain mass balance between all the elements and associated species. In certain cases this will result in elements complexing with others causing a reduction in the equivalent computed cation and anion balance. This is demonstrated between the two sites, where the analytical and computed balances are in good agreement at Worbarrow but show a small divergence at Manor Lane. This reflects the concentration differences between the sites where it was found that low ionic strengths (dilute ≈ 0.045) prevail at the former site in comparison to high ionic strengths (concentrated ≈ 0.15) at the latter site.

With reference to Table 6.6 for Worbarrow Bay, the total alkalinity reflects the pH of the system and shows a similar distribution to that plotted in Figure 4.22b. Broadly this shows a decrease in alkalinity from 0.073 to -0.026 MeqKg⁻¹ downslope of the source unit to the rear of the lobe where a small increase in alkalinity was found (0.023 MeqKg⁻¹). The latter was considered a result of the deposition of weathered slipped materials in this area and the periodic inundation and ingress of sea-salts in to the accumulation lobe. Since an accumulation lobe is prevented from forming at Manor Lane, alkalinity was only found to decrease down-slope of the source areas from approximately 0.4 to 0.2 MeqKg⁻¹ (Table 6.7). Thus it may be argued that either there was an increase in the acidity of the aqueous phase within the mudslides downslope of the source units or that there was an increase in alkalinity immediately following the erosion and weathering of materials (releasing base cations) in the headward regions of the mudslides.

The mole ratios of both sites support the discussion of section 4.421 in identifying the nature of the geochemical system. At Worbarrow Bay the system is dominated by monovalent NaCl-type ionic species, the ratio between these being closest to unity (Table 6.6). When compared with the divalent cations calcium and magnesium, the molality of chloride is shown to be 10-16 times more concentrated. In contrast, Manor Lane is dominated by magnesium, and to a lesser extent calcium, and was thus highly saturated with neutral divalent salts. Although the ratios are based on the chloride anion, the dominant anion at Manor Lane was known to be sulphate (Table 4.17). The ratio for iron indicates that the concentration in the source areas at both sites is an order or two greater than in the feeder track. A more detailed discussion of the

distribution of the dominant ions within each mudslide was given in section 4.421 and will not be further discussed here.

Of greater importance to the modelling of weathering processes is the activity of the aqueous solution for this facilitates the interpretation and description of the chemical environment in which minerals are formed or altered. The activity ratios of the aqueous solution at both sites are practically identical and show a decreasing solubility in order of magnesium, calcium, aluminium, sodium, potassium and ferrous iron, except at Worbarrow where aluminium was found to be more active because the solubility of the divalent cations was lower. This would account for the high proportion of soluble salts at Manor Lane in contrast to Worbarrow Bay (section 4.422). The logarithm of each ratio may be used to construct activity diagrams for each site as a descriptive variable of mineral equilibria (Helgeson et al, 1969).

Ideally, a number of ratios should be used to construct a three dimensional stability field, although typically two-dimensional models are reported. Because mudslides contain an excess of 50 per cent clay and that the bulk chemistry of the clay fraction contains more than 65 per cent silicon dioxide (section 4.44), it was considered that the primary aqueous species was amorphous silica (H_4SiO_4). Thus the activity diagrams are constructed in three ways to take into account the valency of the dominant aqueous phase and the degree of weathering (Al-released) experienced by the system:

1. $\log A(H_4SiO_4)$ versus $\log A(Al/H_2)$
2. $\log A(Mg/H_2)$ versus $\log A(Ca/H_2)$

3. $\text{Log } A(\text{Na}/\text{H}_1)$ versus $\text{Log } A(\text{K}/\text{H}_1)$

where $\text{Log } A$ = activity

H_3 = 3 hydrogen ions

The diagrams are based on those published by Helgeson *et al* (1969). With reference to Figure 6.3, the stability diagram for $\text{Log } A(\text{H}_4\text{SiO}_4)$ versus $\text{Log } A(\text{Al}/\text{H}_3)$, the activity ratios for each slope unit are plotted for both sites. It is clear that the activities of amorphous silica and aluminium were best represented by an association with magnesium saturated montmorillonite clay minerals at both mudslides. When the second diagram was considered, $\text{Log } A(\text{Mg}/\text{H}_2)$ versus $\text{Log } A(\text{Ca}/\text{H}_2)$ presented in Figure 6.4, the activity of the divalent cations suggests an association with micaceous minerals, considerably so at Manor Lane but in combination with montmorillonite clays at Worbarrow.

The final association between the activities of the monovalent cations $\text{Log } A(\text{Na}/\text{H}_1)$ versus $\text{Log } A(\text{K}/\text{H}_1)$ shown in Figure 6.5, would confirm the dominance of montmorillonite clay minerals at Worbarrow and the importance of micaceous clays at Manor Lane, recognised in the mineralogical assessments in section 4.46. The distribution of the activities within each stability field does suggest that montmorillonite clay minerals are particularly prevalent in the source areas of both mudslides, either from *in situ* or formed upon weathering, and that there was a tendency for an increase in mica/illite upon movement down the Manor Lane mudslide. In contrast there was a greater association with kaolinite minerals in preference to mica following the weathering of the Wealden Clay. The instability of the latter over the London Clay was prevalent in the activity diagrams, but both analyses would confirm the distributions of the semi-quantitative assessments given in section 4.46.

Figure 6.3. Mineral stability diagram for the activities of aluminium and amorphous silica.

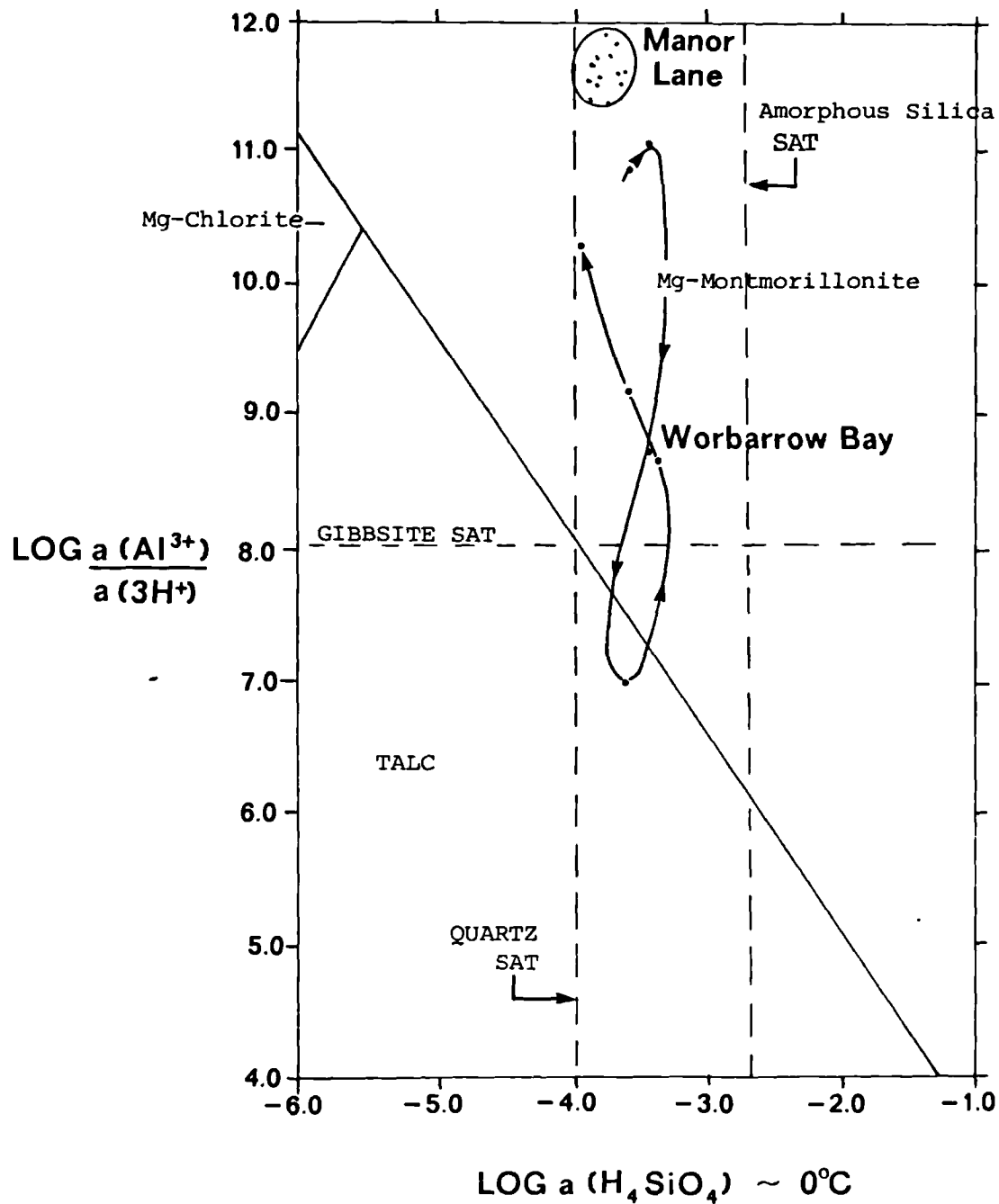
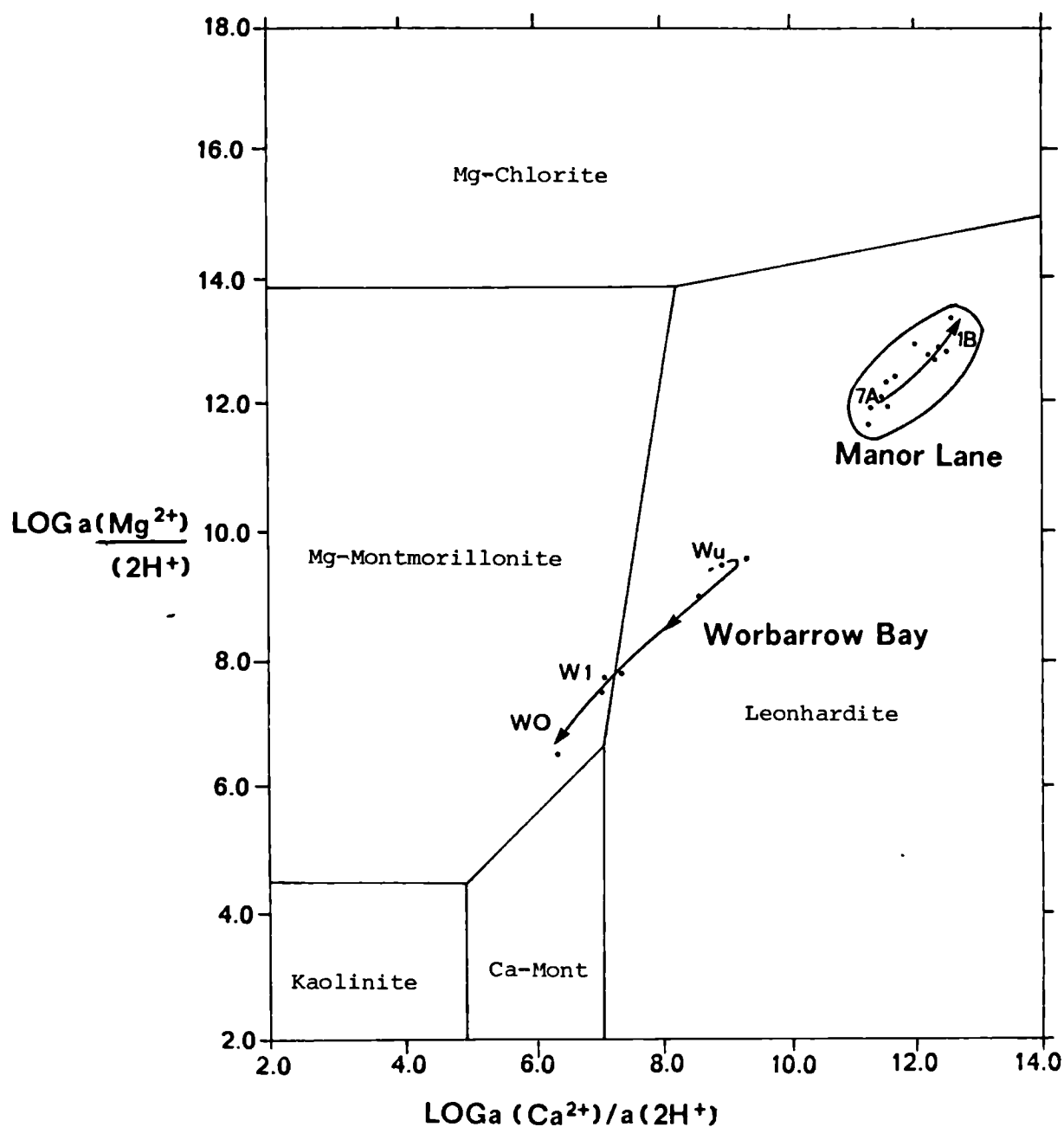


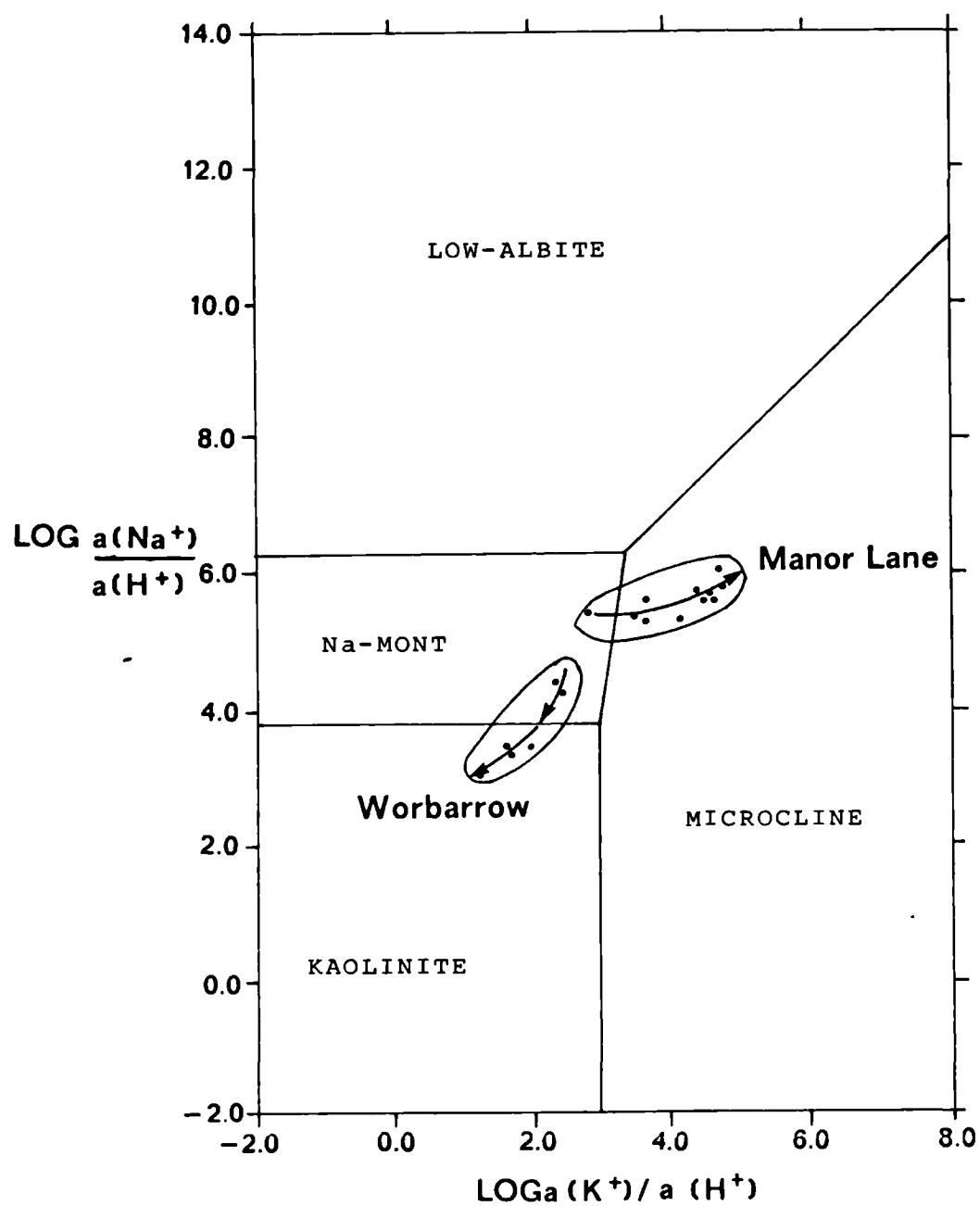
Figure 6.4. Mineral stability diagram for the activities of the divalent magnesium and calcium.



HCl-H₂O-Al₂O₃-CaO-CO₂-MgO-SiO₂

25°C : Log $a \text{H}_4\text{SiO}_4$ = -2.7 saturation

Figure 6.5. Mineral stability diagram for the activities of the monovalent sodium and potassium.



HCl-H₂O-Al₂O₃-CaCO₃-CO₂-MgO-SiO₂

0°C : log a H₄SiO₄ = -3.5 PCO₂ Saturation

The ion activity products of the solid phase provides a direct means of assessing which mineral species control the composition of the pore water. With reference to Tables 6.6 and 6.7, the logarithms of the IAP ratios are reported for the main mineral species associated with both mudslides. As for the activity ratios the speciation is similar for both sites except that the activity products vary for several clays specific to each site.

The minerals predominant in the undisturbed Wealden Beds (WU) show a decreasing association with the aqueous phase in order of:

Magnetite > Hematite > Leonhardite > Montmorillonite > Kaolinite >
K-mica > Illite > Alunite > Amorphous $\text{Fe}(\text{OH})_3$ > Quartz

In contrast the mineral sequence identified for undisturbed London Clay decreases in association as follows:

Magnetite > Hematite > Leonhardite > Montmorillonite > K-mica > Kaolinite
> Illite > Alunite > Amorphous $\text{Fe}(\text{OH})_3$ > Albite > Quartz

The presence of iron and aluminium oxides was recognised in the bulk chemistry of the clay fraction section 4.44 supporting the likely dominance of the first three mineral species. The presence of iron was well documented in the lithostratigraphy of each site (section 3.23). The dominance of magnetite over hematite is probably no more than a reflection of the oxidation state of iron oxide in the weathered zone, Fe_2O_3 (Hematite) in a reduced form with depth, and Fe_3O_4 (Magnetite) in the weathered oxidized state. This would explain the colour change between the blue 'reduced form' London Clay and the brown weathered 'oxidized' London Clay. Evidence of mottling at Worbarrow, and iron-staining along fissures at both sites (section 4.45; Plate 16) would add

strong support to this contention. Little is known, however, about the effects of redox conditions upon the stability of such materials at these sites.

Leonhardite is an aluminosilicate of the form $\text{Ca}_2\text{Al}_4\text{Si}_8\text{O}_{24} \cdot 7\text{H}_2\text{O}$ and would appear to be common to both mudslides in an undisturbed condition in the cliffs backing each landslide. The mineral breaks down upon erosion and weathering at Worbarrow but remains in roughly the same proportion within the mudslide at Manor Lane. The distribution of the minerals directly associated with iron and aluminium show maxima in the source units of both sites, a reduction downslope, and an accumulation at the base of the feeder track and in the accumulation lobe (sections 4.44-4.45).

Of the clay minerals montmorillonite is found to predominate the *in situ* bedrock at both sites. This agrees with the reported clay mineralogy of landslide prone geological strata (Table 4.30; section 4.61). Kaolinite was also an important subsidiary mineral in the Wealden as was muscovite (potassium mica) in the London Clay; the presence of Albite (Na-mica) at Manor Lane demonstrates this fact. Illite was also important at both sites, always subordinate to K-mica, which might suggest its origin from the weathering of the latter.

Alunite, $\text{KAl}_3(\text{SO}_4)_2(\text{OH})_6$, amorphous $\text{Fe}(\text{OH})_3$, and quartz are less abundant but are probably associated with the activity of the aqueous phase as by-products of weathering processes. The ion of importance in alunite, SO_4 , is probably a reflection of the inclusion of sea salts, which are rich in the latter anions. To maintain mass balance sulphate ions are released from the weathering complex with aluminium and potassium to form alunite. At Manor Lane and Worbarrow, the latter mineral is best

associated with the weathered clays than with *in situ* bedrock. Similarly, amorphous $\text{Fe}(\text{OH})_3$ increases upon weathering in the source, decreases downslope, and accumulates towards the base of the feeder track and lobe.

The distribution of the ion activity products (IAP) of the clay minerals within each mudslide shows few variations that may be considered evidence of weathering from one mineral form to another through mudslide processes, although it has been established that micaceous and montmorillonite clays form upon erosion and movement at Manor Lane and Worbarrow, respectively. At Worbarrow the distributions of the IAP for each clay mineral mirror image one another and compare favourably with the distribution of montmorillonite in Figure 4.50, with low values about midslope and large associations in the source and accumulation lobe. This implied a greater divergence from equilibrium between the mineral and aqueous phases in the feeder track, and perhaps a greater degree of chemical instability. In contrast the IAPs at Manor Lane were much more variable, but like Worbarrow the saturation coefficients of each clay have a similar distribution.

Thus it may be concluded that both mudslides show evidence from aqueous phase equilibria of associations with montmorillonite clays *in situ* and upon weathering, magnesium saturated at Manor Lane and sodium saturated at Worbarrow. Weathering reactions and mudslide processes result in an increase in the proportion of illite-mica type clays in place of montmorillonite at Manor Lane whereas there is an increase in montmorillonite upon weathering at Worbarrow. These weathering reactions will be determined by changes in the aqueous phase chemistry, affecting both the stability of the mineral phase as well as the bonding

forces between particles. The causes of such transformations may be simulated using the geochemical model PHREEQE.

6.312 Effects of dilution and salt deposition.

PHREEQE is a computer programme designed to perform a sequence of simulations that enable a variety of solutions to be equilibrated or reacted with the mineral phase. The model solves a set of equations using iterative techniques to simultaneously maintain electrical neutrality, electron balance, mass balance and mineral mass action (Parkhurst *et al*, 1985). Each simulation consists of two separate problems:

1. to process an initial solution or solutions and;
2. to model a reaction (starting from the initial solution(s)).

The model is highly versatile and there are many ways to simulate a geochemical transformation because the model is completely user-definable. For instance, for any particular problem it is necessary to define the chemistry of the starting solution including pH and P_{CO_2} , the phase boundaries (or main mineral species), and the type of reaction required. However, for a more comprehensive description of the capabilities of PHREEQE the reader is referred to Parkhurst *et al* (1985).

In principle it is possible to model the effects of a number of solutions upon mineral stability at both Worbarrow and Manor Lane using the phase boundaries identified in the previous section. Thus the remaining aims (3 and 4) of this section (p.554), to assess the effects of the dilution and the addition of salts upon the weathering behaviour of mudslides,

were modelled using PHREEQE on the University of London Amdahl computer. For simplicity there are two logical stages to the analysis of both systems:

1. to equilibrate the mineral phase with pure water;
2. to mix sea water with the aqueous phase and equilibrate with the mineral phase.

In coastal environments where surface and ground-waters are influenced by sea-salts it was reasonable to assume that these solutions mark the two end points of the range in fluctuations in pore water concentration. Because the model may be simulated by a series of increments, the stability and IAPs of the clay minerals may be related to pore water concentration, so that both the dilution and an increase in salt content may be monitored by the same model.

There are a number of assumptions and constraints to this analysis that were imposed by the amount of time that could be spent modelling these reactions, which include:

- (a) the phase boundaries (or main minerals) were reduced to include magnetite, leonhardite, quartz, alunite and k-mica for both sites in addition to the main clays Mg-montmorillonite and illite at Manor Lane, and Na-montmorillonite and kaolinite at Worbarrow Bay. The IAPs of all other associated minerals were obtained.
- (b) pure water was used as an end point for the theoretically most dilute solution, and sea-water as the theoretically most concentrated pore water solution. Both were held constant throughout all simulations, although it is expected that regional variations in sea-water concentration also occur. The chemistry of sea-water was measured in the laboratory and applied to the model.

- (c) to monitor the effects of the two end points upon weathering sea-water was added to the pure water in increments and equilibrated with the mineral phase until fully saturated.

The results are summarized in Tables 6.8 and 6.9 for Worbarrow and Manor Lane, respectively. The stability of the phase boundaries (delta phase) are presented for the various reactions along with the IAPs of other associated minerals. For both sites increments of 1, 2, 4, 8, 10, 20, 40, 60, 80 and 100 per cent sea-water were equilibrated with the predominant mineral phases identified at each site. As might be expected the ionic strength of the aqueous phase increases proportionally with the addition of sea-water. Similarly with the total alkalinity, although the pH shows a maximum at an effective concentration of 4 per cent sea-water, decreasing rapidly at higher pore water salt contents (60%).

It was possible to relate these results with the activity of the natural aqueous and mineral phase geochemistry, described in the previous section. The ionic strength of the natural pore water solutions were most closely represented an effective sea-water concentration of about 4-8 per cent at Worbarrow, whereas Manor Lane was higher at about 10-20 per cent. In this analysis the stability and IAP coefficients above and below these divisions were considered to represent an addition and dilution of salts in the pore water, respectively. When each solution was equilibrated with the phase boundaries, weathering reactions resulted in the dissolution or precipitation of certain minerals. This is represented by the delta phase coefficient, a negative value indicating precipitation and positive values dissolution.

Table 6.8. Simulated effect of weathering and mineral stability of an increasing concentration of sea water at Worbarrow Bay.

PHREEQE OUTPUT	% SEA WATER COMPOSITION										
	0	1	2	4	8	10	20	40	60	80	100
pH	5.62	8.46	8.51	8.54	8.52	8.51	8.44	8.35	8.30	8.25	8.22
IONIC STRENGTH	0	.007	.014	.028	.056	.070	.139	.276	.412	.547	.685
TOT. ALKALINITY	.246	.952	1.153	1.274	1.392	1.476	1.538	1.654	1.797	1.931	2.410
<u>DELTA PHASE</u>											
Mont-Na	.158	.150	.142	.127	.10	.088	.031	-.092	-.237	-.398	-
Kaolinite	-.230	-.260	-.210	-.192	-.165	-.155	-.126	-.118	-.129	-.145	-
Leonhardite	9.3E-15	-4.7E-7	-1.1E-4	-2.1E-4	-4.3E-4	-5.3E-4	-1.1E-3	-.002	-3.200	-.004	-
Magnetite	1.9E-8	8.3E-7	5.2E-7	4.7E-7	3.9E-7	3.6E-7	2.5E-7	1.5E-7	1.0E-7	7.8E-8	-
Kmica	1.4E-6	-4.5E-5	-2.1E-4	-4.2E-4	-8.4E-4	-1.1E-3	-2.1E-3	4.2E-3	6.3E-3	8.5E-3	-
Mont-Mg	.040	.040	.040	.040	.044	.048	.083	.204	.362	.541	-
Quartz	-.239	-2.270	-.218	-.201	-.174	-.164	-.137	-.134	-.150	-.171	-
<u>LOG IAP/KT</u>											
Mont-Ca	-1.880	-1.88	-1.88	-1.88	-1.879	-1.879	-1.878	-1.876	-1.873	-1.870	-1.312
Mont-BF	4.305	4.601	4.658	4.655	4.649	4.646	4.634	4.616	4.602	4.591	2.630
Illite	2.138	2.138	2.138	2.138	2.137	2.137	2.136	2.133	2.130	2.127	.003
Albite	2.185	2.185	2.185	2.184	2.184	2.183	2.181	2.177	2.172	2.168	-.841
Alunite	-	63.761	64.417	65.118	65.904	66.181	67.111	68.093	68.673	69.09	-4.913
Hematite	6.365	9.364	9.310	9.288	9.245	9.225	9.137	9.022	8.947	8.89	13.283
Goethite	.715	2.202	2.187	2.176	2.155	2.144	2.100	2.042	2.004	1.975	-23.817
Amor. Fe(OH) ₃	-3.115	-1.638	-1.642	-1.650	-1.675	-1.686	-1.730	-1.790	-1.830	-1.861	.333

All values computed in Molality IAP = Ion activity product KT = Equilibrium constant
 Log Pco₂ = fixed at -3.5 Temperature = 10°C Unit of ALKALINITY = MeqKg⁻¹ water
 Negative delta phase indicates precipitation and positive delta phase indicates dissolution
 + + Natural range of ionic strength

Table 6.9. Simulated effect of weathering and mineral stability of an increasing concentration of sea water at Manor Lane.

PHREEQE OUTPUT	% SEA WATER COMPOSITION										
	0	1	2	4	8	10 ↔ 20	40	60	80	100	
pH	5.62	8.41	8.51	8.54	8.52	8.51	8.44	8.354	8.297	8.254	8.22
IONIC STRENGTH	0	.007	.014	.028	.056	.070	.139	.276	.412	.547	.685
TOT. ALKALINITY	.246	.425	.481	.962	1.259	1.421	1.481	1.769	1.844	1.933	2.410
<u>DELTA PHASE</u>											
Mont-Mg	-3.7E-4	-3.7E-3	-6.8E-3	-.011	-.015	-.014	9.0E-3	.109	.246	.404	-
Illite	2.5E-4	-4.1E-4	8.2E-4	6.5E-3	3.3E-3	4.2E-3	8.6E-3	.018	.027	.036	-
Leonhardite	9.1E-12	5.3E-5	1.1E-4	2.1E-4	4.2E-4	5.3E-4	1.1E-3	2.1E-3	3.1E-3	4.2E-3	-
Magnetite	9.6E-12	2.6E-12	1.7E-12	1.4E-12	1.5E-12	1.6E-12	2.0E-12	2.7E-12	3.1E-12	3.4E-12	-
Kmica	-1.5E-4	-2.4E-4	-4.7E-4	9.6E-4	-2.0E-3	-2.5E-3	-5.4E-3	-.012	-.018	-.025	-
Mont-Na	3.4E-4	3.7E-3	6.8E-3	.011	.015	.137	-8.7E-3	-.108	-.244	-.401	-
Quartz	-2.0E-4	-2.2E-4	-4.8E-4	-1.1E-3	-2.3E-3	-2.9E-3	-6.5E-3	-.014	-.023	-.031	-
<u>LOG IAP/KT</u>											
Kaolinite	1.415	1.412	1.415	1.415	1.414	1.414	1.410	1.411	1.409	1.407	-.171
Mont-Ca	-.469	-.469	-.469	-.469	-.469	-.469	-.468	-.468	-.467	-.467	-1.312
Mont-BF	.943	1.162	1.140	1.118	1.098	1.092	1.074	-1.057	1.048	1.042	2.630
Albite	-	-2.092	-2.092	-2.092	-2.091	-2.091	-2.091	-2.089	-2.088	-2.087	-.841
Alunite	-	80.801	82.407	83.925	85.317	85.732	86.912	87.950	88.520	88.910	-4.913
Hematite	4.763	6.592	6.405	6.224	6.054	6.003	5.853	5.717	5.641	5.587	13.283
Goethite	-.086	.829	.735	.645	.560	.534	.458	.389	.351	.323	-23.817
Amor. Fe(OH) ₃	-3.915	-3.000	-3.094	-3.185	-3.270	-3.296	-3.372	-3.443	-3.483	-3.512	.333

All values computed in Molality IAP = Ion activity product KT = Equilibrium constant
 Log Pco₂ = fixed at -3.5 Temperature = 10°C Unit of ALKALINITY = MeqKg⁻¹ water
 Negative delta phase indicates precipitation and positive delta phase indicates dissolution
 ↔ Natural range of ionic strength

At Manor Lane (Table 6.9) low salt concentrations were found to encourage the formation of magnesium saturated montmorillonite, but with an increase in sea-water composition the mineral became unstable, breaking down upon weathering. Illite clay minerals also dissolve with an increase in sea-water content contrary to earlier assessments although k-mica was found to precipitate throughout the entire range of salt concentrations. Thus the greater proportion of mica clay minerals on the lower slopes may be explained by an increasing precipitation of soil mica towards the sea-cliff, and corresponding dissolution of expansive illite and montmorillonite clays. It was noted that in the natural range of ionic concentrations the stability of Mg-montmorillonite is very sensitive to aqueous phase chemistry, and a change in sea-water content of 5 per cent can result in either the dissolution or precipitation of the mineral. At higher pore water salt contents it was evident that montmorillonite became saturated with monovalent sodium cations in preference to divalent magnesium, promoting weathering processes and a likely reduction in the shear strength of mudslide materials.

Quartz is precipitated under the predominant weathering climate increasing with salt content, and although leonhardite is generally unstable and dissolving there was a tendency for the mineral to precipitate at low inherent salt-concentrations and thus immediately upon weathering. The results support the known distribution of the clay minerals and weathering products discussed in the previous section and suggests that both a dilution and an increase in sea-water concentration can result in mineral instability, the latter as a consequence of the presence of Na-montmorillonite on the lower slopes of the mudslide.

Other associated minerals at Manor Lane show little variation in the saturation coefficients, kaolinite and Ca-montmorillonite, in particular, remaining constant throughout the range of concentrations. The most noticeable change to the IAPs is a reduction in hematite and Goethite, FeO(OH) , with a corresponding increase in amorphous iron hydroxide.

The latter by-products of weathering processes may also be seen at Worbarrow Bay (Table 6.8), and along with the highly saturated state of alunite, the transformation of iron and aluminium in the mudslide environment is quite considerable. In comparison to Manor Lane, an increase in pore water concentration was found to cause the precipitation of Na-montmorillonite, and because there was an increase in the proportion of montmorillonite downslope, the Wealden Beds would appear highly susceptible to mass movement through salt deposition and chemical weathering processes in coastal environments.

In simulating the probable weathering reactions taking place in coastal mudslides of this study it has been possible to simulate the likely effects of dilution or an increase in concentration upon the IAP or mineral stability of the component clays. PHREEQE has shown that within the effective pore water salt-contents found in reality, weathering reactions are highly sensitive to small fluctuations in chemistry such that a 2 per cent change in sea-water concentration at Worbarrow can cause a significant precipitation of Na-montmorillonite and the probable development of dispersive conditions. Such fluctuations have major effects upon the residual shear strength of clays. The interactions between the aqueous and mineral phase geochemistry are fundamental to particle interaction, the development of bonding mechanisms, shear strength and the weathering behaviour of coastal mudslides.

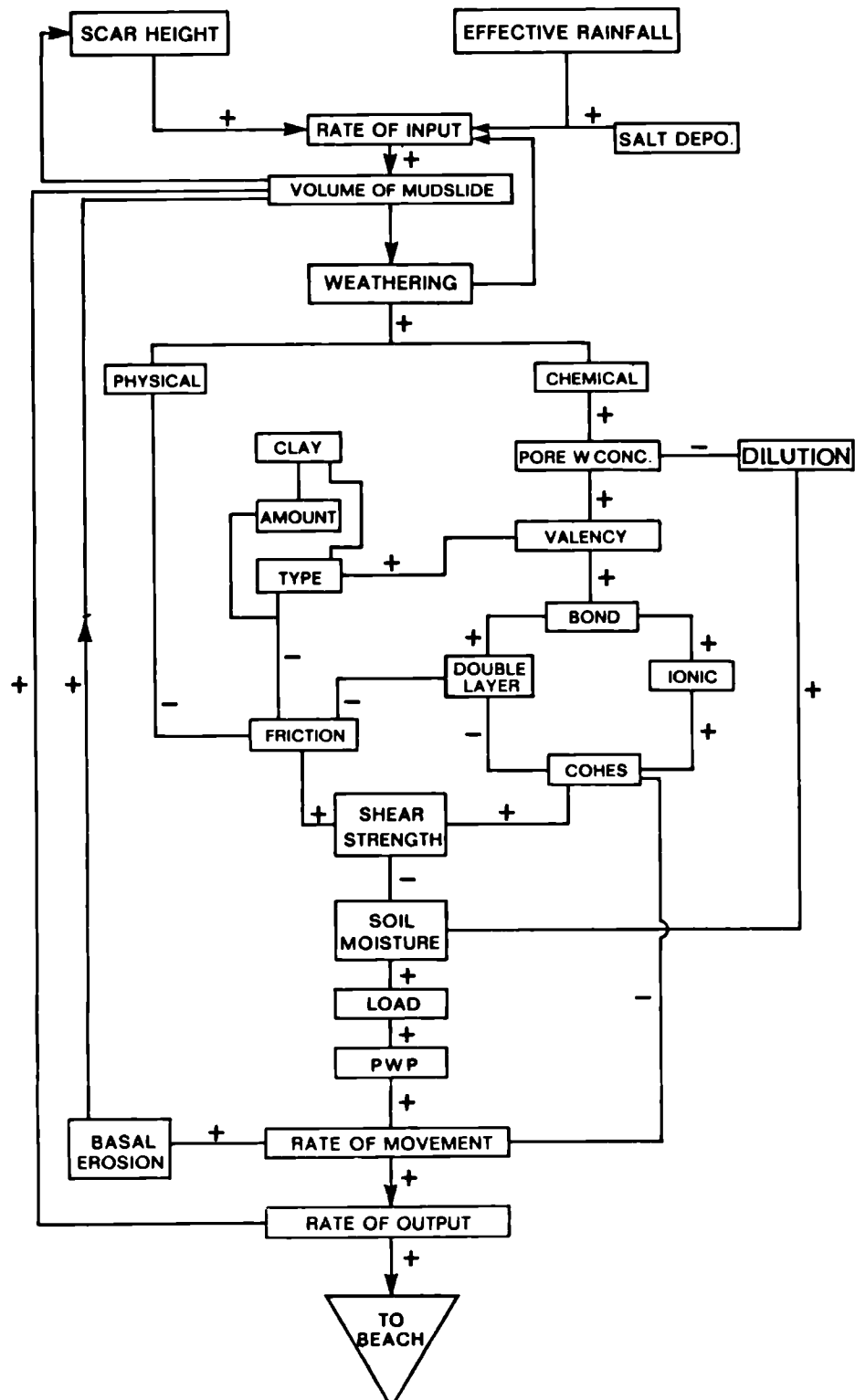
6.32 Geochemical interactions.

In conclusion to the findings of the geochemical modelling, and the static and dynamic distribution of soil properties and behaviour, a process response model is proposed to represent how the findings of this study relate to mudslide behaviour and the stability of coastal slopes. The findings only concern the role of shear strength within the model by Brunsden (Figure 1.5), and how the processes of weathering and geochemistry interact with shear strength, the principle resisting force against mudsliding, and thus the dynamics of mudslide processes. The model is not presented as a detailed summary of this thesis, but merely to demonstrate how the physico-chemical properties of clay interact to determine the stability of slope materials. The model serves as a basis for the detailed stability analyses undertaken in the next section.

It is necessary to consider friction and cohesion separately within this framework, although ultimately they both determine shear strength (Figure 6.6). Principally, three main contributing factors to shear strength are isolated: the nature of the clay fraction, aqueous phase chemistry, and the bonding mechanisms determining the inter- and intra-particle associations. Weathering and soil moisture are the primary factors involved in mudslide processes, and the seasonal variation in shear strength.

Broadly, the model suggests that the presence of clay can result in a significant reduction in friction, the type of clay and the degree of inter-layer substitutions (primary bonds) and the valency of associated cations may further reduce the influence of the frictional component of strength. From a physico-chemical viewpoint the nature of the inter- and

Figure 6.6. Physico-chemical process-response model of mudslide activity.



intra-particle bonding mechanisms is critical. Where there is a high electrolyte concentration of high valency cations, and little soil water, there is a tendency for strong ionic bonds to form between and within particles and cohesion will be strong. When the solution is diluted the bonds are chemically weakened in preference for diffuse double layers, causing the expansion and separation of particles. This in principle reduces both cohesion and the frictional forces of shear strength in clay suspensions.

The dynamics of mudsliding are such that other physical stresses within the slope, and finally movement itself, break down any ionic bonds between particles and especially across shear surfaces. Evidence of creep or small stick-slip type displacements would suggest an element of strain-weakening before the reactivation of mudslide movements. It was considered that ionic bonds reform across shear surfaces over the dry and stable summer months and that these are primarily responsible for supporting this initial stress. When the stresses are too great the bonds snap in a cataclysmic manner. Cohesion at this point is zero and the mudslide is entirely supported by friction and the weaker van der Waals' forces of attraction within the double layers. Thus, movement is negatively related to cohesion, and also to friction through physical weathering processes. The interaction between the components of this model may now be discussed in greater detail with reference to the seasonal stability of both mudslides.

6.4 Slope stability analysis:

Slope stability analysis is conventionally used by geotechnical engineers, and more recently geomorphologists, to obtain a quantitative statement of the potential stability of a slope with known physical properties and hydrological regimes. The results of such modelling can be used to predict the behaviour of slopes under variable conditions, as well as identifying the factors most responsible for past failures, known as back-analysis.

The results of this study may be applied in this manner, although it is noted that most models of stability are primarily based on the physical properties of soils, slope geometry, and pore water pressures; they are a simplification of real processes such that truly accurate models are seldom obtained because soil variability and other important factors, such as the forces of chemical interaction between particles are generally ignored (section 2.32). This is especially true when considering surface translational mudslides developed within normally-consolidated clays. The application of geochemical and clay mineral data to slope instability are unavailable in standard stability models.

However, the success of stability analyses is based on its versatility in application to a wide variety of problems, including many types and dimensions of landslides with varying distributions of stresses within the slope, and the ability to define as many slope units or slices, and sub-zones or horizons within slices as required, of each site under study. In this way a slope stability model can be designed specifically for each site depending on the type of landslide to be modelled and the purpose of the analysis.

Slope stability analyses were undertaken for both Worbarrow Bay and Manor Lane using purposely designed models to enable the incorporation of field and laboratory results at a much enhanced resolution than normally achieved. Additionally, it was possible to relate seasonal changes in residual shear strength with pore water pressures and the effects of undrained loading to obtain a model of the stability of both sites throughout the study period.

Before describing the relative influences of these parameters upon the stability of slopes it is emphasised that such models can only assess the likelihood of failure but not the mechanics of landslide behaviour; these were discussed earlier in section 5.3. Thus the purpose of this analysis was to substantiate and model these findings with respect to seasonal behaviour and further complement this research. Because there are many models of stability, an important pre-requisite to using this type of analysis is the correct identification and design of the most suitable model.

6.41 Choice of model.

Because translational mudslides tend to be relatively shallow with respect to their length and width, the model most typically used is the infinite slope method which is a two-dimensional analysis of a slice with the forces on the sides being equal and opposite in direction and magnitude (Selby, 1982). The thickness and angle of rest are constant and infinite in extent. Thus interslice forces are assumed to be negligible and for each slice a factor of safety is computed by determining the forces resisting movement divided by the forces promoting instability:

$$F = \frac{\text{sum of resisting forces}}{\text{sum of driving forces}} = \frac{\sum Cr' (b/\cos\alpha) + (W\cos\alpha - \mu(b/\cos\alpha)) \tan\phi'}{\sum W\sin\alpha}$$

where:

Cr' = cohesion where r' denotes effective residual parameters (kPa)

ϕ' = the internal friction angle (°)

b = the slice dimension (m)

α = the slope angle of the shear surface (°)

μ = pore water pressure (kPa)

W = the overburden weight (kN/m³).

The sum of the forces from each slice are used to compute a global factor of safety for the entire slope. Where the forces are equal $F = 1$ the slope is termed critical; where $F < 1$ the slope is in a condition for failure; and where $F > 1$ the slope is likely to be stable. Because the factor of safety is a simplification of real processes it is important to realise that not all terms in the model are equally susceptible to change, and parameters such as the length of slice, cohesion and slope angle are the most sensitive parameters in the equation when considering shallow slides. Thus the greatest alterations in F would be found when manipulating these terms, and it must be considered prudent to justify their alteration before discussing the results. However, because the equation has been used in engineering practice for many years it was felt necessary to relate the current findings to the standard framework.

Following discussion with Bromhead (pers.com., 1987) the infinite stability model was chosen and designed for each site to include the slope units defined in Table 4.1 as slices, each containing three sub-zones (or horizons), to obtain a more accurate representation of the density and shear strength parameters recorded in Chapter Four. Typically, models such as the infinite slope and the Janbu methods are

not designed to include a high degree of soil variability and only consider one unit of depth owing to the shallow nature of translational slides and probably due to the sparsity of measured data. Thus a total of 6 slices were included in the Worbarrow stability model (Figure 6.7), whereas 10 were established for Manor Lane, and each model was programmed into a SuperCalc spreadsheet for use on an Apricot Zen microcomputer. By using the spreadsheet, the effects of changing the value of the component variables can be assessed interactively and thus their sensitivity within the model established.

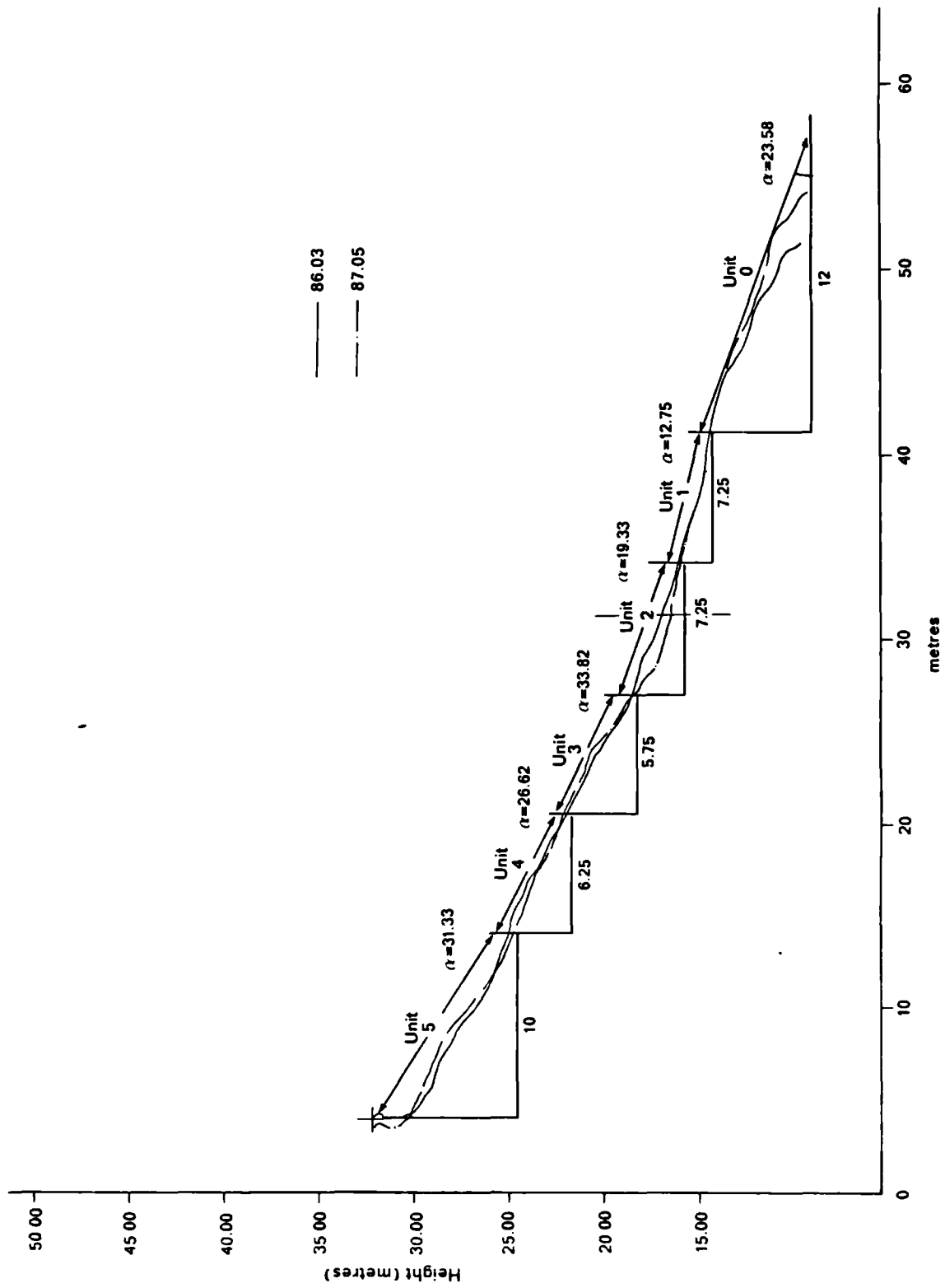
6.42 Local and Global Factor of Safety:

6.421 Peak and residual conditions.

The aims of the analyses of stability for both Worbarrow and Manor Lane may be summarized and discussed with reference to six models of the factor of safety:

1. The peak and residual conditions of stability; and whether cohesion may justifiably be set to zero.
2. The seasonal fluctuation in F caused by variations in pore water pressure.
3. The seasonal fluctuations in F caused by the combined effects of pore water pressure and shear strength.
4. The seasonal variation in F attributable to shear strength.
5. The seasonal fluctuations in F caused by the combined effects of pore water pressure, shear strength and undrained loading.
6. The seasonal variation in F attributable to undrained loading.

Figure 6.7. Worbarrow Bay slope slices used in stability analyses.



The first model of the analysis was to determine the peak and residual factors of safety using the static parameters measured in the laboratory programme (Chapter Four). The shear strength and unit weight parameters measured at the basal shear surface and within the mudslide, respectively, were used to set up the 'standard' factor of safety models. These are summarized in Tables 6.10 and 6.11, presenting the calculation of the local, global and peak values of F . The global factor of safety is only based on the stability of the mudslide and does not include the peak condition.

At Worbarrow Bay the reduction from a peak value in $F = 3.08$ to a global residual value of $F = 1.19$ represents a 61 per cent reduction in the stability of the slope. Similarly at Manor Lane, a reduction in F from a peak value of 2.81 to 1.23 represents a 56 per cent fall in the stability of the slope. These reductions may be accounted for by a corresponding fall in the shear strength parameters (section 4.322). Thus the general conditions of mudslide stability observed at both sites, show a decline in the factor of safety towards unity that is supported by a reduction in the shear strength parameters from peak to residual states, and the coastal slope is permanently exposed to near-critical conditions for failure.

More importantly, the distribution of the local values of F clearly show that at both sites several slices have values of F below unity, including .90 and .70 at Manor Lane, and .82 and .94 at Worbarrow Bay. These values coincide with the positions of the current source in slope unit 6 and a former retrogressive source unit 3A at Manor Lane (section 4.241), in contrast with the toe of the slope (unit 0) and the base of the feeder

Table 6.10. Computed factor of safety at Worbarrow Bay.

Model 1 : Computed factor of safety assuming zero pore water pressure.

SLOPE UNIT	STRENGTH c'	SLICE phi	ANGLE b	MUDSLIDE deg	DEPTH z1	z2	g1	z3	g2	g3	PWP p	FACTOR OF SAFETY top	bot	cos(a)
0	2.87	7.86	12	23.6	.32	14.39	.29	13.14	.45	15.62	0	61.028	74.197	.916
1	3.63	10.4	7.25	12.8	.3	13.8	.32	15.43	.58	13.93	0	49.206	27.558	.975
2	1.90	5.73	7.25	19.3	.26	14.18	.23	13.61	.21	12.03	0	21.010	22.389	.944
3	2.35	12.5	5.75	33.8	.1	12.61	.22	14.06	.17	13.26	0	23.261	21.138	.831
4	2.83	7.38	6.25	26.6	.16	14.51	.17	15.39	.28	11.2	0	25.625	22.594	.894
5	5.27	6.85	10	31.3	.15	14.39	.25	10.81	.28	11.86	0	70.074	42.505	.854
Peak	12.31	23.2	1	25	.46	10.14	.53	9.29	.58	9.07	0	19.350	6.2752	.906

Peak factor of safety = 3.084

Global factor of safety = 1.189

Local factor of safety =

	slice	0
		1
		2
		3
		4
		5

Table 6.11. Computed factor of safety at Manor Lane.

Model 1 : Computed factor of safety assuming zero pore water pressure.

FACTOR OF SAFETY														
SLOPE UNIT	STRENGTH	SLICE ANGLE		MUDSLIDE DEPTH AND UNIT WEIGHT			PWP		FACTOR OF SAFETY					
	c'	phi	b	deg	z1	g1	z2	g2	z3	g3	p	top	bot	cos(a)
1A	2.40	9.54	25.00	16.00	.39	12.60	.31	12.30	.84	12.70	0	140.75	133.65	.96
1B	2.25	6.76	25.50	14.00	.14	12.30	.3	13.00	.29	11.80	0	85.66	55.79	.97
2A	2.64	7.96	15.00	17.00	.17	12.40	.29	11.60	.36	12.13	0	61.14	43.15	.96
2B	2.17	8.98	15.00	20.00	.13	13.20	.26	11.50	.16	10.78	0	48.96	32.99	.94
3A	1.67	7.84	14.50	26.00	.15	11.20	.21	11.60	.23	11.92	0	39.25	43.59	.90
3B	3.93	7.91	15.00	29.00	.07	12.50	.16	11.10	.20	11.43	0	76.40	35.90	.87
4A	2.31	11.36	14.00	32.00	.11	12.20	.2	12.04	.21	11.24	0	52.71	45.33	.85
4B	4.17	11.42	15.00	33.00	.16	13.80	.29	11.75	.23	13.21	0	96.57	70.70	.84
5A	2.80	11.00	10.00	32.00	.06	10.90	.08	11.46	.19	9.81	0	38.68	18.20	.85
6	1.27	11.30	24.50	34.00	.17	10.30	.24	10.64	.22	11.45	0	65.23	93.48	.83
Peak	13.00	15.52	1.00	25.00	.51	11.24	.49	9.76	.45	10.67	0	18.20	6.47	.91

Peak factor of safety = 2.812

Global factor of safety = 1.231

Local factor of safety =

1A	1.053	slice
1B	1.535	
2A	1.417	
2B	1.484	
3A	.9004	
3B	2.128	
4A	1.163	
4B	1.366	
5A	2.125	
6	.6977	

track (unit 2) at Worbarrow, respectively. Although the latter features are truncated by a sea-cliff at Manor Lane it would suggest that at this site instability is more than likely generated from the source units, whereas the lower slopes at Worbarrow show considerable weakness to the rear and front of the accumulation lobe. The lobe itself (unit 1) is the most stable feature of the latter mudslide ($F=1.79$).

These results demonstrate that the processes of erosion and weathering alone can give rise to conditions of instability before other influences such as pore water pressures are considered. The cause of initial failure is normally attributed to basal undercutting in association with high ground water pressures. Once F is reduced to near unity mudsliding is seasonally self-perpetuated as fluctuations in F occur above and below unity. The causes of such fluctuations are considered in the following sections.

Although certain areas of slope are prone to instability, others show values greater than unity and would probably contain the influence of the former slices *en mass* by maintaining the stability of the slope. Thus the dominant values of F within the slope are probably more important in describing the development of instability than implied by the global factor of safety. There can be little doubt that the results of these two independent sites show how coastal slopes of this nature may become extremely sensitive to failure as a consequence of oversteepening by marine erosion and the associated physical disturbance to the soil and geologic materials.

That the model is very sensitive to shear strength is demonstrated if the assumption that cohesion is negligible or zero in the residual state is

Table 6.12. Computed factor of safety at Worbarrow Bay.

Model 2 : Computed factor of safety assuming zero cohesion and pore water pressure.

STRENGTH c'	phi	b	SLICE ANGLE deg	MUDSLIDE DEPTH z1	g1	z2	g2	z3	g3	PWP p	FACTOR OF SAFETY top	bot	cos(a)
0	7.86	12.00	23.60	.32	14.39	.29	13.14	.45	15.62	0	23.44	74.20	.92
0	10.38	7.25	12.80	.30	13.80	.32	15.43	.58	13.93	0	22.22	27.56	.98
0	5.73	7.25	19.30	.26	14.18	.23	13.61	.21	12.03	0	6.42	22.39	.94
0	12.50	5.75	33.80	.10	12.61	.22	14.06	.17	13.26	0	7.00	21.14	.83
0	7.38	6.25	26.60	.16	14.51	.17	15.39	.28	11.20	0	5.84	22.59	.89
0	6.85	10.00	31.30	.15	14.39	.25	10.81	.28	11.86	0	8.40	42.51	.85

Global factor of safety = .349

Local factor of safety =

.316	slice	0
.806		1
.287		2
.331		3
.259		4
.198		5

Table 6.13. Computed factor of safety at Manor Lane.

Model 2 : Computed factor of safety assuming zero cohesion and pore water pressure.

STRENGTH c'	phi	SLICE b	ANGLE deg	MUDSLIDE z1	DEPTH g1	AND z2	UNIT g2	WEIGHT z3	PWP p	FACTOR OF SAFETY top	FACTOR OF SAFETY bot	cos(a)
0	9.54	25.00	16.00	.39	12.60	.31	12.30	.84	12.70	0	78.33	133.65 .96
0	6.76	25.50	14.00	.14	12.30	.3	13.00	.29	11.80	0	26.52	55.79 .97
0	7.96	15.00	17.00	.17	12.40	.29	11.60	.36	12.13	0	19.73	43.15 .96
0	8.98	15.00	20.00	.13	13.20	.26	11.50	.16	10.78	0	14.32	32.99 .94
0	7.84	14.50	26.00	.15	11.20	.21	11.60	.23	11.92	0	12.31	43.59 .90
0	7.91	15.00	29.00	.07	12.50	.16	11.10	.20	11.43	0	9.00	35.90 .87
0	11.36	14.00	32.00	.11	12.20	.2	12.04	.21	11.24	0	14.58	45.33 .85
0	11.42	15.00	33.00	.16	13.80	.29	11.75	.23	13.21	0	21.99	70.70 .84
0	11.00	10.00	32.00	.06	10.90	.08	11.46	.19	9.81	0	5.66	18.20 .85
0	11.30	24.50	34.00	.17	10.30	.24	10.64	.22	11.45	0	27.69	93.48 .83

Global factor of safety = .402

Local factor of safety =

	slice	1A
.586		1B
.475		2A
.457		2B
.434		3A
.282		3B
.251		4A
.322		4B
.311		5A
.311		6
.296		

applied to the model. The results are shown in Tables 6.12 and 6.13, where it may be seen that the global values of F are significantly reduced to .35 and .40 at Worbarrow and Manor Lane, respectively. The results would imply extreme instability throughout the year, which is clearly not the case (section 5.3). This suggests that not only is the assumption of zero cohesion theoretically and practically unjustified (see sections 2.23, 2.32 and 4.321), but wholly inappropriate for estimations of the seasonal stability of translational mudslides. The stability model is more realistic with the inclusion of the laboratory determined cohesive forces which exist between the component particles and across shear surfaces, albeit greatly reduced in the latter case. These forces are known to vary according to the chemistry of the solid and aqueous phases (section 6.223), which are considered later in section 6.432.

6.43 Seasonal fluctuations in the Factor of Safety.

6.431 Effect of pore water pressures.

The 'standard' model described above may be developed further to include the seasonal fluctuations in pore water pressures measured directly in the field (section 5.322, Appendix 12). Values of the phreatic head pressure within the soil were applied to the model, examples of which are given in Tables 6.14 and 6.15 for the theoretical 'worst' case where the phreatic level is at the surface of the fully saturated mudslide. Where artesian pressures exist, such as on the lower slopes at both sites, greater levels may be recorded and similarly applied to the model producing even lower values of F . One assumption is made in this model: a linear relationship exists between the phreatic levels of known points. This is necessary because pore water pressures were not consistently measured in every slope unit.

Table 6.14. Computed factor of safety at Worbarrow Bay.

Model 3 : Computed factor of safety with worst case pwp assuming static residual strength.

STRENGTH														FACTOR OF SAFETY													
c'	phi	b	deg	z1	g1	z2	g2	z3	g3	p	top	bot	cos(a)														
2.87	7.86	12.00	23.60	.32	14.39	.29	13.14	.45	15.62	1.06	59.46	74.20	.92														
3.63	10.38	7.25	12.80	.30	13.80	.32	15.43	.58	13.93	1.20	47.00	27.56	.98														
1.90	5.73	7.25	19.30	.26	14.18	.23	13.61	.21	12.03	.70	20.28	22.39	.94														
2.35	12.50	5.75	33.80	.10	12.61	.22	14.06	.17	13.26	.49	21.98	21.14	.83														
2.83	7.38	6.25	26.60	.16	14.51	.17	15.39	.28	11.20	.61	24.76	22.59	.89														
5.27	6.85	10.00	31.30	.15	14.39	.25	10.81	.28	11.86	.68	69.14	42.51	.85														

Global factor of safety = 1.153

Local factor of safety =

		slice			
.8014				0	
1.705				1	
.9058				2	
1.040				3	
1.096				4	
1.627				5	

Table 6.15. Computed factor of safety at Manor Lane.

Model 3 : Computed factor of safety with worst case pwp assuming static residual strength.

STRENGTH c'	phi	SLICE b	ANGLE deg	MUDSLIDE z1	DEPTH g1	AND z2	UNIT g2	WEIGHT z3	PWP g3	FACTOR OF SAFETY p	top	bot	cos(a)
2.40	9.54	25.00	16.00	.39	12.60	.31	12.30	.84	12.70	1.54	138.11	133.65	.96
2.25	6.76	25.50	14.00	.14	12.30	.3	13.00	.29	11.80	.73	84.78	55.79	.97
2.64	7.96	15.00	17.00	.17	12.40	.29	11.60	.36	12.13	.82	59.97	43.15	.96
2.17	8.98	15.00	20.00	.13	13.20	.26	11.50	.16	10.78	.55	48.06	32.99	.94
1.67	7.84	14.50	26.00	.15	11.20	.21	11.60	.23	11.92	.59	38.36	43.59	.90
3.93	7.91	15.00	29.00	.07	12.50	.16	11.10	.20	11.43	.43	75.73	35.90	.87
2.31	11.36	14.00	32.00	.11	12.20	.2	12.04	.21	11.24	.52	51.50	45.33	.85
4.17	11.42	15.00	33.00	.16	13.80	.29	11.75	.23	13.21	.68	94.97	70.70	.84
2.80	11.00	10.00	32.00	.06	10.90	.08	11.46	.19	9.81	.33	37.94	18.20	.85
1.27	11.30	24.50	34.00	.17	10.30	.24	10.64	.22	11.45	.63	63.74	93.48	.83

Global factor of safety = 1.210

Local factor of safety =

slice	1A
1.033	1B
1.520	2A
1.390	2B
1.457	3A
.8801	3B
2.109	4A
1.136	4B
1.343	5A
2.084	6
.6818	

The values of F associated with the variation in pore water pressures throughout the study are presented in Tables 6.16 and 6.17 for Worbarrow and Manor lane, respectively. At Manor Lane the inclusion of pore water pressures was only found to cause a reduction in the global factor of safety from 1.23 to 1.20 throughout the winter months. The corresponding reduction at Worbarrow was 0.05 to 1.14 suggesting that pore water pressures only have a relatively minor influence upon the overall stability of shallow mudslides, the global values of F remaining above unity. This no doubt reflects the shallow nature of mudslides, because at greater depths such as for deep-seated rotational mudslides pore water pressures are known to be largely responsible for first-time failures and the re-activation of large landslides (Bromhead 1979a). At such depths the model is more sensitive to changes in pore water pressures.

The local factors of safety show a higher degree of variation caused by pore water pressure amounting to a maximum of 0.10 at Manor Lane and 0.13 at Worbarrow with both sites showing the lowest values of F during the months of December to February. At Worbarrow the value of F in slope unit 3 (mid-feeder track) is particularly responsive to variations in pore water pressure reducing to .97 in January but increasing to 1.07 in the drier months of July and August. This change marked a reduction in the local factors of safety to below unity over 50 per cent of the mudslide. Such variation is less pronounced at Manor Lane, although the source areas 5A and 3B do show significant changes in F . Thus, although the global stability of each site was not greatly affected by the inclusion of pore water pressures, in certain areas of the slope the latter are likely to remain a significant and sensitive cause of triggering seasonal movements.

Table 6.16. Seasonal fluctuation in the factor of safety at Worbarrow Bay attributed to pore water pressure.

DATE	SLOPE UNITS						Global
	0	1	2	3	4	5	
Oct 85	.79	1.70	.89	1.00	1.10	1.64	1.15
Nov	.79	1.70	.89	1.00	1.10	1.64	1.15
Dec	.79	1.70	.89	.99	1.09	1.63	1.14
Jan 86	.79	1.69	.88	.97	1.08	1.63	1.14
Feb	.79	1.69	.88	.99	1.09	1.63	1.14
Mar	.79	1.70	.89	1.00	1.10	1.64	1.14
Apr	.80	1.71	.89	1.00	1.09	1.63	1.15
May	.80	1.72	.90	1.02	1.10	1.64	1.15
Jun	.80	1.73	.91	1.05	1.12	1.65	1.16
Jul	.80	1.73	.91	1.07	1.13	1.65	1.17
Aug	.80	1.73	.91	1.07	1.13	1.65	1.17
Sep	.80	1.72	.91	1.04	1.12	1.65	1.16
Oct	.80	1.72	.89	.99	1.09	1.63	1.14
Nov	.80	1.72	.90	1.01	1.09	1.63	1.15
Dec	.80	1.71	.90	1.01	1.09	1.63	1.15
Jan 87	.79	1.70	.89	.99	1.09	1.63	1.14
Feb	.79	1.69	.88	.99	1.09	1.63	1.14
Mar	.79	1.70	.89	.99	1.09	1.63	1.14
Apr	.80	1.72	.90	1.00	1.09	1.63	1.15
May	.80	1.72	.90	1.01	1.10	1.63	1.15
M = 1	.80	1.71	.91	1.04	1.10	1.63	1.15
Variation	.01	.04	.03	.10	.05	.02	.03
Fall in F	.03	.10	.06	.13	.05	.02	.05

M = 1 represents F where the phreatic level is at the ground surface.

Table 6.17. Seasonal fluctuation in the factor of safety at Manor Lane attributed to pore water pressure.

DATE	SLOPE UNITS										Global
	1A	1B	2A	2B	3A	3B	4A	4B	5A	6	
13.10.85	1.03	1.50	1.37	1.42	.86	2.08	1.12	1.34	2.04	.68	1.20
27.10.85	1.03	1.50	1.37	1.42	.86	2.08	1.12	1.34	2.05	.69	1.20
10.11.85	1.03	1.50	1.37	1.42	.86	2.08	1.11	1.34	2.03	.68	1.20
24.11.85	1.03	1.50	1.37	1.42	.86	2.08	1.11	1.34	2.04	.68	1.20
5.12.85	1.03	1.50	1.37	1.42	.86	2.08	1.12	1.34	2.04	.68	1.20
22.12.85	1.03	1.51	1.37	1.42	.86	2.08	1.12	1.34	2.04	.68	1.20
11.01.86	1.03	1.51	1.37	1.42	.86	2.08	1.11	1.34	2.03	.68	1.20
17.01.86	1.03	1.50	1.37	1.42	.86	2.08	1.11	1.34	2.03	.68	1.20
8.02.86	1.03	1.50	1.37	1.42	.86	2.08	1.12	1.34	2.04	.68	1.20
15.02.86	1.03	1.50	1.37	1.42	.86	2.08	1.12	1.34	2.05	.69	1.20
1.03.86	1.03	1.50	1.37	1.42	.86	2.08	1.12	1.34	2.05	.69	1.20
15.03.86	1.03	1.50	1.37	1.42	.86	2.08	1.12	1.34	2.05	.69	1.20
29.03.86	1.03	1.50	1.37	1.42	.86	2.08	1.12	1.34	2.05	.69	1.20
12.04.86	1.03	1.50	1.37	1.42	.86	2.09	1.12	1.34	2.06	.69	1.20
26.04.86	1.03	1.50	1.37	1.42	.86	2.09	1.12	1.34	2.05	.69	1.20
18.05.86	1.03	1.50	1.37	1.43	.87	2.09	1.13	1.35	2.09	.69	1.21
M = 1	1.03	1.52	1.39	1.46	.88	2.11	1.14	1.34	2.08	.68	1.21
Variation	.00	.02	.02	.04	.02	.03	.03	.01	.06	.01	.01
Fall in F	.02	.04	.05	.06	.04	.05	.05	.03	.10	.02	.03

M = 1 represents F where the phreatic level is at the ground surface.

6.432 Effect of residual shear strength.

The calculated fluctuations in residual shear strength attributed to seasonal variations in pore water concentration (section 6.223) were applied to the stability model to assess the influence of shear strength on the seasonal stability of each site. Because the changes in residual strength could not be associated with either friction or cohesion (section 6.223), it was considered appropriate to apply the changes in strength to the cohesion term because the units used are equivalent to an actual change in residual shear strength, and because in theory such changes are probably a consequence of varying intensities of cohesive bonding between particles.

Although the pore water chemistry was only monitored at Worbarrow Bay, it was considered necessary to predict the likely response of residual strength to fluctuations in pore water concentration at Manor Lane, given the differences in site lithology and soil chemistry. Consequently variations in F at both sites caused by fluctuations in shear strength could be considered an important factor in the seasonal instability of mudslides. Thus if the same proportional fluctuations in pore water concentration measured at Worbarrow Bay are assumed to affect the Manor Lane site, changes in residual strength of the London Clay may be calibrated from the laboratory simulation test results (section 6.223) in a similar manner to Wealden Clay.

It is noted that although the simulated change in shear strength with sea-water concentration was less pronounced for the London Clay (Figure 5.34), the initially more concentrated pore water solution underwent much greater seasonal fluctuations in concentration, which consequently

produced a similar change in actual strength when compared with the Worbarrow site. This is no coincidence because it supports the contention that the shear strength of clay soils is dependent on the mineralogy and chemistry of the system. At low inherent pore water concentrations, residual strength is reduced and highly variable between weathered and unweathered states, whereas high pore water salt contents produce greater but less variable strength. Thus for the same proportional change in pore water concentration similar values of strength are found because the fluctuation in concentration is greater in the latter case.

The results are summarized in Tables 6.18-6.21 for both sites, presenting the seasonal change in F attributed to both pore water pressure and shear strength, and shear strength alone. With reference to both Worbarrow and Manor Lane a much greater change in F is noted when shear strength and pore water pressures are combined. This, however, is mostly attributable to shear strength for this term is more sensitive to change than pore water pressures in shallow landslips. At Worbarrow Bay and Manor Lane the global factor of safety undergoes a much more marked seasonal cycle (as might be expected from the findings in Chapter 5), with F reducing 0.11 (1.08) and 0.12 (1.11) by September to October, respectively, and increasing to 1.29 and 1.35 in January to March. The differences between these extremes is entirely accounted for by a change in the resisting forces of residual shear strength.

The reduction in F coincides with the apparent dilution of the pore water from August to October (Figure 5.22) and a subsequent reduction in residual strength, whereas the dramatic increase in F is due to an increase in pore water salt content and shear strength. Such changes in

Table 6.18. Seasonal fluctuation in the factor of safety at Worbarrow Bay attributed to pore water pressure and shear strength.

DATE	SLOPE UNITS						Global
	0	1	2	3	4	5	
Oct 85	.75	1.64	.79	.90	1.00	1.56	1.08
Nov	.77	1.66	.83	.94	1.04	1.59	1.11
Dec	.77	1.67	.84	.94	1.04	1.60	1.11
Jan 86	.79	1.69	.88	.97	1.08	1.62	1.13
Feb	.85	1.78	1.03	1.14	1.24	1.75	1.25*
Mar	.86	1.80	1.05	1.16	1.26	1.77	1.26
Apr	.81	1.73	.92	1.03	1.12	1.66	1.17
May	.83	1.76	.96	1.08	1.16	1.69	1.20
Jun	.81	1.75	.94	1.07	1.15	1.67	1.18
Jul	.83	1.77	.98	1.14	1.20	1.70	1.22
Aug	.76	1.67	.81	.96	1.03	1.57	1.10
Sep	.76	1.66	.80	.94	1.02	1.57	1.09
Oct	.76	1.66	.81	.91	1.01	1.56	1.09
Nov	.78	1.69	.84	.95	1.03	1.58	1.11
Dec	.78	1.69	.85	.96	1.05	1.60	1.12
Jan 87	.88	1.83	1.10	1.21	1.30	1.80	1.29*
Feb	.80	1.71	.91	1.01	1.11	1.65	1.16
Mar	.79	1.69	.87	.98	1.07	1.62	1.13
Apr	.77	1.68	.84	.94	1.04	1.59	1.11
May	.82	1.75	.95	1.07	1.15	1.68	1.19
Variation	.13	.19	.31	.31	.30	.24	.21
Fall in F	.13	.19	.31	.31	.30	.24	.21

* There is an apparent increase in F with residual shear strength consequent upon an increase in pore water salt concentration following major slope movements and from aerial salt deposition (see sections 5.323 and 6.223).

Table 6.19. Seasonal fluctuation in the factor of safety at Worbarrow Bay attributed to shear strength alone.

DATE	SLOPE UNITS						Global
	0	1	2	3	4	5	
Oct 85	.78	1.73	.84	1.00	1.03	1.57	1.12
Nov	.80	1.75	.88	1.04	1.07	1.60	1.15
Dec	.80	1.76	.89	1.05	1.08	1.61	1.15
Jan 86	.82	1.78	.94	1.10	1.13	1.65	1.19
Feb	.88	1.87	1.09	1.25	1.28	1.77	1.29*
Mar	.89	1.88	1.11	1.27	1.30	1.78	1.31
Apr	.84	1.80	.97	1.13	1.16	1.67	1.21
May	.85	1.82	1.00	1.16	1.20	1.70	1.23
Jun	.83	1.80	.96	1.13	1.16	1.67	1.21
Jul	.85	1.83	1.01	1.17	1.20	1.70	1.24
Aug	.78	1.72	.83	.99	1.03	1.57	1.12
Sep	.78	1.73	.84	1.00	1.04	1.57	1.12
Oct	.79	1.74	.86	1.02	1.05	1.58	1.13
Nov	.80	1.75	.88	1.04	1.08	1.60	1.15
Dec	.80	1.76	.89	1.05	1.09	1.59	1.16
Jan 87	.91	1.91	1.15	1.32	1.35	1.82	1.34*
Feb	.83	1.80	.96	1.12	1.16	1.66	1.20
Mar	.82	1.77	.92	1.08	1.12	1.63	1.18
Apr	.80	1.75	.88	1.04	1.08	1.61	1.15
May	.85	1.82	.99	1.16	1.19	1.68	1.23
Variation	.19	.19	.32	.33	.32	.25	.22
Fall in F	.19	.19	.32	.33	.32	.25	.22

* There is an apparent increase in F with residual shear strength consequent upon an increase in pore water salt concentration following major slope movements and from aerial salt deposition (see sections 5.323 and 6.223).

Table 6.20. Seasonal fluctuation in the factor of safety at Manor Lane attributed to pore water pressure and shear strength.

DATE	SLOPE UNITS										Global
	1A	1B	2A	2B	3A	3B	4A	4B	5A	6	
27.10.85	.97	1.37	1.24	1.25	.71	1.92	1.07	1.26	1.98	.63	1.11
24.11.85	1.00	1.43	1.29	1.32	.77	1.98	1.09	1.29	2.00	.65	1.14
22.12.85	1.00	1.44	1.31	1.33	.78	2.00	1.09	1.30	2.00	.66	1.15
17.01.86	1.03	1.50	1.37	1.41	.85	2.08	1.11	1.33	2.03	.68	1.19
15.02.86	1.12	1.69	1.56	1.67	1.09	2.33	1.19	1.47	2.15	.76	1.34*
15.03.86	1.13	1.71	1.58	1.70	1.12	2.36	1.20	1.48	2.17	.77	1.35
12.04.86	1.05	1.54	1.41	1.47	.91	2.14	1.13	1.37	2.08	.70	1.23
18.05.86	1.07	1.58	1.45	1.53	.96	2.20	1.16	1.40	2.13	.73	1.26
Variation	.16	.34	.34	.45	.41	.44	.13	.22	.19	.14	.24
Fall in F	.16	.34	.34	.45	.41	.44	.13	.22	.19	.14	.24

Table 6.21. Seasonal fluctuation in the factor of safety at Manor Lane attributed to shear strength alone.

DATE	SLOPE UNITS										Global
	1A	1B	2A	2B	3A	3B	4A	4B	5A	6	
27.10.85	.99	1.41	1.29	1.31	.74	1.96	1.11	1.28	2.06	.65	1.14
24.11.85	1.02	1.46	1.34	1.38	.81	2.03	1.13	1.32	2.08	.67	1.18
22.12.85	1.02	1.47	1.35	1.40	.82	2.05	1.14	1.32	2.09	.67	1.19
17.01.86	1.05	1.53	1.41	1.48	.90	2.12	1.16	1.36	2.12	.70	1.23
15.02.86	1.14	1.73	1.61	1.74	1.13	2.37	1.24	1.49	2.23	.77	1.37*
15.03.86	1.15	1.75	1.63	1.77	1.16	2.4	1.24	1.50	2.24	.78	1.38
12.04.86	1.07	1.57	1.45	1.53	.95	2.18	1.18	1.39	2.15	.71	1.26
18.05.86	1.09	1.62	1.50	1.59	1.00	2.23	1.19	1.42	2.17	.73	1.29
Variation	.16	.34	.34	.46	.42	.44	.13	.32	.16	.13	.24
Fall in F	.16	.34	.34	.46	.42	.44	.13	.32	.16	.13	.24

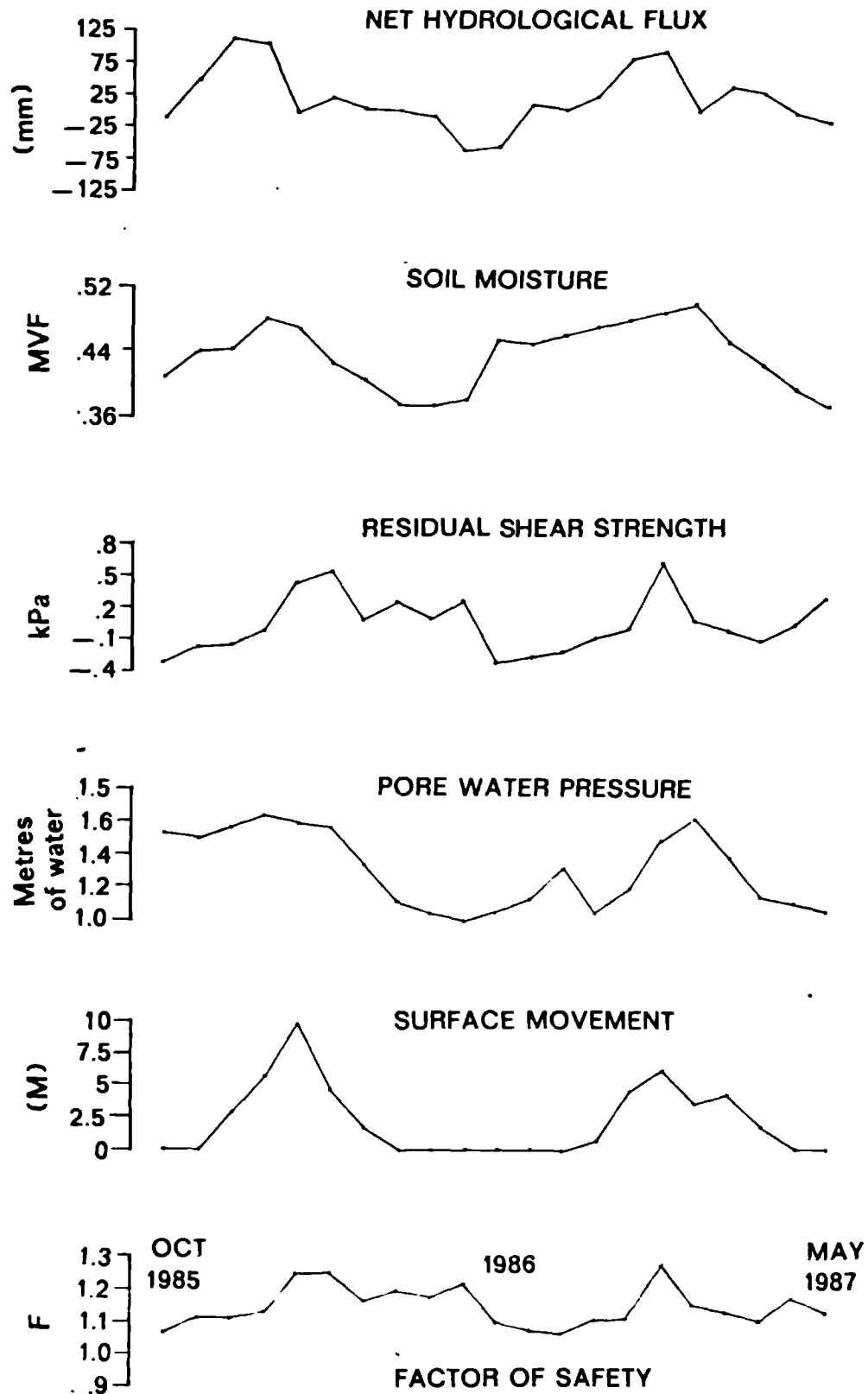
* There is an apparent increase in F with residual shear strength consequent upon an increase in pore water salt concentration following major slope movements and from aerial salt deposition (see sections 5.323 and 6.223).

the value of F suggest that the seasonal variations in strength can in theory and practice play a fundamental role in the seasonal behaviour of translational mudslides (Figure 6.8). Moreover, the shear strength of landslip clays was extremely sensitive to fluctuations in pore water chemistry (section 5.421).

As was found for pore water pressure in the previous section, a much higher degree of variation was found amongst the local factors of safety. With reference to Table 6.18 there was an observable reduction in F downslope from unit 5 to 0, although the central part of the accumulation lobe maintained a value of F above unity (≈ 1.69). In October the combined effects of pore water pressure and shear strength reduce F to below unity over two thirds of the mudslide and under such conditions failure must be imminent. In contrast only one sixth of the slope remained below $F = 1$ from January to March, which might offer an explanation for the cessation of movements by April or May each year, as a consequence of a gain in strength over the stresses promoting instability. A similar response may be recognised at Manor Lane (Table 6.20) where approximately 40 per cent of the slope shows $F < 1$ in October, whereas only 10 per cent remains below 1 in March. The greatest degree of variation (.33) was found in the source area and feeder track at Worbarrow, and similarly at Manor Lane (.45), where the majority of weathering, movement and particle disruption takes place.

That pore water pressures are responsible for triggering instability is demonstrated at Worbarrow, because if the reduction in shear strength was considered alone to trigger failure only 50 per cent (compared with 66%) of the slope was reduced to below 1, and similarly for Manor Lane where only 30 per cent (compared with 40%) of the local factors of safety were

Figure 6.8. Summary of parameters influencing the seasonal instability of mudslides at Worbarrow Bay.



noted below $F=1$. This would confirm the contention that the reduction in shear strength may be considered a primary cause of the seasonal re-activation of mudslide behaviour and that the trigger of failure or instability was the result of an increase in the intensity of climatic and ground water conditions. Ultimately the slope is very sensitive to variations in pore water pressures which control the mechanisms and pattern of movement described in section 5.33.

Because the model was sensitive to fluctuations in shear strength it was of interest to simulate the change in F caused by a reduction in the cohesive force in view of relating such behaviour to the mechanisms of seasonal instability. Thus, the 'static-model' cohesion term was reduced by increments of 10 per cent during the month of November where strength and pore water pressure conditions for failure have been shown to be most critical. The results for both sites are presented in Table 6.22. A high degree of correspondence between sites is noted, and it is found that a mere 10 per cent reduction in the measured cohesive force was required to reduce the global factor of safety to unity; $F = 0.99$ at Worbarrow and $F = 1.00$ at Manor Lane. Further reductions of 10 per cent caused a fall in $F = 0.7$.

At Worbarrow only a 10 per cent reduction in cohesion (or a mean fall of 0.38 kPa in residual strength) was needed to bring the local factors of safety below unity for over 66 per cent of the mudslide. At Manor Lane a reduction of 30 per cent (or a mean fall in strength of 0.77 kPa) was needed to reduce F below unity for over 70 per cent of the slope. These small changes in strength demonstrate the sensitivity of the cohesion parameter within the model, suggesting that the progressive loss of

Table 6.22. Simulated effect of a reduction in cohesion with pore water pressures upon the stability of mudslides.

Site 1. Worbarrow Bay (November 1986).

REDUCTION %	SLOPE UNITS						Global
	0	1	2	3	4	5	
0	.79	1.70	.89	1.00	1.10	1.64	1.15
10	.70	1.55	.73	.83	.91	1.41	.99
20	.66	1.46	.68	.77	.83	1.27	.92
30	.61	1.37	.63	.70	.76	1.13	.84
40	.57	1.28	.57	.63	.68	1.00	.77
50	.52	1.19	.52	.57	.60	.86	.69
60	.48	1.10	.46	.50	.53	.72	.61
70	.43	1.01	.41	.44	.45	.59	.54
80	.39	.92	.36	.37	.37	.45	.46
100	.30	.74	.25	.24	.22	.18	.31
Variation	.49	.96	.64	.76	.88	1.46	.84

Site 2. Manor Lane (24th November 1985).

REDUCTION %	SLOPE UNITS										Global
	1A	1B	2A	2B	3A	3B	4A	4B	5A	6	
0	1.03	1.50	1.37	1.42	.86	2.08	1.11	1.34	2.04	.68	1.20
10	.92	1.23	1.15	1.14	.66	1.72	.92	1.14	1.66	.53	1.00
20	.88	1.15	1.06	1.06	.62	1.55	.85	1.05	1.50	.50	.93
30	.84	1.06	.98	.97	.57	1.38	.78	.95	1.34	.48	.86
40	.80	.97	.90	.88	.52	1.22	.70	.86	1.18	.45	.79
50	.76	.89	.82	.80	.48	1.05	.63	.76	1.02	.42	.72
60	.72	.80	.74	.71	.43	.88	.56	.67	.86	.39	.65
70	.68	.71	.65	.63	.38	.71	.49	.57	.70	.36	.58
80	.64	.62	.57	.54	.33	.54	.42	.47	.54	.34	.51
100	.57	.44	.41	.37	.24	.21	.27	.28	.22	.28	.37
Variation	.46	1.06	.96	1.05	.62	1.87	.84	1.06	1.82	.40	.83

cohesive force at the shear surface could be a fundamental, but generally ignored, causal process of mudslide behaviour.

Most importantly, this observation explains the prevalence of the 'multiple' stick-slip mechanism of movements before subsequent surge behaviour, since the cohesive bonds developed over the summer months are gradually weakened (chemically and physically) until the whole slide is mobilised and under such conditions cohesion may correctly be considered to be zero. The intensity and frequency of movements are controlled by pore water pressures in the source unit, albeit at lower intensities than are involved in the initial reactivation of the slide (Figure 5.31). The mechanisms of movement appeared to correspond with the value of F such that multiple displacements occur when $F \approx 1$, surge movements $F \approx 0.4$, and graded movements may be considered intermediary.

The model also explains why movements are abated following a reduction in the intensity of pore water pressures through drainage and the regain of strength. Movements are interspaced with periods of no displacement (section 5.33; Figure 5.27) such that in April cohesive bonds are able to reform across the shear surface in time, the process being enhanced by an increase in pore water salt concentration and the deposition of salts. Chemically bonds may be formed and weakened, but not broken, such that other stresses are required to bring about their physical destruction. The resultant increase in strength or cohesion of the mudslide materials will increase F and in doing so the mechanism of movement will change, such as from surge to graded displacements for example, although cohesion is lost once-more during movement events. Eventually, the less intense pore water pressures are unable to trigger movements of the mudslide because the resistance to shear is greater than the driving force, and

movements are abated until the strength of the material reduces once more the following season.

6.433 Undrained loading.

The stability model so far has only been discussed in terms of shear strength and pore water pressures. These have shown that under field conditions the global factor of safety was reduced to 1.11 and 1.08 for Manor Lane and Worbarrow, respectively. Although the conditions of slope stability are nearly-critical these values would in theory suggest that stability should prevail and that another factor must be involved in the initial triggering of major movements.

A very important, but as yet undiscussed factor is the role of undrained loading in promoting shallow mudsliding (Hutchinson and Bhandari 1971; section 1.4). Undrained loading occurs as a result of inputs of soil and rock debris and ground water such that the dimensions and pressure regimes are altered, most typically in the source unit, although it is possible to have secondary zones of loading within a cascading mudslide system.

In section 5.212 photogrammetric analyses revealed quite substantial alterations to the dimensions and volume of material in the source unit at Worbarrow Bay, the measurements of which may be used in the stability model of the site to demonstrate the role of undrained loading in promoting mudsliding. It is assumed that this loading either occurred during the critical months preceding reactivation or during November when other variables showed the stability of the slope to be most critical. During this period the mudslide source unit extended inland

TABLE 6.23. Reduction in F with the inclusion of undrained loading in November 1986
with measured pore water pressures and shear strength at Worbarrow Bay.

Model 7 : Computed factor of safety with simulated loading and unloading of the mudslide.

STRENGTH		SLICE ANGLE		MUDSLIDE DEPTH AND UNIT WEIGHT				PWP		FACTOR OF SAFETY			
c'	phi	b	deg	z1	g1	z2	g2	z3	g3	p	top	bot	cos(a)
2.55	7.86	12.00	23.60	.32	14.39	.29	13.14	.45	15.62	1.05	.55.29	74.20	.92
3.31	10.38	7.25	12.80	.30	13.80	.32	15.43	.58	13.93	.96	45.06	27.56	.98
1.58	5.73	7.25	19.30	.26	14.18	.23	13.61	.21	12.03	.87	17.65	22.39	.94
2.02	12.50	5.75	33.80	.10	12.61	.22	14.06	.17	13.26	.77	18.96	21.14	.83
2.50	7.38	6.25	26.60	.37	14.51	.17	15.39	.28	11.20	.68	24.56	31.12	.89
4.95	6.85	14.76	31.30	.55	14.39	.25	10.81	.28	11.86	.59	105.81	106.87	.85

Global factor of safety = .94

Local factor of safety =

		slice	1.00
.75			2.00
1.64			3.00
.79			4.00
.90			5.00
.79			6.00
.99			

by 4.76 metres increasing the slice dimension of unit 5 to 14.76 m, and the volume (depth) by a maximum of 0.61 m. The change in volume was noted to affect both units 5 and 4 corresponding to an average increase in depth of 0.50 and 0.21 m, respectively.

When these values were applied to the stability model (Table 6.23) the global factor of safety revealed that undrained loading, in combination with shear strength and pore water pressures are responsible for reducing F below unity (0.94) predisposing the mudslide to major failure under such conditions. Thus, in November the whole slope was unstable except for the central portion of the accumulation lobe which maintained a relatively high value of $F = 1.64$. That the stability of the slope should be considered a response of a number of processes is demonstrated below in Table 6.24, because like the previous variables, undrained loading alone is not sufficient to reduce F below unity. However, the results demonstrate the sensitivity of the model to loading in the source areas, and would add considerable support to the principle of undrained loading as a precursor to the seasonal reactivation of mudslides.

Table 6.24. The effect of undrained loading and other variables on the stability of the Worbarrow mudslide in November 1986.

VARIABLES	SLOPE UNITS						
	0	1	2	3	4	5	Global
Standard	.82	1.79	.94	1.10	1.13	1.65	1.19
U.Loading	.82	1.79	.94	1.10	.90	1.05	1.04
UL + PWP	.80	1.72	.90	1.01	.87	1.04	1.01
UL+PWP+SS	.75	1.64	.79	.90	.80	.99	.94

UL = Undrained loading PWP = Pore water pressure SS = Shear strength

6.5 Conclusions.

This chapter has demonstrated that residual strength should not be considered a static property and that variations in its spatial and temporal character are fundamentally related to the stability of slopes and the behaviour of mudslides. Correlations of the static properties show that the best associations with the residual strength parameters were found with the chemistry of the soil and pore water solution. The proportion of clay (in excess of 30%) showed poor correlations with the distribution of shear strength although strongly related to the phase relationships, plasticity and density. The unit weight showed a strong relationship with strength at both sites of varying lithology suggesting that the progressive orientation and compaction of materials maybe partly responsible for the reduction in residual shear strength within mudslides and the self-preservation of mudsliding.

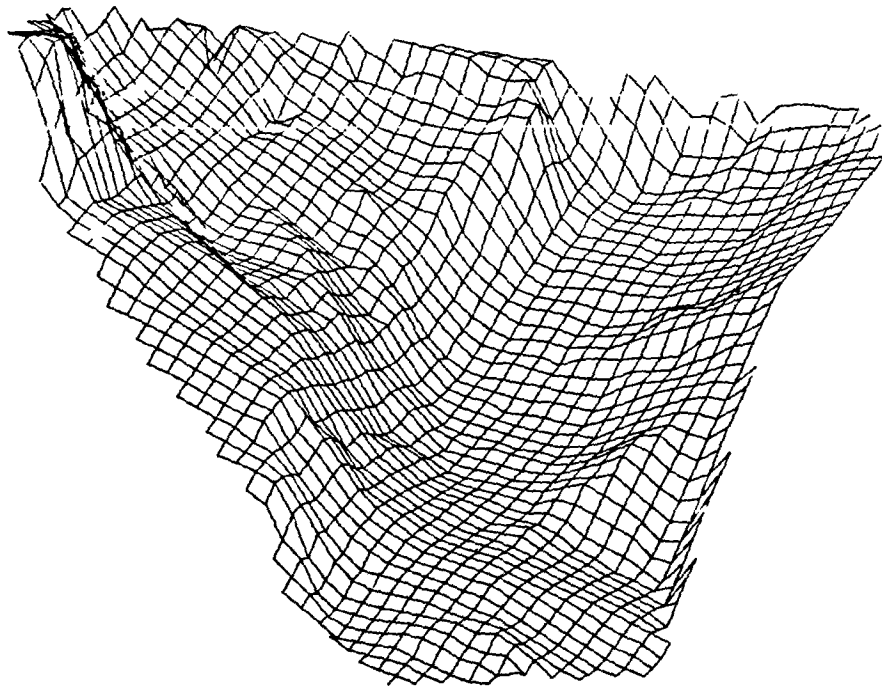
The strongest associations were, however, found with the solubility and concentration of cations associated with mineral hydration shells and the interstitial pore water. The development of diffuse ionic double layers upon weathering were considered to cause the reduction in residual shear strength downslope. Such ideas were supported by geochemical modelling of the aqueous and mineral phases and the identification of preferred weathering reaction paths. Seasonal fluctuations in pore water chemistry were found to have quite considerable effects upon weathering processes, where only 2-5 per cent changes in pore water salt content were required for a mineral to precipitate from a formerly unstable condition.

The nature of physico-chemical interactions of landslides ^{has been} ~~were~~ described and related to the seasonal instability of each mudslide. Correlations between the dynamic parameters showed very strong relationships between effective rainfall and the soil water relations. The latter were even more significantly associated with the movement of the Worbarrow mudslide. When the continuous data-set was used in correlation short time-lags of several days were identified between the effective rainfall, soil moisture and the pore water pressure in the source unit. Pulses of pressure decreasing in magnitude were recognised for up to 4 days following rainfall, with a corresponding increase in pressures in the lobe for several days as undrained loading of the lower slopes and accumulation lobe took place.

Such mechanisms were shown in the stability analysis to be primarily responsible for triggering slope movements. However, alone they were found to be insufficient to cause global instability, even with simulated increases in undrained loading. Only when considered with the seasonal variations in residual shear strength were realistic factors of safety obtained in relation to observed behaviour. Three mechanisms of movement were considered to reflect the strength and type of inter-particle bonding, such that surge movements were associated with zero cohesion, multiple stick-slip movements with strong primary ionic bonds, and graded movements were intermediary. The findings are supported by theoretical and experimental considerations and as such improve our understanding of mudslide behaviour.

Chapter Seven

CONCLUSIONS



7.1 Original contribution to the study of mass movement.

The findings of this thesis have shown the properties of clay soils to be fundamental to mudslide processes and that these may not be assumed to be either temporally or spatially static. Although previous work recognises this concept few have attempted to measure and apply clay mineralogy, solute geochemistry and soil variability as important factors in mudslide behaviour. This thesis provides the first comprehensive study of both the properties and seasonal behaviour of coastal mudslides in relation to physico-chemical and weathering processes.

The original contribution to the study of mass movement is reflected in the multi-disciplinary methodology (section 1.1), since this work includes aspects of geomorphology, geology, engineering geology, soil mechanics, geochemistry, pedology and surveying. This was necessary because researchers have recently shown an increased awareness of clay properties in studies of soil deformation. Thus, this thesis combines knowledge from all these fields to assess the role of soil properties upon the instability of mudslides.

The objectives of the study were derived from two reviews: mass movement (Chapter One) and the physico-chemical properties of landslip clays (Chapter Two). They are outlined in section 2.5, and may broadly be divided into two sections entitled the 'static' properties, and the 'dynamic' behaviour of mudslides. Using the methodology outlined in Chapter Three, results are presented for each of these models, the static analysis in Chapter Four and the dynamic analysis in Chapter Five. The results are discussed and modelled in Chapter Six with respect to pore water chemistry and the seasonal instability of slopes using standard

procedures so that the findings of this work may be readily assessed. The conclusions of the working hypotheses form an original contribution to knowledge. These are briefly summarized below (section 7.1) and outlined in greater detail in the Epilogue (section 7.3) to which cross-reference should be made. The findings are related to associated literature (section 7.1) before suggesting recommendations for further research (section 7.2) with respect to the findings of this work.

This thesis makes the following original contributions to the study of mass movement:

1. it demonstrates a broad regional association between the mineralogy of sediments and landslide distribution in southern and south-east England (see section 7.31);
2. it establishes a clear association between the spatial variability of physico-chemical properties and landslide distribution within the London Clay Basin (section 7.31);
3. it conclusively showed that the weathered mantle of the translational mudslides considered by this study contained far greater proportions of montmorillonite clay minerals than found beneath the basal shear surface and for undisturbed sediments of two contrasting lithologies, the London and Wealden Clays (section 7.32);
4. it establishes the importance of the spatial variability of the physico-chemical properties in association with weathering processes and the characteristic morphological units of mudslides: the influence of physical and chemical properties were related to the mineralogy and shear strength characteristics of each site (section 7.32);

5. it demonstrates that a change from an over-consolidated to a normally-consolidated condition is not only important from a geotechnical point of view, but a fundamental reason for the chemical activity of the weathered mantle (section 7.32);
6. it shows that although monovalent sodium ions are progressively adsorbed onto the exchange sites of clays, the fundamental reason for the chemical instability of the materials was due to an apparent dilution of salts on the exchanger. This was found to have important implications for both the spatial and temporal instability of the study sites (section 7.32):
 - (a) Spatial. There was an increase in the solubility of ions within the mudslides which was considered to represent an increase in double layer activity downslope and a consequent reduction in the strength of bonding between particles.
 - (b) Temporal. The seasonal instability of mudslides was directly related to a reduction in pore water salt concentration and thus a net dilution of the base cations associated with the exchanger of clays, and a reduction in shear strength due to an increase in double layer activity.
7. laboratory simulation tests conclusively showed that residual strength was dependent on the type and quantity of clay minerals and associated pore water cations. For montmorillonite clays in excess of 30 per cent, residual strength was lowest for Na-montmorillonite exchanged clay, increasing in strength linearly with salt concentration (section 7.35).
8. laboratory simulation tests also showed that the residual strength of natural samples of London and Wealden Clay was dependent on the weathered state of the materials: residual strength was lowest for fully weathered clays. The residual strength of both weathered and unweathered samples increased linearly with an increase in pore water salt concentration.

9. analytical results were used in geochemical models of the stability of clay minerals and showed that the mudslide matrix contained high proportions of amorphous materials and 2:1 layered clays. The influence of dilution and the addition of sea-salts was found to be a very sensitive function of pore water concentration; a change in concentration of several per cent resulted in the dissolution of clay minerals from formerly stable conditions. The natural range of concentrations monitored in the field were potentially the most unstable, a decrease in salt content promoting the dispersion of clays, while an increase in sea-water intrusion, or rise in concentration, caused the flocculation of clay particles (section 7.33).
10. the spatial and temporal distributions of soil-water chemistry in combination with laboratory simulation tests demonstrated:
 - (a) a reduction in residual strength downslope associated with the degradation of bonds between clay particles in each mudslide and preceding the reactivation of seasonal slope instability (section 7.34).
 - (b) an increase in residual shear strength and pore water salt concentration following slope movements and aerial salt deposition during the winter months (section 7.35).
11. field-monitoring demonstrated that the dynamics of mudslide behaviour were intrinsically related to weather and climatic conditions (section 7.35). Fluctuations in soil moisture and pore water pressures were distinctly related to the net-hydrological flux. Time-lags of several days were identified between initial weather events and the response in the Worbarrow source unit. Pore water pressures showed quick response times, but soil moisture changed more slowly and uniformly in time.
12. non-contact photogrammetric monitoring showed an overall recession of the mudslide rear-scarp of 1.38 m, although the extent of the source unit varied by as much as 4.76 m (section 7.35). The lateral shear surfaces were confined by underlying bedrock, and only showed minor realignment, although most changes in morphology were considered to be in dynamic equilibrium. A DTM of difference

isolated areas of significant volume changes; skew profiles showed an increase in volume of upto 0.6m in the source and a depletion at the base of the feeder track of 0.9m. These findings demonstrated the influence of undrained loading when incorporated in stability analyses of the site.

13. slope movements varied from small edge displacements of 4 m to a maximum body displacement of 26 m for the 1985/86 season (section 7.35). Displacements were not spatially uniform although a central plug was characterised by equivalent movements on either side.
14. three mechanisms of movement were recognised (section 7.35): a low intensity 'multiple' stick-slip type movement, a medium intensity 'graded' movement, and a low frequency high intensity 'surge'. Each mechanism was found to be associated with the intensity of pore water pressures and prevailing physico-chemical conditions (see points 6 and 10):
 - (a) low intensity (<10 cm) multiple movements were limited to independent displacements of one or two centimetres per hour, and did not show any clear relationship with pore water pressure.
 - (b) graded displacements involved movements of upto 10 cm per hour and were associated with a rise in pore water pressure equivalent to 5 kPa.
 - (c) surge displacements of upto one metre in 10 minutes coincided with pore water pressure changes of upto 10 kPa.
15. stability analyses demonstrated that the pore water pressures measured at Worbarrow and Manor Lane were insufficient to promote slope instability (section 7.35). A reduction in the factor of safety below unity did not occur. Seasonal reactivation at Worbarrow was controlled by several factors, and occurred following a reduction in shear strength and increases in the stresses promoting instability, such as pore water pressure and undrained loading:

16. temporal changes in shear strength were calibrated against laboratory findings and applied to the cohesion term (section 7.35). Although this parameter represented an actual change in shear strength, and not friction or cohesion (the test procedure was unable to differentiate between the parameters except as an assumed value on the Mohr envelope), in reality such changes represented both the degradation of cohesion between particles and a reduction in the influence of friction.
17. the chemical hypothesis also provided an explanation for the mechanisms of movement; surge displacements were associated with zero cohesion and values of $F \approx 0.5$, multiple stick-slip movements with strong primary ionic bonding with values of F above unity, and graded movements intermediary and associated with double layers and relatively weak bonding.
18. an increase in pore water concentration, and thus shear strength, following major weathering and movement events was considered an important factor in promoting the cessation of movement in late March. At this time diagenetic bonds re-develop, due to favourable and more concentrated chemical conditions. This also occurs during periods of no movement. Subsequently, pore water pressures were falling and unable to trigger slope movements. Over the summer months the pore water becomes progressively more dilute because salt deposition is low and ions are not released by movement or induced by weathering, and the primary ionic bonds between particles are weakened and become potentially unstable. An increase in pore water pressure in the winter months exerts a stress in excess of the bond strength; initially small stick-slip movements coincide with gradual bond-breaking along shear surfaces. Eventually, the whole slope is supported by few bonds (\approx zero cohesion) and cataclysmic surge behaviour results.

In relation to the literature, this work contains two detailed reviews to demonstrate the importance of clay and soil physico-chemical processes upon the stability of mudslide materials. This was supported by well established findings of clay research (Van Olphen 1986, Grim 1959, Dixon

and Weed 1977, Yariv and Cross 1979), geochemistry (Garrells and Christ 1965, Lerman 1979, Drever 1982, Krauskopf 1967) and soil science (White 1979, Bear 1964, Brady 1984). It was also noted that many soil mechanics texts (Mitchell 1976, Lambe and Whitman 1969, Craig 1983, Das 1985) consider such properties as important.

The work was also supported by geomorphological literature, notably Yatsu 1966 and 1967, Rosenqvist 1984, Anderson *et al* 1969, Prior and Ho 1970, and Prior 1977, but although these works provide examples where the properties of clay were considered to have influenced the distribution or behaviour of mudslides, no research has been undertaken to directly assess these relationships. The findings of this thesis attempt to bridge this gap in knowledge.

The need for this research was recognised by Brunsden (1984) after Craig (1979) had refuted some findings of Prior *et al* (1971) in associating clay mineralogy with movement rates. McConchie (1986) has since attempted to relate the spatial variability in physical and chemical properties of soil for an 'earth-slide' in New Zealand. The successes of chemical soil stabilization methods (Sherwood 1961, Ingles 1968 and 1970, Handy and Williams 1966, Broms 1984, Arora and Scott 1974, Mearns 1973) suggests that the materials contained within shallow translational mudslides are particularly sensitive to chemical treatments which are designed to improve the physical condition of soils. Thus the reviews add considerable support to the physico-chemical hypothesis of mudslide behaviour. The overall conclusion opens up vital new avenues for applied geomorphology because it should now be possible to base chemical treatments on a detailed understanding of both the chemical and physical parameters in the mass movement system.

7.2 Suggestions for future research.

The findings of this thesis suggests that attention should be given in the following areas to further develop our understanding of the spatial and temporal behaviour of mass movements:

1. further consideration should be given to the distribution of landslides and the mineralogy of associated clays;
2. a comparative thorough investigation of soil properties and landslide generation in non-coastal locations to complement the work of this thesis;
3. the development of monitoring, laboratory and modelling techniques to assess the relevant chemical forces (i.e. the quantitative determination and measurement of cohesion) for application in stability equations;
4. a reconsideration of the Mohr-Coulomb strength equation to provide unbiased applications of the chemical factors associated with slope instability;
5. the development of laboratory methods to improve the simulation of the chemical effects on peak and residual shear strength, especially at low effective stresses for the latter;
6. the application of the theoretical considerations of this thesis to the chemical stabilization of shallow landslides;
7. the application and development of analytical photogrammetry to monitoring large landslides;
8. the development of a photogrammetric-geotechnical data-base for the non-contact monitoring of large landslides;

7.3 Epilogue.

7.31 Regional associations between landslides and clay mineralogy.

A regional survey of the density of landslides and the clay mineralogy of different geological formations was collated from literature sources (section 4.61). Although the surveys have several limitations (p412) a number of conclusions could be made. Apart from the Lias formation, the Cretaceous and Tertiary Beds possess the greatest density of landslides in southern and south-east England, with an apparent decrease in susceptibility with age (section 4.61). The same may be said of the number of translational and unclassified types of landslides for which the London Clay had the greatest association, both for reasons of its susceptibility to mass movement, and probably as a result of the biased research interests shown in this deposit. Both corresponded with an increase in the proportion of 2:1 layered micaceous clay minerals and a relative decrease in the proportion of montmorillonite. It might have been expected from such evidence that landsliding may have been more frequent in past geological environments due to higher montmorillonite clay contents.

When landslides only originating over the last century were considered, the greatest densities of mass movement were related to an increase in the proportion of micaceous clays from 30 to 50 per cent, and a modal proportion of montmorillonite of about 40 per cent. Thus, given the incompleteness of our knowledge of both the distribution of landslides and the clay mineralogy of British sediments, the greatest densities of landslides were found on geological formations containing up to 50 per cent mica/illite clay minerals and 40 per cent montmorillonite. The

dominance of 2:1 sheet minerals were found to have important effects upon weathering and soil deformation processes (section 2.22 and 2.32).

A further survey was conducted to assess the relationship between lithological variation and the distribution of landslides within the London Clay Basin, also from literature sources (section 4.62). The results showed that an increase in the total number of landslides coincided with an increase in clay content from 50 to 74 per cent, and the proportion of montmorillonite clay minerals from 10 to 35 per cent. Towards the coastal fringe the montmorillonite content of weathered mudslide materials was found to be as high as 63 per cent of the clay fraction, averaging 42 per cent at Warden Point. The proportion of micaceous and montmorillonite clays measured on-site was equivalent to that expected for the deposit from the regional survey which suggested that the London Clay was inherently susceptible to landsliding towards the eastern coastline. In addition calcium cations found in undisturbed sediments were exchanged for magnesium ions following weathering and erosion of the coastal cliffs. Ion-exchange of this form was found to promote the instability of the clay materials (sections 2.31, 2.232 and 4.43).

7.32 The spatial variability of physico-chemical properties.

The physico-chemical variability of soil properties was assessed for two mudslides of contrasting lithology based on the findings of the regional survey. These included the London Clay at Manor Lane and the Wealden Beds at Worbarrow Bay (section 3.23). At each site a series of core samples were obtained for laboratory analysis (section 3.31). The number and series of soil tests undertaken are described in section 3.4, the

results of which were used to establish the spatial variability of soil properties with respect to weathering and the morphology of mudslides.

The distribution of clay minerals within and surrounding each mudslide was examined (section 4.46). At Manor Lane there was a greater proportion of montmorillonite clay minerals in the surface layers of undisturbed sediments and weathered mudslide materials, decreasing with depth in the surface weathered horizons by as much as 15.2 per cent. A distinctive reduction across the basal shear surface was particularly prevalent. Upon movement downslope the proportion of montmorillonite decreased by up to 18 per cent and there was a corresponding increase in mica/illite clay minerals. The findings suggested that the surface horizons of the London Clay were very susceptible to mass movement due to a relatively high proportion of montmorillonite clay minerals.

At Worbarrow Bay, there was an increase in the proportion of montmorillonite upon erosion, weathering and inclusion into the mudslide. The Wealden Beds were similarly susceptible to mass movement when compared with Manor Lane because of the considerable inter-stratification between the beds of clay, sandstone and other sediments (section 3.232). The *in situ* results showed a greater proportion of montmorillonite clay minerals above the shear surface, decreasing with depth as for the London Clay. This was especially marked in the source areas of the mudslide where there was a 35.2 per cent reduction in montmorillonite below the shear surface. Thus, as for the London Clay, the materials contained within the moving mudslide are mineralogically more unstable than beneath the shear surface because they contain greater proportions of montmorillonite clay minerals.

Of the particle characteristics of the two mudslides the proportion of clay was found to increase with depth, especially across the shear surface. The association with morphology was also quite distinct showing an increase upon erosion and weathering and a sharp but uniform reduction of 5 per cent downslope at Manor Lane and 11 per cent at Worbarrow Bay (section 4.23).

Similarly with the moisture relations of both sites. At Worbarrow an increase in natural soil moisture of 6 per cent was measured following the disturbance of *in situ* materials. A larger increase of 10 per cent was found at Manor Lane (section 4.241) which was thought to arise from the greater proportion of fines within the London Clay in comparison with the more heterogeneous Wealden Beds. Both sites showed an increase of approximately 10 per cent in natural soil moisture downslope of the source areas. Thus, weathering and mudslide processes accounted for an increase in soil moisture of around 20 per cent above *in situ* levels. In addition the saturated moisture content was found to decrease downslope by upto 5 per cent at Worbarrow and 30 per cent at Manor Lane, suggesting that the materials became progressively more susceptible to saturation.

The phase relationships revealed a high degree of inter-dependence (section 4.242), as might be expected. The specific gravity averaged 2.65 at both sites, which was less than the theoretical value of 2.7 for clay soils (section 2.24). Differences between the sites were found with the void ratio (2.09) and porosity (0.68) at Manor Lane in comparison with (1.51 and 0.59) Worbarrow. The void ratio and porosity increased with depth except below the shear surface where they decreased in value. Within the mudslides the void ratio also decreased downslope

by 0.2 at Manor Lane and 1.3 at Worbarrow, and because the porosity was dependent on the void ratio similar distributions were obtained for this parameter.

The unit weight or particle density was inversely related to both the void ratio and porosity (section 4.243). At both sites the surface layers were found to be more dense than the material immediately below, which was most likely the result of surface crusting. There was also a uniform increase in unit weight with depth, particularly across the shear surface, where a two-fold increase from 12 to 24 kN/m² was measured at both sites. There was also an increase in the unit weight and bulk density downslope at the shear surface amounting to 1.5 kN/m² at Manor Lane and 6.5 kN/m² at Worbarrow, in contrast with the void ratio and mean bulk density which decreased on the lower slopes. This finding demonstrated the independence of shear surfaces within mudslides, where it should be realised that in any study of soil deformation or mudslide behaviour they should receive careful investigation. Once formed shear surfaces self-generate mudsliding across highly orientated, densely packed slickensided surfaces.

The London Clay was found to exhibit greater plasticity than the Wealden Beds with mean values of the plasticity index equal to 40.3 and 35.7 per cent, respectively (section 4.31). The corresponding Atterberg limits were 65.5 and 52.3 for the liquid limit, and 25.2 and 16.6 per cent for the plastic limit. The presence of fine sands at Worbarrow was considered to result in the lower plastic and liquid limits, suggesting that the Wealden Beds were inherently more susceptible to liquefaction. Upon erosion and weathering there was a 10 per cent increase in the liquid limit at Worbarrow in contrast to a 10 per cent reduction at Manor

Lane. Because the phase relationships could not account for this difference it was considered that the increase in montmorillonite clay content at Worbarrow caused an increase in the liquid limit in contrast to the reduction in montmorillonite at Manor Lane. Owing to the presence of fine sand and lower plasticity, the activity ratio at Worbarrow (0.72) was less than Manor Lane (1.28). There was, however, an apparent increase upon weathering and translation at Worbarrow, except for low values of activity for undisturbed and source unit materials. Similarly for Manor Lane although the *in situ* material had a relatively high activity.

The chemical characteristics of the soil from each site varied considerably, as indicated by the pH (section 4.411), which was neutral or alkaline at Manor Lane (7.29) but slightly acidic at Worbarrow (5.69). At both sites the pH remained relatively constant although there was a tendency for alkaline conditions to develop with depth, whereas upon weathering or movement at Worbarrow the pH dropped an equivalent of 1.6 about midslope but attained its original value upon deposition in the lobe. Such associations were also recognised at Manor Lane although the fluctuations were less marked (0.4 pH), confirming the tendency for acidic conditions to develop from the translation and weathering of materials in mudslides.

The conductivity of the soil solution increased with depth at both sites and was found to decrease downslope. This was reflected by the spatial distribution of the means and values measured directly at the shear surface. The variations were relatively large at Manor Lane (4 mS/cm) in comparison with Worbarrow Bay (0.18 mS/cm). The differences suggested that the pore water at Manor Lane was more susceptible to large changes

in electrolyte salt content, whereas at Worbarrow the pore water remained relatively dilute throughout the system. The pH and conductivity were correlated with the density of the materials at both sites (section 6.212); it was found that the tendency for over-consolidated clays to develop a normally-consolidated condition upon weathering was not only important from the physical point of view, but also a fundamental cause of the chemical activity of the system.

There was relatively little organic matter at both sites with 2.8 per cent at Manor Lane and 2.0 per cent at Worbarrow (section 4.412). The difference between these and the respective loss-on-ignition results of 9.3 and 6.5 per cent, represented the amount of bonded water on particle surfaces. An increase in the LOI with depth was measured at both sites as well as a decrease downslope of 1.5 per cent at Manor Lane and 3.2 per cent at Worbarrow.

The mean cation exchange capacity at Manor Lane was 60 meq/100g in comparison with 50 meq/100g at Worbarrow (section 4.43). Both confirmed the influence of the 2:1 layered clay minerals. Although montmorillonite was more common at Worbarrow the contribution of illite and mica clays at Manor Lane to the exchange capacity was greater than the kaolinite minerals found at the former site. The results are variable for both mudslides but tend to show an increase in CEC at the surface upon weathering and erosion, a decrease below the shear surface, and a reduction downslope at Manor Lane in contrast to an increase on the lower slopes at Worbarrow. The distribution corresponds with the clay mineralogy at each site.

The concentration of exchangeable cations were found to be relatively constant for both *in situ* and mudslipped materials (section 4.422). At Manor Lane there was a tendency for an increase in exchangeable cations with depth and a reduction downslope of 0.1 g/l. At Worbarrow there was an increase in exchangeable salts at the surface upon weathering and a further increase downslope equivalent to 0.25 g/l. These differences were thought to reflect the saturated condition of the exchange sites of the materials, giving rise to an increase in exchangeable cations associated with weathered Wealden Clay, particularly with sodium, in contrast to a relative reduction in salt concentration of weathered London Clay.

The exchange reactions were described by several indices in section 4.43. They contrast to a large extent between sites because of chemical differences such as the concentration and valency of ions. The mean per cent base saturation at Manor Lane was 67.9% in comparison with 77.6% at Worbarrow. These values decreased with depth at the former site but increased with depth at the latter. Following weathering and erosion in the source areas a dramatic decrease from 95 to 52 per cent occurred in the feeder track at Manor Lane resulting in the lower mean value, whereas there was a gradual increase in exchangeable base cations to 88 per cent at Worbarrow. The latter was due to an increase in the sodium adsorption ratio from 0.9 to 2.34 in comparison with 0.5 to 1.0 at Manor Lane. The former level of adsorbed sodium could be considered sufficient to cause the deflocculation or dispersion of clay soils. The exchangeable sodium percentage was found to increase downslope from 12 to 25 per cent at Worbarrow and 6 to 10 per cent at Manor Lane. At Manor Lane, however, there was a greater exchange of magnesium for calcium than sodium ions. These exchange reactions supported the contention that the materials

become progressively more susceptible to liquefaction and dispersion following weathering and mudslide processes, and the adsorption of sodium, and demonstrates why the Wealden Beds may experience considerable chemical weathering and dispersion in coastal environments.

At Manor Lane the concentration of salts in the interstitial pore water was much greater (8.19 g/litre) than found at Worbarrow (2.68 g/l). The salt content of groundwater entering the mudslide was less than the pore water with recorded concentrations of 1.25 g/l and 1.65 g/l, respectively (section 4.421). The dominant types of salt vary for both sites, with divalent magnesium and calcium sulphates predominating at Manor Lane and monovalent sodium chloride at Worbarrow. Upon erosion and weathering there was a sharp increase in salt content in the upper slope units at both sites which decreased following deposition on the lower slopes and accumulation lobe at Manor Lane and Worbarrow, respectively. The release of salts through weathering accounts for a three fold increase in concentration in relation to *in situ* conditions with maximum values recorded in the translational zone. Differences were noted in the concentration of iron at both sites with an accumulation on the lower slopes at Manor Lane in contrast to a reduction at Worbarrow. The results confirm that the London Clay was highly saturated with divalent salts whereas at Worbarrow the Wealden Beds are unsaturated with monovalent salts.

The concentration of soluble salts or ions loosely bound to particle surfaces and diffuse double layers (section 4.422), was similarly ~~more~~ *greater* at Manor Lane (0.81 g/l) than at Worbarrow (0.23 g/l). These values are six times more concentrated than for *in situ* conditions suggesting that the processes of mudsliding and weathering causes an

increase in the solubility of salts associated with diffuse double layers and a corresponding reduction in the bonding strength within and between clay particles. There was generally an accumulation of soluble salts with depth reaching a maximum at the shear surface, with a sharp reduction within *in situ* materials below. An exception to this trend was noted for the source areas where high concentrations were found below the basal shear surface. This was thought to reflect a greater degree of chemical instability in the materials of the source areas. Both sites show an increase in concentration of soluble salts with the weathering and movement of material downslope with a resultant increase in double layer activity.

7.33 Effects of weathering.

The chemical structure of the clay minerals was found to remain relatively constant at both sites except for an increase in iron oxide on the lower slopes (section 4.44). This was confirmed by modelling aqueous phase equilibria using WATEQF and PHREEQE to quantify weathering reaction paths (section 6.3). The dominance of iron and aluminium amorphous oxides was recognised in relation to the clay mineralogy previously discussed.

The influence of sea-salts upon the stability of the clay minerals revealed that the natural ionic strength of the pore water was equivalent to 4-8 per cent sea-water at Worbarrow, and 10-20 per cent at Manor Lane (section 6.311). An increase or decrease in ionic strength above or below these limits represented an addition or dilution of salts in the pore water, respectively. A dilution was found to encourage the formation of magnesium-saturated montmorillonite at Manor Lane, but when the sea-water concentration was greater than the range specified the mineral was

unstable and dissolved (section 6.312). A corresponding increase in the precipitation of soil mica was found. This provided a reason for the reduction in montmorillonite downslope at Manor Lane, because the effective sea-water concentration increased towards the high water mark. At Worbarrow an increase in sea-water concentration caused the precipitation of sodium-montmorillonite downslope confirming the clay distributions previously found. Kaolinite was precipitated throughout the range of sea-water concentrations in contrast to the dissolution of divalent forms of montmorillonite and other minerals. The stability of the clay minerals at both sites was found to be very sensitive to changes in pore water concentration in the natural range of ionic strengths, and it was found that a 2 per cent change could cause the dissolution of a mineral from a formerly stable condition.

Analyses of micro-morphology and surface chemistry revealed differences in solute movement and deposition upon clay surfaces and fissures, above and below the basal shear surface (section 4.45). For instance a greater proportion of amorphous silica and aluminium were found on clay surfaces and fissures above the shear surface at Manor Lane. Both were also found to increase downslope. Greater variability was found at Worbarrow, such as an accumulation of amorphous silica above the shear surface downslope from 55 to 70 per cent. In contrast to Manor Lane, a greater proportion of aluminium was found beneath the shear surface at Worbarrow up to 10 per cent in places, which was considered to be evidence of the leaching of weathered products from the overlying mudslide materials. Unlike silica, aluminium was not more abundant in the accumulation lobe at Worbarrow. Amorphous iron showed the greatest variations at both sites with 6 per cent occurring on clay surfaces in comparison with 16 per cent along fissures above and below the shear surface. The deposition along

fissures was found to vary by as much as 700 per cent, in addition to an overall increase downslope at Manor Lane in contrast to a reduction at Worbarrow. Little is known about the effect of iron and redox conditions upon soil deformation processes.

7.34 Association of physico-chemical properties with shear strength.

The spatial distribution of shear strength was established at both sites (section 4.32). Each showed a characteristic reduction in the shear strength parameters from peak to residual, or near-residual condition upon erosion and disruption of *in situ* materials. A further reduction in residual strength was found on the lower slopes confirming that weathering and mudsliding are fundamental in soil deformation processes. The drained peak friction angle at Manor Lane was 15.5° in comparison with 23.2° at Worbarrow. The corresponding peak cohesion terms for both sites equalled 12-13 kN/m².

The mean residual friction angle of the mudslipped materials at Manor Lane was 9.6° in comparison with 8.5° at Worbarrow, ^{where} the lower value was thought to result from the greater proportion of monovalent-montmorillonite at the latter site. However, the residual strength was quite variable at Worbarrow recording a range of values between 12.5° and 5.7°, probably as a consequence of the variability and dispersion of the Wealden Beds. In contrast the residual strength of the London Clay was found to reduce uniformly downslope from 11.3° to 8.0°, with both sites recording small values of residual cohesion within the range of 2-4 kN/m². The reduction from peak to residual states accounted for a 39-64 per cent fall in the frictional term and 74-81 per cent in cohesion. The destruction of primary cohesive bonds in soil deformation was thus

found to be of greater significance than the alteration of the friction angle.

Although shear strength was considered to be a function of friction and cohesion it was evident that the resistance to soil deformation was determined by many soil properties, some directly and others indirectly; the more important parameters have been described. In order to assess which variables were most closely associated with shear strength all parameters were statistically correlated (section 6.21). The analysis isolated the unit weight or particle density and the concentration of both soluble salts and the interstitial pore water as the most significant properties related to the distribution of residual strength. The proportion and type of clay minerals, the saturated moisture content and the void ratio were also found to have important associations with shear strength.

The unit weight was negatively correlated at both sites confirming that the progressive compaction of clay, and probably ^{particle} orientation, are partly responsible for the reduction in residual strength and the perpetuation of mudslides irrespective of lithological variability. However, by far the most significant correlations were found with the chemistry of the soil water and particle interfaces. The development of diffuse ionic double layers as a consequence of an increase in the solubility of salts associated with mineral surfaces was considered to result in a reduction in the strength of bonding or cohesion within and between particles, the expansion between mineral layers and the observed reduction in residual strength downslope. There was an apparent dilution of the hydration shells loosely bonded to particle surfaces following weathering and a consequent increase in interstitial 'free-water' salt concentration.

The concentration of salt in the double layers was found to be the most critical for the mechanisms of bonding between particles and hence shear strength. When dilute, the mineral surfaces are separated by several layers of water causing the expansion of clays and a reduction in friction. Because cohesion was close to zero there was an apparent reduction in the friction angle, or rather a reduction in the influence of friction. Friction will be greatest with poorly developed double layers. Cohesion may similarly re-develop following an increase in pore water salt concentration and a change in bonding mechanism from Van der Waals' and diffuse ionic forces to strong close-range ionic or cohesive bonds.

7.35 Seasonal behaviour of mudslides.

To assess the controlling factors of the dynamic behaviour of mudslides the Worbarrow field-site was comprehensively monitored using standard instrumentation and procedures (section 3.3). Wherever possible automatic recording devices were used to obtain a continuous data-set for weather, soil water and surface movement parameters. Other equipment and techniques were developed in the dynamic analysis of mudsliding that are considered original to the applications of this study. These include the use of analytical photogrammetry for the accurate measurement of morphological change, the design of groundwater samplers and salt gauges for the analysis of atmospheric and pore water chemistry, the re-design of an automatic technique for monitoring surface movement, and the application of simulation tests to model the effects of aqueous chemistry upon the residual shear strength of mudslides.

Analytical photogrammetry was applied to assess morphological change throughout the study using non-contact terrestrial photography (section 3.22). Apart from providing detailed site plans for the planning and location of field instrumentation (section 3.23), temporal changes in the extent, shape and volume of the mudslide were achieved through planimetric and profile analyses (section 5.21). ^{Measurement of the} ~~The~~ movement of targets throughout the entire mudslide complex was possible (section 5.214) for comparison with the continuous record of the automatic movement sensors. Additionally, it was possible to compute a digital terrain model for each survey, and to subtract one from another to obtain a quantitative description of the extent of surface change at the site (section 5.213). The accurate measurement of cliff recession (section 5.211) and volume change (section 5.212) were critical for the stability analyses of the site.

Electronic sensors and recording devices were designed, tested and installed on-site (section 3.32). These included a remote weather station sited close to the cliffs to provide a comprehensive record of weather parameters (section 3.321); specially designed salt gauges (section 3.325) were used to assess the variability of rainfall and salt deposition on the coastal cliffs with respect to micro-climate. Peak salt deposition in November was significantly related to effective south-westerly precipitation (section 5.314); automatic water depth sensors were used with standpipe piezometers and the neutron probe to assess the seasonal variability in pore water pressure and the soil moisture balance (sections 3.322-3.323); pore-water samplers were specially designed, to enable the extraction of soil water from the basal shear surface for chemical analysis (section 3.326). The durability and effectiveness of these samplers proved much greater than standard soil water samplers and

lysimeters; surface movement was monitored by eight automatic sensors located on a 10 metre span gantry across the mudslide (section 3.324) with a new and improved cable link for maintenance purposes.

Distinctive seasonal cycles were observed for most parameters (section 5.3), emphasising the climatic controls upon slope instability. Three mechanisms of movement were identified, confirming recent developments in mass movement studies; these were similarly termed multiple, graded and surge displacements, each varying in frequency and magnitude (section 5.331). The analysis of results demonstrated the association of the soil water relations, shear strength and undrained loading as causal factors of mudslide movements and the instability of slopes (section 5.332).

Field-data were collated at several time-scales (section 3.33) and correlated to establish the antecedent time-lags operating between variables, and which parameters were most closely associated with surface movement (section 6.22). Strong relationships were found between effective rainfall, or the hydrological flux, and the soil water relations, although the latter were even more significantly related to the movement of the mudslide. Pore water chemistry was significantly correlated with movement representing a seasonal change in shear strength. Time-lags of several days were identified between movement and effective rainfall, soil moisture, and pore water pressure. Pulses of pressure of decreasing magnitude were measured in the source unit for up to 4 days following the initial event, and were associated with a gradual rise in pore pressure and undrained loading of the lobe. This behaviour was considered to be evidence of 'kinematic' waves of loading and movement down the mudslide.

Laboratory simulation tests were undertaken to monitor the effects of mineralogy and aqueous chemistry upon the residual strength of pure and natural clay samples (section 3.43). The results showed that residual strength is sensitive to the quantity and type of clay minerals as well as the type, valency and concentration of the pore water solution. For montmorillonite dominated clay soils low concentrations of monovalent cations produced the lowest strengths. An increase in concentration corresponds with a disproportionate increase in strength dependent on the valency of the exchangeable cation being greatest for divalent ions. When natural samples of London and Wealden Clay were used in simulation, the weathered samples supported the lowest residual shear strengths, with strength increasing reversely with concentration. The change in strength was similarly disproportionate and dependent on the weathered state of the material, with the greatest fluctuations occurring in highly weathered materials particularly at low (10 %) sea water concentrations. The residual strength was found to fluctuate by up to 20 per cent through the effects of pore water concentration. Throughout the tests the post-flow chemistry remained relatively constant except at low concentrations when significant proportions of divalent cations were released to the pore water with a change from a divalent to a monovalent aqueous system. As found in the geochemical analysis, the natural range of ionic concentrations was not only sensitive to change with weathering reactions but also with the residual shear strength of mudslipped materials.

Seasonal variation in pore water concentrations were calibrated against laboratory results to establish the likely change in shear strength for field conditions (section 6.223). Fluctuations in residual strength of up to 1.02 kPa at Worbarrow and 1.32 kPa at Manor Lane were accountable

through the effects of pore water chemistry. From June to November 1986 low inherent shear strengths were recorded coincident with low pore water salt contents, soil moisture and zero movement. Shear strength increased dramatically in December 1986 or January 1987 following intense weathering and mudslide movements, triggered by groundwater pressures, and probably as a consequence of the peak aerial salt deposition in November. The interaction between clay minerals and pore water chemistry in relation to the weathering and shear strength of mudslide materials were represented and applied to the process-response model proposed by Brunsden (1973).

Results from the static and dynamic analyses were combined in slope stability models of both sites. An infinite slope model was developed for each site based on the series of slope units and depth zones defined in the static model (section 3.41) enabling the inclusion of a much greater resolution of data than conventionally used. Measured values were input to the model for the residual strength parameters from the basal shear surface, the unit weight for three horizons, along with the geometry of each slice of mudslide. Fluctuations in pore water pressures, shear strength and undrained loading were applied to the static model to obtain the seasonal variation in the factor of safety. Simulated changes in the cohesive strength from zero to measured values were also undertaken to establish the sensitivity of the model to shear strength.

An increase in undrained loading and pore water pressures are traditionally thought to cause the seasonal instability of translational mudslides, but when these were applied to the model they were found to be insufficient to cause global instability at both sites. Only when considered with the seasonal variations in shear strength were realistic

factors of safety obtained in relation to observed behaviour. In addition the three mechanisms of movement were considered to reflect the strength and type of inter-particle bonding, such that surge movements were associated with zero cohesion, multiple 'stick-slip' movements with strong close-range ionic or cohesive bonds, and graded movements intermediary. The findings are supported by theoretical and experimental considerations and suggest that the properties of clay soils should receive careful consideration in studies of mass movement and soil deformation processes.

REFERENCE LIST

- Allen, P. (1972) Wealden detrital tourmaline implications for northwestern Europe. *Quart. J. Geol. Soc. Lond.*, 128(3);273-284.
- Allen, S. (1974) *Chemical analysis of ecological materials*. Blackwell. 565pp.
- Allison, R.J. (1986) *Mass movement and coastal cliff development of the Isle of Purbeck, Dorset*. Unpublished Ph.D. thesis, University of London. 610pp.
- Alther, G.R. (1986) The effect of exchangeable cations on the physico-chemical properties of Wyoming bentonites. *Applied Clay Science*, 1(3);273-284.
- Andersland, D.B. and Douglas, A.G. (1970) Soil deformation and activation energies. *Geotechnique*, 20(1);1-16.
- Anderson, D.M. et al (1969) Bentonite debris flows in Northern Alaska. *Science*, 164;173-174.
- Anderson, M.G. and Burt, T.P. (1978) The role of topography in controlling throughflow generation. *Earth Surface Processes and Landforms*, 3;331-344.
- Anderson, M.G. and Kneale, P.E. (1980) Pore water pressure and stability conditions on a motorway embankment. *Earth Surface Processes and Landforms*, 5;37-46.
- Anderson, M.G. and Richards, K.S. (1987) *Slope Stability*. Wiley. 650pp.
- Anderson, M. and Rubin, A. (1981) Adsorption of inorganics at the solid-liquid interface. Ann Arbor Science Publ., Michigan. 357pp.
- Apted, J.P. (1977) *Effects of weathering on some geotechnical properties of London Clay*. Unpublished Ph.D. thesis, University of London.
- Arkell, W.J. (1947) *The geology of the country around Weymouth, Swanage, Corfe and Lulworth*. Memoirs of the Geological Survey of Great Britain. HMSO, London. 386pp.
- Arora, H.S. and Scott, J.B. (1974) Chemical stabilization of landslides by ion-exchange. *Californian Geologist*, 2;99-107.
- Atkinson, J.H. (1973) Elasticity and plasticity in soils. *Geotechnique*, 23;565.
- Australian Water Resources Council (1974) *Soil moisture measurement and assessment*. Australian Water Resources Council Hydrology Series report No. 9, Victoria. 45pp.
- Avery, B.W. and Bascombe, C.L. (1974) *Soil survey laboratory methods*. Soil Survey of England and Wales Technical Monograph, No. 6, Harpenden, England. 83pp.

- Avery, B.W. and Bullock, P. (1977) *Mineralogy of clayey soils in relation to soil classification*. Soil Survey Technical Monograph, No.10, Harpenden, England. 64pp.
- Aylmore, L.A.G. and Quirk, J.P. (1959) Swelling of clay water systems. *Nature*, 183;1752-1753.
- Aylmore, L.A.G. and Quirk, J.P. (1967) The micro-pore size distribution of clay mineral systems. *Journal of Soil Science*, 18;1-17.
- Bailey, S.W. (1986) Layer silicate structures. In: Cairnes-Smith, A.G. and Hartmann, H. (Eds.) *Clay minerals and the origin of life*, p24-40. Cambridge University Press.
- Bailey, S.W. et al (1971) Summary of national and international recommendations on clay mineral nomenclature. *Clays and clay minerals*, 19;129-133.
- Balteanu, D. (1976) Two case studies of mudflows in the Bazan Sub-Carpathians. *Geografiska Annaler*, 58A; 165-171.
- Barber, C. et al (1977) *Groundwater sampling: the extraction of interstitial water from cores of rock and sediments by high-speed centrifuge*. Rivers Division Water Research Centre Technical report TR 54. p1-17.
- Barden, L. (1972) The influence of structure on deformation and failure in clay soil. *Geotechnique*, 22;159.
- Barrer, R.M. (1984) Sorption and molecular sieve properties of clays and their importance as catalysts. *Philosophical Transactions of the Royal Society, London*, A311;333-352.
- Bascombe, C.L. (1964) A rapid method for the determination of cation exchange capacity of calcareous and non-calcareous soils. *J. Sci. Food and Agr.*, 15;821-823.
- Baver, L.D. et al (1972) *Soil Physics* (4th Ed.). Wiley, New York. 489pp.
- Bear, F.E. (1964) *Chemistry of the soil*. Reinhold, New York. 515pp.
- Begemann, H.K.S.Ph. (1977) Sample disturbance influencing shear strength of cohesive soils. In: Hoshino, K. (Ed.) *Soil sampling*. p123-27, Special publication of the 9th Int. Conf. Soil Mech. Found. Engng., Tokyo.
- Bell, J.P. and McCulloch, J.S.G. (1969) Soil moisture estimation by the neutron method in Britain, a further report. *J. Hydrology*, 7;415-433.
- Bennett, R.H. and Hulbert, M.H. (1986) *Clay micro-structure*. D.Rheidel, Holland. 161pp

- Bentley, S.P. (1985) Monitoring methods and data interpretation. In: Morgan, C.S. (Ed.) *Proceedings of the Symposium on Landslides in the South Wales Coalfield*, p45-58. Polytechnic of Wales, Pontypridd.
- Berner, R.A. (1971) *Principles of chemical sedimentology*. McGraw-Hill, New York. 240pp.
- Bhandari, R.K. and Hutchinson, J.N. (1982) Coastal mudslides in the Oligocene clays of Bouldnor cliff, Isle of Wight. *Reports of the Alma-Ata International Seminar, UNESCO-UNEP, landslides and mudflows, Publications and Information Support*. In: Project (A. Sheko, Ed.), Oct.1981, Moscow Centre of International Projects. GKNi; 176-199.
- Bishop, A.W. et al (1971) A new ring shear apparatus and its application to the measurement of residual strength. *Geotechnique*, 21(4);273-328.
- Bjerrum, L. (1961) The effective shear strength parameters of sensitive clays. *Proceedings of the 5th International Conference on Soil Mechanics and Foundation Engineering*, Paris, 1;23-8.
- Bjerrum, L. (1967) Progressive failure in slopes of over-consolidated plastic clay and clay shales. *Journal of Soil Mechanics and Foundations Division, American Society of Civil Engineering (SM5)*, 93;1-49.
- Black, C.A. (1965) *Methods of soil analysis*. Part 1, Physical and mineralogical methods. Soil Science Society of America, Agronomy monograph No. 9, Wisconsin, USA. 1216pp.
- Blackmore, A.V. and Miller, R.D. (1961) Tactoid size and osmotic swelling in Ca-montmorillonite. *Proceedings of Soil Science Society of America*, 25;169-73.
- Blyth, F.G.H. and de Freitas, M.H. (1974) *A Geology for Engineers*. 6th Edition. Arnold, London. 557pp.
- Bolt, G.H. (1954) *Physico-chemical properties of the electric double layers on planar surfaces*. Unpublished Ph.D. thesis, Cornell University.
- Bolt, G.H. (1955) Ion-adsorption by clays. *Soil, Science* 79;267-276.
- Bolt, G.H. (1956) Physico-chemical analysis of the compressibility of pure clays. *Geotechnique*, 6(2);86-93.
- Bolt, G.H. (1979) *Soil chemistry; B. Physico-chemical models*. Elsevier, Amsterdam. 479pp.
- Brady, N.C. (1984) *The nature and properties of soils*. Collier Macmillan, New York. 750pp.
- Brewer, R. (1964) *Fabric and mineral analysis of soils*. Wiley. New York. 470pp.

- Brindley, G.N. and Brown, G. (1984) *Crystal structures of clay minerals and their X-ray identification*. Mineralogical Society, London. Monograph 5. 504pp.
- British Standards 1377 (1975) *Methods of testing soils for Civil Engineering purposes*. British Standards Institution, HMSO, London. 233pp.
- British Standards 5930 (1981) - *Code of practice for site investigation*. British Standards Institution, HMSO, London.
- Broecker, W.S. (1974) *Chemical oceanography*. Harcourt Brace Jovanovich, New York. 214pp
- Bromhead, E.N. (1979a) Factors affecting the transition between the various types of mass movement in coastal cliffs consisting largely of over-consolidated clay with special reference to southern England. *Quart. J. Engng. Geol.*, 12;291-300.
- Bromhead, E.N. (1979b) A simple ring shear apparatus. *Ground Engineering*, 12;40-44.
- Bromhead, E.N. (1986) *The stability of slopes*. Surrey University Press, London. 373pp.
- Broms, B.B. (1984) *Stabilization of soil with lime columns*. Design handbook, 3rd Edition, Nanyang Technological Institute, Singapore. 51pp.
- Broms, B.B. and Anttikoski, U. (1985) Soil stabilization : chemical stabilization of soft clay and silt. General report of speciality session 9, of the 3rd Int. Geotech. Seminar on soil improvement methods, Singapore 27-29 Nov., p141-153.
- Broms, B.B. and Boman, P. (1977) Stabilization of soil with lime. *Ground Engineering*, 12(4);23-32.
- Brooks, R.H. et al (1956) The effects of various exchangeable cations upon the physical conditions of soils. *Proceedings of Soil Science Society of America*, 20;325-327.
- Brownlow, A.H. (1979) *Geochemistry* (Chp. 3). Prentice-Hall. 498pp.
- Bruce, J.P. and Clark, R.H. (1980) *Introduction to hydrometeorology*. Pergamon Press, Oxford. 323pp.
- Bruckl, E. and Scheidegger, A.E. (1973) Application of the theory of plasticity to slow mudflows. *Geotechnique*, 23;101-107.
- Brunsdon, D. (1973) The application of system theory to the study of mass movement. *Geologia Applicata e Idrogeologia*, Bari, 8;185-207.
- Brunsdon, D. (1974) The degradation of a coastal slope, Dorset, England. *Inst. Brit. Geogr. Spec. Publ. No. 7*, p79-98.
- Brunsdon, D. (1979a) Mass movement. In: Embleton, C. and Thornes, J.B. (Eds.) *Processes in Geomorphology*, p130-186. Edward Arnold.

- Brunsdon, D. (1979b) Weathering. In: Embleton, C. and Thornes, J.B. (Eds.) *Processes in Geomorphology*, p73-129. Edward Arnold.
- Brunsdon, D. (1984) Mudslides. In: Brunsdon, D. and Prior, D.B. (Eds.) *Slope Instability*, p363-418. Wiley, Chichester.
- Brunsdon, D. (1985) Landslide types, mechanisms, recognition and identification. In: Morgan, C.S. (Ed.) *Proceedings of the Symposium on Landslides in the South Wales Coalfield*, p19-28. Polytechnic of Wales, Pontypridd.
- Brunsdon, D. and Goudie, A.S. (1982) *Classic coastal landforms of Dorset*. Landform Guide No.1. Geographical Association, Sheffield. 39pp.
- Brunsdon, D.B. and Jones, D.K.C. (1972) The morphology of degraded landslide slopes in south-west Dorset. *Quart. J. Engng. Geol.*, 5;205-222.
- Brunsdon, D.B. and Thornes, J.B. (1977) *Geomorphology and time*. Methuen, London. 208pp.
- Burnett, A.D. (1972) *Engineering geology of the London Clay in the London and Hampshire Basins*. Unpublished Ph.D thesis, University of London.
- Burnett, A.D. and Fookes, P.G. (1974) A regional engineering geological study of the London Clay in the London and Hampshire Basins. *Quarterly J. Engng. Geol.*, 7(3);257-295.
- Callabresi, G. and Scarpelli, G. (1985) Effects of swelling caused by unloading in over-consolidated clays. *Proceedings of the 11th International Conference on Soil Mechanics and Foundation Engineering (ICSMFE)*, San Francisco, 2;411-414.
- Calladine, C.R. (1971) A micro-structural view of the mechanical properties of saturated clay. Discussion, *Geotechnique*, 22;364.
- Campbell, A.P. (1966) Measurement of movement of an earthflow. *Soil water*, March; 23-24.
- Carroll, D. and Starkey, H.C. (1960) Effects of sea-water on clay minerals. *Clays and clay minerals*, 7;80-101.
- Carson, M.A. (1969) Models of hillslope development under mass failure. *Geogr. Anal.*, 1;76-100.
- Carson, M.A. (1971) Application of the concept of threshold slopes to the Laramide Mts., Wyoming. I.B.G. Special publication No. 3, *Slopes: form and process*, (Brunsdon, D. Ed.) p31-49.
- Carson, M.A. (1975) Threshold and characteristic angles of straight slopes. In: *Mass Wasting*, (Yatsu, E. et al, Eds.) *Proceedings of the 4th Guelph Symposium on Geomorphology*, p19-34.

- Carson, M.A. and Kirkby, M.J. (1972) *Hillslope form and process*. Cambridge. 475pp.
- Carson, M.A. and Petley, D.J. (1970) The existence of threshold slopes in the denudation of the landscape. *Trans. Inst. Brit. Geogr.*, 49;71-92.
- Castellan, G.W. (1971) *Physical chemistry* (2nd Ed.). Addison-Wesley. 436pp.
- Chandler, J.H. et al (1987) Analytical photogrammetry applied to Nepalese slope morphology. *Photogrammetric Record*, 12(70);443-458.
- Chandler, M.P. (1984) *The coastal landslides forming the undercliff of the Isle of Wight*. Unpublished Ph.D. thesis, University of London.
- Chandler, R.J. (1969) The effect of weathering on the shear strength of Keuper Marl. *Geotechnique*, 22;403-31.
- Chandler, R.J. (1972a) Periglacial mudslides in Vestspitsbergen and their bearing on the origin of fossil 'solifluction' shears in low-angled clay slopes. *Quart. J. Engng. Geol.*, 5;223-241.
- Chandler, R.J. (1972b) Lias clay weathering processes and their effect on shear strength. *Geotechnique*, 22(3);403-431.
- Chandler, R.J. (1982) Lias clay slope sections and their implications for the prediction of limiting or threshold slope angles. *Earth Surface Processes and Landforms*, 7;427-438.
- Chandler, R.J. (1984) Recent European experience of landslides in over-consolidated clays and soft rocks. *Proceedings of the 4th International Symposium on Landslides*, Toronto, 1;61-81.
- Chandler, R.J. and Skempton, A.W. (1974) The design of permanent cutting slopes in stiff fissured clays. *Geotechnique*, 24;457-66.
- Chattopadhyay, P.K. (1972) *Residual shear strength of some pure clay minerals*. Unpublished Ph.D. thesis, The University of Alberta, Edmonton, Canada.
- Chen, P. (1977) Table of key lines in X-ray powder diffraction patterns of minerals in clays and associated rocks. *Department of Natural Resources Geological Survey Occasional Paper*, 21. Bloomington, Indiana. 46pp.
- Chorley, R.J. Schumm, S.A. and Sugden, D.E. (1984) *Geomorphology*. Methuen. 605pp.
- Collins, B.J. and Madge, B. (1981) Photo-radiation: a new method for monitoring beach movement. *Chart. Land Surveyor and Chart. Minerals Surveyor*, 3(1);4-11.
- Collins, B.J. and Madge, B. (1985) A note on photo-radiation: a new photogrammetric method. In: Morgan, C.S. (Ed.) *Proceedings of the Symposium on Landslides in the South Wales Coalfield*, p201-203. The Polytechnic of Wales, Pontypridd.

- Colman, S.M. and Dethier, D.P. (1986) *Rates of chemical weathering of rocks and minerals*. Academic Press. 745pp.
- Conway, B.W. (1976) Coastal terrain evaluation and slope stability of the Charmouth-Lyme Regis area of Dorset. *Inst. Geol. Sci., Geophys. Div., Engng. Geol. Unit Report No. EG76/10*.
- Cooke, R.U. (1979) Laboratory simulation of salt weathering processes in arid environments. - *Earth Surface Processes and Landforms*, 4;347-359.
- Cooke, R.U. and Doornkamp, J.C. (1978) *Geomorphology in environmental management*. Clarendon Press, Oxford. 413pp.
- Cooper, M.A.R. (1987) *Control surveys in civil engineering*. Collins, London. 381pp.
- Cooper, M.A.R. et al (1986) The development of photogrammetric techniques for monitoring movements of unstable hillslopes in Nepal. *Transport and Road Research Laboratory Report*, 50. Department of Transport. 79pp.
- Craig, D. (1979) *Some aspects of mudslide stability in east County Antrim, Northern Ireland*. Unpublished Ph.D. thesis, Queen's University of Belfast. 401pp.
- Craig, D. (1981) Mudslide plug flow within channels. *Engng. Geol.*, 17, 273-281.
- Craig, R.F. (1983) *Soil Mechanics*. 3rd Edition. Van Nostrand Reinhold, Wokingham, England. 419pp.
- Crandell, D.R. and Varnes, D.J. (1961) Movement of the Slumgullion earth-flow near Lake City, Colorado. *US Geological Survey Professional Paper*, 424B;136-139.
- Cripps, J.C. and Taylor, R.K. (1981) The engineering properties of mudrocks. *Quart. J. Engng. Geol.*, 14;325-46.
- Crozier, M.J. (1968) *Mass movement in Eastern Otago*. Unpublished Ph.D. thesis, University of Otago, New Zealand. 300pp.
- Crozier, M.J. (1986) *Landslides: causes, consequences and environment*. Croom Helm. 252pp.
- Culling, W.E.H. (1983) Rate process theory in geomorphic soil creep. *Catena Supplement*, 4;191-214.
- Cunningham, M.J. (1972) A mathematical model of the physical processes of an earthflow. *J. Hydrology*, 11;47-54.
- Das, B.M. (1985) *Advanced soil mechanics*. McGraw-Hill, p15-34.
- Davidtz, J.C. and Low, P.F. (1970) Relation between crystal lattice configuration and swelling of montmorillonite. *Clays and clay minerals*, 18(6); p325.

- Davis, A.G. (1936) The London Clay of Sheppey and the location of its fossils. *Proceedings of the Geologist Association*, 47;328-345.
- Davis, A.G. (1937) Additional notes on the geology of Sheppey. *Proceedings of the Geologist Association*, 48;77-81.
- Davis, A.G. and Elliot, G.F. (1957) The palaeogeography of the London Clay Sea. *Proceedings of the Geologist Association*, 69(4);255-277.
- Demek, J. and Embleton, C. (1978) *Guide to medium scale geomorphological mapping*. I.G.U. Commission on geomorphological survey and mapping, Brno. 348pp.
- Denisov, N.J. et al (1941) On the colloid-chemical nature of cohesion in argillaceous rocks. USSR Academie des Sciences, *Comptes Rendus (Doklady)*, 54(6);519-522.
- Denisov, N.J. and Reltov, B.F. (1946) Surface phenomena and landslides of argillaceous formations. *Comptes Rendus, l'Academie des Sciences de l'USSR*, 33(4);295-296.
- Deshpande, T.L. et al (1964) Role of iron oxides in the bonding of soil particles. *Nature*, 201;107-108.
- Dines, H.G. et al (1971) *Geology of the country around Chatham*. Memoir of the Geological survey of Great Britain. HMSO, London. 162pp.
- Dixon, J.B. and Weed, S.B. (1977) *Minerals in soil environments*. Soil Science Society of America, publication. 948pp.
- D.O.E. (1987) *Review of research into landsliding in Great Britain*. Unpublished report prepared by Geomorphological Services Limited for the Department of the Environment, August 1986. Vols. 1-6.
- Drever, J.I. (1977) *Sea-water: cycles of the major elements*. Dowden, Hutchinson and Ross, Stroudsburg Pa. 345pp.
- Drever, J.I. (1982) *The geochemistry of natural waters*. Prentice-Hall, Englewood Cliffs, N.J. 388pp.
- Drever, J.I. (1985) *The chemistry of weathering*. Reidel Publ. Co.; NATO ASI, c149. 384pp.
- Driscoll, R. (1984) The effects of clay volume changes on low-rise buildings. In: Attewell, P.B. and Taylor, R.K. (Eds) *Ground movements and their effects on structures*, p268-302. Surrey University Press-Blackie Group, Glasgow.
- Duchaufour, P. (1982) *Pedogenesis and classification*, p6-7. George Allen and Unwin, London. 448pp.
- Dumbleton, M.J. (1966) Some factors affecting the relation between the clay minerals in soils and their plasticity. *Clay Minerals*, 6;179-93.

- El-Hiti, A.S. (1985) The activation energy for the lattice destruction of Egyptian bentonite. *Journal of the College of Science, King Saud University*, 16(2);265-272.
- Emerson, W.W. and Bakker, A.C. (1973) The comparative effects of exchangeable calcium, magnesium and sodium on some physical properties of red-brown earth subsoils. *Austr. J. Soil Res.*, 11;151-157.
- Emerson, W.W. and Chi, C.L. (1977) Exchangeable Ca, Mg, Na and the dispersion of illites in water. Part 1, *Austr. J. Soil Res.*, 15;243. Part 2, *Austr. J. Soil Res.*, 15;255-262.
- Fisher, R.A. (1970) *Statistical methods for research workers*. Oliver and Boyd Ltd.. 564pp.
- Foster, M.D. (1953) Geochemical studies of clay minerals II: Relation between ionic substitution and swelling in montmorillonites. *America Mineralogist*, 38;994-1006.
- Fowden, L. et al (1984) Clay minerals: their structure, behaviour and use. *Philosophical Transactions of the Royal Soc.*, A311;219-432.
- Francis, S.C. (1987) Slope development through the threshold concept. In: Anderson, M.G. and Richards, K.S. (Eds.) *Slope Stability*, p601-624. Wiley.
- Franzmeier, D.P. et al (1968) Soil swelling: laboratory measurement and relation to other soil properties. *Proceedings of the Soil Science Society of America*, 32; 573-577.
- Freeze, R.A. and Cherry, J.A. (1979) *Groundwater*. Prentice-Hall, New Jersey. Chapters 2 and 3; p14-143.
- Fripiat, J.J. (1965) Surface chemistry and soil science. In: Hallsworth, E.G. and Crawford, D.V. (Eds.) *Experimental pedology*. Butterworth, London. 425pp.
- Fripiat, J.J. et al (1984) Interaction of water with clay surfaces. *Phil. Trans. Royal Soc.*, London, A 311;287-299.
- Fripiat, J.J. (1986) Internal surface of clays and constrained chemical reactions. *Clays and Clay Minerals*, 34(5);501-506.
- Gardiner, V. and Dackombe, R.V. (1983) *Geomorphological field manual*. Allen and Unwin, London, 254pp.
- Garrells, R.M. and Christ, C.L. (1965) *Solutions, minerals and equilibria*. Harper and Row, New York. 450pp.
- Gillott, J.E. (1987) *Clay in Engineering Geology* (2nd Ed.). Elsevier, New York. 468pp.

- Goudie, A.S. (1974) Further experimental investigations of rock weathering by salt and other mechanical processes. *Zeitschrift für Geomorph. Supp.*, 21;1-12.
- Goudie, A.S. (1977) Sodium sulphate weathering and disintegration of Mohenjo-Daro, Pakistan. *Earth Surf. Proc. Landforms*, 2;75-86.
- Goudie, A.S. (1981) *Geomorphological techniques*. Allen and Unwin, London, 395pp.
- Goudie, A.S. (1986) Laboratory simulation of the 'Wick effect' in salt weathering of rock. *Earth Surf. Proc. Landforms*, 11;275-285.
- Goudie, A.S. et al (1970) Experimental investigation of rock weathering by salts. *Area*, 4;2-8.
- Grainger, P. and Harris, J. (1986) Weathering and slope stability on Upper Carboniferous mudrocks in south-west England. *Quart. J. Engng. Geol.*, 19;155-173.
- Grainger, P. and Kalaugher, P.G. (1988) Intermittent surging movements of a coastal landslide. *Earth Surf. Proc. and Landforms*, 12(6);597-603.
- Greacen, E.L. et al (1981) *Soil water assessment by the neutron method*. CSIRO, Victoria, Australia. 140pp.
- Greenkorn, R.A. and Kessler, D.P. (1969) Dispersion in heterogeneous non-uniform anisotropic porous media. *Ind. Eng. Chem.*, 61;14-32.
- Grim, R.E. (1948) Mineral composition in relation to the properties of certain soils. *Geotechnique*, 1;139-147.
- Grim, R.E. (1953) *Clay Mineralogy*. McGraw-Hill, New York. 384pp.
- Grim, R.E. (1959) Physico-chemical properties of soils; Clay Minerals. *Proceedings of the Soil Mechanics and Foundations Division*, Amer. Soc. Civil Eng., (SM2);1-17.
- Grim, R.E. (1962) *Applied Clay Mineralogy*. McGraw-Hill, New York. 422pp.
- Grim, R.E. (1968) *Clay Mineralogy*. 2nd Ed. McGraw-Hill, New York. 596pp.
- Grim, R.E. and Guven, N. (1978) *Bentonites: geology, mineralogy, properties and use*. Developments in Sedimentology 24, Elsevier. 412pp.
- Grove, A.T. (1953) Account of a mudflow on Bredon Hill, Worcestershire. *Proceedings of the Geologist Association*, 64;10-13.

- Handy, R.L. and Williams, W.W. (1966) *Chemical stabilization of an active landslide*, Iowa State University Research Laboratory Report, 66-11;1-15.
- Hansen, M.J. (1984) Strategies for the classification of landslides. In: Brunsden, D. and Prior, D.B. (Eds.) *Slope Instability*, p1-25. Wiley, Chichester.
- Harris, N.T. (1974) *Factors affecting the permeability of clays with particular reference to fissures in London Clay*. Unpublished M.Sc. thesis, Dept. Civil Engineering, Imperial College, University of London.
- Havlicek, J. and Kazda, J. (1961) Soil properties in relation to hydration of exchangeable ions. *Proceedings of the 10th Int. Conf. Soil Mech. Found. Engng.*, 1;137-139.
- Hawkins, A.B. (1985) Geological factors affecting shear strength. *Proceedings of the 9th International Conference and Field Workshop on Landslides*. Tokyo, p239-244.
- Hay, R.K.M. (1981) *Chemistry for agriculture and ecology*. Blackwell. 243pp.
- Head, K.H. (1984) *Manual of soil laboratory testing*. Volume 1, soil classification and compaction tests. ELE Ltd., Pentech Press. 1238pp.
- Helfferich, F. (1962) *Ion-exchange*. McGraw-Hill. 624pp.
- Helgeson, H.C. et al (1969) Evaluation of irreversible reactions in geochemical processes involving minerals and aqueous solutions. II Applications *Geochim. Cosmochim. Acta*, 33;455-481.
- Hendershot, W.H. and Duquette, M. (1986) A simple barium chloride method for determining CEC and exchangeable cations. *Soil Science Society of America*, 50(3);605-608.
- Henderson, P. (1982) *Inorganic geochemistry*. Pergamon Press. 353pp.
- Henkel, D.J. (1955) A landslide at Jackfield, Shropshire in heavily over-consolidated clay. *Geotechnique*, 5;131-137.
- Hillel, D. (1971) *Soil and Water*. Academic Press, New York. 288pp.
- Hodgson, J.M. (1978) *Soil sampling and soil description*. Clarendon Press. 241pp.
- Holdren, G.R. and Berner, R.A. (1979) Mechanism of feldspar weathering: 1, Experimental studies. *Geochim. Cosmochim. Acta*, 43;1161-1171.
- Holland, H.D. (1978) *The chemistry of the atmosphere and oceans*. Wiley-Interscience, N.Y. 351pp.
- Holmes, S.C.A. (1981) *Geology of the country around Faversham*. Institute of Geological Sciences. HMSO, London. 117pp.

- Horn, H.M. and Deere, D.V. (1962) Frictional characteristics of minerals. *Geotechnique*, 12(4);319-335.
- Hutchinson, J.N. (1965) *The stability of cliffs composed of soft rocks, with particular reference to the coasts of south-east England*. Unpublished Ph.D. thesis, University of Cambridge.
- Hutchinson, J.N. (1967) The free degradation of London Clay cliffs. *Proc. Geotech. Conf., Oslo*, 1;113-118.
- Hutchinson, J.N. (1968) Field meeting on the coastal landslides of Kent, 1-3 July, 1966. *Proc. Geol. Ass.*, 79;227-237.
- Hutchinson, J.N. (1969) A reconsideration of the coastal landslides at Folkestone Warren, Kent. *Geotechnique*, 19;6-38.
- Hutchinson, J.N. (1970) A coastal mudflow on the London Clay cliffs at Beltinge, North Kent. *Geotechnique*, 20;412-438.
- Hutchinson, J.N. (1972) *Contribution to Discussion, Session 6*, Roscoe Memorial Symposium, p730-734. Cambridge.
- Hutchinson, J.N. (1973) The response of London Clay cliffs to differing rates of toe erosion. *Geologia Applicata e Idrogeologia*, Bari, 8;221-239.
- Hutchinson, J.N. (1981) Methods of locating slip surfaces in landslides. Simpozijum istraživanja i sanacija klizista. Inst. za puteve zavod za istraživanja is ispitivanja. *Rudarsko Geoloski Fakultet Geotehnika i geofizika*, Beograd. 34pp.
- Hutchinson, J.N. (1983) A pattern in the incidence of major coastal mudslides. *Earth Surface Processes and Landforms*, 8;1-7.
- Hutchinson, J.N. (1984) Landslides in Britain and their countermeasures. *J. Japan Landslide Society*, 21;1-24.
- Hutchinson, J.N. (1986) Cliffs and shores in cohesive materials: Geotechnical and engineering geological aspects. *Proc. Symp. on Cohesive soils*, May 5-7, Burlington Ontario, (Skafel, M.G., Ed.) p1-44, Ass. Comm. for research into shoreline erosion and sedimentation. National Research Council, Canada.
- Hutchinson, J.N. and Bhandari, R. (1971) Undrained loading: a fundamental mechanism of mudflows and other mass movements. *Geotechnique*, 21;353-358.
- Hutchinson, J.N. and Gostelow, T.P. (1976) The development of an abandoned cliff in London Clay at Hadleigh in Essex. *Phil. Trans. of Royal Society*, A283;557-379.
- Hutchinson, J.N. Prior, D.B. and Stephens, N. (1974) Potentially dangerous surges in an Antrim mudslide. *Quart. J. Engng. Geol.*, 7;363-376.

- Hvorslev, M.J. (1960) Physical components of the shear strength of saturated clay. *Proceedings of the American Society of Civil Engineering Research Conference on the shear strength of cohesive soils*, p1-189.
- Ingles, O.G. (1968) Advances in soil stabilization (1961-1967) - A review. *Pure and Applied Chemistry*, 18;291.
- Ingles, O.G. (1970) Mechanisms of clay stabilization with inorganic acids and alkalis. *Australian Journal of Soils Research*, 8;81-95.
- Institute of Hydrology (1981) *User's handbook for the Institute of Hydrology Neutron Probe System*. IOH report No. 79, Wallingford, Oxford. 30pp.
- James, P.M. (1970) *Time effects and progressive failure in clay slopes*. Unpublished P.h.D., University of London.
- Jones, D.K.C. (1981) *South-east and southern England*. Methuen, London. 332pp.
- Jones, J.A.A. (1981) *The nature of soil piping: a review of research*. British Geomorphology Research Group Research Monograph No.3. Geo Books, Norwich. 301pp.
- Jones, M.E. et al (1983) On the relationships between geology and coastal landforms in Central Southern England. *Proc. Dorset Nat. Hist. Archaeol. Soc.*, 105;107-118.
- Kazda, J. (1979) The character of adsorbed water on clayey soils. *Geologica 8th conference on clay minerals and petrology*, Templice. p59-64.
- Keil, K.F.G. and Striegler, W. (1961) Influence of hydrating chemical on Rheological properties of fine grained soils. *Proceedings of the 5th International Conference on Soil Mechanics and Foundation Engineering*, 1;185-188.
- Kelsey, H.M. (1978) Earthflows in Franciscan melange, Van Duzen River basin, California. *Geology*, 6;361-364.
- Kelsey, H.M. (1980) A sediment budget and an analysis of geomorphic process in the Van Duzen River basin, north coastal California, 1941-1975. *Geological Society of America Bulletin*, 91(3);1119-1216.
- Kenney, T.C. (1967a) The influence of mineralogical composition on the residual strength of natural soils. *Proceedings of the Geotechnical Conference on the Shear Strength properties of natural soils and rocks*, Oslo, 1;123-129.

- Kenney, T.C. Moun, J. and Berre, T. (1967b) An experimental study of bonds in a natural clay. *Proc. of the Geotech. Conf. on the shear strength properties of natural soils and rocks*, 1;65-69. Oslo.
- Kenney, T.C. (1977) Residual Strength of mineral mixtures. *Proceedings of the 10th Int. Conf. Soil Mech. Found. Engng.*, 1;155-160.
- Kenney, T.C. (1984) Properties and behaviours of soils relevant to slope instability. In: Brunsden, D. and Prior, D.B. (Eds.) *Slope Instability*, p27-65. Wiley, Chichester.
- Kerpen, W. and Scharpenseel, H.W. (1967) Movement of ions and colloids in undisturbed soil and parent rock columns. *Proceedings of the International Atomic Energy Agency Symposium*, Istanbul, p213-255.
- Kerr, P.F. (1963) Quick Clay. *Scientific American*, 209;132-42.
- Kinniburgh, D.G. and Miles, D.L. (1983) Extraction and chemical analysis of interstitial water from soil and rocks. *Environmental Science and Tech.*, 17(6);362-368.
- Kirkby, M.J. (1978) *Hillslope Hydrology*. Wiley, p56.
- Kirkby, M.J. (1987) General models of long-term slope evolution through mass movement. In: Anderson, M.G. and Richards, K.S. (Eds.) *Slope Stability*, p353-379. Wiley, Chichester.
- Klute, A. (1986) *Methods of Soil analysis*, Part 1, Physical and mineralogical methods. 2nd Edition. Soil Science Society of America, Agronomy monograph No. 9, Wisconsin, USA. 1216pp.
- Kowalski, W. (1970) The interdependence between strength, softening, swelling and shrinkage of cretaceous marls and 'Opokas' and their lithology. *Proceedings of the 1st International Congress of the International Association of Engineering Geology*, Paris, 1;457-464.
- Krauskopf, K.B. (1967) *Introduction to Geochemistry*. McGraw-Hill, 721pp.
- Krizek, R.J. (1977) Fabric effects on strength and deformation of kaolin clay. *Proceedings of the 9th Int. Conf. Soil Mech. Found. Engng.*, 1;169-176.
- Lambe, T.W. (1960) A mechanistic picture of shear strength in clay. *Proceedings of the Amer. Soc. Civil Eng. Research Conference on the shear strength of cohesive soils*, 437pp.
- Lambe, T.W. and Whitman, R.V. (1969) *Soil Mechanics*. Wiley, New York, 553pp.
- Lang, W.D. (1944) Geological notes, 1941-42. *Proc. Dorset Nat. Hist. Archaeol. Soc.*, (1942), 64;129-130. Also in *Geol. Notes*, (1944), 66;129.

- La Rochelle, P. *et al* (1981) Causes of sampling disturbance and design of a new sampler for sensitive soils. *Canadian Geotechnical Journal*, 18(1);52-66.
- Larsson, R. and Jansson, T (1982) Landslide at Tuve. *Swedish Geotechnical Institute Report*, 18. 28pp.
- Lee, I. *et al* (1983) *Geotechnical engineering*. Pitman. 508pp.
- Lerman, A. (1979) *Geochemical processes*. Wiley-Interscience, N.Y. 481pp.
- Likens, G.E. *et al* (1967) The Ca, Mg, K, and Na budgets for a small forested ecosystem. *Ecology*, 48(5);772-85.
- Loughnan, F.C. (1969) *Chemical weathering of the silicate minerals*. Elsevier, New York. 380pp.
- Loveday, J. (1974) *Methods for analysis of irrigated soils*. Commonwealth Agricultural Bureaux technical Communication No. 54 of the Comm. Bur. of Soils. Farnham Royal, England. 208pp.
- Loveland, P.J. (1984) The soil clays of Great Britain: 1. England and Wales. *Clay Minerals*, 19(5);681-707.
- Lupini, J.F. (1980) *The Residual Strength of Soils*. Unpublished Ph.D. thesis, University of London.
- Lupini, J.F. *et al* (1981) The drained residual strength of cohesive soils. *Geotechnique*, 31(2);181-213.
- Ma, Y. (1985) The effect of Ca and Na ions on the stability of montmorillonite colloids. *Acta Mineralogica Sinica*, 5(3);251-256.
- MacEwan, D.M.C. (1954) Short-range electrical force between charged colloid particles. *Nature*, 174;39-40. London.
- Madsen, E.T. (1979) Determination of the swelling pressure of claystones and marlstones using mineralogical data. *Proceedings of the 4th Congress of the International Society of Rock Mechanics*, 1;237-243.
- Manglesdorf, P.C. Jr and Sayles, F.L. (1975) Ion-exchange between sediments and sea-water. *Trans. Amer. Geophys. Union*, 56;1004 (Abstract).
- Marshall, C.E. (1964) *The physical chemistry and mineralogy of soils*. Volume One: Soil Materials. Wiley, New York. 388pp.
- Matsuo, S. and Kamon, M. (1977) Microscopic study on deformation and strength in clays. *Proceedings of the 9th Int. Conf. Soil Mech. Found. Engng.*, 1;201-204.

- McCaig, M. (1986) Soil properties and sub-surface hydrology. p121-140, In: Richards, K.S. et al (Eds.), *Geomorphology and soils*. Allen and Unwin, London.
- McConchie, J.A. (1986) *Earthflows : measurement and explanation*. Unpublished Ph.D. thesis, Victoria University, Wellington, New Zealand. 577pp.
- McGreal, W.S. and Craig, D. (1977) Mass movement activity : an illustration of differing responses to groundwater conditions from two sites in Northern Ireland. *Irish geographer*, 10;28-35.
- McGreavy, J.P. and Whalley, W.B. (1984) Weathering. *Progress in Physical Geography*, 8;543-569.
- McKyes, E. and Yong, R.N. (1971) Three techniques for fabric viewing as applied to shear distortion of clay. *Clays and clay minerals*, 19; 289-293.
- McNeal, B.L. et al (1966a) Effect of solution composition on the swelling of extracted soil clays. *Proceedings of the Soil Science Society of America*, 30;313-317.
- McNeal, B.L. and Coleman, N.T. (1966b) Effect of solution composition on soil hydraulic conductivity. *Proc. Soil Science Soc. Amer.*, 30;308-312.
- Meade, R.H. (1964) Removal of water and rearrangement of particles during the compaction of clayey sediments-review. *U.S. Geological Survey Prof. Paper*; 497-8;23, U.S. Government printing office.
- Mearns, R. (1973) Land stabilization by ion-exchange. *Military Engineer*, 425;158-159.
- Melville, R.V. and Freshney, E.C. (1982) *The Hampshire Basin and adjoining areas*. British Regional Geology, HMSO, London. 146pp.
- Mesri, G. and Olson, R.E. (1970) Shear Strength of montmorillonite. *Geotechnique*, 20(3);261-270.
- Mesri, G. and Olson, R.E. (1971) Mechanisms controlling the permeability of clays. *Clays and clay minerals*, 19;151-158.
- Meteorological Office (1982) *Rules for rainfall observers*. Met. Office leaflet No. 6. Bracknell, Berkshire. 12pp.
- Methley, B.D.F. (1986) *Computational models in surveying and photogrammetry*. Blackie, Glasgow. 346pp.
- Mielenz, R.C. and King, M.E. (1955) Physical-chemical properties and engineering performance of clays. *Clays and Clay Minerals*, 1;196-254.
- Mitchell, J.K. (1956) The fabric of natural clays and its relation to engineering properties. *Proceedings of the Highway Research Board*, 35;693-713.

- Mitchell, J.K. (1960) Fundamental aspects of thixotropy in soils. *Journal of the Soil Mech. Found. Div.*, Amer. Soc. Civil Eng., 86(SM3);19-52.
- Mitchell, J.K. (1964) Shearing resistance of soils as a rate process. *Journal of Soil Mech. Engng. Found. Div.*, ASCE, 90(SM1);29-61.
- Mitchell, J.K. (1976) *Fundamentals of soil behaviour*. Wiley, New York. 422pp.
- Mitchell, J.K. et al (1969) Bonding, effective stress, and strength of soils. *Journal of SMFD*, ASCE, 95(SM5);1219-1246.
- Moore, J.G. et al (1977) The effect of leaching on engineering behaviour of a marine sediment. *Geotechnique*, 27(4);517-531.
- Moore, R. (1985) The chemical status of mudslides and its bearing on remedial and preventative measures. In: Morgan, C.S. (Ed.) *Proceedings of the symposium on landslides in the South Wales Coalfield*, p122-123. The Polytechnic of Wales, Pontypridd.
- Moore, R. (1986) *The Fairlight landslips: the location, form and behaviour of coastal landslides with respect to toe erosion*. Occasional Paper 27, Geography Department, King's College London. 43pp.
- Moorman, R.F. (1939) Notes on the principal 'mud-glacier' at Hampstead. *Proc. Isle of Wight Nat. Hist. Archaeol. Soc.*, 3;148-150.
- Morgenstern, N.R. and Tchalenko, J.S. (1967) Microstructural observations on shear zones from slips in natural clays. *Proceedings of the Geotechnical Conference on the shear strength properties of natural soils and rocks*, Oslo, 1;147-152.
- Mori, R. (1964) Some problems on the chemical stability of soils. *Report of the committee of soil chemistry, Association of electro-chemistry*, Tokyo. 48pp.
- Mottershead, D.N. (1982) Rapid weathering of greenschist by coastal salt spray, east Prawle, south Devon: a preliminary report. *Proc. Ussher Soc.*, 5;347-353.
- Moun, J. and Rosenqvist, I.Th (1961) The mechanical properties of montmorillonite and illitic clays related to the electrolytes of the pore water. *Proceedings of the 5th ICSMFE*, 1;263-267.
- Nadeau, P.H. (1987) Clay particle engineering: a potential new technology with diverse applications. *Applied Clay Science*, 2(1);83-93.
- Nemcok, A. et al (1972) Classification of landslides and other mass movements. *Rock Mechanics*, 4;71-8.
- Nir, S. et al (1986) Specific adsorption of Li, Na, K and Sr to montmorillonite. *Soil Science Society of America Journal*, 50(1);40-52.

- Noble, H.L. (1973) Residual strength and landslides in clay and shale. *Proceedings of the ASCE, Journal of SMFED*, 99;705-19.
- Nordstrom, D.K. et al (1979) A comparison of computerised chemical models for equilibrium calculations in aqueous systems. p857-892 In: *Chemical modelling in aqueous systems*, Ed. Jenne, E.A., A.C.S. Symposium Series 93, Washington D.C..
- Norrish, K. (1954) The swelling of montmorillonite. *Discussions of the Faraday Society*, London, 18;120-134.
- Ogwada, R.A. and Sparks, D.L. (1986) Kinetics of ion-exchange on clay minerals and soil: Parts 1 and 2, *Soil Science Soc. Amer. J.*, 50(5);1158-1162.
- Okumura, T. (1981) *International manual for the sampling of cohesive soils*, Tokyo. Tokai Univ. Press. 129pp.
- Ollier, C.D. (1969) *Weathering*. Oliver and Boyd, Edinburgh. 304pp.
- Olson, R.E. (1962) The shear strength properties of Ca-illite. *Geotechnique*, 12(1);23-43.
- Olson, R.E. (1974) The shearing strength of kaolinite, illite and montmorillonite. *Journal of the Geotechnical Engineering Division*, ASCE, 100(GT11);1215-29.
- Olson, R.E. and Mesri, G. (1970) Mechanisms controlling the compressibility of clays. *Journal of Soil Mechanics and Foundations Division*, ASCE, 96;1863-78.
- Pane, V. et al (1983) Effects of consolidation on permeability measurements for soft clay. *Geotechnique*, 33(1);p67.
- Parkhurst, D.L. et al (1985) PHREEQE, a computer program for geochemical calculations. *U.S. Geol. Surv. Water-resources Investigations*. 80-96. 193pp.
- Peck, R.B. (1972) Observations and instrumentation, some elementary considerations. *Highway Focus*, 4;1-5.
- Perrin, R.M.S. (1971) The clay mineralogy of British sediments. *Mineralogical Society (Clay Minerals group) special monograph*, Queen's Gate, London. 247pp.
- Petley, D.J. (1966) *The shear strength of soils at large strains*. Unpublished Ph.D. thesis, University of London.
- Piper, J. (1987) Interaction forces between soil particles: shear moduli of the <2 μm size fraction. *Journal of Soil Science*, 38(1);1-11.

- Plummer, L.N. and Mackenzie, F.T. (1974) Predicting mineral solubility from rate data: application to the dissolution of magnesian calcite. *Amer. J. Sci.*, 274;61-83.
- Plummer, L.N. (1984) Geochemical modelling: a comparison of forward and inverse methods. *First Canadian/Amer. Conf. on Hydrogeology: practical applications of ground water geochemistry*, Alberta, Canada. Reprint 29pp.
- Plummer, L.N. *et al* (1976) WATEQF a computer programme for calculating chemical equilibrium in natural waters. *US Geol. Surv. Water Res. Invest.*, 76-13. 61pp.
- Prior, D.B. (1973) Coastal landslides and swelling clays at Røsnæs, Denmark. *Geografisk Tidsskrift*, 72;1-15.
- Prior, D.B. (1977) Coastal mudslide morphology and processes on Eocene clays in Denmark. *Geografisk Tidsskrift*, 76;14-33.
- Prior, D.B. Stephens, N. and Archer, D.R. (1968) Composite mudflows on the Antrim coast of north-east Ireland. *Geografiskz Annaler*, 50(A);65-78.
- Prior, D.B. and Ho, C. (1970) Bentonite landslides. *Science*, 167;1014-1015.
- Prior, D.B. Stephens, N. and Douglas, G.R. (1971) *Some examples of mudflow and rockfall activity in north-east Ireland*. Inst. Brit. Geogrs. Spec. Publ. 3;129-140.
- Prior, D.B. and Stephens, N. (1972) Some movement patterns of temperate mudflows: examples from north-east Ireland. *Bull. Geol. Soc. Am.*, 83;2533-2544.
- Prior, D.B. and Eve, R.M. (1973) Coastal landslide morphology at Røsnæs, Denmark. *Geografisk Tidsskrift*, 74;12-20.
- Prior, D.B. and Eve, R.M. (1975) Coastal landslide morphology at Røsnæs, Denmark. *Geografisk Tidsskrift*, 76;12-20.
- Prior, D.B. and Suhayda, J.N. (1979) Submarine mudslide morphology and development mechanisms, Mississippi Delta. *Proc. Offshore Tech. Conf.*, O.T.C. 3482, Houston, Texas. p1055-61.
- Prior, D.B. and Renwick, W.H. (1980) Landslide morphology and processes on some coastal slopes in Denmark and France. *Zeitschrift für Geomorphologie*, S.B., 34;63-86.
- Putnam, W.C. and Sharp, R.P. (1940) Landslides and earthflows near Ventura, Southern California. *Bull. Geol. Rev.*, 30;591-600.
- Quigley, R.M. and Gelinas, P.J. (1976) Soil mechanics aspects of shore-line erosion. *Geoscience Canada*, 3;169-173.
- Quigley, R.M. and Gelinas, P.J. (1977) Cyclic erosion - instability relationships: Lake Erie north shore bluffs. *Canadian Geotechnical Journal*, 14;310-23.

- Quirk, J.P. (1968) Particle interaction and soil swelling. *Israel Journal of Chemistry*, 6;213-234.
- Quirk, J.P. (1986) Soil permeability in relation to sodicity and salinity. *Phil. Trans. Royal Society, London*, A316;297-317.
- Quirk, J.P. and Schofield, R.K. (1955) The effect of electrolyte concentrations on soil permeability. *Journal of Soil Science*, 6;163-178.
- Ramiah, B.K. et al (1970) Influence of chemicals on the residual strength of silty clay. *Soils and foundations*, 10;25-36.
- Raymond, G.P. et al (1971) The effect of sampling on the undrained soil properties of a Leda soil. *Canadian Geotechnical J.*, 8(4);546-557.
- Reeve, R.C. (1957) Factors which effect permeability. In: *Drainage of Agricultural Land. American Society Agronomy Monograph*, 7;404-414.
- Reeve, R.C. et al (1954) A comparison of the effects of exchangeable sodium and potassium upon the physical condition of soils. *Proceedings of the Soil Science Society of America*, 18;130-132.
- Richards, L.A. (1954) *Diagnosis and improvement of saline and alkali soils*. United States Department of Agriculture, Agricultural Handbook No. 60. 160pp.
- Riley, J.P. and Chester, R. (1971) *Introduction to marine chemistry*. Academic Press, N.Y. 465pp.
- Roberson, H.E. (1974) Early diagenesis: expansive soil clay sea-water reactions. *J. Sediment. Petrol.*, 44;441-449.
- Rosenqvist, I.Th. (1959) Physico-chemical properties of soils: soil water systems. *Journal of the SMFED, ASCE*, 85(SM2) Part 1;31-59.
- Rosenqvist, I.Th. (1984) The importance of pore water chemistry on the mechanical and engineering properties of clay soils. *Phil. Trans. Royal Society, London*, A311;369-374.
- Rouse, W.C. (1975) Engineering properties and slope form in granular soils. *Quart. J. Engng. Geol.*, 9;327-38.
- Rouse, W.C. and Farhan, Y.I. (1976) Threshold slopes in South Wales. *Quart. J. Engng. Geol.*, 9;327-338.
- Rowe, P.W. (1972) The relevance of soil fabric to site investigation practice. Twelfth Rankine Lecture in *Geotechnique*, 22(2);195-300.
- Russell, D.J. and Parker, A. (1979) Geotechnical mineralogical and chemical interrelationships in weathering profiles in over-consolidated clays. *Quart. J. Engng. Geol.*, 12;107-16.

- Ruxton, B.P. (1968) Measurements of the degree of chemical weathering of rocks. In: *Landform studies in Australia and New Guinea*, Ed. Jennings, J.N. and Mabbut, J.A. p64-87. Cambridge Univ. Press.
- Sankaran, K.S. et al (1972) The influence of structure on deformation and failure in clay soils. *Geotechnique*, 22;669.
- Sayles, F.L. and Manglesdorf, P.C. Jr. (1977) The equilibration of clay minerals with sea-water: exchange reactions. *Geochim. Cosmochim. Acta*, 41;951-960.
- Sayles, F.L. and Manglesdorf, P.C. Jr. (1979) Cation-exchange characteristics of Amazon River suspended sediment and its reaction with sea-water. *Geochim. Cosmochim. Acta*, 43;767-779.
- Schafer, W.M. and Singer, M.J. (1976) Influence of physical and mineralogical properties on swelling of soils in Yolo County, California. *Soil Science Society of America Journal*, 40;557-562.
- Schafer, G.J. and Trangmar, B.B. (1981) Some factors affecting tunnel gully erosion. *Proc. 10th Int. Conf. Soil Mech. Found. Engng.*, Stockholm, 1;481-486.
- Seed, H.B. et al (1964) Clay mineralogical aspects of the Atterberg limits. *Journal of the SMFED*, ASCE, 90(SM4);107-31.
- Selby, M.J. (1982) *Hillslope materials and processes*. Oxford University Press, 264pp.
- Sergeyev, E.M. and Osipov, V.I. (1977) Structural aspects of shearing resistance of clays. *Proc. 9th Int. Conf. Soil Mech. Found. Engng.*, 1;293-294.
- Shainberg, N.I. et al (1987) Charge density and Na-K-Ca exchange on smectites. *Clays and Clay Minerals*, 35(1);68-73.
- Sharpe, C.F.S. (1938) *Landslides and related phenomena: a study of mass movement of soil and rock*. Columbia University Press, New York, 137pp.
- Sherard, J.L. et al (1976) Identification and nature of dispersive soils. *Journal of the Geotechnical Engineering Division*, ASCE, 102(GT4); Proceedings paper 12052;287-301.
- Sherlock, R.L. (1960) *London and the Thames Valley*. British Regional Geology, Institute of Geological Sciences. HMSO, London.
- Sherwood, P.T. (1961) Soil stabilization by the use of chemical admixtures: a review of the present position. *Roads and Road construction*, 39(460);102-111.
- Shridharan, A. (1968) *Some studies on the strength of partly saturated clays*. Unpublished Ph.D. thesis, Purdue University, Lafayette, Indiana.

- Shridharan, A. et al (1971) Shear strength of montmorillonite. *Geotechnique*, 21;180.
- Shridharan, A. and Venkatappa Rao, G. (1973) Mechanisms controlling volume change of saturated clays and the role of the effective stress concept. *Geotechnique*, 23;359-382.
- Shridharan, A. and Jayadeva, M.S. (1982) Double layer theory and compressibility of clays. *Geotechnique*, 32(2);133-144.
- Sidle, R.C. et al (1985) Soil mass movement: influence of natural factors and land use. *American Geophysical Union Water Resources Monograph 11*. American Geophysical Union, Washington DC.
- Siyag, R.S. et al (1984) Predicting transport of three cations in soil columns under conditions of steady-state flow, India. *Geoderma*, 34;281-292.
- Skempton, A.W. (1948) The rate of softening in stiff fissured clays, with special reference to London Clay. *Proc. 2nd Int. Conf. Soil Mech. Found. Engng.*, Rotterdam, 2;50-53.
- Skempton, A.W. (1950) Soil mechanics in relation to geology. *Proceedings of the Yorkshire Geological Society*, 29(3);33-62.
- Skempton, A.W. (1953) The colloidal activity of clay. *Proc. 3rd Int. Conf. Soil Mech. Found. Engng.*, 1;57-61.
- Skempton, A.W. (1957) Stability of natural slopes in London Clay. *Proc. 4th Int. Conf. Soil Mech. Found. Engng.*, London, 2;378-81.
- Skempton, A.W. (1964) The long term stability of clay slopes. *Geotechnique*, 14;77.
- Skempton, A.W. (1970) First-time slips in over-consolidated clays. *Geotechnique*, 20;320-324.
- Skempton, A.W. (1985) Residual strength of clays in landslides, folded strata and the laboratory. *Geotechnique*, 35(1);3-18.
- Skempton, A.W. and DeLory, F.A. (1957) Stability of natural slopes and embankment foundations. *Proc. 7th Int. Conf. Soil Mech. Found. Engng.*, Mexico; *State-of-the-Art* Volume, p291-340.
- Skempton, A.W. and Hutchinson, J.N. (1969) Stability of natural slopes and embankment foundations. *Proc. 7th Int. Conf. Soil Mech.*, Mexico; *State-of-the-Art* Volume, 291-340.
- Skempton, A.W. and Weeks, A.G. (1976) The quaternary history of the Lower Greensand escarpment and Weald Clay vale near Sevenoaks, Kent. *Phil. Trans. Royal Society*, London, A283;493-526.
- Smith, K.A. (1983) *Soil analysis: instrumental techniques and related procedures*. Marcel Dekker Inc., New York. 562pp.
- Soil Instruments (1986) *Instrumentation for soils and rocks*. Uckfield, England. 107pp.

- Spears, D.A. and Taylor, R.K. (1972) Influence of weathering on the composition and engineering properties of *in situ* Coal Measures Rocks. *Inst. Rock Mech. Mining Sci.*, 9;729-756.
- Sposito, G. (1984) *The surface chemistry of soils*. Oxford University Press, New York. 234pp.
- Sposito, G. et al (1986) Ca-Mg exchange on illite in the presence of adsorbed Na. *Soil Science Soc. Amer. J.*, 50(4);905-909.
- Statham, I. (1979) *Earth surface sediment transport*. Clarendon Press, Oxford. pp184.
- Steward, H.E. (1983) *Links between geochemical and engineering properties of weathered pyritic shales*. Unpublished Ph.D. thesis, University of Sheffield.
- Steward, H.E. and Cripps, J.C. (1983) Some engineering implications of chemical weathering of pyritic shale. *Quarterly Journal of Engineering Geology*, 16;281-289.
- Stuckl, J.W. and Banwart, W. (1980) *Advanced chemical methods for soil and clay minerals research*. Rheidel, Holland. 477pp.
- Stumm, W. and Morgan, J.J. (1981) *Aquatic chemistry* (2nd Ed.). Wiley-Interscience, New York. 780pp.
- Sutton, B.H.C. (1984) *Solution of problems in soil mechanics*. Pitman, London. 310pp.
- Tavenas, F. et al (1983) The permeability of natural soft clays: Part 2, permeability characteristics. *Canadian Geotechnical Journal*, 20;645-660.
- Taylor, A.W. (1959) Physico-chemical properties of soils: ion-exchange phenomena. *Proc. Soil Mech. Found. Div., ASCE*, (SM2);19-29.
- Taylor, R.K. and Cripps, J.C. (1987) Weathering effects: Slopes in mudrocks and over-consolidated clays. In: Anderson, M.G. and Richards, K.S. (Eds), *Slope Stability*, p405-445. Wiley.
- Taylor, R.K. and Smith, T.J. (1986) The engineering geology of clay minerals: swelling, shrinking, and mudrock breakdown. *Clay Minerals*, 21;235-260.
- Tchalenko, J.S. (1968) The microstructure of London Clay. *Quart. J. Engng. Geol.*, 1(3);155-168.
- Terzaghi, K. (1929) The mechanics of adsorption and of the swelling of Gels. *Colloid Symposium Monograph*, p58-78. Chemical Catalogue Co. Inc., New York.
- Terzaghi, K. (1931) The influence of elasticity and permeability on the swelling of two phase systems. In: Alexander, J. (Ed.), *Colloid Chemistry*, 8;65-88. Chemical Catalogue Company, New York.

- Terzaghi, K. (1936) The shearing resistance of saturated soils and the angles between the planes of shear. *Proc. 1st Int. Conf. Soil Mech. Found. Engng.*, 1;54-56.
- Terzaghi, K. (1950) Mechanisms of landslides. Geological Society of America, *Engineering Geology*, 83;123.
- Thornes, J.B. and Brunsden, D. (1977) *Geomorphology and time*. Methuen, London. 208pp.
- Torrance, (1983) Towards a general model of quick clay development. *Sedimentology*, 30;547-555.
- Townsend, R.P. (1984) Thermodynamics of ion exchange in clays. *Phil. Trans. Royal Society*, London, A311;301-314.
- Trenhaile, A.S. and Mercan, D.W. (1984) Frost weathering and the saturation of coastal rocks. *Earth Surf. Proc. Land.*, 9;321-331.
- Trudgill, S.T. (1976) Rock weathering and climate: quantitative and experimental aspects. In: Derbyshire, E. (Ed.), *Geomorphology and climate*, p59-99. Wiley, London.
- Trudgill, S.T. (1986) *Introduction to Solute Processes*. Wiley, Chichester. 512pp.
- Van Olphen, H. (1977) *An Introduction to Clay Colloid Chemistry*. 2nd Edition. Wiley, New York. 318pp.
- Van Olphen, H. (1986) Long-range forces: flocculation, deflocculation and osmotic swelling. In: Cairnes-Smith, A.G. and Hartmann, H. (Eds.) *Clay minerals and the origin of life*, p57-63. Academic Press.
- Varnes, D.J. (1958) Landslide types and processes. In: Eckel, E.B. (Ed.) *Landslides and engineering practice*. Highway Research Board Special Report, 29, NAS-NRC Publication, 544;20-47. Washington D.C.
- Varnes, D.J. (1975) Slope movements in the Western United States. In: *Mass Wasting*, Proc. 4th Guelph Symp., Geo Abstracts. p1-17.
- Vaughan, P.R. (1973) The measurement of pore water pressure with piezometers. In: Penman, A.D.M. (Ed.) *Field instrumentation in geotechnical engineering*, p411-422. Butterworths, London.
- Vickers, B. (1983) *Laboratory work in soil mechanics*. Granada. 170pp.
- Visvalingham, M. and Tandy, J.D. (1972) The neutron method for measuring soil moisture content: a review. *J. of Soil science*, 23;499-509.

- Walsh, J.N. (1982) Whole rock analysis by Inductively Coupled Plasma. *Inst. Min. Metal.*, 79;91.
- Ward, R.C. (1975) *Principles of Hydrology*. (2nd Edition), McGraw-Hill, London. 367pp.
- Warkentin, B.P. and Bozozuk, M. (1961) Shrinking and swelling properties of two Canadian clays. *Proc. 5th Int. Conf. Soil Mech. Found. Engng.*, Paris, 1;851-55.
- Weaver, C.E. and Pollard, L.D. (1975) *The Chemistry of Clay Minerals*. Elsevier, Amsterdam. 213pp.
- Webb, D.A. et al (1986) Thermal analysis of ion-exchanged montmorillonite. *Particle Science and Technology* (U.S. Bureau of mines), 4;131-142.
- Weeks, A.G. (1961) The stability of natural slopes in south-east England as affected by periglacial activity. *Quart. J. Engng. Geol.*, 2;49-62.
- Wesley, L.D. (1977) Shear strength properties of halloysite and allophane clays in Java, Indonesia. *Geotechnique*, 27(2);125-136.
- White, R.E. (1979) *Introduction to the principles and practice of soil science*. Blackwell, Oxford. 198pp.
- White, W.A. (1955) *Water sorption properties of homoionic clay minerals*. Unpublished Ph.D. thesis, University of Illinois, Urbana.
- Williams, A.A.B. and Donaldson, G.W. (1980) Building on expansive soils in South Africa, 1973-1980. *Proc. 4th Int. Conf. on Expansive Soils*, ASCE, Denver, p834-844.
- Williams, G.M. (1971) *The stratigraphy and micro-palaeontology of the London Clay*, Unpublished Ph.D. thesis, University of London.
- Williams, R.B.G. and Robinson, D.A. (1981) Weathering of sandstones by the combined action of frost and salt. *Earth Surf. Proc. Landf.*, 6;1-9.
- Wolf, P.R. (1985) *Elements of photogrammetry*, 2nd Edition. McGraw-Hill, London. 628pp.
- Wooding, R.A. and Schafer, G.J. (1979) Studies on erosion rates in soil. *Working papers workshop on soil physics and field heterogeneity*. CSIRO Division of environmental mechanics. p19-28. Canberra, Australia.
- Wooldridge, S.W. and Linton, D.L. (1955) *Structure, surface and drainage in south-east England*. George Philip and Son Ltd., London. p1-176.

- Yariv, S. and Cross, H. (1979) *Geochemistry of colloid systems*, p287-302. Springer-Verlag, Berlin.
- Yatsu, E. (1966) *Rock control in geomorphology*. Sozosha, Tokyo. 347pp.
- Yatsu, E. (1967) Some problems on mass movements. *Geogr. Ann. Ser. A.*, 49 (2-4);396-401.
- Yong, R.N. (1961) Characteristic and limiting slope angles. *Zeitschrift für Geomorphologie*, 5;126-31.
- Yong, R.N. and Warkentin, B.P. (1966) *Introduction to soil behaviour*. Macmillan, New York. 451pp.
- Yong, R.N. and Warkentin, B.P. (1975) *Soil properties and behaviour*. Elsevier, Amsterdam. p335-359.
- Yong, R.N. and Sethi, A.J. (1977) Influence of amorphous material on soil performance and its relation to environmental weathering. p437-450, *Proceedings of a Special Session on Geotechnical and Environmental Control*. The 9th Int. Conf. Soil Mech. Found. Engng., Tokyo. MAA publishing company.
- Zaruba, Q. and Mencl, V. (1969) *Landslides and their control*. Academia and Elsevier, Prague, 205pp.
-

APPENDIXES

Appendix 1

CORE-SAMPLING TECHNIQUE: FIELD PROCEDURE

Equipment and materials:

1. thin-walled open-drive core sampler with percussion head;
2. pre-cut plastic sample tubes 0.75-1.5 m in length;
3. aluminium density tubes 110 mm by 30 mm, end caps and percussion sampler;
4. parafilm sealing material, marker pens and 3 m tape;
5. cotton bags, sealing wax and rubber bands;
6. a 15lb sledge hammer and smaller club hammer;
7. spades and trowels, and;
8. hand-drill with 7 mm bit.

Method:

- a. locate pre-arranged sampling position and survey using theodolite;
- b. prepare site for sampling by removing surface vegetation and debris;
- c. take surface density sample using a pre-weighed and labelled density tube and sampler. The tube was inserted flush with the ground level with regular blows using the percussion drive. The tube was then extracted using a trowel, and the ends are sealed with parafilm and end caps;
- d. adjacent to the density sample a core sample tube was placed vertically with cutting edge down, and the sampler percussion head placed on top (ensuring the air vent was free with a 7mm drill bit). Using the sledge hammer, the tube was driven into the ground as quickly and continuously as possible. The tube was inserted to the basal shear surface and beyond. This was noticed by a marked change in the resistance to penetration beyond the shear zone;
- e. following insertion, the percussion head was removed and the top end of the core sealed with parafilm and covered with a protective cotton bag;
- f. the core sample was retrieved by excavating the surrounding material, taking care not to damage or disturb the tube;
- g. the ground surface level and position of the basal shear surface were marked on the tube along with the core catalogue number;
- h. the core was moved to shear the soil below the tube end, lifted from the hole, and the lower end sealed with parafilm and protective cotton bags;
- i. a second density tube sample was taken from the base of the excavated hole using a pre-weighed and labelled density tube and drive sampler;
- j. the weight of the density tubes (to 3 decimal places) was established in the field after cleaning, and further sealed for transportation;
- k. each core sample was doubly sealed with parafilm, cleaned, and the ends protected with padded cotton bags for transportation.

Appendix 2

LABORATORY DETERMINATION OF PARTICLE-SIZE DISTRIBUTION

Introduction:

Traditionally the particle-size distribution is measured using standard wet and dry sieving and sedimentation techniques (BS 1377, 1975). It is also common practice to analyse the coarse component separately from the fines. The coarse particles are best and most accurately assessed by dry sieving; fine particles are less satisfactorily measured and generally use sedimentation methods based on the principle of Stoke's law. Errors arise from the latter method since Stoke's law assumes the sedimentation of spherical particles with a uniform particle density. Fines containing a large proportion and variety of platy clay particles are, thus, likely to be underestimated because of shape and mineralogical differences.

Recent advances in analytical methods have shown that laser diffraction techniques may significantly improve the estimation of fine particles. Since an accurate estimation of the proportion of clay particles was required for a large number of samples, a two-stage analysis was adopted in this study: following sample pre-treatment to disperse particle aggregations, the coarse fraction ($>500\text{ }\mu\text{m}$) was separated from the fines, and measured by dry sieving. The fine component was analysed and computerised by a Malvern Particle Sizer, and the sample particle-size distribution re-calculated to include the coarse component.

Equipment and materials:

1. a nest of British Standard sieves ($>50\text{ }\mu\text{m}$);
2. a mechanical sieve shaker;
3. a Malvern Particle Sizer and computer;
4. weighing balance to 3 decimal places and foil dishes;
5. drying oven set at 105°C ;
6. a riffle-sampler;
7. dispersants: 27-30% H_2O_2 , 10% Calgon, 2M HCl;
8. distilled water.

Pre-treatments:

- a. 250 g of sample was riffled to approximately 120 g, and accurately weighed (w_1);
- b. the sample was transferred to a large beaker, to which 100 ml of H_2O_2 was added. The combustion of organic matter was observed for 30 minutes and the beaker and sample gently heated and stirred. Further applications of 20 ml were added until no reaction was observed. The sample was left to dry over-night, and re-weighed (w_2). The loss in weight (w_1-w_2) was expressed as the % organic matter.
- c. the sides of the beaker were washed down with distilled water, and the sample diluted to 200 ml. 50 ml of Calgon dispersant was added and the sample vigorously stirred in a homogenizer for 30 minutes. 25 ml of HCl was added to breakdown any amorphous oxides and the sample further agitated;
- d. the dispersed slurry was passed through a B.S. 0.5 mm aperture sieve, and washed with distilled water. The particles retained

were quantitatively transferred to a foil dish, dried in an oven, and weighed. Likewise, the slurry passing through the sieve was transferred to a foil dish, dried and weighed. The two separates were stored in sealed and labelled plastic bags for future analysis.

Sieve analysis of the coarse component:

1. the coarse particles were measured using three mesh sizes: 0.5 mm, 1 mm and 2 mm. The nest of sieves were cleaned and prepared for use on the mechanical shaker. The coarse sample was carefully placed on the 2 mm sieve, covered, and shaken for 30 minutes;
2. the weight of particles retained on each mesh was quantitatively measured by carefully brushing them onto a foil weighing dish. Pebbles greatly in excess of 2 mm in diameter were weighed and measured independently;
3. the per cent of particles retained on each sieve was calculated from the total weight of coarse particles separated after pre-treatment.

Laser diffraction of the fine component:

1. using a Malvern Particle Sizer, the sample powders separated following pre-treatment, were analysed over the range 0.5mm (500 μ m) to 0.5 μ m, using three optical lenses. The apparatus was operated using the Easy Sizer computer menu, and the ultrasonic bath was primed. After controlled experiments the lens-range most suitable for this application was found to be 188 μ m-1.9 μ m because all particles were found to fall below 100 μ m;
2. about 1.0 g of powdered sample was added to the ultrasonic water bath to which 10 ml of Calgon was added. The intensity of detection of the sample in the water bath was monitored and displayed by the computer enabling the adjustment of the quantity of sample added to optimum conditions. The sample was left for 5 minutes to ensure the complete breakdown of aggregates. For untreated samples a longer period of disaggregation is recommended to ensure accurate estimations of the proportion of clay.
3. the suspended sample was analysed by laser diffraction integrated over a 20 second timescale. The computer processed the data to provide (1) a completely calculated and tabulated results sheet, (2) the particle size distribution, and if requested (3) a bar histogram. Further data analysis was possible since the sample results were stored on floppy discs.

References: Loveday (1974); British Standards 1377 (1975); Vickers (1983).

Appendix 3

MOISTURE CONTENT DETERMINATIONS AND FIELD BULK DENSITY

Introduction.

The accurate determination of moisture content was required for a large number of laboratory tests and field samples. Samples obtained directly from the field and those retained in the cores were assessed using standard techniques in a variety of states: natural, saturated, and air-dry. The procedures are outlined below, followed by the method used to determine field bulk density.

Equipment and materials:

1. 30 mm by 200 mm aluminium density tubes and rubber end caps;
2. parafilm sealing material;
3. balance accurate to three decimal places with foil dishes;
4. drying oven set at 105°C, and;
5. vacuum desiccator;

Method A. Natural moisture content:

- a. samples set aside from the core sub-sampling programme were immediately placed on pre-weighed (w1) foil dishes and weighed to 3 d.p. (w2).
- b. the sample and dish were placed in a drying oven for 48 hours.
- c. after drying the sample was transferred to a desiccator and allowed to cool.
- d. the sample WAS re-weighed when cool (w3).
- e. the per cent natural moisture content Wn was calculated as follows:

$$Wn = \frac{w2 - w3}{w3 - w1} * 100\%$$

Method B. Air-dry moisture content:

The same procedure and calculations were used in the assessment of air-dry moisture content (Wa), except air-dried samples set aside for chemical tests were used. These samples had been placed in large foil dishes, covered, and allowed to 'air-dry' in the laboratory for fourteen days before measurement.

Method C. Saturated moisture content:

The saturation percentage was assessed from the addition of a known volume of water to a sample of air-dry soil of known moisture content.

- a. approximately 20 g of air-dry soil was weighed to 3 d.p. (w2) in a pre-weighed mixing cup (w1).
- b. distilled water was added from a graduated burette until the soil became saturated. At saturation the soil glistened, and flowed slightly upon tipping the cup. The sample was sealed and left to

- stand for one hour.
- c. if the soil was still glistening after one hour, the cup and sample were weighed to 3 d.p. (w3) and placed in a drying oven for 48 hours. If not, further water was added and the sample left to mature for a further hour until completely saturated. Finally the volume of water added was noted from the burette.
 - d. after 48 hours and when cool, the dry weight of sample was measured to 3 d.p. (w4).
 - e. the saturated moisture content was calculated as follows:

$$1. \text{ Total H}_2\text{O (g)} = T = \text{wght of H}_2\text{O} + W_a * [(w2-w1) - (w4-w1)]$$

$$2. W_s = \frac{(T)}{w4 - w1} * 100\%$$

Method D. Determination of field bulk density:

Density tube samples were obtained, weighed (w2) and measured in the field as described in Appendix 1. Each tube was of known weight (w1) and volume (v).

- a. on reception at the laboratory the tube and sample were re-weighed to 3 d.p. (w3). The tube and sample were placed in a drying oven for 48 hours.
- b. the tube and sample were transferred to a desiccator and allowed to cool before weighing (w4).
- c. the field moisture content and bulk density were calculated as follows:

$$W_n = \frac{w2 - w4}{w4 - w1} * 100\%$$

$$BD = \frac{w2 - w1}{v}$$

References: British Standards 1377 (1975); Richards (1954).

Appendix 4

DETERMINATION OF SPECIFIC GRAVITY

Equipment and materials:

1. 50 ml capacity density bottles with stoppers, numbered and calibrated;
2. vacuum desiccator and vacuum supply;
3. constant water bath maintained at 25°C;
4. drying oven kept at 105°C;
5. balance to 4 d.p.;
6. wash bottle with de-aired distilled water;
7. plastic gloves;
8. small riffle sampler.

Procedure:

- a. thoroughly clean and dry density bottles and stoppers.
- b. weigh bottle and stopper to 4 d.p. (w1).
- c. prepare an oven dried (80°C) <2 mm specimen sample.
- d. the sample was riffled into three and placed in separate density bottles.
- e. weigh each bottle, stopper and sample to 4 d.p. (w2)
- f. add ≈20 ml de-aired distilled water sufficient to cover sample, and apply vacuum.
- g. the sample was agitated every hour until air was completely removed, leaving over night.
- h. completely fill density bottle with de-aired distilled water and transfer to a temperature bath at 25°C for one hour.
- i. if the volume of water decreases after one hour, remove stopper and top-up, and repeat if necessary.
- j. remove bottle and dry exterior, and weigh to 4 d.p. (w3).
- k. thoroughly clean bottle and stopper, fill with de-aired distilled water, and weigh to 4 d.p. (w4).
- l. the specific gravity was calculated using a computer program based on the following calculation:

$$G_s = \frac{w_2 - w_1}{(w_2 + w_4) - (w_1 + w_3)}$$

- m. with a knowledge of the natural and saturated moisture contents of the sample, the phase relationships were further analysed by computer to include:

void ratio $e = G_s * W_s$

porosity $n = \frac{e}{1 + e}$

unit weight (UW) $\gamma = \frac{G_s(1 + W_n)}{1 + e} * \gamma_w$ where $\gamma_w = 9.81 \text{ kN/m}^3$
unit weight of water.

bulk density $\rho = \frac{G_s(1 + W_n)}{1 + e} * \rho_w$ where $\rho_w = 100 \text{ kg/m}^3$
density of water.

References: British Standards 1377 (1975); Craig (1983); Head (1984).

Appendix 5

Consistency limits.

Equipment and materials:

1. liquid limit apparatus (cone penetrometer and timer) and sample cups;
2. plastic boards;
3. spatulas and palette knives;
4. vernier callipers, and;
5. distilled water.

Method A. Liquid limit:

- a. samples of natural soil set aside for residual strength testing were also used for the assessment of the liquid and plastic limits. A 100g sample placed on a plastic board was cut into small pieces with a cheese wire and moistened with distilled water. The sample was left to mature for 30 minutes.
- b. after 30 minutes the sample was thoroughly remoulded using a palette knife. Where necessary more water was added to ease this process. A small 20g sample was set aside for plastic limit determination (Method B) before adding too much water.
- c. the sample was worked into a homogeneous paste with the addition of more water; any coarse particles were removed. The sample was covered and left to mature for 2 hours.
- d. the cone penetrometer was primed and calibrated.
- e. soil paste was pressed into the sample cup. Every effort was made to prevent trapping air by adding soil to the side walls until the container was full. The sample was finally pressed down and the surface smoothed off level with the rim of the cup.
- f. the cone and support was lowered carefully until the tip of the cone just touched the sample surface. By moving the sample slightly sideways the cone tip just marked the surface. The dial gauge reading was set to zero.
- g. the timer was triggered and the cone allowed to fall for 5 seconds. The cone was automatically locked and the penetration measured by the dial gauge to the nearest 0.1 mm.
- h. the cone was cleaned and the sample re-levelled. The penetrometer was re-set and a second measurement taken. This was repeated five times for each stage of the test providing the variation of recordings did not exceed 1 mm. A small sample was then transferred to a pre-weighed foil dish and the moisture content determined using the method outlined in Appendix 3A.
- j. the sample was then further wetted and the next sample of higher moisture content similarly measured by the cone penetrometer, as in f above.
- k. the regression of the mean penetration versus moisture content was plotted with five increments of moisture content for each sample, and the liquid limit interpolated as the per cent moisture content enabling a penetration of 20 mm.

Method B. Plastic limit:

- a. the sample set aside at the beginning of the liquid limit determination was moulded into a ball once sufficiently plastic to facilitate this process. If not, more water was added and the sample allowed to mature. The sample was split into four equal segments.
- b. each sample was rolled-into a thread about 6 mm in diameter using the thumb and first finger of each hand. The thread must be intact and homogeneous. By rolling the thread between the hand and plastic board, with slight pressure the diameter of the thread was reduced to 3 mm. A uniform rolling pressure was maintained throughout, and callipers used to measure the diameter of the threads for accuracy.
- c. this process was repeated for all samples until the thread started to crumble at 3 mm in diameter. The crumbs were transferred to a foil dish and weighed and the moisture content determined using the method outlined in Appendix 3A.
- d. an average moisture content was calculated from the four samples, which defined the % plastic limit.

The liquid and plastic limits were used to calculate the plasticity index (Ip) and activity ratio (AR) using the following equations:

$$I_p = LL - PL \%$$

$$AR = \frac{I_p}{\%Clay}$$

References: Head (1984); British Standards 1377 (1975); Vickers (1983).

Appendix 6

DETERMINATION OF DRAINED SHEAR STRENGTH PARAMETERS

Equipment and materials:

1. triaxial compression apparatus (sample lathe & confining sheaths).
2. Bromhead ring-shear apparatus with proving ring and weight accessories;
3. two electronically recording load cells;
4. an interface unit linking the load cells to a BBC metrawatt chart recorder;
5. constant head tank and tubing connections to the ring-shear sample cell, and;
6. an adapted ring-shear sample cell to allow the introduction and collection of pore water fluids during strength testing.

Method A. Triaxial compression determination of τ_p or τ_{cv} .

- a. trim each specimen to approximately 80 mm in length by 38 mm in diameter using the soil lathe, enclose in a rubber membrane with porous stones at both ends, and place in the triaxial cell.
- b. seal the cell and fill with water and adjust the cell pressure to establish a principle or confining stress.
- c. allow the sample to saturate by manipulating the cell and pore water pressures until fully saturated and equilibrium established; the confining and pore water pressures were monitored throughout the test.
- d. once equilibrium was established the first increment of effective stress was applied. In the tests undertaken in this research the first increment was set at 100 kPa. Further increments of stress were set at 200 kPa and 300 kPa for the remaining test specimens.
- e. the total vertical or principle stress σ_1 and the confining stress σ_3 were used to calculate the deviatoric stress (or the additional load applied to the proving ring to initiate sample failure). For each increment of load Mohr circles of stress were plotted to obtain the peak strength envelope of each sample.

Method B. Standard measurement of residual shear strength:

- a. material set aside from each core sample was used to determine the residual strength parameters. Each sample was tested by remoulding material into the annular sample cell cavity, and levelled flush with the cell rim.
- b. an offcut of the material was placed on a foil dish and assessed for moisture content using the method outlined in Appendix 3A.
- c. the lower sample cell was secured to the ring shear with two thumb screws and the loading platen positioned on top. The loading arm was brought into contact with the loading platen and the vertical dial gauge set to zero. The load cell jacks were positioned to locate the loading platen lugs using the innermost positions for low stress levels.
- d. the previously calibrated load cells were set to zero via an interface unit and a base line established on the chart recorder.
- e. the sample bath was filled with distilled water and the first

- increment of load applied via the 10:1 ratio lever arm.
- f. following initial rapid consolidation, the sample turret was rotated through a minimum of 720° to develop a shear surface and the residual condition. The sample was left for 2 hours to equilibrate.
- g. the sample was then sheared at a displacement of 0.032° per minute, and the load transmitted through the sample was traced on the chart recorder. Once the load registered had reached a constant value, further weights were placed on the lever arm to the next increment of normal load. The change in stress transmitted through the sample was continuously monitored via the interface and chart recorder.
- h. seven increments of load were used to establish the shear strength envelope, and immediately following test the final moisture content was assessed using the procedure outlined in Appendix 3A.
- i. the increments of load used in the standard tests were 100, 200, 400, 600, 800, 1000, and 1200 newtons. The effective normal load and residual shear strength were calculated from the load cell calibrations and the following equations using a BASIC computer programme:

$$1. \text{ residual strength } \tau = \frac{3 (F_1 + F_2) L}{4\pi (R_2 - R_1)}$$

where F = load transmitted (two load cells)
R = the inner and outer sample radius (R₂=inner)
L = distance between load cell jacks.

$$2. \text{ effective normal stress } \sigma' = \frac{P}{\pi(R_2 - R_1)}$$

where P = vertical load applied.

3. the ratio of strength to effective stress was also computed (eq.1 / eq.2), and assuming cohesion to be zero, the residual friction angle ϕ_r' was calculated from the Mohr-Coulomb relationship (section 2.32):

$$\text{residual shear strength } \tau_r = c_r' + \sigma' \tan \phi_r'$$

Method C. Simulation of strength under different chemical conditions.

- a. as for stages a and b in Method B above.
- b. a rubber gasket was placed under the cell secured with the thumb screws to allow the flow of solution up through the sample cavity.
- c. the ring-shear was primed as for the standard procedure, except that proving rings were used in place of the load cells. The rings were set to zero.
- d. the constant head bath was filled with solution of known chemistry, and positioned 1 metre above the sample. The bath was connected to the cell with plastic tubing via a stopcock valve and a 4-way connector to four brass-nippled inlets on the lower cell block. Solution was allowed to flow through the sample under the small head-pressure. The sample cell was de-aired via a stopcock valve on the upper loading platen, and post-flow solution collected via four outlet tubes.
- e. weights were placed on the lever arm and the residual condition

- established as in f above.
- f. the sample was sheared at 0.032° per minute until the load transmitted to the proving rings was constant. Stress readings were recorded and a post-flow sample collected for future chemical analysis.
 - g. at this stage a solution of different chemistry was allowed to flow through the sample; the composite flow system was thoroughly washed with distilled water to prevent contamination. However, distilled water was not flushed through the sample for reasons discussed in section 2.312.
 - h. pH and conductivity readings were routinely taken for the pre- and post-flow solutions.
 - i. the normal load used in test was 1000N and was held constant for all tests. The effective normal load and shear stress were calculated using purpose-written computer programmes as in stage 1 in Method B, above.

References: Bromhead (1979); Steward (1983); Steward and Cripps (1983).

Appendix 7

CLAY MINERAL IDENTIFICATION AND MICRO-FABRIC ANALYSIS

Introduction:

Particular attention was given to the identification of clay minerals and the micro-fabric of intact soil material. Quantitative estimations of clay minerals are rarely obtained and only possible with extensive analysis and cross-referencing with standard minerals. Semi-quantitative assessments are most commonly employed in laboratory practice and may be obtained using less comprehensive and time-consuming methods. A variety of tests may be used in such analysis mostly revolving around X-ray diffraction techniques. Based on Bullock and Loveland (1974), Method A was adopted in this study to enable a large number of analyses to be undertaken with reasonable accuracy and reproducibility. A scanning electron microscope and micro-probe were used to study the micro-fabric of intact core specimens and the procedures used are detailed in Method B. Assessments and comparisons of each technique were also facilitated from chemical calculations (see section 4.46).

Equipment and materials:

1. Philips X-ray diffractometer;
2. Hitachi scanning electron microscope and micro-probe;
3. clay mineral separation (Appendix 9E, part a);
4. microscope glass plates and pressed powder holders;
5. ultrasonic stirrer and 10% calgon;
6. platinum/gold preparation facilities for intact SEM stubs;
7. 1N potassium and magnesium exchange solutions;
8. furnace set at 110°C, 330°C and 550°C;
9. disposable glass pipettes;
10. distilled water;

Method A Semi-quantitative estimation of clay minerals:

- a. following the pre-treatment and separation of clay minerals described in Appendix 2 and Appendix 9E, respectively, the crystalline minerals were identified by X-ray diffraction. A variety of slides were prepared to enable a process of elimination of the various clay minerals.
- b. powdered clay was pressed onto an indented microscope slide and covered with a glass plate. The sample was analysed by XRD by rotating the sample from 2° from the horizontal to 55°.
- c. ultrasonically dispersed clay was applied to three glass plates and the particles allowed to develop a preferred orientation. One of these plates was left to dry naturally, another dried in a glycolated atmosphere, and the other heated to 550°C. The first specimen was rotated through 30°, and the latter two through 13°.
- d. ultrasonically dispersed clay was also treated with saturated solutions of potassium and magnesium. Four slides were prepared with potassium-saturated solution and allowed to orientate naturally. One was left to air-dry, and the other three were heated to 110°C, 330°C and 550°C, respectively. All samples were rotated through 13°. Magnesium-saturated dispersed clay was allowed to orientate naturally on two more glass plates, one was air-dried and the other dried in a warm glycolated atmosphere.

Others were heated as for the potassium-saturated samples. The orientated Mg-saturated sample was analysed by XRD from 2° to 30°, and the glycolated plate from 2° to 13°.

- c. the clay mineral species were identified by observing and comparing the spacing and peaks of the diffractometer traces. Ethylene glycol differentiates smectite from vermiculite and chlorite. Vermiculite and smectite collapse on heating to 330°, and kaolinite on heating to 550°. Potassium and magnesium exchangers are used to emphasise the kaolinite and smectite peaks.
- d. a semi-quantitative estimate of the proportions of the different clay mineral groups was established from peak areas, peak intensities and supplementary chemical and physical analyses. The relative proportions of expansible mineral and mica groups were obtained by comparing the 10Å reflection of a glycolated sample with that after heating to 330° and dividing the difference by 2. Relative peaks show which expansible minerals are present. Non-exchangeable K₂O values (Method 9E) give an approximate indication of the amount of mica present. Kaolinite and chlorite are weighted in relation to mica by dividing their peak areas by 3 and 2 respectively. Cation exchange capacity may also be used to supplement X-ray diffraction data in the following manner:

Kaolinite- <3.5% K₂O, CEC <30 me/100g, dominant on XRD trace

Smectite- >45me/100g and more smectite than vermiculite

vermiculite- >45me/100g and more vermiculite than smectite

micaceous- other clays with > 3.5% K₂O

mixed- other clays

Method B Micro-fabric observation and micro-probe analysis:

- a. in-tact specimens of core sample were set aside for SEM analysis (section 3.411). Using a sharp edge the sample was split exposing an unsmear surface. The sample was placed on a stub and coated with a platinum/gold conductive coating. The samples were kept in a desiccator for 48 hours before analysis.
- b. a routine was established that involved the observation of each stub in the SEM, the isolation of fabric and particles of interest, followed by an area and fissure point chemical analysis by the microprobe to note any preferential staining along discontinuities. A data sheet was designed to catalogue sample details, photograph numbers, and the probe analytical details.

References: Avery and Bascombe (1974); Avery and Bullock (1977); Brindley and Brown (1984); Chen (1977).

Appendix 8

DETERMINATION OF ORGANIC MATTER

Equipment and materials:

1. muffle furnace set at 850°C;
2. vitreosil crucibles, tongues and protective gloves;
3. balance to 3 d.p.;
4. vacuum desiccator;
5. 10% H₂O₂;
6. drying oven;
7. fume cupboard, and;
8. heating plate and stirrer.

Method A. Loss on ignition:

- a. labelled vitreosil crucibles were placed in a pre-heated furnace at 850°C for one hour.
- b. the crucibles were transferred to a desiccator, allowed to cool and weighed to 3 d.p. (w1).
- c. 1 g of soil was accurately weighed in the crucible to 3 d.p. (w2), and placed in the furnace for one hour.
- d. after 1 hour the sample was transferred to a desiccator, and allowed to cool. When cool the crucible and sample were weighed to 3 d.p. (w3).
- e. the loss on ignition was calculated as follows:

$$LOI = \frac{w2 - w3}{w2 - w1} * 100\%$$

Method B. Organic or wet combustion by hydrogen peroxide.

This method has already been described in Appendix 2, under the pre-treatment methods for the particle size analysis, to which the reader is referred.

References: Avery and Bascombe (1974); Loveday (1974).

Appendix 9

SOIL-WATER CHEMICAL ANALYSIS

Equipment and materials:

1. bench centrifuge; -
2. polyethylene centrifuge tubes and caps (30 ml & 100 ml capacity);
3. balance accurate to 3 d.p.;
4. vitreosil crucibles;
5. shaker;
6. flame photometer;
7. atomic adsorption spectrometer;
8. Dionex ion-chromatograph and base solutions;
9. auto continuous flow analyser;
10. inductively coupled plasma source spectrometer;
11. micro-burette and titration equipment;
12. double-distilled water;
13. Arklone immiscible fluid;
14. 0.5M BaCl₂;
15. 0.01M MgSO₄;
16. concentrated Hydrofluoric acid;
17. concentrated Hydrochloric acid;
18. Ferrozine reagent;
19. Thioglycollic acid;
20. Catechol violet reagent;

Method A. Interstitial water extraction (centrifuge method):

- a. weigh a clean labelled 100 ml centrifuge tube and lid (w1) and add ~150g of saturated sample and reweigh (w2). An offcut was set aside and the moisture content (Wn) assessed using the method already described (Appendix 3A).
- b. add 20 ml of Arklone (1,1,2 - trichloro - 1,2,2 - trifluoroethane) to cover soil surface and secure lid. This stage should be carried out in a fume cupboard, because Arklone has a low boiling point (40°C) and is denser than water. Thus pore water was separated from the clay interface.
- c. centrifuge at 4000 r.p.m for 2 hrs. To improve results a refrigerated centrifuge at 10,000 r.p.m. is preferable.
- d. remove centrifuge tube and decant free water from the surface of the Arklone to a pre-weighed sample bottle (w3) and accurately weigh extract (w4). The extract was chemically analysed (Method 9F).
- e. the yield of extract was calculated from the equation:
 1. wt of water in sample SW(g) = (w2 - w1) * Wn
where totally saturated Wn = Ws = 1.
 2. wt of water extract SE(g) = w4 - w3
 3. % yield = $\frac{SE}{SW} * 100\%$

Method B. Water soluble cations:

- a. in a weighed (w1) and labelled 30 ml centrifuge tube accurately weigh 10 g of <2mm air-dried soil (w2). Add 20 ml distilled water and shake for 30 minutes.
- b. transfer tube and sample to a bench centrifuge and spin at 1500 r.p.m. for 10 minutes. Collect supernatant for chemical analysis (Method F).

Method C. Exchangeable cations:

- c. weigh the tube and soil cake (w3), and add 20 ml of 0.5M BaCl₂ and agitate for 30 minutes.
- d. transfer tube and sample to centrifuge and spin at 1500 r.p.m. for 10 minutes. Collect supernatant for chemical analysis (Method F).

Method D. Cation-exchange capacity:

- e. weigh the tube and soil cake (w4). Agitate and wash soil cake with distilled water. Centrifuge and discard supernatant. Re-wash until all traces of BaCl₂ have dispersed. If excessive amounts of carbonates are present further pre-treatment is required as described in Appendix 2.
- f. add to the sample 20 ml 0.01 MgSO₄ and agitate for 30 minutes.
- g. transfer to centrifuge and spin at 1500 r.p.m. for 10 mins.
- h. collect supernatant and assess the concentration of magnesium (Method F) in addition to samples of the original solutions.
- i. weigh soil cake (w5) and discard.

Volume adjustments are made to calculate the final concentrations:

$$\text{where [Conc. of water soluble cations]} = \frac{\text{Reading (mg/l) [R]}}{\text{Dilution factor [DF]}}$$

$$\text{For Method B: DF} = \frac{10\text{g (soil)} - W_a(w2-w1)}{20\text{g (water)} - (w3-w2)}$$

$$\text{For Method C: DF} = \frac{10\text{g (soil)} - W_a(w2-w1)}{20\text{g (water)} - (w4-w3)}$$

$$\text{For Method D: DF} = \frac{10\text{g (soil)} - W_a(w2-w1)}{20\text{g (water)} - (w5-w4)}$$

Method E. Bulk chemistry of the clay fraction:

- a. a small sample of <10μ fine material was separated by dispersing 5g of <500μ soil in distilled water. The sample was agitated and allowed to settle. The supernatant liquid was discarded and the clay particles removed from the surface of the soil cake and dried.
- b. to a labelled vitreosil crucible 1g of clay size sample was added and placed in a pre-heated furnace set at 850°C for 30 minutes.
- c. the crucibles were transferred to a vacuum desiccator and allowed

- to cool. The sample was transferred to a labelled glass sample tube for storage.
- d. 0.100g of sample and powdered standards were accurately weighed into clean crucibles.
 - e. 3ml of a 1:2 mixture of perchloric/hydrofluoric acid were added to each in a fume cupboard with extreme care. Place the crucibles on a hotplate and evaporate to dryness.
 - f. remove from hotplate and allow to cool. Add 1ml of hydrochloric acid to each sample and fill to 3/4 full with distilled water. Return to hotplate and allow to warm for no more than 15 minutes.
 - g. remove from hotplate and allow to cool. Transfer with care to a 10ml capacity sample tube and make up to 10.2g by weight, cap and leave for a minimum of 14 days for reliable aluminium results.
 - h. each sample was run through an inductively coupled plasma source spectrophotometer interfaced with a PDP-11/03 minicomputer. The samples were automatically assessed for the majors in per cent of oxide and the trace elements were given in mg/l. A computer print-out detailed each sample number and standards and tabulated the results. The concentration of the major cations were calculated from the per cent oxide using standard conversion factors (see Tables 4.23-4.24).

Method F. Analysis of rain, pore water and supernatant solutions:

- a. a flame photometer was used to measure the concentration of Na^+ and K^+ . The FP was set up individually for each cation and calibrated between 0-50 ppm using pre-prepared standards. Distilled water was aspirated in the nebuliser to establish the baseline or 0 ppm. Samples were individually aspirated and the intensity of emission from the nebuliser displayed and recorded. If samples were too concentrated for the calibration range, they were accurately diluted, and re-measured. The final concentrations in mg/l were calculated using a computer program by interpolating the FP readings from the calibration curve and adjusting for any dilution.
- b. an atomic adsorption spectrometer was used to assess the concentrations of Mg^{2+} and Ca^{2+} . The AAS was individually set for the best sensitivity at the required wavelength for each cation, and was calibrated between 0-0.5 ppm for magnesium and 0-5 ppm for calcium. Distilled water was used as the 0 baseline. Samples were aspirated in a 2000°C air-acetylene flame and the intensity of adsorption integrated over 10 seconds, displayed and recorded. If samples were too concentrated for the calibration range, they were accurately diluted, and re-measured. The final concentrations in mg/l were calculated using a computer program by interpolating the AAS readings from the least squares fit calibration and adjusting for any dilution.
- c. the major anions Cl^- , SO_4^{2-} , and NO_3^{2-} were analysed on a Dionex ion-chromatograph. The specific conductance of samples was measured against background reagents (made from double-distilled water), and the intensity automatically traced on a chart recorder. The ion-chromatograph was set by allowing reagent solutions to flow through the analyser, by turning on a pump linked to a compressor, and by priming the chart recorder. Once a base line was established, standard solutions were injected simultaneously at ≈ 7 minute intervals and the deflections registered on the chart trace. Seven peaks were noted for each sample which occurred in order of fluoride, chloride, nitrite,

- phosphate, bromide, nitrate and sulphate. The optimum calibration range was established between 0-10 ppm although chloride, nitrate and sulphate were extended to 40 ppm. All samples were diluted into the calibration range and injected into the analyser through a 45 μ filter. The intensity of the anion deflections was measured and interpolated from the least squares fit calibration curve by a computer programme. Adjustments were made for the dilution factors and the final concentration reported to the nearest whole number.
- d. an auto-continuous flow analyser was used to measure ferric and total iron and aluminium. Ferrous ions react with ferrozine reagent to produce an intense purple complex which was measured at 560nm by a colorimeter interfaced with a chart recorder. 20ml of sample and standards were treated with 2 ml of thioglycolic acid and heated at 80°C for 1 hour on a hotplate. The samples were transferred to the auto sampler and analysed. Standards between 0-5 ppm were used to establish a calibration and the deflections of the emission for each sample were measured. The final concentration was interpolated from the calibration curve to the nearest mg/l by a purpose written computer programme. Aluminium reacts with Catechol violet and was measured at 580nm. Samples were pre-treated with 1% hydrochloric acid and transferred to the auto-sampler. Standards were used between 0-5ppm to calibrate the readings. The final concentrations were calculated in the same way as for ferrous iron.
- e. bicarbonate ions were assessed using a standard titration technique. Samples were titrated against 0.01M sulphuric acid while the pH was monitored throughout. A point of inflection on the titration curve in the region of pH 4.5 marked the end point. 25 ml of filtered sample was used and the pH measured. Acid was slowly added until the pH fell below 6. Acid was then added in aliquots of 0.5ml down to pH 4 recording the pH and volume after each addition. A graph was plotted over the range pH 6-4 against total volume added. The volume of acid corresponding to the point of inflection was noted and the alkalinity of the sample expressed as bicarbonate calculated from the equation:

$$\text{HCO}_3^- \text{ mg/l} = V * 122.03 * A * \frac{1000}{25}$$

where V = volume added, and;

A = the actual molarity of sulphuric acid.

References: Smith (1983); Bascombe (1964); Kinniburgh and Miles (1983); Walsh (1982); Klute (1985); Allen (1974).

APPENDIX 10

CORE SAMPLE LOG-SHEETS

Appendix 10

SOIL CORE LOG-SHEET 1

SITE : Manor Lane

CORE NUMBER : 1A

CORING METHOD : Thin walled open drive

GROUND LEVEL : 10.312 m OD

TUBE DIAMETER : 110 mm

COORDINATES (x,y) : 1031.67,
1057.63

TUBE PENETRATION : 1.411 m

DATE : 15 March 86

CORE PROFILE				SUMMARY OF PROPERTIES				
DESCRIPTION	LEGEND	LEVEL	SAMPLES	PARAMETER	S1	S2	S3	S4
			FD	Wn%	39	37	44	37
very saturated				Ws%	70	71	75	70
brown CLAY with				Gs	2.66	2.57	2.72	2.63
some pebbles		9.877	S1	VR	1.9	1.8	2.0	1.8
				P	0.65	0.65	0.67	0.65
				UW kN/m ²	12.6	12.3	12.7	12.4
occasional pebble				BD kg/m ³	1285	1251	1292	1269
deposits				Ø _r '			9.5	
				LL %			73	
saturated matrix		9.677	S2	PL %			22	
of brown/blue CLAY			RS1	PSA%				
with small peds of				<500µ	98	97	100	100 [*]
in-situ blue CLAY				<100µ	98	96	100	100
fissures present				<20µ	78	71	69	77
				<4µ	33	24	25	29
		9.457	FW					
dark brown Clay		9.427	S3	Org %	2.4	1.3	2.3	2.4
with silt/sand &				pH	7.2	7.3	7.3	7.3
pebble inclusions				Cond. mS/cm	2.0	1.5	2.2	2.3
				mg/ltr				
saturated blue/		9.227	S4	FW.cations			1876	
brown CLAY		9.197	RS2	FW.anions			4700	
Sample end	-----	9.147		S.cations	202	194	304	332
				S.anions	535	507	847	857
				Ex.cations	810	761	809	824
				CEC	54	56	57	55
Shear surface	---	9.060		Minerals %				
				mica/illite	38	33	41	39
Depth of hole	---	8.901		Kaolinite	12	12	23	18
				swelling	50	55	37	43

KEY

S1 : sample zone

FW : saturated extract for free water

RS : residual strength sample

F/BD: field and bulk density assessment

... : sample shear surface(s)

--- : sample extent

_ _ : field levels and shear surface

Gs : specific gravity

VR : void ratio

P : porosity

Org : organic matter content

CEC : cation exchange capacity
in Meq/100g

Cond : conductivity

Appendix 10

SOIL CORE LOG-SHEET 2

SITE : Manor Lane

CORE NUMBER : 1B

CORING METHOD : Thin walled open drive

GROUND LEVEL : 10.290 m OD

TUBE DIAMETER : 110 mm

COORDINATES (x,y) : 1027.03,
1058.62

TUBE PENETRATION : 0.998 m

DATE : 15 March 86

CORE PROFILE				SUMMARY OF PROPERTIES				
DESCRIPTION	LEGEND	LEVEL	SAMPLES	PARAMETER	S1	S2	S3	S4
isaturated brown		10.247	FD1	Wn%	39	37	44	37
CLAY			S1	Ws%	70	71	75	70
light brown/yellow				Gs	2.62	2.62	2.64	2.64
brown peds of CLAY		10.087		VR	2.0	1.8	2.1	2.3
in matrix of dark				P	0.67	0.64	0.68	0.7
brown remoulded		10.007	S2	UW kN/m ²	12.3	13.0	11.8	10.4
CLAY			RS1	BD kg/m ³	1256	1327	1205	1057
traces of organic				Ø _r '			6.8	
litter				LL %			76	
pebble deposits		9.842	FW	PL %			28	
		9.812	S3	PSA%				
sample shear plane	9.782	RS2	<500µ	100	100	100	100
				<100µ	100	100	100	100
dark brown/blue		9.657	S4	<20µ	70	78	84	79
overconsolidated				<4µ	26	33	36	35
CLAY with fissures	---	9.563		Org %	2.3	2.1	2.8	2.6
sample end	-----	9.517		pH	7.3	7.3	7.3	8.0
				Cond. mS/cm	1.9	2.3	2.1	1.5
				mg/ltr				
				FW.cations			1712	
				FW.anions			4144	
				S.cations	240	320	238	151
depth of hole	---	9.292	FD2	S.anions	675	966	678	362
				Ex.cations	883	857	879	885
				CEC	58	59	51	57
				Minerals %				
				mica/illite	41	40	40	43
				Kaolinite	23	23	22	19
				swelling	37	37	38	38

KEY

S1 : sample zone
 FW : saturated extract for free water
 RS : residual strength sample
 F/BD: field and bulk density assessment
 ... : sample shear surface(s)
 --- : sample extent
 _ _ : field levels and shear surface

Gs : specific gravity
 VR : void ratio
 P : porosity
 Org : organic matter content
 CEC : cation exchange capacity
 in Meq/100g
 Cond : conductivity

Appendix 10

SOIL CORE LOG-SHEET 3

SITE : Manor Lane CORE NUMBER : 2A
 CORING METHOD : Thin walled open drive GROUND LEVEL : 15.425 m OD
 TUBE DIAMETER : 110 mm COORDINATES (x,y) : 1028.88,
 1042.97
 TUBE PENETRATION : 0.962 m DATE : 15 March 86

CORE PROFILE				SUMMARY OF PROPERTIES				
DESCRIPTION	LEGEND	LEVEL	SAMPLES	PARAMETER	S1	S2	S3	S4
saturated light brown CLAY with traces of organic litter highly remoulded/slurried CLAY saturated brown/yellow Clay with dark brown/blue CLAY inclusions		15.369	FD1 S1	Wn%	45	39	46	31
				Ws%	76	79	80	83
				Gs	2.63	2.63	2.68	2.63
				VR	2.0	2.1	2.2	2.2
				P	0.68	0.67	0.68	0.69
				UW kN/m ³	12.4	11.6	12.1	10.6
				BD kg/m ³	1270	1188	1238	1083
		15.119	S2	0 _r '			8.0	
				LL %			75	
				PL %			28	
saturated brown/blue CLAY		14.908	FW	PSA%				
		14.868	S3	<500μ	100	100	100	100
	14.848	RS	<100μ	100	100	100	100
				<20μ	70	82	88	91
				<4μ	26	34	37	41
stiff plastic blue fissured blue CLAY sample end		14.779	S4					
	---	14.719		Org %	3.2	2.6	2.4	3.2
	-----	14.609		pH	7.4	7.3	7.2	7.7
				Cond. mS/cm	2.4	2.6	3.0	1.8
				mg/ltr				
depth of hole				FW.cations			2141	
				FW.anions			5391	
		14.463	FD2	S.cations	330	303	337	240
				S.anions	1020	921	1023	609
				Ex.cations	841	799	889	909
				CEC	58	55	54	57
				Minerals %				
				mica/illite	41	40	41	43
				Kaolinite	16	20	27	19
				swelling	43	40	32	38

KEY

S1 : sample zone
 FW : saturated extract for free water
 RS : residual strength sample
 F/BD: field and bulk density assessment
 ... : sample shear surface(s)
 --- : sample extent
 _ _ : field levels and shear surface

Gs : specific gravity
 VR : void ratio
 P : porosity
 Org : organic matter content
 CEC : cation exchange capacity
 in Meq/100g
 Cond : conductivity

Appendix 10

SOIL CORE LOG-SHEET 4

SITE : Manor Lane

CORE NUMBER : 2B

CORING METHOD : Thin walled open drive

GROUND LEVEL : 15.480 m OD

TUBE DIAMETER : 110 mm

COORDINATES (x,y) : 1018.61,
1045.06

TUBE PENETRATION : 0.773m

DATE : 14 March 86

DESCRIPTION	CORE PROFILE		SAMPLES	PARAMETER	SUMMARY OF PROPERTIES			
	LEGEND	LEVEL			S1	S2	S3	S4
saturated brown CLAY with some peds of blue CLAY		15.429	FD1 S1	Wn%	49	41	36	30
				Ws%	73	83	86	74
				Gs	2.63	2.65	2.68	2.65
				VR	1.9	2.2	2.3	2.0
fissured brown CLAY		15.249	FW	P	0.66	0.69	0.7	0.66
			S2	UW kN/m ²	13.2	11.5	10.8	11.4
				BD kg/m ³	1341	1174	1100	1161
saturated active shear plane	15.179	RS1	ϕ_r			9.0	
slickensided shear in brown/blue CLAY	15.102	S3	LL %			80	
			RS2	PL %			30	
				PSA%				
highly fissured stiff blue CLAY		15.049	S4	<500 μ	100	100	100	100
				<100 μ	100	100	100	100
				<20 μ	75	87	75	89
				<4 μ	32	38	32	40
sample end	---	14.930		Org %	2.9	2.5	2.7	2.0
	---	14.879		pH	7.3	7.3	7.3	7.5
depth of hole		14.707	FD2	Cond. mS/cm	2.5	2.5	2.3	1.7
				mg/ltr				
				FW.cations			2047	
				FW.anions			5560	
				S.cations	371	440	360	287
				S.anions	1143	1296	1085	694
				Ex.cations	829	839	818	798
				CEC	56	61	56	53
				Minerals %				
				mica/illite	41	42	42	42
				Kaolinite	23	25	25	23
				swelling	35	33	34	35

KEY

S1 : sample zone
 FW : saturated extract for free water
 RS : residual strength sample
 F/BD: field and bulk density assessment
 ... : sample shear surface(s)
 --- : sample extent
 _ _ : field levels and shear surface

Gs : specific gravity
 VR : void ratio
 P : porosity
 Org : organic matter content
 CEC : cation exchange capacity
 in Meq/100g
 Cond : conductivity

Appendix 10

SOIL CORE LOG-SHEET 5

SITE : Manor Lane CORE NUMBER : 3A
 CORING METHOD : Thin walled open drive GROUND LEVEL : 21.172 m OD
 TUBE DIAMETER : 110 mm COORDINATES (x,y) : 1033.1,
 1029.03
 TUBE PENETRATION : 0.903 m DATE : 9 March 86

CORE PROFILE				SUMMARY OF PROPERTIES				
DESCRIPTION	LEGEND	LEVEL	SAMPLES	PARAMETER	S1	S2	S3	S4
friable brown/blue weathered CLAY		21.116	FD1 S1	Wn%	32	35	41	33
				Ws%	79	76	80	84
				Gs	2.73	2.63	2.73	2.62
				VR	2.2	2.0	2.2	2.2
saturated brown/yellow CLAY above slickensided shear		20.916	S2 RS1	P	0.68	0.67	0.69	0.69
				UW kN/m ²	11.2	11.6	11.9	10.6
				BD kg/m ³	1141	1183	1216	1086
				ϕ_r'			7.8	
fissured dark brown CLAY - main shear		20.816	FW	LL %			76	
staining along	20.766	S3	PL %			28	
fissures with red/brown/yellow amorphous deposit		20.681	RS2	PSA%				
				<500 μ	100	100	100	100*
				<100 μ	400	100	100	100
				<20 μ	86	90	72	87
blue/brown softened CLAY		20.579	S4	<4 μ	38	43	31	39
large fissure		20.571		Org %	3.0	3.0	2.2	2.7
stiff blue plastic CLAY		20.496		pH	7.1	7.1	7.2	7.1
				Cond. mS/cm	3.2	2.8	3.1	3.2
sample end		20.416		mg/ltr				
				FW.cations			2247	
depth of hole		20.269	FD2	FW.anions			5944	
				S.cations	347	387	334	573
				S.anions	1028	1178	943	1760
				Ex.cations	867	1017	919	917
				CEC	57	73	63	58
				Minerals %				
				mica/illite	41	43	36	39
				Kaolinite	10	27	28	22
				swelling	49	31	36	39

KEY

S1 : sample zone
 FW : saturated extract for free water
 RS : residual strength sample
 F/BD: field and bulk density assessment
 ... : sample shear surface(s)
 --- : sample extent
 - - : field levels and shear surface

Gs : specific gravity
 VR : void ratio
 P : porosity
 Org : organic matter content
 CEC : cation exchange capacity
 in Meq/100g
 Cond : conductivity

Appendix 10

SOIL CORE LOG-SHEET 6

SITE : Manor Lane

CORE NUMBER : 38

CORING METHOD : Thin walled open drive

GROUND LEVEL : 22.085 m OD

TUBE DIAMETER : 110 mm

COORDINATES (x,y) : 1012.71,
1030.86

TUBE PENETRATION : 0.744 m

DATE : 17 March 86

CORE PROFILE				SUMMARY OF PROPERTIES				
DESCRIPTION	LEGEND	LEVEL	SAMPLES	PARAMETER	S1	S2	S3	S4
brown/yellow silty			FD1	Wn%	47	39	43	33
CLAY with some very		22.068	S1	Ws%	77	85	85	81
fine sand-saturated				Gs	2.6	2.61	2.63	2.62
			S2	VR	2.0	2.2	2.2	2.1
highly saturated		21.918	RS1	P	0.67	0.69	0.69	0.68
weathered brown				UW kN/m ²	12.5	11.1	11.4	11.0
CLAY with peds of				BD kg/m ³	1274	1134	1167	1121
blue CLAY			FW	Ø _r '			7.9	
			S3	LL %			70	
active shear plane	21.730	RS2	PL %			27	
over softened blue	---	21.655		PSA%				
CLAY				<500µ	99	100	100	100
fissured stiff				<100µ	99	100	100	100
plastic blue CLAY		21.533	S4	<20µ	82	83	80	86
amorphous staining				<4µ	35	34	34	33
along fissures	-----	21.438						
sample end				Org %	3.3	2.7	2.3	2.7
depth of hole	---	21.341	FD2	pH	7.3	7.4	7.4	7.3
				Cond. mS/cm	0.98	1.62	2.2	2.6
				mg/ltr				
				FW.cations			2163	
				FW.anions			5242	
				S.cations	99	260	309	251
				S.anions	233	688	919	701
				Ex.cations	961	769	784	898
				CEC	64	57	51	57
				Minerals %				
				mica/illite	35	39	41	43
				Kaolinite	18	22	27	26
				swelling	47	39	32	31

KEY

S1 : sample zone

FW : saturated extract for free water

RS : residual strength sample

F/BD: field and bulk density assessment

... : sample shear surface(s)

--- : sample extent

_ _ : field levels and shear surface

Gs : specific gravity

VR : void ratio

P : porosity

Org : organic matter content

CEC : cation exchange capacity
in Meq/100g

Cond : conductivity

Appendix 10

SOIL CORE LOG-SHEET 7

SITE : Manor Lane

CORE NUMBER : 4A

CORING METHOD : Thin walled open drive

GROUND LEVEL : 30.170 m OD

TUBE DIAMETER : 110 mm

COORDINATES (x,y) : 1034.67,
1015.38

TUBE PENETRATION : 0.759 m

DATE : 17 March 86

CORE PROFILE				SUMMARY OF PROPERTIES				
DESCRIPTION	LEGEND	LEVEL	SAMPLES	PARAMETER	S1	S2	S3	S4
sandy gravel in			FD1	Wn%	40	37	35	32
saturated brown		30.120	S1	Ws%	75	73	81	92
CLAY with yellow/				Gs	2.6	2.58	2.72	2.59
brown/grey mottling				VR	1.9	1.9	2.2	2.4
saturated dark				P	0.66	0.65	0.69	0.7
brown CLAY with			S2	UW kN/m ²	12.2	12.0	11.2	9.9
deposits of pebbles		29.94	RS1	BD kg/m ³	1241	1229	1147	1008
smell of sulphide/				Ø _r '			11.4	
rotting litter		29.765	FW	LL %			68	
active shear plane			S3	PL %			26	
dark brown CLAY	29.757	RS2	PSA%				
softened blue CLAY				<500µ	94	99	100	100.
stiff blue CLAY	---	29.636		<100µ	94	99	100	100
with silt stained		29.60	S4	<20µ	82	76	86	89
fissures				<4µ	37	32	29	37
		29.54						
sample end				Org %	3.4	2.8	3.6	2.9
				pH	6.1	7.5	7.2	7.3
depth of hole	---	29.411	FD2	Cond. mS/cm	0.35	0.49	0.78	1.57
				mg/ltr				
				FW.cations			977	
				FW.anions			1942	
				S.cations	57	82	55	256
				S.anions	44	32	147	858
				Ex.cations	865	815	844	883
				CEC	59	53	58	54
				Minerals %				
				mica/illite	28	38	38	43
				Kaolinite	9	16	24	28
				swelling	63	46	38	28

KEY

S1 : sample zone
 FW : saturated extract for free water
 RS : residual strength sample
 F/BD: field and bulk density assessment
 ... : sample shear surface(s)
 --- : sample extent
 -- : field levels and shear surface

Gs : specific gravity
 VR : void ratio
 P : porosity
 Org : organic matter content
 CEC : cation exchange capacity
 in Meq/100g
 Cond : conductivity

Appendix 10

SOIL CORE LOG-SHEET 8

SITE : Manor Lane CORE NUMBER : 4B
 CORING METHOD : Thin walled open drive GROUND LEVEL : 28.995 m OD
 TUBE DIAMETER : 110 mm COORDINATES (x,y) : 1015.11,
 1015.97
 TUBE PENETRATION : 0.920 m DATE : 9 March 86

CORE PROFILE				SUMMARY OF PROPERTIES				
DESCRIPTION	LEGEND	LEVEL	SAMPLES	PARAMETER	S1	S2	S3	S4
saturated brown/ yellow CLAY with peds of brown/blue CLAY - some pebbles gravel and sand in dark brown CLAY some rotting litter saturated brown CLAY with pebbles softened blue/brown CLAY stiff blue plastic CLAY fissured with polished surfaces sample end		28.95	FD1 S1	Wn%	37	37	34	29
				Ws%	60	75	61	101
				Gs	2.67	2.55	2.65	2.6
				VR	1.6	1.9	1.6	2.6
				P	0.62	0.66	0.62	0.73
				UW kN/m ³	13.8	11.8	13.2	9.1
		28.75	S2	BD kg/m ³	1406	1199	1348	926
		28.71	RS1	Ø _r '			11.4	
			FW	LL %			75	
		28.63	S3 RS2	PL %			24	
depth of hole			PSA%				
				<500µ	91	78	92	100*
		28.47	S4	<100µ	91	78	92	100
				<20µ	75	68	73	89
	-----	28.35		<4µ	29	25	28	41
	---	28.317						
				Org %	2.6	3.3	1.9	2.2
				pH	7.2	7.4	7.0	7.8
				Cond. mS/cm	0.95	0.73	0.97	1.55
				mg/ltr				
depth of hole		28.075	FD2	FW.cations			2127	
				FW.anions			4982	
				S.cations	108	68	85	213
				S.anions	244	129	176	451
				Ex.cations	856	839	945	857
				CEC	54	55	61	54
				Minerals %				
				mica/illite	29	26	30	39
				Kaolinite	9	15	15	32
				swelling	62	59	55	28

KEY

S1 : sample zone
 FW : saturated extract for free water
 RS : residual strength sample
 F/BD: field and bulk density assessment
 ... : sample shear surface(s)
 --- : sample extent
 _ _ : field levels and shear surface

Gs : specific gravity
 VR : void ratio
 P : porosity
 Org : organic matter content
 CEC : cation exchange capacity
 in Meq/100g
 Cond : conductivity

SITE : Manor Lane CORE NUMBER : 5A
 CORING METHOD : Thin walled open drive GROUND LEVEL : 36.588 m OD
 TUBE DIAMETER : 110 mm COORDINATES (x,y) : 1041.22,
 1008.16
 TUBE PENETRATION : 0.551 m DATE : 16 March 86

CORE PROFILE				SUMMARY OF PROPERTIES				
DESCRIPTION	LEGEND	LEVEL	SAMPLES	PARAMETER	S1	S2	S3	S4
1 brown/yellow silty		36.574	S1 FD1	1 Wn%	34	35	29	25
1 CLAY saturated/with				1 Ws%	82	77	90	92
1 fine sand & gravel		36.504	S2 FW	1 Gs	2.58	2.59	2.6	2.58
1 amorphous yellow/	36.464	RS1	1 VR	2.1	2.0	2.3	2.4
1 orange stains				1 P	0.68	0.67	0.7	0.7
1 soft dark brown				1 UW kN/m ²	10.9	11.5	9.8	9.4
1 CLAY		36.314	S3	1 BD kg/m ³	1110	1169	1001	958
1 fissured/crumbley	---	36.254		1 ϕ_r			11.0	
1 brown/blue CLAY				1 LL %			41	
1 blue/brown stiff				1 PL %			21	
1 plastic CLAY with		36.134	S4	1 PSA%				
1 polished & stained	-----	36.094		1 <500 μ	100	96	100	100
1 fissured surfaces				1 <100 μ	100	96	100	100
1 selenite crystal	---	36.037	FD2	1 <20 μ	91	82	81	84
1 depth of hole				1 <4 μ	38	32	33	34
				1 Org %	2.7	3.0	2.9	2.7
				1 pH	7.7	7.7	7.3	7.4
				1 Cond. mS/cm	0.64	0.86	2.59	2.32
				1 mg/ltr				
				1 FW.cations			757	
				1 FW.anions			1527	
				1 S.cations	67	92	239	248
				1 S.anions	90	155	878	695
				1 Ex.cations	938	974	1006	972
				1 CEC	57	63	64	62
				1 Minerals %				
				1 mica/illite	30	31	38	43
				1 Kaolinite	19	19	32	41
				1 swelling	51	50	30	16

KEY

S1 : sample zone
 FW : saturated extract for free water
 RS : residual strength sample
 F/BD: field and bulk density assessment
 ... : sample shear surface(s)
 --- : sample extent
 _ _ : field levels and shear surface

Gs : specific gravity
 VR : void ratio
 P : porosity
 Org : organic matter content
 CEC : cation exchange capacity
 in Meq/100g
 Cond : conductivity

SITE : Manor Lane CORE NUMBER : 5B
 CORING METHOD : Thin walled open drive GROUND LEVEL : 36.568 m OD
 TUBE DIAMETER : 110 mm COORDINATES (x,y) : 1036.27,
 1005.88
 TUBE PENETRATION : 0.837 m DATE : 10 March 86

CORE PROFILE				SUMMARY OF PROPERTIES				
DESCRIPTION	LEGEND	LEVEL	SAMPLES	PARAMETER	S1	S2	S3	S4
crumbly brown/blue		36.494	FD1 S1	Wn%	30	32	35	34
CLAY amorphous				Ws%	71	86	83	84
yellow silt stains				Gs	2.72	2.63	2.66	2.64
				VR	1.9	2.3	2.2	2.2
wet dark brown CLAY				P	0.66	0.69	0.69	0.69
with red/yellow		36.314	S2	UW kN/m ²	11.8	10.4	11.0	10.8
'iron' staining		36.254	RS1	BD kg/m ³	1205	1059	1123	1100
				Ø _r '			11.1	
				LL %			43	
				PL %			20	
saturated brown/		36.094	FW	PSA%				
blue CLAY matrix			S3	<500µ	100	100	100	100
with peds of blue				<100µ	100	100	100	100
in-situ CLAY	36.056	RS2	<20µ	84	88	88	94
				<4µ	35	33	28	35
softened blue/brown	---	35.943						
CLAY		35.926	S4					
stiff plastic blue				Org %	2.9	3.1	3.0	3.7
CLAY - some pyrite	-----	35.844		pH	7.4	7.4	7.6	6.7
sample end				Cond. mS/cm	1.58	2.79	2.09	3.65
depth of hole	---	35.731	FD2	mg/ltr				
				FW.cations			2177	
				FW.anions			5914	
				S.cations	194	298	255	555
				S.anions	526	528	698	210
				Ex.cations	802	721	757	979
				CEC	55	55	54	69
				Minerals %				
				mica/illite	39	39	36	41
				Kaolinite	22	16	19	30
				swelling	40	45	45	31

KEY

S1 : sample zone
 FW : saturated extract for free water
 RS : residual strength sample
 F/BD: field and bulk density assessment
 ... : sample shear surface(s)
 --- : sample extent
 _ _ : field levels and shear surface

Gs : specific gravity
 VR : void ratio
 P : porosity
 Org : organic matter content
 CEC : cation exchange capacity
 in Meq/100g
 Cond : conductivity

SITE : Manor Lane

CORE NUMBER : 6

CORING METHOD : Thin walled open drive

GROUND LEVEL : 37.115 m OD

TUBE DIAMETER : 110 mm

COORDINATES (x,y) : 1031.81,
1003.1

TUBE PENETRATION : 0.832 m

DATE : 9 March 86

CORE PROFILE				SUMMARY OF PROPERTIES				
DESCRIPTION	LEGEND	LEVEL	SAMPLES	PARAMETER	S1	S2	S3	S4
brown weathered		37.055	FD1 S1	Wn%	32	34	33	25
CLAY with deposits				Ws%	88	85	76	91
of fine sand & silt				Gs	2.63	2.59	2.68	2.61
brown/yellow CLAY			S2	VR	2.3	2.2	2.0	2.4
dark brown CLAY &		36.905	RS1	P	0.7	0.69	0.67	0.7
some litter				UW kN/m ³	10.3	10.6	11.5	9.5
saturated brown			FW	BD kg/m ³	1048	1086	1169	969
CLAY to yellow/			S3	ϕ_r			11.3	
brown slurry	36.75	RS2	LL %			43	
softened brown CLAY				PL %			22	
blue/brown stiff				PSA%				
CLAY with yellow		36.615	S4	<500 μ	100	100	98	100*
silt/fine sand				<100 μ	100	100	98	100
lined fissures	-----	36.505		<20 μ	87	86	85	91
fissured blue CLAY	---	36.488		<4 μ	37	38	31	36
sample end				Org %	3.5	2.6	2.9	3.0
				pH	7.6	7.7	7.5	7.2
				Cond. mS/cm	0.58	0.59	0.81	2.61
depth of hole	---	36.283	FD2	mg/ltr				
				FW.cations			969	
				FW.anions			2466	
				S.cations	119	50	78	344
				S.anions	49	60	143	920
				Ex.cations	883	841	825	849
				CEC	56	67	67	61
				Minerals %				
				mica/illite	42	40	35	43
				Kaolinite	16	17	17	35
				swelling	42	44	48	22

KEY

S1 : sample zone
 FW : saturated extract for free water
 RS : residual strength sample
 F/BD: field and bulk density assessment
 ... : sample shear surface(s)
 --- : sample extent
 _ _ : field levels and shear surface

Gs : specific gravity
 VR : void ratio
 P : porosity
 Org : organic matter content
 CEC : cation exchange capacity
 in Meq/100g
 Cond : conductivity

SITE : Manor Lane

CORE NUMBER : 7U

CORING METHOD : Thin walled open drive

GROUND LEVEL : 43.732 m OD

TUBE DIAMETER : 110 mm

COORDINATES (x,y) : 1009.77,
999.82

TUBE PENETRATION : 1.595 m

DATE : 9 March 86

DESCRIPTION	CORE PROFILE		SAMPLES	SUMMARY OF PROPERTIES				
	LEGEND	LEVEL		PARAMETER	S1	S2	S3	S4
shallow soil with			FD1	Wn%	33	35	29	26
yellow mottled CLAY		43.632	S1	Ws%	78	97	81	61
and organic litter				Gs	2.62	2.61	2.62	2.62
blue/grey and green				VR	2.1	2.5	2.1	1.6
CLAY with yellow		43.492		P	0.67	0.72	0.68	0.61
staining - organic	~~~~~			UW kN/m ²	11.2	9.8	10.7	12.5
horizon				BD kg/m ³	1147	996	1088	1271
reduced mottling				Op'			15.5	
weathered light		43.352	S2	LL %			74.5	
brown CLAY matrix			SS1	PL %			23.8	
with peds of dark				PSA%				
brown CLAY /nodules				<500μ	100	100	100	100*
of fine sand-quartz				<100μ	100	100	100	100
saturated zone	43.132	FW	<20μ	83	89	94	91
dark brown densely				<4μ	31	36	30	25
fissured CLAY with		43.072	S3					
yellow/brown stains		42.992	SS2	Org %	3.8	3.1	2.6	1.4
along slickensided				pH	5.1	8.0	7.4	7.3
surfaces				Cond. mS/cm	1.98	3.57	4.88	6.42
				mg/ltr				
crumbly dark brown		42.802	S4	FW.cations			390	
fissured CLAY -less				FW.anions			857	
staining with depth		42.712		S.cations	68	46	41	99
Stiff brown CLAY				S.anions	51	49	60	137
				Ex.cations	798	920	933	909
				CEC	52	67	57	61
plastic brown/blue				Minerals %				
CLAY	-----	42.303		mica/illite	30	30	36	38
sample end				Kaolinite	9	11	13	13
depth of hole	↓↓↓↓↓	42.137	FD2	swelling	62	58	51	49

KEY

S1 : sample zone
 FW : saturated extract for free water
 RS : residual strength sample
 F/BD: field and bulk density assessment
 ... : sample shear surface(s)
 --- : sample extent
 _ _ : field levels and shear surface

Gs : specific gravity
 VR : void ratio
 P : porosity
 Org : organic matter content
 CEC : cation exchange capacity
 in Meq/100g
 Cond : conductivity

Appendix 10

SOIL CORE LOG-SHEET 13

SITE : Worbarrow Bay CORE NUMBER : WO
 CORING METHOD : Thin walled open drive GROUND LEVEL : 13.453 m LD
 TUBE DIAMETER : 110 mm COORDINATES (x,y) : 93.89,
 127.44
 TUBE PENETRATION : 1.368 m DATE : 16 April 86

CORE PROFILE				SUMMARY OF PROPERTIES				
DESCRIPTION	LEGEND	LEVEL	SAMPLES	PARAMETER	S1	S2	S3	S4
saturated yellow			FD1	Wn%	23	29	28	31
SAND		13.039		Ws%	46	59	42	59
plastic red CLAY				Gs	2.68	2.68	2.64	2.63
saturated red CLAY		12.979	S1	VR	1.2	1.6	1.1	1.5
with paler mottling				P	0.55	0.61	0.53	0.61
& organic deposits				UW kN/m²	14.4	13.1	15.6	13.3
				BD kg/m³	1468	1341	1593	1356
uniform sticky		12.839	S2	φ _r '			7.9	
plastic purple/red				LL %			51	
CLAY				PL %			17	
saturated light red				PSA%				
CLAY with pale		12.679	FW	<500μ	97	97	93	97
yellow/blue mottles				<100μ	97	97	93	97
		12.539	S3	<20μ	80	81	81	88
yellow/orange silt		12.489	RS1	<4μ	37	38	34	42
and fine sand in a								
red CLAY matrix				Org %	2.5	1.2	1.2	2.5
				pH	7.3	6.6	6.0	5.4
purple/red stiff				Cond. mS/cm	0.82	0.64	0.56	0.61
plastic CLAY		12.353	S4	mg/ltr				
		12.309	RS2	FW.cations			701	
grey/blue sandy				FW.anions			1271	
SILT and CLAY - dry	---	12.196		S.cations	387	306	209	52
and crumbly	----	12.169		S.anions	125	97	73	100
sample end				Ex.cations	578	464	427	579
				CEC	61	58	64	62
				Minerals %				
depth of hole	---	11.985	FD2	mica/illite	23	21	17	23
				Kaolinite	8	12	12	13
				swelling	68	67	70	64

KEY

S1 : sample zone
 FW : saturated extract for free water
 RS : residual strength sample
 F/BD: field and bulk density assessment
 ... : sample shear surface(s)
 --- : sample extent
 -- : field levels and shear surface

Gs : specific gravity
 VR : void ratio
 P : porosity
 Org : organic matter content
 CEC : cation exchange capacity
 in Meq/100g
 Cond : conductivity

SITE : Worbarrow Bay CORE NUMBER : W1
 CORING METHOD : Thin walled open drive GROUND LEVEL : 16.657 m LD
 TUBE DIAMETER : 110 mm COORDINATES (x,y) : 89.83,
 135.08
 TUBE PENETRATION : 1.364 m DATE : 16 April 86

CORE PROFILE				SUMMARY OF PROPERTIES				
DESCRIPTION	LEGEND	LEVEL	SAMPLES	PARAMETER	S1	S2	S3	S4
			FD1	Wn%	20	18	21	14
saturated red CLAY				Ws%	48	37	48	40
				Gs	2.66	2.64	2.65	2.61
uniform wet purple/red CLAY		16.507	S0	VR	1.3	1.0	1.3	1.1
				P	0.56	0.5	0.56	0.51
saturated grey/yellow and green				UW kN/m³	13.8	15.4	13.9	14.2
mottled CLAY some sand lenses		16.337	S1	BD kg/m³	1408	1575	1422	1448
				ϕ _r %			22.0	
				LL %			42	
		16.217	RS1	PL %			16	
plastic grey/green and yellow CLAY				PSA%				
deep yellow SANDS & sandstone		16.107	S2	<500μ	99	91	86	100
				<100μ	99	91	86	100
				<20μ	80	79	77	80
				<4μ	33	34	33	39
saturated sand base			FW	Org %	1.9	0.8	1.0	1.0
red/purple stiff			S3	pH	5.2	5.4	5.4	6.4
plastic CLAY with polished surfaces		15.907	RS2	Cond. mS/cm	0.58	0.59	0.53	0.52
				mg/ltr				
light blue/buff		15.767	S4	FW.cations			613	
grey SILT and CLAY				FW.anions			1235	
dry and crumbly		15.637		S.cations	120	115	125	136
sample end				S.anions	109	92	90	79
				Ex.cations	673	515	635	628
				CEC	54	65	52	47
				Minerals %				
basal shear		15.453		mica/illite	19	12	17	13
surface				Kaolinite	7	T	3	T
depth of hole	↓↓↓↓↓	15.293		swelling	75	88	80	87

KEY

S1 : sample zone
 FW : saturated extract for free water
 RS : residual strength sample
 F/BD: field and bulk density assessment
 ... : sample shear surface(s)
 --- : sample extent
 _ _ : field levels and shear surface

Gs : specific gravity
 VR : void ratio
 P : porosity
 Org : organic matter content
 CEC : cation exchange capacity
 in Meq/100g
 Cond : conductivity

Appendix 10

SOIL CORE LOG-SHEET 15

SITE : Worbarrow Bay CORE NUMBER : W2
 CORING METHOD : Thin walled open drive GROUND LEVEL : 20.603 m LD
 TUBE DIAMETER : 110 mm COORDINATES (x,y) : 86.3,
 145.64
 TUBE PENETRATION : 0.871 m DATE : 20 April 86

CORE PROFILE				SUMMARY OF PROPERTIES				
DESCRIPTION	LEGEND	LEVEL	SAMPLES	PARAMETER	S1	S2	S3	S4
coarse SAND in sat.			FD1	Wn%	17	20	22	17
red CLAY matrix		20.521	SO	Ws%	43	49	61	51
				Gs	2.66	2.66	2.60	2.65
saturated red CLAY/				VR	1.2	1.3	1.6	1.4
SAND				P	0.53	0.56	0.61	0.58
saturated pale grey			S1 FW	UW kN/m ³	14.2	13.6	12.0	13.0
green and yellow	20.341	RS1	BD kg/m ³	1447	1389	1227	1324
mottled CLAY under				Ø _r '			5.7	
active shear plane				LL %			62	
				PL %			19	
softened dark grey		20.161	S2	PSA%				
blue mottled CLAY				<500µ	98	100	100	100
stiff dark grey				<100µ	98	100	100	100
CLAY - yellow/red			S3	<20µ	88	83	94	93
& grey mottled CLAY	20.021	RS2	<4µ	41	39	50	50
lower-consolidated								
with silt lined	---	19.907		Org %	0.8	1.9	2.5	2.4
fissures				pH	5.0	5.5	5.1	6.3
dark grey stiff		19.841	S4	Cond. mS/cm	0.5	0.59	0.65	0.53
plastic clay with				mg/ltr				
slight mottling	-----	19.771		FW.cations			812	
sample end	---	19.732	FD2	FW.anions			1634	
depth of hole				S.cations	88	87	101	88
				S.anions	87	85	116	81
				Ex.cations	802	812	899	926
				CEC	48	54	57	56
				Minerals %				
				mica/illite	22	17	23	18
				Kaolinite	12	9	23	13
				swelling	66	74	55	70

KEY

S1 : sample zone
 FW : saturated extract for free water
 RS : residual strength sample
 F/BD: field and bulk density assessment
 ... : sample shear surface(s)
 --- : sample extent
 -- : field levels and shear surface

Gs : specific gravity
 VR : void ratio
 P : porosity
 Org : organic matter content
 CEC : cation exchange capacity
 in Meq/100g
 Cond : conductivity

Appendix 10

SOIL CORE LOG-SHEET 16

SITE : Worbarrow Bay CORE NUMBER : W3
 CORING METHOD : Thin walled open drive GROUND LEVEL : 22.00 m LD
 TUBE DIAMETER : 110 mm COORDINATES (x,y) : 86.48,
 148.4
 TUBE PENETRATION : 0.855 m DATE : 20 April 86

CORE PROFILE				SUMMARY OF PROPERTIES				
DESCRIPTION	LEGEND	LEVEL	SAMPLES	PARAMETER	S1	S2	S3	S4
			FD1	Wn%	26	25	21	19
brown sandy grey				Ws%	61	49	51	51
CLAY - deep yellow		21.913	S1	Gs	2.72	2.62	2.63	2.65
layers of coarse				VR	1.7	1.3	1.4	1.4
SAND - saturated		21.822	FW	P	0.62	0.56	0.58	0.58
pale purple mottled				UW kN/m³	12.6	14.1	13.3	13.1
CLAY with yellow			S2	BD kg/m³	1287	1434	1353	1333
sand inclusions	21.691	RS	Ø _r %			12.5	
				LL %			53	
softened grey/green				PL %			15	
yellow mottled CLAY		21.572	S3	PSA%				
basal shear surface	---	21.518		<500µ	90	96	98	100
stiff plastic pale				<100µ	90	96	98	100
grey/yellow CLAY		21.427	S4	<20µ	83	85	84	86
over-consolidated				<4µ	35	37	39	42
with silt and sand								
lined fissures	-----	21.327		Org %	1.2	1.4	1.7	2.1
sample end				pH	5.4	5.2	4.7	5.0
				Cond. mS/cm	0.58	0.67	0.59	0.64
				mg/ltr				
depth of hole	---	21.145	FD2	FW.cations			939	
				FW.anions			1652	
				S.cations	68	80	65	71
				S.anions	50	116	92	102
				Ex.cations	706	712	827	811
				CEC	61	48	54	48
				Minerals %				
				mica/illite	24	26	19	21
				Kaolinite	10	14	14	14
				swelling	67	60	67	65

KEY

S1 : sample zone
 FW : saturated extract for free water
 RS : residual strength sample
 F/BD: field and bulk density assessment
 ... : sample shear surface(s)
 --- : sample extent
 -- : field levels and shear surface

Gs : specific gravity
 VR : void ratio
 P : porosity
 Org : organic matter content
 CEC : cation exchange capacity
 in Meq/100g
 Cond : conductivity

SITE : Worbarrow Bay CORE NUMBER : W4
 CORING METHOD : Thin walled open drive GROUND LEVEL : 24.104 m LD
 TUBE DIAMETER : 110 mm COORDINATES (x,y) : 87.66,
 152.88
 TUBE PENETRATION : 0.865 m DATE : 15 April 86

CORE PROFILE				SUMMARY OF PROPERTIES				
DESCRIPTION	LEGEND	LEVEL	SAMPLES	PARAMETER	S1	S2	S3	S4
dark brown sandy SOIL (some humus)		24.044	FD1 S1	Wn%	18	26	30	23
				Ws%	42	42	75	65
				Gs	2.67	2.63	2.61	2.58
sandy brown/purple CLAY with yellow/blue mottling		23.909	S2	VR	1.1	1.1	2.0	1.7
				P	0.53	0.53	0.66	0.63
occasionally sandy purple/red sandstone		23.784	FW	UW kN/m ³	14.5	15.4	11.2	11.7
rock in saturated			S3	BD kg/m ³	1480	1571	1143	1190
red CLAY with silt	23.729	RS	Q _r			7.4	
and sand lenses				LL %			36	
				PL %			21	
				PSA%				
				<500μ	99	88	100	100
softened dark grey CLAY -yellow/green		23.569	S4	<100μ	99	87	100	100
mottling -some silt	---	23.499		<20μ	83	72	95	96
blue/grey stiff plastic CLAY	-----	23.469		<4μ	30	30	50	51
sample end				Org %	2.2	1.7	2.9	3.1
				pH	6.0	5.5	5.1	6.0
				Cond. mS/cm	0.58	0.65	0.73	0.63
				mg/ltr				
depth of hole	---	23.239	FD2	FW.cations			994	
				FW.anions			1688	
				S.cations	44	156	51	60
				S.anions	83	70	123	112
				Ex.cations	656	499	893	804
				CEC	42	46	57	49
				Minerals %				
				mica/illite	22	11	24	24
				Kaolinite	11	T	23	19
				swelling	67	89	54	57

KEY

S1 : sample zone
 FW : saturated extract for free water
 RS : residual strength sample
 F/BD: field and bulk density assessment
 ... : sample shear surface(s)
 --- : sample extent
 -- : field levels and shear surface

Gs : specific gravity
 VR : void ratio
 P : porosity
 Org : organic matter content
 CEC : cation exchange capacity
 in Meq/100g
 Cond : conductivity

SITE : Worbarrow Bay CORE NUMBER : W5
 CORING METHOD : Thin walled open drive GROUND LEVEL : 26.445 m LD
 TUBE DIAMETER : 110 mm COORDINATES (x,y) : 83.07,
 154.38
 TUBE PENETRATION : 0.842 m DATE : 17 April 86

CORE PROFILE				SUMMARY OF PROPERTIES				
DESCRIPTION	LEGEND	LEVEL	SAMPLES	PARAMETER	S1	S2	S3	S4
saturated red/grey and yellow mottled CLAY with some silt		26.348	S1	FD1 Wn%	25	27	21	20
				Ws%	59	77	63	57
				Gs	2.68	2.62	2.66	2.63
				VR	1.2	2.0	1.7	1.5
saturated purple/ red CLAY with sand		26.187	FW	P	0.55	0.67	0.63	0.6
		26.147	S2	UW kN/m³	14.4	10.8	11.9	12.4
				BD kg/m³	1468	1103	1210	1268
buried organic SOIL dry and sandy		26.064		φ _r %			6.9	
				LL %			55	
				PL %			18	
softened blue/red mottled CLAY -shear.....		25.967	S3 RS	PSA%				
surface				<500μ	100	100	100	100
consolidated stiff		25.886	S4	<100μ	100	100	100	100
plastic grey/red				<20μ	90	91	93	92
CLAY with fissures		25.807		<4μ	49	51	55	54
sample end		25.763						
basal shear				Org %	2.7	2.8	2.7	2.5
				pH	4.9	5.0	6.3	6.4
				Cond. mS/cm	0.55	0.59	0.69	0.62
depth of hole		25.603	FD2	mg/ltr				
				FW.cations			862	
				FW.anions			1562	
				S.cations	42	46	56	44
				S.anions	86	91	106	90
				Ex.cations	636	674	694	656
				CEC	61	47	44	43
				Minerals %				
				mica/illite	14	14	16	14
				Kaolinite	7	7	8	8
				swelling	79	79	76	78

KEY

S1 : sample zone
 FW : saturated extract for free water
 RS : residual strength sample
 F/BD: field and bulk density assessment
 ... : sample shear surface(s)
 --- : sample extent
 _ _ : field levels and shear surface

Gs : specific gravity
 VR : void ratio
 P : porosity
 Org : organic matter content
 CEC : cation exchange capacity
 in Meq/100g
 Cond : conductivity

Appendix 10

SOIL CORE LOG-SHEET 19

SITE : Worbarrow Bay CORE NUMBER : WU
 CORING METHOD : Thin walled open drive GROUND LEVEL : 26.403 m LD
 TUBE DIAMETER : 110 mm COORDINATES (x,y) : 97.53,
 150.79
 TUBE PENETRATION : 1.456 m DATE : 17 April 86

CORE PROFILE				SUMMARY OF PROPERTIES				
DESCRIPTION	LEGEND	LEVEL	SAMPLES	PARAMETER	S1	S2	S3	S4
			FD1	Wn%	15	17	15	14
crumbly red/grey				Ws%	74	89	81	83
mottled CLAY highly		26.658	S1	Gs	2.69	2.68	2.65	2.69
cracked & weathered				VR	2.0	2.3	2.4	2.2
				P	0.67	0.69	0.7	0.69
paler grey/green &				UW kN/m²	10.1	9.3	9.1	10.1
red mottled CLAY		26.483		BD kg/m³	1035	948	926	1027
	~~~~~	26.411	S2	Ø _r %			23.2	
dark grey/blue CLAY				LL %			39.0	
mottled yellow/				PL %			22.7	
green -few fissures				PSA%				
		26.246		<500µ	100	100	100	100
pale grey/blue				<100µ	100	100	100	100
green and yellow		26.178		<20µ	94	97	98	97
mottled CLAY/silt				<4µ	45	43	45	47
			FW					
purple/red plastic	-----	26.023	S3	Org %	1.6	2.0	2.2	2.8
CLAY some pale grey			SS	pH	5.9	5.9	6.2	6.4
mottling				Cond. mS/cm	0.59	0.62	0.66	0.69
				mg/ltr				
				FW.cations			355	
nodules of sand in				FW.anions			1292	
red CLAY matrix		25.80		S.cations	107	108	100	99
grey/blue stiff	-----			S.anions	249	241	278	282
CLAY with some silt			SS	Ex.cations	616	627	656	663
dry loosely packed	-----	25.672	S4	CEC	63	67	49	59
pale grey/blue SILT				Minerals %				
and fine sand				mica/illite	29	37	30	34
sample end	--↓--	25.366		Kaolinite	14	16	18	13
depth of hole	↓_↓	25.282	FD2	swelling	58	47	52	53

## KEY

S1 : sample zone  
 FW : saturated extract for free water  
 RS : residual strength sample  
 F/BD: field and bulk density assessment  
 ... : sample shear surface(s)  
 --- : sample extent  
 _ _ : field levels and shear surface

Gs : specific gravity  
 VR : void ratio  
 P : porosity  
 Org : organic matter content  
 CEC : cation exchange capacity  
 in Meq/100g  
 Cond : conductivity

**APPENDIX 11**

**CHEMICAL EQUILIBRIA OF WATER-SOLUBLE AND EXCHANGEABLE IONS**

Manor Lane.

CORE #	Ion balance n = 2	ZONE ONE		ZONE TWO		ZONE THREE		ZONE FOUR		MEAN	
		S	E	S	E	S	E	S	E	S	E
1A	Na	2.35	3.74	2.83	4.22	3.48	4.61	3.91	4.96	3.13	4.39
	K	0.54	0.51	0.39	0.39	0.62	0.49	0.69	0.51	0.56	0.49
	Mg	4.33	27.08	3.92	25.25	6.83	29.0	6.75	28.50	5.50	27.5
	Ca	3.66	18.49	3.27	16.88	5.76	16.39	6.54	16.98	4.83	17.17
	Cl	0.96		1.27		1.27		1.24		1.18	
	SO ₄	10.44		9.63		16.71		16.94		13.44	
	Total (+)	10.88	49.82	10.40	46.73	16.68	50.49	17.89	50.95	14.02	49.55
1B	Total (-)	11.40		10.90		17.98		18.18		14.62	
	HCO ₃	-0.52		-0.50		-1.29		-0.28		-0.6	
	Na	2.0	3.22	3.09	3.96	3.30	5.70	3.74	8.91	3.04	5.44
	K	0.59	0.49	0.62	0.46	0.69	0.59	0.74	1.0	0.67	0.64
	Mg	5.42	29.08	7.83	32.17	4.92	31.08	1.42	25.83	4.92	29.58
	Ca	5.17	21.51	6.39	17.66	3.71	17.17	0.93	16.15	4.05	18.15
	Cl	0.68		0.85		0.99		0.65		0.79	
2A	SO ₄	13.56		19.50		13.40		7.06		13.38	
	Total (+)	13.18	54.30	17.93	54.25	12.62	54.54	6.83	51.89	12.68	53.81
	Total (-)	14.24		20.35		14.38		7.71		14.16	
	HCO ₃	-1.06		-2.42		-1.76		-0.88		-1.49	
	Na	2.78	4.22	2.91	4.83	4.04	5.22	4.78	7.70	3.65	5.48
	K	0.77	0.54	0.72	0.51	0.90	0.64	0.95	0.90	0.85	0.64
	Mg	8.42	31.75	8.0	30.92	8.25	34.92	3.50	28.67	7.08	31.58
2B	Ca	6.59	16.68	5.46	14.49	5.37	15.85	2.49	17.22	4.98	16.05
	Cl	1.27		1.35		1.55		0.82		1.24	
	SO ₄	20.31		18.19		20.17		12.08		17.69	
	Total (+)	18.55	53.19	17.09	50.74	18.56	56.63	11.72	54.48	16.56	53.75
	Total (-)	21.58		19.54		21.72		12.9		18.93	
	HCO ₃	-3.03		-2.45		-3.16		-1.18		-2.37	
	Na	4.17	5.83	5.52	6.22	4.35	6.30	5.65	7.57	4.91	6.48
3A	K	1.13	0.67	1.28	0.67	1.0	0.72	1.15	0.82	1.15	0.72
	Mg	10.0	30.67	10.08	32.92	8.83	30.58	4.0	24.50	8.25	29.67
	Ca	5.42	14.68	6.93	13.42	5.61	13.56	3.12	14.54	5.27	14.05
	Cl	1.38		1.69		1.75		0.99		1.47	
	SO ₄	22.79		25.75		21.31		13.73		20.90	
	Total (+)	20.72	51.84	23.81	53.22	19.79	51.17	13.93	47.42	19.59	50.91
	Total (-)	24.17		27.44		23.06		14.72		22.36	
3B	HCO ₃	-3.46		-3.63		-3.27		-0.79		-2.78	
	Na	3.87	6.30	4.04	7.17	4.48	6.83	7.17	7.83	4.91	7.04
	K	1.10	0.80	1.13	0.90	1.23	0.74	1.18	0.74	1.15	0.80
	Mg	8.08	34.67	9.50	39.75	6.92	35.50	12.5	34.33	9.25	36.08
	Ca	5.76	13.42	6.63	16.59	4.88	14.98	10.34	14.44	6.93	14.88
	Cl	1.27		1.27		0.87		1.38		1.21	
	SO ₄	20.48		23.60		19.0		35.65		24.69	
3C	Total (+)	18.81	55.18	21.31	64.41	17.50	58.05	31.19	57.34	22.24	58.80
	Total (-)	21.75		24.87		19.87		37.03		25.90	
	HCO ₃	-2.94		-3.57		-2.37		-5.83		-3.65	

All values in milliequivalents per litre (meq/l) where S = soluble & E = exchangeable ions  
 (+) : sum of the major cations (-) : sum of major anions  
 HCO₃ : assumed difference between cations and anions.



CORE #	Ion balance n = 2	ZONE ONE		ZONE TWO		ZONE THREE		ZONE FOUR		MEAN	
		S	E	S	E	S	E	S	E	S	E
3B	Na	2.22	4.22	3.09	4.09	2.65	5.35	4.04	7.17	3.0	5.22
	K	0.13	0.26	0.54	0.44	1.08	0.74	0.90	0.82	0.67	0.56
	Mg	1.33	31.08	5.42	24.75	7.50	26.33	4.92	32.83	4.83	28.75
	Ca	1.32	23.46	5.02	17.61	5.66	15.42	3.12	14.98	3.81	17.85
	Cl	0.79		0.82		1.07		1.18		0.96	
	SO ₄	4.27		13.73		18.35		13.73		12.52	
	Total (+)	5.00	59.02	14.07	46.88	16.89	47.84	12.98	55.80	12.31	52.39
	Total (-)	5.06		14.55		19.42		14.91		13.48	
	HCO ₃	-0.07		-0.48		-2.54		-1.93		-1.17	
4A	Na	0.48	2.61	0.61	2.87	1.35	3.61	2.96	4.09	1.35	3.30
	K	0.80	0.23	1.21	0.28	0.13	0.31	0.56	0.51	0.67	0.33
	Mg	1.25	30.08	1.75	23.42	0.83	21.67	4.58	26.92	2.08	25.50
	Ca	0.01	21.22	0.01	22.29	0.44	23.85	5.42	21.76	1.46	22.29
	Cl	0.37		0.37		0.51		0.87		0.54	
	SO ₄	0.65		0.40		2.69		17.23		5.25	
	Total (+)	2.53	54.14	3.57	48.86	2.75	49.44	13.52	53.27	5.56	51.43
	Total (-)	1.01		0.76		3.20		18.10		5.79	
	HCO ₃	1.52		2.81		-0.45		-4.58		-0.22	
4B	Na	1.96	3.48	1.57	3.09	1.91	3.35	4.52	6.30	2.48	4.04
	K	0.15	0.26	0.18	0.26	0.13	0.23	0.87	0.82	0.33	0.36
	Mg	1.75	24.92	1.08	24.0	1.08	33.42	2.67	24.42	1.67	26.67
	Ca	1.76	22.78	0.59	22.93	1.12	22.34	2.10	18.88	1.42	21.76
	Cl	0.56		0.51		0.51		1.32		0.73	
	SO ₄	4.67		2.31		3.29		8.42		4.67	
	Total (+)	5.62	51.43	3.41	50.27	4.25	59.34	10.16	50.42	5.89	52.83
	Total (-)	5.23		2.82		3.80		9.74		5.40	
	HCO ₃	0.39		0.59		0.45		0.42		0.49	
5A	Na	1.87	4.35	2.04	4.22	3.13	4.09	3.35	4.22	2.61	4.22
	K	0.05	0.13	0.05	0.15	0.46	0.41	0.51	0.46	0.21	0.28
	Mg	0.50	20.25	1.25	22.00	1.25	30.25	4.25	33.25	1.83	26.42
	Ca	0.78	28.78	1.37	29.61	6.54	26.00	4.88	22.34	3.42	26.68
	Cl	0.82		0.9		1.16		1.30		1.04	
	SO ₄	1.27		2.56		17.44		13.52		8.71	
	Total (+)	3.20	53.51	4.71	55.98	11.38	60.75	12.99	60.27	8.06	57.60
	Total (-)	2.09		3.46		18.59		14.82		9.75	
	HCO ₃	1.11		1.25		-7.21		-1.83		-1.69	
5B	Na	1.48	2.48	3.35	3.96	2.87	3.74	4.61	5.35	3.09	3.87
	K	0.82	0.56	0.87	0.51	0.90	0.59	1.31	0.69	0.97	0.59
	Mg	4.92	27.92	4.92	31.25	6.17	29.67	16.5	42.0	8.17	32.8
	Ca	3.37	18.93	6.24	11.46	3.90	14.24	9.76	15.85	5.81	15.12
	Cl	0.20		0.73		0.90		1.24		0.76	
	SO ₄	10.81		10.46		13.88		3.46		9.65	
	Total (+)	10.58	49.89	15.38	47.18	13.84	48.24	32.17	63.89	18.03	52.33
	Total (-)	11.01		11.19		14.78		4.70		10.41	
	HCO ₃	-0.43		4.19		-0.94		27.48		7.63	

All values in milliequivalents per litre (meq/l) where S = soluble & E = exchangeable ions

(+) : sum of the major cations

(-) : sum of major anions

HCO₃ : assumed difference between cations and anions.

CORE #	Ion balance n = 2	ZONE ONE		ZONE TWO		ZONE THREE		ZONE FOUR		MEAN	
		S	E	S	E	S	E	S	E	S	E
6	Na	1.0	3.74	1.52	3.87	1.83	3.61	3.78	4.35	2.04	3.91
	K	1.44	0.31	0.36	0.33	0.18	0.33	0.92	0.54	0.72	0.39
	Mg	3.33	23.08	0.58	21.33	0.83	21.58	9.17	33.67	3.50	24.92
	Ca	0.01	24.78	0.05	23.56	0.93	22.93	5.42	15.81	1.61	22.31
	Cl	0.45		0.48		0.96		1.16		0.76	
	SO ₄	0.69		0.90		2.27		18.31		5.54	
	Total (+)	5.77	51.91	2.51	49.10	3.77	48.45	19.29	54.36	7.87	51.53
	Total (-)	1.14		1.38		3.23		19.47		6.30	
	HCO ₃	4.64		1.14		0.54		-0.18		1.57	
7U	Na	0.48	2.35	1.35	3.74	1.39	5.09	3.04	5.83	1.57	4.26
	K	0.95	0.41	0.21	0.28	0.03	0.31	0.46	0.31	0.41	0.33
	Mg	1.67	16.67	0.50	18.08	2.33	20.17	0.75	21.75	1.33	19.17
	Ca	0.01	25.76	0.05	29.56	0.01	27.42	0.10	24.49	0.04	26.83
	Cl	0.42		0.37		0.68		2.23		0.93	
	SO ₄	0.75		0.75		0.75		1.21		0.88	
	Total (+)	3.10	45.18	2.10	51.67	3.76	52.98	4.35	52.37	3.35	50.59
	Total (-)	1.17		1.12		1.43		3.43		1.81	
	HCO ₃	1.93		0.99		2.33		0.92		1.54	
X	Na	2.04	3.87	2.65	4.35	2.91	4.78	4.30	6.17	2.98	4.79
	K	0.72	0.44	0.64	0.44	0.62	0.51	0.85	0.67	0.71	0.52
	Mg	4.25	27.25	4.58	27.17	4.67	28.67	5.92	29.75	4.86	28.21
	Ca	2.83	20.88	3.51	19.66	3.66	19.17	4.54	17.81	3.64	19.38
	Cl	0.76		0.87		1.01		1.21		0.96	
	SO ₄	9.23		10.65		12.44		13.44		11.44	
	Total (+)	9.84	52.43	11.39	51.61	11.85	53.13	15.60	54.4	12.17	52.89
	Total (-)	9.99		11.52		13.45		14.65		12.40	
	HCO ₃	-0.15		-0.13		-1.6		0.96		-0.23	

Worbarrow Bay.

WO	Na	10.48	6.70	5.52	4.83	5.39	3.96	1.91	4.96	5.83	5.13
	K	3.28	0.44	4.21	0.46	1.80	0.49	0.10	0.51	2.35	0.49
	Mg	1.50	9.17	1.25	8.50	1.25	8.17	0.25	10.92	1.08	9.17
	Ca	0.01	14.49	0.01	11.37	0.01	10.68	0.05	15.32	0.02	12.98
	Cl	1.89		1.66		1.41		1.75		1.69	
	SO ₄	1.21		0.79		0.48		0.79		0.81	
	Total (+)	15.26	30.79	10.98	25.15	8.44	23.29	2.32	31.70	9.25	27.76
	Total (-)	3.10		2.45		1.89		2.54		2.50	
	HCO ₃	12.17		8.52		6.55		-0.22		6.76	
W1	Na	4.09	10.78	3.91	11.52	3.65	11.13	3.30	10.65	3.74	11.04
	K	0.36	0.31	0.33	0.26	0.72	0.33	1.13	0.44	0.64	0.33
	Mg	1.00	16.17	1.00	11.75	1.08	15.75	1.33	12.25	1.10	14.0
	Ca	0.01	10.68	0	4.83	0	8.63	0	10.68	0.01	8.73
	Cl	2.09		2.06		1.78		1.24		1.79	
	SO ₄	0.73		0.40		0.56		0.73		0.60	
	Total (+)	5.45	37.94	5.25	28.36	5.45	35.85	5.77	34.02	5.48	34.11
	Total (-)	2.81		2.45		2.34		1.97		2.39	
	HCO ₃	2.63		2.79		3.12		3.80		3.08	

CORE #	Ion balance n = 2	ZONE ONE		ZONE TWO		ZONE THREE		ZONE FOUR		MEAN	
		S	E	S	E	S	E	S	E	S	E
W2	Na	2.74	11.52	2.70	10.65	3.22	12.0	2.65	12.74	2.83	11.74
	K	0.33	0.51	0.33	0.51	0.36	0.62	0.39	0.64	0.35	0.56
	Mg	1.0	17.25	1.00	16.58	1.0	16.67	1.00	16.75	1.0	16.83
	Ca	0.01	15.12	0.01	16.98	0.05	19.46	0.01	19.85	0.02	17.85
	Cl	1.80		1.63		1.97		1.52		1.73	
	SO ₄	0.48		0.56		0.96		0.56		0.65	
	Total (+)	4.07	4.41	4.03	44.72	4.63	48.75	4.04	49.98	4.19	46.99
	Total (-)	2.28		2.19		2.93		2.08		2.37	
	HCO ₃	1.79		1.83		1.70		1.95		1.82	
W3	Na	2.26	11.78	2.70	11.04	2.09	10.52	2.35	12.74	2.35	11.52
	K	1.26	0.49	0.23	0.49	0.23	0.59	0.23	0.56	0.49	0.54
	Mg	0.58	17.08	0.67	14.50	0.58	17.50	0.60	14.50	0.17	15.92
	Ca	0.01	10.29	0.05	12.93	0.05	17.17	0.05	15.71	0.04	14.05
	Cl	0.99		2.28		1.61		1.69		1.63	
	SO ₄	0.31		0.73		0.73		0.88		0.67	
	Total (+)	4.10	39.65	3.64	38.96	2.95	45.78	3.20	43.51	3.47	42.03
	Total (-)	1.30		3.01		2.34		2.57		2.30	
	HCO ₃	2.80		0.63		0.62		0.65		1.18	
W4	Na	1.65	12.0	1.04	9.78	1.74	6.30	2.17	10.78	1.65	9.74
	K	0.10	0.41	3.08	0.41	0.15	0.51	0.13	0.62	0.87	0.49
	Mg	0.17	14.33	1.0	11.50	0.25	19.75	0.25	20.92	0.42	16.67
	Ca	0.01	9.37	0	5.85	0.10	23.95	0.10	13.71	0.05	13.22
	Cl	1.58		1.55		2.17		1.52		1.72	
	SO ₄	0.56		0.31		0.96		1.21		0.77	
	Total (+)	1.93	36.11	5.12	27.55	2.24	50.52	2.65	46.02	2.99	40.11
	Total (-)	2.14		1.86		3.13		2.73		2.49	
	HCO ₃	-0.21		3.26		-0.89		-0.08		0.50	
W5	Na	1.61	5.44	1.78	5.44	2.13	5.70	1.65	4.61	1.78	5.30
	K	0.08	0.69	0.05	0.33	0.10	0.51	0.10	0.51	0.08	0.51
	Mg	0.17	14.75	0.17	12.83	0.17	13.42	0.17	12.25	0.17	13.33
	Ca	0.01	14.98	0.05	18.63	0.05	18.63	0.01	18.68	0.02	17.76
	Cl	1.66		1.80		2.23		1.78		1.86	
	SO ₄	0.56		0.56		0.56		0.56		0.56	
	Total (+)	1.86	35.85	2.05	37.24	2.45	38.26	1.93	36.06	2.05	36.91
	Total (-)	2.23		2.37		2.79		2.34		2.42	
	HCO ₃	-0.37		-0.32		-0.34		-0.41		-0.37	

All values in milliequivalents per litre (meq/l) where S = soluble & E = exchangeable ions  
 (+) : sum of the major cations (-) : sum of major anions  
 HCO₃ : assumed difference between cations and anions.

CORE #	Ion balance n = 2	ZONE ONE		ZONE TWO		ZONE THREE		ZONE FOUR		MEAN	
		S	E	S	E	S	E	S	E	S	E
WU	Na	3.78	7.78	3.91	7.70	3.44	7.22	3.30	7.39	3.61	7.52
	K	0.23	0.49	0.18	0.33	0.23	0.46	0.28	0.36	0.23	0.41
	Mg	0.67	17.75	0.58	18.33	0.67	20.58	0.58	21.75	0.67	19.58
	Ca	0.15	10.0	0.20	10.59	0.20	10.98	0.24	10.63	0.20	10.54
	Cl	4.68		4.79		5.80		5.72		5.24	
	SO ₄	1.73		1.48		1.50		1.65		1.58	
	Total (+)	4.83	36.02	4.87	36.95	4.53	39.24	4.41	40.13	4.70	38.05
	Total (-)	6.41		6.27		7.30		7.36		6.82	
	HCO ₃	-1.58		-1.40		-2.78		-2.95		-2.12	
X	Na	1.96	9.44	1.83	8.7	1.87	8.13	1.87	9.13	1.88	8.85
	K	1.31	0.49	1.49	0.41	0.8	0.51	0.26	0.51	0.97	0.48
	Mg	0.42	15.25	0.5	13.42	0.42	16.0	0.33	15.58	0.42	15.06
	Ca	0.02	12.15	0.05	11.61	0.05	15.66	0.05	14.93	0.04	13.59
	Cl	1.97		2.14		2.31		2.06		2.12	
	SO ₄	0.79		0.69		0.81		0.92		0.80	
	Total (+)	3.70	37.32	3.86	34.13	3.13	40.30	2.51	40.15	3.30	37.98
	Total (-)	2.76		2.83		3.12		2.97		2.92	
	HCO ₃	0.94		1.03		0.01		-0.47		0.38	

=====

All values in milliequivalents per litre (meq/l) where S = soluble & E = exchangeable ions  
 (+) : sum of the major cations      (-) : sum of major anions  
 HCO₃ : assumed difference between cations and anions.

APPENDIX 12

MANOR LANE DISPLACEMENT AND PHREATIC LEVEL DATA SUMMARY

DATE	MOVEMENT									PHREATIC LEVEL	
	1	2	3	4	5	6	7	8	9	SOURCE	LOBE
<u>1985</u>											
13.10	0	0	0	0	0	0	0	0	0	55	164
27.10	0	0	0	0	0	0	0	0	0	50	164
10.11	0	0	0	0	0	0	0	0	0	64	162
24.11	0	0	0	0	0	0	0	0	0	59	163
05.12	0	0	0	0	0	0	0	0	0	54	161
22.12	0	6	4	49	62	167	62	46	0	59	151
<u>1986</u>											
11.01	0	17	19	208	283	743	523	480	1	68	149
17.01	0	24	32	325	348	1167	666	622	1	67	157
08.02	0	29	40	617	431	1988	818	824	1	56	165
15.02	0	103	199	826	567	2416	1056	1068	1	48	169
01.03	0	168	327	985	708	2748	1258	1265	1	43	174
15.03	0	224	445	1151	812	3057	1423	1431	1	46	175
29.03	0	251	502	1233	862	3236	1518	1529	1	47	172
12.04	0	269	546	1287	897	3341	1579	1590	1	40	168
26.04	0	274	553	1301	909	3355	1593	1606	1	43	166
18.05	0	274	553	1301	910	3358	1594	1606	1	15	167

=====

All values in centimetres

Movement is presented as the cumulative displacement of surface peglines

Location of targets given in Figure 3.10

Phreatic level is calculated as the head of water above the basal shear surface

**APPENDIX 13**

**CORRECTIONS TO FORTRAN 4 PROGRAMME WATEQF**

```

*****
File WORKING: CUDAA230JORIGINAL_WATEQF.FOR;1
  125      INTEGER D,E,DD,RBIT,CORALK,Z(120),PRT(4)
  126      INTEGER PECALC,PECK
*****
File WORKING: CUDAA230JEDITED_WATEQF.FOR;2
  125      INTEGER D,E,DD,RBIT,CORALK,Z(120),PRT(4),RUNCOU
  126      INTEGER PECALC,PECK
*****
*****
File WORKING: CUDAA230JORIGINAL_WATEQF.FOR;1
  129      REAL NSPEC(120),NREACT(200)
  130      COMMON MI,KT,LOGKT,LOGKTO,KW,D,E,DD,C,R,T,F,TEMP,A,B,PE,PES,PEDO,P
*****
File WORKING: CUDAA230JEDITED_WATEQF.FOR;2
  129      REAL*8 NSPEC(120),NREACT(200)
  130      COMMON MI,KT,LOGKT,LOGKTO,KW,D,E,DD,C,R,T,F,TEMP,A,B,PE,PES,PEDO,P
*****
*****
File WORKING: CUDAA230JORIGINAL_WATEQF.FOR;1
  138      JJ=0
*****
File WORKING: CUDAA230JEDITED_WATEQF.FOR;2
  138      RUNCOU=0
  139      JJ=0
*****
*****
File WORKING: CUDAA230JORIGINAL_WATEQF.FOR;1
  148      ICK=0
*****
File WORKING: CUDAA230JEDITED_WATEQF.FOR;2
  149      RUNCOU=RUNCOU+1
  150      WRITE(6,*)
  151      WRITE(6,*) 'OUTPUT FOR RUN',RUNCOU
  152      WRITE(6,*)
  153      WRITE(7,*)
  154      WRITE(7,*) 'DATA CARDS FOR RUN ',RUNCOU
  155      WRITE(7,*)
  156      WRITE(7,*) 'DATA FOR CARD ONE IS:'
  157      WRITE(7,70) TITL
  158      ICK=0
*****
*****
File WORKING: CUDAA230JORIGINAL_WATEQF.FOR;1
  166      50  FORMAT (5X,A8,2X,I2,3X,F10.4,1X,F4.1)
  167      60  FORMAT (5X,A8,2X,2F10.4)
*****
File WORKING: CUDAA230JEDITED_WATEQF.FOR;2
  176      50  FORMAT (5X,A8,2X,I2,2X,F10.4,1X,F4.1)
  177      60  FORMAT (5X,A8,2X,2F10.4)
*****
*****
File WORKING: CUDAA230JORIGINAL_WATEQF.FOR;1
  181      REAL NSPEC(120),NREACT(200)
  192      COMMON MI,KT,LOGKT,LOGKTO,KW,D,E,DD,C,R,T,F,TEMP,A,B,PE,PES,PEDO,P
*****
File WORKING: CUDAA230JEDITED_WATEQF.FOR;2
  191      REAL*8 NSPEC(120),NREACT(200)
  192      COMMON MI,KT,LOGKT,LOGKTO,KW,D,E,DD,C,R,T,F,TEMP,A,B,PE,PES,PEDO,P
*****

```

```

*****
File WORKING:[UDAA230]ORIGINAL_WATEQF.FOR;1
  241      IFLAG=FLAG
*****
File WORKING:[UDAA230]EDITED_WATEQF.FOR;2
  251      WRITE(7,*) 'DATA FOR CARD TWO IS:'
  252      WRITE(7,*) TEMP,PH,EHM,EHMC,EMFZ,DENS,DOX,FLAG,CORALK,
  253      1PECALC,IGD,(PRT(I),I=1,4),IDAV=S,ISPEC,IMIN
  254      IFLAG=FLAG
*****
*****
File WORKING:[UDAA230]ORIGINAL_WATEQF.FOR;1
  271      IF (ISPEC.GT.0) READ(5,590) (KSPEC(I),I=1,ISPEC)
  272      IF (IMIN.GT.0) READ(5,590) (KMIN(I),I=1,IMIN)
  273      80  READ(5,690) WORD,(INT(I),VAL(I),I=1,5)
  274      IF (WORD.NE.CARD(1)) GO TO 100
  275      DO 90 I=1,5
*****
File WORKING:[UDAA230]EDITED_WATEQF.FOR;2
  284      WRITE(7,*) 'DATA FOR CARD THREE IS:'
  285      WRITE(7,*) (CUNITS(INPT(I)),I=1,6)
  286      WRITE(7,*) 'DATA FOR CARD FOUR IS:'
  287      WRITE(7,*) (CUNITS(INPT(I)),I=7,12)
  288      IF (ISPEC.GT.0) READ(5,590) (KSPEC(I),I=1,ISPEC)
  289      IF (ISPEC.GT.0) WRITE(7,*) 'DATA FOR OPTIONAL CARD TYPE ONE IS:'
  290      IF (ISPEC.GT.0) WRITE(7,*) (KSPEC(I),I=1,ISPEC)
  291      IF (IMIN.GT.0) READ(5,590) (KMIN(I),I=1,IMIN)
  292      IF (IMIN.GT.0) WRITE(7,*) 'DATA FOR OPTIONAL CARD TYPE ONE IS:'
  293      IF (IMIN.GT.0) WRITE(7,*) (KMIN(I),I=1,IMIN)
  294      80  READ(5,690) WORD,(INT(I),VAL(I),I=1,5)
  295      IF (WORD.NE.CARD(1)) GO TO 100
  296      WRITE(7,*) 'DATA FOR OPTIONAL CARD TYPE TWO IS:'
  297      WRITE(7,*) WORD,(INT(I),VAL(I),I=1,5)
  298      DO 90 I=1,5
*****
*****
File WORKING:[UDAA230]ORIGINAL_WATEQF.FOR;1
  289      GO TO 100
*****
File WORKING:[UDAA230]EDITED_WATEQF.FOR;2
  312      WRITE(7,*) 'DATA FOR OPTIONAL CARD TYPE TWO IS:'
  313      WRITE(7,*) WORD,(INT(I),VAL(I),I=1,5)
  314      GO TO 100
*****
*****
File WORKING:[UDAA230]ORIGINAL_WATEQF.FOR;1
  300      GO TO 110
*****
File WORKING:[UDAA230]EDITED_WATEQF.FOR;2
  325      WRITE(7,*) 'DATA FOR OPTIONAL CARD TYPE TWO IS:'
  326      WRITE(7,*) WORD,(INT(I),VAL(I),I=1,5)
  327      GO TO 110
*****
*****
File WORKING:[UDAA230]ORIGINAL_WATEQF.FOR;1
  311      GO TO 130
*****
File WORKING:[UDAA230]EDITED_WATEQF.FOR;2
  338      WRITE(7,*) 'DATA FOR OPTIONAL CARD TYPE TWO IS:'
  339      WRITE(7,*) WORD,(INT(I),VAL(I),I=1,5)

```



```

340          GO TO 130
*****
*****
File WORKING:[UDAA230]ORIGINAL_WATEQF.FOR;1
348          GO TO 180
*****
File WORKING:[UDAA230]EDITED_WATEQF.FOR;1
377          WRITE(7,*) "DATA FOR OPTIONAL CARD TYPE TWO IS:"
378          WRITE(7,*) WORD,(INT(I),VAL(I),I=1,5)
379          GO TO 180
*****
*****
File WORKING:[UDAA230]ORIGINAL_WATEQF.FOR;1
353          GO TO 220
*****
File WORKING:[UDAA230]EDITED_WATEQF.FOR;2
384          WRITE(7,*) "DATA FOR OPTIONAL CARD TYPE TWO IS:"
385          WRITE(7,*) WORD,(INT(I),VAL(I),I=1,5)
386          GO TO 220
*****
*****
File WORKING:[UDAA230]ORIGINAL_WATEQF.FOR;1
576          REAL NSPEC(120),NREACT(200)
577          COMMON MI,KT,LOGKT,LOGKTO,KW,D,E,DD,C,R,T,F,TEMP,A,B,PE,PES,PEDO,P
*****
File WORKING:[UDAA230]EDITED_WATEQF.FOR;2
609          REAL*8 NSPEC(120),NREACT(200)
610          COMMON MI,KT,LOGKT,LOGKTO,KW,D,E,DD,C,R,T,F,TEMP,A,B,PE,PES,PEDO,P
*****
*****
File WORKING:[UDAA230]ORIGINAL_WATEQF.FOR;1
670          REAL NSPEC(120),NREACT(200)
671          DIMENSION NPAIR(5),L1M(9),L1K(9),L1C(9),L1A(9),L2M(13),L2K(13),L2C
*****
File WORKING:[UDAA230]EDITED_WATEQF.FOR;2
703          REAL*8 NSPEC(120),NREACT(200)
704          DIMENSION NPAIR(5),L1M(9),L1K(9),L1C(9),L1A(9),L2M(13),L2K(13),L2C
*****
*****
File WORKING:[UDAA230]ORIGINAL_WATEQF.FOR;1
1298         REAL NSPEC(120),NREACT(200)
1299         COMMON MI,KT,LOGKT,LOGKTO,KW,D,E,DD,C,R,T,F,TEMP,A,B,PE,PES,PEDO,P
*****
File WORKING:[UDAA230]EDITED_WATEQF.FOR;2
1331         REAL*8 NSPEC(120),NREACT(200)
1332         COMMON MI,KT,LOGKT,LOGKTO,KW,D,E,DD,C,R,T,F,TEMP,A,B,PE,PES,PEDO,P
*****
*****
File WORKING:[UDAA230]ORIGINAL_WATEQF.FOR;1
1469         REAL NSPEC(120),NREACT(200)
1470         COMMON MI,KT,LOGKT,LOGKTO,KW,D,E,DD,C,R,T,F,TEMP,A,B,PE,PES,PEDO,P
*****
File WORKING:[UDAA230]EDITED_WATEQF.FOR;2
1502         REAL*8 NSPEC(120),NREACT(200)
1503         COMMON MI,KT,LOGKT,LOGKTO,KW,D,E,DD,C,R,T,F,TEMP,A,B,PE,PES,PEDO,P
*****
*****
File WORKING:[UDAA230]ORIGINAL_WATEQF.FOR;1
1501         77),LIST7(98),LIST7(99),LIST7(100),LIST7(101)/64,116,117,58,67,59,6
1502         81,150,55,45,142,115,54,102,37,10,101,147,143,38,66,62,32,60,107,14

```

*****

File WORKING: CUDAA230JEDITED_WATEQF.FOR;2

1534 *7),LIST7(98),LIST7(99),LIST7(100),LIST7(101)/

1535 *64,116,117,58,67,59,6

1536 81,150,55,45,142,115,54,102,37,10,101,147,143,38,66,62,32,60,107,14

*****

*****

File WORKING: CUDAA230JORIGINAL_WATEQF.FOR;1

1645 DO 100 I=1,102

1646 IF (IMIN.EQ.0) GO TO 80

*****

File WORKING: CUDAA230JEDITED_WATEQF.FOR;2

1679 DO 100 I=1,101

1680 IF (IMIN.EQ.0) GO TO 80

*****

Number of difference sections found: 19

Number of difference records found: 48

DIFFERENCES /IGNORE=()/MERGED=1/OUTPUT=WORKING: CUDAA230JCHANGES.DAT;1-

WORKING: CUDAA230JORIGINAL_WATEQF.FOR;1-

WORKING: CUDAA230JEDITED_WATEQF.FOR;2